VOLUME 67
NUMBER 4 / NUMÉRO 4
APRIL / AVRIL
2010

Canadian Journal of FISHERIES AND AQUATIC SCIENCES

cjfas.nrc.ca

Journal canadien des SCIENCES HALIEUTIQUES ET AQUATIQUES

jcsha.cnrc.ca

An NRC Research Press
JOURNAL
Une REVUE des
Presses scientifiques du CNRC

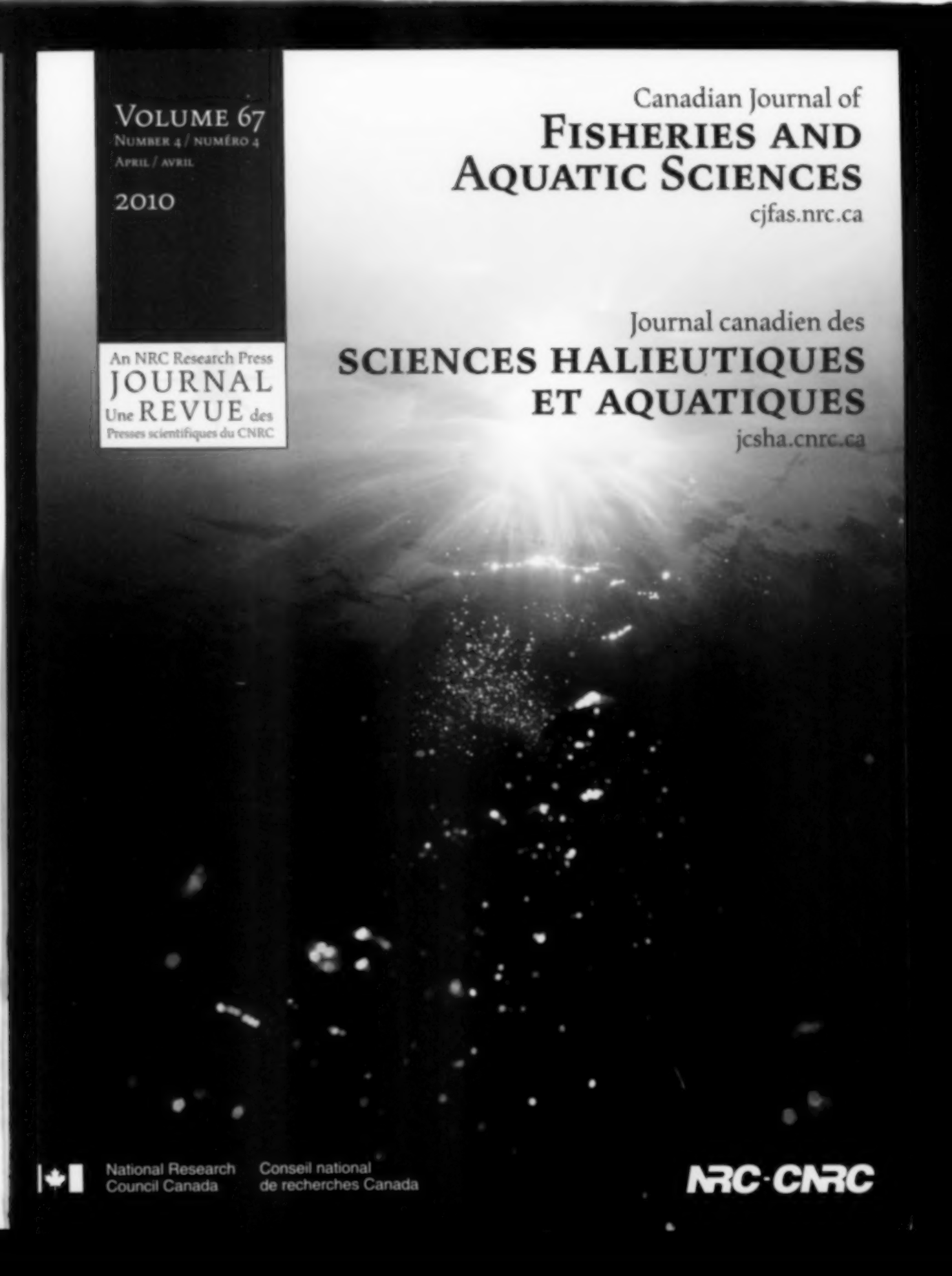

National Research Council Canada
Conseil national de recherches Canada
NRC·CNRC

ISSN 0706-652X / CJFSDX 67(4) 597–768 (2010)

The *Canadian Journal of Fisheries and Aquatic Sciences*, previously published as *Contributions to Canadian Biology* 1901–1925, *Contributions to Canadian Biology and Fisheries* 1926–1934, *Journal of the Biological Board of Canada* 1934–1937, and *Journal of the Fisheries Research Board of Canada* 1938–1979, is issued monthly to form annual volumes of 12 numbers plus supplements.

Editorial policy. The Journal publishes original research articles, perspectives (syntheses, critiques, reevaluations), discussions (comment and reply), and rapid communications. Manuscripts may concern cells, organisms, populations, communities, ecosystems, or processes that affect aquatic systems. They may cover a range of disciplines including biology and ecology of marine and freshwater organisms, limnology, oceanography, physiology, toxicology, genetics, economics, disease, and management. Preference will be given to manuscripts that emphasize understanding of observed phenomena and interpretation of experimental results. The Journal encourages papers that lead from clearly stated purpose or rationale and from testable hypotheses, concepts, or questions to identifiable conclusions or syntheses. Such papers may amplify, modify, question, or redirect accumulated knowledge embodied in contemporary perceptions of a particular state of aquatic sciences. The Journal discourages papers that are essentially descriptive, except in emerging disciplines; have only site-specific or local applications (a certain year, place, taxon, chemical compound, etc.); only confirm previously established principles; or apply standard techniques without breaking new methodological ground.

Manuscripts for publication should be submitted to the Editorial Office via NRC Research Press' online submission and peer review system (**OSPREY**) at pubs.nrc-cnrc.gc.ca/cjfas/osprey. Alternatively, manuscripts may be submitted by mail to Editorial Office, *Canadian Journal of Fisheries and Aquatic Sciences*, Department of Ecology and Evolutionary Biology, University of Toronto, Toronto, ON M5S 3G5, Canada (tel.: 416-946-0609; fax: 866-523-4174 (Canada and United States) or 416-946-0509; e-mail: cjfas@utoronto.ca).

Submissions in either English or French are acceptable. The information must be original, that is, not copyrighted, published, or submitted elsewhere except in abstract form or unless by written consent of the Editors.

Correspondence concerning accepted manuscripts and corrected proofs should be sent to NRC Research Press, National Research Council of Canada, Ottawa, ON K1A 0R6, Canada (fax: 613-952-7656; e-mail: pubs@nrc-cnrc.gc.ca).

Instructions to Authors are published at cjfas.nrc.ca. The **Publishing Policy** of NRC Research Press is available at pubs.nrc-cnrc.gc.ca.

The ***Canadian Journal of Fisheries and Aquatic Sciences***, **ISSN 0706-652X**, is published **Monthly**, **12 times per year**, by **NRC Research Press, c/o USACAN Media Dist. Srv. Corp.** at 26 Power Dam Way, Suite S1-S3, Plattsburgh, NY 12901, USA. Periodicals postage paid at Plattsburgh, NY. POSTMASTER: Send address changes to ***Canadian Journal of Fisheries and Aquatic Sciences***, c/o NRC, P.O. Box 2888, Plattsburgh, NY 12901, USA.

Publié sans interruption depuis 1901, le *Journal canadien des sciences halieutiques et aquatiques* a paru sous plusieurs titres : *Contributions to Canadian Biology* 1901–1925, *Contributions to Canadian Biology and Fisheries* 1926–1934, *Journal of the Biological Board of Canada* 1934–1937, et *Journal of the Fisheries Research Board of Canada* 1938–1979. Le Journal paraît tous les mois, formant ainsi un volume de 12 numéros, et offre en plus jusqu'à deux suppléments par année.

Politique éditoriale. On publie, dans le Journal, des articles rendant compte de recherche originale, des perspectives (synthèses, critiques et réévaluations), des discussions (commentaires et réponses) et des communications rapides. Les documents peuvent porter sur les cellules, organismes, populations, communautés, écosystèmes ou processus qui affectent les systèmes aquatiques. Ils peuvent relever de divers domaines y compris la biologie et l'écologie des organismes marins et d'eau douce, la limnologie, l'océanographie, la physiologie, la toxicologie, la génétique, l'économie, la pathologie et la gestion. On accorde la préséance aux articles qui contribuent à la compréhension de phénomènes observés et à l'interprétation de résultats expérimentaux. On invite les auteurs à soumettre des articles ayant des objectifs précis ou relevant d'hypothèses, de concepts ou de questions vérifiables et se terminant par de solides conclusions ou d'utiles synthèses. Ces articles enrichissent, changent, mettent en question ou réorientent les connaissances acquises sur divers aspects des sciences aquatiques. On décourage toutefois la soumission d'articles simplement descriptifs (à moins qu'il ne s'agisse de nouvelles disciplines), d'application très limitée (applicables à une seule année, une seule région ou un seul taxon, portant sur un unique composé chimique, etc.); d'articles qui ne font que reprendre les principes énoncés dans des articles précédents; et d'articles rendant compte de l'application de normes sans gain de méthodologie.

Les auteurs sont invités à soumettre leur **manuscrit** au Bureau de la rédaction par le truchement du Système de soumission et d'examen en direct des articles (**OSPREY**) des Presses scientifique du CNRC au pubs.nrc-cnrc.gc.ca/jcsha/osprey. Sinon, ils peuvent transmettre leur manuscrit par la poste au Bureau de la rédaction, *Journal canadien des sciences halieutiques et aquatiques*, Département d'écologie et de biologie évolutive, Université de Toronto, Toronto, ON M5S 3G5, Canada (tél. : 416-946-0609; téléc. : 866-523-4174 (Canada et États-Unis) ou 416-946-0509; courriel : cjfas@utoronto.ca).

Les contributions peuvent être en anglais ou en français. Elles doivent être originales, c.-à.-d. qu'elles ne doivent pas avoir fait l'objet d'un copyright, avoir été publiées ou soumises ailleurs, sauf sous forme abrégée ou avec le consentement des rédacteurs en chef.

La correspondance ayant trait aux manuscrits acceptés et les épreuves corrigés doivent être envoyées aux Presses scientifiques du CNRC, Conseil national de recherches du Canada, Ottawa, ON K1A 0R6, Canada (téléc. : 613-952-7656; courriel : pubs@nrc-cnrc.gc.ca).

Les **Recommandations aux auteurs** sont publiées au jcsha.cnrc.ca. La **Politique éditoriale** est disponible auprès des Presses scientifiques du CNRC ou au pubs.nrc-cnrc.gc.ca.

This Journal is indexed or abstracted in / Cette revue est signalée ou résumée dans

Aqualine; Aquatic Sciences and Fisheries Abstracts; BIOBASE; Biological and Agricultural Index; BIOSIS; CAB Abstracts; Canadian Fisheries Abstracts; Chemical Abstracts; Current Awareness in Biological Sciences; Current Abstracts; Current Contents; General Science Index; Oceanic Abstracts; PASCAL; Pollution Abstracts; Referativnyi Zhurnal; Science Citation Index; Water Resources Abstracts

Volume 67, Number 4, April 2010

Canadian Journal of Fisheries and Aquatic Sciences

Published by the National Research Council of Canada

Volume 67, numéro 4, avril 2010

Journal canadien des sciences halieutiques et aquatiques

Publié par le Conseil national de recherches du Canada

Editors / Rédacteurs en chef **Don Jackson and Rolf Vinebrooke**

Assistant to the Editors / Adjointe au rédacteur en chef **Holly Foster**

Associate Editors / Comité de rédaction

M.J. Bradford, *DFO/MPO and Simon Fraser University*
D. Brickman, *DFO/MPO, Dartmouth*
S.E. Campana, *DFO/MPO, Dartmouth*
X. Chen, *Shanghai Fisheries University, Shanghai, China*
Y. Chen, *University of Maine, Orono, Maine*
I. Fleming, *Memorial University of Newfoundland*
D. Fraser, *Concordia University*
B. Gillanders, *University of Adelaide, Australia*
J.W.A. Grant, *Concordia University*
M.M. Hansen, *Aarhus University, Denmark*
R. Hilborn, *University of Washington*
J.M. Jech, *NFSC/NOAA, Woods Hole, Mass.*
B. Jonsson, *Norwegian Institute for Nature Research, Oslo, Norway*
J. Karlsson, *Umeå University*
K.A. Kidd, *University of New Brunswick*
C. Kraft, *Cornell University, Ithaca, N.Y.*
D.L. MacLatchy, *University of New Brunswick, Saint John*
P. Magnan, *Université du Québec à Trois Rivières*
C.T. Marshall, *University of Aberdeen*
P. Moran, *Universidad de Vigo*
J. Post, *University of Calgary*
Y.T. Prairie, *Université du Québec à Montréal*
T.J. Quinn II, *University of Alaska–Fairbanks, Juneau, Alaska*
C.W. Ramcharan, *Laurentian University*
J.S. Richardson, *The University of British Columbia*
M.-J. Rochet, *IFREMER, Nantes, France*
K. Rose, *Louisiana State University, Baton Rouge, La.*
J. Rosenfeld, *British Columbia Ministry of Fisheries*
B. Sainte-Marie, *DFO/MPO, Mont-Joli*
R.E.H. Smith, *University of Waterloo*
S.J. Smith, *DFO/MPO, Dartmouth*
W.G. Sprules, *University of Toronto at Mississauga*
E.B. Taylor, *The University of British Columbia*
W. Tonn, *University of Alberta*
M. Trudel, *DFO/MPO, Pacific Biological Station, Nanaimo*
A. Vasemägi, *University of Turku, Turku, Finland*
C.J. Walters, *The University of British Columbia*
G. Weyhenmeyer, *Uppsala University, Sweden*

NRC Research Press / Presses scientifiques du CNRC

Fax / Télécopieur : 613-952-7656; e-mail / courriel : pubs@nrc-cnrc.gc.ca; URL / URL : pubs.nrc-cnrc.gc.ca

Editor-in-Chief / Directeur de la publication **Bruce P. Dancik**
Deputy Editor-in-Chief / Sous-directrice de la publication **Cindy E. Prescott**
Publisher / Éditeur **Cameron D. Macdonald**
Deputy Director / Directrice adjointe **Suzanne Kettley**

Business Manager / Gestionnaire des affaires commerciales **Mike Boroczki**
Advertising / Annonces publicitaires **Roxanne Landriault** (613-990-2254)
Subscriptions / Abonnements **Eileen Evans-Nantais** (613-990-7873), **Scott Bryant** (613-993-9084)

Manager, Journals Program / Gestionnaire du Programme des revues **Carolyn Brown**
Managing Editor / Directrice de la rédaction **Cecily M. Pearson** (613-993-9099)
Scientific Publishing Editors / Réviseurs de publications scientifiques **Jennifer McColl, Peter Burke**
Editorial Publication Technicians / Techniciens à la publication éditoriale **Diana Leck**
Editorial Applications Training and Support Officer / Agente de formation et de soutien à l'éditique **Susanne Lantos**

Production Manager / Gestionnaire de la production **Judy Hum**
Application Support Technician / Technicien au soutien de la production **Greg Boyce**
e-Publishing Technician / Technicien à l'édition électronique **Cory Klinkenberg**
Graphics Technician / Technicien en graphisme **Dario Ferrara**
Web Technician / Technicien Web **Dennis Cafferty**

The National Research Council of Canada accepts no responsibility for statements or opinions expressed by a contributor. Acceptance of an advertisement, announcement, or other material does not imply endorsement by either the Journal's Editors or the National Research Council of Canada.

© 2010 National Research Council Canada or its licensors

For articles published in 2009 and later, copyright remains with the authors, whereas for articles published before 2009, copyright is held by the National Research Council Canada.

No part of the NRC Research Press journals may be reproduced, stored, or transmitted in any form or by any means, without the written permission of the publisher, except as stated below.

Under the Canadian *Copyright Act*, individuals may download or print single copies of articles for personal research or study. Any person may reproduce short excerpts from articles in the journals for any purpose that respects the moral rights of authors, provided that the source is fully acknowledged. As a courtesy, the consent of authors of such material should be obtained directly from the author.

Authorization to reproduce items for other than personal research or study, as stated above, may be obtained by clicking on the "Reprints and Permissions" link in the table of contents of the electronic article in question or via Access Copyright (www.accesscopyright.ca).

NRC Research Press also extends certain additional rights to authors.

The above rights do not extend to copying or reproduction for general distribution, for advertising or promotional purposes, for creating new collective works, or for resale. For such copying or reproduction, arrangements must be made with NRC Research Press (National Research Council Canada, Ottawa, ON K1A 0R6, Canada).

Subscription information

The *Canadian Journal of Fisheries and Aquatic Sciences* (ISSN 0706-652X) is published monthly by the National Research Council of Canada. The 2010 subscription rates are as follows. Institutional: electronic $1180; print, $1365; electronic + print, $1700. Personal: electronic, $305, print + electronic, $415. For all orders outside Canada, rates are in U.S. dollars. Print subscriptions include second class postage. For air mail add US$204 to the foreign rate. Canadian customers please include GST (business no. 12149 1807 RT 0275). Subscriptions are entered for the calendar year. Remittances should be made payable to the Receiver General for Canada, credit NRC. Price for regular single issues: institutional, $120.00; personal, $40.00. Supplements will be priced separately. Special rates apply to members of Canadian scientific and engineering societies if they subscribe through their respective societies.

Issues of the *Canadian Journal of Fisheries and Aquatic Sciences* are available on the Web. Pricing information can be found at pubs.nrc-cnrc.gc.ca.

There are no refunds on cancelled subscriptions once delivery has begun. Claims for missing issues should be made within four months (North America) or six months (outside North America) following the date of publication. The publisher expects to supply missing issues only when losses have occurred in transit and when the reserve stock will permit. For change of address and subscription enquiries: Subscription Office, NRC Research Press, National Research Council of Canada, Ottawa, ON K1A 0R6, Canada; tel.: 613-993-9084; fax: 613-952-7656; e-mail: pubs@nrc-cnrc.gc.ca.

Microform backfiles are available from UMI, P.O. Box 1346, Ann Arbor, MI 48106-1346, USA, and Micromedia Ltd., 20 Victoria St., Toronto, ON M5C 2N8, Canada.

Le Conseil national de recherches du Canada ne se tient en aucune façon responsable des opinions exprimées par un collaborateur ou des déclarations que pourrait faire ce dernier. La publication d'annonces publicitaires, d'avis et autres n'implique pas l'endossement de leur contenu par les rédacteurs en chef de la Revue ou le Conseil national de recherches du Canada.

© 2010 Presses scientifiques du CNRC ou ses concédants de licence

Les auteurs détiennent les droits d'auteur sur les articles publiés en 2009 et plus tard, tandis que les Presses scientifiques du CNRC détiennent les droits d'auteurs sur les articles publiés avant 2009.

Il est interdit de reproduire, de sauvegarder ou de transmettre toute partie des revues des Presses scientifiques du CNRC dans quelque format ou de quelque façon que ce soit sans le consentement écrit de l'éditeur, sauf dans les cas énoncés ci-après.

Aux termes de la *Loi sur le droit d'auteur* du Canada, les particuliers peuvent télécharger ou imprimer des copies individuelles d'articles pour leurs études ou leurs recherches personnelles. Toute personne peut reproduire de courts extraits des articles d'une revue pourvu que les droits moraux de l'auteur soient respectés et que la source soit clairement indiquée. Il convient de demander directement à l'auteur son consentement.

On peut obtenir l'autorisation de reproduire du contenu à d'autres fins que l'usage personnel (tel que décrit ci-dessus), en cliquant sur le lien « Réimpressions et autorisations » dans la table des matières de l'article électronique en question ou par l'intermédiaire d'Access Copyright (www.accesscopyright.ca).

Les Presses scientifiques du CNRC accordent aussi des privilèges supplémentaires aux auteurs.

Les droits ci-dessus ne s'appliquent pas à la reproduction à grande échelle aux fins de distribution générale, de publicité ou de promotion, de compilation de nouveaux ouvrages collectifs ou de revente, par exemple. Les droits de reproduction de ce genre doivent faire l'objet d'une entente particulière avec les Presses scientifiques du CNRC (Conseil national de recherches du Canada, Ottawa, ON K1A 0R6, Canada).

Renseignements sur l'abonnement

Journal canadien des sciences halieutiques et aquatiques (ISSN 0706-652X) est une publication mensuelle du Conseil national de recherches du Canada. En 2010, les tarifs d'abonnement pour les organismes sont les suivants : 1180 $ pour la version électronique; 1365 $ pour l'imprimé; 1700 $ pour les deux versions. Pour leur part, les particuliers paient les tarifs suivants : 305 $ pour la version électronique; 415 $ pour la version électronique et l'imprimé. Les tarifs des commandes provenant de l'extérieur du Canada sont en dollars des États-Unis. L'abonnement à l'imprimé comprend le tarif du courrier de deuxième classe. L'expédition par avion exige des frais de 204 $US en sus du prix d'abonnement à l'étranger. Les clients du Canada doivent ajouter la TPS (numéro d'entreprise 12149 1807 RT 0275). Les abonnements sont pour l'année civile. Tout paiement doit être adressé au Receveur général du Canada, crédit du CNRC. Le prix par numéro régulier est de 120,00 $ pour les organismes et de 40,00 $ pour les particuliers. Le prix des hors-série varie. Les membres des sociétés canadiennes de sciences et de génie bénéficient de taux préférentiels en s'abonnant via leurs sociétés respectives.

Tous les numéros de *Journal canadien des sciences halieutiques et aquatiques* sont accessibles sur le Web. On trouvera des renseignements sur les tarifs au pubs.nrc-cnrc.gc.ca.

Aucun remboursement ne sera accordé, ni aucune annulation acceptée, une fois que les livraisons auront commencé. Les réclamations de numéros manquants devront être soumises dans les quatre mois (Amérique du Nord) ou dans les six mois (à l'extérieur de l'Amérique du Nord) suivant la date de publication. L'éditeur ne fournira de numéros manquants que si le document a été perdu pendant l'expédition et que si les réserves le permettent. Adressez tout changement d'adresse ou toute question quant à l'abonnement au Bureau des abonnements, Presses scientifiques du CNRC, Conseil national de recherches Canada, Ottawa, ON K1A 0R6, Canada; tél. : 613-993-9084; téléc. : 613-952-7656; courriel : pubs@nrc-cnrc.gc.ca.

On peut obtenir les fichiers rétrospectifs sur **microforme** auprès de UMI, P.O. Box 1346, Ann Arbor, MI 48106-1346, USA, et auprès de Micromedia Ltée, 20, rue Victoria, Toronto, ON M5C 2N8, Canada.

Patterns and magnitude of Zn:Ca in otoliths support the recent phylogenetic typology of Salmoniformes and their sister groups

Karin E. Limburg and Mikael Elfman

Abstract: Fish otolith chemistries are used to associate fishes with specific environments. However, otolith chemistry may also have potential as a tool in phylogenetic research, as demonstrated here in salmoniform fishes and related taxa. Two-dimensional maps of Zn:Ca otolith chemistry displayed annual oscillations in magnitude in members of the Salmoniformes (with salmons differing from whitefishes). These are also detectable in esocids, but not strongly in osmerids or in more distantly related taxa. Further, Zn:Ca magnitudes were highest in salmonids and declined in other taxa: salmonids (salmons, grayling, and whitefishes) > esocids > osmerids > other. We performed spatial analysis on sagittal section Zn:Ca maps, dividing them into five zones and obtaining means within each zone, as well as grand means. Discriminant function analysis of the different otolith zones was better able to separate taxonomic groups, but showed pike grouping more closely with salmonids and osmerids with the out-group. Zn:Ca incorporation in otoliths may be a trait under phylogenetic control, and recent re-ordering of the systematics of Salmoniformes and their sister groups may be supported by otolith Zn:Ca chemistry.

Résumé : La chimie des otolithes de poissons sert à associer les poissons à des environnements spécifiques. La chimie des otolithes peut aussi potentiellement servir d'outil dans la recherche phylogénétique, comme nous le démontrons ici chez les poissons salmonidés et les taxons apparentés. Des cartes bidimensionnelles de la chimie de Zn:Ca dans les otolithes montrent des oscillations annuelles d'amplitude chez des membres des salmoniformes (les saumons se distinguant des corégones). Celles-ci se décèlent aussi chez les ésocidés, mais pas de façon marquée chez les osméridés, ni chez les autres taxons moins apparentés. De plus, les amplitudes de Zn:Ca sont maximales chez les salmonidés et diminuent chez les autres taxons : salmonidés (saumons, ombres et corégones) > ésocidés > osméridés > autres. Une analyse spatiale sur des cartes en coupe sagittale de Zn:Ca les divise en cinq zones et fournit les moyennes de chaque zone ainsi que les moyennes totales. Une analyse des fonctions discriminantes des différentes zones d'otolithes sépare encore mieux les groupes taxonomiques, mais montre que les brochets s'associent de plus près aux salmonidés et les osméridés au groupe externe. L'incorporation de Zn:Ca dans les otolithes peut être un trait sous contrôle phylogénétique et la chimie de Zn:Ca des otolithes peut venir appuyer la réorganisation récente de la systématique des salmoniformes et de leurs groupes-sœurs.

[Traduit par la Rédaction]

Introduction

Fish otoliths, or earstones, are routinely used for ageing studies of fish populations. A second, rapidly growing area of inquiry is the use of otolith microchemistry to understand ecological questions such as migration history or stock discrimination through the identification of "chemical fingerprints" (Campana and Thorrold 2001). Although comparative otolith morphologies have proven valuable for systematics studies (e.g., Nolf 1993; Assis 2003), few, if any, have linked otolith chemical composition to phylogeny. We report here on a striking set of patterns we noticed and suggest that they might be a window on phylogenetic relationships within the protacanthopterygians. Namely, we documented (Limburg et al. 2001; but see also Halden et al. (2000) and Arai et al. (2007)) oscillatory patterns in zinc found in otoliths of salmoniform fishes. Furthermore, the magnitudes of zinc (normalized to calcium) are higher than in other taxa we examined; in fact, in most fish otoliths, Zn is very low (see below).

Our studies were conducted with a nuclear microprobe using proton-induced X-ray emission (micro-PIXE; Elfman et al. 1999, 2000) at the Lund Nuclear Microprobe Facility. Our setup is optimized for Sr detection and is less sensitive to other trace elements. Hence, we often do not measure trace elements at levels that might be detected with higher sensitivity instrumentation, e.g., inductively coupled plasma mass spectrometry. Our aim is generally to map out Sr (rel-

Received 5 May 2009. Accepted 10 February 2010. Published on the NRC Research Press Web site at cjfas.nrc.ca on 10 March 2010. J21183

Paper handled by Associate Editor Bronwyn Gillanders.

K.E. Limburg.[1] Faculty of Environmental and Forest Biology, State University of New York, College of Environmental Science and Forestry, Syracuse, NY 13210, USA.
M. Elfman. Department of Nuclear Physics, Lund University, SE-223 62 Lund, Sweden.

[1]Corresponding author (e-mail: Klimburg@esf.edu).

Fig. 1. Zn:Ca maps of (*a*) Atlantic salmon (*Salmo salar*), (*b*) European whitefish (*Coregonus lavaretus*) (otolith is broken), (*c*) northern pike (*Esox lucius*), and (*d*) rainbow smelt (*Osmerus eperlanus*). All except (*c*) are sagittal sections; the pike otolith is a transverse section. Horizontal bars = 1 mm. Scale is in units of Zn counts per Ca counts ($\times 10^{-3}$).

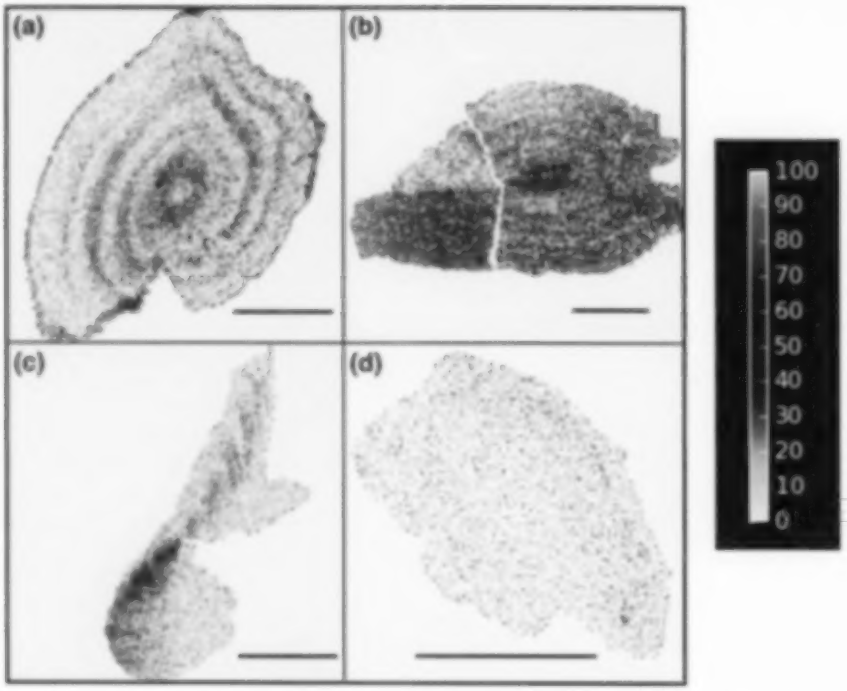

Fig. 2. Otolith of a brown trout (*Salmo trutta*) analyzed by microPIXE. Otoliths grow from a central core and continue to grow throughout a fish's life. Sagittal section shown here; the tip of the rostrum was broken off (lower right). (*a*) Optical image; (*b*) map of strontium to calcium ration; (*c*) map of zinc to calcium ratios. Zn:Ca has same scale as in Fig. 1, units of Zn counts per Ca counts ($\times 10^{-3}$); Sr:Ca scale ranges from 0 to 400 Sr counts per Ca counts ($\times 10^{-3}$).

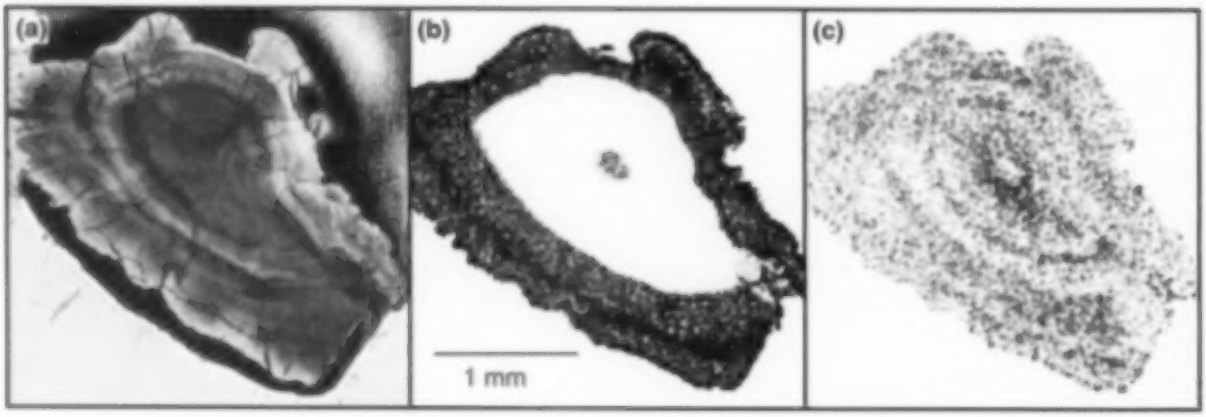

ative to Ca) concentrations in sectioned otoliths, but occasionally we detect other elements as well. We distinguish between biologically meaningful measurements and contamination by the fact that the former follow the growth form of the otolith (Figs. 1 and 2). Zinc in otoliths is thought to be bound to protein (Miller et al. 2006) rather than being incorporated into the aragonite structure.

We first noticed the oscillatory pattern in Zn:Ca in studies of Baltic Sea brown trout (*Salmo trutta*) (Limburg et al. 2001); at that time, we were studying patterns in Sr:Ca and relating these to migratory histories. The Sr:Ca and Zn:Ca patterns were independent of one another, but Zn:Ca matches well with seasonal zonation patterns (Fig. 2). Specifically, Zn:Ca appears to vary in a periodically repeating

Table 1. Summary of taxa examined in this study.

Family	Subfamily	Species	Common name	Origin	Number analyzed	Mean Zn:Ca × 1000
Salmonidae	Salmoninae	*Oncorhynchus mykiss*	Rainbow trout	Gotland, Sweden	1	33.7
Salmonidae	Salmoninae	*Oncorhynchus tshawytscha*	Chinook salmon	Pacific Northwest	1	30.8
Salmonidae	Salmoninae	*Oncorhynchus kisutch*	Coho salmon	Pacific Northwest	1	28.9
Salmonidae	Salmoninae	*Oncorhynchus clarki*	Cutthroat trout	Arkansas	1	44.3
Salmonidae	Salmoninae	*Salmo trutta*	Brown trout	Gotland, Sweden	2	37.7
Salmonidae	Salmoninae	*Salmo salar*	Atlantic salmon	New York, USA	2	22.4
Salmonidae	Salmoninae	*Salvelinus fontinalis*	Brook trout	New York, USA	1	30.5
Salmonidae	Salmoninae	*Salvelinus namaycush*	Lake trout	Pacific Northwest	1	17.2
Salmonidae	Thymallinae	*Thymallus arcticus*	Arctic grayling	Pacific Northwest	1	47.6
Salmonidae	Coregoninae	*Coregonus laurettae*	Bering cisco	Pacific Northwest	1	25.7
Salmonidae	Coregoninae	*Coregonus nasus*	Broad whitefish	Pacific Northwest	1	37.7
Salmonidae	Coregoninae	*Coregonus oidschian*	Humpback whitefish	Pacific Northwest	1	28.3
Salmonidae	Coregoninae	*Coregonus sardinella*	Least cisco	Pacific Northwest	1	27.3
Salmonidae	Coregoninae	*Coregonus lavaretus*	European whitefish	Gotland, Sweden	3	36.7
Salmonidae	Coregoninae	*Prosopium cylindraceum*	Round whitefish	Pacific Northwest	1	27.7
Salmonidae	Coregoninae	*Stenodus leucichthys*	Sheefish	Pacific Northwest	1	38.8
Esocidae		*Esox lucius*	Northern pike (average only)	Gotland, Sweden	3	27.1
Esocidae		*Esox niger*	Chain pickerel	NYS	2	11.1
Osmeridae		*Allosmerus elongatus*	Whitebait smelt	Pacific Northwest	2	7.3
Osmeridae		*Hypomesus pretiosus*	Surf smelt	Pacific Northwest	2	12.9
Osmeridae		*Osmerus mordax*	Rainbow smelt	NYS	3	11.2
Osmeridae		*Osmerus eperlanus*	European smelt	Belgium	3	11.2
Osmeridae		*Osmerus eperlanus*	European smelt	Sweden	2	12.1
Osmeridae		*Spirinchus lanceolatus*	Longfin smelt	Pacific Northwest	3	9.4
Gadidae		*Gadus morhua*	Atlantic cod	North Sea	1	4.4
Centrarchidae		*Lepomis macrochirus*	Bluegill sunfish	New York, USA	1	4.5
Percidae		*Perca flavescens*	Yellow perch	New York, USA	1	5.6

Published by NRC Research Press

manner, with increases in spring–summer and declines in fall–winter. We also saw this pattern in Atlantic salmon (*Salmo salar*). We did not observe Zn in other species that we were studying, including members of the families Anguillidae, Clupeidae, Siluridae, Ictaluridae, Gadidae, Moronidae, Centrarchidae, Percidae, and Gobiidae.

When Halden et al. (2000) published their report on annual Zn oscillations in Arctic char (*Salvelinus alpinus*), also measured by micro-PIXE, we began to think that there might be a genetic basis for this pattern that was detectable by this method. We had the opportunity to analyze a number of other salmoniform otoliths (Table 1) from a broad latitudinal range (ca. 35°N–66°N) of different ages and both sexes and found elevated, oscillating Zn patterns in all of them. However, the patterns differed. We also discovered, in a separate study (K.E. Limburg, M. Elfman, and P. Landergren, unpublished data), that northern pike (*Esox lucius*) otoliths also showed annual Zn oscillations (e.g., Fig. 1*c*).

Ishiguro et al. (2003) analyzed mitochondrial genomic data for 34 species within the protacanthopterygian fishes, an assemblage of primitive taxa. Their analysis yielded a new typology of phylogenetic relationships in which Osmeroides (smelts) are replaced by Esociformes (pikes) as the closest sister group to salmoniforms. Ramsden et al. (2003) took this a step further and suggested that this lent support to the proposition that the group has freshwater origins. We cannot comment on this but note that in the Baltic Sea drainage, there appear to be sympatric populations of obligate freshwater and marine forms along with anadromous forms of northern pike (Westin and Limburg 2002).

Given Ishiguro et al.'s (2003) analysis and our observations of Zn oscillations in salmons, whitefishes, and pike, we enlarged our study and include smelts, as well as an out-group, to test whether Zn concentrations and patterns could, in fact, support the new proposed phylogeny. Specifically, we hypothesized that salmoniform otoliths (*i*) had higher Zn:Ca than other taxa and (*ii*) that patterns of uptake varied in different regions (dorsal, ventral, anterior, posterior) in salmoniforms and that these differed strongly between whitefishes and other salmoniforms.

Materials and methods

Otolith preparation and analysis

Otoliths (Table 1) from eight salmon species (Atlantic and Pacific salmons and chars), seven whitefish species, Arctic grayling (*Thymallus arcticus*), two species of esocids, and four species of osmerids were included in the study, along with three species (cod (*Gadus morhua*), bluegill sunfish (*Lepomis macrochirus*), and yellow perch (*Perca flavescens*)) that together formed an out-group (this based on our previous observations of very low Zn counts in otoliths of non-salmoniform–esocid species that we analyzed; see Introduction). Species were represented by one to five individuals (Table 1).

With the exception of northern pike, all otoliths were sectioned in the sagittal plane, ground, and polished to expose the core. The northern pike otoliths ($n = 3$) were sectioned in the transverse plane, which meant that although oscillations could be observed, we could not include them in the spatial analysis, described below, that examined directional accumulations of Zn.

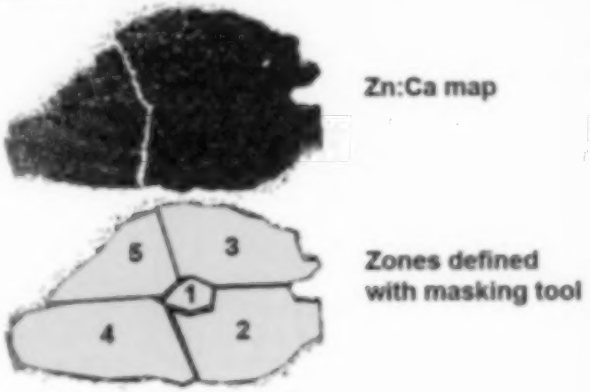

Fig. 3. Zn:Ca map from an otolith of European whitefish (*Coregonus lavaretus*). Bottom panel shows use of masking tool to define zones for extracting data.

Otoliths were analyzed with micro-PIXE; methods can be found in Elfman et al. (1999, 2000) and Limburg et al. (2001), but briefly, a proton beam of 20–50 μm was rastered across the surface of the sample, which excites the electrons and causes them to fluoresce (X-ray fluorescence, XRF). Each element fluoresces at characteristic wavelengths and can thus be quantified individually. In this manner, spatial maps of detectable elements could be constructed. Concentrations of Zn were normalized to Ca, the major element detectable in otoliths. Whereas other methods, such as synchrotron-based XRF, have also detected Zn:Ca oscillations in salmoniform otoliths (e.g., Bilderback et al. 2003), we have restricted this analysis to our own micro-PIXE work to eliminate potential biases due to use of different instrumentation.

Data analysis

Because spatial heterogeneity was evident (Fig. 1), we used a geographic information system (GIS) tool, ArcMap (ESRI 2008), to extract data from the otolith maps. The maps, which were matrices of 128 × 128 or 256 × 256 rows and columns, were input as raster maps into the GIS. A masking tool was then used to define regions of interest (zones) on the otolith (Fig. 3), and the Spatial Analyst subroutine was used to extract summary statistics from the zones, which were exported into database files for further handling. The five zones were the core (zone 1), dorsal and ventral halves of the posterior region (zones 2 and 3), and rostrum (zone 4) and anti-rostrum (zone 5) regions.

Mean Zn:Ca for the entire otolith, as well as mean Zn:Ca for each of the five zones, were collected for all otoliths except for the three northern pike maps, which had been measured in the transverse plane and therefore lacked posterior and anterior (rostrum, anti-rostrum) measurements. In addition, a semiquantitative metric was included to capture the oscillatory nature of the Zn:Ca banding. Clearly visible banding was assigned a 1, no visible banding was assigned a zero, and weakly visible banding was assigned a value of 0.5.

Table 2. Probabilities associated with post-hoc comparisons (unequal *N*, honestly significant difference (HSD)) of analysis of variance (ANOVA) of mean whole otolith Zn:Ca.

	Grayling	Salmon	Coregonine	Esocid	Osmerid	Out-group
Grayling	1	0.479189	0.632059	0.073501	**0.004922**	**0.000927**
Salmon		1	0.976984	0.210472	**0.000131**	**0.000580**
Coregonine			1	0.068597	**0.000130**	**0.000242**
Esocid				1	0.189216	0.061874
Osmerid					1	0.890614
Out-group						1

Note: Significantly different comparisons ($p < 0.05$) indicated by bold type.

Fig. 4. Box plots of mean Zn:Ca in salmoniforms, esocids, osmerids, and "other" (out-group species).

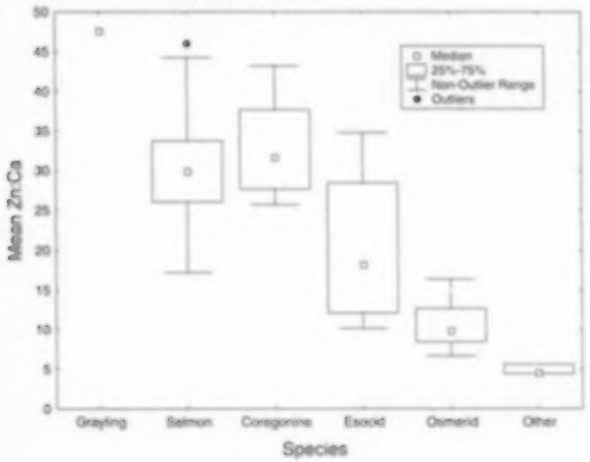

Univariate and multivariate analyses were performed in STATISTICA (StatSoft Inc. 2003) and SYSTAT (Systat Software Inc. 2008). Analysis of variance (ANOVA) was used to test whether mean Zn:Ca alone could distinguish among salmons, whitefish, grayling, pikes, smelts, and the out-group species. Principal components analysis (PCA) was performed to examine associations of the different otolith zones. Discriminant function analysis (DFA) was then used to test whether the zonal statistics and ring visibility could further distinguish among the groups. DFA with the jackknife option was used in SYSTAT to sequentially classify individuals to group (salmon + grayling, whitefishes, pike, smelt, and out-group). Groupings of zones were created based on the PCA and were re-analyzed with discriminant function analysis.

Results

Differences in whole otolith mean Zn:Ca were highly significant (ANOVA, $F_{[5,37]} = 23.53$, $p < 10^{-6}$). Post-hoc comparison showed that smelts and the out-group were significantly different from grayling, salmons, and whitefishes but not from each other (Table 2; Fig. 4). Zones 1–5 also showed similar groupings and displayed heterogeneity of variances (Levene's test, $p < 0.05$).

Principal components analysis indicated that zones 1, 2, and 4 (core and ventral side of the otolith) and zones 3 and 5 (dorsal side of the otolith) grouped together. This helped us to form discriminant function models. A number of models were explored and classification results of three models are presented (Table 3). All models were highly significant, with correct classification rates > 60%. Interestingly, models that did not group zone 1 with zones 2 and 4 performed better than those that did. The criterion of Zn:Ca ring visibility, when included, caused more separation between [osmerids + out-group] and the other groups (Fig. 5).

From examination of the canonical root plots, it was seen that DFA produced two major groupings: [salmon–grayling + coregonine + esocids] and [osmerid + out-group], with some models producing misclassifications of one esocid (chain pickerel) as an osmerid and one Atlantic salmon as an esocid. Lake trout was classified as an osmerid in models that included mean Zn:Ca; it had the lowest mean Zn:Ca of all the salmonines (Table 1).

Discussion

Zn:Ca is generally higher in salmoniform otoliths than in the other taxa we measured. The spatial orientation of otolith Zn:Ca accumulation is different among the salmon and whitefish subfamilies and suggests different patterns of zinc deposition during otolith growth. Namely, *Salmo* spp. deposit Zn more or less uniformly throughout a given growth band, albeit sometimes with less Zn detectable in the ventral posterior region. In contrast, coregonine Zn deposition is concentrated within the anterior (rostral) region. This appeared to be the case in all seven whitefish species we examined, as well as within multiple individuals of European whitefish. These are real patterns and not an accident of poor sample preparation: we inadvertently re-analyzed one of the sectioned whitefish otoliths on its back side and found the same Zn:Ca pattern. We also analyzed otoliths of two *Salvelinus* species, four *Oncorhynchus* species, and Arctic grayling (*Thymallus arcticus*), but not enough specimens of either individual species or groups to conclude anything about depositional patterns, save for the fact that oscillatory patterns are visible.

The only other species in which we detected Zn:Ca annual oscillations are esocids. We also looked for Zn:Ca oscillations within rainbow smelt and European smelt but did not find any. Likewise, other smelt species have lower otolith Zn:Ca, although all of the Pacific smelt species we analyzed appeared to have very weak banding. Fishes more distantly related (gadid, centrarchid, percid) had lowest Zn:Ca and no evidence of annual oscillations at all, even though these fish were several years old.

We find it striking that our observations of Zn oscillatory

Table 3. Classifications into taxonomic groupings with discriminant function analysis (DFA).

	Coregonine	Esocid	Osmerid	Other	Salmon	% correct
(*a*) DFA with zones 1–5 and mean Zn:Ca						
Classification matrix						
Coregonine	**8**	0	0	0	2	80
Esocid	0	**2**	0	0	0	100
Osmerid	0	0	**12**	3	0	80
Other	0	0	0	**3**	0	100
Salmon	0	1	1	0	**8**	80
Total	8	3	13	6	10	83
Jackknifed classification matrix						
Coregonine	**8**	0	0	0	2	80
Esocid	0	**1**	1	0	0	50
Osmerid	1	1	**9**	4	0	60
Other	0	0	0	**3**	0	100
Salmon	1	2	1	0	**6**	60
Total	10	4	11	7	8	68
(*b*) DFA with grouped zones 2–4 and 3–5 and mean Zn:Ca						
Classification matrix						
Coregonine	**9**	0	0	0	0	100
Esocid	0	**1**	1	0	0	50
Osmerid	0	0	**14**	1	0	93
Other	0	0	0	**3**	0	100
Salmon	1	1	1	0	**8**	73
Total	10	2	16	4	8	88
Jackknifed classification matrix						
Coregonine	**9**	0	0	0	0	100
Esocid	0	**1**	1	0	0	50
Osmerid	0	0	**14**	1	0	93
Other	0	0	0	**3**	0	100
Salmon	1	1	1	0	**8**	73
Total	10	2	16	4	8	88
(*c*) DFA with zones 1–5, Zn:Ca, and visible Zn:Ca rings						
Classification matrix						
Coregonine	**9**	0	0	0	0	100
Esocid	0	**2**	0	0	0	100
Osmerid	0	0	**8**	7	0	53
Other	0	0	0	**3**	0	100
Salmon	0	2	0	0	**9**	82
Total	9	4	8	10	9	78
Jackknifed classification matrix						
Coregonine	**7**	0	0	0	2	78
Esocid	0	**2**	0	0	0	100
Osmerid	0	0	**7**	8	0	47
Other	0	0	0	**3**	0	100
Salmon	2	2	0	0	**7**	64
Total	**9**	4	7	11	9	65

Note: "Salmon" also includes the Arctic grayling. Correct classifications are in bold. For the classification matrix, cases in row categories are classified into columns.

patterns used to group these fishes agree with the phylogenetic typology suggested by Ishiguro et al. (2003). We do not understand the mechanism of Zn incorporation in otoliths, although Zn can be taken up through the gills (Hogstrand et al. 1998) or via direct consumption and trophic transfer (Willis and Sunda 1984). Some workers (e.g., Arai et al. 2007) have concluded that Zn, like Sr, can be used as a tracer of past environments used by individual fishes. In contrast, we analyzed dozens of brown trout otoliths from fish that used multiple environments over their lifetimes (Limburg et al. 2001) and found that whereas otolith Sr:Ca varied with environment, Zn:Ca had regular, annual patterns of increase and decrease (Fig. 2) regardless of where they had lived. We also analyzed a dozen Atlantic salmon (unpublished data) from both Sweden and North America and observed the same phenomenon. The same is also true of the northern pike we analyzed (K.E. Limburg, M. Elfman, and P. Landergren, unpublished data), which were anadro-

Fig. 5. Plots of primary canonical roots of discriminant function model that used zones 2 + 4 and 3 + 5 and the presence of visible rings as classifiers. Key to symbols: diamonds, coregonines; asterisks, salmonines; squares, esocids; triangles, osmerids; ×, outgroup.

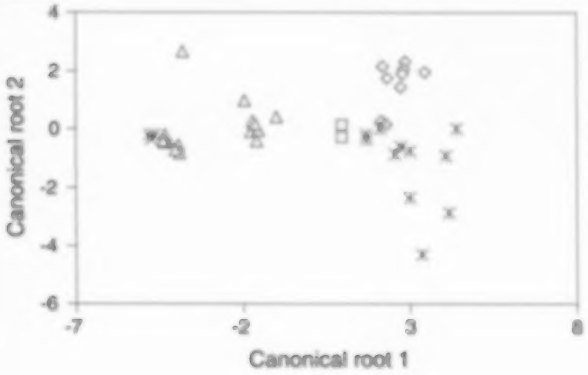

mous based on Sr:Ca patterns but which showed annual patterns of Zn:Ca. We suggest that this provides support for a genetic basis of the Zn:Ca oscillations observed in salmoniforms and esocids.

We also note that other species may in fact show annual patterns in zinc within otoliths, but our criterion for quantifying Zn:Ca was to use a particular method (microPIXE) implemented with relatively short scanning times (ca. 9–18 s per pixel) for this study. Longer scanning times or different, more sensitive instrumentation (e.g., laser ablation combined with ICPMS) can doubtless quantify lower zinc concentrations. Indeed, one of us (K.E.L.) has quantified seasonal oscillations of zinc in cod otoliths, but with synchrotron-based XRF and fivefold longer scanning times (K.E. Limburg, unpublished data).

Otolith formation is under genetic control (Söllner et al. 2003). We suggest that otolith proteins, which can be extracted by decalcifying the otoliths (e.g., Miller et al. 2006), or the genes that code for these proteins might provide useful material for phylogenetic analysis. Further research on otolith Zn might help to identify more highly resolved groupings within the salmoniforms, and in general, the affinity for metal uptake by these proteins may show genetic control in other taxa as well. Finally, we suggest that this approach might also be applied to other trace elements in fish otoliths, particularly those for which environmental control does not appear to be a factor.

Acknowledgments

The authors thank J.J. Dodson for pointing out the revised phylogeny and for reading an early draft, R. Brown, A. Cushing, J. Guelinckx, P. Landergren, S. Parker, L. Resseguie, A. Siniscal, E. Taylor, and H. Wickström for providing specimens, S. Stehman for confirming the statistical analyses and for discussions about interpretation, and T. Hayden, D. Stewart, and J. Waldman for comments on the manuscript. This work was supported by grants from FORMAS (No. 217-2006-1048) and the National Science Foundation (DEB-021838).

References

Arai, T., Ohji, M., and Hirata, T. 2007. Trace metal deposition in teleost fish otolith as an environmental indicator. Water Air Soil Pollut. **179**(1–4): 255–263. doi:10.1007/s11270-006-9229-4.

Assis, C.A. 2003. The lagenar otoliths of teleosts: their morphology and its application in species identification, phylogeny and systematics. J. Fish Biol. **62**(6): 1268–1295. doi:10.1046/j.1095-8649.2003.00106.x.

Bilderback, D.H., Huang, R., Kazimirov, A., Kriksunov, I.A., Limburg, K., and Fontes, E. 2003. Monocapillary optics developments and applications. Adv. X-ray Anal. **46**: 320–325.

Campana, S.E., and Thorrold, S.R. 2001. Otoliths, increments, and elements: key to a comprehensive understanding of fish populations. Can. J. Fish. Aquat. Sci. **58**(1): 30–38. doi:10.1139/cjfas-58-1-30.

Elfman, M., Limburg, K.E., Kristiansson, P., Malmqvist, K., and Pallon, J. 1999. Application of microPIXE to fish life history analyses: trace element analysis of otoliths. Nucl. Instrum. Methods Phys. Res. B, **150**(1–4): 272–276. doi:10.1016/S0168-583X(98)01006-4.

Elfman, M., Limburg, K.E., Kristiansson, P., Svedäng, H., Westin, L., Wickström, H., Malmqvist, K., and Pallon, J. 2000. Complex life histories of fishes revealed through natural information storage devices: case studies of diadromous events as recorded by otoliths. Nucl. Instrum. Methods Phys. Res. B, **161–163**: 877–881. doi:10.1016/S0168-583X(99)00923-4.

ESRI. 2008. ArcGIS 9.2. ESRI, Redlands, California. Available at www.esri.com.

Halden, N.M., Mejia, S.R., Babaluk, J.A., Reist, J.D., Kristofferson, A.H., Campbell, J.L., and Teesdale, W.J. 2000. Oscillatory zinc distribution in Arctic char (*Salvelinus alpinus*) otoliths: the result of biology or environment? Fish. Res. **46**(1–3): 289–298. doi:10.1016/S0165-7836(00)00154-5.

Hogstrand, C., Webb, N., and Wood, C.M. 1998. Covariation in regulation of affinity for branchial zinc and calcium uptake in freshwater rainbow trout. J. Exp. Biol. **201**(11): 1809–1815. PMID:9576891.

Ishiguro, N.B., Miya, M., and Nishida, M. 2003. Basal euteleostean relationships: amitogenomic perspective on the phylogenetic reality of the "Protacanthopterygii." Mol. Phylogenet. Evol. **27**(3): 476–488. doi:10.1016/S1055-7903(02)00418-9. PMID: 12742752.

Limburg, K.E., Landergren, P., Westin, L., Elfman, M., and Kristiansson, P. 2001. Flexible modes of anadromy in Baltic sea trout: making the most of marginal spawning streams. J. Fish Biol. **59**(3): 682–695. doi:10.1111/j.1095-8649.2001.tb02372.x.

Miller, M.B., Clough, A.M., Batson, J.N., and Vachet, R.W. 2006. Transition metal binding to cod otolith proteins. J. Exp. Mar. Biol. Ecol. **329**(1): 135–143. doi:10.1016/j.jembe.2005.08.016.

Nolf, D. 1993. A survey of perciform otoliths and their interest for phylogenetic analysis, with an iconographic synopsis of the Percoidei. Bull. Mar. Sci. **52**: 220–239.

Ramsden, S.D., Brinkmann, H., Hawryshyn, C.W., and Taylor, J.S. 2003. Mitogenomics and the sister of Salmonidae. Trends Ecol. Evol. **18**(12): 607–610. doi:10.1016/j.tree.2003.09.020.

Söllner, C., Burghammer, M., Busch-Nentwich, E., Berger, J., Schwarz, H., Rickel, C., and Nicolson, T. 2003. Control of crystal size and lattice formation by starmaker in otolith biomineralization. Science (Washington, D.C.), **302**(5643): 282–286. doi:10.1126/science.1088443. PMID:14551434.

StatSoft Inc. 2003. STATISTICA (data analysis software system). Version 6. StatSoft Inc., Tulsa, Oklahoma. Available at statsoft.com.

Systat Software Inc. 2008. SYSTAT. Version 12. Systat Software Inc., Chicago, Illinois. Available at systat.com.

Westin, L., and Limburg, K.E. 2002. Newly discovered reproductive isolation reveals sympatric populations of *Esox lucius* in the Baltic. J. Fish Biol. **61**: 1647–1652.

Willis, J.N., and Sunda, W.G. 1984. Relative contributions of food and water in the accumulation of zinc by two species of marine fish. Mar. Biol. (Berl.), **80**(3): 273–279. doi:10.1007/BF00392822.

Thermal dynamics of ovarian maturation in Atlantic cod (*Gadus morhua*)

Olav Sigurd Kjesbu, David Righton, Maria Krüger-Johnsen, Anders Thorsen, Kathrine Michalsen, Merete Fonn, and Peter R. Witthames

Abstract: The timing and success of spawning in marine fish are of fundamental importance to population persistence and distribution and, for commercial species, sustainability. Their physiological processes of reproduction are regulated, in part, by water temperature, and therefore changes in marine climate may have dramatic effects on spawning performance. Using adult Atlantic cod (*Gadus morhua*) as a case study, we examined the links between water temperature, body size, vitellogenesis, and spawning time by conducting extensive laboratory and field studies. Our experiments documented that vitellogenesis generally starts at autumnal equinox and that oocyte growth and investment are greater in cod held at warmer temperatures. Furthermore, spawning occurred earlier when oocyte growth was more rapid. Large females spawned earlier than smaller females at warmer temperatures, but this effect vanished at colder temperatures. The experimental results were confirmed by measurements of oocyte growth collected from wild-caught cod in northern (Barents Sea) and southern (Irish Sea and North Sea) populations. The established, general model of oocyte maturation was consistent with published egg production curves of cod from these waters, considering relevant in situ temperatures recorded by individual data-storage tags on cod. These findings have considerable relevance for future studies of fish recruitment in relation to climate change.

Résumé : Le calendrier et le succès de la fraie chez les poissons marins sont d'importance fondamentale pour la persistance, la répartition et, chez les espèces commerciales, la durabilité de la population. Leurs processus de régulation physiologique sont contrôlés, en partie, par la température de l'eau, si bien que des changements dans le climat marin peuvent avoir des effets considérables sur la performance de la fraie. Nous servant de la morue franche (*Gadus morhua*) comme espèce de cas, nous examinons les liens entre la température, la taille corporelle, la vitellogenèse et le moment de la fraie au cours d'expériences en laboratoire et d'études de terrain d'envergure. Nos expériences démontrent que la vitellogenèse débute généralement à l'équinoxe d'automne et que la croissance des oocytes et l'investissement reproductif sont plus importants chez les morues gardées aux températures plus élevées. De plus, la fraie se produit plus tôt lorsque la croissance des oocytes est plus rapide. Aux températures plus élevées, les femelles de plus grande taille fraient plus tôt que les femelles plus petites, mais ce phénomène ne se produit pas aux températures plus basses. Nos résultats expérimentaux sont confirmés par des mesures de la croissance des oocytes réalisées chez des morues capturées en nature dans des populations du nord (mer de Barents) et du sud (mers d'Irlande et du Nord). Le modèle général établi de maturation des oocytes s'accorde avec les courbes publiées de production d'œufs de morues dans ces eaux, compte tenu des températures pertinentes enregistrées in situ par des étiquettes enregistreuses individuelles sur les morues. Ces résultats sont d'une grande pertinence pour les études futures du recrutement des poissons en fonction du changement climatique.

[Traduit par la Rédaction]

Introduction

Current scenarios of climate change are based on extensive analyses of a suite of environmental variables and have led to the conclusion that many natural systems are being affected by regional climate changes, particularly temperature increases (Intergovernmental Panel of Climate Change (IPCC) 2007). The focus on temperature has resulted in many studies examining the link between species distributions and climate change (Parmesan and Yohe 2003). The marine environment is no exception, with some authors suggesting that the southern limits of species distributions are rapidly moving northwards (Perry et al. 2005).

Although species distributions are likely to change, many populations will persist under suboptimal conditions and

Received 1 April 2009. Accepted 11 December 2009. Published on the NRC Research Press Web site at cjfas.nrc.ca on 9 March 2010. J21136

Paper handled by Associate Editor C. Tara Marshall.

O.S. Kjesbu,[1] **M. Krüger-Johnsen, A. Thorsen, K. Michalsen, and M. Fonn.** Institute of Marine Research, P.O. Box 1870, N-5817 Bergen, Norway.
D. Righton and P.R. Witthames.[2] Centre for Environment Fisheries and Aquaculture Science, Pakefield Road, Lowestoft, Suffolk NR330HT, UK.

[1]Corresponding author (e-mail: olav.kjesbu@imr.no).
[2]Present address: Fecund Fish Consultancy, 40 Plumtrees, Lowestoft, Suffolk, NR32 3JH, UK.

therefore it is also necessary to understand how changes in marine climate will affect vital processes (Drinkwater 2005; Pörtner et al. 2008). This can be achieved by undertaking process-oriented and mechanistic studies and placing the results in the framework of metabolic ecology (Brown et al. 2004; Sousa et al. 2008). For example, based on studies on eelpout (*Zoarces viviparous*) and Atlantic cod (*Gadus morhua*), Pörtner et al. (2008) concluded that temperatures beyond pejus ("turning worse") are first felt at the whole-organism level (because of oxygen-limited thermal tolerance), followed by reductions in growth and reproductive investment. Thus the physiological effects of extreme warming seas are likely to have far-ranging effects on population dynamics (Brander 2007).

Atlantic cod is a species of high commercial and socio-economic value that occurs throughout the North Atlantic in waters predicted to be among those showing the largest temperature rises in the world (Drinkwater 2005; IPCC 2007). Cod grow faster, become fatter, mature at an earlier age, and are distributed further north with increasing environmental temperature (Dutil and Brander 2003; Drinkwater 2005; Sundby and Nakken 2008). The reproductive performance of cod is also sensitive to temperature. Overall fecundity seems to increase with temperature (Kjesbu et al. 1998; Pörtner et al. 2001), but the quality of the eggs may be reduced beyond ~10 °C (Pepin et al. 1997; Geffen et al. 2006; van der Meeren and Ivannikov 2006). The physiological links between water temperature and reproductive success are likely traceable to the aerobic demands of their large reproductive organs (up to 20% of body weight) (Pörtner and Farrell 2008; Pörtner et al. 2008). The ovary of a spawning cod is highly active in sequestering vitellogenin from the plasma, i.e., during spawning, there is a significant increase in the transport of protein from the white muscle via the liver to the high number of developing oocytes (Kjesbu et al. 1991, 1996).

In addition to the number and quality of eggs, the timing of spawning behaviour is also critical to reproductive success (Wright and Trippel 2009). Cod spawn earlier in the year in the warmer (more southerly) areas of the species' distribution (Brander 2005), which appears to be the result of the interaction between three main factors. First, the environmental conditions suitable for larval development occur earlier in the year in warmer seas (Planque and Fredou 1999). Second, the onset of sexual maturation in cod is related to day length (Bromage et al. 2001; Norberg et al. 2004; Davie et al. 2007). Finally, the temperature that cod experience during the vitellogenic period influences the timing of egg release (Kjesbu 1994), with egg release being delayed in colder waters.

Developing a clearer and more precise understanding of the exogenous factors regulating reproductive development and their interactions is a necessary prerequisite for predicting the effect of warming seas on reproductive success in marine fish. To do so requires a comprehensive, process-oriented analysis based on existing knowledge combined with new information from experimental and field studies. We took advantage of recent advances in image analysis and ovary sampling techniques (Kjesbu et al. 1996; Thorsen and Kjesbu 2001; Witthames et al. 2009) to track oocyte growth in cod under experimentally controlled conditions. Our target was to determine the underlying principles regulating the natural maturity cycle of cod under different environmental conditions and to establish an accurate and precise oocyte growth curve ideally applicable to all stocks. Gonad growth apparently commences around the time of autumnal equinox (Woodhead and Woodhead 1965; Kjesbu 1991; Davie et al. 2007), but more exact information is required to pinpoint the time of vitellogenesis initiation in the year. Likewise, the rate of development of oocytes under different temperature regimes has not yet been adequately shown but has been modelled using physiological principles (Kjesbu 1994). Secondly, we integrated this understanding with temperature data collected using electronic archival tags on wild cod under natural conditions to enable us to answer the question of how trade-offs between body growth and reproductive performance are influenced in different thermal environments, addressing in particular the effect of temperature on variation in reproductive traits such as fecundity and size-specific spawning time. Finally, the overall spawning time model should, as far as possible, be simple to run, i.e., be based on mechanistic principles rather than new raw data, and be properly tested by consulting published egg production curves for cod in different waters.

Materials and methods

Laboratory study

Main protocol

The experiment took place at the Institute of Marine Research (IMR) in Bergen, Norway, between 1 June 2005 and 26 January 2006 using reared local Norwegian coastal cod brought to the laboratory for acclimation in December 2004. The fish were produced semi-extensively at the IMR marine pond facility Parisvatnet, Øygarden, west of Bergen (Blom et al. 1994), in the spring of 2003, and were subsequently vaccinated against vibrosis and transported to the IMR Austevoll Research Station in March 2004 for further growth. At arrival in Bergen, an equal number of fish were placed into two identical semirectangular 30 m^3 outdoor concrete tanks (water depth, 1.8 m). The top of the tank was covered by a net to reduce light intensity (by about 70%). Sea water was continuously supplied from the bottom of the nearby deep fjord, after sand filtration and degassing, to refresh the water in each tank. In January 2005, all individuals were anaesthetized (60 ppm benzocaine in oxygenated sea water), their sex was determined by gonad catheterization ("biopsied") using a Pipelle de Cornier endometrial suction curette (Witthames et al. 2009), and then they were all PIT-tagged. As expected (Svåsand et al. 1996), all of these 2-year-olds were sexually mature; both running males and maturing–running females were noted. During the period at Austevoll, the fish were given dry feed (Amber Neptun; www.skretting.no) consisting of 52% protein, 18% fat, and 9.6% nitrogen-free extracts, with a total energy content of 21.0 $MJ \cdot kg^{-1}$. In late spring 2005, a special broodstock feed (Vitalis Repro Cod) from the same producer was used to speed up recovery after the completion of the first spawning season.

At the start of the experiment, all fish were mixed together and randomly reassigned to the same tanks used pre-

viously. In one of the tanks (n = 80), the water was consistently maintained at ambient temperature (AT), i.e., at approximately 9–10 °C throughout the year, whereas in the other tank (n = 75), the temperature was gradually reduced overnight to 5 °C; this tank was designated as low temperature (LT). Thus, the guidelines of Schmidt-Nielsen (1983) for further Q_{10} studies (see below) were followed strictly, including that the experimental temperatures should be "sufficiently far apart" but still fall within the natural temperature range of the fish (Sundby 2000; Brander 2005). Fish were hand-fed ad libitum three times per week (Kjesbu et al. 1991) using the standard dry feed described above, but no food was given 2–5 days before the fish were weighed. Care was taken to stop feeding when appetite dropped markedly. The amount of uneaten pellets (waste feed) was judged from the number of pellets remaining on the tank bottom 1 h after feeding at the maximum stocking density of 8 kg·m^{-3}. The tank was vacuum-cleaned to remove any waste feed and excreta once per week.

Every month (1 June (day 0), 5 July (day 35), 3 August (day 64), 6 September (day 98), 6 October (day 128), 2 November (day 155), 6 December (day 189), and 10 January (day 224)), all specimens were anaesthetized, weighed (W, to within 1 g), and measured for total length (TL, 0.5 cm below). In total, 75 LT and 74 AT individuals (both genders) could be successfully followed over the whole experiment. Biopsies were taken from day 128 onwards to establish oocyte growth curves (Kjesbu 1994). Initiation of spermiation was tested by hand-stripping. Oocyte sizes, measured on day 224, together with established oocyte growth rates, were used to define the time for termination of the experiment, with the aim that the groups would consist of both prespawning ("prespawners") and spawning females ("spawners"). Consequently, all specimens were exposed to a lethal dose of anaesthetic and killed on day 240 (26 January) by a blow to the head. Total length and whole body weight were measured and the whole gonad, liver, and remaining viscera were carefully removed and weighed (to within 0.1 g). Apart from a few exceptions, only data from the females are presented here.

Analysis of ovarian biopsies

About 0.25 g of ovarian tissue (n = 344) was collected from each female on days 128, 155, 189, 224, and 240, removing a total of ≤1% of the final ovary weight measured on day 240. The samples were fixed in 3.6% phosphate-buffered formaldehyde (Bancroft and Stevens 1996), stored, and analysed automatically for oocyte diameter >200 µm (Thorsen and Kjesbu 2001). Of the 200 normal oocytes (follicles) measured per sample, the largest 10% was defined as the leading cohort (LC) and the corresponding mean diameter (LC diameter) was used to specify the maturity phase (West 1990; Kjesbu 1994; Thorsen and Kjesbu 2001). Similar data on the smallest 10% of oocytes were taken to reflect the smallest cohort (SC diameter) to study hiatus (gap) development between previtellogenic (≤250 µm) and vitellogenic (>250 µm) oocytes (Sivertsen 1935) and thereby termination of oocyte recruitment. Some caution should be expressed for data between 200 and 250 µm because of contrast problems during the automated procedure. The vitellogenic oocyte distribution of cod should be considered as unimodal and homogeneous throughout the ovary (Witthames et al. 2009). The width of this distribution, reported as standard deviation (SD_{diam}), was included to strengthen the understanding of oocyte growth dynamics and to indicate portion of eggs spawned, seen by a gradual fall in SD_{diam} (Kjesbu et al. 1990). Hydrated or ovulated oocytes, used as spawning markers, were noted but not measured. Individual fecundity was given from oocyte packing density (number of oocytes per gram), estimated from the mean diameter of all 200 oocytes, multiplied by whole-ovary weight, i.e., the autodiametric method (Thorsen and Kjesbu 2001). To test for normal oocyte development, a limited numbers of samples were processed histologically using conventional protocols, i.e., Technovit as embedding medium and 2% toluidine blue and 1% sodium tetraborate as stain.

Experimental definitions and calculations

Data on body growth were split by gender and tank (LT and AT), and spawning status (prespawners or spawners) was added as a third category when considering reproductive information. Common expressions were applied in all calculations. Growth analyses included (*i*) specific growth rate (G, in percentage), $G = (\ln W_2 - \ln W_1)/(t_2 - t_1) \times 100$, where W_1 is initial weight at time t_1 and W_2 is final weight at time t_2, and (*ii*) daily length increment (DLI, in mm·day^{-1}), $DLI = (TL_2 - TL_1)/(t_2 - t_1) \times 10$ (Svåsand et al. 1996), with TL_1 and TL_2 corresponding to total length at t_1 and t_2, respectively. To be able to compare overall G with previous studies, males were also included in the calculation.

Reproductive investment was defined as (*i*) fecundity (F, the number of vitellogenic oocytes); (*ii*) relative fecundity (RF, the number of vitellogenic oocytes·whole-body weight^{-1}); or (*iii*) gonadosomatic index (GSI, 100 × gonad weight·whole-body weight^{-1}). Fish condition was presented either as liver (hepatosomatic) index (HSI, 100 × liver weight·whole-body weight^{-1}), or Fulton's condition factor (K, 100 × whole-body weight·total length^{-3}). Occasionally, ovary-free weight (somatic weight) replaced whole-body weight, indicated by the subscript S. The influence of experimental temperature on daily growth in LC diameter was established by (*i*) common linear regression analysis at either the group (tank) or the individual level and (*ii*) estimation of the Q_{10} value, $Q_{10} = (R_2/R_1)^{10/(T_2-T_1)}$ (Schmidt-Nielsen 1983), where estimated slopes (rates) from the previous regressions were labelled as $R_{1,LT}$ and $R_{2,AT}$, and corresponding temperatures were labelled as $T_{1,LT}$ and $T_{2,AT}$. A new rate (R_{new}) at another temperature (T_{new}) was determined after rearrangement of the standard Q_{10} formula: $R_{new} = R_{1,LT} \times Q_{10}^{(T_{new}-T_{1,LT})/10}$ (or $R_{new} = R_{2,AT} \times Q_{10}^{(T_{new}-T_{2,AT})/10}$) (Schmidt-Nielsen 1983). Final maturation for the presently fixed oocytes was set to start (eccentric germinal vesicle (GV)) and end (GV breakdown) at LC diameters of 875 and 1000 µm, respectively, found after conversion (Thorsen and Kjesbu 2001) of fresh oocyte data (Kjesbu et al. 1996). The length of the vitellogenic period, i.e., from 250 to 875 µm, was given as $625/R_{1,LT}$ and $625/R_{2,AT}$ (days).

Feeding ration (FR) was calculated for each of the eight successive periods between fish measurements and for the whole experiment. In the first situation, FR was calculated

as the total amount of feed eaten during each period divided by estimated total fish biomass in the tank midway in the period ($(\Sigma W_1 + \Sigma W_2)/2$) and the number of days in question ($t_2 - t_1$). FR for the whole experiment was the weighted mean periodic feeding ration.

Experimental water temperature was reported as the grand mean weekly temperature based on three to seven, usually five, measurements per week. Temperatures limited to the vitellogenic period (T_{vit}) were given separately.

Field study

DST-recorded temperatures

Information on temperatures experienced during the length of the maturation cycle, recorded by data storage tags (DSTs), was acquired from previous projects studying free-ranging cod. The temperature data were compiled from the longest DST records available in the English Channel (Channel), southern North Sea and Irish Sea (southern waters), and the Barents Sea (northern waters).

In the case of the northern individuals ($n = 6$), all appear in Godø and Michalsen (2000) showing the following total length at release (tag number in parentheses) in March 1996: 64 (246), 74 (117), 72 (131), 65 (204), 73 (206), and 81 cm (44). Successful recording times were 12 ± 1 month. The last fish mentioned was tagged at the spawning ground in Lofoten, i.e., considered to be sexually mature, whereas the others were tagged at the Finnmark coast and most were believed to be sexually immature. However, the majority were likely to be sexually mature at recapture in 1997, seen by consulting the corresponding length-at-age key and maturity-at-age ogive reflecting a probability of 73%–93% (International Council for the Exploration of the Seas (ICES) Advisory Committee 2008). The DST was attached externally and temperature was recorded (precision: ±0.2 °C) in weekly cycles of every 2 h for the first 6 days and every 12 h on the 7th day. In southern waters, DST data (accuracy: ±0.1 °C; precision: 0.03 °C) collected from 10 specimens tagged between 1999 and 2005 showed recording times comparable with those given above for the Barents Sea cod but using a higher measuring frequency of once per 10 min (Neat and Righton 2007). Data were collected from tags either attached externally or implanted internally, but the difference in site was considered unimportant (Righton et al. 2006). Also, any between-year variation recorded was considered negligible in relation to within-year fluctuation (Neat and Righton 2007). Thus, to ease visual comparison, monthly resolved data, including also data for the cod in the north, were plotted within a single year. The tagged cod in southern waters were released in February, except for the largest fish measured, i.e., an 86 cm Channel cod, which was released in March. The total length for the other nine specimens ranged from 47 to 66 cm. The examined Channel and North Sea cod showed 75%–100% probability of being sexually mature (R.D.M. Nash, IMR, P.O. Box 1870 Nordnes, N-5817 Bergen, Norway, unpublished data, RASER (EU project Q5RS-2002-01825)), whereas the one examined from the Irish Sea certainly was sexually mature (Armstrong et al. 2004).

CTD-recorded temperatures

IMR Barents Sea CTD (conductivity, temperature, and depth) files were consulted to indicate the effect of annual variation in environmental temperature on gonad maturation. More specifically, the average temperature in August–September (1998–2007) in the Vardø North Transect (72°15′N–74°15′N, 31°E; depth, 50–200 m) was compared with development in maturity stage as observed 6–7 months later. Considered temperatures correlated well with bottom temperatures (R. Ingvaldsen, IMR, P.O. Box 1870 Nordnes, N-5817 Bergen, Norway, personal communication, 2008) in the centre of the cod distribution (Sundby 2000) just before or at initiation of vitellogenesis (Kjesbu 1991).

In one case, Vardø North Transect temperature was contrasted with similar types of information from DSTs. Transect temperature measured in August–September 1996 and January 1997 were averaged and related to average DST temperatures between 1 September 1996 and 1 February 1997 for each of the above-mentioned six Barents Sea cod.

Fish sampling and analyses

Adult cod were collected from both northern and southern waters using very much the same protocols, although in the last situation, the sampling was spread over several days, including into the spawning season. Northern fish were worked up just after landing of the catch, whereas this procedure took place onboard for the southern fish.

The sampling in the northern area was part of the regular "Andenes fecundity time series" (Kjesbu et al. 1998; Thorsen et al. 2006), i.e., examining females ($n = 486$) captured by commercial vessels over a period of 1–2 days in early to mid-March (calendar days 57–74) off the Vesterålen region, northern Norway (69°19′N, 16°09′E). The Andenes study was limited to Barents Sea (Northeast Arctic) cod, excluding 5%–30% of the material classified from the otolith as coastal cod. Otoliths were also used for reading of age and spawning zones (Rollefsen 1934). Presently eight years spanning from 1999 to 2008 were included. Thus, only ovarian samples analysed after the introduction of the autodiametric method (see above) were considered. Generally, close to 100% of the fish were prespawners, i.e., only a few spawners were detected based on the presence of hyaline or ovulated oocytes. In 2006, an extra sample was taken in mid-February (calendar days 43–44, early 2006) to be compared with the standard sample (calendar days 66–67, late 2006). To further evaluate representativeness of the adopted sampling scheme, year-specific length-at-age data were contrasted with similar types of data available from the statutory Lofoten–Vesterålen survey in mid-March to late April (Korsbrekke et al. 2001; ICES Advisory Committee 2008). However, as these data were not resolved by sex, the present comparison was limited to 2005–2007, i.e., in years when the Andenes program was extended to include males. Each fish was physically characterized by its total length (1 cm below), weight of the whole body (10 g), ovary, liver, and viscera (1 g). Viscera consisted of all organs left in the body cavity after removing the ovary and liver and as much as possible of the esophagus. Any stomach content was judged by dominant species. Cases in which the stomachs were devoid of contents were noted as a special category.

Fish from the southern area were collected in 2004 in the central North Sea ($n = 41$) and the eastern Irish Sea ($n = 38$) from catches made with IBTS gear (North Sea) or a com-

mercial rock-hopper trawl (Irish Sea). Because of low catchability, the collection of specimens was stretched over 34 days (22 January – 24 February) and 10 days (10–19 February), respectively. Hence special emphasis was placed on the establishment of relevant maturity standardization techniques, as detailed in Results. Only total lengths (1 cm below) with measured oocyte data (see below) were considered. Spawners showed either hydrated–ovulated oocytes or recent postovulatory follicles. The latter structures were detected in resin sections specially designed for this purpose, i.e., using PAS–Mallory's trichrome stain (Witthames et al. 2009). As previously, final oocyte maturation was set to be introduced at 875 μm as there were no indications of any deviation.

Analysis of ovarian subsamples

All sampling was carried out from the right ovarian lobe using either a plastic pipette with a wide opening (IMR) or a standardized Wiretrol II pipette (Drummond Scientific Company, Broomall, Pennsylvania) (Cefas) (Witthames et al. 2009). The corresponding LC diameter was added to the established fish database and supplemented with mean oocyte diameter for Barents Sea cod to estimate fecundity. Variation in LC diameter across the whole ovary was about ±10 μm (standard error, SE), tested on seven Barents Sea cod (total length, 89–111 cm) in the standard Andenes program (2003), cf. also fig. 1 in Witthames et al. (2009). Calibration tests performed between institutes showed that the two image analysis programs used were fully compatible (Witthames et al. 2009).

Field-related definitions and calculations

The following relationship was established between weight of viscera with empty stomach (VW_{empty}, g) and total length (TL, cm) for Barents Sea fish:

$$(1)\quad VW_{empty} = 1.38 \times 10^{-5} \times TL^{3.722} \quad (r^2 = 0.940,\ df = 1, 56, p < 0.001,\ TL = 58 - 124\,cm)$$

Prior to antilogarithm, the constant had a logarithmic value of –11.19 and an associated SE of 0.57. SE for the exponent was 0.126. No year effect was noted (late 2006 vs. 2008) (slope, $p = 0.074$; intercept, $p = 0.178$) (analysis of covariance, ANCOVA). Thus, whole-body weight (W, g) could be corrected ($W_{corrected}$, g) for varying stomach content:

$$(2)\quad W_{corrected} = W - (VW - VW_{empty})$$

where VW is recorded weight of viscera (g). At a given length, based on all standard Andenes samples, expected body weight ($W_{expected}$, g) was

$$(3)\quad W_{expected} = 2.76 \times 10^{-3} \times TL^{3.266} \quad (r^2 = 0.970,\ df = 1, 445,\ p < 0.001,\ TL = 54 - 128\,cm)$$

The constant showed a logarithmic value of –5.89, with SE equal to 0.12. The exponent SE was 0.027.

Based on these approaches, viscera condition ($C_{viscera}$) and fish condition (C_{weight}) were defined as $C_{viscera} = VW/VW_{empty}$ and $C_{weight} = W_{corrected}/W_{expected}$. The latter expression was used to handle problems with size dependency in condition (Scott et al. 2006), simultaneously cancelling out any noise in the data caused by varying stomach content. Specific growth rate was found from the standard formula (see above) defining W_1 and W_2 as $W_{corrected,\ age\ 8}$ and $W_{corrected,\ age\ 9}$, respectively, and $(t_2 - t_1)$ as 365 days, i.e., studying separate cohorts (Dutil and Brander 2003). Annual total length increment (ALI) was estimated as total length divided by the corresponding age (cm·year^{-1}).

Light cycle

The duration of daylight from 1 June 2005 to 26 January 2006 (i.e., the present experimental period) at Guernsey (49°27′N, 02°33′W) (Channel), Isle of Man (54°15′N, 04°30′W) (Irish Sea), Bergen (60°24′N, 05°18′E) (experiment), and Bear Island (74°27′N, 19°02′E) (Barents Sea) was taken from the Astronomical Applications Department of the US Naval Observatory, USA (http://aa.usno.navy.mil). For plotting purposes, the number of minutes was transformed into decimal fraction of an hour. Total duration refers to when any portion of the sun is above the horizon. This was found for all days corresponding to experimental measurements days ($n = 9$) but adding summer and winter solstice and autumnal equinox.

Statistics

All statistical analyses were performed with Systat 12 (Systat Software, Inc. 2007), and the graphs were produced with SigmaPlot 10 (Systat Software, Inc. 2007). Prior to any statistical test, each subset of data was examined for normal distribution by the Shapiro–Wilk test and the Anderson–Darling test (default options). For proportions, normality was in some cases achieved by arcsine transformation (Sokal and Rohlf 1981). Equality of variances was tested with the F test (including the Levene test). Coefficient of variation (CV) was presented as 100 × standard deviation (SD)/mean (%). Tests between or among groups included both nonparametric (Mann–Whitney test and Kruskal–Wallis test) and parametric methods (Student's t test). For ANCOVA, the assumption of homogeneity of slopes was tested prior to any test on intercepts, using natural-log-transformed data when required. In regression analysis, standard error was attached to each regression coefficient and r^2 was replaced with adjusted r^2 at low numbers of observations. For multiple regressions, the entry of an independent variable was based as far as possible on biological relevance consulting experimental findings when establishing field models. Unless specially mentioned, any predictor adopted showed a significant contribution (an absolute value of $t > 2.0$) and a tolerance > 0.1, the latter to exclude highly correlated predictors (Systat Software, Inc. 2007). The Akaike information criterion (AIC) was consulted when appropriate, searching for the lowest AIC (Systat Software, Inc. 2007). In tracking studies on the same experimental individuals across time (i.e., balanced design), observed changes were tested with linear mixed models (LMM) and (or) repeated-measures analysis of variance (ANOVA). To clarify the specific influence of a given category at specific points within such time series, hypothesis test (effects) ANOVA was used. For LMM, fixed factors were tank, time (month), gender (if relevant), and tank × month, and the random factor was fish × tank. The default first-order autoregressive structure was included to adjust for autocorrelation with time. Resulting adjusted p values for fixed effects were consulted and presented. Rejection of null hypothesis was always set at $p < 0.05$.

Fig. 1. Experimental conditions in low-temperature (LT, solid circles) and ambient-temperature (AT, open circles) tanks as described by (*a*) water temperature (*T*), (*b*) feeding ration (FR), and (*c*) resulting mean specific growth rate (*G*) (± standard error, SE) and (*d*) mean Fulton's condition factor (*K*) (±SE). Vitellogenesis (shaded area) refers to females with developing oocytes. Inserted numbers in (*a*) are mean vitellogenic temperature at LT (lower position) and AT (upper position); arrow reflects a transient problem with the temperature cooler. Solid and broken lines in (*b*) show weighted mean FR at LT and AT, respectively; overlapping lines in (*c*) show mean *G* for the whole experiment in the two tanks. Day 0, 1 June 2005; day 240, 26 January 2006.

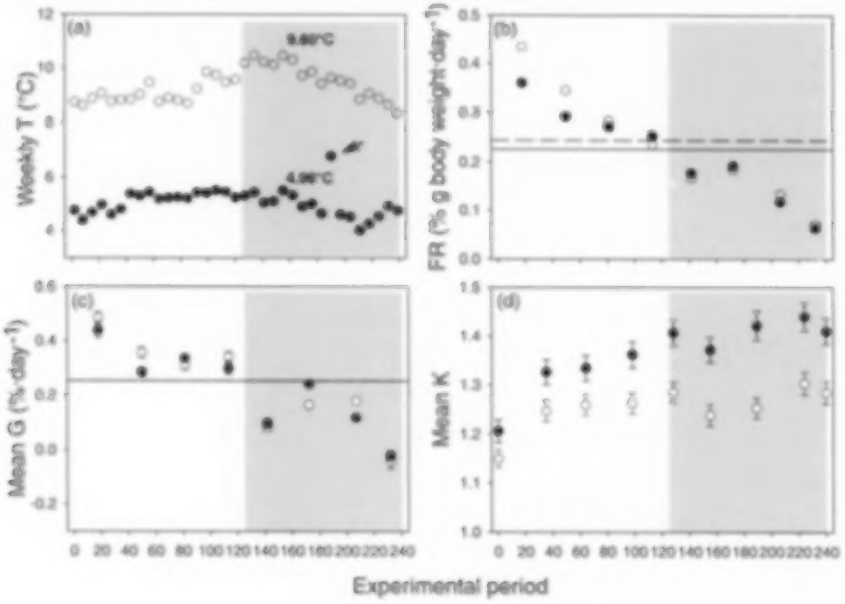

Results

Laboratory study

Water temperature and food intake

Grand mean (SD) temperature during the length of the experiment (240 days) was 5.05 (0.49) °C at LT (low temperature) and 9.33 (0.59) °C at AT (ambient temperature). Variation in temperature within a week was typically ±0.5 °C. The smallest between-tank difference in temperature was 2.9 °C, the largest was 5.2 °C (Fig. 1*a*). Daily temperature showed evidence of synchrony between tanks (r = 0.474, $p < 0.001$).

Weighted mean feeding rations (FR) for the eight measurement periods at LT and AT were 0.226 and 0.244 g dry feed·g wet fish^{-1}·day^{-1}, respectively, i.e., not significantly different (p = 0.774) (Student's t test). Periodic FR declined over time in both tanks (Fig. 1*b*). There were indications that the AT fish took more feed initially (days 0–64), but later, appetites in the two tanks were similar. There was a transitory drop in interest in food between days 128 and 155, coinciding with initiation of vitellogenesis (see below).

Fish growth and condition

Individual growth in body weight showed evidence of tank (p = 0.011), month ($p < 0.001$), gender (p = 0.017), and tank × month ($p < 0.001$) effects (LMM). Despite this, overall specific growth rate (*G*) did not vary statistically between tanks, but overall daily length increment (DLI) did vary, showing the highest figures for AT (Table 1). Fish at LT and AT were similar in size at the start of the experiment, in terms of both mean length and weight (Table 1). After 224 days, their mean lengths were statistically different (Table 1).

More in-depth analyses demonstrated that the specific growth rate varied periodically. Both tanks demonstrated a strong positive relationship between mean periodic *G* and periodic FR (LT, r^2_{adj} = 0.889, df = 1,6, $p < 0.001$; AT, r^2_{adj} = 0.829, df = 1,6, p = 0.001; both genders). The fall in mean periodic *G* (Fig. 1*c*) essentially mimicked the one for FR (Fig. 1*b*), whereas the pattern of change across time for *G* differed between tanks (p = 0.007) (repeated-measures ANOVA). There was evidence of a trade-off between initial body weight and subsequent growth rate (LT, r = –0.448, p = 0.009; AT, r = –0.382, p = 0.018). Around the time of the initiation of spawning (see below), *G* generally became negative (Fig. 1*c*).

AT fish developed a significantly lower condition factor (*K*) than those at LT (Fig. 1*d*). The interaction month × tank was highly significant ($p < 0.001$; repeated-measures ANOVA). As a consequence, mean *K* at LT and AT became increasingly significantly different (day 0, p = 0.057; days 35–98, $p \leq 0.017$; days 128–240, $p < 0.001$; hypothesis test ANOVA). Analysis of somatic condition factor (K_S) gave a similar result for the last measurement point (day 240) (LT vs. AT prespawners, $p < 0.001$; Student's t test).

Initiation of spawning

A higher proportion of AT fish (34%) than LT fish (6%) started to spawn on day 240, indicated by either running eggs

Table 1. Summary of experimental results on female coastal cod (*Gadus morhua*) held at low (LT) and ambient (AT) temperatures during their second maturation cycle, i.e., from the age of ~2 1/2 to 3 years. In one case, both genders were analysed for comparison with published results.

			LT		AT		Between-tank comparison
	Category	No. of days	*n*	Mean (SD)	*n*	Mean (SD)	(*P* value)
Growth							
W (g)	Female	0	33	1861 (298)	38	1866 (350)	0.955
	Female	224	33	3348 (482)	38	3469 (589)	0.351
TL (cm)	Female	0	33	53.6 (3.4)	38	54.4 (3.2)	0.317
	Female	224	33	61.5 (3.8)	38	64.2 (3.9)	0.004
G (%·day^{-1})	Both genders	224	75	0.252 (0.052)	74	0.253 (0.059)	0.624
	Female	224	33	0.263 (0.036)	38	0.278 (0.045)	0.086
DLI (mm·day^{-1})	Female	224	33	0.35 (0.05)	38	0.44 (0.08)	<0.001
Reproduction							
W (g)	Female, prespawner	0	31	1855 (306)	25	1774 (304)	0.328
	Female, spawner	0	2	1961 (—)	13	2042 (377)	—
	Female, prespawner	224	31	3354 (496)	25	3340 (535)	0.921
	Female, spawner	224	2	3257 (—)	13	3717 (629)	—
K	Female, prespawner	224	31	1.42 (0.15)	25	1.28 (0.15)	0.001
	Female, spawner	224	2	1.68 (—)	13	1.34 (0.11)	—
GSI (%)	Female, prespawner	240	30	11.8 (3.0)	25	14.1 (3.7)	0.013
	Female, spawner	240	2	15.7 (—)	13	22.2 (4.1)	—
HSI (%)	Female, prespawner	240	31	13.2 (1.5)	25	11.0 (1.2)	<0.001
	Female, spawner	240	2	12.7 (—)	13	10.1 (1.4)	—
F (millions)	Female, prespawner	240	30	3.72×10^6 (0.70×10^6)	25	4.32×10^6 (1.02×10^6)	0.017
RF (g^{-1})	Female, prespawner	240	30	1117 (167)	25	1307 (242)	0.003

Note: *W*, whole-body weight; TL, total length; *G*, specific growth rate; DLI, daily length increment; *K*, Fulton's condition factor; GSI, gonadosomatic index; HSI, hepatosomatic index; *F*, fecundity; RF, relative fecundity; *n*, number of fish; SD, standard deviation. Prespawner and spawner refer to females that became these categories towards the end of the experiment (day 224).

or hydrated oocytes. All ovaries were in a normal state. Freely running (spermiating) males were first noted on day 224.

GSI, HSI, and fecundity regulation

Prespawners held at AT showed, on average, significantly higher gonadosomatic index (GSI), fecundity (*F*), and relative fecundity (RF) than their LT counterparts at day 240 but a significantly lower hepatosomatic index (HSI) (Table 1). Only the LT regime showed evidence of any influence of maturity status, represented by LC diameter, on somatic relative fecundity (RF_S), but fish in both regimes developed a negative trend in RF_S with increasing LC diameter (LT, $r = -0.518$, $p = 0.003$; AT, $r = -0.271$, $p = 0.189$) (Fig. 2). Exclusion of a statistical outlier at AT (Fig. 2) associated with an uncertain measurement did not influence the conclusion. AT prespawners demonstrated a significantly higher LC diameter-specific RF_S than LT prespawners (intercept, $p < 0.001$; slope, $p = 0.458$ (0.604, without outlier); ANCOVA).

In testing the temporal influence of body size on fecundity, multiple regression analysis consistently revealed no significant effect of TL ($p \gg 0.05$) when *W* was used as the other independent variable. Hence, this type of analysis did not expose any condition effect as such on fecundity. Use of *W* as the only independent variable explained up to 36% of the variance (r^2) in *F* for LT and 40% for AT, referring to *W* on days 224 and 240, respectively (Fig. 3). The level of significance was, however, rather similar throughout the experiment for AT ($0.001 < p < 0.004$) but steadily increasing for LT (*p* falling from 0.054 to 0.001). Inclusion of vitellogenic LC diameter (see below) contributed significantly to the regression for LT ($p \leq 0.046$) but not so for AT ($p \geq 0.077$) (Fig. 3). In the first case, r^2 reached 0.681 on day 240. The relative influence of LC diameter versus *W* on *F*, taken as the ratio of the corresponding absolute standard coefficients, increased for LT from ~50% on day 155 to ~75% on day 240 but was rather stable around 40% for AT. In all cases, *W* contributed positively to *F*, whereas LC diameter contributed negatively. The respective *F* formulae (millions) based on *W* (g) and LC diameter (μm), all referring to day 240, for LT and AT were

$$F = 3.08\,(\mathrm{SE}\pm 0.74) + 9.87 \times 10^{-4}\,(\mathrm{SE}\pm 1.61\times10^{-4})\times W - 4.14 \times 10^{-3}\,(\mathrm{SE}\pm 0.92\times10^{-3})\times \mathrm{LC} \quad (\mathrm{LT},\ r^2 = 0.681,\ \mathrm{df} = 1, 25,\ p < 0.001) \tag{4}$$

$$F = 2.70\,(\mathrm{SE}\pm 0.76) + 8.46 \times 10^{-4}\,(\mathrm{SE}\pm 2.16\times10^{-4})\times W - 2.12 \times 10^{-3}\,(\mathrm{SE}\pm 1.28\times10^{-3})\times \mathrm{LC} \quad (\mathrm{AT},\ r^2 = 0.481,\ \mathrm{df} = 1, 18,\ p = 0.004) \tag{5}$$

For the sake of comparison, LC was withheld in eq. 5, despite its insignificant statistical contribution: at an LC of

Fig. 2. Relative somatic fecundity (RF_S) versus leading cohort (LC) oocyte diameter on day 240 (experimental end) for prespawners held at low (LT) or ambient (AT) temperatures. LT prespawners are represented by solid circles; AT prespawners, open circles. Separate regression lines are included (LT, solid line; AT, broken line), excluding an outlier (arrow) in one case.

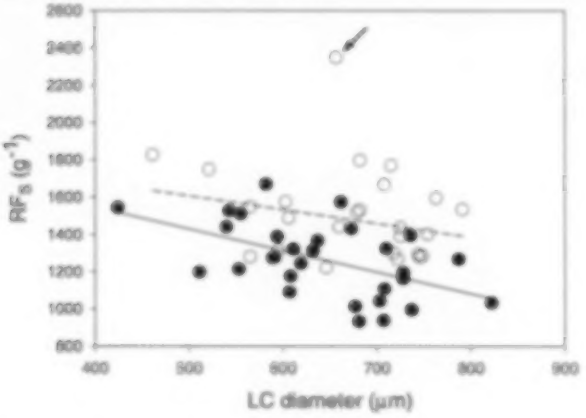

500 µm for a standard female of 3500 g, the fecundity was 3% higher at AT than at LT, but this difference increased to 23% at an LC of 800 µm.

Data on oocyte diameter frequency distributions showed differences in oocyte recruitment dynamics both between tanks and between prespawners and spawners. The width of the oocyte distribution (SD_{diam}) increased markedly over time but significantly more in AT prespawners than in LT prespawners (day 189, $p = 0.163$; day 224, $p = 0.017$; day 240, $p < 0.001$; Student's t test) (Fig. 4*a*). A comparable situation appeared between AT prespawners and spawners (day 189, $p = 0.003$; day 224, $p = 0.013$), but the difference disappeared (day 240, $p = 0.393$) when the spawners experienced a fall in SD_{diam} related to initiation of spawning (Student's t test). This analysis was not testable at LT. Indications of differences in SD_{diam} between AT prespawners and spawners appeared early (day 155, $p = 0.051$) but not so between LT and AT prespawners (day 155, $p = 0.820$; Mann–Whitney test). When ignoring the subdivision into prespawners and spawners, the pooled SD_{diam} data showed no differences between the two temperature regimes on day 155 ($p = 0.330$; Mann–Whitney test) but diverged by days 189 ($p = 0.009$) and 224 ($p < 0.001$; Student's t test). Corresponding data on the smallest cohort of oocytes (SC) revealed that the process of oocyte recruitment had ceased on day 189, i.e., mean SC was then well above 250 µm (Fig. 4*b*), though a few individuals apparently recruited oocytes up to day 224. Any difference in SC development between LT and AT prespawners could not be fully confirmed (days 155–240, $p > 0.062$; Student's t test), but examples of such differences existed when contrasting AT prespawners and spawners (day 155, $p = 0.504$; day 189, $p = 0.009$; day 224, $p = 0.054$; day 240, $p = 0.001$; Mann–Whitney test). The pooled SC data demonstrated tank differences on day 155 ($p = 0.009$) but not later ($p > 0.687$) (Mann–Whitney test).

LC oocyte diameter as maturation criterion

The observation that AT females showed a reasonable mixture of prespawners and spawners on the last day of the experiment made it possible to test the assumption that individuals with larger LC diameter spawn first. This appeared to be generally true: on day 224, females that subsequently spawned within the next two weeks showed, on average, an LC diameter of 694 µm (SE, ±17) compared with 585 µm (SE, ±16) for those that did not spawn within that period of time, i.e., a significant difference ($p < 0.001$; Student's t test).

Fig. 3. Explanatory power (r^2) of potential fecundity on day 240 (experimental end) for prespawners at low (LT, solid line) or ambient (AT, broken line) temperatures regressed on either body weight (W) alone or combined with leading cohort (LC) diameter (W + LC) at different measurement points during the experiment. Mean LC diameter is attached to each relevant analysis point. W-based regressions are indicated by solid circles for LT and open circles for AT; W + LC regressions are indicated by solid and open crosses, respectively. An AT outlier was excluded.

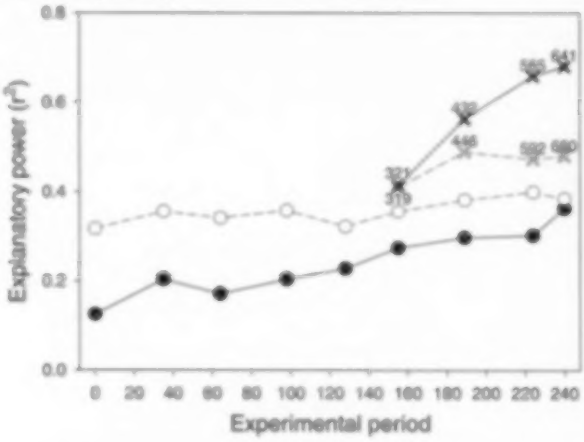

Overall oocyte growth rate

LT and AT females tracked over time showed significantly different oocyte growth trajectories ($p < 0.001$; repeated-measures ANOVA) resulting in significant differences in mean LC diameter (LC_{group}) at late vitellogenesis (Fig. 5). More explicitly, the two data sets differed statistically from day 189 onwards (day 128, $p = 0.521$; day 155, $p = 0.075$; day 189, $p = 0.011$; day 224, $p = 0.005$; day 240, $p = 0.003$; Mann–Whitney test or Student's t test). Dropping spawners from the analysis caused the observed differences on days 189 and 224 to disappear ($p = 0.298$ and 0.154, respectively) and nearly so on day 240 ($p = 0.048$). On day 128, 10% of the LT females and 6% of the AT females contained developing oocytes (LC diameter > 250 µm). This figure increased sharply to 66% and 76% on day 155, respectively. Hence, in relative terms, more AT females entered vitellogenesis between days 128 and 155. The detailed individual tracking study revealed an example of extreme slow oocyte growth. Exclusion of this LT female did not affect the above statistical conclusions. LC_{group} diameter (µm) increased between days 128 and 240 (Fig. 5) as

$$(6) \quad LC_{group} = 3.43\,(SE \pm 0.20) \times ED - 197\,(SE \pm 39)$$

$$(LT,\ r^2 = 0.990,\ df = 1, 3,\ p < 0.001)$$

Fig. 4. Development in mean values (± standard error, SE) of (*a*) the width of the developing oocyte frequency distribution (SD_{diam}) and (*b*) the diameter of the smallest cohort of oocytes (SC) in low-temperature prespawners (solid circles) and ambient-temperature prespawners (open circles) and spawners (crosses) between days 155 and 240 (2 November – 26 January). In (*b*), the vertical distance from maximum previtellogenic oocyte diameter (horizontal broken line) to each measurement point indicates oocyte gap size formation.

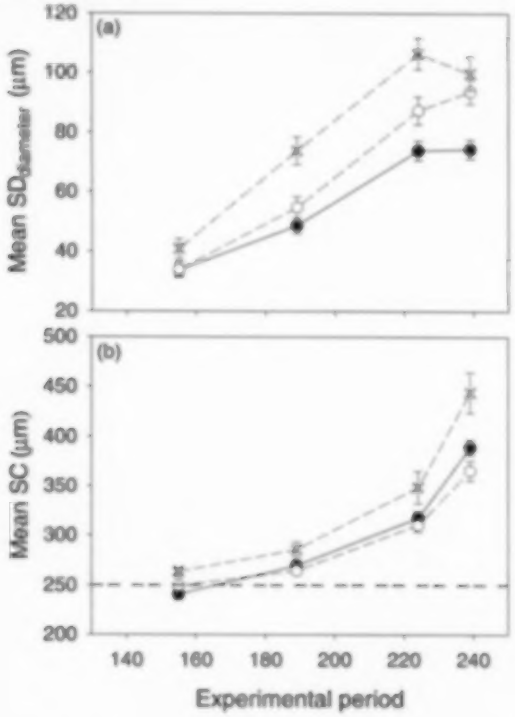

$$LC_{group} = 4.10\,(SE \pm 0.15) \times ED - 281\,(SE \pm 30) \quad (AT,\ r^2 = 0.996,\ df = 1, 3,\ p < 0.001) \tag{7}$$

where ED is elapsed days since day 0. The use of a power function in place of a linear function increased r^2 even closer to 1, but had no practical implications. The typical oocyte growth rate (R) of AT females was 19.5% higher than for LT females, i.e., 3.43 µm·day^{-1} at LT vs. 4.10 µm·day^{-1} at AT.

Individual oocyte growth rate

Studies of individual LC diameter data showed that the time of entrance to vitellogenesis in the autumn influenced when each female would likely start to spawn in the subsequent spring. This was most clearly seen for the earliest and latest spawners: females with the largest LC diameter on day 240 were all vitellogenic on day 155 (LC diameter > 380 µm), whereas none of the females with the smallest LC values on day 240 had yet commenced vitellogenesis on day 155 (LC diameter ≤ 250 µm). A regression analysis on the complete individual-based data sets indicated that predicted spawning time for both temperature regimes showed similar

Fig. 5. Growth in mean leading cohort (LC) oocyte diameter (± standard error, SE) at the group level (LC_{group} diameter) at low (solid circles) and ambient (open circles) temperatures between days 128 and 240 (6 October – 26 January. The same females were tracked over time.

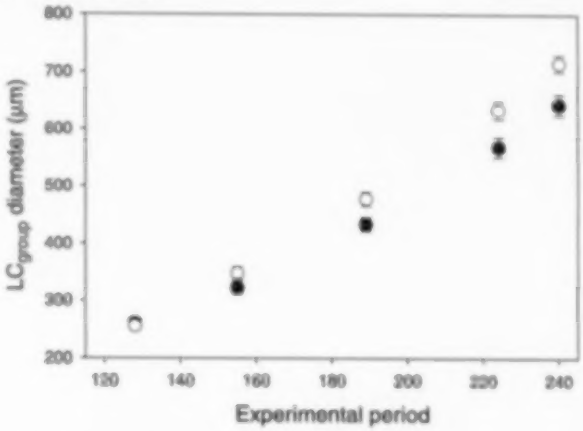

dependence on the time of entrance to vitellogenesis (intercept) and subsequent oocyte growth rate (slope) (R), i.e., LC diameter on day 155 and R influenced final LC diameter (day 224) by 57%–58% and 42%–43%, respectively. A few of the tracked females deviated from the rest by showing a fall in R after day 155. Likewise, some apparently had a temporarily increased R, mainly between days 224 and 240, cf. appearance of spermiating males. Nevertheless, the high individual stability in R preceding the process of egg release was confirmed by separate regression analysis (LT, mean r^2 = 0.979 (SE, ±0.010); AT, mean r^2 = 0.993 (SE, ±0.001)), where each fish was represented with four successive LC diameter measurement points. In one single case, the r^2 was much lower, i.e., 0.717. Subsequent histology showed a fully normal ovary.

The average individual R per tank was 3.56 µm·day^{-1} (SE, ±0.15) and 4.21 µm·day^{-1} (SE, ±0.12), i.e., about 3%–4% higher compared with the corresponding group-based parameter values given in eqs. 6 and 7, respectively. The R appeared to be statistically independent (p = 0.928) on when the females entered vitellogenesis in the autumn, being testable for AT (middle vs. late entrance, Mann–Whitney test).

Estimated R values reflected a general vitellogenic Q_{10} value of 1.44 (1.47) and a length of the vitellogenic period of 176 (182) days at LT and 148 (152) days at AT, with the results from eqs. 6 and 7 given in parentheses. Thus, the respective ovaries matured typically for 6 and 5 months before initiation of spawning, or stated in another way, LT females showed a delay in spawning time of 1 month compared with AT females. Based on these findings, R_{new} (µm·day^{-1}), i.e., the oocyte growth rate at another environmental temperature (T_{new}) than the present ones, can be predicted by the following expression:

$$R_{new} = 4.21 \times 1.44^{(T_{new} - 9.60)/10} \tag{8}$$

As noted, input data are from AT, and the Q_{10} value refers to vitellogenic females. The alternative use of input data from LT would logically give the same result.

Size-specific oocyte growth

Only AT females showed a significant relationship between LC diameter on day 224 and body weight and length measurements during the course of the experiment. Of the two explanatory variables, *W* had, with the exception of days 64–98, a higher predictive power than TL, but both r^2 values showed generally falling values with time (TL: day 0, 0.34; day 224, 0.19; *W*: day 0, 0.37; day 224, 0.27). All these regressions were significant for AT (TL, $p \leq 0.007$; *W*, $p \leq 0.001$), but none were significant for LT (TL, $p \geq 0.653$; *W*, $p \geq 0.082$). Exclusion of the above-mentioned LT female with extremely slow oocyte growth had no statistical relevance. All slopes were positive, except for two LT outputs, which were considered irrelevant because of their insignificant nature. In consequence, those AT females that turned out to be spawners before the end of the experiment had on day 0 a significantly larger body size than their accompanying prespawners (*W*, $p = 0.023$; TL, $p = 0.026$ (mean, 56.0 vs. 53.6 cm); Student's *t* test) (Table 1). However, these prespawners, compared with the other time periods tested ($p \geq 0.677$), showed indications of a higher specific growth rate between days 35 and 98 ($0.171 < p < 0.181$; Mann–Whitney test). This probably contributed to the finding that AT spawners and prespawners became just insignificantly different in mean body weight on day 224 (Table 1) ($p = 0.060$), whereas their corresponding mean lengths (65.0 vs. 63.8 cm) evidently had turned statistically similar ($p = 0.365$; Student's *t* test). Too few LT spawners existed for such a test. More comprehensive multivariate analyses did not locate any other additional variables such as hepatosomatic index or expressions of body growth (*G* and DLI), which significantly increased the understanding of variation in prespawning LC diameter.

The underlying reason for any potential influence of body size on prespawning LC diameter was tested by regressing oocyte growth rate (*R*, μm·day^{-1}) on initial length, with no relationship for LT ($p >> 0.05$) but a noticeable relationship for AT (Fig. 6):

$$(9)\quad R_{size} = 10.42 \times 10^{-2}\,(\mathrm{SE} \pm 3.40 \times 10^{-2}) \times \mathrm{TL} - 1.50\,(\mathrm{SE} \pm 1.87)\ (\mathrm{AT},\ r^2 = 0.232,\ \mathrm{df} = 1, 31,\ p = 0.005,\ 46 < \mathrm{TL\,(day\,0)} < 61\ \mathrm{cm})$$

For clarity, *R* was relabelled as R_{size}. Using initial body weight instead of length as the predictor gave similar results. This significant relationship persisted until both days 128 and 224 when studying the same individuals:

$$(10)\quad R_{size} = 8.24 \times 10^{-2}\,(\mathrm{SE} \pm 2.94 \times 10^{-2}) \times \mathrm{TL} - 0.90\,(\mathrm{SE} \pm 1.83)\ (\mathrm{AT},\ r^2 = 0.202,\ p = 0.009,\ 51 < \mathrm{TL\,(day\,128)} < 68\ \mathrm{cm})$$

$$(11)\quad R_{size} = 8.02 \times 10^{-2}\,(\mathrm{SE} \pm 2.85 \times 10^{-2}) \times \mathrm{TL} - 0.97\,(\mathrm{SE} \pm 1.85)\ (\mathrm{AT},\ r^2 = 0.204,\ p = 0.008,\ 53 < \mathrm{TL\,(day\,224)} < 70\ \mathrm{cm})$$

These two latter regressions were included because of practical applications in the field study below. Next, the following formula was established including both the above temperature (eq. 8) and body size effect (eqs. 9, 10, or 11, depending on the time in the autumn):

$$(12)\quad \mathrm{LC}_2 = R_{size} \times 1.44^{(T_{acc} - 9.60)/10} \times (t_2 - t_1) + \mathrm{LC}_1$$

Thus, measured developing LC diameter (LC_1) on any day t_1 can, in effect, be transferred (standardized) to developing LC diameter (LC_2) on day t_2 in a warm temperature situation resembling the one of the AT regime.

Fig. 6. Individual oocyte growth rate (*R*) between days 155 and 224 (2 November – 10 January) at low (LT) (solid circles) and ambient (AT) (open circles) temperatures in relation to total length (TL) as measured on day 0 (1 June). Associated regression lines (LT, solid line; AT, broken line) are included, but excluding an outlier (arrow) in the case of LT.

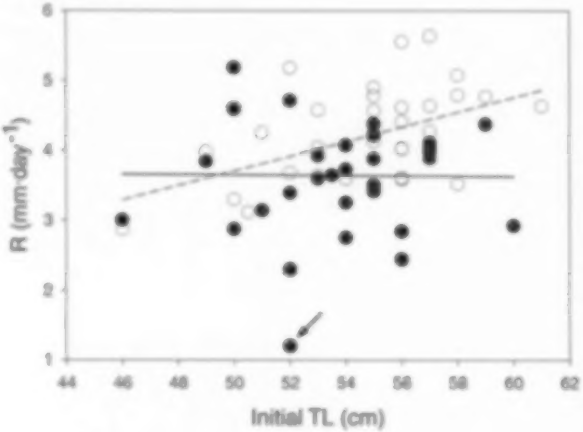

Field study

DST-recorded temperatures in the different waters

Temperature information gathered from DSTs showed that adult cod in the northern and southern waters stayed in highly different temperatures throughout the year but without any evident trend in selected temperature by fish size. Monthly temperature profiles from the Channel, North Sea, and Irish Sea clearly differed from those from the Barents Sea (Fig. 7). After the supposed spawning season, cod from the southern category went into significantly warmer water, whereas those belonging to the northern category generally entered cooler water, including temperatures below zero. Both categories showed less variation around expected time of spawning, but particularly the northern one, i.e., between March and May, the temperatures experienced by the present individuals of Barents Sea cod were concentrated around 4 °C, which was far below the introduced threshold value of 9.6 °C thought to imply impaired spawning if met or exceeded (Fig. 7). This was not the case for the three southern stocks, showing examples of individuals quite close to this critical line in the months of interest, i.e., January to March. The data indicated that the overall temperature between 1 September and 1 February, assumed to overlap to a large extent with the period of vitellogenesis, was centred on 2 °C (range, 1–3.5 °C) and 11 °C (range, 9–13 °C) for cod in the north and south, respectively (Fig. 8). There was no

Fig. 7. Data storage tag (DST) recorded temperatures (T) (monthly mean ± standard deviation, SD) in released-and-recaptured individual cod in southern waters, i.e., the Channel (crosses), southern North Sea (open squares), and Irish Sea (open triangles) and the Barents Sea (solid circles). Length of spawning season in southern (left box) and northern (right box) waters is from Brander (1994) and Pedersen (1984), respectively. Temperatures at or above the horizontal line (9.6 °C) are considered to result in reduced egg fertilization and normal development (van der Meeren and Ivannikov 2006).

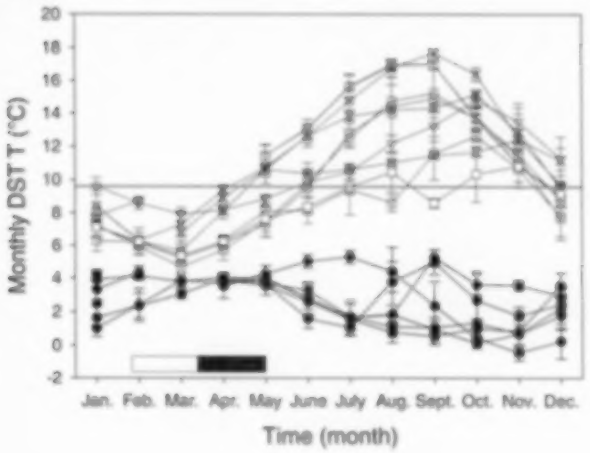

Fig. 8. Data storage tag (DST) recorded temperatures (mean, minimum, and maximum values) between 1 September and 1 February for cod in northern and southern areas in relation to total length (TL) at release (same material as in Fig. 7). The selected period of time is assumed to encompass the major part of the vitellogenic period and thereby vitellogenic temperature (T_{vit}). Open crosses, open squares, open triangles, and solid circles represent the Channel, North Sea, Irish Sea, and Barents Sea, respectively.

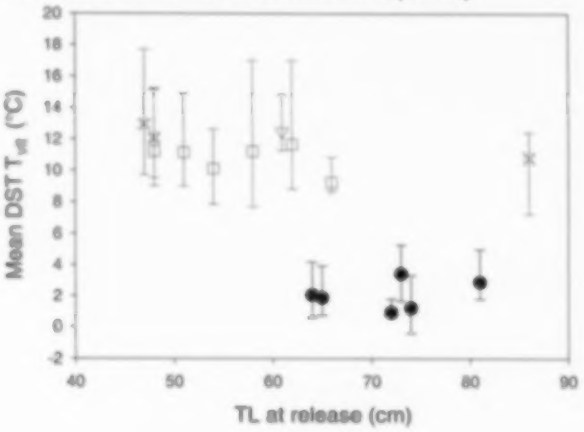

obvious fish size dependency as analysed within the Channel, North Sea, and Barents Sea cod stocks (for the Irish Sea, only one fish was recorded).

Barents Sea database

Data from this area included physical descriptors (total length, viscera condition ($C_{viscera}$) and body condition (C_{weight}); Table 2; Fig. 9) and CTD-recorded temperature in August to September (Vardø North Transect, T_{VN}; Fig. 9). All three physical descriptors demonstrated significant annual variations within the standard time series ($p < 0.001$; Kruskal–Wallis test), although the length data (54–128 cm) should be treated with some caution due to likely examples of nonrandom sampling. The early and late (standard) 2006 samples also deviated significantly in length ($p = 0.032$) and viscera condition ($p < 0.001$) but not in body condition ($p = 0.172$) (Mann–Whitney test). Viscera condition was included to reflect feeding activity, finding two major peaks 2003 and late 2006 (Fig. 9).

To assess the representativeness of the various data, our fish measurement data were first compared with similar survey data but also with present experimental growth data, followed by a study on CTD data in relation to similar DST data, finding some deviations. The comparison with the extensive length-at-age database from the Lofoten–Vesterålen survey showed that the presently sampled cod, focusing on the main age groups 8 and 9 (combined sexes), were consistently 5%–10% larger between 2005 and 2007. Corresponding specific growth rate (females only) varied typically from about 0.05%·day^{-1} within the period 1999–2005 to about 0.12%·day^{-1} within the period 2006–2007. Thus, indicated growth in body weight was roughly half, or less, of the above experimental values. Transect temperature during the autumn of 1996 (3.1 °C) was about 1 °C higher than the corresponding average DST temperature. However, the individual range in DST temperature (Fig. 8) showed an overlap with this CTD record.

Fecundity regulation in the Barents Sea cod

The pooled analysis on standard Andenes samples (i.e., excluding early 2006) showed that the fecundity represented by F (millions) was significantly influenced ($p < 0.001$) by TL (cm), C_{weight} (without unit), LC diameter (μm), and T_{VN} (°C):

$$(13)\quad F = 1.95 \times 10^{-4} \times \mathrm{TL}^{3.726} \times C_{weight}^{1.729} \times \mathrm{LC}^{-1.141} \times T_{VN}^{0.325} \quad (r^2 = 0.921,\ \mathrm{df} = 1,445,\ p < 0.01)$$

The constant had a logarithm value of –8.54 (SE, 0.65). The SEs of the exponents were 0.054, 0.098, 0.093, and 0.091, respectively. The corresponding standard coefficients were 0.928, 0.246, –0.166, and 0.050, implying that the absolute relative contributions were 66.8, 17.7, 11.9, and 3.6%, respectively. Thus, TL and T_{VN} contributed clearly the most ($t = 69.01$) and least ($t = 3.59$) to F, respectively. Tolerance was ≥0.92. Inclusion of ALI as an expression of growth resulted in the same AIC, i.e., its contribution was barely insignificant ($t = -1.85$ or $p = 0.065$) and therefore excluded. F for a standard female of 85 cm with LC diameter of 750 μm ($F_{85\ cm,\ 750\ \mu m}$) ranged from 2.3 million (1999) to 3.1 million (2007).

The fecundity of each sample could be described successfully ($p < 0.001$) by the linear combination of body weight ($W_{corrected}$) and LC diameter: r^2 ranged from –0.85 (1999) to –0.94 (early 2006 and 2008). The higher r^2 in the field com-

Table 2. Overview of samples, split into prespawners and spawners, used to explore the relationship between leading cohort (LC) oocyte diameter and total length (TL) in the different waters of study.

					TL (cm)		LC (μm)		Regression analysis: LC vs. TL			
Year	Area	Calendar day	*n*	Category	Mean	SD	Grand mean	Grand mean SD	r^2	*P*	*a* (±SE)	*b* (±SE)
Northern area												
1999	Barents Sea	69–70	90	Prespawner	85.2	9.7	752	62	0.001	0.758	—	—
2000	Barents Sea	74	79	Prespawner	80.8	9.4	792	64	0.007	0.456	—	—
2003	Barents Sea	62	48	Prespawner	84.9	14.7	732	64	0.002	0.793	—	—
2004	Barents Sea	57	51	Prespawner	86.1	16.1	722	52	0.086	**0.037**	0.95 (0.44)	640 (39)
2005	Barents Sea	59	45	Prespawner	89.7	13.4	717	65	0.038	0.199	—	—
2006, early	Barents Sea	43–44	38	Prespawner	90.5	14.8	680	76	0.001	0.825	—	—
2006, late	Barents Sea	66–67	40	Prespawner	82.1	17.9	724	59	0.158	**0.011**	1.31 (0.49)	613 (54)
2007	Barents Sea	67	49	Prespawner	91.3	17.8	785	79	0.180	**0.002**	1.88 (0.58)	613 (54)
2008	Barents Sea	58–59	46	Prespawner	92.8	14.7	725	64	0.004	0.687	—	—
Southern area												
2004	North Sea	22–55	17	Prespawner	**60.9**	**16.1**	706	94				
			24	Spawner	**78.9**	**15.3**	≥875	—				
2004	Irish Sea	41–50	15	Prespawner	62.7ns	14.6ns	822	44				
			23	Spawner	65.9ns	12.4ns	≥875	—				

Note: *n*, number of females; SD, standard deviation. For the Barents Sea, cod year-specific regressions were established. If significant, slope (*a*) and intercept (*b*) values (± standard error, SE) are given. In 2006, both early and late samples were taken. LC diameter data for the Barents Sea are observed values; North Sea and Irish Sea LC diameter data are standardized to the last day of sampling on the cruise. Bold type denotes a significant result; ns denotes an insignificant result (for TL only).

Published by NRC Research Press

Fig. 9. Descriptors (mean ± standard deviation, SD) of the Andenes-caught Barents Sea cod females, i.e., (*a*) total length (TL), (*b*) viscera condition ($C_{viscera}$), and (*c*) body condition (C_{weight}) using solid circles for standard samples and open circles for extra samples, and (*d*) CTD temperature (mean only) in the Vardø North Transect (T_{VN}) in August–September (early vitellogenesis). Extreme values in (*b*) refer mainly to predation on adult capelin (*Mallotus villosus villosus*) but also to adult herring (*Clupea harengus*) and unidentified fish species. Horizontal lines in (*b*) and (*c*) are the normalized reference lines.

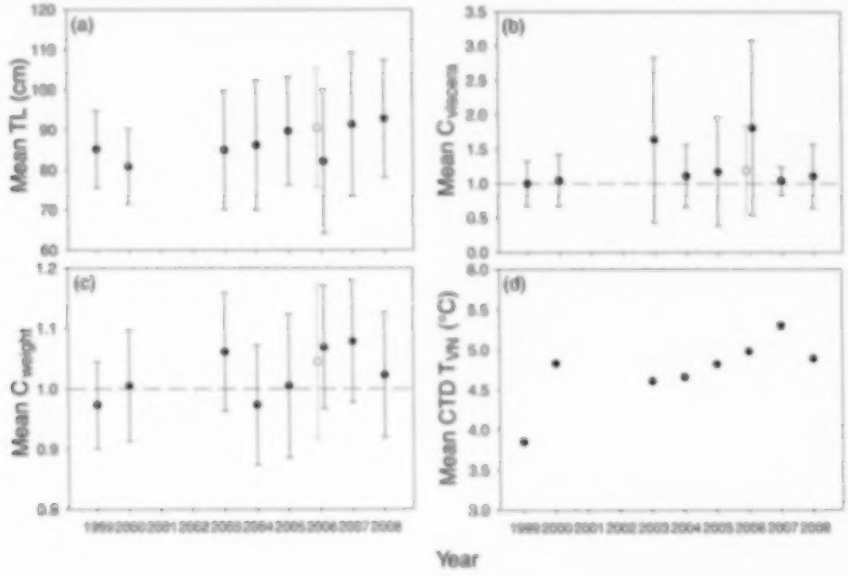

pared with in the laboratory (Fig. 3) was the result of the longer range in body size of wild specimens. Mean C_{weight} of a sample effectively predicted mean $F_{5500\ g\_750\ \mu m}$ (r^2 = 0.911, $p < 0.001$), 5500 g corresponding to $W_{expected}$ of a 85 cm fish (eq. 3).

Overall oocyte growth rate of the Barents Sea cod

Development in mean LC diameter (LC_{group}) over time as observed in the Andenes samples agreed largely with experimental, low-temperature results, although giving somewhat lower LC values at a given calendar day (Fig. 10). The proper establishment of the field-based equation was complicated by two outliers (late 2006 and 2007) and one case of large leverage (early 2006). The statistical use of all field data showed an oocyte growth rate (R) of 3.45 μm·day^{-1} (SE, ±1.76) and an intercept of −214 μm (SE, ±196) (r^2 = 0.770, p = 0.002). Avoiding the problem of presenting the year 2006 twice by leaving out late 2006 in the test gave comparable outputs (R, 3.69 μm·day^{-1} (SE, ±0.59); intercept, −278 μm (SE, ±163); r^2 = 0.866, $p < 0.001$). Based on the data in Fig. 9, the biggest positive residual in LC_{group} diameter (2007) was associated with nonfeeding larger fish, which apparently had experienced the highest vitellogenic temperature. The corresponding most negative residual (late 2006) referred to the most actively feeding fish, which were also among the smallest in size.

Individual oocyte growth rate of the Barents Sea cod

The individual-based study of all standard Andenes samples combined revealed that only about 5%–7% of the total variation in LC diameter residuals could be explained by the above defined physical descriptors and transect temperature.

Fig. 10. Grand mean of leading cohort oocyte diameter (LC_{group}) as observed in the Andenes sampling program on Barents Sea cod (solid circles with year attached) plotted versus calendar day of sampling (solid line) in comparison with similar experimental data at 5 °C (short-dashed line, cf. eq. 14) and 9.6 °C (long-dashed line, cf. eq. 15) and conceptually modelled data (3.4 °C) (dotted line). Shaded area refers to oocyte final maturation.

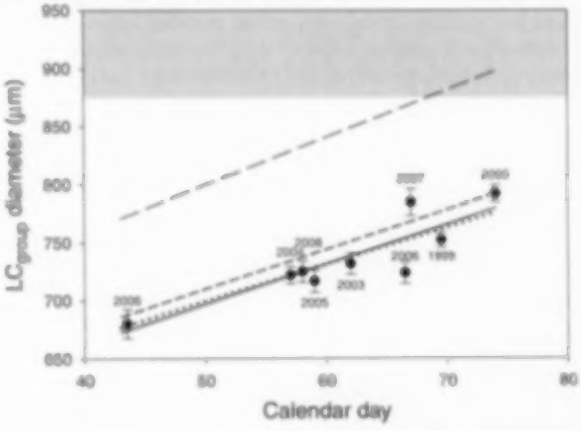

These multiple regressions were, however, highly significant ($p < 0.001$), which should be seen in light of the high number of females examined (df = 1,445). Temperature data (Vardø North, T_{VN}) as such did not meet the t value > 2 requirement (t = 1.58), but clearly did so when multiplied with length (TL) (t = 3.03) to form an interaction term (t = 3.66). The standard coefficients pointed to TL × T_{VN} being about

1.6 times more influential than C_{weight} (t = 2.26). The addition of $C_{viscera}$ resulted in another significant but negative contribution (t = –2.96). Dropping out $C_{viscera}$, the comparable contribution by ALI was t = 1.94, i.e., very close to being significant (p = 0.053).

Size-specific spawning time in the different waters

For the Barents Sea cod, only three of eight annual standard samples showed evidence of any relationship between LC diameter and total length of each individual fish (Table 2). More specifically, 9% of the variation in 2004 and 16%–18% in 2006–2007 could be explained, otherwise a few percent at most. The extra sample in early 2006 did not demonstrate such a positive relationship. Year 2000, referring to the latest sample taken in the spring (mid-March), showed 12 spawners. Spawners were not significantly different in length from prespawners (p = 0.536; Student's t test). Also, the regression behaved similarly (p = 0.415) when spawners were included, rounding off their LC diameters to 875 μm to avoid getting false relationships driven by large, swelling oocytes. Similarly, inclusion of five spawners in 2007 did not bias the given regression, i.e., gave p = 0.003 instead of p = 0.002. Replacement of $W_{corrected}$ with TL throughout the time series gave similar conclusions, whereas age and number of spawning zones did not significantly (p > 0.05) influence LC diameter at any point, despite the large spread in observed values (age, 5–13 years (plus one at 18 years); spawning zones, 0–6 (plus one at 7 and 12)).

Both the North Sea and Irish Sea samples showed examples of individuals lagging behind in maturation, but in contrast to the Barents Sea samples, these were generally concentrated more towards the lower part of the size range. In the North Sea, the observed spawners were significantly larger in size than their accompanying prespawners (p = 0.003; Mann–Whitney test), i.e., typically by 18 cm (Table 2). This was much less clear for the Irish Sea (p = 0.476), where the spawners were, on average, only 3 cm larger (Student's t test). However, in this case, a meaningful comparison was complicated because prespawners were also very close to spawning, as seen by their large LC_{group} diameter (822 μm) (Table 2). Prior to standardization using eqs. 11 and 12, both the North Sea and Irish Sea data showed a significant positive fish size dependency (North Sea, r^2 = 0.137, df = 1,33, p = 0.029; Irish Sea, r^2 = 0.238, df = 1,35, p = 0.002). Following standardization, this significance still prevailed (North Sea, r^2 = 0.152, df = 1,39, p = 0.012; Irish Sea, r^2 = 0.155, df = 1,36, p = 0.014), setting the LC diameter of spawners to 875 μm, as above.

Light cycle in the different waters

The light cycle in the Barents Sea differs markedly from the other areas of interest and is characterized by continuous light during the summer followed by a steep decline in day length to continuous darkness in the winter, i.e., with a much larger amplitude in day length than the Channel, the Irish Sea, and the experimental location (Fig. 11). These latter three show quite similar light cycles, although following the general pattern of a larger temporal range in day length northwards, as expected.

Fig. 11. Duration of daylight at four areas of study (Channel, crosses; Irish Sea, solid triangles; experimental location, open squares; Barents Sea, solid circles) as reported by the US Naval Observatory (http://aa.usno.navy.mil) at present experimental measurement days (days 0–240, 1 June 2005 – 26 January 2006). Time of summer and winter solstice and autumnal equinox are added, as well as the time when the sun went below the horizon for the first time after the period of continuous light in the Barents Sea. Horizontal line is inserted to mark autumnal equinox.

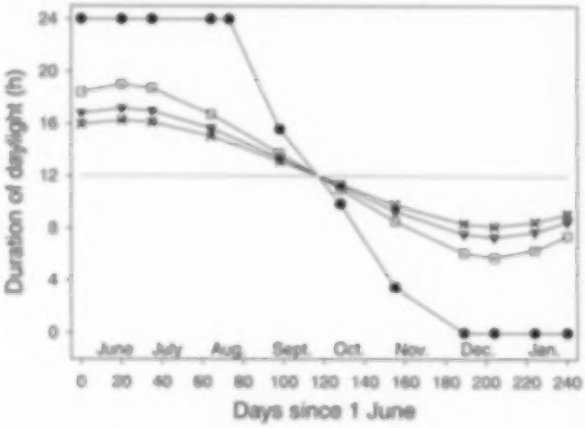

Conceptual maturation model

Approaches taken

The fact that the oocyte growth curves of the low-temperature experimental cod and the Barents Sea cod were close (Fig. 10) despite the great difference in light cycle suggested that autumnal equinox could be a collective starting point for vitellogenesis, simply because this was the only point between summer and winter time when their day lengths were exactly equal (Fig. 11). The inference of an underlying similar oocyte growth pattern following temperature adjustments was strengthened because the LT curve referred to 5 °C (Fig. 5), whereas the Barents Sea cod likely stayed in somewhat cooler water (Figs. 8 and 9); the plotted field curve should be located somewhat below the experimental LT one (as noticed in Fig. 10). Detailed examinations of eqs. 6 and 7 showed that these two experimental curves intersected on day 130 (8 October) corresponding to an LC_{group} diameter of 250 μm (LT, 249 μm; AT, 252 μm) followed in both cases by initiation of vitellogenic oocyte growth. This was seen from the combination of the following points, each point being described in full above: (*i*) 250 μm is the maximum previtellogenic oocyte diameter; (*ii*) oocyte growth is linear; and (*iii*) vitellogenesis is well established on day 155. Thus, the roughly 2-week period from autumnal equinox on day 114 (22 September) to this intersection point was defined as response time (latency), and eqs. 6 and 7 are rewritten as

$$(14)\quad LC_{group} = 3.43\,(\mathrm{SE} \pm 0.20) \times ED_{eq} + 250 \qquad (\mathrm{LT})$$

$$(15)\quad LC_{group} = 4.10\,(\mathrm{SE} \pm 0.15) \times ED_{eq} + 250 \qquad (\mathrm{AT})$$

where ED_{eq} is number of days after 8 October (therefore, ED_{eq} in the following year will be 84 + calendar day). As a

consequence, the problem of locating the intercept value, known to be important (see above), was assumed solved. A remaining problem was to clarify the actual vitellogenic temperature (T_{vit}) of the present Barents Sea cod bearing in mind that the above data indicated some differences in CTD and DST temperature records. Accordingly, T_{vit} was considered unknown and indicated by adjusting the oocyte growth rate, R_{acro}, in the general equation $LC_{group} = R_{acro} \times ED_{vit} + 250$ to achieve a fit between this curve and the field-based one. This happened when R_{acro} was 3.36 μm·day^{-1} (Fig. 10), reflecting a temperature of 3.4 °C, found by re-arranging eq. 8. Thus, the Andenes cod apparently stayed mostly in the upper part of the relevant DST temperature range (Fig. 8), i.e., consistently in colder water than indicated by the CTD Vardø North Transect (Fig. 9).

Resulting output

The combined use of eq. 8 and the expression $ED_{vit} = 625/R_{acro}$ made it possible to model the start of spawning (i.e., LC = 875 μm) in the year for an individual female cod in response to a range in T_{vit} (Fig. 12). As can be seen, eq. 8 was extrapolated by 3–4 °C on each side of the range to include higher and lower temperatures than used experimentally and adopting the associated level of uncertainty. Any dependency on fish size was tested in a warm water situation (see above) using eq. 10 followed by the previous standard procedure setting the temperature to 11 °C, i.e., the typical DST T_{vit} seen for southern waters (Fig. 8). However, the low r^2 of eq. 10 implied considerable prediction bands (not shown) and thereby gave an uncertain conclusion about the actual levels of response (Fig. 12).

Realism test

The conceptual model, excluding any body size effects, was tested by consulting published spawning curves (seasonal pelagic egg production curves) of the Barents Sea (Lofoten area; Pedersen 1984) and Irish Sea (Armstrong et al. 2001) cod. Thus, start of spawning (egg release) was known, meaning that the matching T_{vit} could be found from Fig. 12 and validated with available oceanographic data (Barents Sea cod) or DST information (Irish Sea cod). Resulting vitellogenic temperatures agreed well with expected environmental water temperatures encountered by the fish; however, in the case of the Barents Sea cod, these earliest spawners (calendar day 75) likely originated from local waters. More specifically, T_{vit} equaled 7.5 °C, corresponding with the typical autumnal temperature of 7 to 8 °C seen in Atlantic water masses (50–200 m) off Lofoten in the Gimsøy Transect (68°24′N, 14°04′E – 70°24′N, 08°12′E) (Dr. K.A. Mork, Institute of Marine Research, P.O. Box 1870 Nordnes, N-5817 Bergen, Norway, personal communication, 2008). In the case of the Irish Sea, start of spawning (calendar day 45) referred to a T_{vit} of 13 °C, which was possible (Fig. 8).

Discussion

Our study on reproductively competent Atlantic cod has revealed the interaction between the main factors influencing the maturity (oocyte growth) dynamics of this species. The strong dependence between day length and the initiation of vitellogenesis enabled us to develop temperature-specific maturity formulae based on general physiological principles, i.e., not requiring any new data to run the model in future operations. We were then able to use these formulae to predict convincingly the variation in start of spawning time in cod of several different stocks. Thus, other factors affecting oocyte growth rate such as condition variation and body size did not significantly bias this calculation. These results now make it possible to better understand the variation in cod spawning time as a consequence of past marine climate and allow us to make forecasts about what may happen in the future as climate changes.

Fig. 12. Conceptual modelled relationship (±2 × standard error, SE) between start of spawning (i.e., leading cohort oocyte diameter equals 875 μm) and vitellogenic temperature (T_{vit}) for an individual cod female. Spawning times of a large (65 cm, large circle) and a small (55 cm, small circle) warm-water (southern) cod are indicated.

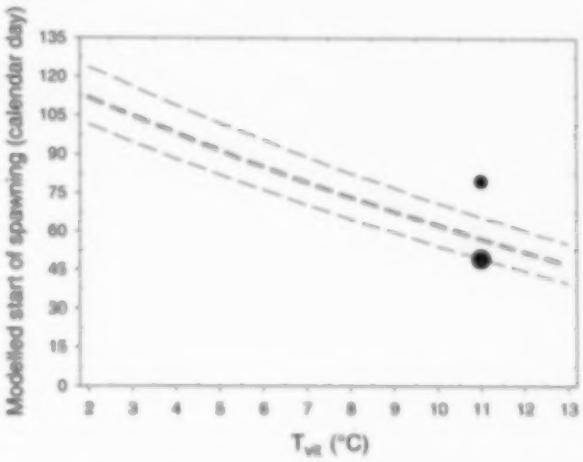

The effect of the autumnal equinox on maturity

Here we demonstrate experimentally that autumnal equinox is the starting point of vitellogenesis in Atlantic cod. This can be deduced from the fact that the fish in two different tanks were maintained at very different temperatures from summer onwards but did not display any sign of different oocyte growth trajectories until 8 October. The models that we fitted to the data show that the growth curves for oocytes in each experimental tank intersected at 250 μm corresponding to the upper previtellogenic oocyte (PVO) diameter described in other studies (Sivertsen 1935; Kjesbu 1991). This result concurs with Woodhead and Woodhead's (1965) conclusion, based on observation of a concurrent sharp increase in thyroid follicle cell height and increase in size and numbers of late PVOs (circumnuclear phase oocytes), that autumnal equinox is the time of "spawning migration and gonad maturation" for the Barents Sea cod. Previously, Woodhead and Woodhead's work has received little attention, possibly because the spawning migration of the Barents Sea cod starts much later, i.e., in December–January (Bergstad et al. 1987), and so is easily disassociated from gonad maturation in this stock. However, the regulation of thyroid hormone production was further explored by Comeau et al. (2001), who observed a significant increase in

these hormones around the equinox in the southern Gulf of St. Lawrence cod. Their results on estradiol-17β and testosterone show a (minor) pulse around that time. Surprisingly, sentinel catches in the western part of this Gulf area consistently peaked on exactly the same date as the present oocyte growth intersection point, 8 October (2–13 October) followed by another catch peak about two weeks later in the eastern part of the Gulf when the migrating cod arrived. Comeau et al. (2001) conclude that "thyroid hormones may facilitate the onset of the autumn migration by enhancing metabolism, sensory biology and swimming capacity." Although it is new information that vitellogenic oocyte growth in cod typically commences after a latency of about two weeks following autumnal equinox, studies related to cod aquaculture, especially on photoperiod manipulation, agree with our conclusion as these report increased levels of sex steroids and gonad growth from October onwards in the normal day group (Norberg et al. 2004; Skjæraasen et al. 2004; Davie et al. 2007). Such experimental designs also reflect that the oocyte growth rate can show a great level of plasticity (Hansen et al. 2001; Davie et al. 2007), but in a field situation, the photoperiodicity should be considered constant between years, ignoring the possible effect of variation in cloud covers. Our study is exceptional in that it finds an almost perfect matching of laboratory and field data on the temperature dependence of oocyte growth, which (*i*) emphasizes the success of our experimental design and the accuracy of both the experimental and field data sets and (*ii*) opens the road for similar experiments to take place for other fish species.

Present results showed that the experimental cod lost their appetite and grew less between 6 October and 2 November. Skjæraasen et al. (2004) observed a similar sudden drop in food intake for cod held on natural light and considered the following decline in appetite up to spawning to be a consequence of sexual maturation, although information shows that cod may take food during spawning (Fordham and Trippel 1999; Michalsen et al. 2008). Hence, the time around autumnal equinox is obviously a period when major changes take place in the physiology of adult cod, including a switch in energy allocation patterns to support further gonad growth. The experimentally delayed and compressed seasonal photoperiod data in Norberg et al. (2004) show that testosterone levels for both female and male cod consistently increase when the day length falls below 12 h. For females, the corresponding estradiol-17β pattern lags slightly behind, which is as expected; testosterone is "aromatized" into estradiol-17β (see Norberg et al. 2004). Thus, it is not the calendar as such that determines the onset of maturity, but the time when the duration of darkness first exceeds 12 h in the autumn, presumably through the mechanism of melatonin accumulation (Migaud et al. 2007). The present outlined day length threshold value and subsequent vitellogenic response is remarkably similar to mechanisms demonstrated in the marine annelid *Nereis virens* (Olive et al. 1998).

The experimental oocyte growth data do, however, show a variation in initiation of vitellogenesis of about ±1 month. Thus, a few individuals start to show evidence of oocyte growth in September, whereas others start in November, corresponding to day lengths of 14 and 10 h, respectively. Consequently, early spawners (those that require only 10 h of darkness to start oocyte growth) should be considered to be less sensitive to light than late spawners (requiring 14 h of darkness). One applied consequence of this discovery is that considerable savings could likely be made in the cod aquaculture industry by replacing the current practise of continuous light (24 h light – 0 h dark) to prevent sexual maturation (Taranger et al. 2006) to obviously somewhat shorter day lengths to reduce the electricity bill.

The effect of temperature on reproductive investment and condition factor

We found ample experimental evidence of an influence of temperature on reproductive investment, temporal variation in body growth, and condition factor. Earlier in the experiment, females held at the higher, ambient temperature (AT) showed indications of better appetite compared with females held at the lower, cooled temperature (LT), although the overall feeding ration for the whole length of the experiment was not statistically different. In both treatments, oocyte recruitment ended during the late autumn, with a few exceptions, as is usually observed for determinate spawners such as cod (Kjesbu 2009). However, despite indications of a higher food intake, AT females had a lower condition index (Fulton's *K*) than LT females. This is in contrast to previous field studies across cod stocks that report higher *K* at higher temperatures (Rätz and Lloret 2003). In our experiment, the main reason appears to be generally more investment in length growth at AT but similar overall weight growth at LT, putting the estimated *K* for AT downwards. This finding was further supported by the following facts: (*i*) tests on somatic *K*, i.e., following subtraction of ovary weight from the expression, also gave a significant difference, and (*ii*) these differences in *K* were already in place in early October, i.e., before gonad growth was well established. Regression analyses standardized for maturity demonstrated that differences in relative fecundity between the two categories of females was established early in the maturity cycle (LC diameter ≈ 400 μm), pointing to an increased production of PVOs at AT compared with at LT. The noted higher fecundity at AT apparently came at the expense of reduced liver size. In contrast, LT females appeared to "over-recruit" oocytes and later significantly reduced the number of developing oocytes as vitellogenesis (LC diameter) progressed, a process known as down-regulation through vitellogenic atresia (Witthames et al. 2009). These different patterns might suggest that the AT regime is more "effective" in terms of oocyte recruitment, i.e., assumed to be closer to the upper pejus temperature (Pörtner et al. 2001, 2008): a vitellogenic temperature of 9 °C enabled the AT females to reduce investment in the liver to boost egg production, whereas the LT group retained investment in the liver at a less "optimal" temperature of 5 °C. Taken together these results show that interpretation of *K* data on cod (for example, from field surveys) requires a good understanding of feeding conditions, as well as thermal experience, and therefore such data should be treated with caution. Conversely, our findings support the conclusion of Skjæraasen et al. (2006) that the period of early vitellogenesis is important for the resulting fecundity of cod, but here we clarify that the underlying oocyte regulation pattern depends on temperature and thereby varies with temperature and can be traced back to as early as summer.

The effect of temperature and other factors on oocyte and ovary growth

Unlike previous work (Kjesbu 1989) to estimate Q_{10}, our experiments were conducted during the vitellogenic period rather than during the spawning season. The rates of growth of oocytes, and thereby the corresponding Q_{10} values, are therefore lower because the estimates of growth were not made during the period when oocytes swell with water (Kjesbu et al. 1996). As a result, our experiments enabled us for the first time to establish a robust relationship between the rate of oocyte growth and temperature during the full maturity period, paying special attention to the assessment of the Q_{10} value and its underlying rate-specific error terms.

In any experiment of this nature, it is not possible or desirable to totally negate uncontrolled effects on oocyte growth created by, e.g., variation in fish condition (Kjesbu 2009) or a potential trade-off with somatic growth (Yoneda and Wright 2005). However, the modelled specific growth rates (G) of cod (of the size used in our experimental tanks) are almost constant over the temperature ranges we selected (as per Björnsson and Steinarsson 2002) and should cancel out any overall difference in body growth, as we found. More specifically, the present overall G values of LT and AT fell between two earlier published records, one from the laboratory (Björnsson and Steinarsson 2002; Icelandic cod), which was 17% and 9% above, and one from the field (Clark et al. 2003; North Sea), which was 15% and 20% below, respectively. Similarly, the applied ad libitum feeding protocol should, in theory, remove any general condition effect as such. Thus, the measurements of leading cohort (LC) diameter over time at 5 °C and 9 °C can be considered to very much reflect the actual, typical effect of these two temperature regimes on oocyte growth. Our experiments therefore provide us with overall oocyte growth rates that were, as far as is possible, solely related to temperature.

In consequence, we were able to derive accurate models for maturity (expressed as LC diameter growth) at standard (5–9 °C) and extrapolated (2–13 °C) temperatures. These did not reveal any deviation from the observed spawning curves in the northern or southern stocks (as derived from field sampling). In addition, the temperature data collected from the electronic tagging experiments showed that the temperatures at the upper limit of this extrapolation can be considered normal for wild cod at the southern end of their distribution. Thus it seems likely that changes in spawning time, based on the maturity curves, can be predicted at these higher temperatures. We are, however, more uncertain about the validity of this model at the other end of the temperature scale (from 2 °C to 5 °C) because the directly measured thermal experience of cod in the southern stocks has rarely fallen this low (Neat and Righton 2007, D. Righton, personal communication, 2009). Historical data on water temperatures at the southern limits of cod distribution suggest that such circumstances have occurred in the past (Bigg et al. 2008).

One potentially important problem not accounted for in the present maturity models is that mature fish in poor condition are known to delay spawning time by up to two weeks (see review in Kjesbu 2009). This length of time compares with what was seen in the Andenes time series in terms of total residual variation in LC_{group} diameter (when considering the relevant oocyte growth rate). Only 5%–7% of this variation could, however, be explained by the set of selected predictors in this work, including relative condition. This result was markedly different from the corresponding fecundity model where almost all of the variation (92%) could be explained by the same predictors. In other words, fecundity and spawning time show fundamentally different main regulatory principles, as implied in the above discussion on the dominating role of day light for subsequent spawning time. Other candidates for creating bias when running the present oocyte growth models might be any additional effect of age (Ramsay and Witthames 1996; Dover sole (*Solea solea*) from the English Channel) or spawning experience. These single effects could not be assessed in the experiment because all fish had the same origin. However, the Andenes cod showed large variations in these parametric values but no trace of any relevant implications. Nevertheless, to reduce any uncertainty in the application of the present maturity equations, this potential age effect should be further explored, at least in warmer water. Note here that we did find a temperature-specific effect of body size, dealt with later. Further tests on the maximum vitellogenic LC diameter in relation to fish size (Ramsay and Witthames 1996), presently set to 875 µm, should also be considered for fine-tuning the present model.

The effect of temperature on the timing of spawning

Validations showed that our models of oocyte growth were able to predict convincingly the variation in start of spawning time of northern and southern cod stocks in the Northeast Atlantic. Thus, spawning time in the southern stocks always occurred earlier than in the northern stocks, and because the variation in thermal experience during vitellogenesis was greater to the south, spawning time was more variable than in the north. Furthermore, our model can help to explain variation in spawning time for stocks outside our study region. For example, the observed water temperature and spawning time information presented for cod off Newfoundland (Hutchings and Myers 1994) also agree well with our models, despite very low ambient temperatures and a different definition of time of spawning. However, for unknown reasons, our model does not seem suitable for the Eastern Baltic Sea cod, which may also spawn in the early autumn even though the experienced temperatures do not seem to be particularly cold (Wieland et al. 2000). This situation might be explained by the long Baltic spawning season (March–September), which is a special adaptation to the extreme fluctuating environmental conditions in this ecosystem (MacKenzie et al. 1996). Also the Baltic tribe is an outlier both physiologically (in terms of egg formation) and genetically (Kjesbu and Witthames 2007), as well as by its more pelagic lifestyle than typical for adult cod (Tomkiewicz et al. 1998).

Understanding the spawning dynamics of cod stocks

In most areas, the progression of the spawning season in cod is observed as a gradual and accelerating increase in egg density to a peak and a subsequent deceleration (the "spawning curve"). The experiments that we conducted show that the start of vitellogenesis is imprinted (Otterå et

al. 2006; Greives et al. 2008; Paul et al. 2008) but the subsequent oocyte growth rate is adjusted by environmental temperature (Olive et al. 1998). Thus, autumnal equinox acts as the oocyte growth trigger, and temperature acts as the main oocyte growth regulator. These results lead to a new perspective of the principles involved in the formation of what appears as this typical spawning curve, as seen for instance in the Lofoten area (Pedersen 1984). The first part of this curve should consist of eggs shed by fish coming from the warmest water followed progressively by fish coming from colder and colder water. In the case of Lofoten, this would indicate that local cod (i.e., Coastal cod) eggs are generally spawned first, followed later by eggs from the Barents Sea cod.

Secondly, our data support the contention that the spawning time of larger females in relation to smaller females is advanced in the warmer water but that this phenomenon vanishes in the colder water. The underlying reasons for size dependency are, however, unclear (Wright and Trippel 2009). According to Pörtner et al. (2008), a larger ectothermic body enhances thermal sensitivity based on allometrical considerations: "oxygen supply becomes restricted earlier than in a smaller specimen." For the Barents Sea cod, the size dependency seems labile; in a few years, larger cod are more developed; in most other years, they are not. For the Irish Sea and North Sea, both data sets indicate that the larger cod spawn first, although less convincing for the Irish Sea than the North Sea, possibly due to the less successful sampling program but also to truncated age and length distribution following the stock collapse in the Irish Sea stock. Taken together, this suggests that size-specific spawning time apparently has an underlying physiological reason related to thermal window dynamics, found experimentally to relate back to body size in summer time at AT. In this article, the information from DSTs suggests that the spawning temperature (window) is around 7 °C for cod in southern waters, the Irish Sea and North Sea, and the Channel and around 4 °C for cod in northern waters, the Barents Sea. Thus, the two spawner categories seem adapted to different thermal windows, as expected (Pörtner et al. 2008). However, more data are needed to stretch this argument any further, e.g., earlier findings suggest that the Barents Sea cod may spawn at between 4 and 6 °C (Ellertsen et al. 1989).

Predicting the effects of climate change on cod reproductive ecology

In summary, the results of our work show that we are now able to explain and predict the maturity (oocyte growth) and likely fecundity and reproductive success of cod in different areas. The tool box of equations that we derived should now make it possible to better understand the variation in cod spawning time as a consequence of future climate change that, in turn, will have great prospects in further recruitment studies. For instance, one could now examine if the effects of climate-mediated changes in the zooplankton community (e.g., Beaugrand et al. 2000), coupled with changes in the time of spawning, could lead to a more frequent mismatch between the critical feeding period for cod larvae and the time of greatest abundance of copepod nauplii. Also, the consequences of warming on the success of ovulation and egg quality in different waters should be further examined, paying special attention to the critical threshold value of 9.6 °C for cod seen in the aquaculture-related work of van der Meeren and Ivannikov (2006).

Conversely, temperatures suitable for optimal vitellogenesis may be actively selected by adult cod, assuming that these temperatures also allow for sufficient food intake to permit sufficient investment in the gonads and therefore mediate the effect of any climate change by shifting the relative positions of feeding and spawning habitats. By turning the present series of arguments around, our findings may suggest that observations of spawning curves can be used to indicate the temperatures that adult cod have been experiencing, i.e., the ovaries of cod could be used as a "biological thermometer."

Altogether, we show that the underlying oocyte growth and energy allocation patterns of cod are strongly influenced by environmental temperature, opening up a fascinating field of research, and that the issues discussed in this paper will be central research areas for marine fish reproductive physiologists in the years to come.

Acknowledgements

This study is a consequence of the project ECOBE (Effects of North Atlantic Climate Variability on the Barents Sea Ecosystem) funded by the Research Council of Norway (RCN) (no. 155930/700, 2003-6) and was coordinated by Svein Sundby, Institute of Marine Research (IMR), Bergen. The actual preparation of the manuscript was supported by the RCN project ECOFISH (Ecosystem Dynamics and Fish Stocks) (no. 173536/i30) coordinated by Kjellrun Hiis Hauge and Nils Olav Handegard, IMR. The authors thank Gunnar Larsen, Sjoanlegget A/S, Andenes, for locating commercial samples and laboratory space during the hectic Lofoten fishery and Ørjan Karlsen and James Kennedy for commenting on an earlier draft. This article was encouraged by discussions with and the terms of reference of the NAFO Working Group on Reproductive Potential and COST Action Fish Reproduction and Fisheries (FRESH, FA0601). All experimental work was undertaken in accordance with animal welfare conventions and guidelines. The authors also thank the referees for their most constructive comments.

References

Armstrong, M.J., Connolly, P., Nash, R.D.M., Pawson, M.G., Alesworth, E., Coulahan, P.J., Dickey-Collas, M., Milligan, S.P., O'Neill, M.F., Witthames, P.R., and Woolner, L. 2001. An application of the annual egg production method to estimate the spawning biomass of cod (*Gadus morhua* L.), plaice (*Pleuronectes platessa* L.) and sole (*Solea solea* L.) in the Irish Sea. ICES J. Mar. Sci. **58**(1): 183–203. doi:10.1006/jmsc.2000.1001.

Armstrong, M.J., Gerritsen, H.D., Allen, M., McCurdy, W.J., and Peel, J.A.D. 2004. Variability in maturity and growth in a heavily exploited stock: cod (*Gadus morhua* L.) in the Irish Sea. ICES J. Mar. Sci. **61**(1): 98–112. doi:10.1016/j.icesjms.2003.10.005.

Bancroft, J.D., and Stevens, A. 1996. Theory and practice of histological techniques. Churchill Livingstone, New York.

Beaugrand, G., Reid, P.C., Ibañez, F., and Planque, B. 2000. Biodiversity of North Atlantic and North Sea calanoid copepods. Mar. Ecol. Prog. Ser. **204**: 299–303. doi:10.3354/meps204299.

Bergstad, O.A., Jørgensen, T., and Dragesund, O. 1987. Life history and ecology of the gadoid resources of the Barents Sea. Fish. Res. **5**(2–3): 119–161. doi:10.1016/0165-7836(87)90037-3.

Bigg, G.R., Cunningham, C.W., Ottersen, G., Pogson, G.H., Wadley, M.R., and Williamson, P. 2008. Ice-age survival of Atlantic cod: agreement between paleoecology models and genetics. Proc. R. Soc. Lond. B Biol. Sci. **275**(1631): 163–172. doi:10.1098/rspb.2007.1153.

Bjørnsson, B., and Steinarsson, A. 2002. The food-unlimited growth rate of Atlantic cod (*Gadus morhua*). Can. J. Fish. Aquat. Sci. **59**(3): 494–502. doi:10.1139/f02-028.

Blom, G., Svåsand, T., Jørstad, K.E., Otterå, H., Paulsen, O.I., and Holm, J.C. 1994. Comparative survival and growth of two strains of Atlantic cod (*Gadus morhua*) through the early life stages in a marine pond. Can. J. Fish. Aquat. Sci. **51**(5): 1012–1023. doi:10.1139/f94-101.

Brander, K.M. 1994. The location and timing of cod spawning around the British Isles. ICES J. Mar. Sci. **51**(1): 71–89.

Brander, K. 2005. Spawning and life history information for North Atlantic cod stocks. ICES Cooperative Research Report No. 274, Copenhagen, Denmark.

Brander, K.M. 2007. Climate change and food security special feature. Global fish production and climate change. Proc. Natl. Acad. Sci. U.S.A. **104**(50): 19709–19714. doi:10.1073/pnas.0702059104. PMID:18077405.

Bromage, N., Porter, M., and Randall, C. 2001. The environmental regulation of maturation in farmed finfish with special reference to the role of photoperiod and melatonin. Aquaculture, **197**(1–4): 63–98. doi:10.1016/S0044-8486(01)00583-X.

Brown, J.H., Gillooly, J.F., Allen, A.P., Savage, V.M., and West, G.B. 2004. Towards a metabolic theory of ecology. Ecology, **85**(7): 1771–1789. doi:10.1890/03-9000.

Clark, R.A., Fox, C.J., Viner, D., and Livermore, M. 2003. North Sea cod and climate change — modelling the effects of temperature on population dynamics. Glob. Change Biol. **9**(11): 1669–1680. doi:10.1046/j.1365-2486.2003.00685.x.

Comeau, L.A., Campana, S.E., Chouinard, G.A., and Hanson, J.M. 2001. Timing of Atlantic cod *Gadus morhua* seasonal migrations in relation to serum levels of gonadal and thyroidal hormones. Mar. Ecol. Prog. Ser. **221**: 245–253. doi:10.3354/meps221245.

Davie, A., Porter, M.J.R., Bromage, N.R., and Migaud, H. 2007. The role of seasonally altering photoperiod in regulating physiology in Atlantic cod (*Gadus morhua*). Part I. Sexual maturation. Can. J. Fish. Aquat. Sci. **64**(1): 84–97. doi:10.1139/F06-169.

Drinkwater, K.F. 2005. The response of Atlantic cod (*Gadus morhua*) to future climate change. ICES J. Mar. Sci. **62**(7): 1327–1337. doi:10.1016/j.icesjms.2005.05.015.

Dutil, J.-D., and Brander, K. 2003. Comparing productivity of North Atlantic cod (*Gadus morhua*) stocks and limits to growth production. Fish. Oceanogr. **12**(4–5): 502–512. doi:10.1046/j.1365-2419.2003.00243.x.

Ellertsen, B., Fossum, P., Solemdal, S., and Sundby, S. 1989. Relation between temperature and survival of eggs and first-feeding larvae of Northeast Arctic cod (*Gadus morhua* L.). Rapp. P.-v. Réun. Cons. Perm. Int. Explor. Mer, **191**: 209–219.

Fordham, S.E., and Trippel, E.A. 1999. Feeding behavior of cod (*Gadus morhua*) in relation to spawning. J. Appl. Ichthyol. **15**(1): 1–9. doi:10.1046/j.1439-0426.1999.00098.x.

Geffen, A.J., Fox, C.J., and Nash, R.D.M. 2006. Temperature-dependent development rates of cod *Gadus morhua* eggs. J. Fish Biol. **69**(4): 1060–1080. doi:10.1111/j.1095-8649.2006.01181.x.

Godø, O.R., and Michalsen, K. 2000. Migratory behaviour of north-east Arctic cod, studied by use of data storage tags. Fish. Res. **48**(2): 127–140. doi:10.1016/S0165-7836(00)00177-6.

Greives, T.J., Kriegsfeld, L.J., Bentley, G.E., Tsutsui, K., and Demas, G.E. 2008. Recent advances in reproductive neuroendocrinology: a role for RFamide peptides in seasonal reproduction? Proc. R. Soc. Lond. B Biol. Sci. **275**(1646): 1943–1951. doi:10.1098/rspb.2008.0433.

Hansen, T., Karlsen, Ø., Taranger, G.L., Hemre, G.-I., Holm, J.C., and Kjesbu, O.S. 2001. Growth, gonadal development and spawning time of Atlantic cod (*Gadus morhua*) reared under different photoperiods. Aquaculture, **203**(1–2): 51–67. doi:10.1016/S0044-8486(01)00610-X.

Hutchings, J.A., and Myers, R.A. 1994. Timing of cod reproduction: interannual variability and the influence of temperature. Mar. Ecol. Prog. Ser. **108**: 21–31. doi:10.3354/meps108021.

Intergovernmental Panel of Climate Change. 2007. Climate change 2007: synthesis report. Contributions of Working Groups I, II and III to the Fourth Assessment Report of the Intergovernmental Panel of Climate Change. Intergovernmental Panel of Climate Change (IPCC), Geneva, Switzerland.

International Council for the Exploration of the Sea Advisory Committee. 2008. Report of the Arctic Fisheries Working Group (AFWG). ICES CM 2008/ACOM:01.

Kjesbu, O.S. 1989. The spawning activity of cod, *Gadus morhua* L. J. Fish Biol. **34**(2): 195–206. doi:10.1111/j.1095-8649.1989.tb03302.x.

Kjesbu, O.S. 1991. A simple method for determining the maturity stages of Northeast Arctic cod (*Gadus morhua* L.) by *in vitro* examination of oocytes. Sarsia, **75**(4): 335–338.

Kjesbu, O.S. 1994. Time of start of spawning in Atlantic cod (*Gadus morhua*) females in relation to vitellogenic oocyte diameter, temperature, fish length and condition. J. Fish Biol. **45**(5): 719–735. doi:10.1111/j.1095-8649.1994.tb00939.x.

Kjesbu, O.S. 2009. Applied fish reproductive biology: contribution of individual reproductive potential to recruitment and fisheries management. *In* Fish reproductive biology: implications for assessment and management. *Edited by* T. Jakobsen, M.J. Fogarty, B.A. Megrey, and E. Moksness. John Wiley and Sons, Hoboken, New Jersey. pp. 293–332.

Kjesbu, O.S., and Witthames, P.R. 2007. Evolutionary pressure on reproductive strategies in flatfish and groundfish: relevant concepts and methodological advancements. J. Sea Res. **58**(1): 23–34. doi:10.1016/j.seares.2007.02.001.

Kjesbu, O.S., Witthames, P.R., Solemdal, P., and Greer Walker, M. 1990. Ovulatory rhythm and a method to determine the stage of spawning in Atlantic cod (*Gadus morhua*). Can. J. Fish. Aquat. Sci. **47**(6): 1185–1193. doi:10.1139/f90-138.

Kjesbu, O.S., Klungsøyr, J., Kryvi, H., Witthames, P.R., and Greer Walker, M. 1991. Fecundity, atresia, and egg size of captive Atlantic cod (*Gadus morhua*) in relation to proximate body composition. Can. J. Fish. Aquat. Sci. **48**(12): 2333–2343. doi:10.1139/f91-274.

Kjesbu, O.S., Kryvi, H., and Norberg, B. 1996. Oocyte size and structure in relation to blood plasma steroid hormones in individually monitored, spawning Atlantic cod. J. Fish Biol. **49**(6): 1197–1215. doi:10.1111/j.1095-8649.1996.tb01789.x.

Kjesbu, O.S., Witthames, P.R., Solemdal, P., and Greer Walker, M. 1998. Temporal variations in the fecundity of Arcto-Norwegian cod (*Gadus morhua*) in response to natural changes in food and temperature. J. Sea Res. **40**(3–4): 303–321. doi:10.1016/S1385-1101(98)00029-X.

Korsbrekke, K., Mehl, S., Nakken, O., and Pennington, M. 2001. A survey-based assessment of the Northeast Arctic cod stock. ICES J. Mar. Sci. **58**(4): 763–769. doi:10.1006/jmsc.2001.1064.

MacKenzie, B., St. John, M., and Wieland, K. 1996. Eastern Baltic cod: perspectives from existing data on processes affecting growth and survival of eggs and larvae. Mar. Ecol. Prog. Ser. **134**: 265–281. doi:10.3354/meps134265.

Michalsen, K., Johannesen, E., and Bogstad, B. 2008. Feeding of mature cod (*Gadus morhua*) on the spawning grounds in Lofoten. ICES J. Mar. Sci. **65**(4): 571–580. doi:10.1093/icesjms/fsn019.

Migaud, H., Davie, A., Martinez Chavez, C.C., and Al-Khamees, S. 2007. Evidence for differential photic regulation of pineal melatonin synthesis in teleosts. J. Pineal Res. **43**(4): 327–335. doi:10.1111/j.1600-079X.2007.00480.x. PMID:17910600.

Neat, F., and Righton, D. 2007. Warm water occupancy by North Sea cod. Proc. R. Soc. Lond. B Biol. Sci. **274**(1611): 789–798. doi:10.1098/rspb.2006.0212.

Norberg, B., Brown, C.L., Halldorsson, A., Stensland, K., and Bjørnsson, B.T. 2004. Photoperiod regulates the timing of sexual maturation, spawning, sex steroid and thyroid hormone profiles in the Atlantic cod (*Gadus morhua*). Aquaculture, **229**(1–4): 451–467. doi:10.1016/S0044-8486(03)00393-4.

Olive, P.J.M., Rees, S.W., and Djunaedi, A. 1998. Influence of photoperiod and temperature on oocyte growth in the semelparous polychaete *Nereis* (*Neanthes*) *virens*. Mar. Ecol. Prog. Ser. **172**: 169–183. doi:10.3354/meps172169.

Otterå, H., Agnalt, A.-L., and Jørstad, K.E. 2006. Differences in spawning time of captive Atlantic cod from four regions of Norway, kept under identical conditions. ICES J. Mar. Sci. **63**(2): 216–223. doi:10.1016/j.icesjms.2005.11.004.

Parmesan, C., and Yohe, G. 2003. A globally coherent fingerprint of climate change impacts across natural systems. Nature (London), **421**(6918): 37–42. doi:10.1038/nature01286. PMID:12511946.

Paul, M.J., Zucker, I., and Schwartz, W.J. 2008. Tracking the seasons: the internal calendars of vertebrates. Philos. Trans. R. Soc. Lond. B Biol. Sci. **363**(1490): 341–361. doi:10.1098/rstb.2007.2143. PMID:17686736.

Pedersen, T. 1984. Variation of peak spawning of Arcto-Norwegian cod (*Gadus morhua* L.) during the time period 1929–1982 based on indices estimated from fishery statistics. *In* Proceedings of the International Symposium, Arendal, Norway, 14–17 June 1983: The Propagation of Cod *Gadus morhua* L. *Edited by* E. Dahl, D.S. Danielssen, E. Moksness, and P. Solemdal. Flødevigen rapportser 1, 1984, Institute of Marine Research, Flødevigen Biological Station, Arendal, Norway. pp. 301–316.

Pepin, P., Orr, D.C., and Anderson, J.T. 1997. Time to hatch and larval size in relation to temperature and egg size in Atlantic cod (*Gadus morhua*). Can. J. Fish. Aquat. Sci. **54**(Suppl. 1): 2–10. doi:10.1139/cjfas-54-S1-2.

Perry, A.L., Low, P.J., Ellis, J.R., and Reynolds, J.D. 2005. Climate change and distribution shifts in marine fishes. Science (Washington, D.C.), **308**(5730): 1912–1915. doi:10.1126/science.1111322. PMID:15890845.

Planque, B., and Fredou, T. 1999. Temperature and the recruitment of Atlantic cod (*Gadus morhua*). Can. J. Fish. Aquat. Sci. **56**(11): 2069–2077. doi:10.1139/cjfas-56-11-2069.

Pörtner, H.O., and Farrell, A.P. 2008. Ecology: physiology and climate change. Science (Washington, D.C.), **322**(5902): 690–692. doi:10.1126/science.1163156. PMID:18974339.

Pörtner, H.O., Berdal, B., Blust, R., Brix, O., Colosimo, A., De Wachter, B., Giuliani, A., Johansen, T., Fischer, T., Knust, R., Lannig, G., Naevdal, G., Nedenes, A., Nyhammer, G., Sartoris, F.J., Serendero, I., Sirabella, P., Thorkildsen, S., and Zakhartsev, M. 2001. Climate induced temperature effects on growth performance, fecundity and recruitment in marine fish: developing a hypothesis for cause and effect relationships in Atlantic cod (*Gadus morhua*) and common eelpout (*Zoarces viviparus*). Cont. Shelf Res. **21**(18–19): 1975–1997. doi:10.1016/S0278-4343(01)00038-3.

Pörtner, H.O., Bock, C., Knust, R., Lannig, G., Lucassen, M., Mark, F.C., and Sartoris, F.J. 2008. Cod and climate in a latitudinal cline: physiological analyses of climate effects in marine fishes. Clim. Res. **37**(2–3): 253–270. doi:10.3354/cr00766.

Ramsay, K., and Witthames, P. 1996. Using oocyte size to assess seasonal ovarian development in *Solea solea* (L.). J. Sea Res. **36**(3–4): 275–283. doi:10.1016/S1385-1101(96)90796-0.

Rätz, H.-J., and Lloret, J. 2003. Variation in fish condition between Atlantic cod (*Gadus morhua*) stocks, the effect on their productivity and management implications. Fish. Res. **60**(2–3): 369–380. doi:10.1016/S0165-7836(02)00132-7.

Righton, D., Kjesbu, O.S., and Metcalfe, J. 2006. A field and experimental evaluation of the effect of data storage tags on the growth of cod. J. Fish Biol. **68**(2): 385–400. doi:10.1111/j.0022-1112.2006.00899.x.

Rollefsen, G. 1934. The cod otolith as a guide to race, sexual development and mortality. Rapp. P.-v. Réun. Cons. Perm. Int. Explor. Mer, **88**(2): 1–5.

Schmidt-Nielsen, K. 1983. Animal physiology: adaptation and environment. Cambridge University Press, Cambridge, UK.

Scott, B.E., Marteinsdottir, G., Begg, G.A., Wright, P.J., and Kjesbu, O.S. 2006. Effects of population size/age structure, condition and temporal dynamics of spawning on reproductive output in Atlantic cod (*Gadus morhua*). Ecol. Model. **191**(3–4): 383–415. doi:10.1016/j.ecolmodel.2005.05.015.

Sivertsen, E. 1935. Torskens gytning. Med særlig henblikk på den årlige cyklus i generasjonsorganenes tilstand. Fisk. Hav. **4**(10): 1–29.

Skjæraasen, J.E., Salvanes, A.G.V., Karlsen, Ø., Dahle, R., Nilsen, T., and Norberg, B. 2004. The effect on sexual maturation, appetite and growth in wild Atlantic cod (*Gadus morhua* L.). Fish Physiol. Biochem. **30**(2): 163–174. doi:10.1007/s10695-005-4319-6.

Skjæraasen, J.E., Nilsen, T., and Kjesbu, O.S. 2006. Timing and determination of potential fecundity in Atlantic cod (*Gadus morhua*). Can. J. Fish. Aquat. Sci. **63**(2): 310–320. doi:10.1139/f05-218.

Sokal, R.R., and Rohlf, F.J. 1981. Biometry: the principles and practice of statistics in biological research. W.H. Freeman and Company, New York.

Sousa, T., Domingos, T., and Kooijman, S.A.L.M. 2008. From empirical patterns to theory: a formal metabolic theory of life. Philos. Trans. R. Soc. Lond. B Biol. Sci. **363**(1502): 2453–2464. doi:10.1098/rstb.2007.2230. PMID:18331988.

Sundby, S. 2000. Recruitment of Atlantic cod stocks in relation to temperature and advection of copepod populations. Sarsia, **85**(4): 277–298.

Sundby, S., and Nakken, O. 2008. Spatial shifts in spawning habitats of Arcto-Norwegian cod related to multidecadal climate oscillations and climate change. ICES J. Mar. Sci. **65**(6): 953–962. doi:10.1093/icesjms/fsn085.

Svåsand, T., Jørstad, K.E., Otterå, H., and Kjesbu, O.S. 1996. Differences in growth performance between Arcto-Norwegian and Norwegian coastal cod reared under identical conditions. J. Fish Biol. **49**(1): 108–119. doi:10.1111/j.1095-8649.1996.tb00008.x.

Systat Software, Inc. 2007. Systat 12. Systat Software, Inc., San Jose, California.

Tarunger, G.L., Aardal, L., Hansen, T., and Kjesbu, O.S. 2006. Continuous light delays sexual maturation and increases growth of Atlantic cod (*Gadus morhua* L.) in sea cages. ICES J. Mar. Sci. **63**(2): 365–375. doi:10.1016/j.icesjms.2005.10.014.

Thorsen, A., and Kjesbu, O.S. 2001. A rapid method for estimation of oocyte size and potential fecundity in Atlantic cod using a computer-aided particle analysis system. J. Sea Res. **46**(3–4): 295–308. doi:10.1016/S1385-1101(01)00090-9.

Thorsen, A., Marshall, C.T., and Kjesbu, O.S. 2006. Comparison of various potential fecundity models for north-east Arctic cod *Gadus morhua* L. using oocyte diameter as a standardizing factor. J. Fish Biol. **69**(6): 1709–1730. doi:10.1111/j.1095-8649.2006.01239.x.

Tomkiewicz, J., Lehmann, K.M., and St. John, M.A. 1998. Oceanographic influences on the distribution of Baltic cod, *Gadus morhua*, during spawning in the Bornholm Basin of the Baltic Sea. Fish. Oceanogr. **7**(1): 48–62. doi:10.1046/j.1365-2419.1998.00051.x.

van der Meeren, T., and Ivannikov, V.P. 2006. Seasonal shift in spawning of Atlantic cod (*Gadus morhua* L.) by photoperiod manipulation: egg quality in relation to temperature and intensive larval rearing. Aquat. Res. **37**(9): 898–913. doi:10.1111/j.1365-2109.2006.01510.x.

West, G. 1990. Methods of assessing ovarian development in fishes: a review. Aust. J. Mar. Freshwater Res. **41**(2): 199–222. doi:10.1071/MF9900199.

Wieland, K., Jarre-Teichmann, A., and Horbowa, K. 2000. Changes in the timing of spawning of Baltic cod: possible causes and implications for recruitment. ICES J. Mar. Sci. **57**(2): 452–464. doi:10.1006/jmsc.1999.0522.

Witthames, P.R., Thorsen, A., Murua, H., Saborido-Rey, F., Greenwood, L.N., Dominguez, R., Korta, M., and Kjesbu, O.S. 2009. Advances in methods for determining fecundity: application of the new methods to some marine fishes. Fish. Bull. (Washington, D.C.), **107**(2): 148–164.

Woodhead, A.D., and Woodhead, P.M.J. 1965. Seasonal changes in the physiology of the Barents Sea cod, *Gadus morhua* L., in relation to its environment. I. Endocrine changes particularly affecting migration and maturation. ICNAF Spec. Publ. **6**: 691–715.

Wright, P.J., and Trippel, E.A. 2009. Fishery-induced demographic changes in the timing of spawning: consequences for reproductive success. Fish Fish. **10**: 283–304.

Yoneda, M., and Wright, P.J. 2005. Effects of varying temperature and food availability on growth and reproduction in first-time spawning female Atlantic cod. J. Fish Biol. **67**(5): 1225–1241. doi:10.1111/j.1095-8649.2005.00819.x.

Hydrogeomorphic effects on bedload scour in bull char (*Salvelinus confluentus*) spawning habitat, western Washington, USA

Jeffrey G. Shellberg, Susan M. Bolton, and David R. Montgomery

Abstract: We investigated the vulnerability of fall-spawned bull char (*Salvelinus confluentus*) embryos to redd scour during winter rain and rain-on-snow flood discharges in western Washington, USA. It was hypothesized that the magnitude of bedload scour at bull char redds is reduced by the provision and selection of stable refugia habitat controlled by local-, reach-, or subcatchment-scale variables such as hydraulic habitat unit and channel type. Bedload scour and channel change were measured using 96 scour monitors and 34 elevational transects in three catchments over 2 to 4 years. Scour to cited egg burial depths of bull char did not commence until discharge typically exceeded the 2-year recurrence interval. At a local scale, scour varied significantly among side channel, protected main channel, and unprotected main channel redd sites. Unprotected gravel patches in simplified channel types with moderate gradients were most susceptible to deep scour, especially if coupled with the transient supply and storage of sand and gravel from mass wasting. Partially transport-limited reaches had reduced scour due to lower stream power and armored gravel beds. Complex spawning habitat (i.e., with abundant large woody debris and side channels) was important in providing refuge from deep scour and in buffering embryos against inhospitable hydrologic or sediment regimes.

Résumé : Nous examinons la vulnérabilité des embryons d'ombles à tête plate (*Salvelinus confluentus*) produits en automne à l'affouillement des frayères durant les débits de crue d'hiver dus à la pluie ou la pluie sur la neige dans l'ouest de l'état de Washington, É.-U. Nous avons émis l'hypothèse selon laquelle l'ampleur de l'affouillement causé par les alluvions de fond sur les frayères des ombles à tête plate est réduite par l'établissement et la sélection d'habitats de refuge stables contrôlés par des variables à l'échelle du site, de la section et du sous-bassin, tels que l'unité d'habitat hydraulique et le type de chenal. Nous avons mesuré l'affouillement causé par les alluvions de fond, ainsi que les modifications du chenal, à l'aide de 96 moniteurs d'affouillement et de 34 transects des relevés des élévations dans trois bassins versants pendant 2 à 4 ans. L'affouillement aux profondeurs connues d'enfouissement des œufs d'ombles à tête plate ne se produit pas ordinairement aux débits inférieurs à ceux de l'intervalle de récurrence de 2 années. À l'échelle locale, l'affouillement varie significativement selon qu'il s'agit de frayères situées sur un chenal latéral, sur un chenal principal protégé ou sur un chenal principal exposé. Les bancs de gravier exposés dans des chenaux de type simplifié avec des gradients modérés sont les plus vulnérables à un affouillement profond, particulièrement s'il existe concurremment un apport et une rétention transitoires de sable et de gravier provenant de mouvements en masse. Les sections à transport partiellement limité ont un affouillement réduit à cause de la puissance diminuée du cours d'eau et des bancs de gravier blindés. Les habitats de fraie complexes (c'est-à-dire avec de nombreux débris ligneux et des chenaux latéraux) sont importants car ils fournissent un refuge contre l'affouillement profond et ils protègent les embryons des régimes hydrologiques ou sédimentaires inhospitaliers.

[Traduit par la Rédaction]

Introduction

Salmonids have adapted to the natural discharge regimes of fluvial ecosystems (Lytle and Poff 2004). However, embryos of many salmonid species are present in the streambed before and during flood events that transport bedload, e.g., with fall-spawned embryos and winter floods or spring-spawned embryos and early summer floods. Streambed

Received 14 March 2009. Accepted 29 December 2009. Published on the NRC Research Press Web site at cjfas.nrc.ca on 10 March 2010.
J21104

Paper handled by Associate Editor Jordan Rosenfeld.

J.G. Shellberg[1,2] **and S.M. Bolton.** University of Washington, School of Forest Resources, Forest Hydrology, Box 352100, Seattle, WA 98195, USA.
D.R. Montgomery. University of Washington, Department of Earth and Space Sciences and Quaternary Research Center, Box 351310, Seattle, WA 98195, USA.

[1]Corresponding author (e-mail: j.shellberg@griffith.edu.au).
[2]Present address: Australian Rivers Institute, Griffith University, 170 Kessels Road, Nathan, Queensland 4111, Australia.

scour (lowering of the streambed elevation) and fill during bedload transport can result in high mortality of incubating salmonids (e.g., Seegrist and Gard 1972; Erman et al. 1988).

The effects of scour on salmonid distribution and abundance at local to regional scales depends on fish size, life history strategy (i.e., iteroparity vs. semelparity), spawn time, amount of spawning and rearing habitat, local hydraulics, geomorphic reach type, sediment supply, discharge regime, and disturbance history. Montgomery et al. (1999) hypothesized that salmonids will not be able to persist in channel reaches with predictable deep scour during the incubation period ("bed scour hypothesis") unless fish locally bury their eggs below typical scour depths or spawn in sites with locally reduced scour. In low-gradient pool–riffle gravel-bed streams, large-bodied salmon avoid streambed scour by burying their eggs below typical scour depths during bankfull discharge (Montgomery et al. 1996). Bedload disturbance depths in low-gradient gravel-bed streams are on average less than two times the 90th percentile surface particle size ($2 \cdot D_{90}$) (DeVries 2002).

In coarse mountain channels where the supply of spawning gravel is limited and transport capacity is high, smaller-bodied salmonids with shallow to moderate egg burial depths may not be able to bury their eggs deep enough to avoid scour disturbance (i.e., below $2 \cdot D_{90}$). In addition, bedload transport and scour processes in channels where smaller-bodied salmonids typically spawn may be different than those active in pool–riffle or plane-bed channels where larger salmon spawn (Montgomery et al. 1999). Alternatively, at the local scale, many aquatic species avoid disturbance by selecting habitats that provide refuge from disturbance, preventing species exclusion at higher spatial scales (reach, segment, or catchment; Sedell et al. 1990).

The specific biology and life history of a salmonid can affect their exposure to scouring floods. For example, migratory bull char (*Salvelinus confluentus*) in western Washington spawn in cold mountain streams during the fall (September to December), peaking in October (Johnson 1991). They are medium-sized (300–800 mm in length), iteroparous, and long-lived (7–12 years) (US Fish and Wildlife Service 1998). Egg burial depths for migratory females average 10–15 cm (DeVries 1997; Shellberg 2002), which is less than larger fall-spawning Pacific salmon (15–25 cm) (DeVries 1997). Egg and alevin gravel residence times are prolonged and temperature-dependent, with hatching after 90–145 days at 2–4 °C (McPhail and Murray 1979; Shepard et al. 1984) and up to 220 days until gravel emergence (Goetz 1989; Stutsman and Ogg 2002; Shellberg 2002). These biologic factors put bull char eggs and alevins at high mortality risk from scour during late-fall and early-winter peak flood events. However, bull char iteroparity may spread the risk of offspring mortality over multiple years.

Numerous studies have measured the patterns and processes of scour and fill in the spawning habitat of salmonids (e.g., Rennie and Millar 2000; Schuett-Hames et al. 2000; DeVries 2002; and others). However, most of these studies investigated sediment transport and scour patterns in low-gradient, pool–riffle channel types typically used by large-bodied salmon. Sediment transport in steeper mountain streams has been examined in detail (e.g., Bathurst et al. 1983; Gintz et al. 1996), but only a few studies have measured scour and fill in gravel patches used by smaller salmonids in mountain channel types (Kondolf et al. 1991; Barta et al. 1994).

The aim of this study was to investigate the previously undocumented vulnerability of bull char embryos to scour and fill of spawning gravels during fall and winter floods in mountain drainage basins of western Washington State, USA. It was hypothesized that the magnitude of bedload scour at bull char redds is reduced by the presence and selection of stable habitat refugia controlled by local-, reach-, or subcatchment-scale hydrogeomorphic variables. For example, energy dissipation around large woody debris (LWD) structures may reduce the effective shear stress available for bed scour in spawning gravels upstream or downstream of LWD. This habitat refugia component of the bed scour hypothesis (Montgomery et al. 1999) has not been explicitly tested for bull char or most salmonids in general. Therefore, selected hydrogeomorphic variables (hydraulic habitat unit, channel type, discharge magnitude and frequency, sediment transport regime) influencing measured scour and fill depths in bull char spawning locations were analyzed in three contrasting catchments in western Washington.

Materials and methods

Study reaches

Three study catchments were chosen from known spawning populations of migratory bull char in western Washington, USA: the upper Cedar River, North Fork (NF) Skykomish River, and South Fork (SF) Skokomish River. All three catchments are located in high-relief mountainous terrain in the Cascade or Olympic mountains, with moderate to dense conifer forest cover but different geology and forest land use (Table 1). Within each of the three catchments, two adjacent primary spawning reaches were chosen for detailed analysis, providing six reaches in total with contrasting reach-scale (100–1000 m) channel types (Table 1; sensu Montgomery and Buffington 1997).

The pool–riffle reaches of the upper Cedar River (including the Rex River) in the western Cascade Mountains are low-gradient channels with gravel beds armoured in patches and well-connected floodplains (Table 1). Obstructions such as LWD are rare, which is at least partially a result of historic riparian timber harvest. The varying yet abundant supply of gravel-sized particles and local gravel armouring lead to the presumption that gravel-sized bedload is at least partially transport-limited as compared with the available stream power (sensu Bravo-Espinosa et al. 2003). Char spawning typically occurs on straight riffles, riffle crests, or occasionally, side channels without other competing fall-spawning species. These reaches are located near the seasonal inundation zone of the large regulated Chester Morse Lake; however, backwater did not affect the stage, discharge, or water surface slope during the measured winter flood events in the study period.

The forced pool–riffle reaches of the NF Skykomish River below Goblin Creek in the western Cascade Mountains are moderate-gradient, cobble- and boulder-bed channels with numerous LWD, boulder, and bedrock obstructions. The associated floodplains are coarse-grained

Table 1. Summary of physical conditions in different study catchments and reaches.

	North Fork Skykomish		South Fork Skokomish		Upper Cedar	
	Lower Goblin Creek	Below Goblin Creek	Above Church Creek	Below Church Creek	Cedar River near Camp 18	Rex River near Boulder Creek
Channel type	Forced step–pool	Forced pool–riffle	Forced pool–riffle	Forced pool–riffle	Pool–riffle	Pool–riffle
Gradient, %	1.5–3.5	0.7–1.5	0.8–1.5	0.8–1.0	0.2–0.7	0.2–0.5
Substrate framework	Boulder/cobble	Cobble/boulder	Cobble/gravel	Cobble/gravel	Gravel/cobble	Gravel/cobble
Spawning locations	Gravel pockets, pool tails	Gravel pockets, lateral bars, side channels	Lateral bars, gravel pockets	Lateral bars, gravel pockets	Gravel riffles, riffle crests	Gravel riffles, riffle crests
Scour monitors						
Selected	7	7	10	8	11	12
Nonselected	5	11	8	0	10	7
Catchment area, km^2	12.8	88.4	35.6	52.0	105.4	56.7
Elevation range, m	549–2134	488–2134	305–1524	274–1524	475–1644	475–1341
Reach coordinates	47°55′10.93″N 121°18′38.03″W	47°54′11.02″N 121°18′59.70″W	47°28′27.16″N 123°26′56.91″W	47°27′1.99″N 123°25′45.15″W	47°22′12.03″N 121°37′25.63″W	47°22′17.67″N 121°41′16.76″W
Catchment geology	Metamorphic rock, granodiorite, volcaniclastic deposits	Metamorphic rock, granodiorite, volcaniclastic deposits	Marine sandstone, marine basalt, glacial–fluvial terrace deposits	Marine sandstone, marine basalt, glacial–fluvial terrace deposits	Volcaniclastic deposits, andesite flows, Quaternary alluvium	Volcaniclastic deposits, andesite flows, Quaternary alluvium
Land-use history	Mostly wilderness	Wilderness, logging/roads	Mostly wilderness	Logging/roads, wilderness	Logging/roads, water supply	Logging/roads, water supply

Published by NRC Research Press

and well connected with abundant side channels created by large LWD jams or overflow channels. The forced step–pool tributary Goblin Creek is a steep-gradient, cobble- and boulder-bed channel, where pools are forced by LWD jams, boulder obstructions, and bedrock. The armoured cobble- and boulder-bed thalwegs and periodic marginal deposits of gravel in these channel types suggest that gravel particles are supply-limited (sensu Bravo-Espinosa et al. 2003) and only persist in local zones of reduced unit stream power. Char spawning typically occurs on lateral bar gravel deposits, pocket gravels above or below obstructions, and in side channels.

The forced pool–riffle reaches of the SF Skokomish River in the southern Olympic Mountains are moderate-gradient, cobble-bed channels with pools forced by LWD or boulders. These reaches are laterally active with side channels and occasional braids, which build coarse-grained floodplains and erode into glacial–fluvial terrace deposits. The supply of gravel-sized particles is from highly episodic mass wasting and terrace erosion. Transient gravel patches overlying an armoured cobble and boulder bed suggest that gravel particles are supply-limited in these reaches with abundant stream power (sensu Bravo-Espinosa et al. 2003). Char spawning typically occurs on lateral bar gravel deposits or pocket gravels above or below obstructions.

Hydrology of study reaches

In the Cedar and Rex rivers, hydrologic data are available from existing US Geological Survey (USGS) stream gages within the study reaches. In the NF Skykomish and SF Skokomish catchments, existing USGS gages were more than 30 km downstream. Therefore, automatic stage recorders were installed along study reaches with adequate local-scale (1–10 m) and reach-scale (~100 m) geomorphic control (Goblin Creek (NF Skykomish) and SF Skokomish River above Church Creek). Stage-discharge rating curves were developed for each gage according to standard techniques (Rantz 1982).

At USGS gages (Cedar and Rex rivers), the frequency or recurrence interval (RI) of annual peak discharge magnitudes was calculated from gage records in Sumioka et al. (1998). At non-USGS gages, the event frequency was estimated from regional regression equations using basin area and basin mean annual precipitation developed by Sumioka et al. (1998). Flood frequency regression data at non-USGS gages had standard error of prediction of ±50%. Therefore, flood frequency values at downstream USGS gages were used to validate estimates at non-USGS gages upstream.

Bedload scour and fill measurements

Sliding-ball scour monitors were used to measure scour and fill. They consisted of durable perforated-plastic golf balls, 4 cm in diameter, strung on 3 mm stainless steel cable, attached to an anchor, and inserted into the streambed (Schuett-Hames et al. 1999; DeVries 2000). Scour and fill depths were measured at 4 cm intervals, with an estimated error of ±2.5 cm, which is slightly larger than that reported by DeVries (2000) due to an uneven heterogeneous bed. Scour and fill depths were measured both incrementally (i.e., from individual floods) and cumulatively (from multiple flood events). The cumulative maximum scour or fill depth for the incubation season is defined as the maximum extent of scour or fill over the period regardless of smaller, intermediate cycles of scour and fill. In minor flood situations where scour was less than the distance to the first scour monitor ball, only net scour or fill could be measured.

Ninety-six scour monitors were installed in the three main catchments (Table 1). Fifty-five monitors were located adjacent to selected bull char redd sites and 41 were located at nonselected sites (see local site selection below). Reference points on all scour monitors were surveyed into local benchmarks to determine their relative elevation and bed elevations after each event. Thirty-four permanent elevational transects were (re)surveyed at scour monitor locations to document net cross-sectional channel change and the stability of scour monitors following distinct flood events. All sites were monitored over two water years (WY) and incubation seasons: WY 2001 and WY 2002. Sites on the Cedar and Rex rivers also were monitored into WY 2003 and WY 2004 to include a wider range of temporal variation in flood magnitude at these sites.

Local site selection

Scour monitors were installed during late summer 2000 and 2001 prior to spawning to avoid disturbing adults or eggs. A grid pattern of scour monitors (Schuett-Hames et al. 1999) was not used because of the unsuitability of much of the coarse substrate for spawning and the low density of bull char spawning activity. Scour monitor and transect installation locations were chosen according to qualitative assessment of potential char spawning sites (based on depth, velocity, substrate, cover, habitat unit) and local advice from fisheries biologists on recent past (1–2 years) spawning locations. Scour data from only one monitor per spawning patch was used in the analysis.

After fall spawning, scour monitor sites were classified as either selected (S) by bull char or nonselected (NS). Scour data were discarded under the rare instance that monitors were disturbed by spawning fish ($n = 3$). Sites designated as selected were within 2 m of the redd pit within the same homogenous substrate patch, under the assumption that scour processes were similar between the redd and adjacent bed (Rennie and Millar 2000). Nonselected sites were typically not representative of high quality bull char spawning sites based on habitat-preference data (i.e., depth, velocity, substrate size, distance to wetted edge, distance to cover, temperature, vertical hydraulic gradient) collected during spawning conditions and reported in Shellberg (2002). However, nonselected sites were generally suitable for salmonid spawning as many had been locations of redds by other salmonids in other years (e.g., *Oncorhynchus kisutch*, personal observation by J. Shellberg). Nevertheless, nonselected sites did not represent the full range of habitat conditions throughout a spawning reach (which were not systematically sampled), but were biased toward sites assessed a priori to have a higher probability of spawning.

The site-selection parameters used are distance to wetted edge and proximity to cover (hydraulic obstructions), both normalized by wetted width. These variables were chosen because of their relation to the main hypothesis that scour is reduced by the availability and selection of stable refugia habitat provided by channel margins or in-channel obstruc-

tions. Owing to a lack of systematic sampling of reach habitat conditions, distances to cover and wetted edge were normalized to channel dimensions.

All scour monitor sites (selected and nonselected) were classified by hydraulic habitat unit type (Barta et al. 1994). Based on observations at all stages, hydraulic habitat units were classified as either (*i*) gravel pockets upstream of obstructions, (*ii*) gravel pockets downstream of obstructions, (*iii*) lateral bars, (*iv*) straight bars (riffle crests and riffles), or (*v*) side channels. Obstructions consisted of single large wood pieces, LWD jams, or large boulders (>1024 mm). Neither scour monitors nor redds were located immediately under or around obstructions where much localized vortex scour typically occurs. All five hydraulic habitats were not always present in each channel type.

Channel hydraulics

At specific scour monitor sites and longitudinally up- and down-stream, Velcro crest gages (DeVries 2000) were established along channel margins to determine maximum stage heights and water surface slopes. Continuous stage data were established for each crest gage from their relationships with nearby continuous stream gages. Water surface slopes were measured for discharge events at a local scale (12 m centered on cross section) and a reach scale (120 m).

Total boundary shear stress, τ_0 ($N \cdot m^{-2}$), was estimated at each scour monitor site using the depth–slope product:

$$(1) \qquad \tau_0 = \rho_w g d S$$

where ρ_w is the fluid density ($kg \cdot m^{-3}$), g is the acceleration of gravity ($m \cdot s^{-2}$), d is the local flow depth (m), and S is the local water surface slope ($m \cdot m^{-1}$). Equation 1 assumes a steady uniform flow, a flow depth equal to the hydraulic radius in a wide, rectangular channel, and a water surface slope equal to the friction slope (Henderson 1966). Local water surface gradient was used as the appropriate gradient to estimate shear stress (Zimmermann and Church 2001).

In mountainous or forested channels, actual or effective bed shear stress can be reduced by momentum and energy losses due to obstructions, bed forms, bank friction, channel bends, and channel width changes (Buffington and Montgomery 1999*a*). Initial attempts were made to estimate local effective bed shear stress during flood events using vertical velocity profiles (e.g., Wilcock 1996); however, snow and road closures hampered access during all but a few flood events. Furthermore, total shear stress estimates were not partitioned mathematically because of the lack of supporting data in highly complex mountain channels. Thus, analyses of the driving forces of sediment transport were restricted to total shear stress and flood magnitude–frequency.

Total shear stress measurements were nondimensionalized for comparison by using the Shields' equation:

$$(2) \qquad \tau^* = \frac{\tau_0}{D_{50}(\rho_s - \rho_w)g}$$

where τ^* is the dimensionless Shields' parameter, τ_0 is the total boundary shear stress ($N \cdot m^{-2}$), ρ_s and ρ_w are the sediment and fluid densities ($kg \cdot m^{-3}$), g is the acceleration of gravity ($m \cdot s^{-2}$), and D_{50} is the median bed-surface grain size (m) (Henderson 1966). Substrate size distributions in selected and nonselected spawning patches were measured during low discharge periods. Pebble counts consisted of at least 100 particles located entirely in local, relatively homogenous substrate patches (Kondolf 1997), excluding within-patch areas disturbed by spawning.

Statistical analysis

Differences in cumulative maximum scour depths between hydraulic habitat units were analyzed using the nonparametric Kruskal–Wallis (KW) one-way analysis of variance because of small sample sizes, unequal variances, and non-normality. The χ^2 distribution was used instead of the Kruskal–Wallis H distribution because of the differing sample sizes (Zar 1999). Differences in scour depth between habitat types were assessed within the selected and nonselected groups but were not compared between groups (selected vs. nonselected) because of the varying representativeness of nonselected sites. The KW test was also used to compare normalized distance to wetted edge distributions with a uniform distribution, representing no selection preference. Linear regression t tests were used to determine whether regression slopes were significantly different from zero. All statistical results were considered to be significant at $\alpha \leq 0.05$.

Results

Hydrology

Bedload scour and egg mortality within salmonid redds are highly dependent on the probability of peak flood events occurring during the incubation period (October to March). Shellberg (2002) and Gibbins et al. (2008) provide an assessment of discharge regimes in regional bull char catchments and determine the inherent probabilities of flooding during incubation. From their analysis, catchments dominated by rain or rain-on-snow peak flood events such as the SF Skokomish River have a high probability of peak discharges occurring during the incubation period of bull char. Catchments at a slightly higher elevation such as the upper Cedar and Skykomish rivers have a moderate probability of peak discharges occurring during this period because of the influence of seasonal snow packs. The timing of different flood events and their different flood-producing mechanisms (rain, rain-on-snow, snowmelt) are evident in the study area hydrographs (Fig. 1).

During the study period, WY 2001 was one of the driest winters on record, with peak discharges at or less than the 1-year recurrence interval (RI) in all study catchments. In contrast, WY 2002 had normal precipitation and discharge, and WYs 2003 and 2004 experienced above-average precipitation and peak discharge (Fig. 1).

Local bedload scour at redd sites

During the WY 2001 drought (Fig. 1), minimal bedload transport at all selected (S) and nonselected (NS) scour monitor sites resulted in shallow scour depths (<5 cm), lack of channel change, and high survival to emergence of char (e.g., Stutsman and Ogg 2002). After additional spawning site selection during the WY 2002 char spawning season, sites selected by bull char during both WY 2001 and WY 2002 were combined as one data set for analysis because of

Fig. 1. Instantaneous discharge ($m^3 \cdot s^{-1}$) during study period: (*a*) Cedar River (USGS 12115000), (*b*) Rex River (USGS 12115500), (*c*) Goblin Creek (North Fork Skykomish), (*d*) Skykomish River (USGS 12134500), (*e*) South Fork Skokomish above Church Creek, (*f*) South Fork Skokomish (USGS 12060500). Note that the *x* and *y* axes have different scales for different gage sites. RI, flood recurrence interval (years).

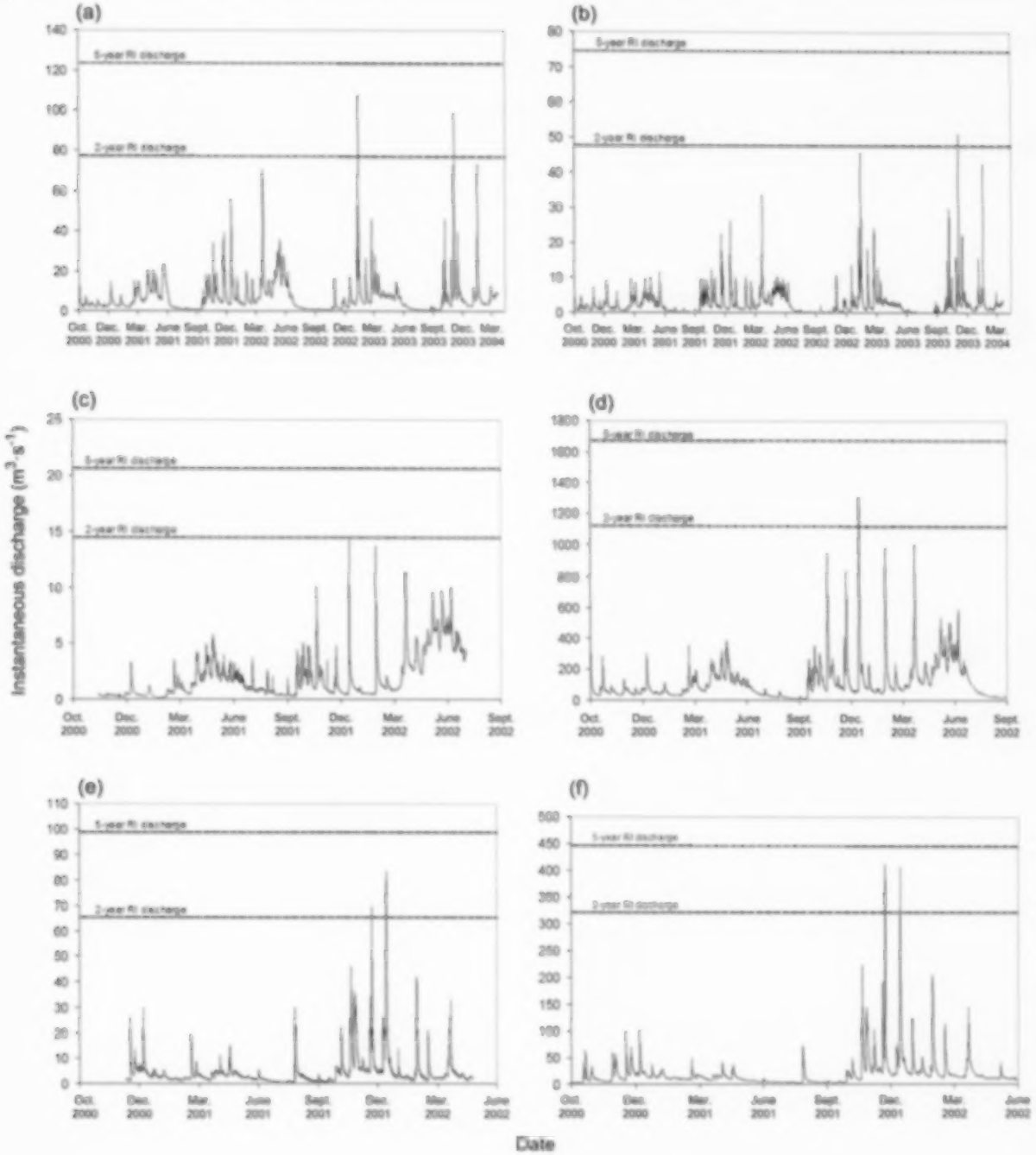

the low number of selected sites for any given year and the unchanged bed morphology from the previous year.

NF Skykomish River

Three flood events (14 November 2001, 7 January 2002, and 22 February 2002) occurred during WY 2002 (Figs. 1*c*–*d*), which had RIs ranging from approximately 1 to 3 years. The cumulative maximum scour depth for the entire WY 2002 winter egg incubation period (October to March) was significantly different between hydraulic habitat units selected (KW $p \leq 0.03$) and not selected (KW $p \leq 0.02$) by bull char (Fig. 2*a*). Among selected sites, lateral bars experienced the greatest scour depths (>10–15 cm) at or beyond cited egg burial depths (DeVries 1997). Sites downstream of obstructions such as LWD and boulders had moderate amounts of scour (generally <10 cm), whereas selected side-channel spawning sites were stable with a tendency toward fill. These results support the hypothesis that specific hydraulic habitat units such as side channels and units near obstructions can provide incubation environments with reduced scour.

SF Skokomish River

Cumulative maximum scour depths during WY 2002 were dominated by events on 16 December 2001 and 7 January 2002, which were both between the 2- and 4-year RI. Scour depths at many selected and nonselected sites were at or well beyond the 10–15 cm cited egg burial depths (Fig. 2*b*), indicating that substantial egg loss could result at these discharge magnitudes, as supported by Stutsman and Ogg (2002). Selected sites upstream of LWD obstructions experienced significantly less scour (KW $p \leq 0.02$), as these sites continued to be deposition zones for locally eroded gravel. Sites downstream of obstructions were initially stable in December 2002, but eventually scoured during the observed mobility of modest diameter LWD. Although these results partially support the hypothesis that obstructions can provide incubation environments with reduced scour, they also demonstrate that site-specific discharge thresholds exist at which in-channel obstructions can become mobilized (especially modest-sized LWD), ending their role as energy and scour reducers.

Upper Cedar River

Scour and channel change were monitored for two additional years in the Cedar and Rex rivers (WYs 2003 and 2004), providing additional data for the relationship between scour depth and flood recurrence interval. Cumulative maximum scour depths during both WY 2001 and WY 2002 were shallower than cited egg burial depths except for a few extremes (Fig. 3). Cumulative maximum scour during WY 2002 was dominated by one flood event on 14 April 2002 (Cedar River, 1.8-year RI; Rex River, 1.3-year RI), when slight fill was just as common as scour and a majority of the bed was not mobilized. During WYs 2001 and 2002, abundant production of bull char was determined from qualitative observations of juveniles (J.G. Shellberg and local biologists' personal observations). Each year from 2001 to 2004 generally had progressively higher peak discharge magnitudes (Figs. 1*a* and 1*b*) resulting in progressively deeper scour depths at or beyond the 10–15 cm egg burial range during WY 2004 (Fig. 3). However, this deep scour (>15 cm; Fig. 3) was only common during 2004, which had the highest flood durations above the 1.5-year RI during the study (see below). Data from 2001–2003 support the bed scour hypothesis that vertical refugia may exist below 2-D_{50} during common flood events in partially transport-limited, pool–riffle channel types with abundant gravel and local gravel armour layers.

Fig. 2. Cumulative maximum scour or fill depth at (*a*) North Fork Skykomish River and Goblin Creek during WY 2002 (maximum 2.0 - to 2.7-year flood recurrence interval (RI)), and (*b*) South Fork Skokomish River during WY 2002 (maximum 3.8-year RI). Negative values represent cumulative fill. *N*, sample size; S, selected (darker shaded boxes); NS, nonselected (lighter shaded boxes).

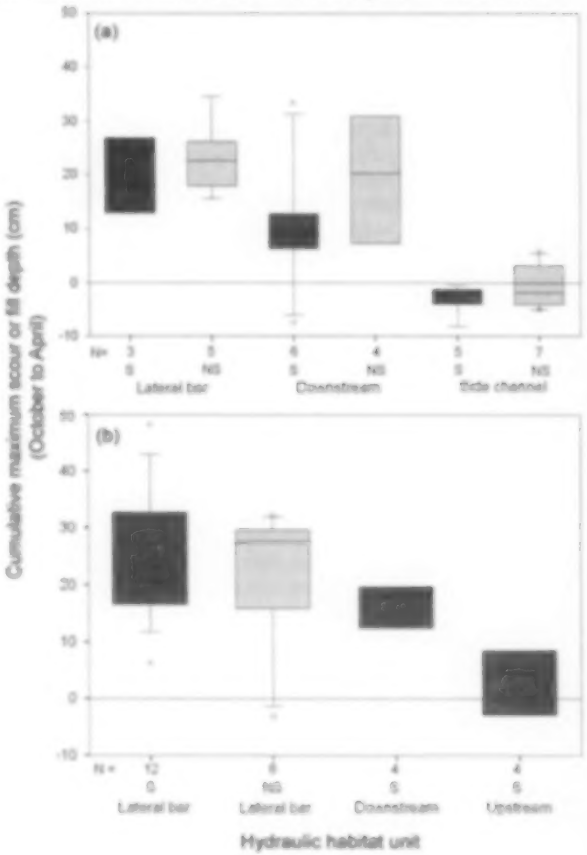

Shear stress at scour monitor sites

In the NF Skykomish catchment, scour depth data at side-channel, downstream, and lateral bar habitat units were correlated as one group against estimates of total bed shear stress from the depth–slope product during the largest flood event in WY 2002 (7 January 2002) (Fig. 4). Although the above habitat units were characterized by systematically different local shear stresses, the units were situated on an increasing gradient of exposure to shear stress, as supported by local velocity profiles in Shellberg (2002). Therefore, they were analyzed together to develop a common relation-

Fig. 3. Cumulative maximum scour depth at the Cedar and Rex rivers along straight bars (riffle crests and riffles) during WY 2001 to WY 2004. *N*, sample size; RI, flood recurrence interval (years); S, selected (darker shaded boxes); NS, nonselected (lighter shaded boxes).

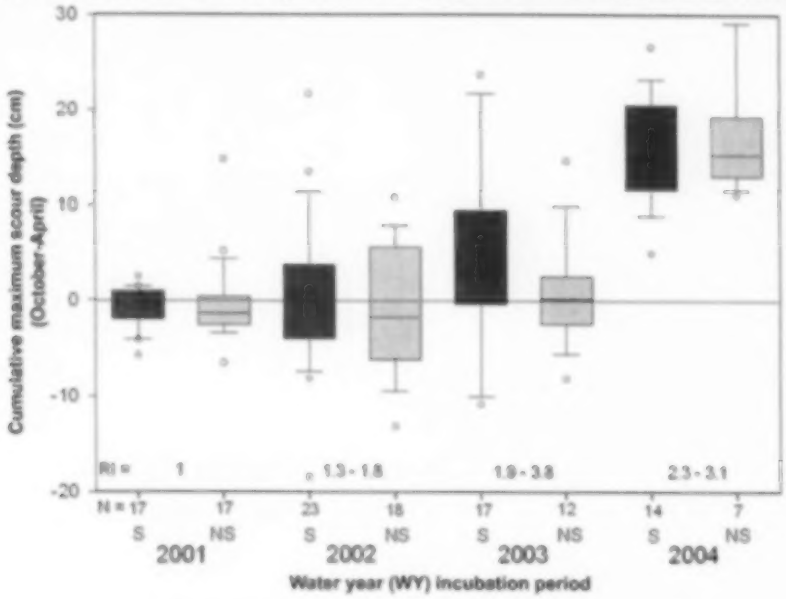
Cumulative maximum scour depth (cm) (October-April)
30
20
10
0
-10
-20
RI = 1 1.3 - 1.8 1.9 - 3.8 2.3 - 3.1
N = 17 17 23 18 17 12 14 7
S NS S NS S NS S NS
2001 2002 2003 2004
Water year (WY) incubation period

Fig. 4. North Fork Skykomish River and Goblin Creek scour depth (scaled to D_{50}) vs. total dimensionless shear stress during the largest flood event during WY 2002 (2.0- to 2.7-year flood recurrence interval). Lateral bar (open squares), side channel (plus signs), downstream (open diamonds).

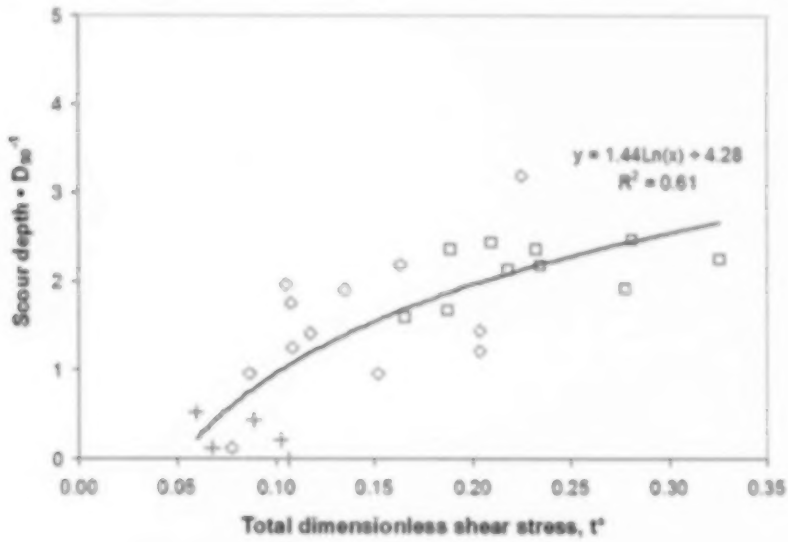

ship between shear stress and scour depth (Fig. 4). Overall, the surface of lateral bars had the highest total shear stress estimates and experienced the deepest scour, but deep scour beyond 2.5-D_{50} was uncommon. The best-fit logarithmic trend suggests an asymptotic trend with a limit on potential scour depth; however, this needs to be confirmed by sampling scour over a larger range of discharges and shear stresses than observed in this study. According to these total shear stress estimates, the initiation of scour (motion) began at a dimensionless shear stress value of ~0.05, similar to values reported elsewhere (Buffington and Montgomery 1997).

In contrast with the NF Skokomish, the relationship between shear stress and scour depth in the SF Skykomish varied between habitat types because of large differences in local depth and slope and presumably differences in energy dissipation (Fig. 5); therefore, units were analyzed separately. In all habitat units, scour depth (scaled to D_{50}) increased significantly with dimensionless shear stress, but

Fig. 5. South Fork Skokomish River scour depth (scaled to D_{84}) vs. total dimensionless shear stress during the largest flood event during WY 2002 (3.8-year flood recurrence interval). Lateral bar (open squares), upstream (asterisks), downstream (open diamonds).

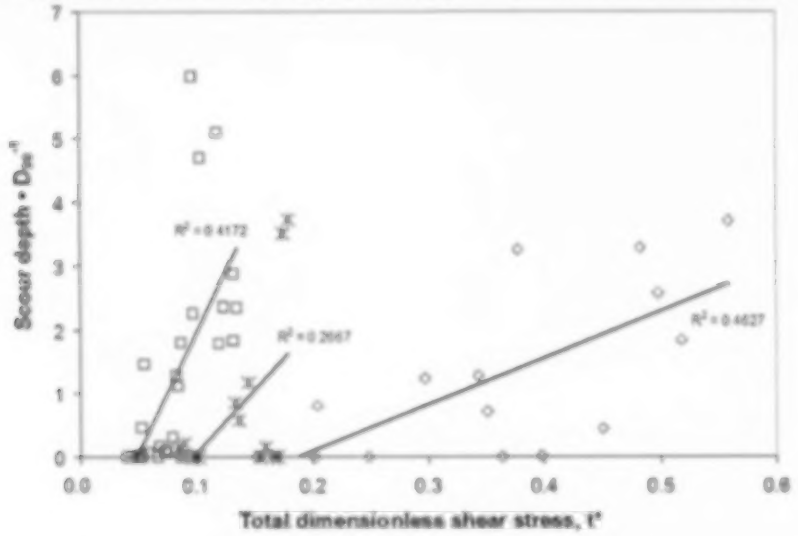

the rate of increase varied among different hydraulic habitat units. Lateral bar sites with relatively little structural energy dissipation had total dimensionless shear stresses closest to the presumed local effective stress (i.e., initiation of scour at ~0.05) (Fig. 5). Scour at sites upstream and downstream of obstructions began at higher dimensionless boundary shear stresses of ~0.1 and 0.2, respectively, indicating that actual effective shear stresses were greatly reduced by energy dissipation around these structures and (or) that the local depth–slope product greatly overestimated total shear stress in these locales.

In the upper Cedar River reaches, cumulative maximum scour depth increased ($r^2 = 0.21$, $p < 0.0001$) with increasing total dimensionless shear stress estimated for the largest flood event of each year (Fig. 6). The initiation of scour (motion) also began at dimensionless shear stress values near ~0.05, which was likely due to the dearth of obstructions influencing energy loss in these pool–riffle channel types. However, the variability in the relationship between scour and shear stress was considerable due to the tendency for both scour and fill in these channel types, plus the lack of more precise data on local sediment supply imbalances and local effective shear stress.

Despite the lack of local effective shear stress measurements, total shear stress measurements applied locally in these different channel types and hydraulic habitat units demonstrate that both shear stress and scour are reduced in spawning gravels near in-channel obstructions and in side channels. These habitats provide scour refugia for incubating bull char embryos according to the main hypothesis. Data from the pool–riffle channels of the upper Cedar River highlight that other factors beyond obstructions can influence shear stress and resultant scour and fill, e.g., alternating bedforms (pools and riffles) and storage of abundant gravel.

Reach-scale bed mobility

In the NF Skykomish catchment, data from elevational transects before and after floods confirmed that the framework structure of the channel bed (i.e., large interlocked cobbles and boulders) was stable during common flood events (<3-year RI). Annual net change in cross-sectional area ranged from –1.3% to 4.4% (median of 1.1%, $n = 6$) (positive values indicate degradation). However, local exposed and unprotected gravels in lateral bars were mobile and experienced scour (Fig. 2*a*), indicating a different threshold of mobility for habitat units with contrasting particle sizes (e.g., Gintz et al. 1996; Zimmermann and Church 2001).

The transects of the Cedar and Rex rivers also were generally stable in their morphology during four years of monitoring, despite patchy local scour and fill in spawning riffles (Fig. 3). During WY 2002, net annual change in channel cross-sectional area ranged from –2.3% to 8.6% (median of 0.5%, $n = 11$). From WY 2003 to WY 2006, cumulative net change in channel cross-sectional area increased (range, –9.6% to 14.8%), but the median value remained low (–0.3%, $n = 11$). Local gravel armor layers were only breached during events greater than the 2-year RI. It remains unknown whether larger discharges (i.e., >4.0-year RI) would produce even greater channel change and scour depths, or whether this relationship would break down because of the difficulty of shearing abundant gravel to great depths in pool–riffle channel types (DeVries 2000, 2008).

In contrast to other catchments, the SF Skokomish transects showed considerable reach-scale bed mobility. Above Church Creek, temporary sediment transport imbalances were associated with eroding terrace deposits at cut banks. Initial aggraded material (sand, gravel, cobble, LWD) was stable and attractive to spawning bull char in an otherwise course cobble-bedded reach. Spawning gravels were partially unstable during the first few floods of the year (1- to 2-year RI), when the change in cross-sectional area ranged from –2.7% to 7.4% (median, 1.9%; $n = 5$). These gravels were later exported during larger events (3.8-year RI), re-

Fig. 6. Cedar and Rex rivers cumulative maximum scour depth (scaled to D_{50}) vs. total dimensionless shear stress at straight bars (riffle crests and riffles) during the largest flood event of each year from WY 2001 to WY 2004 (maximum 3.8-year flood recurrence interval).

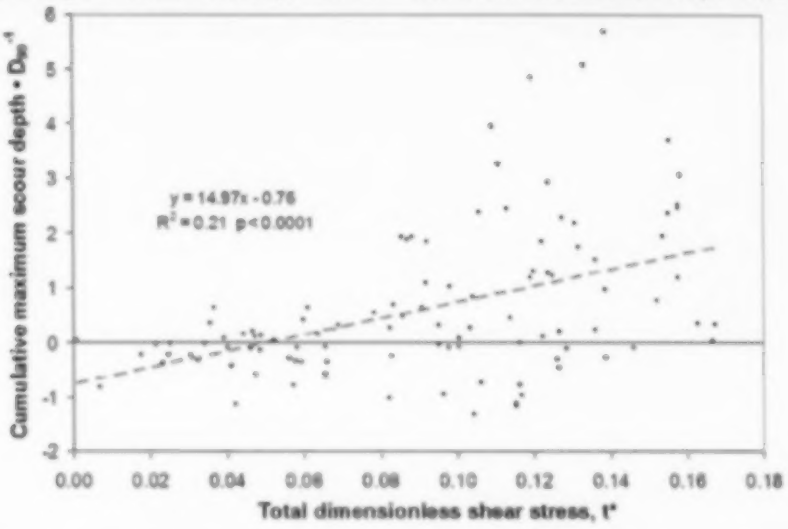

sulting in scour (Fig. 2*b*) and net increases in cross-sectional area (range, –16.6% to 19.3%; median, 6.0%; $n = 5$). Newly recruited sediment from terrace deposits re-initiated the cycle of bed aggradation and degradation. Below Church Creek, additional coarse and fine sediment was delivered from both upstream terrace cut bank erosion and anthropogenically enhanced erosion of landslide material (e.g., Church Creek). This reach adjusted more frequently to its imposed sediment supply, resulting in initial scour at or beyond the cited egg burial depths (Fig. 2*b*), which was later followed by massive aggradation and decreases in net cross-sectional area (range, –15.0% to –69.6%; median, –58.0%; $n = 5$).

These channel change data suggest that hydrogeomorphic conditions beyond local in-channel obstructions or egg burial depth can influence embryo vulnerability to scour and fill, specifically the stochastic supply, storage, and transport of sand and gravel bed material. Thus, local refugia at the reach scale may be inadequate for scour protection in isolation, and channel segment or subcatchment scale refugia may play an important role.

Redd site selection and scour refugia

Redd distances to wetted edge, normalized by wetted width, were typically less than 0.30 for both the NF Skykomish and upper Cedar sites, suggesting that fish generally avoided the center 40% of these channels. However, selected sites did not have distributions significantly different from a uniform distribution (NF Skykomish, KW $p > 0.5$; upper Cedar, KW $p < 0.12$), indicating that any width selection preference was slight. In contrast, the SF Skokomish had normalized distances to wetted edge values less than 0.10. Selected sites differed significantly (KW $p < 0.0001$) from a uniform distribution, suggesting a strong selection preference for channel margins. However, avoidance of deep thalwegs in the SF Skokomish also was partially influenced by limited gravel availability in these areas.

Redd distance to cover was largest in the pool–riffle reaches of the upper Cedar River (median, 12.2 m; range, 1.2–21.3 m), where the forced pool–riffle channels of the NF Skykomish (median, 2.9 m; range, 1.8–5.5 m) and SF Skokomish (median, 5.5 m, range 2.3–8.8 m) had lower values. In comparison to available habitat, values normalized to wetted width were lowest in the SF Skokomish (median, 0.21; range, 0.16–0.49), intermediate in the NF Skykomish (median, 0.55; range, 0.07–0.70), and highest in the upper Cedar River (median, 0.62; range, 0.10 –1.09).

Site selection in proximity to potential scour refugia (channel margins or obstructions) was most pronounced in the SF Skokomish River, less pronounced in the NF Skykomish, and relatively absent in the pool–riffle reaches of the upper Cedar River. It is interesting to note that the scour sites and reaches in the SF Skokomish in the Olympic Mountains had the deepest scour depths, the greatest degree of reach-scale bed mobility, and the most inhospitable discharge regime (Figs. 1*e*, 1*f*; Gibbins et al. 2008), supporting the hypothesis that bull char were actively selecting spawning sites to avoid redd scour.

Flood discharge and scour

The three catchments and channel types had median scour depths at or beyond the cited egg burial depths (10–15 cm) during 2- to 4-year RI events, suggesting that bull char redds are indeed vulnerable to scour during common flood events. When grouping scour data for all study sites, positive trends existed for increasing scour or median scour with increasing RI, respectively ($r^2 = 0.20$, $p < 0.0001$; $r^2 = 0.70$, $p < 0.0001$) (Fig. 7*a*). However, the distribution of local scour depths differed at the hydraulic habitat unit scale and between channel types (Figs. 2–6), presumably due to variations in local shear stress and sediment supply. The exception of increasing median scour with increasing RI was the Cedar River, where the largest flow magnitude during WY 2003 (3.8-year RI) was higher than during WY

Fig. 7. (*a*) Scour depth (cm) versus flood recurrence interval (RI) for all study sites. Shaded broken line represents raw data trend (R^2 = 0.20; $p < 0.0001$; $y = 5.37x - 4.06$). Black continuous line represents median data trend ($R^2 = 0.70$; $p < 0.0001$; $y = 5.81x - 5.70$). (*b*) Scour depth (cm) versus flood duration (hours) > 1.5-year recurrence interval (RI) for all study sites. Shaded broken line represents raw data trend ($R^2 = 0.21$; $p < 0.0001$; $y = 0.40x + 1.94$). Black continuous line represents median data trend ($R^2 = 0.86$; $p < 0.0001$; $y = 0.47x + 0.13$). Small shaded rectangles represent all raw data from all catchments; solid symbols represent median values: triangles, Cedar River; circles, Rex River; diamonds, North Fork Skykomish; squares, South Fork Skokomish.

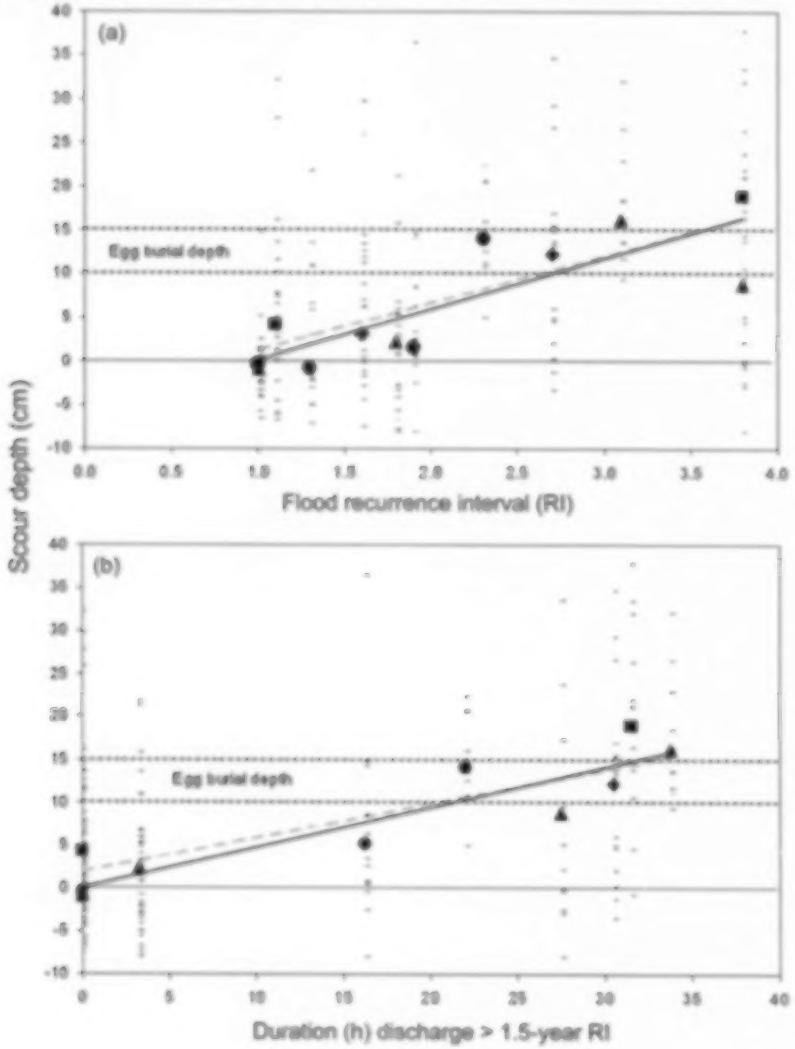

2004 (3.1-year RI) (Fig. 1*a*), whereas the opposite was true for scour depths. However, the total time duration that discharge exceeded the 1.5-year RI was greater in 2004 than in 2003. Positive trends also existed between scour or median scour and flood duration ($r^2 = 0.21$, $p < 0.0001$, and $r^2 = 0.86$, $p < 0.0001$, respectively) (Fig. 7*b*). Although total flood duration greater than the 1.5-year RI is intuitively a more meaningful hydrologic metric to relate to net scour over an entire water year (rather than one peak flood RI value), the correlation with scour only improved slightly, partially due to the positive correlation between annual peak RI and total flood duration ($r^2 = 0.73$).

Discussion

The results show that fall-spawned bull char redds are indeed vulnerable to bedload disturbance and scour in rain or rain-on-snow dominated catchments in western Washington during relatively common flood events (2- to 4-year RI). However, redd scour is dependent on many site-specific hydrogeomorphic factors that vary between different catchments, channel types, habitat units, and discharge and sediment regimes. In support of the main hypothesis, bull char did select sites that provided reduced bedload scour such as local sites near LWD and boulders or in side chan-

nels created by complex fluvial processes at the reach scale. In addition, egg burial depth below gravel armour layers and typical scour depths appeared to be a viable refuge strategy during common flood events in pool–riffle channel types with few in-channel obstructions. Certain catchment discharge regimes (i.e., winter rain or rain-on-snow dominated), sediment supply regimes (i.e., enhanced mass wasting), reach-scale channel types (i.e., supply-limited reaches), and habitat units (i.e., unprotected gravel patches) appear to be high-risk areas for bull char spawning.

Influence of reach type and local habitat type

Reach-scale channel type and morphology strongly influenced the type, availability, and stability of local spawning gravel, as suggested by Montgomery et al. (1999) and Buffington et al. (2004). Gravel deposits were more transient in supply-limited reaches (forced pool–riffle and forced step–pool in this study) compared with partially transport-limited reaches (pool–riffle). Forced pool–riffle reaches influenced by locally high but transient gravel supply and reduced wood loads from altered riparian zones had more mobile channel beds than reaches with modest sediment supplies and abundant large wood. Gravel deposits associated with energy dissipating structures (LWD or boulders) experienced reduced scour magnitudes, as suggested by Kondolf et al. (1991) and Barta et al. (1994). In pool–riffle reaches, abundant gravel and local gravel armor layers partially mitigated against deep scour (>15 cm) beyond egg burial depth (e.g., DeVries 2000, 2002, 2008), implying that other mechanisms besides in-channel obstructions also can provide refugia from egg scour. Quantitative data in the NF Skykomish and qualitative data in the upper Cedar and SF Skokomish catchments indicate that side channels were the most stable spawning areas utilized by bull char due to dampened stream power across complex floodplain habitat.

Site selection

Bull char spawning site selection indicated a slight to strong preference toward channel margins. Elevational transect and scour data demonstrated that gravel patches along channel center lines and thalwegs were less stable than channel margin areas, especially in compound cross sections, similar to the findings of other studies (Lapointe et al. 2000; Ames and Beecher 2001; Haschenburger 2006). Ames and Beecher (2001) have labeled the relatively scour-free channel margin areas "flood protection zones" (FPZ) because of the high relative survival of salmonid eggs and alevins in these areas. However, in higher gradient channel types, it remains unclear whether spawning site selection is a result of increased spawning gravel availability along channel margins in otherwise coarse channels or selective pressures to avoid sediment transport (scour) along the channel center line during predictable floods (i.e., SF Skokomish). Regardless, there are significant mortality trade-offs between spawning high in a cross section near the channel edge to avoid bedload scour and spawning low in a cross section near the thalweg to avoid redd dewatering or sedimentation (Den Boer 1968; Ames and Beecher 2001; Gibbins et al. 2008).

Successful spawning in pool–riffle reaches with few in-channel obstructions indicates that selection of hydraulic cover is not essential in channel types with generally low scour depths. However, site selection near local cover that provides hydraulic shelter (LWD, boulders) or in reach-scale side channels may enhance the protection of bull char offspring from deep scour, especially in channel types with higher stream power. Where suitable hydraulic complexity exists at the reach scale, it is hypothesized that the wide site selection proclivities of bull char should result in at least some redds being constructed in areas protected from scour during large floods (i.e., risk-spreading at the subpopulation level). Females occasionally construct multiple redds within a reach (J.G. Shellberg, personal observation), which may also be a site-selection risk-spreading technique at the individual level.

Frequency of disturbance

Sediment transport and scour depths generally increased with discharge magnitude and shear stress, similar to other studies (Emmett and Leopold 1965; Carling 1987; Haschenburger 2006), with flood discharge RI and duration accounting for up to 20% of variation in scour depths. In catchments in this study, scour to cited egg burial depths did not typically commence until flood events exceeded the 2-year RI. The frequency of disturbance needed to entrain the entire bedload of these reaches and (re)create complex habitat across the channel and floodplain was greater than the 4-year RI, similar to studies on other regional rivers (e.g., Ham and Church 2000; 5-year RI). Floods larger than these observed magnitudes are needed to deposit well-sorted gravel patches below newly formed LWD jams and other obstructions to provide stable habitat during smaller floods. Even larger floods are needed to reset floodplain habitat mosaics and create side channels important for spawning refugia during common floods (e.g., Wondzell and Swanson 1999; Whited et al. 2007). Adapting the intermediate disturbance hypothesis to habitat heterogeneity rather than species diversity (Richards et al. 2002), channel-changing flood events occurring at an intermediate frequency are important in creating and maintaining complex habitat (e.g., gravel pockets near obstructions and side channels) for aquatic organisms such as bull char.

Shear stress

In addition to flood magnitude and duration, estimates of total boundary shear stress generally improved predictions of scour depth, explaining up to 60% of the variability in scour at some sites. However, other factors such as local effective (grain) shear stress and local sediment supply to specific spawning patches likely explain much of the remaining variability. Future detailed measurements of local hydraulic and velocity conditions (e.g., Wilcock 1996; Crowder and Diplas 2002) should improve local effective shear stress and scour predictions in mountain channel types.

Changes in hydrology and sediment supply

Bull char typically spawn in cold mountain valleys where catchment water, sediment, and LWD production are sensitive to proximal land surface and land use conditions (Church 2002). Building road networks and timber harvesting on potentially unstable slopes can increase the magnitude and frequency of sediment production (e.g., Beschta

1978) and bed mobility in response to altered sediment regimes (e.g., Tripp and Poulin 1986; Madej and Ozaki 1996; Lisle et al. 2000). Changing land cover can also alter water yield (e.g., Harr et al. 1975; Bosch and Hewlett 1982; Harr 1986) and increase the magnitude of common peak flood events (i.e., <1- to 2-year RI up to the 10-year RI) in small- and medium-sized catchments (e.g., Jones and Grant 1996, 2001; Lewis et al. 2001). During this study, scour to cited egg burial depths occurred during these sensitive common peak flood events, as found in other studies (Montgomery et al. 1996; Haschenburger 2006). Changes in event magnitude and frequency could increase the frequency of disturbance of scour in char spawning areas (Tonina et al. 2008), especially if coupled with increased production of transient bed sediment and loss of instream LWD structure.

In this study, the catchments of the NF Skykomish and SF Skokomish above Church Creek remain relatively undisturbed from human activities and produce moderate to low (respectively) numbers of bull char. In contrast, the SF Skokomish River below Church Creek has been affected by the delivery of large amounts of coarse sediment (sand and gravel) from road building and timber harvesting on steep, erodible slopes, resulting in increased bed mobility. Although the upper Cedar River catchment also has been densely roaded and logged, the low-gradient pool–riffle reaches are partially decoupled (sensu Church 2002) from upstream water and sediment supply disturbances. Low stream power, gravel armor layers, and abundant gravel appear to mitigate scour depths in these pool–riffle reaches (e.g., DeVries 2000, 2002, 2008), which support high numbers of bull char. Fine sediment (clay, silt, fine sand) throughput and deposition may be a greater mortality factor in these channel types (DeVries 2008).

From these observations, we hypothesize that anthropogenically increased production of transient bed sediment to supply-limited reaches, especially sand and poorly sorted gravel, increases the frequency of spawning gravel mobility and scour to egg burial depths during relatively common flood events (i.e., 1- to 4-year RI). Bed texture and mobility are sensitive to sediment supply (Buffington and Montgomery 1999*b*; Lisle et al. 2000). Though large sustained influxes of gravel could force changes in channel type, anthropogenically increased bed material supplies more commonly produce episodic fluxes of poorly sorted sediment that is highly transient. In contrast, the well-sorted spawning gravels that salmonids have adapted to in mountain channels are created as gravel lag deposits in preferential deposition zones that are flushed of finer, more mobile sediment over geomorphic time scales. Thus the caliber and quantity of contemporary sediment supply and bed mobility may be good indicators of spawning habitat integrity. Other studies have noted a negative relationship between land use intensity (i.e., riparian harvest and roads disturbance) and char population abundance (Baxter et al. 1999).

Loss of roughness

Reduced LWD hydraulic roughness has been predicted to result in reach-scale bed-surface coarsening and a reduction in both the availability and retention of quality spawning substrate (Buffington and Montgomery 1999*a*; Buffington et al. 2004). Abundant LWD can provide spatial spawning habitat heterogeneity that salmonids actively select for and improve the redd carrying capacity of a reach (Merz 2001), in addition to reducing velocity and shear stress (this study). Bed stability has been shown to decrease following wood removal (Bilby 1984; Smith et al. 1993) and where LWD is undersized and mobile (McHenry et al. 1998; Schuett-Hames et al. 2000; Fox et al. 2002). A loss in the quality, quantity, and diversity of LWD roughness due to riparian logging, instream wood removal, and (or) increased hydrologic flushing may reduce the availability or quality of bull char spawning habitat (Hauer et al. 1999), especially in sediment supply limited reaches with high stream power.

Implications

This study emphasizes the importance of habitat heterogeneity and refugia availability in sustaining salmonid populations at multiple spatial scales: from catchment-scale (10–1000 km) discharge regime heterogeneity and flood disturbance probability, to reach-scale (100–1000 m) channel type complexity, to local-scale (1–10 m) site selection and structural energy dissipation. The distribution and abundance of bull char in western Washington could have been influenced by a loss of complex fluvial spawning habitat (e.g., LWD roughness), especially in streams with limited supplies of quality gravel and harsh discharge regimes during incubation (rain or rain-on-snow dominated). Processes that form complex habitat in association with LWD (Beechie et al. 2000) may partially mitigate against unfavorable discharge regimes, water and sediment yield alterations due to land-use, or future climate change (e.g., Battin et al. 2007).

Acknowledgements

Field support for this project was provided by Carrie Furman, Jeff Bash, Ashley Adams and others, whose company and hard work are greatly appreciated. Local field advice and support by Dwayne Paige, Heidy Barnett, and Bill Belknap (Seattle Public Utilities), Mike Stutsman, Larry Ogg, and Anthony Taiber (US Forest Service), and Curt Kraemer (Washington Department of Fish and Wildlife) were essential for project success. Input from four anonymous reviewers substantially improved the manuscript, as did initial comments from Thomas Quinn and Paul DeVries. The study was funded by the US Forest Service, Pacific Northwest Research Station, and the Washington Fly Fishing Club.

References

Ames, J., and Beecher, H. 2001. Incorporating flood risk into controlled spawning flow regimes for Pacific salmon: an example using the Cedar River sockeye salmon. Washington Department of Fish and Wildlife, Olympia, Wash.

Barta, A.F., Wilcock, P.R., and Shea, C.C.C. 1994. The transport of gravels in boulder-bed streams. *In* Hydraulic Engineering '94. *Edited by* G.V. Controneo and R.R. Rumer. American Society of Civil Engineers, New York. pp. 780–784.

Bathurst, J.C., Graf, W.H., and Cao, H.H. 1983. Initiation of sediment transport in steep channels with coarse bed material. *In* Mechanics of Sediment Transport, Proceedings of Euromech 156 Colloquium, Istanbul, Turkey, 12–14 July 1982. *Edited by* B.M. Sumer and A. Muller. A.A. Balkema (Taylor and Francis), London, UK. pp. 207–213.

Battin, J., Wiley, M.W., Ruckelshaus, M.H., Palmer, R.N., Korb,

E., Bartz, K.K., and Imaki, H. 2007. Projected impacts of climate change on salmon habitat restoration. Proc. Natl. Acad. Sci. U.S.A. **104**(16): 6720–6725. doi:10.1073/pnas.0701685104. PMID:17412830.

Baxter, C.V., Frissell, C., and Hauer, F.R. 1999. Geomorphology, logging roads, and the distribution of bull trout spawning in a forested river basin: implications for management and conservation. Trans. Am. Fish. Soc. **128**(5): 854–867. doi:10.1577/1548-8659(1999)128<0854:GLRATD>2.0.CO;2.

Beechie, T., Pess, G., Kennard, P., Bilby, R., and Bolton, S. 2000. Modeling recovery rates and pathways for woody debris recruitment in northwestern Washington streams. N. Am. J. Fish. Manage. **20**(2): 436–452. doi:10.1577/1548-8675(2000)020<0436:MRRAPF>2.3.CO;2.

Beschta, R.L. 1978. Long-term patterns of sediment production following road construction and logging in the Oregon Coast Range. Water Resour. Res. **14**(6): 1011–1016. doi:10.1029/WR014i006p01011.

Bilby, R.E. 1984. Removal of woody debris may affect stream stability. J. For. **82**: 609–613.

Bosch, J.M., and Hewlett, J.D. 1982. A review of catchment experiments to determine the effect of vegetation changes on water yield and evpotranspiration. J. Hydrol. (Amst.), **55**(1–4): 3–23. doi:10.1016/0022-1694(82)90117-2.

Bravo-Espinosa, M., Osterkamp, W.R., and Lopes, V.L. 2003. Bedload transport in alluvial channels. J. Hydraul. Eng. **129**(10): 783–795. doi:10.1061/(ASCE)0733-9429(2003)129:10(783).

Buffington, J.M., and Montgomery, D.R. 1997. A systematic analysis of eight decades of incipient motion studies, with special reference to gravel-bedded rivers. Water Resour. Res. **33**: 1993–2029.

Buffington, J.M., and Montgomery, D.R. 1999*a*. Effects of hydraulic roughness on surface textures of gravel-bed rivers. Water Resour. Res. **35**(11): 3507–3521. doi:10.1029/1999WR900138.

Buffington, J.M., and Montgomery, D.R. 1999*b*. Effects of sediment supply on surface textures of gravel-bed rivers. Water Resour. Res. **35**(11): 3523–3530. doi:10.1029/1999WR900232.

Buffington, J.M., Montgomery, D.R., and Greenberg, H.M. 2004. Basin-scale availability of salmonid spawning gravel as influenced by channel type and hydraulic roughness in mountain catchments. Can. J. Fish. Aquat. Sci. **61**(11): 2085–2096. doi:10.1139/f04-141.

Carling, P.A. 1987. Bed stability in gravel streams, with reference to stream regulation and ecology. *In* River channels: environment and process. *Edited by* K. Richards. Blackwell, Oxford, UK. pp. 321–347.

Church, M. 2002. Geomorphic thresholds in riverine landscapes. Freshw. Biol. **47**(4): 541–557. doi:10.1046/j.1365-2427.2002.00919.x.

Crowder, D.W., and Diplas, P. 2002. Vorticity and circulation: spatial metrics for evaluating flow complexity in stream habitats. Can. J. Fish. Aquat. Sci. **59**(4): 633–645. doi:10.1139/f02-037.

Den Boer, P.J. 1968. Spreading of risk and stabilization of animal numbers. Acta Biotheor. **18**: 163–194.

DeVries, P. 1997. Riverine salmonid egg burial depths: review of published data and implications for scour studies. Can. J. Fish. Aquat. Sci. **54**(8): 1685–1698. doi:10.1139/cjfas-54-8-1685.

DeVries, P. 2000. Scour in low gradient gravel bed streams: patterns, processes, and implications for the survival of salmonid embryos. Ph.D. dissertation, University of Washington, College of Engineering, Seattle, Wash.

DeVries, P. 2002. Bedload layer thickness and disturbance depth in gravel bed streams. J. Hydraul. Eng. **128**(11): 983–991. doi:10.1061/(ASCE)0733-9429(2002)128:11(983).

DeVries, P. 2008. Bed disturbance processes and the physical mechanisms of scour and fill in salmonid spawning habitat. *In* Salmon spawning habitat in rivers: physical controls, biological responses and approaches to remediation. *Edited by* D. Sear and P. DeVries. AFS Symp. No. 65. pp. 121–147.

Emmett, W.W., and Leopold, L.B. 1965. Downstream pattern of river-bed scour and fill. *In* Proceedings Federal Inter-agency Sedimentation Conference. USDA ARS Misc. Pub. No. 170. pp. 399–408.

Erman, D.C., Andrews, E.D., and Yoder-Williams, M. 1988. Effects of winter floods on fishes in the Sierra Nevada. Can. J. Fish. Aquat. Sci. **45**(12): 2195–2200. doi:10.1139/f88-255.

Fox, M.J., Bolton, S., and Conquest, L. 2002. Reference conditions for instream wood in western Washington. *In* Restoration of Puget Sound rivers. *Edited by* D.R. Montgomery, S. Bolton, D. Booth, and L. Wall. University of Washington Press, Seattle, Wash. pp. 361–393.

Gibbins, C., Shellberg, J., Moir, H., and Soulsby, C. 2008. Hydrological influences on adult salmonid migration, spawning and embryo survival. *In* Salmon spawning habitat in rivers: physical controls, biological responses and approaches to remediation. *Edited by* D. Sear and P. DeVries. AFS Symp. No. 65. pp. 195–223.

Gintz, D., Hassan, M.A., and Schmidt, K.H. 1996. Frequency and magnitude of bedload transport in a mountain river. Earth Surf. Process. Landf. **21**(5): 433–445. doi:10.1002/(SICI)1096-9837(199605)21:5<433::AID-ESP580>3.0.CO;2-P.

Goetz, F.A. 1989. Biology of bull trout, *Salvelinus confluentus*: a literature review. US Department of Agriculture, Forest Service, Willamette National Forest, Eugene, Oregon.

Ham, D.G., and Church, M. 2000. Bed-material transport estimated from channel morphodynamics: Chilliwack River, British Columbia. Earth Surf. Process. Landf. **25**(10): 1123–1142. doi:10.1002/1096-9837(200009)25:10<1123::AID-ESP122>3.0.CO;2-9.

Harr, R.D. 1986. Effects of clearcutting on rain-on-snow runoff in western Oregon: a new look at old studies. Water Resour. Res. **22**(7): 1095–1100. doi:10.1029/WR022i007p01095.

Harr, R.D., Harper, W.C., Krieger, J.T., and Hsieh, F.S. 1975. Changes in storm hydrographs after road building and clear-cutting in the Oregon Coast Range. Water Resour. Res. **11**(3): 436–444. doi:10.1029/WR011i003p00436.

Haschenburger, J.K. 2006. Observations of event-based streambed deformation in a gravel bed channel. Water Resour. Res. **42**(11): W11412. doi:10.1029/2006WR004985.

Hauer, F.R., Poole, G.C., Gangemi, J.T., and Baxter, C.V. 1999. Large woody debris in bull trout (*Salvelinus confluentus*) spawning streams of logged and wilderness watersheds in Northwest Montana. Can. J. Fish. Aquat. Sci. **56**(6): 915–924. doi:10.1139/cjfas-56-6-915.

Henderson, F.M. 1966. Open channel flow. Macmillan, New York.

Johnson, T.H. 1991. Bull trout studies in Washington, 1989. Washington Department of Wildlife, Fisheries Management Division, Port Townsend, Wash.

Jones, J.A., and Grant, G.E. 1996. Peak flow responses to clear-cutting and roads in small and large basins, Western Cascades, Oregon. Water Resour. Res. **32**(4): 959–974. doi:10.1029/95WR03493.

Jones, J.A., and Grant, G.E. 2001. Comment on "Peak flow responses to clear-cutting and roads in small and large basins, Western Cascades, Oregon: a second opinion" by R.B. Thomas and W.F. Megahan. Water Resour. Res. **37**(1): 175–178. doi:10.1029/2000WR900276.

Kondolf, G.M. 1997. Application of the pebble count: notes on purpose, method and variants. J. Am. Water Resour. Assoc. **33**(1): 79–87. doi:10.1111/j.1752-1688.1997.tb04084.x.

Kondolf, G.M., Cada, G.F., Sale, M.J., and Felando, T. 1991. Dis-

tribution and stability of potential salmonid spawning gravels in steep boulder-bed streams of the eastern Sierra Nevada. Trans. Am. Fish. Soc. **120**(2): 177–186. doi:10.1577/1548-8659(1991)120<0177:DASOPS>2.3.CO;2.

Lapointe, M., Eaton, B., Driscoll, S., and Latulippe, C. 2000. Modeling the probability of salmonid egg pocket scour due to floods. Can. J. Fish. Aquat. Sci. **57**(6): 1120–1130. doi:10.1139/cjfas-57-6-1120.

Lewis, J., Mori, S.R., Keppeler, E.T., and Ziemer, R.R. 2001. Impacts of logging on storm peak flows, flow volumes and suspended sediment loads in Casper Creek, California. *In* Land use and watersheds: human influences on hydrology and geomorphology in urban and forest areas. *Edited by* M.S. Wigmosta and S.J. Burges. American Geophysical Union, Water Science and Application No. 2, Washington, D.C. pp. 85–125.

Lisle, T.E., Nelson, J.M., Pitlick, J., Madej, M.A., and Barkett, B.L. 2000. Variability of bed mobility in natural, gravel-bed channels and adjustments to sediment load at local and reach scales. Water Resour. Res. **36**(12): 3743–3755. doi:10.1029/2000WR900238.

Lytle, D.A., and Poff, N.L. 2004. Adaptation to natural flow regimes. Trends Ecol. Evol. **19**(2): 94–100. doi:10.1016/j.tree.2003.10.002. PMID:16701235.

Madej, M.A., and Ozaki, V. 1996. Channel response to sediment wave propagation and movement, Redwood Creek, California, USA. Earth Surf. Process. Landf. **21**(10): 911–927. doi:10.1002/(SICI)1096-9837(199610)21:10<911::AID-ESP621>3.0.CO;2-1.

McHenry, M.L., Shott, E., Conrad, R.H., and Grette, G.B. 1998. Changes in the quantity and characteristics of large woody debris in streams of the Olympic Peninsula, Washington, U.S.A. (1982–1993). Can. J. Fish. Aquat. Sci. **55**(6): 1395–1407. doi:10.1139/cjfas-55-6-1395.

McPhail, J.D., and Murray, C. 1979. The early life history and ecology of Dolly Varden (*Salvelinus malma*) in the Upper Arrow Lakes. Report to B.C. Hydro Power Authority and Kootenay Department of Fish and Wildlife, Vancouver, B.C., by the Department of Zoology, University of British Columbia.

Merz, J.E. 2001. Association of fall-run chinook salmon redds with woody debris in the lower Mokelumne River, California. Calif. Fish Game, **87**: 51–60.

Montgomery, D.R., and Buffington, J.M. 1997. Channel-reach morphology in mountain drainage basins. Geol. Soc. Am. Bull. **109**(5): 596–611. doi:10.1130/0016-7606(1997)109<0596:CRMIMD>2.3.CO;2.

Montgomery, D.R., Buffington, J.M., Peterson, N.P., Schuett-Hames, D., and Quinn, T.P. 1996. Stream-bed scour, egg burial depths, and the influence of salmonid spawning on bed surface mobility and embryo survival. Can. J. Fish. Aquat. Sci. **53**(5): 1061–1070. doi:10.1139/cjfas-53-5-1061.

Montgomery, D.R., Beamer, E.M., Pess, G., and Quinn, T.P. 1999. Channel type and salmonid distribution and abundance. Can. J. Fish. Aquat. Sci. **56**: 377–387. doi:10.1139/cjfas-56-3-377.

Rantz, S.E. 1982. Measurement and computation of streamflow. US Geol. Surv. Water Supply Paper No. 2175, Washington, D.C.

Rennie, C.D., and Millar, R.G. 2000. Spatial variability of stream bed scour and fill: a comparison of scour depth in chum salmon (*Oncorhynchus keta*) redds and adjacent bed. Can. J. Fish. Aquat. Sci. **57**(5): 928–938. doi:10.1139/cjfas-57-5-928.

Richards, K., Brasington, J., and Hughes, F. 2002. Geomorphic dynamics of floodplains: ecological implications and a potential modelling strategy. Freshw. Biol. **47**(4): 559–579. doi:10.1046/j.1365-2427.2002.00920.x.

Schuett-Hames, D., Conrad, R., Pleus, A.E., and Lautz, K. 1999. Salmonid spawning gravel scour survey. NW Indian Fisheries Commission, Timber Fish and Wildlife Report No. TFW-AM9-99-008, Olympia, Wash.

Schuett-Hames, D.E., Peterson, N.P., Conrad, R., and Quinn, T.P. 2000. Patterns of gravel scour and fill after spawning by chum salmon in a western Washington stream. N. Am. J. Fish. Manage. **20**(3): 610–617. doi:10.1577/1548-8675(2000)020<0610:POGSAF>2.3.CO;2.

Sedell, J.R., Reeves, G.H., Hauer, F.R., Stanford, J.A., and Hawkins, C.P. 1990. Role of refugia in recovery from disturbances: modern fragmented and disconnected river systems. Environ. Manage. **14**(5): 711–724. doi:10.1007/BF02394720.

Seegrist, D.W., and Gard, R. 1972. Effects of floods on trout in Sagehen Creek, California. Trans. Am. Fish. Soc. **101**(3): 478–482. doi:10.1577/1548-8659(1972)101<478:EOFOTI>2.0.CO;2.

Shellberg, J.G. 2002. Hydrologic, geomorphic, and biologic influences on redd scour in bull char (*Salvelinus confluentus*) spawning streams. M.S. thesis, University of Washington, College of Forest Resources, Seattle, Wash.

Shepard, B.B., Pratt, K., and Graham, P.J. 1984. The life histories of westslope cutthroat and bull trout in the upper Flathead River Basin, Montana. Montana Department of Fish, Wildlife and Parks, Kalispell, Montana.

Smith, R.D., Sidle, R.C., and Porter, P.E. 1993. Effects on bedload transport of experimental removal of woody debris from a forest gravel-bed stream. Earth Surf. Process. Landf. **18**(5): 455–468. doi:10.1002/esp.3290180507.

Stutsman, M.R., and Ogg, L.W. 2002. Summary report of the Olympic National Forest Bull Trout Recovery Project 1995–2001. USDA Forest Service, Olympic National Forest, Hoodsport, Wash.

Sumioka, S.S., Kresch, D.L., and Kasnick, K.D. 1998. Magnitude and flood frequency in Washington. US Geological Survey, Water Resources Investigations Report No. 97-4277, Tacoma, Wash.

Tonina, D., Luce, C.H., Rieman, B., Buffington, J.M., Goodwin, P., Clayton, S.R., Ali, S.M., Barry, J.J., and Berenbrock, C. 2008. Hydrological response to timber harvest in northern Idaho: implications for channel scour and persistence of salmonids. Hydrol. Process. **22**(17): 3223–3235. doi:10.1002/hyp.6918.

Tripp, D.B., and Poulin, V.A. 1986. The effects of logging and mass wasting on salmonid spawning habitat in streams on the Queen Charlotte Islands. B.C. Ministry of Forest Lands, Land Management Report No. 50, Vancouver, B.C., Canada.

US Fish and Wildlife Service. 1998. Bull trout interim conservation guidance. US Fish and Wildlife Service (USFWS), Lacey, Wash.

Whited, D.C., Lorang, M.S., Harner, M.J., Hauer, F.R., Kimball, J.S., and Stanford, J.A. 2007. Climate, hydrologic disturbance, and succession: drivers of floodplain pattern. Ecology, **88**(4): 940–953. doi:10.1890/05-1149. PMID:17536710.

Wilcock, P.R. 1996. Estimating local bed shear stress from velocity observations. Water Resour. Res. **32**(11): 3361–3366. doi:10.1029/96WR02277.

Wondzell, S.M., and Swanson, F.J. 1999. Floods, channel change, and the hyporheic zone. Water Resour. Res. **35**(2): 555–567. doi:10.1029/1998WR900047.

Zar, J.H. 1999. Biostatistical analysis. 4th ed. Prentice Hall, Upper Saddle River, New Jersey.

Zimmermann, A., and Church, M. 2001. Channel morphology, gradient profiles and bed stresses during flood in a step–pool channel. Geomorphology, **40**(3–4): 311–327. doi:10.1016/S0169-555X(01)00057-5.

Estimating detection probabilities of tagged fish migrating past fixed receiver stations using only local information

Michael C. Melnychuk and Carl J. Walters

Abstract: We developed a method to predict the probability of detecting acoustic tags crossing a receiver station using only detection information at that station. This method is suitable for acoustic or radio telemetry studies in which individually tagged animals migrate past fixed stations (where a station may consist of one or more receivers). It is based on fitting attenuation models to sequences of detections and missed transmissions of individually coded tags in fish migrating past stations of the Pacific Ocean Shelf Tracking Project (POST). We used estimated attenuation model parameters from detected fish at each station to predict the number of fish that crossed the station undetected, which in turn was used to calculate the local detection probability. This estimator was correlated (r = 0.54–0.81 in river and coastal habitats) with mark–recapture estimates of detection probability (p_{mr}) that use nonlocal detection information at stations further along migration routes. This local detection probability estimate can be used as a covariate of p_{mr} in mark–recapture models and can predict approximate values of p_{mr} at final detection stations where p_{mr} is not estimable because of the lack of recaptures further along migration routes.

Résumé : Nous mettons au point une méthode pour prédire la probabilité de détection d'une étiquette acoustique lors du passage près d'une station de réception à l'aide de la seule information détectée à cette station. Cette méthode convient aux études acoustiques et aux travaux de radiotélémétrie dans lesquels des animaux marqués individuellement migrent en passant près de stations fixes (une station peut comporter un ou plusieurs récepteurs). La méthode se base sur un ajustement de modèles d'atténuation à des séquences de détections et de transmissions manquées d'étiquettes codées individuellement portées par des poissons qui migrent près des stations du Projet de surveillance de la plate-forme du Pacifique (POST). Nous utilisons les paramètres estimés du modèle d'atténuation des poissons détectés à chaque station pour prédire le nombre de poissons qui sont passés près de la station sans être détectés, ce qui nous sert alors à calculer la probabilité de détection locale. Cet estimateur est en corrélation (r = 0,54–0,81 dans les habitats des rivières et des côtes) avec les estimations, faites par marquage et recapture, de la probabilité de détection (p_{mr}) à l'aide de renseignements de détection non locaux provenant de stations plus éloignées sur la route de migration. Cette estimation de la probabilité de détection locale peut être utilisée comme covariable de p_{mr} dans les modèles de marquage et de recapture et peut prédire des valeurs approximatives de p_{mr} aux stations de destination finale lorsque p_{mr} ne peut y être estimée à cause du manque de recaptures plus loin sur la route de migration.

[Traduit par la Rédaction]

Introduction

Mark–recapture methods such as Cormack–Jolly–Seber (CJS) models (Cormack 1964; Jolly 1965; Seber 1965) are commonly used to estimate survival rates of fish populations. These methods were developed for repeated, time-based sampling where, at a particular recapture occasion, a tagged animal is either recaptured or not. Survival and recapture probabilities are estimated from these recapture data over several occasions. Similarly, a spatial approach to CJS models is often used for migrating animals, where fish tagged with individually coded transmitters may be detected at successive detection stations (lines or grids of receivers) along migration routes (Burnham et al. 1987). Routes are partitioned into segments between stations, with survival in each segment and detection probability at each station estimated jointly. In some of these spatial approaches, detection data may be limited to whether or not a tag was detected at a particular station, e.g., passive integrated transponder (PIT) tags detected in dam bypass channels. In other spatial approaches, if fish are tagged with radio (Skalski et al. 2001) or acoustic (Welch et al. 2009) tags and pass detection stations, additional information may be available other

Received 5 March 2009. Accepted 11 December 2009. Published on the NRC Research Press Web site at cjfas.nrc.ca on 12 March 2010. J21094

Paper handled by Associate Editor Stephen Smith.

M.C. Melnychuk[1,2] and C.J. Walters. Department of Zoology and Fisheries Centre, University of British Columbia, 2202 Main Mall, Vancouver, BC V6T 1Z4, Canada.

[1]Corresponding author (e-mail: mikem@zoology.ubc.ca).
[2]Present address: School of Aquatic and Fishery Sciences, University of Washington, Box 355020, Seattle, WA 98195-5020, USA.

than simply a binary outcome. Radio and acoustic tag transmissions are often detected multiple times as a tagged fish passes a stationary receiver during its migration or on multiple receivers at a station. Sequential patterns of detections during a crossing event may provide additional information about the probability of detection at a station.

Estimating a mark–recapture detection probability for fish migrating past a station of interest (p_{mr}, the probability of detecting a tagged fish as it crosses a detection station) requires detection data at station(s) further along a migration route. The parameter is estimated as the ratio of the number of fish detected at the line of interest to the estimated number alive and available for detection at the line, the latter derived from detection information after the line of interest. Detection probability at the final detection station along a migration route, and survival to that final station, are confounded in classic CJS models. This presents a problem for many radio or acoustic tracking studies in which survival to the final detection station is often of biological interest, but budgetary or logistical factors limit the number of detection stations that can be deployed. A fixed value can be assumed for the final p_{mr} (Welch et al. 2009), but this could result in substantial bias in the resulting estimate of the final survival probability. Incorporating a covariate as a predictor of p_{mr} (Pollock et al. 1984), however, allows the final station's p_{mr} to be estimated through its relationship with p_{mr} at other stations. Covariates that explain variation in p_{mr} among detection stations can therefore be of great use in survival estimation. Though classic CJS models assume instantaneous sampling occasions with a single opportunity to detect or capture an animal that is alive, telemetry data generally provide several opportunities to detect a tagged animal crossing a station, with a variable probability of detecting transmissions during a crossing event.

Here, we present a method to estimate p_{mr} based on the sequence of detections and known missed tag signals of individual fish that swim past a station. Essentially, we attempt to estimate the proportion of fish not detected while crossing a station from the detection patterns of fish that were detected. Detection probabilities of individual tag transmissions may "attenuate" with increasing tag-to-receiver distance. We fit attenuation models to crossing sequences of individual fish and use estimated model parameters to calculate a local detection probability estimate, p'_{loc}. This estimate uses only information at the detection station of interest, not at stations further along a migration route. Specifically, we consider detection data from migrating juvenile salmon tagged with acoustic tags passing stations of one or more acoustic receivers, but the method could be used for other telemetry systems that log the time when individually coded tags are detected on stationary receivers. We also consider the predictive ability of two other types of local-information detection probability estimates: fitting probability distributions to frequency distributions of the length of crossing sequences, and subsetting data from a multireceiver line. We analyze crossing sequences at stations and estimate p'_{loc} across five habitat types: a large river, small rivers, estuaries, inshore coastal areas, and the outer coast. We compare p'_{loc} with CJS detection probability estimates ($\tilde{p}_{mr}$) at the same detection stations to evaluate the predictive ability of p'_{loc}.

Materials and methods

Tag and tracking technology

Detection data from juvenile coho (*Oncorhynchus kisutch*), steelhead (*Oncorhynchus mykiss*), sockeye (*Oncorhynchus nerka*), and Chinook (*Oncorhynchus tshawytscha*) salmon released in 2004–2006 (9–16 populations each year) under the Pacific Ocean Shelf Tracking Project (POST; www.postcoml.org) were used for this study. Coded acoustic tags (VEMCO V7 or V9; VEMCO Division, AMIRIX Systems Inc., Halifax, Nova Scotia, Canada) were surgically implanted into salmon smolts during their downstream migration (for wild fish) or immediately prior to migrating, at hatcheries. Acoustic receivers (VEMCO VR-2) were deployed at successive stations along migratory routes to detect tagged fish. About half of the tagged populations each year migrated out of the Fraser River, whereas the other half originated from smaller rivers in British Columbia, Canada. In rivers and estuaries, receivers were deployed as single or paired units and, on the ocean seabed, were arranged in transect lines perpendicular to typical migration routes, spaced approximately 700–900 m apart. These tags can typically be detected up to 400–500 m from a fixed station in relatively calm conditions with low levels of background noise (D. Welch, Kintama Research Corp., 10–1850 Northfield Road, Nanaimo, BC V9R 5S5, Canada, unpublished data); this range can be substantially less in suboptimal conditions, especially in rivers (Voegeli et al. 1998; Simpfendorfer et al. 2008). The two tags used differ in acoustic power output (V7 tags, 136 dB re 1 μPa at 1 m; V9 tags, 142 dB), which affects detection range and hence the probability of being detected. On average, tags transmitted a signal every 62 s. As tagged smolts were usually <200 mm long and swim at up to a few body lengths per second (reviewed in Groot and Margolis 1991), a tag generally transmits several signals as the fish crosses a receiver station. The number of signals transmitted within the detection range of a receiver while crossing a station depends on several factors: (*i*) noise levels, bubbles, and suspended matter in the water during the time of crossing, as these affect detection range (as well as the probability of detection within this range); (*ii*) speed of the fish, including assistance by river or tidal currents; (*iii*) chord length of the crossing position, as this varies depending on whether fish pass directly over a receiver or in the gap between two receivers (Welch et al. 2003); and (*iv*) random variation in the intervals between signals during the crossing event. Tags are often programmed with a random interval between signals to minimize the chance of repeated collisions with other tags. By chance, more or fewer signals than average can be transmitted during a crossing event.

Constructing sequences of detections and missed transmissions

Most tags used by POST for juvenile salmon had random uniform intervals of 30–90 s between coded signals. Each signal is a train of 7–8 pulses that takes approximately 2 s to transmit (the intervals between pulses contain the information for unique codes). The time between the start of successive signals therefore ranged from 32 to 92 s, with an average of 62 s. We arranged in chronological order all of

the detections of a given fish at a given station. When a tag was heard more than once at a station, successive detections were often 32–92 s apart, but sometimes several minutes apart, indicating that an unknown number of transmissions was not detected between these times. If >60 min elapsed between successive detections, we parsed the sequence and considered only the first part as a crossing event. For stations with multiple receivers, if a tag was detected simultaneously on two or more receivers, we removed all but one of the simultaneous detections from the list as the interest was in detection sequences for the line as a whole, not for each individual receiver. A sequence of n detections remained.

From the temporal detection sequence, we created a crossing sequence of detected signals (1s) and missed signals (0s). Because tags were programmed with random intervals, it was not possible to determine the exact number of missed signals between recorded detections. The distribution of intervals between signals is uniform, however, so we estimated the number of misses simply by comparing the actual time between successive detections with multiples of the average signal interval (62 s). Beginning with the time of actual first detection (t_1), we constructed a hypothetical sequence of signal times that incremented by the average interval. Whichever hypothetical time was closest to the next actual detection time (t_2), we assigned that time a 1 in the corresponding crossing sequence. We assigned all hypothetical times between the two detections a 0 in the crossing sequence to represent signals not detected. We repeated this algorithm beginning with the next actual detection time (t_2) until the last actual detection time (t_n) was reached. Sequences of 1s and 0s were of length m, containing n detections and $m - n$ misses. Sequence length ranged from 1 (a single detection of a tag crossing a station) to >2000 (where a fish likely stopped in proximity of a station). For estimation purposes, we added a sequence of 50 zeros before and after the main sequence to represent the signals that were not detected as a fish approached and left the station before and after its first and last detection. This choice of 50 zeros was arbitrary but was generally robust to different numbers of zeros considered (e.g., 10 or 100) in terms of parameter and detection probability estimates (pseudocode for constructing crossing sequences is shown in Appendix A).

Several filtering steps were taken to ensure that the local detection probability estimates derived from crossing event data were representative of migrating fish so that they would be comparable to mark–recapture detection probabilities and also to reduce variability in the estimates as a result of variation in tag technology. We only considered V7 or V9 low-power tags with a random interval of 30–90 s between transmitted signals. We only included tag codes for smolts tagged under POST. Some sequences from remaining tags were excluded for the following reasons. (*i*) Detections thought to be false positives were identified in an independent data screening based on the number of detections of a tag at a station, the presence of other tags on the detecting receiver around the time of the detection, and the plausibility of the detection with respect to migration routes and legitimate detection times at other stations. False detections were rare and were likely the result of tag collisions (overlap in pulse trains of two or more tags) when they did occur; all were excluded before constructing detection sequences. (*ii*) Some tags were detected sporadically or continuously from some point in time until the end of the study when receivers were retrieved. These were likely from fish that died close enough to a receiver to be detected. All sequences of the tag at the station were excluded. (*iii*) Only the first crossing event of a particular tag at a particular station was considered novel. Another series of detections a few hours later potentially represented milling behaviour around the station rather than continual migration across and beyond it. These later sequences were excluded, with the following two exceptions. (*a*) If a fish moved from station *i* to station *ii* and then back to station *i*, the first crossing sequence after returning from the other station was also considered novel. (In this case, we would consider three crossing events to be novel, at *i*, *ii*, and again at *i*.) (*b*) If more than 24 h elapsed between detections at a station, we considered the crossing event after this period to also be novel, as the fish had likely travelled somewhere else over that period instead of milling near the station. (*iv*) If a crossing event lasted more than 4 h, this was also considered likely to be milling instead of migratory behaviour. Less than 2% of all remaining crossing events lasted more than 4 h, and these were excluded from analyses. After applying these filters, 4918 sequences of crossing events remained.

Fitting detection probability attenuation models to crossing sequences

Each constructed sequence of detections and missed transmissions as a fish approached, passed over, and left a station is temporal. Assuming a steady rate of travel past a station, the sequence can also be considered quasi-spatial. The sequence represents a continuum of movement across the station, although the specific point in the sequence of passing by the closest receiver at the station is unknown. We modelled this quasi-spatial detection process, albeit without knowing the true distances from tag to station at which transmissions were detected or missed.

During a crossing event, the probability of detecting a single tag transmission may vary ($0 \leq p_{\text{ping}} \leq 1$). Rather than a near-uniform probability out to a maximum detection range (A.J. Hobday, CSIRO Marine and Atmospheric Research, GPO Box 1538 Hobart, TAS 7001, Australia, and D. Pincock, VEMCO Division, AMIRIX Systems Inc., 211 Horseshoe Lake Dr., Halifax, NS B3S 0B9, Canada, unpublished data), p_{ping} may decrease with increasing tag-to-station distance. We might expect p_{ping} to increase as a fish approaches a station, be at its maximum as it passes over the station (somewhere near the middle of the crossing sequence), and decrease as the fish moves away. That is, we might expect a greater proportion of signals missed near the beginning and end of a crossing sequence than in the middle. Such data on signals detected and signals missed can be described by attenuation models in a probabilistic framework.

We fit five different detection probability attenuation models (details in Appendix B) to each of the 4153 crossing sequences that contained ≥2 detections (the 765 remaining sequences with $n = 1$ do not contain enough information to properly fit attenuation models). We define $\boldsymbol{X}$ as the vector of 1s and 0s for a given crossing sequence, comprised of n detections and $m - n$ misses, and X_i as an individual transmission. Excluding the 50 zeros before and after the main

Table 1. List of symbols used throughout the text.

Symbols and model parameters	Definitions
Detection probabilities	
$\bar{p}_{\text{rec},j}$	Estimate of mark–recapture detection probability at a particular combination j of station, year, and tag type (requires nonlocal information)
$p'_{\text{rec},j}$	Estimator of detection probability at j using only local information
p_{ping}	Probability of detecting a single tag transmission during a crossing event
Crossing sequences	
$\boldsymbol{X}$	Crossing sequence vector of 1s and 0s
n	Number of detections in $\boldsymbol{X}$
m	Length of $\boldsymbol{X}$ including n 1s and $n - m$ 0s
X_i	Individual signal transmitted within $\boldsymbol{X}$; i ranges from (1 − 50) to (m + 50)
$[M_{\text{logit}}p_{\text{ping}}]$ model	
$p_{\max}$	Maximum p_{ping} during a crossing event
$x_{\min}$	Value of X_i (not necessarily an integer) at the first inflection point
ω	Distance in units of $\boldsymbol{X}$ between the inflection points
σ	Steepness^{-1} around each inflection point
Calculations of p'_{rec}	
$\bar{p}^*_{\text{seq}}$	Probability of detecting at least one tag transmission during a hypothetical crossing event, given the parameter set describing its detected crossing event.
$p'_{\max,j}$	Extrapolated $p_{\max}$ at j for $\boldsymbol{X}$ containing $n = 1$
$N_{n,j}$	Number of fish detected at combination j of station, year, and tag type, with $\boldsymbol{X}$ containing n detections
$\bar{N}^-_{n,j}$	Estimated number of fish passing by undetected at j, corresponding to fish detected with $\boldsymbol{X}$ containing n detections
F_j	Correction factor to standardize differences among j in the time within detection range during a crossing event

sequence, X_i ranges from X_1 to X_m. All models involved an increase in p_{ping} from X_1 towards approximately the middle of $\boldsymbol{X}$, followed by a decrease in p_{ping} from this approximate middle towards X_m. All models contained either a centring parameter (x_c) or two centre-bounding parameters, where the centre point x_c represented the hypothesized point along $\boldsymbol{X}$ of minimum distance to the station during the crossing event. This centre point was somewhere near but not necessarily equal to the middle of $\boldsymbol{X}$, $X_{m/2}$. Likewise, the increase in p_{ping} in the initial part of $\boldsymbol{X}$ and decrease in p_{ping} in the later part were symmetric about x_c, but not necessarily about $X_{m/2}$ (it is possible to relax the assumption of symmetry about x_c). All five models had a single parameter in common, $p_{\max}$, which represented the maximum p_{ping} during the crossing event ($p_{\max}$ occurred at x_c or its equivalent in all models). In two models, $p_{\max}$ also extended from x_c some distance in both directions to represent a threshold effect of p_{ping} with distance. The values of $p_{\max}$ or other parameters were not constrained to be equal among models. Definitions of symbols for detection probabilities and model parameters are listed in Table 1.

The first model, $[M_{\text{lin}}p_{\text{ping}}]$, was a simple linear decrease in p_{ping} with increasing tag-to-station distance (Simpfendorfer et al. 2002; Topping et al. 2006), from $p_{\max}$ at the centre point, x_c, towards either end of $\boldsymbol{X}$ (Fig. 1). The second model, $[M_{\text{norm}}p_{\text{ping}}]$, was a normal-shaped decrease in p_{ping} from $p_{\max}$ at x_c towards either end of $\boldsymbol{X}$. Two other models were mechanistic, predicting a decrease in p_{ping} with increasing tag-to-station distance according to physical properties of underwater attenuation of acoustic energy. One of these, $[M_{si}p_{\text{ping}}]$, assumed that p_{ping} was proportional to acoustic intensity and so decayed with distance from x_c as a result of geometrical spreading and absorption (Richards et al. 1996; Leighton 1998). The other, $[M_{si\text{-}thr}p_{\text{ping}}]$, involved similar assumptions but had greater flexibility by incorporating a threshold of constant p_{ping} (at or near $p_{\max}$) over some distance bracketing x_c, beyond which p_{ping} decreased. The fifth model, $[M_{\text{logit}}p_{\text{ping}}]$, also incorporated a threshold effect of p_{ping} with distance. It allowed constant p_{ping} ($\approx p_{\max}$) to a certain distance, and beyond this point, p_{ping} followed a logistic decrease towards either end of $\boldsymbol{X}$ (Szedlmayer and Schroepfer 2005; Fig. 1).

A likelihood equation was constructed for each model, and a nonlinear search routine was used to find the parameter values that maximized this likelihood. Model selection procedures (Burnham and Anderson 2002) were used to compare the five attenuation models in their balance between goodness-of-fit to the data (because likelihood values differed among models) and the number of parameters required to achieve that fit (which also differed). Model $[M_{\text{logit}}p_{\text{ping}}]$ had the most support in the data among these models (Appendix B). This model alone is used for estimating p'_{rec} in the remainder of this paper, but the other four p_{ping} models are described and compared in Appendix B.

Model $[M_{\text{logit}}p_{\text{ping}}]$ is a four-parameter model ($p_{\max}$, $x_{\min}$, ω, σ) that predicts a logistic-shaped increase in p_{ping} during the early portion of the crossing sequence $\boldsymbol{X}$ towards $p_{\max}$ and a symmetrical decrease in p_{ping} in the later portion of $\boldsymbol{X}$:

$$(1)\qquad p_{\text{ping},i} = p_{\max}\left(\frac{1}{1+e^{-\left(\frac{X_i - x_{\min}}{\sigma}\right)}}\right)\left(1 - \frac{1}{1+e^{-\left(\frac{X_i - x_{\min} - \omega}{\sigma}\right)}}\right)$$

The first term in parentheses controls the increasing phase of p_{ping} during the approach to the station, and the second term controls the decreasing phase during departure. Between these regions of increase and decrease is a flat portion of

Fig. 1. Five p_{ping} attenuation models fit to a crossing sequence of detections and missed transmissions. The main sequence, X, of 1s and 0s ranges from X_1 to X_m, with 50 zeros added to either end of X (some 0s not shown). Parameters for model $[M_{logit}p_{ping}]$, p_{max}, x_{min}, ω, and σ, are indicated.

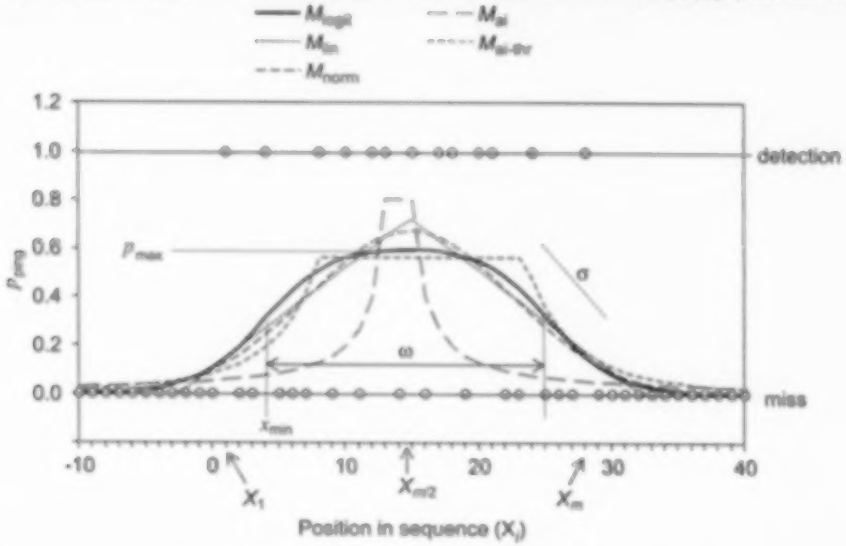

variable width, with $p_{ping} \approx p_{max}$ (Fig. 1). The value of X_i (not necessarily an integer value) at the first logistic inflection point is represented by x_{min}. The width of the curve between the two inflection points (in units of X) is represented by ω (alternative parameterizations to ω could include a second inflection point, x_{max}, where $x_{max} = x_{min} + \omega$, or a centering parameter, x_c, where $x_c = x_{min} + \omega/2$). The slope around each inflection point is determined by the standard deviation, σ. Smaller values of σ result in a greater change in p_{ping} with change in X_i. The portion of the curve where p_{ping} is flat (and $\approx p_{max}$) is wider when ω is greater and (or) σ is smaller. Flexibility in the width of this flat portion of the curve (Appendix C) implies a variable threshold effect, ranging from a p_{max} with no distance threshold (i.e., shaped like a normal density function) to a near-constant p_{max} with a knife-edged distance threshold (i.e., a near-uniform density function). Note that the early increase in p_{ping} and later decrease in p_{ping} (Fig. 1) do not need to be symmetrical. Separate σ parameters could be modelled for the approach and departure phases if there was reason to suspect that fish speed or detection processes would vary between approach and departure phases. In eq. 1, the first σ would be replaced by $\sigma_{approach}$ and the second σ would be replaced by $\sigma_{departure}$, increasing the total parameter count to five. The following constraints were placed on the parameters for numerical estimation purposes: $0.001 < p_{max} < 1$; $0 \leq \omega$; $0.1 < \sigma$. In addition, the two terms in parentheses were each constrained to be $\in (1.0 \times 10^{-9}, 0.999999999)$.

Predicted p_{ping} models were fit to the observed binary detection sequence data by maximizing the following binomial log-likelihood for each crossing sequence with $n \geq 2$:

$$(2) \qquad \ln(L) = \sum_{i=(1-50)}^{(m+50)} \ln\left(p_{ping,i}^{X_i} \times (1 - p_{ping,i})^{(1-X_i)}\right)$$

The summed terms of eq. 2 represent the likelihood of each observed value, X_i, including the m observations in X, as well as the 50 zeros before and after X (hence the indexing starting at –49 and ending at $m + 50$). Individual terms and thus $\ln(L)$ are negative quantities. Smaller values of $\ln(L)$ are expected for longer sequences and poorer fits to the detection data. Sequences of $n = m = 1$ were excluded from model selection comparisons as these events do not contain enough information to discriminate among models.

Estimating local-information detection probability from attenuation models

The proportion of tagged fish crossing a station undetected ($1 - p_{str}$) is unknown. Using only local information from a station, we estimated a detection probability from detection data of tags that were detected while crossing the station. For every detected crossing sequence, we have a set of maximum likelihood estimates (MLEs) of the four parameters that characterize the best-fit $[M_{logit}p_{ping}]$ model to the data for that crossing sequence. These model parameters, specific to detected crossing events at a particular station, contain sufficient information to predict an overall probability of crossing a station undetected. We identify crossing sequences as belonging to a particular combination j of station, year, and tag type in this analysis.

For each crossing sequence where a fish was detected, there is a corresponding nonzero probability that the fish, hypothetically, would not have been detected while passing the station. We define $\widehat{p}^{*}_{seq}$ as the probability that a fish would again be detected during a hypothetical crossing of the station, given the parameter set and sequence length describing its detected crossing event. This is calculated differently depending on whether 1 or ≥2 tag transmissions were detected during the crossing event:

$$(3) \qquad \widehat{p}^{*}_{seq} = \begin{cases} \widehat{p}^{j}_{max,j} & \text{if } X \text{ has } n = 1 \\ 1 - \prod_{i=(1-50)}^{(m+50)} 1 - p_{ping,i} & \text{if } X \text{ has } n \geq 2 \end{cases}$$

For $\boldsymbol{X}$ with $n \geq 2$, $\hat{p}^{*}_{\text{seq}}$ can be estimated directly from the best-fit logistic curve. Because $p_{\text{ping},i}$ describes the probability of detecting a single transmission at position X_i of the sequence, there is a chance $1 - p_{\text{ping},i}$ that the transmission would not again be detected (again, the 50 $p_{\text{ping},i}$ corresponding to the 0s before and after $\boldsymbol{X}$ are included in the sum). If we consider the $p_{\text{ping},i}$ independent during a crossing event, the product of the probabilities of not detecting each of the m transmissions in $\boldsymbol{X}$ results in $1 - \hat{p}^{*}_{\text{seq}}$ (eq. 3). Generally, sequences that are long or have $p_{\max} \approx 1$ will have a near-zero probability of passing the station undetected in a corresponding hypothetical crossing event. For $\boldsymbol{X}$ with $n = 1$, attenuation models cannot be properly fit, but $\hat{p}^{*}_{\text{seq}}$ can instead be estimated by using information from other crossing events at j. Because $p_{\max}$ is simply p_{ping} at the shortest tag-to-station distance during a crossing event, for a crossing event with $n = 1$, $\hat{p}^{*}_{\text{seq}}$ is simply $p_{\max}$. Although $p_{\max}$ is not estimable for single-detection crossings, we extrapolated $p_{\max}$ from those of sequences with $n = 2$–20 using a simple least-squares regression (Fig. 2; lines were fit separately for each j). For these relatively short sequences, $p_{\max}$ generally decreased as n decreased, likely because near the edges of station detection ranges, crossing times are expected to be shorter and $p_{\max}$ is concurrently expected to be less. Extrapolated values of $p_{\max,j}$, $\hat{p}^{'}_{\max,j}$, were constrained at $0.01 \leq \hat{p}^{'}_{\max,j} \leq 1$ in case predicted values were outside the probability scale. Values of $\hat{p}^{*}_{\text{seq}}$ with $n = 1$ in $\boldsymbol{X}$ tended to be smaller than those with $n \geq 2$. Across all combinations j, $\hat{p}^{'}_{\max,j}$ ranged from 0.29 to 1.

The number of fish passing a station undetected ($\hat{N}^{-}_{j}$) is estimated from the number of fish detected at j (N_j) for a given crossing sequence n and $\hat{p}^{*}_{\text{seq},j}$ at that same n. This method explicitly accounts for nonlinear variation in N_j and $\hat{p}^{*}_{\text{seq},j}$ with n, which is expected from variation in detection ranges and crossing positions of fish past the receivers at a station (because $[M_{\text{logit}}\, p_{\text{ping}}]$ parameters vary with n, see Results). At a given n, the mean $\hat{p}^{*}_{\text{seq},j}$, $\overline{\hat{p}^{*}_{\text{seq},n,j}}$, is calculated from all crossing events, and by rearranging $\overline{\hat{p}^{*}_{\text{seq},n,j}} = N_{n,j}/(N_{n,j} + \hat{N}^{-}_{n,j})$, it follows that

$$(4) \qquad \hat{N}^{-}_{n,j} = \left(\frac{N_{n,j}\left(1 - \overline{\hat{p}^{*}_{\text{seq},n,j}}\right)}{\overline{\hat{p}^{*}_{\text{seq},n,j}}}\right)\left(\frac{1}{F_j}\right)$$

In the case of $\boldsymbol{X}$ with $n = 1$, $\overline{\hat{p}^{*}_{\text{seq},n,j}}$ is simply $\hat{p}^{'}_{\max,j}$. A correction factor, F_j, is applied because habitat differences involving river currents (and, to a lesser extent, tag-type differences) lead to expected differences in the time within detection range during a crossing event. Crossing sequence length, m, and duration, ω, are both measures of this time. The estimate of undetected fish, $\hat{N}^{-}_{n,j}$, is considered proportional to the known $N_{n,j}$, but under swift flow conditions, the ratio of $\hat{N}^{-}_{n,j} : N_{n,j}$ is expected to be higher than under low flow conditions (the same is true for weaker tags compared with stronger tags). That is, $\hat{N}^{-}_{n,j}$ is conditioned on $N_{n,j}$, but this relationship is sensitive to time-within-range differences among j. Weaker tags or tags in swift rivers are generally associated with lower m and ω, so F_j helps to standardize $\hat{N}^{-}_{n,j} : N_{n,j}$ in terms of time within detection range. We chose to standardize predictions to crossing events involving V9 tags at an inner coastal station in relatively calm conditions, the outer Howe Sound line (HSout). The choice of a standardizing term is arbitrary — it could be an average of ocean stations or a different station in calm conditions. Four measures of F_j were considered in addition to an uncorrected model with $F_j = 1$: (*i*) $\overline{m_j}/\overline{m_{\text{HSout}}}$ (means), (*ii*) $\tilde{m}_j/\tilde{m}_{\text{HSout}}$ (medians), (*iii*) $\overline{\omega_j}/\overline{\omega_{\text{HSout}}}$, and (*iv*) $\tilde{\omega}_j/\tilde{\omega}_{\text{HSout}}$. The mean (and median) of crossing events at HSout was 44.5 (26.0) for m and 37.0 (17.4) for ω. Those at other stations tended to be shorter, especially in rivers, but were occasionally longer.

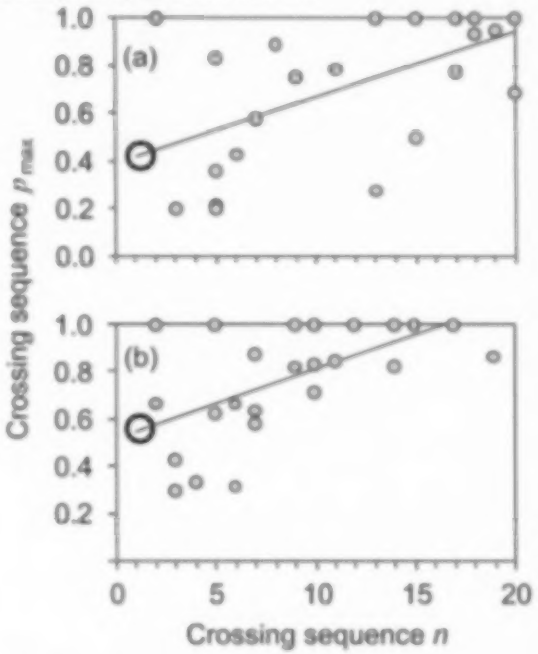

Fig. 2. Two examples of $p_{\max}$ extrapolation to crossing sequences with $n = m = 1$. Small points represent $p_{\max}$ estimates for crossing sequences with $n = 2$–20 at the same station, year, and tag-type combination: (*a*) inner Howe Sound line (inner coast), 2006, V9 tags; (*b*) lower Squamish River, 2006, V9 tags. Large points represent extrapolated $p_{\max}$ values for $n = 1$.

The estimated number of fish crossing undetected for each given n, $\hat{N}^{-}_{n,j}$, is used to calculate the detection probability estimate across all n:

$$(5) \qquad p^{'}_{\text{loc},j} = \frac{\sum_{n=1}^{\infty} N_{n,j}}{\sum_{n=1}^{\infty}\left(N_{n,j} + \hat{N}^{-}_{n,j}\right)}$$

The estimator $p^{'}_{\text{loc},j}$ was calculated for each unique combination j of station, year, and tag type (at Fraser River stations, j was stock-specific as well).

Other local-information estimates of detection probability

Two alternative types of detection probability estimates that use only local information at a detection station were also considered and compared with $\hat{p}_{\text{mr},j}$. First, the same crossing sequences $\boldsymbol{X}$ were used, but instead of fitting p_{ping} models to $\boldsymbol{X}$, a $0 \rightarrow \infty$ probability distribution was fit di-

rectly to the frequency distributions of m at each particular station, year, and tag-type combination j. These frequency distributions contain values of m from $1 \rightarrow \infty$ (actually to 240 after filtering, but this makes little difference). The missing frequency at $m = 0$, i.e., the number of fish at j that crossed the line undetected, is the value required for estimating detection probability. Five probability distributions were modelled in an attempt to find the best overall fit to m rather than strictly adhering to whether the probability distribution properly describes the processes behind m. The Poisson distribution (discrete, with a single parameter, λ; $[M_{\text{Poisson}}]$), which describes the number of detectable transmissions m during a crossing event, would apply if the expected m were the same across all fish. As this is unlikely because of variable detection ranges and locations of crossing a station relative to receiver(s), the variance-to-mean ratio is likely higher than provided by the Poisson distribution, so the negative binomial distribution (discrete, with two parameters, p and r; $[M_{\text{neg-binom}}]$), used in cases of overdispersion, may more reasonably describe this process. We also considered the geometric distribution (discrete, with a single parameter, p; $[M_{\text{geom}}]$) and two continuous distributions that could reasonably fit the pattern of frequency distributions of m at j: the log-normal distribution (with two parameters, μ and σ; $[M_{\text{log-norm}}]$), and the gamma distribution (with two parameters, κ and θ; $[M_{\text{gamma}}]$). The probability mass at $m = 0$ for the discrete distributions, or the area under the probability density functions from $m = 0 \rightarrow 1$ for the continuous distributions, represents the probability of a fish passing undetected. For each probability distribution, the maximum-likelihood fit was obtained, and the cumulative probability at $m = 1$ was calculated to give the estimated zero proportion. The parameters of these distributions are not as easily interpretable as those of p_{ping} models for describing crossing events, but this method is simpler compared with fitting p_{ping} models to crossing sequences and estimating $p'_{\text{loc},j}$ using eqs. 3–5.

The second alternative local detection probability estimate was possible for stations that contained multiple receivers arranged in a line. Detection data from independent subsets of receivers on a line can be used to calculate $p'_{\text{loc},j}$ if at least some fish tend to be detected on more than one receiver while crossing a line. For example, subsets of odd-numbered and even-numbered receivers can be taken, splitting the detection data at the station among these subsets accordingly. A probability $p'_{\text{loc},j(\text{odd})}$ is calculated as the proportion of individual fish detected on even-numbered receivers that were also detected on odd-numbered receivers (i.e., (even∩odd)/even, and vice versa). Treating these components as independent, we estimate an overall $p'_{\text{loc},j}$ for this model, $[M_{\text{odd-even subset}}]$, as

$$(6) \qquad p'_{\text{loc},j} = 1 - \left(1 - p'_{\text{loc},j(\text{odd})}\right)\left(1 - p'_{\text{loc},j(\text{even})}\right)$$

This is the probability of detecting a fish on only odd, only even, or both odd- and even-numbered receivers. A similar approach was used by Melnychuk (2009) to assess the redundancy of receivers on a multireceiver line when detection data at receiver stations further along migration routes are included as well. This method could also be applied to situations where two single-receiver detection stations are close enough that 100% survival between stations can be reasonably assumed. The probability of a fish crossing both stations undetected is equal to the product of the probabilities of crossing each station undetected.

Mark–recapture detection probabilities

Mark–recapture $\tilde{p}_{\text{mr},j}$ were estimated independently of the local estimators, $p'_{\text{loc},j}$, for the same combinations of j. Stocks and species sharing the same tag type were similarly pooled for estimating $\tilde{p}_{\text{mr}}$ at a particular station in a particular year (Melnychuk 2009). This pooling was not done in the Fraser River, as p_{mr} decreased over the migration season as a result of increasing water flow. Instead, stock-specific $\tilde{p}_{\text{mr},j}$ were estimated using a river level covariate paired with stock-specific run timing values (Melnychuk 2009). Note that $\tilde{p}_{\text{mr},j}$ estimates were not possible for the final inner coast stations in the POST study area or for outer coast stations, where no or insufficient detection data were available beyond station j. This limits the comparison of $\tilde{p}_{\text{mr},j}$ and $p'_{\text{loc},j}$ in coastal areas to three stations prior to the final stations. Only $p'_{\text{loc},j}$ with $N_j \geq 10$ were compared with $\tilde{p}_{\text{mr},j}$ to reduce bias from small sample size in either measure of p. In total, the number of combinations j at which both $\tilde{p}_{\text{mr},j}$ and $p'_{\text{loc},j}$ were estimated was, by habitat: Fraser River (25), smaller rivers (33), estuaries (3), and inner coast (15), except for the multireceiver $[M_{\text{odd-even subset}}]$ $p'_{\text{loc},j}$ estimator, where only the inner coast comparisons were possible.

Results

Crossing sequences

After filtering out detections that were likely false, 16% of all crossing sequences had a single detection (Table 2). The proportion of single-detection crossing events was greater at river stations than at coastal detection stations. Related measures, the mean number of detections in a crossing sequence (n) and the mean length of crossing sequences including missed transmissions (m), were smaller in river habitats than in coastal habitats. Excluding the 765 crossing sequences with $n = m = 1$, 23% of crossing sequences with $n \geq 2$ had no missed signals within $\boldsymbol{X}$ (i.e., $n = m$; Table 2). Again, the proportion of crossing events without a miss was larger in river habitats than in coastal habitats. The number of detected signals in a row in these sequences ranged from 2 to >100.

Crossing events consisted primarily of short sequences, with 73% of sequences containing $n \leq 15$ (Fig. 3*a*) and 57% containing $m \leq 15$ (Fig. 3*b*). As the time between X_i and X_{i+1} was about 1 min on average, $m \leq 60$ denotes a crossing event shorter than 1 h, which was true for 87% of all sequences. When separated by habitat type (shown later), histograms for crossing sequences at stations in small and large rivers were skewed more towards smaller n and m relative to the trend shown in Fig. 3, whereas those at stations in estuaries and coastal areas were skewed towards larger n and m. This is reflected in the smaller mean n and mean m, as well as the greater proportion of sequences with single detections, in the two river categories compared with estuary or coastal stations (Table 2).

Table 2. Summary of number of detections (n) in crossing sequences (X), as well as sequence length (m) including missed signals, separated by habitat type.

Habitat	Total X	Mean n	Mean m	No. of X with $n = m = 1$	% of X with $n = m = 1$	No. of X with $n = m \geq 2$	% of X with $n = m \geq 2$
Fraser River	945	9.8	18.2	199	21.1	188	25.2
Smaller rivers	1277	10.2	15.5	265	20.8	530	52.4
Estuaries	565	14.9	36.4	100	17.7	47	10.1
Inner coast	1751	19.3	31.7	170	9.7	166	10.5
Outer coast	380	17.1	32.0	31	8.2	42	12.0
All	4918	13.8	25.5	765	15.6	973	23.4

Fig. 3. Histograms and cumulative probability distributions of 4918 crossing sequences: (*a*) number of detections in a sequence, n; (*b*) sequence length, m, including missed transmissions. Cumulative distributions are shown in both plots for comparison: continuous shaded line with circles corresponds with n and broken line corresponds with m.

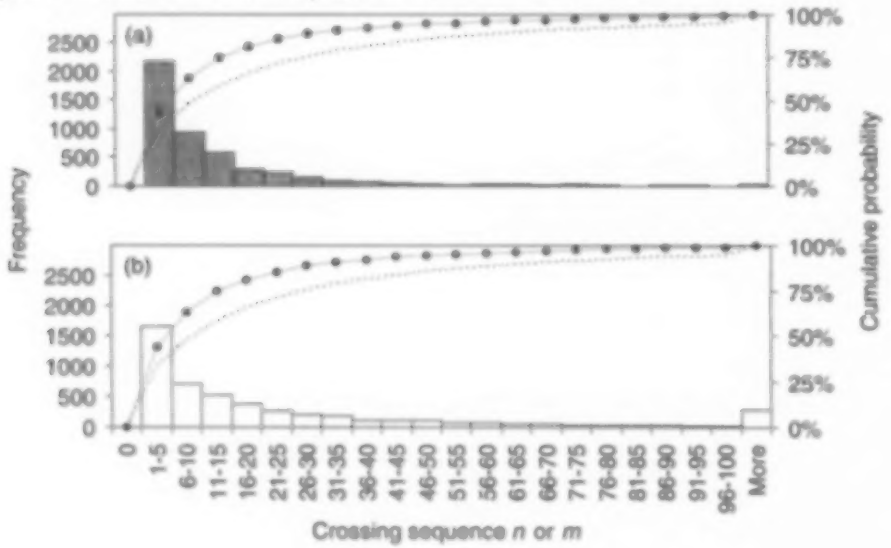

$[M_{\text{logit}} p_{\text{ping}}]$ parameter estimates

For each of the 4153 crossing sequences (excluding the 765 sequences with $n = m = 1$), a set of four parameters was estimated for $[M_{\text{logit}} p_{\text{ping}}]$. Histograms and co-plots of the MLEs of these parameters are shown in Fig. 4 (n is not a parameter but is also included to show covariation with model parameters). Apart from ω, which was roughly log-normally distributed, the three other parameters showed bimodal (σ and $p_{\max}$) or strongly skewed distributions, with parameter estimates often at or near boundaries. Because X were preceded by 50 zeros, $x_{\min}$ was typically near 50 (but was sometimes greater for long sequences when σ was also high). The width of the curve, ω, was typically proportional to n. The steepness^{-1} around the inflection points, σ, was estimated at the lower boundary of 0.1 in 46% of sequences, especially short ones, which resulted in a logistic curve that approximated a uniform density function. Higher σ were generally estimated for longer sequences. Nearly 45% of crossing sequences had $p_{\max}$ estimated at >0.99, especially for sequences that had $n = m$. This parameter showed little consistent variation with n, $x_{\min}$, or σ but was negatively correlated with ω (Fig. 4).

The general patterns of covariation between parameter estimates (Fig. 4) hold if sequences are separated by tag type and (or) by the five habitat categories, although there are some differences in parameter distributions. Sequence length (m) and duration (ω) tended to be longer for V9 tags than for V7 tags except in the Fraser River, where they were similar (Table 3). There was no consistent difference among tag types in $x_{\min}$ (as expected) or in $p_{\max}$, although σ tended to be slightly higher for V9 tags. Comparing habitats, m, ω, and σ were all smaller in rivers than in estuaries or coastal areas. In rivers, $p_{\max}$ was slightly higher on average than in coastal areas, and there was little consistent difference among habitats in $x_{\min}$ (Table 3).

Using eqs. 3–5, frequency distributions of n and m (Fig. 3) can be extrapolated to the unknown $n = m = 0$ category. The estimated number of crossing events at a combination j of station, year, and tag type during which no transmissions were detected is represented by the $\sum_{n=1}^{\infty} \hat{N}_{n,j}$ term in eq. 5. Summing these estimates across j within each habitat gives $\hat{N}_{\overline{\text{hab}}}$, i.e., $\hat{N}_{\text{hab}}$ with $n = m = 0$ (Fig. 5). Frequency counts at $n = 1$–20 are the same as those shown in

Fig. 4. Histograms (on the diagonal) and co-plots of maximum likelihood estimates of $[M_{\text{logit}} p_{\text{ping}}]$ parameters fit to crossing sequences. The number of detections in the crossing sequence, n, is also shown for $n \geq 2$. Three parameters and n are log-transformed. A Lowess fit line with smoothing parameter 0.2 is shown in each co-plot. Correlation coefficients between parameters or n are shown above the diagonal.

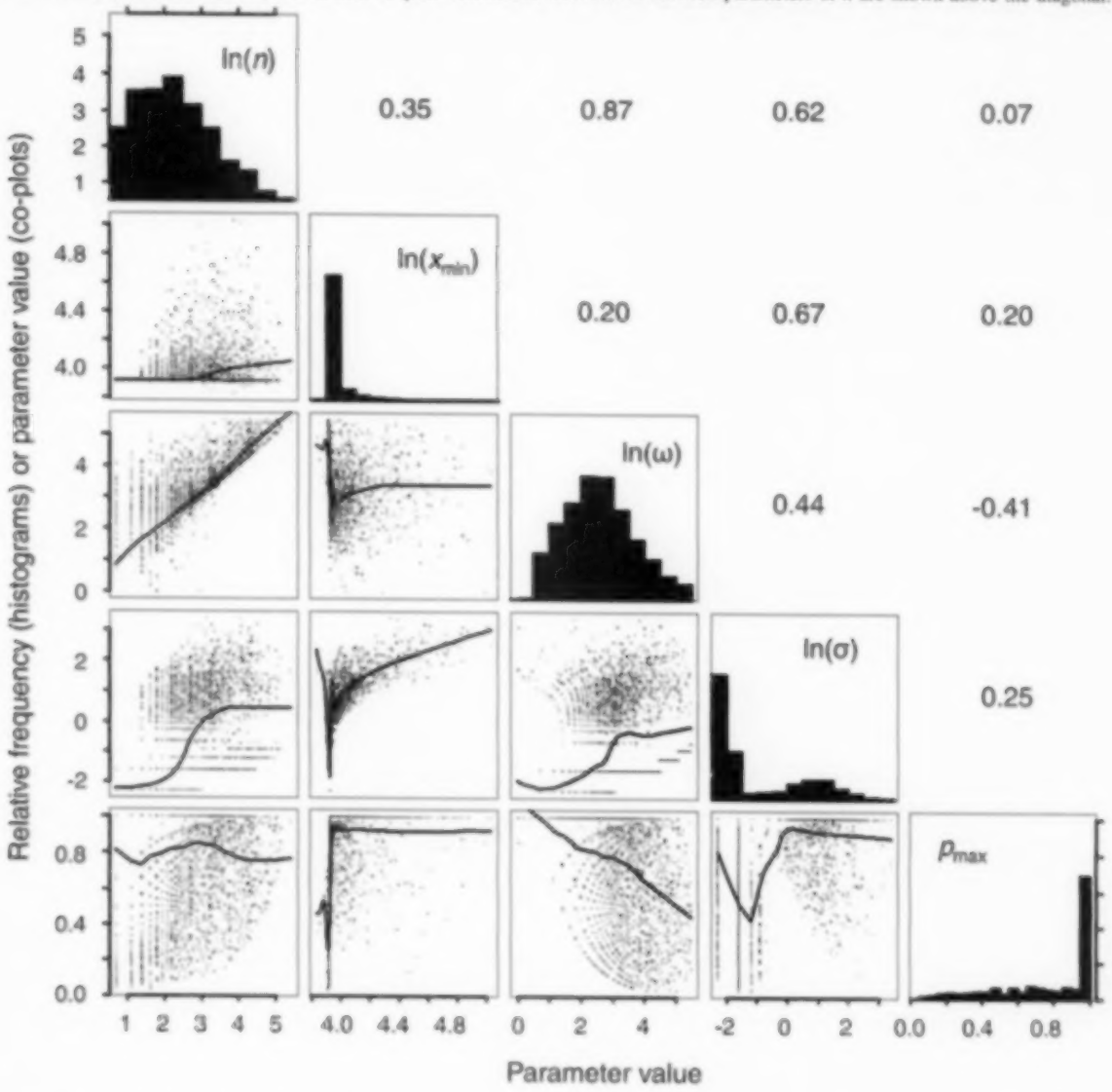

Fig. 3, separated by habitat. Predicted $\widehat{N}_{\text{hab}}$ values seemed to follow the general trends of the frequency distributions from $n = 1$–20. The $n = 0$ category was the most frequent in all habitats. The increase from N_{hab} at $n = 1$ to $\widehat{N}_{\text{hab}}$ was least for estuary and outer coast stations and greatest for Fraser River stations (Fig. 5).

Comparison of p'_{inc} estimators with p_{mr} estimates

Paired estimates of the $p'_{\text{inc},j}$ estimators with $\widehat{p}_{\text{mr},j}$ had correlation coefficients ranging from 0.28 to 0.54 at Fraser River stations, from 0.53 to 0.76 at smaller river stations, and from 0.38 to 0.81 at inner coast stations (Table 4). Among the $[M_{\text{logit}} p_{\text{ping}}]$ models, the four corrected models tended to have higher r than the model with $F_j = 1$. The two models that had the highest overall correlations across habitats were those with $F_j = \overline{m_j}/\overline{m_{\text{HStout}}}$ ($r = 0.54$, 0.75, and 0.81 for Fraser River, smaller rivers, and inner coast, respectively; Fig. 6) and $F_j = \widetilde{m}_j/\widetilde{m_{\text{HStout}}}$ ($r = 0.47$, 0.72, and 0.78 for Fraser River, smaller rivers, and inner coast, respectively). Local-information estimators based on direct fits of probability distributions to frequency distributions of crossing sequence m tended to have poorer overall correlations with $\widehat{p}_{\text{mr},j}$ than estimators based on the corrected $[M_{\text{logit}} p_{\text{ping}}]$ models (Table 4). The Poisson distribution was the poorest of these and the negative binomial distribution, better able

Table 3. Means (and medians in parentheses) of crossing sequence lengths, m, and $[M_{\text{logit}}p_{\text{ping}}]$ model parameters fit to 4153 sequences (765 sequences of $n = m = 1$ are excluded), separated by habitat and tag type.

Habitat	Tag type	Total X	m	ω	σ	p_{mean}	x_{mean}
Fraser River	V7	152	24.0 (10)	20.5 (8.0)	0.86 (0.10)	0.73 (0.79)	52.1 (50.5)
	V9	594	22.4 (11)	18.1 (9.0)	0.98 (0.10)	0.80 (0.89)	52.4 (50.5)
Smaller rivers	V7	313	16.1 (6)	14.7 (6.0)	0.50 (0.10)	0.88 (1.00)	51.2 (50.5)
	V9	699	20.7 (8)	18.6 (7.1)	0.56 (0.10)	0.86 (1.00)	51.4 (50.5)
Estuaries	V7	32	25.9 (10)	20.1 (8.5)	1.44 (0.10)	0.71 (0.67)	52.4 (50.5)
	V9	433	45.4 (27)	38.5 (20.7)	1.48 (0.20)	0.62 (0.67)	53.9 (50.5)
Inner coast	V7	224	28.4 (18)	22.4 (13.1)	1.30 (0.20)	0.66 (0.67)	53.6 (50.5)
	V9	1 357	36.5 (22)	29.6 (16.6)	1.57 (0.20)	0.75 (0.86)	53.9 (50.5)
Outer coast	V7	0					
	V9	349	34.4 (23)	27.1 (19.0)	1.69 (0.20)	0.81 (0.92)	54.1 (50.5)

Fig. 5. Frequency distributions of the number of detections per crossing sequence, n, separated by habitat. Only sequences with $n \leq 20$ are shown. Symbols from $n = 1$–20 are from sequence data, whereas large symbols at $n = 0$ are estimates of the number of fish crossing stations undetected, $\hat{N}_{\text{hab}}$, under model $[M_{\text{logit}}p_{\text{ping}}]$ with $F_j = \overline{m_j/m_{\text{release}}}$.

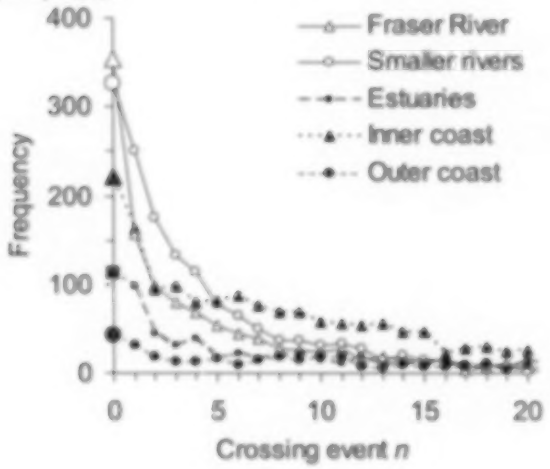

to deal with overdispersion, was somewhat more correlated with $\tilde{p}_{\text{mr},j}$. Of these five models, on average, the geometric distribution best fit the pattern across habitats ($r = 0.48$, 0.57, and 0.64 for Fraser River, smaller rivers, and inner coast, respectively). Applying a correction factor $F_j = \overline{m_j/m_{\text{release}}}$ or $F_j = \overline{m_j}/m_{\text{release}}$ to these direct-fit distribution models improved the overall correlation across habitats slightly (not shown), but the corrected direct-fit distribution models were still less correlated with $\tilde{p}_{\text{mr},j}$ than the corrected $[M_{\text{logit}}p_{\text{ping}}]$ models. At multireceiver inner coast stations, the correlation for $[M_{\text{mbh-even subset}}]$ was intermediate between the corrected $[M_{\text{logit}}p_{\text{ping}}]$ models and the direct-fit distribution models (Table 4). Because there were only three paired estimates of $p'_{\text{loc},j}$ and $\tilde{p}_{\text{mr},j}$ in estuaries, we do not present correlation or regression results for these stations. Similarly, no comparisons were possible for outer coast stations as $\tilde{p}_{\text{mr},j}$ is not estimable. Both tag types are included in this paired analysis, because V7 tags generally had a lower p than V9 tags for both $p'_{\text{loc},j}$ and $\tilde{p}_{\text{mr},j}$.

Local detection probability estimates were generally high compared with $\tilde{p}_{\text{mr},j}$ (i.e., were likely biased upward) as regressions between $p'_{\text{loc},j}$ and $\tilde{p}_{\text{mr},j}$ all had intercepts greater than 0 (a, ranging from 0.18 to 1) and slopes less than 1 (b, ranging from 0 to 0.72; Table 4). This was especially true for the uncorrected $[M_{\text{logit}}p_{\text{ping}}]$ model and the five direct-fit distribution models. The corrected $[M_{\text{logit}}p_{\text{ping}}]$ models tended to have a closer to 1 and b closer to 0, i.e., $p'_{\text{loc},j} : \tilde{p}_{\text{mr},j}$ ratios closer to 1:1 (Fig. 6). Again, at multireceiver inner coast stations, $[M_{\text{mbh-even subset}}]$ was intermediate between the corrected $[M_{\text{logit}}p_{\text{ping}}]$ models and the direct-fit distribution models in terms of a and b (Table 4). Comparing the best overall $p'_{\text{loc},j}$ (the $[M_{\text{logit}}p_{\text{ping}}]$ model with $F_j = \overline{m_j/m_{\text{release}}}$) and $\tilde{p}_{\text{mr},j}$ in different habitats, correlation between estimators was lower but the relationship was closer to 1:1 for Fraser River stations (Fig. 6*a*). Conversely, correlation was higher but the relationship was furthest from 1:1 at inner coast stations (Fig. 6*c*; the range of both measures of p was much less compared with river habitats, which may have contributed to the higher correlation). Smaller river stations had correlation intermediate between these, as well as intermediate a and b (Table 4), although the fit was degraded by two estimates that had high leverage, with $\tilde{p}_{\text{mr},j} = 0.27$–$0.30$ and $p'_{\text{loc},j} \approx 1$ (Fig. 6*b*).

Paired comparisons (Table 4; Fig. 6) were limited to $p'_{\text{loc},j}$ based on $N_j \geq 10$. However, $10 \leq N_j \leq 20$–30 may still be a low number of crossing events on which to base an estimate of detection probability. Small sample sizes can lead to biases in both $p'_{\text{loc},j}$ and $\tilde{p}_{\text{mr},j}$, so $p'_{\text{loc},j}$ is likely a less reliable predictor of $\tilde{p}_{\text{mr},j}$ when $N_j \leq 20$–30 compared with when $N_j \geq 30$. Using $p'_{\text{loc},j}/\tilde{p}_{\text{mr},j}$ as an indicator of bias in the predictive relationship, this ratio deviates from 1 at smaller numbers of N_j (Fig. 7). A doubling or halving of the ratio is not uncommon at $N_j \leq 20$, but this ratio stabilizes near 1 as N_j increases.

Discussion

Utility of p'_{loc} as a predictor of $\tilde{p}_{\text{mr}}$

The detection probability estimator presented here is based on patterns of detected and missed signal transmissions from fish tags that were detected while migrating past a station. From this local information, inferences are made about the proportion of fish not detected. It is assumed that these fish not detected at a station could have been, otherwise mark–recapture estimates of $\tilde{p}_{\text{mr},j}$ would be biased and

Table 4. Comparison of $\hat{p}_{mr,j}$ and estimators of $p'_{loc,j}$: five $[M_{logit}\,p_{ping}]$ models (four with a correction factor, F_j), five probability distribution fits to crossing sequence m histograms, and one receiver subsetting method.

	Fraser River			Smaller rivers			Inner coast		
	r	*b*	*a*	*r*	*b*	*a*	*r*	*b*	*a*
$[M_{logit}\,p_{ping}]$ model									
Uncorrected ($F_j = 1$)	0.31	0.14	0.80	0.65	0.21	0.78	0.64	0.19	0.77
$F_j = \overline{m_j}/\overline{m_{Mixed}}$	0.54	0.71	0.20	0.75	0.60	0.37	0.81	0.44	0.51
$F_j = \tilde{m}_j/\tilde{m}_{Mixed}$	0.47	0.68	0.18	0.72	0.72	0.23	0.78	0.41	0.54
$F_j = \overline{\omega_j}/\overline{\omega_{Mixed}}$	0.52	0.66	0.23	0.75	0.59	0.38	0.53	0.35	0.59
$F_j = \tilde{\omega}_j/\tilde{\omega}_{Mixed}$	0.45	0.59	0.29	0.73	0.66	0.31	0.60	0.30	0.65
Direct fits to crossing sequence m									
$M_{Poisson}$	0.32	0.10	0.90	0.53	0.26	0.75	0.38	0.00	1.00
$M_{neg\text{-}binom}$	0.34	0.19	0.67	0.70	0.32	0.52	0.44	0.16	0.78
M_{geom}	0.48	0.35	0.56	0.57	0.29	0.58	0.64	0.11	0.84
$M_{log\text{-}norm}$	0.34	0.15	0.80	0.76	0.25	0.70	0.47	0.10	0.89
M_{gamma}	0.28	0.11	0.79	0.66	0.19	0.70	0.42	0.12	0.85
Multireceiver subsetting method									
$M_{odd\text{-}even\ subset}$		—			—		0.57	0.50	0.48

Note: Criteria for comparison include correlation coefficients (r), slopes (b), and intercepts (a) of a linear regression of $p'_{loc,j}$ against $\hat{p}_{mr,j}$.

the local estimator would be less reliable. For example, consider two situations: (*i*) a dense line of multiple receivers stretches only halfway across an inshore strait, but migration routes of fish are uniformly distributed across this strait; (*ii*) a dense multireceiver line is deployed on an outer coast, but only half of the fish from a tagged group cross over the line, whereas the other half goes around it, further offshore. In both cases, assume that there are sufficient detection stations further along the migration route to estimate $\hat{p}_{mr}$ at this station. Even if all fish that crossed over the receivers were detected, $\hat{p}_{mr}$ would only be 0.5 because half of the fish did not cross over the receivers. Conversely, p'_{loc} would be based on the fish that were detected at the station, so might be closer to 1. Using $p'_{loc,j}$ as a predictor of $\hat{p}_{mr,j}$ therefore assumes that receivers are deployed close enough to one another and cover the full range of possible migration routes across some point so that every fish migrating past that point has a nonzero probability of being detected. In other words, $p'_{loc,j}$ conditions on any tagged fish crossing the station transmitting at least once while within range of a receiver.

The best local estimator considered here, $[M_{logit}\,p_{ping}]$ with $F_j = \overline{m_j}/\overline{m_{Mixed}}$, predicted mark–recapture detection probabilities reasonably well considering that it uses only local information. The primary purpose of using a local estimator would be to address situations in which $\hat{p}_{mr,j}$ is not known or precisely estimable, however, so correlations of $p'_{loc,j}$ and $\hat{p}_{mr,j}$ would not necessarily be routinely quantified. Instead, the local estimator could be used as either a covariate of $p_{mr,j}$ in mark–recapture models or an absolute predictor of $p_{mr,j}$; which of these is most appropriate may depend on the sample size of the study and magnitude of p_{mr}. If $N_j \leq 50$–100 at stations along migration routes as a result of moderate tag sample sizes, moderate $p_{mr,j}$, or mortality during the migration before arriving at later stations, the estimator could be used as a covariate where $\hat{p}_{mr,j}$ is constrained to be a function of $p'_{loc,j}$. (Similarly, $p'_{loc,j}$ could be used as a prior estimate of $p_{mr,j}$ in Bayesian formulations.) This could result in more parsimonious mark–recapture models for estimating $p_{mr,j}$ and survival probabilities, in contrast to using more general CJS models with $p_{mr,j}$ estimated independently for each j. At modest N_j, however, the ratio of $p'_{loc,j}/\hat{p}_{mr,j}$ may have a large enough bias in either direction that absolute predictions of $p_{mr,j}$ are not reliable. Further, estimating $p'_{loc,j}$ for use as either a covariate or prior parameter from the same detection data set as that used for mark–recapture analyses can be susceptible to overfitting, and the precision of constrained $\hat{p}_{mr,j}$ can be overestimated, so caution should be used if using $p'_{loc,j}$ as a covariate. Conversely, if sample sizes are large, $p_{mr,j}$ is high, and mortality levels are low to moderate during the migration such that $N_j \geq 100$ even at stations later in the migration, the local estimator could be used as an absolute predictor of $p_{mr,j}$ at the final detection station, where p cannot be estimated with mark–recapture methods. For large N_j, if the ratio $p'_{loc,j}/\hat{p}_{mr,j}$ does actually stabilize near 1, the possible bias in this absolute prediction could be acceptable. In making an absolute prediction for the final station, however, either a covariate $p'_{loc,j}$ should be used across all stations or correlations between $p'_{loc,j}$ and $\hat{p}_{mr,j}$ should be assessed to ensure that the prediction for the final station is likely reasonable. Whether $p'_{loc,j}$ is used as a covariate of $\hat{p}_{mr,j}$ or as an absolute predictor of $\hat{p}_{mr,j}$ at the final detection station, in both cases, this allows the survival probability in the final segment to be estimable, conditioned on the final $\hat{p}_{mr,j}$.

Establishing a minimum N_j for making comparisons between $p'_{loc,j}$ and $\hat{p}_{mr,j}$ can reduce biases in either estimate of p from small sample sizes. Although $N_j \geq 10$ was used as a threshold in our comparisons, we found that $N_j \geq 30$ would have resulted in a ratio of $p'_{loc,j}/\hat{p}_{mr,j}$ closer to 1. The trade-off with increasing the N_j threshold is that in studies with

Fig. 6. Comparison of local-information detection probability estimates ($p'_{\mathrm{loc},j}$) from [$M_{\mathrm{tvpt}}p_{\mathrm{tvmt}}$] model and mark–recapture detection probability estimates ($\hat{p}_{\mathrm{mr},j}$) at the same station, year, and tag type (in the Fraser River, estimates are stock-specific as well). Paired estimates are separated by habitat: (*a*) Fraser River, (*b*) smaller rivers, and (*c*) inner coast. Open circles show uncorrected $p'_{\mathrm{loc},j}$ and shaded circles show $p'_{\mathrm{loc},j}$ with $F_j = \overline{m_j}/\overline{m_{\mathrm{detect}}}$. Regression lines (continuous lines) are shown for shaded circles. Dotted lines show 1:1 relationship.

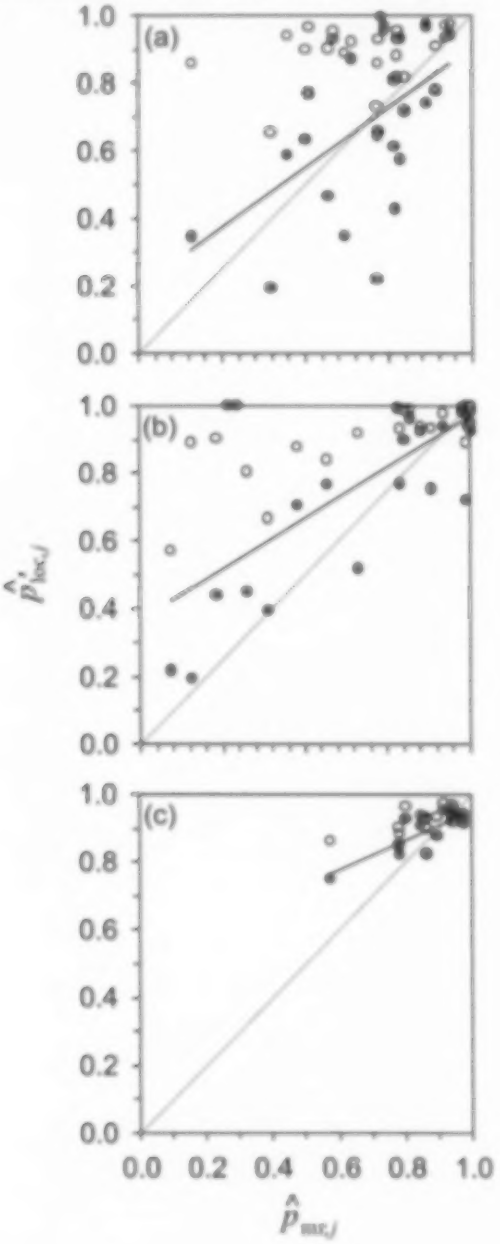

small or moderate sample sizes, fewer paired estimates will be available for assessing the correlation within a given habitat, or fewer $p'_{\mathrm{loc},j}$ will be available for use as a covariate. If we had used $N_j \geq 30$ (or 20), the number of paired estimates of p would have decreased from 25 to 7 (or 10) in the Fraser River, from 33 to 22 (or 26) in smaller rivers, and from 15 to 13 (or 14) at inner coast stations. If N_j is generally large even at later stations in the migration route, or if enough stations or years of study are used, then a higher threshold of N_j may be used while still leaving enough paired estimates to establish a relationship between $p'_{\mathrm{loc},j}$ and $\hat{p}_{\mathrm{mr},j}$. Conversely, if few crossing events occur above some N_j threshold, there will be missing covariate values of the estimator at some stations.

Among the three habitats where $p'_{\mathrm{loc},j}$ was compared with $\hat{p}_{\mathrm{mr},j}$, the relationship was most variable at Fraser River stations. This is likely at least partly the result of a strong relationship between $p_{\mathrm{mr},j}$ and river flow (Melnychuk 2009). These $\hat{p}_{\mathrm{mr},j}$ are estimates for an entire release group (combination of station, year, tag type, and stock), but individual fish within a group may cross the station at different times and may therefore have a variable probability of being detected (the crossing time of fish not detected is not known but can be treated as a random variable in Bayesian formulations of CJS models; Muthukumarana et al. 2009). In contrast, the $p'_{\mathrm{loc},j}$ estimators are assessed from detection data of crossing events of individual fish, so by definition, these reflect the river flow levels at the time of crossing. If heterogeneity in $p_{\mathrm{mr},j}$ exists, methods to account for it can improve mark–recapture estimates (Pledger et al. 2003). The local estimator accounts for heterogeneity among detected individuals; the researcher could assess whether $\tilde{p}^*_{\mathrm{seq},j}$ changes under varying environmental conditions like increasing river flow during a migration season. Similarly, the estimator could be used to evaluate other assumptions of mark–recapture models such as the partial-sampling scenarios from incomplete detection stations described above. If $p'_{\mathrm{loc},j}$ at some j is unusually high relative to $\hat{p}_{\mathrm{mr},j}$, that might suggest that some proportion of the tagged population is not available to be detected at j, thereby biasing $\hat{p}_{\mathrm{mr},j}$.

Assumptions of p'_{loc} attenuation models

In considering the temporal sequence of detections and missed transmissions as quasi-spatial to fit attenuation models, continuous travel at constant speed of tagged fish migrating past stations was assumed. If fish speed changes during a crossing event, or if direction changes to lateral or diagonal movement along a multireceiver station rather than perpendicular movement across it, the quasi-spatial units of sequence length will not be proportional to actual distances from tag to receiver. The method is therefore best suited for species that consistently migrate with little chance of residing near detection stations where residency could be misinterpreted as long crossing events. Long detection sequences or repeated sequences at the same station can be easily identified; we excluded all non-novel and long (>4 h) crossing events before calculating $p'_{\mathrm{loc},j}$.

Travel rate across stations was also assumed to be constant among individual fish. Slower fish, as a result of either shorter body length or a greater proportion of time not continually swimming, are expected to have longer crossing sequence lengths than faster fish. The probability of a fish crossing a line undetected is higher for faster fish; because

Fig. 7. Ratio of $p'_{\text{loc},j}$ (model $[M_{\text{logit}}\, p_{\text{ping}}]$ with $F_j = \overline{m_j}/\overline{m_{\text{HStout}}}$) to $\hat{p}_{\text{mr},j}$ at the same station, year, and tag type (and in the Fraser River stock as well). Points are plotted against the number of detected crossing events, N_j (only paired estimates with $N_j \geq 10$ are shown), and separated by habitat type: Fraser River (△), smaller rivers (○), and inner coast (▲). Note log scale. The horizontal line at 1 shows where $p'_{\text{loc},j} = \hat{p}_{\text{mr},j}$.

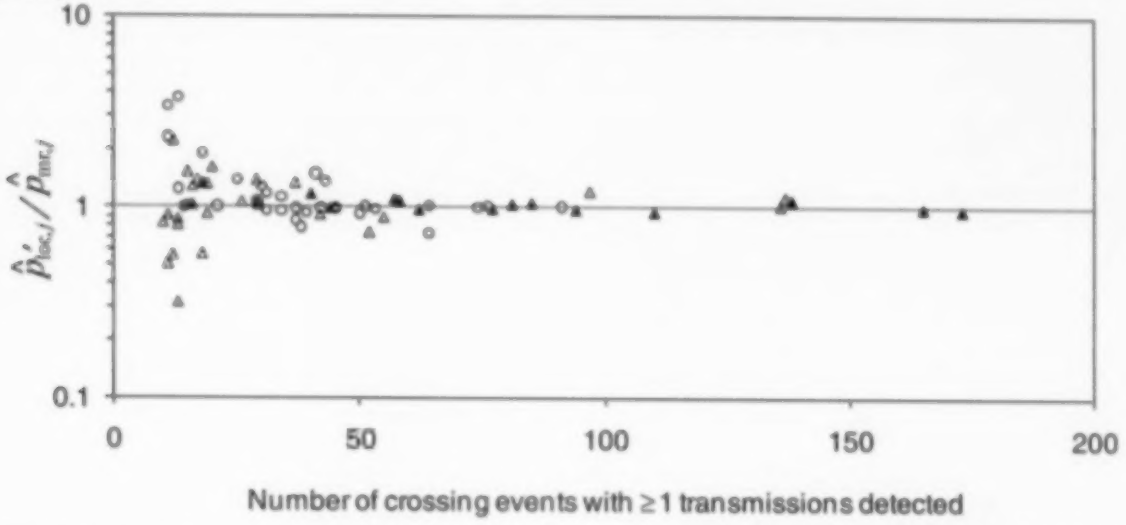

slower fish contribute disproportionately more crossing sequences at j, $p'_{\text{loc},j}$ may underestimate $p_{\text{mr},j}$ (although we found that $p'_{\text{loc},j} \geq \hat{p}_{\text{mr},j}$ rather than $p'_{\text{loc},j} \leq \hat{p}_{\text{mr},j}$ most of the time).

The five p_{ping} attenuation models all involved decrease in p_{ping} with increasing tag-to-station distance (although two had a threshold effect of constant p_{ping} to some distance). This assumption differs from other suggestions that at any given moment (i.e., a crossing event), the density function of p_{ping} with increasing distance is nearly uniform, with $p_{\text{ping}} \approx 1$ to some threshold distance, beyond which p_{ping} declines sharply to zero (A.J. Hobday, CSIRO Marine and Atmospheric Research, GPO Box 1538 Hobart, TAS 7001, Australia, and D. Pincock, VEMCO Division, AMIRIX Systems Inc., 211 Horseshoe Lake Dr., Halifax, NS B3S 0B9, Canada, unpublished data). We found some support for the assumption of a simple uniform density function in sequences with $n \geq 2$: (*i*) 23% of sequences were uniform with $n = m$, (*ii*) 46% of sequences had $[M_{\text{logit}}\, p_{\text{ping}}]$ parameter σ estimated at the lower boundary of 0.1, and (*iii*) 45% of sequences had p_{max} estimated at >0.99 (21% of sequences met all three criteria). Remaining sequences, however, involved more of a gradual increase in p_{ping} with decreasing tag-to-receiver distance. The two threshold p_{ping} models, including the logistic model used, are flexible in that the shape of their probability curves can be near-uniform if warranted by the detection data (Appendix C).

Crossing sequences were treated independently when fitting p_{ping} attenuation models, which resulted in a set of three to five parameters estimated for each crossing event (e.g., four parameters in the case of model $[M_{\text{logit}}\, p_{\text{ping}}]$) and thus a large number of total estimated parameters over all crossing events at j. Alternative approaches could involve modelling parameter values at j as random effects or moving to a Bayesian hierarchical model with $[M_{\text{logit}}\, p_{\text{ping}}]$ parameters described by hyperparameters. This could allow information sharing between parameters at j while still maintaining a local information-only approach to estimation of $p'_{\text{loc},j}$.

The predictive ability of $p'_{\text{loc},j}$ from $[M_{\text{logit}}\, p_{\text{ping}}]$ as an index of $\hat{p}_{\text{mr},j}$ is sensitive to the choice of the correction factor, F_j. The uncorrected model with $F_j = 1$ was not as good a predictor as models with F_j standardized to a station with calm, relatively low net current conditions. Logistic models based on mean or median m ($F_j = \overline{m_j}/\overline{m_{\text{HStout}}}$ or $F_j = \tilde{m}_j/\tilde{m}_{\text{HStout}}$) gave similar and, overall, the best predictions of $\hat{p}_{\text{mr},j}$ among the set of 10 models considered. Inclusion of F_j (which standardizes for variation in average crossing times) in the calculation of $p'_{\text{loc},j}$ is reasonably justified as $\hat{N}^{-}_{a,j}$ is based on the number of fish detected at j; the ratio $\hat{N}^{-}_{a,j} : N_{a,j}$ varies as a result of not only $[M_{\text{logit}}\, p_{\text{ping}}]$ fits to $\boldsymbol{X}$ of fish that were detected, but also time-within-range factors that result in variation in $N_{a,j}$. Several approaches could be used to determine an appropriate F_j for other studies. If there is variation across habitats where receiver stations are placed, a reference station in calm waters could be chosen, as we did. Studies that are conducted only in rivers may not have a comparable low-current station that can be used for F_j. Alternative approaches are to use either the station with lowest flow or the combination of station, year, and tag type (and possibly stock) that have the highest $\overline{m_j}$ as the denominator. We do not consider use of F_j to be a violation of our "only local information" approach. The denominator is constant across all j and could instead be replaced by a constant. If a relationship between $p'_{\text{loc},j}$ and $\hat{p}_{\text{mr},j}$ as close to 1:1 is desired (rather than simply using $p'_{\text{loc},j}$ as an index for prediction) and choice of F_j based on environmental characteristics is not deemed to be important by the researcher, then a constant F_j could instead be found through optimization routines that generate as close to a 1:1 relationship as possible.

Crossing sequences and $[M_{\text{logit}}p_{\text{ping}}]$ parameters

There was considerable variation among crossing sequences in MLEs of $[M_{\text{logit}}p_{\text{ping}}]$ model parameters and in covariation among parameters. This is expected because of variation in environmental conditions during fish crossing events and the specific position of crossing the station (i.e., closest distance from tag to receiver during the crossing event). The sequence length, m, or duration of the $[M_{\text{logit}}p_{\text{ping}}]$ curve, ω, are expected to be shorter if fish cross the station near the edge of the detection range or in the gap between two receivers or if travel speed is faster. High values of $p_{\max}$ are expected when fish pass close to a station or if acoustic conditions are favourable so that most or all transmissions are detected. A low σ resulting in a near-uniform p_{ping} probability curve could arise when acoustic conditions are such that p_{ping} near $p_{\max}$ is expected until some short detection range away, after which p_{ping} drops sharply toward 0 (low σ was typically associated with low n). Crossing positions cannot be estimated easily from the data, but expected variation in these positions leads to the variation in parameter estimates and covariation among them.

Variation in detection processes among habitats was evident in both the length of crossing sequences and MLEs of $[M_{\text{logit}}p_{\text{ping}}]$ parameters. Crossing sequences at river stations had a higher proportion of single detections and a higher proportion of uniform probability curves at $n = m \geq 2$ than those from inner or outer coastal areas. This corresponds with the lower σ and higher $p_{\max}$ estimated for river stations. Crossing sequences at river stations also had shorter mean n, m, and ω than those from coastal stations. Because the minimum distance from tag to station should be shorter in rivers than at coastal stations (where fish can cross in the gaps between two receivers), this might explain why rivers showed a greater proportion of sequences without a missed detection, even if those sequences were shorter on average. Similar differences in sequence length and model parameters were seen between tag types, with crossing sequences of the weaker V7 tags having shorter m and ω and smaller σ than V9 tags. This relates to time-within-detection range differences among habitats and tag types, which were standardized by using F_j in the calculation of $\hat{N}^{\cdot}_{n,j}$. A greater contribution of $\hat{N}^{\cdot}_{n,j}$ comes from $p^{\cdot}_{\max,j}$ extrapolations at $n = 1$ than from hypothetical $\hat{p}^{\cdot}_{\text{seq},j}$ at $n \geq 2$. Summing over all crossing sequences n and combinations j in each habitat, $\hat{N}^{\cdot}_{\text{hab}}$ at least appears to follow the general trend from known crossing sequences at $n = 1$–20.

The choice of the number of zeros added before and after X (50) was arbitrary but did not have a large effect on estimates of $p_{\max}$ for sequences with $n = 1$–20 or on $\hat{p}^{\cdot}_{\text{seq}}$ for sequences with $n \geq 2$; estimates when $[M_{\text{logit}}p_{\text{ping}}]$ was fit to sequences with 50 zeros before and after X were similar to those involving 10 or 100 zeros. The largest deviations were observed for long sequences with 10 zeros before and after X, as the tails of $[M_{\text{logit}}p_{\text{ping}}]$ were not as "rooted" to zero before and after X. Deviations in these long sequences, however, had little effect on $\hat{p}^{\cdot}_{\text{seq}}$ as $\hat{p}^{\cdot}_{\text{seq}}$ is already near zero for long sequences and had little effect on the $p_{\max}$ extrapolation because they were relatively few.

The possibility of false detections resulting from tag collisions and other factors leads to the common suggestion for acoustic or radio telemetry studies that single detections of a tag at a station be excluded from analyses. That may be appropriate for fish that spend considerable time near a station, but migrating fish may be within detection range of a station for enough time to transmit only a few signals, especially in rivers where travel speeds are assisted by currents. Our results show that such exclusions would likely lead to biases of $\hat{p}_{mr,j}$ for migrating fish: 16% of all crossing events that were considered legitimate in this POST data set involved only a single detection. If these detections were excluded from mark–recapture analyses, $\hat{p}_{mr,j}$ would be underestimated because legitimate detections would be treated as nondetection at j. If fish are not detected after j, survival probabilities to j could be either overestimated (because $\hat{p}_{mr,j}$ is underestimated) or underestimated (because evidence of survival to j would be excluded), depending on the degree of bias in $\hat{p}_{mr,j}$. The trade-off between willingness to accept a possible false single detection and exclusion of a legitimate single detection occurs along a continuum. If telemetry studies have direct relevance to estimating parameters important to fisheries management issues, risk assessments could be used to identify appropriate locations along this continuum in terms of optimal policy recommendations.

Acknowledgements

Simon Bonner, Josh Korman, two anonymous reviewers, and Stephen Smith provided helpful comments on the manuscript. Villy Christensen, Steve Martell, Rob Ahrens, Carl Schwarz, and Simon Bonner provided useful comments during discussions. Kintama Research and POST members provided general support and field work. M.M. was supported by a Canada Graduate Scholarship from the Natural Sciences and Engineering Research Council of Canada.

References

Burnham, K.P., and Anderson, D.R. 2002. Model selection and multi-model inference: a practical information-theoretic approach. Springer-Verlag, New York.

Burnham, K.P., Anderson, D.R., White, G.C., Brownie, C., and Pollock, K.H. 1987. Design and analysis methods for fish survival experiments based on release–recapture. American Fisheries Society Monograph No. 5, Bethesda, Maryland.

Cormack, R.M. 1964. Estimates of survival from the sighting of marked animals. Biometrika, **51**: 429–438.

Groot, C., and Margolis, L. 1991. Pacific salmon life histories. UBC Press, Vancouver, British Columbia, Canada.

Jolly, G.M. 1965. Explicit estimates from capture–recapture data with both death and immigration-stochastic model. Biometrika, **52**: 225–247. PMID:14341276.

Leighton, T.G. 1998. Fundamentals of underwater acoustics. *In* Fundamentals of noise and vibration. *Edited by* F.J. Fahy and J.G. Walker. Taylor & Francis, London, UK. pp. 373–444.

Melnychuk, M.C. 2009. Estimation of survival and detection probabilities for multiple tagged salmon stocks with nested migration routes, using a large-scale telemetry array. Mar. Freshw. Res. **60**: 1231–1243.

Muthukumarana, S., Schwarz, C.J., and Swartz, T.B. 2009. Bayesian analysis of mark–recapture data with travel time-dependent survival probabilities. Can. J. Stat. **36**(1): 5–21. doi:10.1002/cjs.5550360103.

Pledger, S., Pollock, K.H., and Norris, J.L. 2003. Open capture–recapture models with heterogeneity: I. Cormack–Jolly–Seber model. Biometrics, **59**(4): 786–794. doi:10.1111/j.0006-341X.2003.00092.x. PMID:14969456.

Pollock, K.H., Hines, J.E., and Nichols, J.D. 1984. The use of auxiliary variables in capture–recapture and removal experiments. Biometrics, **40**(2): 329–340. doi:10.2307/2531386.

Richards, S.D., Heathershaw, A.D., and Thorne, P.D. 1996. The effect of suspended particulate matter on sound attenuation in seawater. J. Acoust. Soc. Am. **100**(3): 1447–1450. doi:10.1121/1.415991.

Seber, G.A.F. 1965. A note on the multiple recapture census. Biometrika, **52**: 249–259. PMID:14341277.

Simpfendorfer, C.A., Heupel, M.R., and Hueter, R.E. 2002. Estimation of short-term centers of activity from an array of omnidirectional hydrophones and its use in studying animal movements. Can. J. Fish. Aquat. Sci. **59**(1): 23–32. doi:10.1139/f01-191.

Simpfendorfer, C.A., Heupel, M.R., and Collins, A.B. 2008. Variation in the performance of acoustic receivers and its implication for positioning algorithms in a riverine setting. Can. J. Fish. Aquat. Sci. **65**(3): 482–492. doi:10.1139/F07-180.

Skalski, J.R., Lady, J., Townsend, R., Giorgi, A.E., Stevenson, J.R., Peven, C.M., and McDonald, R.D. 2001. Estimating in-river survival of migrating salmonid smolts using radiotelemetry. Can. J. Fish. Aquat. Sci. **58**(10): 1987–1997. doi:10.1139/cjfas-58-10-1987.

Szedlmayer, S.T., and Schroepfer, R.L. 2005. Long-term residence of red snapper on artificial reefs in the northeastern Gulf of Mexico. Trans. Am. Fish. Soc. **134**(2): 315–325. doi:10.1577/T04-070.1.

Topping, D.T., Lowe, C.G., and Caselle, J.E. 2006. Site fidelity and seasonal movement patterns of adult California sheephead *Semicossyphus pulcher* (Labridae): an acoustic monitoring study. Mar. Ecol. Prog. Ser. **326**: 257–267. doi:10.3354/meps326257.

Voegeli, F.A., Lacroix, G.L., and Anderson, J.M. 1998. Development of miniature pingers for tracking Atlantic salmon smolts at sea. Hydrobiologia, **371/372**: 35–46. doi:10.1023/A:1017014903313.

Welch, D.W., Boehlert, G.W., and Ward, B.R. 2003. POST — the Pacific Ocean Salmon Tracking Project. Oceanol. Acta, **25**(5): 243–253. doi:10.1016/S0399-1784(02)01206-9.

Welch, D.W., Melnychuk, M.C., Rechisky, E.R., Porter, A.D., Jacobs, M.C., Ladouceur, A., McKinley, R.S., and Jackson, G.D. 2009. Freshwater and marine migration and survival of endangered Cultus Lake sockeye salmon (*Oncorhynchus nerka*) smolts using POST, a large-scale acoustic telemetry array. Can. J. Fish. Aquat. Sci. **66**: 736–750. doi:10.1139/F09-032.

Appendix A. Pseudocode for constructing a sequence of detections and missed emissions

Consider the following detections of two tags at a receiver station, arranged in chronological order:

Tag no.	Date	Time
555	25–05–2004	16:49:02
555	25–05–2004	16:50:54
555	25–05–2004	16:51:38
555	25–05–2004	16:53:22
555	25–05–2004	16:56:17
2222	25–05–2004	17:30:12
2222	25–05–2004	17:31:29

Note: Date is expressed in day–month–year; time is expressed in hours : minutes : seconds.

The goal is to construct the most likely sequence of 1s and 0s representing detections and missed transmissions, respectively, of tag 555 during this time period.

The variables are defined as follows: r, average repeat rate or time between the start of successive transmissions (62 s); cut, threshold for parsing detection data into separate crossing sequences (60 min); and i, row index, starting with 1.

The procedure is as follows.

1. Read in tag code$_i$ and (date+time)$_i$ from row i of detection times and assign this detection a corresponding 1 in a crossing sequence.
2. If tag code$_{i+1}$ on row $i + 1$ is the same, calculate Δtime = (date+time)$_{i+1}$ − (date+time)$_i$. If tag code$_{i+1}$ on row $i + 1$ is not the same, end sequence.
3. If Δtime < cut, construct a hypothetical sequence of transmission times beginning with (date+time)$_i$ and incrementing by r.
4. Find the closest match between (date+time)$_{i+1}$ and all possible times in the hypothetical transmission sequence and assign a 1 in the crossing sequence corresponding to this best-matched time in the transmission sequence.
5. Reset this best-matched time in the transmission sequence to (date+time)$_{i+1}$.
6. Assign a 0 in the crossing sequence corresponding to all hypothetical transmission times between (date+time)$_i$ and (date+time)$_{i+1}$.
7. Increase i by 1 and go to number 1.

The results are as follows:

Detection time		Hypothetical transmission time		
Date	Time	Date	Time	Crossing sequence
25–05–2004	16:49:02	**25–05–2004**	**16:49:02**	1
		25–05–2004	16:50:04	0
25–05–2004	16:50:54	**25–05–2004**	**16:50:54**	1
25–05–2004	16:51:38	**25–05–2004**	**16:51:38**	1
		25–05–2004	16:52:40	0
25–05–2004	16:53:22	**25–05–2004**	**16:53:22**	1
		25–05–2004	16:54:24	0
		25–05–2004	16:55:26	0
25–05–2004	16:56:17	**25–05–2004**	**16:56:17**	1

Note: Date is expressed in day–month–year; time is expressed in hours : minutes : seconds.

Boldfaced hypothetical transmission times are those that were reset to the actual detection time after the process of finding a closest match. We can calculate n as the number of detections of a tag crossing a station during a crossing event and m as the sequence length of the crossing event including both detections and missed transmissions. By definition $n \leq m$, and in this case, $n = 5$ and $m = 9$. For stations with multiple receivers, the detections from all receivers at the station would first be sorted in chronological order, all but one simultaneous detection on multiple receivers would be excluded, and the same procedure would then be followed. Finally, a large number of 0s (e.g., 50–100) would be added to either end of the crossing sequence for numerical estimation purposes.

Appendix B. Alternate p_{ping} attenuation model descriptions and comparison

Four p_{ping} attenuation models are described in this appendix. These models, along with $[M_{logit}p_{ping}]$, are then compared using information-theoretic methods. The general forms of the five models fit to an example crossing sequence are shown in Fig. 1 of the main text.

(*i*) $[M_{lin}p_{ping}]$

This is a three-parameter model (p_{max}, x_c, b) that predicts a linear increase in p_{ping} from the early portion of $\boldsymbol{X}$ towards the centre point, x_c:

$$p_{ping,i} = p_{max}\begin{pmatrix} 1 + b(X_i - x_c) & \text{if } X_i < x_c \\ 1 - b(X_i - x_c) & \text{if } X_i > x_c \end{pmatrix} \quad \text{(B1)}$$

At x_c, $p_{ping} = p_{max}$. A linear decrease is symmetrical about x_c, with p_{ping} decreasing towards the later portion of $\boldsymbol{X}$. The slope of the increase in p_{ping} is b (and $-b$ for the decrease in p_{ping}). Greater b implies a more rapid increase towards p_{max} and decrease away from p_{max}. Typically, x_c occurs near the middle of $\boldsymbol{X}$, $X_{mi/2}$, although asymmetrical patterns of detections and missed signals can draw x_c to one side or another of $X_{mi/2}$. Constraints were placed on the parameters for numerical estimation purposes: $0.001 < p_{max} < 1$; $0.01 < b < 200$; $X_1 < x_c < X_m$. Additionally, p_{ping} was constrained to be $\in (1.0 \times 10^{-9}, 0.999999999)$, which prevented negative values of predicted p_{ping} ouside of $\boldsymbol{X}$ but within the range of the 50 zeros to either side of $\boldsymbol{X}$.

(*ii*) $[M_{norm}p_{ping}]$

This is a three-parameter model (p_{max}, μ, σ) that predicts a bell-shaped increase in p_{ping} from the early part of $\boldsymbol{X}$ towards μ (the centre point, μ, is equivalent to x_c in the linear model, but we use typical notation for the normal probability distribution here):

$$p_{ping,i} = p_{max}\left(\frac{1}{\sigma\sqrt{2\pi}}e^{-\left(\frac{X_i-\mu^2}{2\sigma^2}\right)}\right) \quad \text{(B2)}$$

At μ, $p_{ping} = p_{max}$. As X_i increases, the rate of increase in p_{ping} towards p_{max} at μ or decrease in p_{ping} away from μ is determined by the standard deviation of the normal curve, σ. Similar to the logistic model, smaller values of σ imply a more rapid change in p_{ping} with change in X_i. Constraints were placed on the parameters: $0.001 < p_{max} < 1$; $0.1 < \sigma$; $X_1 < \mu < X_m$. The normal probability density at X_i was standardized by dividing this quantity by the normal density at μ so that the maximum standardized density of the curve was 1 before multiplication with p_{max}.

(*iii*) $[M_{sl}p_{ping}]$

This is a four-parameter model ($p_{max}, x_c, \alpha, \beta$) that predicts a decrease in p_{ping} with increasing tag-to-receiver distance according to physical properties of underwater attenuation and spreading of acoustic intensity. We assume that p_{ping} is proportional to intensity, so p_{ping} decreases exponentially from p_{max} toward zero as the absolute distance from X_i to x_c increases:

$$p_{ping,i} = p_{max}\begin{pmatrix} e^{\left(\frac{2\cdot\alpha\cdot(X_i - x_c)}{20\cdot\log_{10}(e)}\right)} & \text{if } X_i < x_c \\ e^{\left(\frac{-2\cdot\alpha\cdot(X_i - x_c)}{20\cdot\log_{10}(e)}\right)} & \text{if } X_i > x_c \end{pmatrix} \quad \text{(B3)}$$

The attenuation coefficient, α, and exponent, β, together control the steepness of attenuation with increasing distance. For 69 kHz transmissions in seawater, typical measurements of α are 0.015–0.025 dB·m^{-1} (Leighton 1998). Although attenuation in pure water is less, the effect of suspended sediments and microbubbles can drastically increase attenuation, so overall attenuation may be higher in rivers that contain turbulent flow (Richards et al. 1996). Attenuation in seawater resulting from microbubbles under windy or surf conditions has been measured around 4–5 dB·m^{-1} (Richards and Leighton 2003; Leighton et al. 2004). The exponent β determines the geometrical attenuation of the wavefront through the water as the result of spreading: $\beta = 2$ implies spherical spreading and $\beta = 1$ implies cylindrical spreading, which may be more appropriate for riverine attenuation. Despite the lack of theory to support it, to better fit the data we also chose to consider cases in which β ranges as low as 0.01 to reduce the importance of the geometrical spreading effect (at $\beta = 0$, intensity decreases with distance are solely due to absorptive attenuation). The form of eq. B3 is slightly different than typically presented for intensity attenuation as it involves α in units of dB·m^{-1} rather than Nepers·m^{-1} and so requires the conversion (dB·m^{-1}) = $20\cdot\log_{10}e^1$ (Np·m^{-1}). Parameters were constrained as follows: $0.001 < p_{max} < 1$; $0.01 < \alpha < 4$ dB·m^{-1}; $0.01 < \beta < 2$; $X_1 < x_c < X_m$. (Note that a constraint of $1 \leq \beta \leq 2$ would have resulted in an even poorer fit relative to model $[M_{logit}p_{ping}]$.) Additionally, $p_{ping,i}$ was constrained to be $\in (1.0 \times 10^{-9}, 0.999999999)$.

(*iv*) $[M_{sl\text{-}thr}p_{ping}]$

This is a five-parameter model ($p_{max}, x_c, \alpha, \beta, I_{max}$) that is similar to model *iii* but also includes the parameter I_{max} that allows a threshold effect:

$$p_{ping,i} = p_{max}\begin{pmatrix} \frac{I_{max}e^{\left(\frac{2\cdot\alpha\cdot(X_i - x_c)}{20\cdot\log_{10}(e)}\right)}}{(-(X_i - x_c))^\beta} & \text{if } X_i < x_c \\ \frac{I_{max}e^{\left(\frac{-2\cdot\alpha\cdot(X_i - x_c)}{20\cdot\log_{10}(e)}\right)}}{(X_i - x_c)^\beta} & \text{if } X_i > x_c \end{pmatrix} \quad \text{(B4)}$$

Instead of assuming that p_{ping} is directly proportional to intensity across all tag-to-receiver distances, in this model we assume a uniform p_{ping} out to some distance threshold to either side of x_c, beyond which p_{ping} decreases at a similar rate as in model (*iii*). There is no physical interpretation of I_{max}, but it extends p_{max} out to this threshold distance. Parameters were constrained for numerical estimation purposes: $0.001 < p_{max} < 1$; $0.01 < \alpha < 4$ dB·m^{-1}; $0.01 < \beta < 2$; $1 \leq I_{max}$; $X_1 < x_c < X_m$, as well as $p_{ping,i} \in (1.0 \times 10^{-9}, 0.999999999)$.

Comparison of p_{ping} models

Model $[M_{logit}p_{ping}]$ was the most parsimonious among the five models considered in terms of AIC scores (Table B1). The total number of parameters and total likelihood represent sums over all 4153 crossing sequences (crossing sequences were treated independently when fit-

Table B1. Information-theoretic comparison of p_{ping} models fit independently to 4153 crossing sequences (765 sequences of $n = m = 1$ are excluded), with number of parameters (k), log-likelihood, and AIC values given.

Model	k per sequence	Total k*	Total ln(L)	AIC	ΔAIC
$M_{logit}\,p_{ping}$	4	16 612	–65 814	164 853	0
$M_{norm}\,p_{ping}$	3	12 459	–80 494	185 907	21 054
$M_{lin}\,p_{ping}$	3	12 459	–81 159	187 237	22 384
$M_{ai\text{-}thr}\,p_{ping}$	5	20 765	–73 302	188 134	23 281
$M_{ai}\,p_{ping}$	4	16 612	–90 160	213 543	48 690

*Total parameters are counted as k per sequence × 4135 sequences. Alternative parameter counts of k per sequence × the number of unique sequences in the data set change AIC scores of all models somewhat, but that of $[M_{logit}\,p_{ping}]$ is lowest under either count.

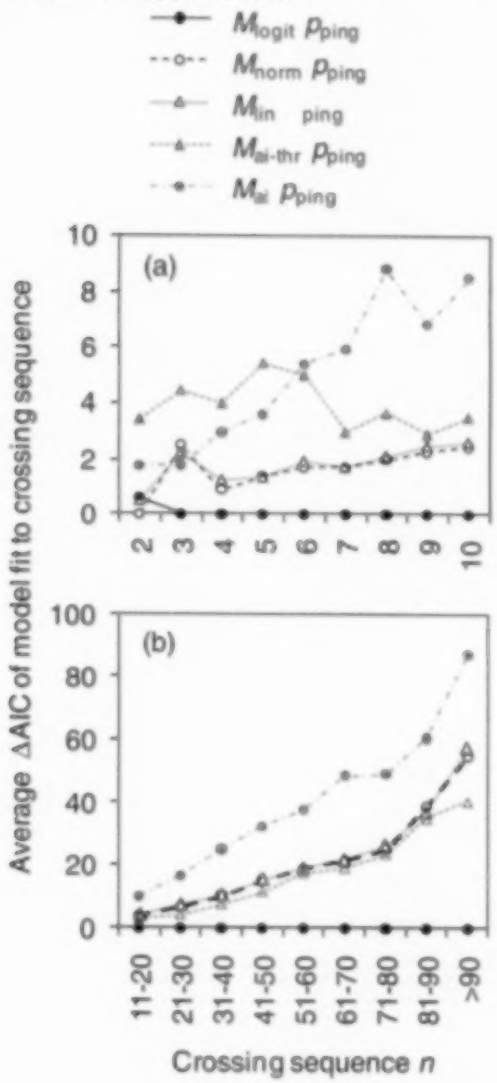

Fig. B1. Average ΔAIC values of p_{ping} attenuation models fit to 4153 crossing sequences, separated by number of detections in sequence: (*a*) n = 2–10; (*b*) n = 11–90+.

ting each model, hence the large AIC and ΔAIC values). Models $[M_{norm}\,p_{ping}]$, $[M_{lin}\,p_{ping}]$, and $[M_{ai\text{-}thr}\,p_{ping}]$ had relatively similar levels of support compared with the large difference between $[M_{logit}\,p_{ping}]$ and these three models (ΔAIC = 21 054 – 23 281). Alternative parameter counts involving the number of unique sequences rather than total sequences change these values and ranking somewhat (ΔAIC = 18 567 for $[M_{ai\text{-}thr}\,p_{ping}]$, 25 768 for $[M_{norm}\,p_{ping}]$, and 27 868 for $[M_{lin}\,p_{ping}]$), but AIC of $[M_{logit}\,p_{ping}]$ is still much lower than these. Model $[M_{ai}\,p_{ping}]$ had the least support among these models.

The number of total parameters estimated varies with sample size, as a set of parameters is estimated for each sequence or unique sequence. To compare models on a per-sequence basis rather than over all sequences, the average AIC can be calculated as AIC/4153, which helps to remove this dependency. The average ΔAIC values for these models are as follows: $[M_{logit}\,p_{ping}]$, 0; $[M_{norm}\,p_{ping}]$, 5.1; $[M_{lin}\,p_{ping}]$, 5.4; $[M_{ai\text{-}thr}\,p_{ping}]$, 5.6; and $[M_{ai}\,p_{ping}]$, 11.7. This ranked pattern of average ΔAIC values generally held across sequences of different length or different numbers of detections (Fig. B1; longer sequences are expected to have greater AIC values as they involve more terms in the log-likelihood summation). For shorter sequences (n = 3–10), $[M_{logit}\,p_{ping}]$ had a lower average AIC than other models and was similar to $[M_{norm}\,p_{ping}]$ and $[M_{lin}\,p_{ping}]$ at n = 2 (Fig. B1*a*). For longer sequences ($n \geq 11$), $[M_{logit}\,p_{ping}]$ performed increasingly better than the other models as n increased (Fig. B1*b*). This ranked pattern also held when crossing sequences were separated by habitat, with $[M_{logit}\,p_{ping}]$ having a lower AIC than all other models in all habitats (not shown; the smallest habitat-specific average ΔAIC was 3.5 for $[M_{norm}\,p_{ping}]$ fit to Fraser River crossing sequences).

References

Leighton, T.G. 1998. Fundamentals of underwater acoustics. *In* Fundamentals of noise and vibration. *Edited by* F.J. Fahy and J.G. Walker. Taylor & Francis, London, UK. pp. 373–444.

Leighton, T.G., Meers, S.D., and White, P.R. 2004. Propagation through nonlinear time-dependent bubble clouds and the estimation of bubble populations from measured acoustic characteristics. Proc. R. Soc. Lond. A Math. Phys. Eng. Sci. **460**(2049): 2521–2550. doi:10.1098/rspa.2004.1298.

Richards, S., and Leighton, T.G. 2003. High frequency sonar performance predictions for littoral operations — the effects of suspended sediments and micro-bubbles. J. Defence Sci. **8**(1): 1–7.

Richards, S.D., Heathershaw, A.D., and Thorne, P.D. 1996. The effect of suspended particulate matter on sound attenuation in seawater. J. Acoust. Soc. Am. **100**(3): 1447–1450. doi:10.1121/1.415991.

Appendix C. Example fits of $[M_{logit}p_{ping}]$ to crossing sequence data

Fig. C1. Four examples of $[M_{logit}p_{ping}]$ model maximum-likelihood fits to crossing sequence data. In each plot, the top row of points represents detections ($p_{ping} = 1$) and the bottom row represents missed transmissions ($p_{ping} = 0$), with the logistic curve ranging between these rows, as in Fig. 1. Crossing sequence data involve the following: (*a*) $n = m = 6$; (*b*) $n = 2$, $m = 4$; (*c*) $n = 35$, $m = 59$; (*d*) $n = 35$, $m = 141$. Note that 20 zeros on either side of X in (*d*) are not shown.

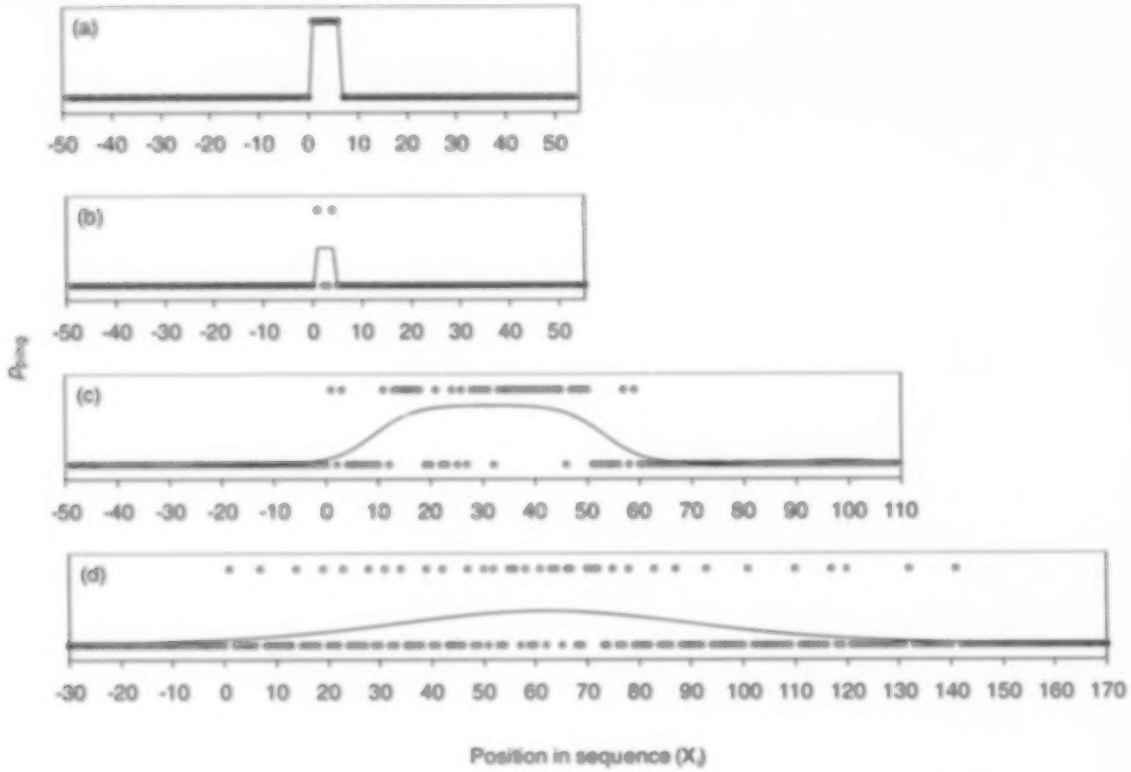

Impact of macroinvertebrate diet on growth and fatty acid profiles of restocked 0+ Atlantic salmon (*Salmo salar*) parr from a large European river (the Allier)

Aurélie Descroix, Christian Desvilettes, Alexandre Bec, Patrick Martin, and Gilles Bourdier

Abstract: The influence of macroinvertebrate diet on growth and fatty acid profiles of Atlantic salmon (*Salmo salar*) parr released at the fry stage in three different riffles was studied in a large temperate river (Allier, France). Comparisons were made between sites and between restocked parr and hatchery-reared counterparts fed with a traditional fish diet. Significant differences were observed along the longitudinal gradient of the river and between restocked and hatchery-reared parr. Growth performance and nutritional status were higher in the hatchery and in downstream riffles and low in the most upstream site. These differences appeared to be related to different types of diet and consequently to variations in polar and neutral lipid intakes. The most favorable site for optimum growth appeared to be the intermediary riffle, with values close to those achieved in the hatchery. Simuliids and baetids, preferentially consumed in downstream sites, constitute an interesting type of food, showing quite different fatty acid composition from vegetable oils. This could be of interest for composing a new diet formula for young salmon intended for river restocking, imitating these macroinvertebrate fatty acid profiles.

Résumé : L'influence de la consommation de proies naturelles sur la croissance et les profils d'acides gras de tacons de saumon atlantique (*Salmo salar*) déversés dans différents radiers a été étudiée sur un grand cours d'eau européen : l'Allier, France. Des comparaisons ont été effectuées entre trois sites de déversement étagés de l'amont vers l'aval, ainsi qu'entre les tacons relâchés et leurs homologues maintenus en salmoniculture et nourris d'aliments artificiels formulés à partir de farines de poissons. Les meilleures performances de croissance et de statut nutritionnel ont été observés en salmoniculture ainsi que dans les radiers aval, tandis que les plus faibles ont été enregistrées sur le radier situé le plus en amont. Ces observations semblent être liées aux différences de régime alimentaire, et par conséquent, à des teneurs variables en lipides neutres et polaires. Le radier le plus favorable à la croissance des tacons semble être le site intermédiaire qui présente des performances proches de celles observées en salmoniculture. En outre, les simulidés et les baetidés, proies préférentiellement consommées dans les sites aval, semblent constituer une nourriture intéressante pour les juvéniles en raison de leurs profils particuliers d'acides gras. Ces diptères pourraient ainsi permettre de formuler de nouveaux aliments artificiels destinés aux tacons de repeuplement.

Introduction

Salmonid farming in France traditionally uses diets based on marine fish meal and oil because farmed species are commonly carnivorous. This is also the case in rearing young Atlantic salmon (*Salmo salar*), even though juveniles and parr are known to be freshwater residents and in their natural environment would encounter a diet consisting mainly of freshwater invertebrates (Thonney and Gibson 1989). However, according to several studies (Ghioni et al. 1996; Sushchik et al. 2003; Torres-Ruiz et al. 2007), the fatty acid (FA) compositions of such insect larvae are quite different from those of the fish oils used in farm diets. Invertebrates showed higher levels of 18:2*n*–6 and 18:3*n*–3, intermediate levels of 20:5*n*–3 and 20:4*n*–6, and lower levels, if any, of 22:6*n*–3 than found in fish-oil based diets. Lipids from freshwater invertebrates consumed by wild salmon parr presented FA profiles closer to those of vegetable oil than of fish oil diets (Bell et al. 1997). However, despite obvious economic and environmental arguments, vegetable oils are still little used in the production of salmon for river restocking: in general, salmonid aquaculture prefers the traditional diet based on marine fish oil.

Studies on anadromous salmonids have shown that the FA composition of wild parr and smolts differs from that of farmed counterparts (Bergström 1989; Ahlgren et al. 1994).

Received 16 March 2009. Accepted 9 February 2010. Published on the NRC Research Press Web site at cjfas.nrc.ca on 12 March 2010. J21105

A. Descroix,[1] **C. Desvilettes, A. Bec, and G. Bourdier.** Clermont Université, Université Blaise Pascal, LMGE, UMR CNRS 6023, Équipe "Fonctionnement des Réseaux Trophiques Aquatiques", F-63177 Aubière CEDEX, France.
P. Martin. Conservatoire National du Saumon Sauvage, 43300 Chanteuges, France.

[1]Corresponding author (e-mail: aurelie.descroix@univ-bpclermont.fr).

Farmed salmon fed with fish oil based diets were particularly rich in *n*–3 highly unsaturated FA (HUFA) and had a high *n*–3 to *n*–6 polyunsaturated FA (PUFA) ratio (Bell et al. 2002), whereas wild parr and farmed parr fed with vegetable oils showed more C_{18} PUFA, less *n*–3 HUFA, and a lower *n*–3 to *n*–6 PUFA ratio (Bell et al. 1998, 2003*b*). However, the most important fact is that these differences in diet may affect parr–smolt transformation (Bell et al. 1997; Bendiksen et al. 2003), a primordial stage in the salmonid life cycle. Fish oil based diets can inhibit the desaturase activity in parr and thus affect smoltification, whereas vegetable oil based diets seem to prevent this inhibition (Tocher et al. 2000). They also seem to enhance the ability of the fish to osmoregulate and thus to adapt to salinity changes (Sargent et al. 1999). Dietary FA must also provide enough energy to ensure sufficient parr growth, whether in the form of monounsaturated FA (MUFA) (mainly 18:1*n*–9, 22:1*n*–9) or other easily catabolized compounds (18:3*n*–3) (Henderson 1996, Bell et al. 2003*b*). Studies on salmonids undergoing parr–smolt transformation also showed that 18:1*n*–9, 22:1*n*–9, 18:3*n*–3, and 18:2*n*–6 were used differently depending on their contribution to different dietary formulae (Tocher et al. 2000; Bendiksen et al. 2003). They can be used as selective substrates either for β-oxidation and (or), in the case of both 18:3*n*–3 and 18:2*n*–6, for bioconversion into HUFA when dietary 22:6*n*–3 and 20:4*n*–6 are insufficient (Henderson 1996; Bell et al. 1997). It therefore seems wasteful to continue to use marine fish oil diets to raise young salmon for river restocking.

In the wild, just a few insect orders (Diptera, Ephemeroptera, Plecoptera, and Trichoptera) are consumed by parr due to special habitat (riffle), morphological, and energetic constraints (Wankowski and Thorpe 1979; Keeley and Grant 1997). Moreover, the diversity and composition of available prey, which have been shown to vary along the upstream–downstream gradient in a large European river (Descroix et al. 2009), could affect parr lipid metabolism. Kaushik et al. (2006) observed that differences in prey diversity between the upper and lower reaches of the River Nivelle could explain the upstream–downstream differences in FA composition recorded in parr. This means that freshwater invertebrates are more diverse in their FA composition than is generally thought, a fact that recent studies tend to confirm (Sushchik et al. 2007; Torres-Ruiz et al. 2007). Mainly MUFA and PUFA content differed among macroinvertebrate taxa. In addition, Trichoptera (Hydropsychidae) and Ephemeroptera (Ephemerillidae) exhibited high percentages of *n*–3 FA (e.g., eicosapentaenoic acid: 10%–23%) and low percentages of *n*–6 FA, while Diptera (Chironomidae) and Oligochaeta generally had low percentages of 18:2*n*–6 and 18:3*n*–3 (Ghioni et al. 1996; Torres-Ruiz et al. 2007). Young salmon will therefore encounter different dietary FA intakes from one site to another, which could affect growth, overwintering, and subsequent smoltification in the wild (Nordgarden et al. 2002).

In this context, the objective of the present study was to investigate the dietary origin of the main FA accumulated by restocked *S. salar* parr during their high-growth period, which will be involved in overwintering and further migration processes. The influence of natural food (aquatic macroinvertebrates) on salmon growth and the FA composition of whole-body neutral lipids (NL) and polar lipids (PL) was analyzed. Emphasis was placed on 16:0 (known to be incorporated into PL), 16:1*n*–7, 18:1*n*–9 (used as oxidation substrate for energy; Bell et al. 1997), and C_{18} PUFA, 20:4*n*–6, 20:5*n*–3, and 22:6*n*–3 (regarded as essential dietary FA). The study was undertaken in three restocking riffles located along the upstream–downstream gradient in the River Allier (France), but comparisons were also performed between hatchery-reared parr fed with a traditional diet based on marine fish oil and the restocked parr from the same broodstock (Chanteuges salmon hatchery). Our aim was to evaluate the importance of natural food, where FA composition varies over time and between sites, compared with hatchery feed, where composition is constant.

Materials and methods

Study sites

The study was undertaken from June to October 2006 in the River Allier, which belongs to the upstream river network of the Loire basin (France) (Fig. 1). The Loire–Allier axis is famous for its wild salmon population, the last in Europe able to make long-distance migration in freshwater (900 km). The wild population is therefore reinforced by restocking the river with 0+ parr (in May) and 1+ smolts (in April) from the Chanteuges salmon hatchery (Haute-Loire, France; see Fig. 1).

Our sampling sites were located in Haut-Allier, the upper part of the River Allier, historically known as a natural breeding area for *S. salar*. There, the river is a fourth- to fifth-order stream (Strahler 1957) with a watershed of 2900 km^2. Three sites were selected according to their upstream–downstream distribution along the river's longitudinal gradient. Site 1 offers middle-rhithron habitats belonging to the trout zone (Huet 1959). Site 2 is located in the grayling zone with lower-rhithron stream characteristics. Site 3 is typical of the upper-potamon fluvial areas located in the barbel zone. Sampling was only performed in riffles where no natural spawning had been observed during the previous autumn (2005). A detailed description of riffle habitats in each site can be found in Descroix et al. (2009).

Fish rearing and field sampling

Fish samples

All parr analyzed in this study originated from artificial spawning of wild *S. salar* caught each autumn in the River Allier. In the Chanteuges salmon hatchery (see Fig. 1) and after yolk sac resorption, juveniles were reared in circular 400 L fibreglass tanks with 18 000 fish per tank. Constant water flow (pumped from the River Allier) and a current speed of 8–10 $cm \cdot s^{-1}$ in the periphery and close to 0 $cm \cdot s^{-1}$ in the center were maintained in all tanks under natural photoperiod. Fish were fed to apparent satiation eight times daily with commercial pelleted food (Nutra HP 0.3, Skretting, France). This diet contains 57% crude protein, 17% lipids, 8.5% carbohydrates, 10% ash, 0.5% cellulose, 1.3% phosphorus, and 19.9 $MJ \cdot kg^{-1}$ digestible energy.

In May, an initial sample of these juvenile farm salmon (15 fish, total length ranging from 3 to 4 cm) was collected prior to the beginning of the experiment. Remaining juveniles were

Fig. 1. Prey relative abundance in the stomachs of Atlantic salmon parr sampled in three riffles from the upper River Allier. Prey items: hatched, others; black, baetids; grey, simuliids; white, chironomids; ND, no data. Sampling riffles (stars) are located on the map as site 1, site 2, and site 3. The circle indicates the location of the Chanteuges salmon hatchery. (Modified from Descroix et al. 2009.)

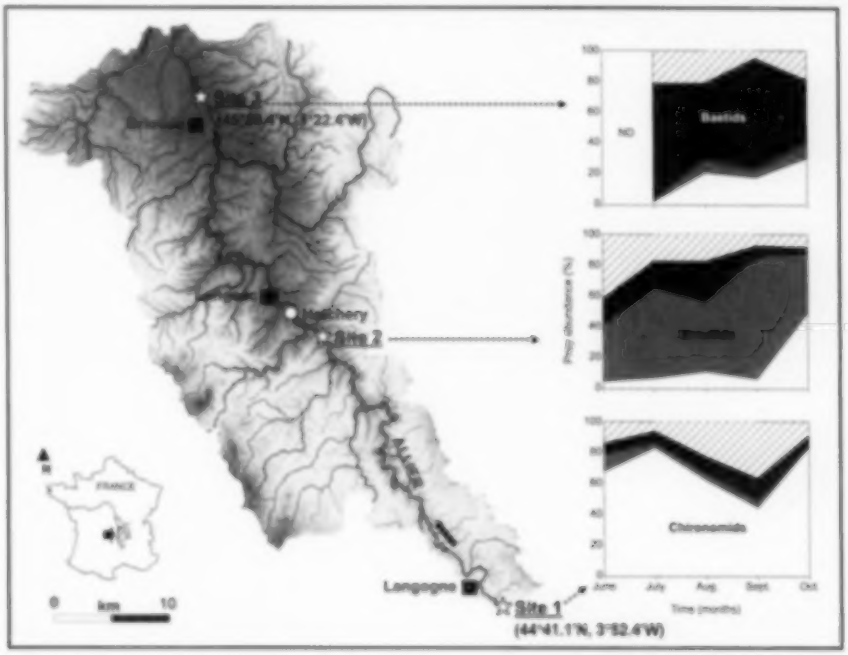

then restocked in the river, except for one batch, which was isolated from the rest and randomly divided between three 1000 L tanks containing 1250 fish each, i.e., hatchery-reared. Their diet consisted of fish oil based pellets (Nutra HP 1.0, Skretting, France) containing 53% crude protein, 19% lipids, 10.5% carbohydrates, 10% ash, 0.5% cellulose, 1.3% phosphorus, and 20.1 MJ·kg^{-1} digestible energy (more details of the FA composition of this artificial diet are given in Table 1). Parr were fed six times a day until the end of the experiment (October). A mean of seven reared salmon were collected each month from June to October. All fish were anaesthetized and immediately frozen in liquid nitrogen prior to lyophilization, dry weight determination, and lipid analysis.

All other batches of juveniles were released in the river in late May 2006. In the three selected riffles, release densities were around 10–15 fry·m^{-2}. After 3 weeks of acclimatization, sampling started and was conducted monthly during the same period as for hatchery-reared parr (June–October). At each site and date, six to nineteen 0+ parr were captured by backpack electrofishing. Stomach contents were extracted by pulsed gastric lavage and diet materials were preserved in 4% formaldehyde. A total of 130 restocked parr were thus collected, of which 69 were immediately frozen in liquid nitrogen pending lyophilization, dry weight determination, and lipid analysis.

Stomach content analysis and macroinvertebrate samples

Restocked salmon food items were identified and enumerated under a binocular microscope. Macroinvertebrate prey were identified to the genus level for Diptera, Ephemeroptera, and Trichoptera and to the family level for other taxa. Each item's contribution to stomach fullness was described as percentage prey abundance (%A_i) (Amundsen et al. 1996):

$$\%A_i = (\Sigma S_i/\Sigma S_t) \times 100$$

where S_i is the stomach content (in this case, number) for prey i and S_t is the total stomach content for all prey categories in the fish. Although prey proportions varied between sites, baetid nymphs and chironomid and simuliid larvae predominated over the survey as a whole (Descroix et al. 2009), and these three families were therefore specifically analyzed for FA composition. They were collected from a minimum of four locations within each riffle using a Surber benthic sampler fitted with a 250 µm mesh net. All sampled macroinvertebrates were kept overnight in a tank filled with river water at 4 °C to achieve gut clearance. The next morning, all baetid, chironomid, and simuliid specimens were carefully hand-sorted and counted. Specimens of each family were pooled in preweighed vials to obtain appropriate biomass for lipid analysis. When possible, three replicated samples were formed for each taxon, freeze-dried, weighed (Mettler AE163 electrobalance, sensitivity 0.001 mg), and stored at –40 °C prior to lipid extraction.

Lipid analysis

Lipids were analyzed in whole salmon parr, natural food (insect larvae), and artificial pellets. Total lipids were extracted with chloroform–methanol according to the method of Folch et al. (1957). For each sample, NL were separated from PL (mainly phospholipids) in prepacked solid-phase silica columns (SPE Strata NH_2). Columns were precondi-

Table 1. Fatty acid composition (weight % of total fatty acids) in total lipids extracted from commercial pellets and freshwater invertebrates.

Fatty acid	Nutra pellets	Baetids	Simulids	Chironomids	*P*
14:0	6.19±0.10a	2.55±0.32b	1.32±0.10d	3.99±0.21c	<0.001
16:0	17.73±0.20a	25.43±2.42b	20.83±0.48ab	17.44±0.36a	<0.01
18:0	3.48±0.00a	10.67±2.25b	7.41±0.41ab	11.20±0.83b	<0.001
Total SFA	30.13±0.30a	41.84±3.50b	36.71±0.84ab	39.91±1.06b	<0.01
14:1	0.06±0.00a	0.04±0.02a	4.53±0.33b	0.58±0.08a	<0.001
16:1*n*–7	6.47±0.10a	10.36±1.33b	9.88±0.34ab	7.30±0.48ab	<0.05
18:1*n*–9	9.71±0.40a	4.14±0.48b	11.99±0.46d	6.28±0.33c	<0.001
18:1*n*–7	2.53±0.10a	5.37±0.63b	3.86±0.24b	2.43±0.22a	<0.001
20:1*n*–9	2.91±0.40a	0.06±0.02b	0.15±0.04b	0.14±0.05b	<0.001
22:1*n*–9	3.14±0.10a			0.03±0.01b	<0.001
22:1*n*–7	0.09±0.00a				<0.001
Total MUFA	25.67±1.30a	22.12±1.68b	31.35±0.82c	20.33±0.59b	<0.001
16:2*n*–4	1.00±0.10a	10.84±4.57b	0.38±0.07a	1.65±0.24a	<0.01
16:3*n*–4	1.29±0.10a	0.22±0.06b		0.53±0.06c	<0.001
16:4*n*–3	0.17±0.01a	0.13±0.04a	0.12±0.03a	0.86±0.11b	<0.001
18:2*n*–6	8.47±0.10a	1.96±0.25b	5.18±0.27d	7.09±0.28c	<0.001
20:2*n*–6	0.17±0.01ab	0.10±0.09 b	0.08±0.03b	0.55±0.17a	<0.05
20:4*n*–6	0.82±0.01a	0.55±0.15a	2.27±0.32b	0.77±0.09a	<0.001
Total *n*–6 PUFA	10.16±0.10a	2.91±0.38b	8.01±0.45c	9.07±0.39ac	<0.001
18:3*n*–3	1.33±0.00a	7.74±1.25b	9.48±0.71b	17.12±0.84c	<0.001
18:4*n*–3	2.24±0.10a	0.76±0.13b	0.92±0.06b	0.89±0.10b	<0.001
20:4*n*–3	0.62±0.00a	0.11±0.04b	0.10±0.02b	0.52±0.12a	<0.001
20:5*n*–3	12.27±0.60a	7.49±0.99b	10.60±0.40a	6.33±0.48b	<0.001
22:5*n*–3	1.43±0.10a				<0.001
22:6*n*–3	10.30±0.60a		0.06±0.02b		<0.001
Total *n*–3 PUFA	29.13±0.20a	17.17±1.83b	21.31±0.84bc	25.90±1.11ac	<0.001
Total PUFA	43.73±0.50a	32.42±3.88b	31.14±1.08b	38.74±0.95ab	<0.01
n–3/*n*–6	2.87±0.10	11.78±5.05	2.85±0.17	2.98±0.24	0.08
Unidentified	0.48±0.01	3.64±2.39	0.79±0.22	1.04±0.25	0.24

Note: Values are mean ± SE. Sites and months are pooled and results of ANOVA are shown. Different letters indicate significant differences between each type of food. SFA, saturated fatty acids; MUFA, monounsaturated fatty acids; PUFA, polyunsaturated fatty acids.

tioned with hexane and total lipid extract dissolved in chloroform was then added. The NL fraction was eluted with chloroform–2-propanol (2:1 *v/v*) and PL were eluted with diethylether–acetic acid (100:2 *v/v*) followed by methanol. After solvent evaporation, lipid extracts were methyled with BF_3 (14% *w/v* in methanol) to convert FA into their corresponding methyl esters (FAME). Samples were heated at 100 °C for 45 min, resuspended in hexane, and concentrated under N_2. FAME were separated and analyzed on a Chrompack CP9001 gas chromatograph fitted with a Supelco Omegawax column and an FID detector (split injection; injector temperature 260 °C, carrier gas helium, oven rise from 140 to 245 °C at 3 °C·min^{-1}). Individual FAME were identified by comparing retention times with those obtained from Supelco and our own laboratory standards and quantified using 13:0 as internal standard added just before FA derivatization. Peaks registering less than 0.1% of total area were considered nondetected. GC/MS was used to confirm identification of some FA. FAME were injected in a GC6850 Agilent gas chromatograph fitted with a 5975B Agilent mass spectrometer. Spectra separated with a DB wax column were identified using our own spectrum library and the American Oil Chemists' Society's lipid library (http://www.lipidlibrary.co.uk).

Data analysis

The statistical analyses were performed on the most important encountered FA: 16:0, 16:1*n*–7, and 18:1*n*–9, known as a specific oxidation substrate for energy especially during the seaward migration, 18:2*n*–6, which is converted into 20:4*n*–6, and 18:3*n*–3, which is elongated and desaturated to 20:5*n*–3 and then to 22:6*n*–3 (Tocher et al. 2000; Bell et al. 2003*a*; Bendiksen et al. 2003). FA 20:4*n*–6 and 20:5*n*–3 are involved in eicosanoid synthesis and therefore in adaptation to salinity changes (Sargent et al. 1999).

Means and standard errors were calculated to characterize FA concentrations (milligrams per gram dry weight) in farmed and restocked parr, commercial pellets, and natural prey. Site/hatchery, date, and invertebrate taxon effects were analyzed by analysis of variance (ANOVA) followed where appropriate by Tukey's post hoc test to determine significant differences. All data were checked for normality and variance homogeneity before analysis and log transformed when necessary. Discriminant function analysis was

performed to differentiate parr groups that tended to have similar FA concentrations according to growth period location (hatchery, site 1, site 2, or site 3). One discriminant function analysis was performed for FA in NL and another for FA in PL. All statistical analyses used XLStat-Pro software (Addinsoft, Paris, France). Differences were considered significant at $P < 0.05$.

Results

Feeding, growth, and total FA content in farmed and restocked parr

Feeding

Over the entire survey, 25 prey taxa, mostly aquatic insects (mean = 99%), were identified in parr stomachs. In the three riffles, the predominant prey were Diptera larvae (A_i = 72% on average) and Ephemeroptera nymphs (A_i = 22%) (Fig. 1). More specifically, chironomid larvae (Orthocladiinae, Chironominae, and Tanypodinae) provided major contributions to salmon diet in site 1 (A_i = 71%), simuliid larvae (*Simulium* and *Prosimulium*) in site 2 (A_i = 58%), and baetid nymphs (*Baetis rhodanii*, *Acentrella sinaica*, and *Procloeon bifidum*) in site 3 (A_i = 60%). Others prey items, such as Coleoptera (*Elmis*), Gastropoda (*Ancylus fluviatilis*), Oligochaeta, Plecoptera (*Capnia* spp. and Leuctridae), and Trichoptera (*Psychomyia pusilla*, *Hydropsyche* spp., and *Rhyacophila* sensu stricto), were also consumed but generally constituted no more than an average of 14% of the diet and were therefore regarded as secondary or occasional prey (Fig. 1).

Growth

Significant variation in mean parr dry weight (Fig. 2) was found between restocking riffles and hatchery (ANOVA and post hoc Tukey's tests: $F_{[3,\ 172]} = 16.60$, $P < 0.01$). At the end of the survey, the maximum dry weights were reached in sites 2 (2.12 ± 0.24 g) and 3 (1.83 ± 0.32 g), with lower values in the most upstream site, site 1 (0.64 ± 0.06 g). In the hatchery, the maximum dry weight of reared fish was greater than for restocked fish, reaching 4.31 ± 1.09 g in October ($F_{[3,\ 31]} = 6.89$, $P < 0.01$). Furthermore, it is of interest to note that growth in the intermediate riffle (site 2) was the closest to that observed in the hatchery, although individual dry weight increased more regularly in the latter. Significant monthly variations were also recorded in each restocking riffle and hatchery tank ($F_{[5,\ 172]} = 18.36$, $P < 0.01$): growth rates were low during the first 2 months after restocking (June and July) and increased over time as of July (Fig. 2).

Total FA content

During the 2 months following restocking, NLFA storage (milligrams per gram dry weight) was higher in hatchery-reared parr than in restocked fish in any riffle (ANOVA and post hoc Tukey's tests: $F_{[3,\ 122]} = 20.48$, $P < 0.01$) (Fig. 2). On the other hand, at the end of the study, no significant differences in NLFA amounts were observed between restocking riffles and hatchery salmon ($F_{[3,\ 13]} = 2.46$, $P = 0.12$). Significant monthly variations were observed in fish from each restocking riffle and from the hatchery ($F_{[5,\ 75]} = 23.96$, $P < 0.01$). After a marked decrease between May and June, these FA increased and stabilized around 28 mg·g dry weight^{-1} in all sites except in site 3 (16 mg·g dry weight^{-1}) (Fig. 2).

PLFA relative concentrations decreased from May to August in the hatchery and in each restocking riffle ($F_{[5,\ 74]} = 42.55$, $P < 0.01$). At the end of the survey, PLFA contents in farmed fish were the closest to those observed in site 2, i.e., slightly lower than in fish growing in sites 1 and 3 (Fig. 2).

FA analysis of natural food versus commercial pellets

The FA composition of total lipids extracted from each type of food (prey and commercial pellets) is shown in Table 1. Saturated FA represented 30% of total FA in Nutra pellets and more than 36% in invertebrate prey. FA 16:0 was the predominant saturated FA, ranging between 17% and 25%, with quite similar proportions in Nutra pellets and chironomid and simuliid larvae (around 17%–21%). FA 18:0 was also present but at smaller values and was more abundant in insect larvae (7%–11%).

MUFA generally represented 20%–32% of total FA in all diets. FA 16:1*n*–7 was the most abundant MUFA in both baetids and chironomids, while 18:1*n*–9 predominated in both hatchery diet and simuliids. Significant differences were also recorded with 20:1*n*–9 and 22:1*n*–9, which were present in pellets (2%–3%) but were found in low or negligible concentrations in insect larvae (Table 1).

PUFA were more abundant in the hatchery (44% of total FA) compared with wild diets (31%–39%). FA 18:2*n*–6 was detected in low proportions in baetids (<2%) and in larger proportions in pellets (8%), chironomids (7%), and simuliids (5%). FA 18:3*n*–3 was found in greater percentages in invertebrates (7%–17%), especially chironomids, than in hatchery diet (<2%). In contrast, 18:4*n*–3 was observed in negligible proportions in larvae and represented just 2% of the total FA in pellets. Negligible proportions of 20:4*n*–6 were also found in all diets, except in simuliids (2%). On the other hand, 20:5*n*–3 was present in abundance, particularly in hatchery diet and simuliids (11%–12%). In baetids and chironomids, this component represented 6%–7% of total FA. The most remarkable differences were observed for 22:6*n*–3: Nutra pellets showed about 10 times as much 22:6*n*–3 as did insect larvae, which seemed to contain only small proportions or none at all. In general, *n*–3 PUFA were always more abundant than *n*–6 PUFA in all types of diet. The sums of *n*–3 and *n*–6 PUFA, however, were higher in pellets and chironomids than in other diets, although the *n*–3 to *n*–6 ratio showed no significant difference between types of food (Table 1).

NLFA and PLFA compositions of farmed and restocked parr: differences and temporal changes

Based on the eight selected FA (16:0, 16:1*n*–7, 18:1*n*–9, 18:2*n*–6, 18:3*n*–3, 20:4*n*–6, 20:5*n*–3, and 22:6*n*–3), discriminant function analysis differentiated groups of parr that tended to have similar FA concentrations in NL and PL (Fig. 3). In NLFA and PLFA, the first two discriminant analysis functions explained 97% and 100% of intergroup variance, respectively (NLFA: Wilks' $\lambda = 0.00$, $P < 0.01$; PLFA: Wilks' $\lambda = 0.01$, $P < 0.01$). In NLFA, 79% of the variance was observed on the first discriminant function and

Fig. 2. Mean temporal changes (May–October) in (*a*) dry weights and mean amounts of total fatty acids extracted from (*b*) neutral lipids (NLFA) and (*c*) polar lipids of hatchery-reared Atlantic salmon parr and restocked parr (sites 1–3). Results of two-way ANOVA and Tukey's post hoc tests are shown with different letters indicating significant differences between months in each site. ND, no data.

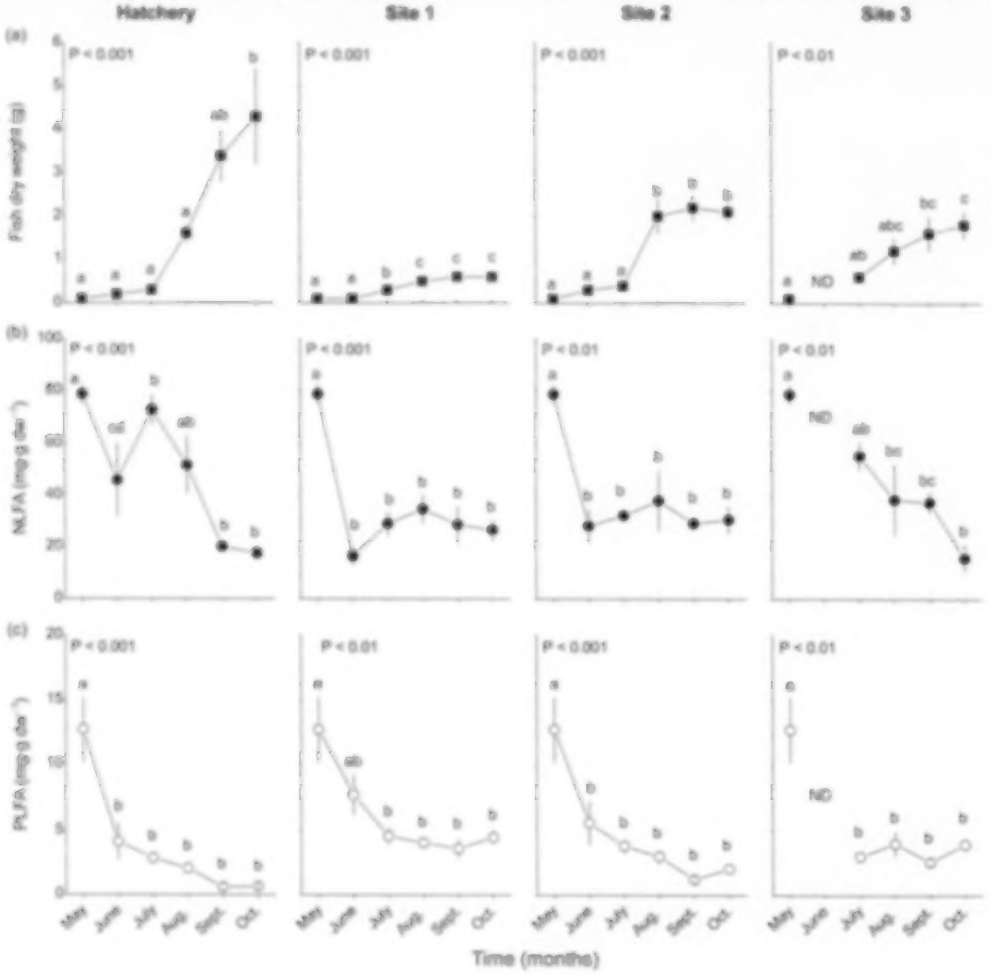

Fig. 3. First two components of the discriminant function analysis with individual fatty acids (mg·g dry weight^{-1}) extracted from Atlantic salmon (*a*) neutral lipids and (*b*) polar lipids as covariates and sample location (hatchery and sites 1–3) as grouping variable.

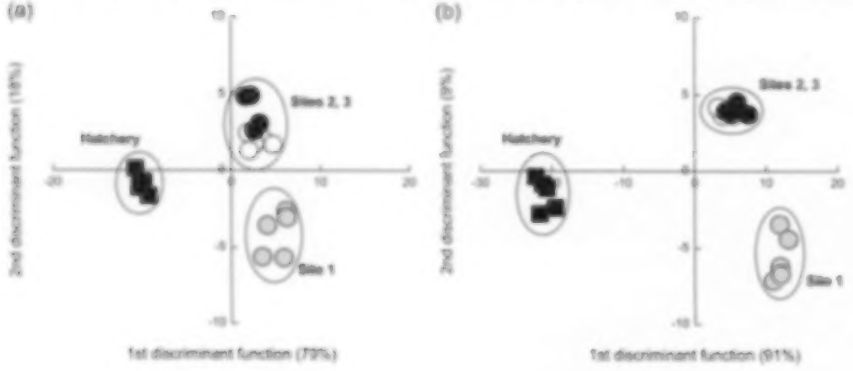

separated the FA concentrations of parr fed with Nutra pellets in the hatchery from those released in the upper Allier riffles. The second discriminant function showed a less pronounced difference (18% of intergroup variance), discriminating the FA composition of salmon collected in the most upstream riffle (site 1) from those sampled in the other sites (sites 2 and 3). These same significant differences were observed with PLFA, the first axis explaining 91% of intergroup variance and the second axis 9%. Thus, some NLFA and PLFA showed significantly different evolution between hatchery-reared parr and their counterparts released in riffles (Fig. 3).

At the beginning of the survey (June–July), the concentrations of 18:1*n*–9, 18:2*n*–6, 20:5*n*–3, and 22:6*n*–3 appeared to be higher in the NL of farmed than in those of restocked parr (Fig. 4). The same trend was observed with 16:0, 16:1*n*–7, and 20:4*n*–6, although not significant in these cases. On the other hand, farmed parr contained smaller amounts of 18:3*n*–3 (0.69 ± 0.11 mg·g dry weight^{-1}) in their NL in June–July than did those released in riffles (range 2.03 ± 0.80 to 6.98 ± 1.50 mg·g dry weight^{-1}). At the end of the study (in October), these values did not show significant differences between farmed and restocked parr, except for 18:1*n*–9, 18:3*n*–3, and 20:4*n*–6. FA 18:1*n*–9 was more abundant in NL of farmed (3.06 ± 0.38 mg·g dry weight^{-1}) than in those of restocked parr (range 1.22 ± 0.39 to 2.16 ± 0.36 mg·g dry weight^{-1}). Restocked parr contained significantly higher amounts of 18:3*n*–3 (range 1.39 ± 0.51 to 3.42 ± 0.85 mg·g dry weight^{-1}) and 20:4*n*–6 (range 0.21 ± 0.09 to 0.39 ± 0.06 mg·g dry weight^{-1}) than farmed parr (0.16 ± 0.03 and 0.13 ± 0.02 mg·g dry weight^{-1}, respectively) (Fig. 4).

For PLFA, no significant differences were recorded from June to July between hatchery and restocked salmon, except for 18:2*n*–6, 18:3*n*–3, and 20:5*n*–3 (Fig. 5). Restocked parr showed higher levels of these PUFA than did farmed parr. In October, on the other hand, all of the various FA were more abundant in restocked than in farmed parr. Moreover, these FA concentrations seemed to be higher in the first riffle (site 1) than in the others, except for 20:5*n*–3 (Fig. 5).

Diet effects on FA composition in farmed and restocked salmon parr

The potential contribution of the NLFA and PLFA supply of the different foods (Nutra pellets and insect larvae) eaten by salmon parr in the hatchery and natural reaches during the entire survey is shown in Fig. 6. In the hatchery, all FA were primarily provided in the form of NL in pellets, except 18:2*n*–6 which, was also provided as PL (1.49 mg·g dry weight^{-1}). For parr collected in riffles, a significant proportion of FA came from NL prey (chironomids in site 1, simuliids in site 2, and baetids in site 3) but also from PL prey, especially in sites 2 and 3. Moreover, in these sites, FA were provided as PL by more than one type of prey. NL 16:0 and NL 16:1*n*–7 were particularly abundant in the prey predominating in the stomach contents of restocked parr from sites 2 and 3. In contrast, their contribution remained lower in parr from site 1 and hatchery, especially with respect to PL input. The second MUFA, 18:1*n*–9, was strongly represented in the NL of artificial food. It was also found in large quantities in the NL and PL of simuliids and markedly in the PL of baetids ingested by parr from site 2. Concerning *n*–3 PUFA, the main difference was observed for 18:3*n*–3 and 22:6*n*–3. PUFA 18:3*n*–3 was, logically, recorded in small quantities in pellets but was found in abundance in the natural diet of restocked parr, especially in the first riffle, in the form of either NL or PL. In contrast, 22:6*n*–3 was absent from macroinvertebrate NL and PL (Table 1). PUFA 20:5*n*–3 was provided in large quantities by the NL from Nutra pellets and chironomid larvae, whereas huge quantities of 20:5*n*–3 were detected in the PL from baetids and simuliids consumed by parr from site 2 and to a lesser extent from site 3. Finally, for *n*–6 PUFA, diet was rich in 18:2*n*–6 whatever the place of growth (hatchery or riffles), whereas only simuliids ingested by parr in site 2 provided significant amounts of 20:4*n*–6, in the form of both PL and NL (Fig. 6).

Discussion

Despite the variety of prey potentially available in the riffle habitats of the River Allier, only three prey families predominated in the stomach contents of restocked *S. salar* parr: baetid nymphs and chironomid and simuliid larvae. These macroinvertebrate prey have been reported as being a major part of salmon parr diet in numerous studies undertaken in reaches of temperate and northern streams (Thonney and Gibson 1989; Keeley and Grant 1997). However, 0+ parr feeding varied in the River Allier along the upstream–downstream gradient. Thus, chironomid larvae were the predominant prey ingested in the upstream riffle (site 1), simuliid larvae in the intermediary riffle (site 2), and baetid nymphs in the downstream riffle (site 3). In sites 1 and 2, parr fed mostly on larvae that predominated in the benthic fauna in terms of numerical abundance (chironomids or simuliids; Descroix et al. 2009). This was not the case in the last riffle (site 3) where the main prey ingested (baetids) was a significant but not predominant taxon in the benthos (Descroix et al. 2009). The importance of secondary prey as a source of FA could not be taken into account in the present study. However, apart from two site-specific sampling dates (September for site 1 and June for site 2), all secondary prey taken together never exceeded 20% of the diet.

Significant variations in parr growth performance and NLFA contents were observed between riffles and between parr reared in the hatchery and those released in the river. Such differences suggest variable growth conditions along the longitudinal gradient of the river sufficient to influence body composition. This could primarily be related to differences in the type of prey ingested as well as differential energy expenditure linked to intra- and interspecies competition (Descroix et al. 2009). It is only at the beginning of the study (June–July) that restocked parr accumulated less NLFA than hatchery-reared salmon. This could not be attributed to difficulties encountered in prey capture by inexperienced released juveniles. According to Reiriz et al. (1998), naïve restocked salmon parr acquire in 6–7 days, the appropriate prey selection criteria usually exhibited by their wild counterparts. From a nutritional viewpoint, it is likely that the type of prey ingested influenced the growth of restocked salmon along the longitudinal gradient in the present study. But, it is difficult to attribute these growth

Fig. 4. Monthly variations in the average amounts of fatty acids extracted from neutral lipids of hatchery-reared Atlantic salmon parr and restocked parr (sites 1–3). Results of two-way ANOVA and Tukey's post hoc tests are shown with different letters indicating significant differences between months in each site. ND, no data.

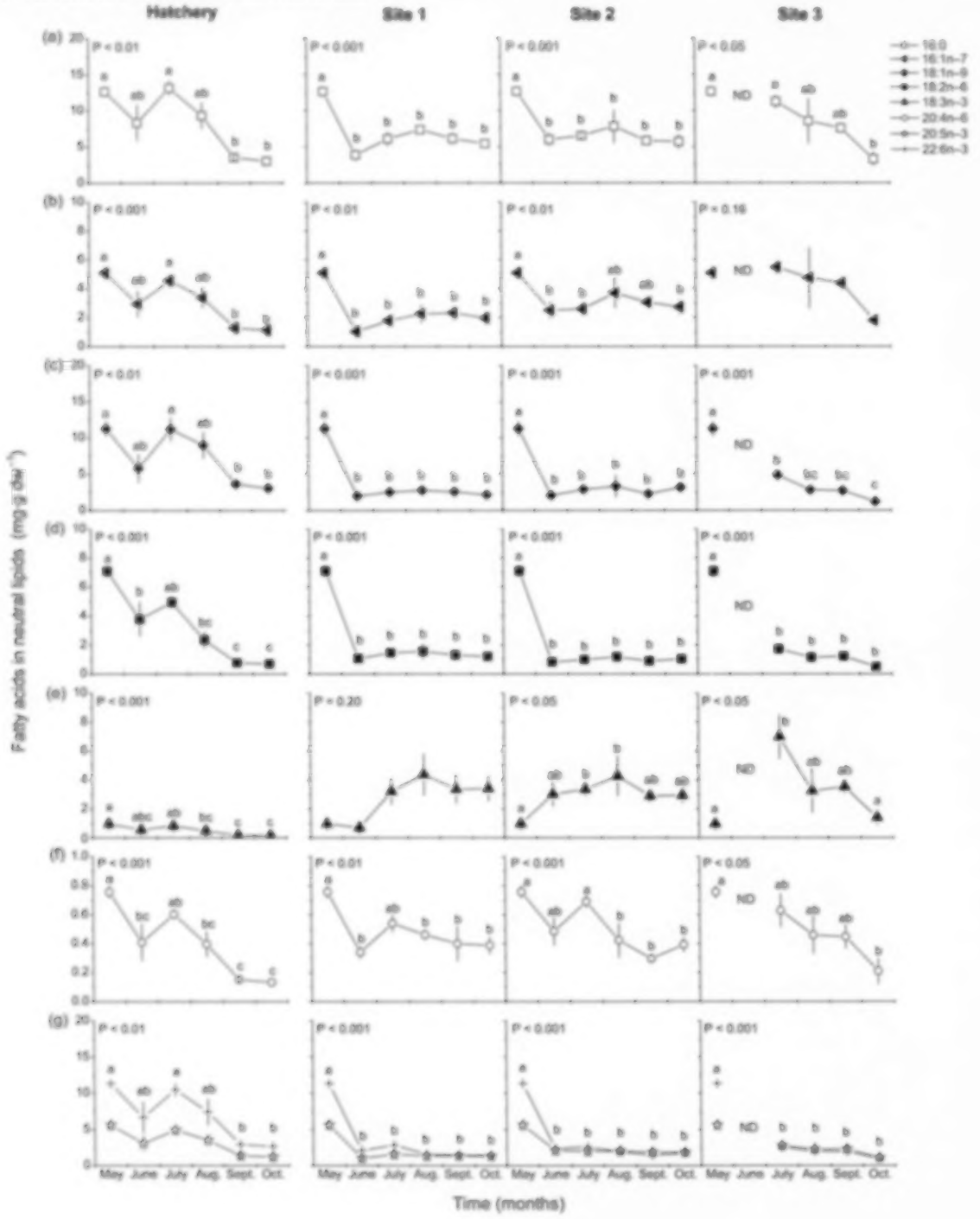

Fig. 5. Monthly variations in the average amounts of fatty acids extracted from polar lipids of hatchery-reared Atlantic salmon parr and restocked parr (sites 1–3). Results of two-way ANOVA and Tukey's post hoc tests are shown with different letters indicating significant differences between months in each site. ND, no data.

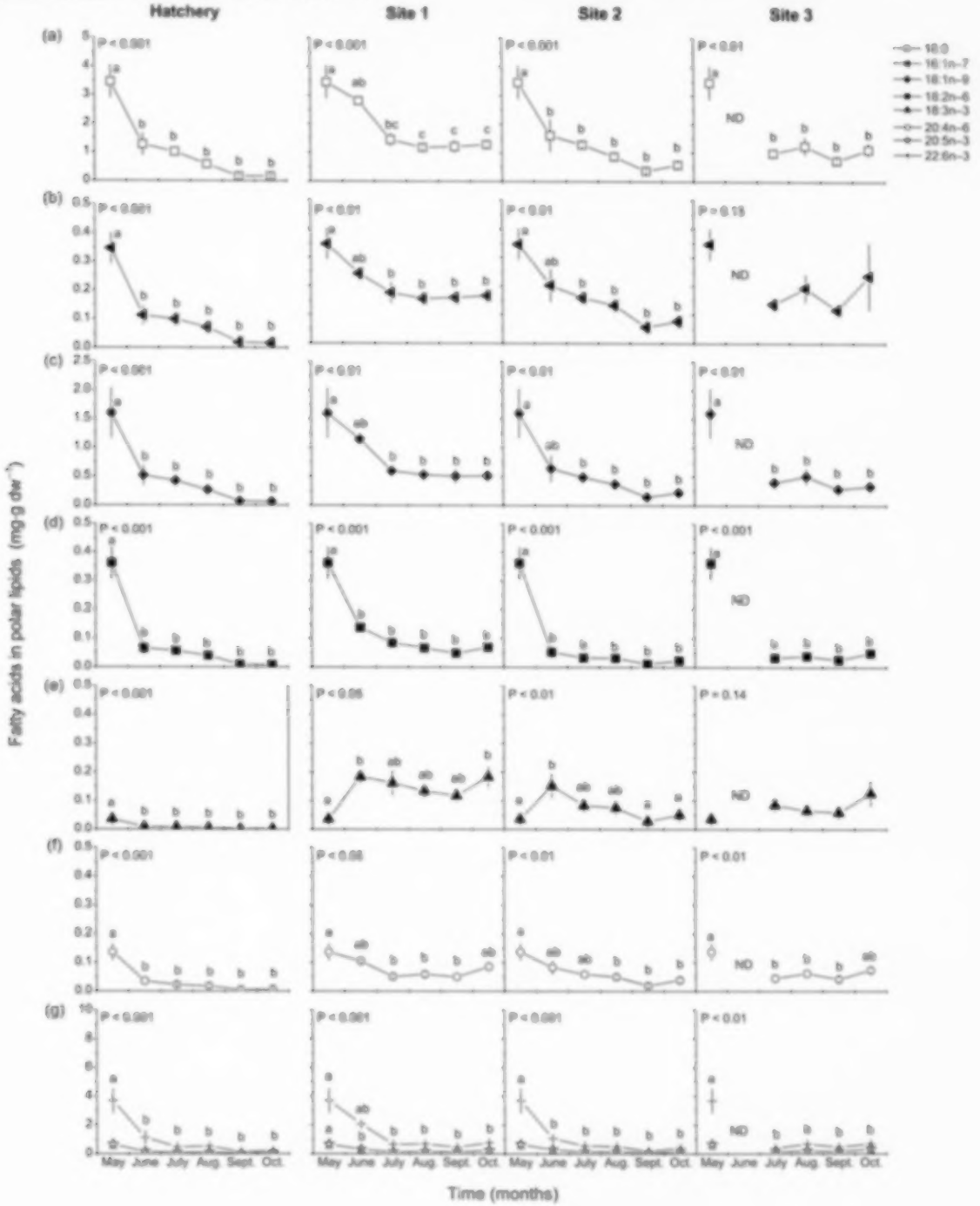

Fig. 6. Mean selected dietary fatty acid inputs from commercial pellets (left column, hatchery) and from the three predominant macroinvertebrate prey (right columns, sites 1–3). For macroinvertebrates, values were recalculated as a function of the average proportion of each prey type encountered throughout the survey in the stomach contents of parr from sites 1–3. NLFA, neutral lipid fatty acids; PLFA, polar lipid fatty acids.

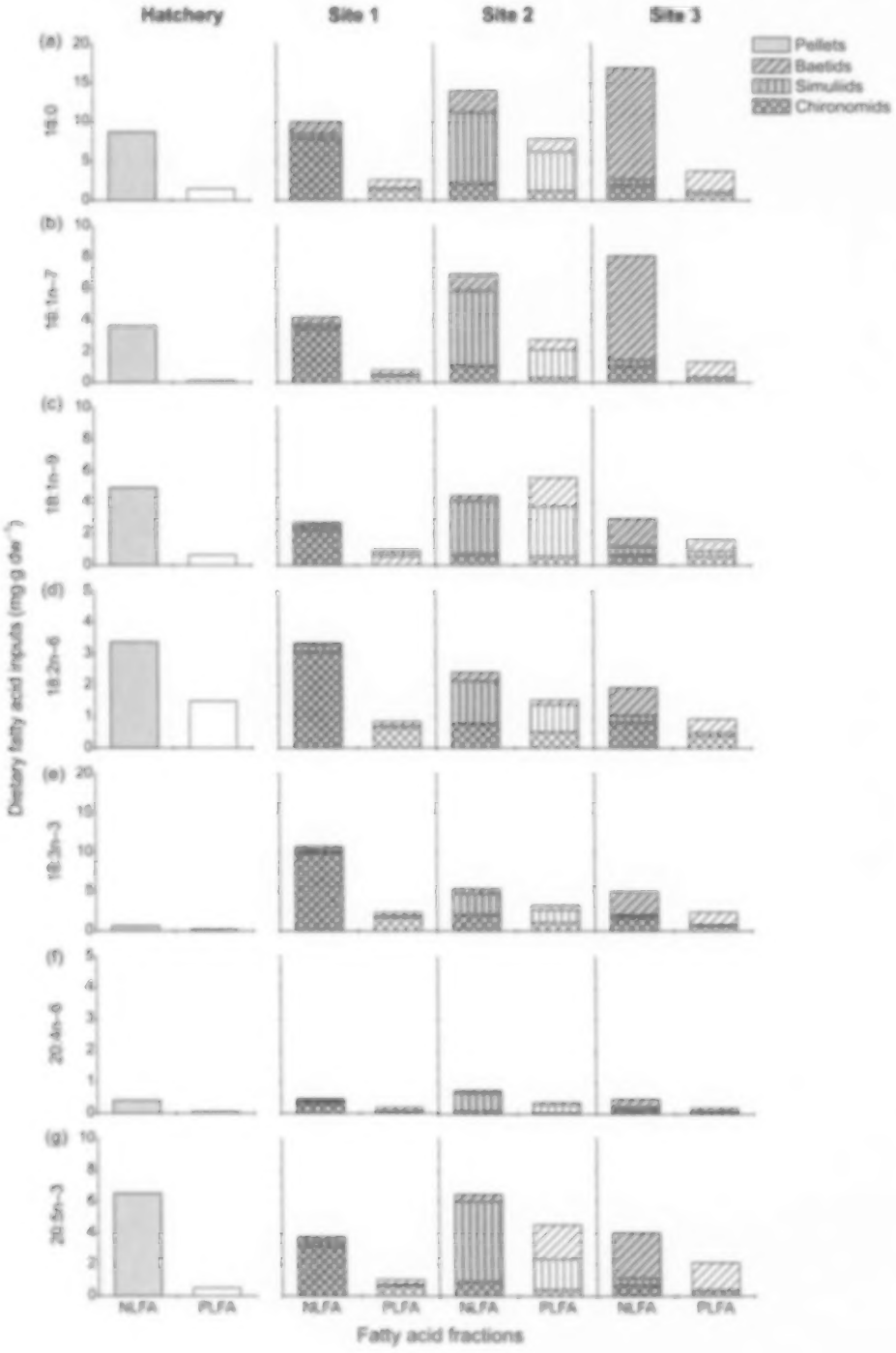

differences solely to variations in the FA composition of baetids, chironomids and simuliids because the digestibility of these prey and their calorific values and carbohydrate and protein contents probably differ (Gupta and Pant 1983; Batzer et al. 1993). Furthermore, many experimental studies have shown that when only the FA composition of artificial diets is modified (replacing fish oil by vegetable oil), the growth performances of parr or smolt remain unchanged and fish health and welfare are not affected (Robin et al. 2003; Miller et al. 2007). On the other hand, such experimental practices generally cause substantial change in the flesh FA composition of salmon parr and of several other species of anadromous salmonid (Bendiksen et al. 2003; Huang et al. 2008). Thus, one of the main reasons for conducting the present study was to assess whether different prey types would at least influence the body lipid FA composition, if not growth, of restocked salmon parr previously raised on artificial diet. In fact, the FA composition of freshwater aquatic insects turned out to be more diverse than we had thought, a fact that recent studies tend to corroborate (Sushchik et al. 2007; Torres-Ruiz et al. 2007).

For instance, MUFA and PUFA contents differed between the macroinvertebrates predominantly consumed by restocked parr. Baetid nymphs and chironomid larvae contained higher lipid levels of 16:1*n*–7 and simuliid larvae of 18:1*n*–9. These FA were reported to be the predominant monounsaturates in chironomid larvae and ephemeropteran nymphs (Bell et al. 1994; Ghioni et al. 1996). Concerning PUFA, the *n*–3 series were the principal components observed in all taxa (17%–26%), confirming previous observations by Bell et al. (1994). However, *n*–6 PUFA were detected in appreciable amounts (3%–9%), especially 18:2*n*–6. This FA exhibited the highest levels in chironomids and the lowest in baetids, which is consistent with observations by Sushchik et al. (2003). In contrast, only simuliid larvae had significant proportions of 20:4*n*–6, the major precursor of eicosanoids (Sargent et al. 1999). Another FA that may be involved in the synthesis of eicosanoids is 20:5*n*–3. This component was reported to be the most abundant *n*–3 PUFA in several taxa of freshwater insects, including Plecoptera and Ephemeroptera (Ghioni et al. 1996). This was particularly true for simuliids in this study, while 20:5*n*–3 appeared to be less abundant than 18:3*n*–3 in chironomids. Negligible amounts of 22:6*n*–3 were recorded in all analyzed prey, as previously reported (Bell et al. 1994; Goedkoop et al. 2000). It appeared from the present study that the FA composition of taxa such as simuliids and baetids was not so close to that of vegetable oil. They contained more 16:0, 18:0, and 16:1*n*–7 and less 18:1*n*–9 than rapeseed and linseed oils (Tocher et al. 2000). Regarding *n*–3 and *n*–6 PUFA, simuliid larvae showed larger amounts of 20:4*n*–6 and 20:5*n*–3. Finally, only the FA profiles of chironomids seemed to be close to those of vegetable oil, with high percentages of 18:2*n*–6 and 18:3*n*–3 and a low percentage of 20:5*n*–3.

Discriminant function analysis distinguished restocked parr in the three riffles from the hatchery-reared parr. This clearly indicates that artificial versus river insect diet significantly affected NLFA and PLFA patterns in juvenile Atlantic salmon throughout the survey. From June to August, the levels of 16:0, 16:1*n*–7, 18:1*n*–9, and 18:2*n*–6 were lower in restocked than in hatchery-reared parr. We assume that these FA were readily mobilized to compensate for the increase in energy expenditure when young salmon were released into the riffles. FA such as 18:1*n*–9 and 18:2*n*–6 are known to be the major substrates for β-oxidation in salmonids (Henderson 1996; Bell et al. 2002), while 16:0 is preferentially incorporated into PL (Tocher et al. 2008). Restocked salmon have to adapt quickly to their new environment, confronting new stimuli generally absent or limited in a hatchery environment: variable water velocity, live prey to seek and capture, etc. At the end of the survey (September–October), differences in the concentration of these FA between farmed and restocked parr tended to disappear. FA 16:1*n*–7 and 18:1*n*–9 were provided in variable but appreciable quantities, whether by natural prey or pellets. However, compared with 18:1*n*–9, 16:1*n*–7 was not detected in abundance in NLFA and PLFA, especially in restocked salmon. This specific trend seems to suggest that 16:1*n*–7 was selectively catabolized by parr living in the riffles, in preference to 18:1*n*–9. This could be a relatively new finding, since 18:1*n*–9 has often been regarded as the predominant FA used for energy cover by hatchery-reared salmon fed on various experimental diets (Bell et al. 2003*b*). FA 16:1*n*–7 is a typical diatom FA (Desvilettes and Bec 2009) that is probably more abundantly produced than 18:1*n*–9 in river ecosystems and therefore more easily transferred to higher levels in a food web (Sushchik et al. 2006).

The most pronounced differences in FA pattern linked to ingested food concerned *n*–6 and *n*–3 PUFA contents. The high level of 18:2*n*–6 in the artificial diet (8%) was linked to the incorporation of small quantities of poultry fat into Nutra pellet oil. Farmed parr had a greater amount of 18:2*n*–6 in their NL than did restocked parr, while 20:4*n*–6 was less abundant. At the end of the survey, in October, the amount of 20:4*n*–6 in the PL of hatchery-reared parr was significantly lower than that of any restocked parr. Hatchery-reared parr did not seem to biosynthesize this component, probably due to the abundant dietary supply of 20:5*n*–3 and 22:6*n*–3. Dietary HUFA (including 20:4*n*–6) are known to partially inhibit FA desaturase activity in salmonids (Tocher et al. 2006). The high level of 22:6*n*–3, logically detected in pellets and in the NL of hatchery parr, may well have affected the conversion of 18:3*n*–3 and probably of 18:2*n*–6 into 20:4*n*–6 (Bendiksen et al. 2003). Concerning released salmon, it is interesting to note that parr from site 2, which obtained significant levels of 20:4*n*–6 from their simuliid prey, contained lower levels of this FA in their PL than did parr in either of the other sites. Our suggestion is that dietary 20:4*n*–6 may have inhibited the bioconversion of 18:2*n*–6 into 20:4*n*–6, which was not the case with the other restocked parr, owing to low levels of 20:4*n*–6 obtained from baetid or chironomid prey. Moreover, the lack of 22:6*n*–3 in prey ingested by restocked parr would in theory enable C_{18} PUFA bioconversion activity to be maintained. However, 18:2*n*–6 could have probably been used as the principal Δ6-desaturase endogenous conversion substrate because 18:3*n*–3 levels accumulated in the NL of restocked parr. According to Bell et al. (2003*b*), these results might suggest that 18:3*n*–3 was stored for future β-oxidation during anadromous migration or, presumably, during overwintering. Similar observations were reported in a study using

deuterated 18:3*n*–3, which showed that catabolism via β-oxidation was preferred to conversion to 22:6*n*–3 in juvenile rainbow trout (*Oncorhynchus mykiss*) (Bell et al. 2001). In the present study, 22:6*n*–3 was recorded in very large quantities in Nutra pellets and not in macroinvertebrate prey. On the other hand, the PL of restocked parr contained similar amounts of this HUFA to those observed in the PL of farmed salmon. FA 22:6*n*–3 synthesis occurs via the Sprecher pathway from 20:5*n*–3 originating from ingested prey and converted into C_{24} PUFA that are further retroconverted into 22:6*n*–3 (Miller et al. 2007). Because Δ6-desaturase also catalyses conversion of 18:3*n*–3 into 18:4*n*–3 and of 24:5*n*–3 into 24:6*n*–3, dietary 20:5*n*–3 is easily converted into 24:5*n*–3. Thus, 18:3*n*–3 and 24:5*n*–3 compete for Δ6-desaturase, inhibiting 18:3*n*–3 desaturation in restocked parr (Ruyter et al. 2000; Zheng et al. 2005).

The last interesting observation highlighted by the present study was that many FA, such as 16:1*n*–7, 18:1*n*–9, 18:2*n*–6, 18:3*n*–3, and 20:5*n*–3, were provided in sites 2 and 3 in the form of PL. Intact PL are required for optimal growth, development, and survival in larval and early juvenile fish of both marine and freshwater species (Coutteau et al. 1997). Indeed, Tocher et al. (2008) reported that the quantitative PL requirements of larval and juvenile salmon ranged from about 2% to 6% of the diet and apparently decreased with age. If no requirement has been observed in salmon greater than 7.5 g, this may be due to the short-term nature of the studies performed. Thus, in Atlantic salmon cultured over a 24-month growth cycle, low dietary phospholipid levels might induce growth depression and other effects over this longer period of culture (Tocher et al. 2008). In this context, it can be suggested that the high growth performances recorded from August to October at sites 2 and 3 could be partly related to the high input of these dietary PL. Indeed, salmon parr from site 1, which exhibited the lowest final growth, received the bulk of their FA in the form of NL (except 18:3*n*–3). In fish larvae and juveniles feeding on NL-rich diets, insufficient dietary PL limits lipoprotein synthesis, leading to impaired FA transport to tissue (Tocher et al. 2008). In contrast, hatchery-reared salmon had the best growth, although their diet contained mostly NLFA and few PLFA. This could indicate that there is probably some minimal level of dietary PL required by salmon parr that could be covered by Nutra pellets but not chironomid-based diet of site 1 parr. Once this minimal level of PL is met, there is probably little additional benefit for salmon. Obviously, further investigations on macroinvertebrate phospholipid structure are needed to confirm or not our suggestion and whether simuliid larvae and baetid nymphs could be of greater nutritional interest than chironomid larvae.

In conclusion, our results show that the type of prey ingested and growth performance of restocked Atlantic salmon parr varied along the longitudinal gradient of the River Allier. Site 1 can be considered as the extreme upstream limit for 0+ salmon restocking. The low growth recorded in this area could be detrimental to overwintering survival and subsequent smoltification. This can be supported by the significant percentage (12%) of parr that delay migration in the most upstream parts of the River Allier (Cuinat 1986) and by problems encountered by their future smolts to achieve complete downstream migration (P. Martin et al., unpublished data). In contrast, the most favorable site for growth was the intermediate riffle (site 2), with values close to those achieved in hatchery-reared parr. Simuliid larvae and baetid nymphs seem to be an interesting type of food. Therefore, from an ecological viewpoint, maintaining the integrity of riffle macroinvertebrate assemblages in a large river can be of great importance for salmon parr, as those insects are thought to be less tolerant to habitat and water quality degradation than chironomid larvae (Lautenschläger and Kiel 2005). Finally, simuliid larvae and baetid nymphs exhibit FA composition not so close to that of vegetable oils, as frequently postulated with freshwater insects. Because during the 2 months following restocking, NLFA storage was lower in restocked fish (in any site), it would therefore be useful to think of a new diet formula based on the FA profiles of these two families of freshwater insect. Moreover, it would be of interest to test whether such diets could be beneficial to salmon fry or parr intended for river restocking rather than commercial aquaculture and human consumption.

Acknowledgements

We thank the Conservatoire National du Saumon Sauvage for their helpful contribution to electrofishing operations and hatchery samples. We are grateful to B. Misson and J. Sauvanet for their help during the analysis of stomach contents and macroinvertebrate identification. We express our gratitude to L. Jouve and C. Lemarchand for help and support during the study. The English was revised by I. McGill.

References

Ahlgren, G., Blomqvist, P., Boberg, M., and Gustafsson, I.-B. 1994. Fatty acid content of the dorsal muscle — an indicator of fat quality in freshwater fish. J. Fish Biol. **45**(1): 131–157.

Amundsen, P.-A., Gabler, H.-M., and Staldvik, F.J. 1996. A new approach to graphical analysis of feeding strategy from stomach contents data — modification of the Costello (1990) method. J. Fish Biol. **48**(4): 607–614.

Batzer, D.P., McGee, M., Resh, V.H., and Smith, R.R. 1993. Characteristics of invertebrates consumed by mallards and prey response to wetland flooding schedules. Wetlands, **13**(1): 41–49. doi:10.1007/BF03160864.

Bell, G., Ghioni, C., and Sargent, J. 1994. Fatty acid compositions of 10 freshwater invertebrates which are natural food organisms of Atlantic salmon parr (*Salmo salar*): a comparison with commercial diets. Aquaculture, **128**(3–4): 301–313. doi:10.1016/0044-8486(94)90319-0.

Bell, J.G., Tocher, D.R., Farndale, B.M., Cox, D.I., McKinney, R.W., and Sargent, J.R. 1997. The effect of dietary lipid on polyunsaturated fatty acid metabolism in Atlantic salmon (*Salmo salar*) undergoing parr–smolt transformation. Lipids, **32**(5): 515–525. doi:10.1007/s11745-997-0066-4. PMID:9168458.

Bell, J.G., McEvoy, J., Webster, J.L., McGhee, F., Millar, R.-M., and Sargent, J.R. 1998. Flesh lipid and carotenoid composition of Scottish farmed Atlantic salmon (*Salmo salar*). J. Agric. Food Chem. **46**(1): 119–127. doi:10.1021/jf970581k. PMID:10554206.

Bell, J.G., Henderson, R.J., Tocher, D.R., McGhee, F., Dick, J.R., Porter, A., Smullen, R.P., and Sargent, J.R. 2002. Substituting fish oil with crude palm oil in the diet of Atlantic salmon (*Salmo salar*) affects muscle fatty acid composition and hepatic

fatty acid metabolism. J. Nutr. **132**(2): 222–230. PMID: 11823582.

Bell, J.G., McEvoy, L.A., Estevez, A., Shields, R.J., and Sargent, J.R. 2003*a*. Optimising lipid nutrition in first-feeding flatfish larvae. Aquaculture, **227**(1–4): 211–220. doi:10.1016/S0044-8486(03)00504-0.

Bell, J.G., Tocher, D.R., Henderson, R.J., Dick, J.R., and Crampton, V.O. 2003*b*. Altered fatty acid compositions in atlantic salmon (*Salmo salar*) fed diets containing linseed and rapeseed oils can be partially restored by a subsequent fish oil finishing diet. J. Nutr. **133**(9): 2793–2801. PMID:12949367.

Bell, M.V., Dick, J.R., and Porter, A.E.A. 2001. Biosynthesis and tissue deposition of docosahexaenoic acid (22:6*n*–3) in rainbow trout (*Oncorhynchus mykiss*). Lipids, **36**(10): 1153–1159. doi:10.1007/s11745-001-0826-1. PMID:11768160.

Bendiksen, E.A., Arnesen, A.M., and Jobling, M. 2003. Effects of dietary fatty acid profile and fat content on smolting and seawater performance in Atlantic salmon (*Salmo salar* L.). Aquaculture, **225**(1–4): 149–163. doi:10.1016/S0044-8486(03)00286-2.

Bergström, E. 1989. Effect of natural and artificial diets on seasonal changes in fatty acid composition and total body lipid content of wild and hatchery-reared Atlantic salmon (*Salmo salar* L.) parr–smolt. Aquaculture, **82**(1–4): 205–217. doi:10.1016/0044-8486(89)90409-2.

Coutteau, P., Geurden, I., Camara, M.R., Bergot, S., and Sorgeloos, P. 1997. Review on the dietary effects of phospholipids in fish and crustacean larviculture. Aquaculture, **155**(1–4): 153–168.

Cuinat, R. 1986. Atlantic salmon in an extensive French river system: the Loire-Allier. *In* Atlantic salmon: planning for the future. *Edited by* D. Mills and D. Piggins. Croom Helm. London, U.K. pp. 389–399.

Descroix, A., Desvilettes, C., Martin, P., Anneville, O., Bec, A., and Bourdier, G. 2009. Feeding, growth and nutritional status of restocked salmon parr along the longitudinal gradient of a large European river: the Allier. Ecol. Freshwat. Fish, **18**(2): 282–296. doi:10.1111/j.1600-0633.2008.00345.x.

Desvilettes, C., and Bec, A. 2009. Formation and transfer of fatty acids in aquatic microbial food webs — role of heterotrophic protists. *In* Lipids in aquatic ecosystems. *Edited by* M.T. Arts, M.T. Brett, and M. Kainz. Springer-Verlag, New York. pp. 25–42. doi:10.1007/978-0-387-89366-2_.

Folch, J.M., Lees, M., and Sloane Stanley, G.H. 1957. A simple method for the isolation and purification of total lipides from animal tissues. J. Biol. Chem. **226**(1): 497–509. PMID: 13428781.

Ghioni, C., Bell, J.G., and Sargent, J.R. 1996. Polyunsaturated fatty acids in neutral lipids and phospholipids of some freshwater insects. Comp. Biochem. Physiol. B Biochem. Mol. Biol. **114**(2): 161–170. doi:10.1016/0305-0491(96)00019-3.

Goedkoop, W., Sonesten, L., Ahlgren, G., and Boberg, M. 2000. Fatty acids in profundal benthic invertebrates and their major food resources in Lake Erken, Sweden: seasonal variation and trophic indications. Can. J. Fish. Aquat. Sci. **57**(11): 2267–2279. doi:10.1139/cjfas-57-11-2267.

Gupta, P.K., and Pant, M.C. 1983. Seasonal variation in the energy content of benthic macroinvertebrates of Lake Nainital, U.P., India. Hydrobiologia, **99**(1): 19–22. doi:10.1007/BF00013713.

Henderson, R.J. 1996. Fatty acid metabolism in freshwater fish with particular reference to polyunsaturated fatty acids. Arch. Tierernahr. **49**(1): 5–22. PMID:8766969.

Huang, S.S.Y., Fu, C.H.L., Higgs, D.A., Balfry, S.K., Schulte, P.M., and Brauner, C.J. 2008. Effects of dietary canola oil level on growth performance, fatty acid composition and ionoregulatory development of spring chinook salmon parr, *Oncorhynchus tshawytscha*. Aquaculture, **274**(1): 109–117. doi:10.1016/j.aquaculture.2007.11.011.

Huet, M. 1959. Profiles and biology of western European streams as related to fish management. Trans. Am. Fish. Soc. **88**(3): 155–163. doi:10.1577/1548-8659(1959)88[155:PABOWE]2.0.CO;2.

Kaushik, S.J., Corraze, G., Radunz-Neto, J., Larroquet, L., and Dumas, J. 2006. Fatty acid profiles of wild brown trout and Atlantic salmon juveniles in the Nivelle basin. J. Fish Biol. **68**(5): 1376–1387. doi:10.1111/j.0022-1112.2006.01005.x.

Keeley, E.R., and Grant, J.W.A. 1997. Allometry of diet selectivity in juvenile Atlantic salmon (*Salmo salar*). Can. J. Fish. Aquat. Sci. **54**(8): 1894–1902. doi:10.1139/cjfas-54-8-1894.

Lautenschläger, M., and Kiel, E. 2005. Assessing morphological degradation in running waters using Blackfly communities (Diptera, *Simuliidae*): can habitat quality be predicted from land use? Limnologica, **35**(2): 262–273.

Miller, M.R., Nichols, P.D., and Carter, C.G. 2007. Replacement of dietary fish oil for Atlantic salmon parr (*Salmo salar* L.) with a stearidonic acid containing oil has no effect on omega-3 long-chain polyunsaturated fatty acid concentrations. Comp. Biochem. Physiol. B Biochem. Mol. Biol. **146**(2): 197–206. doi:10.1016/j.cbpb.2006.10.099. PMID:17134928.

Nordgarden, U., Hemre, G.-I., and Hansen, T. 2002. Growth and body composition of Atlantic salmon (*Salmo salar* L.) parr and smolt fed diets varying in protein and lipid contents. Aquaculture, **207**(1–2): 65–78. doi:10.1016/S0044-8486(01)00750-5.

Reiriz, L., Nicieza, A.G., and Brañta, F. 1998. Prey selection by experienced and naive juvenile Atlantic salmon. J. Fish Biol. **53**(1): 100–114. doi:10.1111/j.1095-8649.1998.tb00113.x.

Robin, J.H., Regost, C., Arzel, J., and Kaushik, S.J. 2003. Fatty acid profile of fish following a change in dietary fatty acid source: model of fatty acid composition with a dilution hypothesis. Aquaculture, **225**(1–4): 283–293. doi:10.1016/S0044-8486(03)00296-5.

Ruyter, B., Rosjo, C., Masoval, K., Einen, O., and Thomassen, M.S. 2000. Influence of dietary *n*–3 fatty acids on the desaturation and elongation of [1-^{14}C] 18:2*n*–6 and [1-^{14}C] 18:3*n*–3 in Atlantic salmon hepatocytes. Fish Physiol. Biochem. **23**(2): 151–158. doi:10.1023/A:1007893317923.

Sargent, J., Bell, G., McEvoy, L., Tocher, D., and Estevez, A. 1999. Recent developments in the essential fatty acid nutrition of fish. Aquaculture, **177**(1–4): 191–199. doi:10.1016/S0044-8486(99)00083-6.

Strahler, A.N. 1957. Quantitative analysis of watershed geomorphology. Trans. Am. Geophys. Union, **38**: 913–920.

Sushchik, N.N., Gladyshev, M.I., Moskvichova, A.V., Makhutova, O.N., and Kalachova, G.S. 2003. Comparison of fatty acid composition in major lipid classes of the dominant benthic invertebrates of the Yenisei River. Comp. Biochem. Physiol. B Biochem. Mol. Biol. **134**(1): 111–122. doi:10.1016/S1096-4959(02)00191-4. PMID:12524039.

Sushchik, N.N., Gladyshev, M.I., Kalachova, G.S., Makhutova, O.N., and Ageev, A.V. 2006. Comparison of seasonal dynamics of the essential PUFA contents in benthic invertebrates and grayling *Thymallus arcticus* in the Yenisei River. Comp. Biochem. Physiol. B Biochem. Mol. Biol. **145**(3–4): 278–287. doi:10.1016/j.cbpb.2006.05.014. PMID:16996285.

Sushchik, N.N., Gladyshev, M.I., Kravchuk, E.S., Ivanova, E.A., Ageev, A.V., and Kalachova, G.S. 2007. Seasonal dynamics of long-chain polyunsaturated fatty acids in littoral benthos in the upper Yenisei River. Aquat. Ecol. **41**(2): 349–365. doi:10.1007/s10452-006-9065-z.

Thonney, J.-P., and Gibson, R.J. 1989. Feeding strategies of brook trout (*Salvelinus fontinalis*) and juvenile Atlantic salmon (*Salmo salar*) in a Newfoundland river. Can. Field-Nat. **103**: 48–56.

Tocher, D.R., Bell, J.G., Dick, J.R., Henderson, R.J., McGhee, F., Michell, D., and Morris, P.C. 2000. Polyunsaturated fatty acid metabolism in Atlantic salmon (*Salmo salar*) undergoing parr–smolt transformation and the effects of dietary linseed and rapeseed oils. Fish Physiol. Biochem. **23**(1): 59–73. doi:10.1023/A:1007807201093.

Tocher, D.R., Dick, J.R., MacGlaughlin, P., and Bell, J.G. 2006. Effect of diets enriched in Δ6 desaturated fatty acids (18:3*n*–6 and 18:4*n*–3), on growth, fatty acid composition and highly unsaturated fatty acid synthesis in two populations of Arctic charr (*Salvelinus alpinus* L.). Comp. Biochem. Physiol. B Biochem. Mol. Biol. **144**(2): 245–253. doi:10.1016/j.cbpb.2006.03.001. PMID:16630735.

Tocher, D.R., Bendiksen, E.A., Campbell, P.J., and Bell, J.G. 2008. The role of phospholipids in nutrition and metabolism of teleost fish. Aquaculture, **280**(1–4): 21–34. doi:10.1016/j.aquaculture.2008.04.034.

Torres-Ruiz, M., Wehr, J.D., and Perrone, A.A. 2007. Trophic relations in a stream food web: importance of fatty acids for macroinvertebrate consumers. J. N. Am. Benthol. Soc. **26**(3): 509–522. doi:10.1899/06-070.1.

Wankowski, J.W.J., and Thorpe, J.E. 1979. Spatial distribution and feeding in Atlantic salmon, *Salmo salar* L. juveniles. J. Fish Biol. **14**(3): 239–247. doi:10.1111/j.1095-8649.1979.tb03515.x.

Zheng, X., Torstensen, B.E., Tocher, D.R., Dick, J.R., Henderson, R.J., and Bell, J.G. 2005. Environmental and dietary influences on highly unsaturated fatty acid biosynthesis and expression of fatty acyl desaturase and elongase genes in liver of Atlantic salmon (*Salmo salar*). Biochim. Biophys. Acta, **1734**(1): 13–24. PMID:15866479.

Parvicapsula minibicornis infections in gill and kidney and the premature mortality of adult sockeye salmon (*Oncorhynchus nerka*) from Cultus Lake, British Columbia

Michael J. Bradford, Jan Lovy, David A. Patterson, David J. Speare, William R. Bennett, Allen R. Stobbart, and Christine P. Tovey

Abstract: In recent years, large losses of migrating adult sockeye salmon (*Oncorhynchus nerka*) from the Fraser River, British Columbia, Canada, have resulted in reductions in catches and productivity. We investigated patterns of mortality and the occurrence of the myxosporean parasite *Parvicapsula minibicornis* in adult sockeye salmon from Cultus Lake, tributary to the Fraser River. Using data from a captive broodstock program, we found that early migrants to Cultus Lake had less severe *P. minibicornis* infections and were more likely to survive to maturity than those fish that arrived later after they had presumably held in the warmer Fraser River. We found *P. minibicornis* in kidneys and gills of spawners. In some fish, significant histopathology in the gills that included severe inflammation and hyperplasia of the gill lamellae was observed; the severity of the disease was correlated with the severity of *P. minibicornis* infections. Kidney and gill pathologies were more prevalent and more severe in fish that died before spawning compared with those that matured successfully. Gill disease associated with *P. minibicornis* infections had not been previously identified in Fraser River sockeye salmon, and its role in the loss of spawners needs further investigation.

Résumé : Ces dernières années, de lourdes pertes de saumons rouges (*Oncorhynchus nerka*) adultes migrateurs dans le fleuve Fraser, Colombie-Britannique, Canada, ont causé des réductions des prises et de la productivité. Nous examinons les patrons de mortalité et l'occurrence de la myxosporidie parasite *Parvicapsula minibicornis* chez les saumons rouges adultes du lac Cultus qui se déverse dans le fleuve Fraser. À l'aide de données provenant d'un programme impliquant un stock reproducteur captif, nous observons que les migrateurs précoces dans le lac Cultus ont des infections à *P. minibicornis* moins sévères et qu'ils sont plus susceptibles de survivre jusqu'à la maturité que les poissons qui arrivent plus tard après avoir vraisemblablement été retenus dans les eaux plus chaudes du fleuve Fraser. Nous avons trouvé *P. minibicornis* dans les reins et les branchies des reproducteurs. Nous avons observé chez certains poissons une importante histopathologie des branchies et, en particulier, une inflammation sévère et une hyperplasie des lamelles branchiales; la gravité de la maladie est en corrélation avec la sévérité des infections de *P. minibicornis*. Les pathologies des reins et des branchies sont plus fréquentes et plus graves chez les poissons qui sont morts avant la fraie, par comparaison à ceux qui ont frayé avec succès. On n'avait pas signalé auparavant la maladie des branchies associée à *P. minibicornis* chez les saumons rouges du fleuve Fraser et il faudra étudier plus au fond son rôle dans la perte des reproducteurs.

[Traduit par la Rédaction]

Introduction

The Fraser River in British Columbia, Canada, is home to numerous sockeye salmon (*Oncorhynchus nerka*) populations that are the mainstay of commercial, sports, and aboriginal fisheries in the region. Since 1995, the timing of entry of many adult sockeye salmon into the Fraser River from the ocean has advanced a month or more, for reasons that are still unknown (Cooke et al. 2004). A group of populations known as the "late runs" have been most affected by the change in behaviour, and high rates of adult mortality have been observed in some years (Cooke et al. 2004). Prior

Received 16 June 2009. Accepted 31 December 2009. Published on the NRC Research Press Web site at cjfas.nrc.ca on 17 March 2010. J21260

M.J. Bradford[1] and D.A. Patterson. Fisheries and Oceans Canada and School of Resource and Environmental Management, Simon Fraser University, Burnaby, BC V5A 1S6, Canada.
J. Lovy and D.J. Speare. Atlantic Veterinary College, University of Prince Edward Island, 550 University Ave., Charlottetown, PEI C1A 4P3, Canada.
W.R. Bennett. Fisheries and Oceans Canada, Pacific Biological Station, 3190 Hammond Bay Rd., Nanaimo, BC V9T 6N7, Canada.
A.R. Stobbart. Fisheries and Oceans Canada, Inch Creek Hatchery, 38260 Bell Rd., Dewdney, BC V0M 1H0, Canada.
C.P. Tovey. Fisheries and Oceans Canada, Cultus Lake Salmon Laboratory, 4222 Columbia Valley Hwy., Cultus Lake, BC V2R 5B6, Canada.

[1]Corresponding author (e-mail: mike.bradford@dfo-mpo.gc.ca).

to 1995, late runs arrived at the mouth of the Fraser River in August but held in the estuary and delayed their entry into the river until late September. However, many of these fish now enter the Fraser River without delay in August and early September. This change in migration timing exposes migrants to higher river temperatures and flows than would have occurred historically (Patterson et al. 2007). English et al. (2005) and Farrell et al. (2008) both found that earliest migrants of the run were the least likely to reach their spawning grounds compared with those whose timing most resembled the historic pattern. Temperature stress, energy depletion, and disease have all been hypothesized as mechanisms linking the change in migration timing to adult mortality (Cooke et al. 2004; Farrell et al. 2008).

Included among late-run populations are sockeye salmon that spawn in Cultus Lake, located in the lower Fraser valley. This population had been trending downwards since the mid-1970s but took a precipitous decline in the late 1990s largely because of two successive years of >80% mortality of adults prior to spawning in the lake (Cooke et al. 2004). The myxosporean parasite *Parvicapsula minibicornis* is very prevalent in spawners from Cultus Lake and was thought to have contributed to that mortality (St-Hilaire et al. 2002). *Parvicapsula minibicornis* becomes abundant in the glomeruli of the kidney and renal failure has been speculated as cause of death (Raverty et al. 2000); however, the exact mechanism has not been established. The population has since been assessed and is now considered endangered by the Committee on the Status of Wildlife Species in Canada (2003). The reoccurrence of adult mortality events will likely imperil the already diminished population (Committee on the Status of Endangered Wildlife in Canada 2003), so a captive broodstock and hatchery supplementation program was initiated in 2001 to increase the number of spawners returning to the lake.

In the fall of 2006, field crews noticed that fish being collected at Cultus Lake for the hatchery program were particularly lethargic, and spawners were observed swimming at the surface of the lake, behaviours not normally observed. Subsequently, a large number of dead unspawned fish were collected from the lake, suggesting that another bout of premature adult mortality was occurring. These observations led to some opportunistic sampling of fish in 2006 and a more structured sampling program in 2007 in an attempt to understand the patterns of mortality and its causes.

The objective of this paper is to describe the mortality and histopathology of maturing Cultus Lake sockeye salmon. The presence of the captive broodstock program allowed us to follow the progression of *P. minibicornis* infections and disease in a more controlled environment than was previously possible from the examination of field collections. We used broodstock fish to compare the severity of infection and disease in fish that successfully matured relative to those that died before spawning.

Materials and methods

Study site

Cultus Lake (49°03′N, 121°59′W) is a small monomictic (6.4 km^2) lowland lake (elevation 46 m) located in southwestern British Columbia (Fig. 1). It has a maximum depth of 48 m and a relatively limited littoral zone. Surface water of the lake reaches temperatures >20 °C in the summer and a strong thermocline develops at 15–20 m depth. Temperatures below the thermocline remain at 6–8 °C (Shortreed 2007). In recent years, hypolimnetic oxygen depletion occurs over the fall, and by late fall, oxygen levels decrease to <6 mg·L^{-1} at 30 m depth (<50% of saturation; Shortreed 2007). The lake becomes isothermal and mixes in late fall (Pon et al. 2010).

Cultus Lake is drained by Sweltzer Creek, which flows 3 km north from the lake to the Vedder River. The Vedder River flows a further 13 km to its confluence with the lower Fraser River 99 km upstream from the ocean (Fig. 1). Water temperatures in the Fraser River can reach 20 °C in August but begin to decline in September (Fig. 2). The Vedder River is generally cooler than the Fraser River at the time of migration. Sweltzer Creek is very warm (>20 °C) during the summer and fall, as it is supplied by surface water from the lake (Fig. 2).

The timing of marine migrations of adult Cultus Lake sockeye salmon is only known from tagging studies conducted in the 1930s (Foerster 1936). Those studies found that adults arrived at the mouth of the Fraser River in August, but their progression up the Fraser was delayed to September, as was the case for other late-run populations. Historically, sockeye arrived at Cultus Lake in October and November (Fig. 3). However, since 1995, fish now enter the lake in August and September (Fig. 3). After entering the lake, spawners hold below the thermocline in 6–8 °C water (Pon et al. 2010). Spawning peaks in late November (Brannon 1987) and takes place on submerged gravel beds along the margins of the lake at depths ranging from 1 to 30 m. Little, if any, creek spawning takes place.

Fish sampling

A salmon counting weir is located in Sweltzer Creek near Cultus Lake and it has been operated annually since 1923 (Foerster 1936). Adults were collected from the weir for the captive broodstock program and we utilized these fish to observe the progression of disease and mortality. Fish were collected throughout the run and were immediately transferred to large, circular concrete ponds at the adjacent Cultus Lake Salmon Research Laboratory. These ponds are supplied with 6–8 °C aerated hypolimnetic water from Cultus Lake. Each fish received a unique passive integrated transponder tag for tracking purposes and was injected with 0.3 mL of Liquamycin LA 200 (oxytetracyline). The holding ponds were treated with Parasite S formalin solution (Syndel Laboratories, 100 ppm for 60 min) three times per week to minimize infections from external protozoans and fungi.

Holding ponds were examined each weekday for mortalities, which were then removed for passive integrated transponder tag recovery. In 2007, but not 2006, samples from premature mortalities were taken for assessment with histopathology. Once fish began to ripen, they were examined for maturity once per week from mid-November to early January. Females were killed at the time of spawning; males were returned to the holding ponds for subsequent spawning. Ovarian fluid from spawned females was tested for infectious haematopoetic necrosis virus using the cell culture method described by Traxler et al. (1997). Ovarian fluid was used,

Fig. 1. Map of the study area in southwestern British Columbia (BC), Canada.

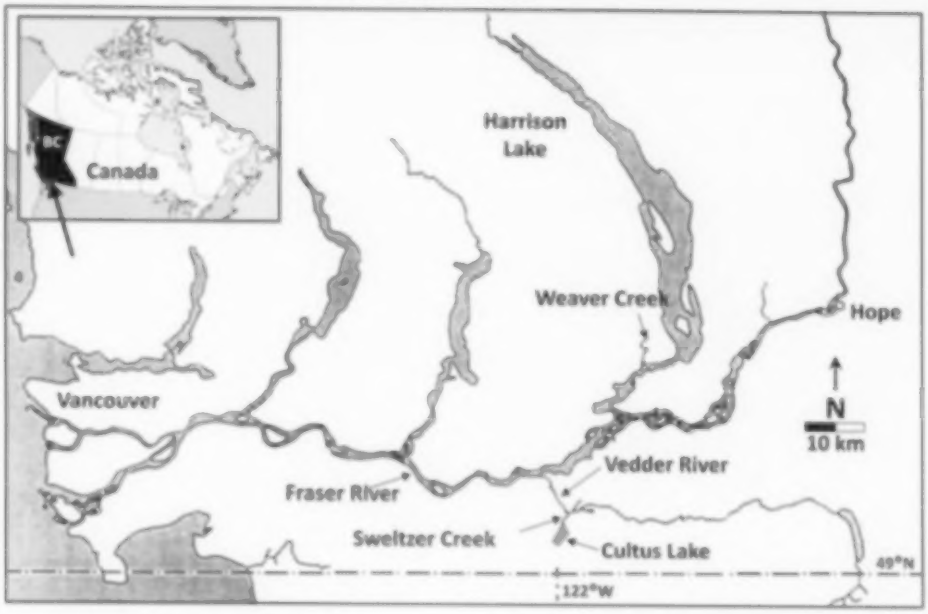

Fig. 2. Mean daily temperatures of (*a*) Fraser River (near Hope, British Columbia) and (*b*) Sweltzer Creek and the Vedder River. Solid line, 2006; dotted line, 2007; dashed line, 2008.

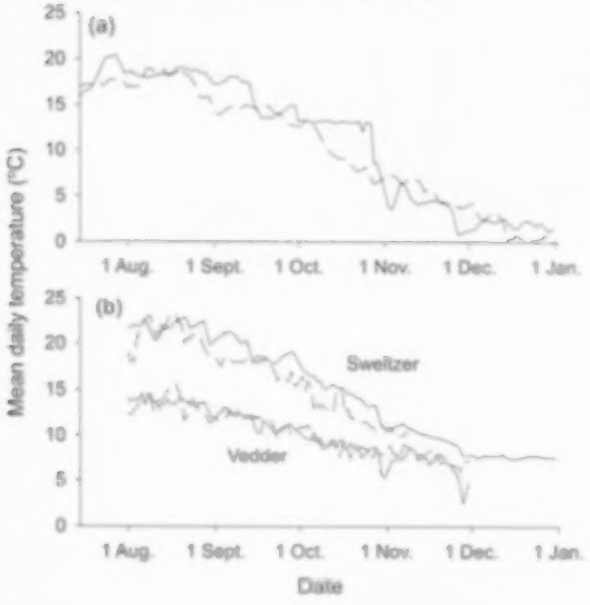

as viral particles are more stable than in tissue samples. All fish sampled were negative for this virus. Kidney tissues were also tested for bacterial kidney disease using the ELISA assay (Pascho et al. 1991). In 2006, 110 of 121 females were considered negative (pptical absorbance <0.08); the remaining 11 females had low-level infections (absorbances ranged from 0.086 to 0.13; Pascho et al. (1991) considered optical densities <0.2 to be a low-level infection). In 2007, all 75 females tested negative. Spawned-out fish in both years were retained for disease examinations.

In 2007, moribund or fresh dead (defined as having pink or red gills) prespawning mortalities that were recovered from field surveys of the lake were sampled for histopathology. We also present data on the arrival and mortality of spawners in 2008, but disease investigations were not conducted in this year.

Histopathology

In 2006, only gill and posterior kidney samples from successfully spawned fish from the captive broodstock program were taken. In 2007, samples of posterior kidney, gill, liver, spleen, and heart were taken from all fish. All tissues were initially fixed in formalin for 24 h and were then transferred to 70% ethanol or isopropanol. Tissues were then dehydrated through a graded series of ethanols and were embedded in parafin wax. Five micrometre sections were mounted on glass slides and stained with haematoxylin and eosin. In 2006, the slides were interpreted at the Pacific Biological Station (Nanaimo, British Columbia); the 2007 material was read at the Atlantic Veterinary College (Charlottetown, Prince Edward Island). In both cases, the readers were blind to the origins of the fish. Unfortunately, scoring systems used each year were different, which precluded comparisons across years.

For the 2006 samples, the gills and kidneys were examined for the presence of abnormalities. A 0–3 scoring system was used that depended on a visual assessment of the the proportion of abnormal tissue on the slide. Scores were assigned as 0: no abnormalities, 1: <10%, 2: 10%–50%, and 3: >50%.

In 2007, a more quantitive scheme was devised to describe histopathology. For kidney, 25 glomeruli from each fish were examined and the number of glomeruli that contained *P.*

Fig. 3. Sockeye salmon gills. (*a*) Severely affected gills with diffuse lamellar fusion and inflammation in both the gill filaments and lamellae; this gill would receive a score of 3 in the quantitative analysis. Scale bar = 200 μm. (*b*) Developmental stages of the parasite (arrows) localized beneath the gill epithelium (arrowhead). Scale bar = 10 μm. (*c*) Gill lamella with a parasite within a pillar channel (arrow) and eosinophilic material filling the lumen of the channel (asterisk). Scale bar = 10 μm.

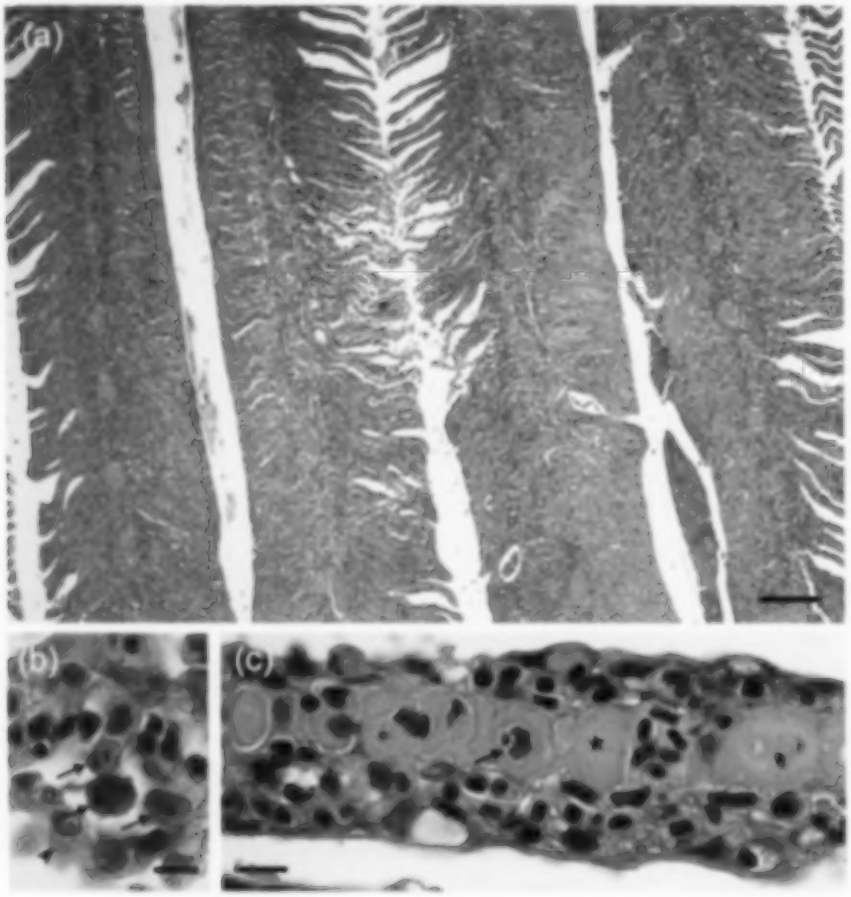

minibicornis parasites was recorded following the procedure of Jones et al. (2003). A glomeruli score was defined as the proportion of the 25 that were positive for the parasite. Additionally, 100 renal tubules were examined in each fish by analyzing about 10 microscope fields under the 40× objective, and the renal tubule score was defined as the proportion that contained *P. minibicornis* in the lumen.

Analysis of gill tissue collected in 2007 was done by a 0–3 scoring system. A gill score of 0 was given if no inflammation or lamellar fusion was observed, a 1 if focal lamellar fusion affecting four or less lamellae and mild infiltration of inflammatory cells was observed in <10% of the tissue on the slide, a 2 if focal lamellar fusion extended to over four lamellae and an inflammatory infiltrate was observed in the gill filament affecting between 10% and 25% of the tissue, and a 3 for a severe inflammatory response that included both the gill filaments and lamellae and lamellar fusion that affected over 25% of the gill tissue (see Fig. 3). Additionally, roughly 10 lamellae of a gill filament were observed with the 40× objective to quantify the number of parasites present in the gills. A score of 0 was given if no parasites were observed, a 1 if one to nine parasites were observed, a 2 if 10–19 parasites were observed, and a 3 if over 20 parasites were seen. In a subsample of fish, the in situ hybridization procedure of Jones et al. (2004) was used to confirm the presence of *P. minibicornis* in the gills.

The bulbus arteriosus of the heart was examined for the presence of *Loma* xenomas and all other tissues were screened for abnormalities.

Results

Spawning in Cultus Lake

A total of 3797 sockeye salmon arrived at the counting fence in 2006, with the first arrival on 31 July. Most of the run had entered the lake by the beginning of October (Fig. 4). The broodstock program retained 277 fish that were taken between 25 August and 21 November.

Field crews made the first observations of abnormal behaviour of spawners in the lake in mid-October 2006. Adults were observed swimming slowly at the surface of the lake and along its margins. Fall rains increased flows to small

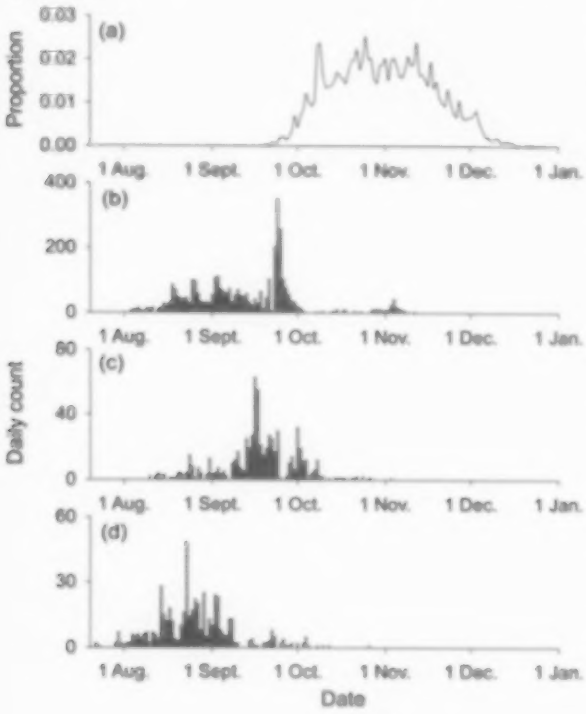

Fig. 4. Timing of the arrival of spawners at the Sweltzer Creek counting weir. (*a*) Historical data are averaged over 1941–1994 (Schubert et al. 2002). Recent counts are for (*b*) 2006, (*c*) 2007, and (*d*) 2008 and are Fisheries and Oceans Canada unpublished data (M. Bradford, Fisheries and Oceans Canada, Burnaby, British Columbia).

streams draining into the lake and salmon were observed attempting to swim into the rapidly flowing water. A total of 78 dead unspawned females were collected from the lake between 31 October and 24 November by boat and foot surveys. Heavy rains in late November raised lake levels and added turbidity and debris to the water, which largely prevented the recovery of carcasses after that point. Because spawning takes place deep in the lake and spawned-out carcasses are not easily captured, obtaining a reliable estimate of the rate of prespawning mortality is not possible for the Cultus Lake population.

A total of 649 spawners returned to Cultus Lake in 2007; the run began on 10 August and was complete on 4 November. Most fish arrived at the fence in mid-September (Fig. 4). The hatchery program retained 151 fish. Only nine unspawned females were found in the lake; field crews did not observe any abnormal behaviours or surface swimming in 2007.

The 2008 return was the earliest on record. The run began in July and was largely complete by early September. A total of 360 fish arrived at the lake and 159 were retained for the captive broodstock program. This was the only year in which broodstock were collected in early August. Eight unspawned females were collected from the lake.

Mortality in the captive broodstock

In 2006, 81 salmon (29% of the total) died before spawning in the broodstock holding ponds. In 2007, the mortality rate was 12%, and in 2008, 21% died prematurely. Mortality was a function of the date of arrival at the counting fence: fish arriving before October generally suffered low mortality (Fig. 5). When analyzed with a logistic regression, the timing of mortality in 2006 and 2007 was similar ($P > 0.3$). The arrival date that resulted in an expectation of 50% mortality for these years was 25 October. In 2008, the mortality pattern was somewhat different, as fish collected in early August suffered high mortality but those collected after that followed a similar pattern to the other years. Logistic regression fitted to the 2008 data was significantly different from that of 2006 and 2007 ($P < 0.001$ using data after 15 August) with the predicted date of 50% mortality of 30 September. There was no effect of sex on the timing of mortality ($P > 0.3$).

Histopathology

Parvicapsula minibicornis infections were frequent in kidneys, and in many instances, every glomerulus that was inspected was heavily infected with parasites. *Parvicapsula minibicornis* was observed both in the visceral layer of Bowman's capsule and within Bowman's space. There was no noticeable cellular host response around or within infected glomeruli, although the infection was associated with eosinophilic material throughout Bowman's capsule and into Bowman's space (Fig. 6). Both parasites and eosinophilic material were also observed in the lumen of renal tubules (Fig. 6).

In gills, pathological lesions ranged from absent to severe. In severe cases, lesions included multifocal to diffuse areas of lamellar fusion and an inflammatory infiltrate composed of neutrophils, macrophages, and lymphocytes in the gill filament and lamellae (Fig. 3*a*). *Parvicapsula minibicornis* was found in three anatomical locations within the gill. The first was within the hyperplastic epithelium of the gill lamellae and in this case were accompanied by an inflammatory infiltrate. The second location was in unfused gill lamellae and in these situations were localized underneath the lamellar epithelium sandwiched between the lamellar epithelium and the basement membrane of the pillar system (Fig. 3*b*). Finally, the parasite was observed directly within pillar channels of the lamellae (Fig. 3*c*), and in these instances, the lumen of the pillar channels contained eosinophilic material, which appeared to occlude the lumen (Fig. 3*c*). In situ hybridization confirmed that the commonly observed parasite observed within gills was *P. minibicornis* (Fig. 7).

Although the myxosporean *Ceratomyxa shasta* is present in the lower Fraser River (Ching and Munday 1984) and uses the same invertebrate host as *P. minibicornis* (Bartholomew et al. 2006), it was not found in fish examined in this study.

Microsporidial infections likely caused by *Loma salmonae* were observed in many fish. *Loma* infections were most frequently found in the bulbus arteriosus of the heart, although they were also observed in gills and spleen. Infections in the bulbus arteriosis ranged from a single xenoma to heavy infections of up to 20 xenomas within a single section. In some cases, the bulbus arteriosis was positive for *Loma*,

Fig. 5. Relationship between the probability of a fish in the captive broodstock dying before spawning and the date of its collection from the Sweltzer Creek weir. Lines are logistic model fits to individual fate data; histograms are the proportion of fish that died before spawning by semimonthly interval. Sample sizes are indicated above the bars. Data from 2006 and 2007 are combined (solid line and solid bars), as there was no statistical difference between years; the dashed line and shaded bars are for 2008. Data from the first half of August 2008 were not used to fit the logistic model.

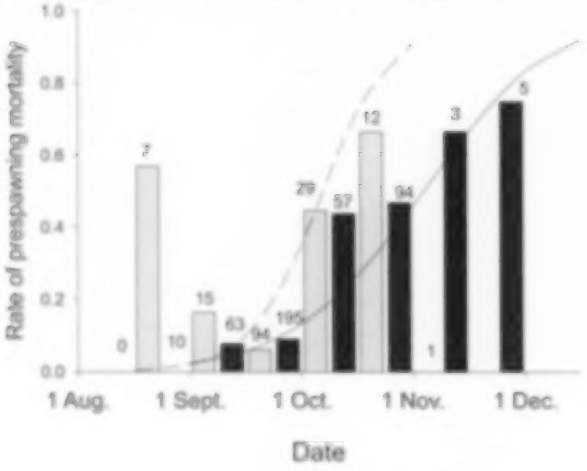

while the parasite was not detected in the gills of the same fish.

There was little liver pathology throughout the sample. One interesting finding was the observation of single cell necrosis through the liver of nine fish. We observed necrotic hepatocytes in various stages of degeneration surrounded by healthy cells. The cause of this condition is unknown.

Quantitative analysis of infection and pathology

In 2006, tissue samples were only collected from successfully spawned fish from the captive broodstock program. Abnormalities were observed in 64% of kidneys and 89% of gills that were examined. Both kidney and gill scores were positively correlated with the date of capture at the fence (kidney: $r = 0.32$, $P = 0.003$, $N = 86$; gill: $r = 0.51$, $P < 0.001$, $N = 110$), suggesting that the severity of disease at the time of spawning was related to the timing of migration to Cultus Lake. Gill and kidney scores were positively related to each other within fish ($r = 0.49$, $P < 0.001$, $N = 84$).

After the 2007 slides were read, the data were organized into three groups: broodstock fish that matured successfully, broodstock fish that died prematurely, and fish recovered from the lake that had died before spawning. The prevalence of *P. minibicornis* in kidney and gill and the prevalence of pathology were consistently highest in the two groups of fish that died before spawning (Table 1). Nonetheless, *Parvicapsula* was identified in nearly half of the fish that were successfully spawned. The prevalence of *Loma* in the heart and spleen was low and unrelated to spawner fate.

There were significant differences in mean scores between the three groups of fish for glomeruli, renal tubule, gill pathology, and gill parasite scores (one-way ANOVA, all $P < 0.001$, $N = 81$–96; in Fig. 8, successful broodstock fish are separated by the date of spawning). In all cases, a post hoc contrast indicated that scores were significantly lower for the successful spawners compared with fish that had died prematurely in the broodstock or the lake (all $P < 0.001$).

Egg takes for the captive broodstock program spanned a 7-week period (Fig. 8). There was no significant variation in mean pathology scores among sampling periods (ANOVA, all $P > 0.2$, $N = 56$–59) but there appeared to be a weak increasing trend in some measures (Fig. 8). These weak trends were confirmed with regressions of pathology scores on the date of sampling (glomeruli: $r = 0.21$, $P = 0.12$; renal tubules: $r = 0.22$, $P = 0.10$; gill pathology: $r = 0.26$, $P = 0.06$; gill parasites: $r = 0.27$, $P = 0.04$).

For captive broodstock fish, three pathology scores were positively correlated with the date that they were captured at the counting fence (glomeruli: $r = 0.62$, $P < 0.001$; gill pathology: $r = 0.59$ $P < 0.001$; gill parasites: $r = 0.48$, $P = 0.002$). Fish arriving at Cultus Lake after mid-October had heavy *P. minibicornis* infections in the glomeruli at the time of sampling (Fig. 9). All three scores were negatively correlated with the date of death (all $P < 0.001$) largely because most of the premature broodstock mortalities, which had the highest disease scores, occurred before the egg takes took place. Scores for renal tubules were not related to the date of arrival ($r = 0.14$, $P = 0.23$, $N = 74$) or the date of sampling ($r = 0.06$, $P = 0.64$).

The severity of infections in renal tubules and gill scores were positively correlated with glomeruli scores (all $r > 0.6$, $P < 0.001$, $N > 80$) (Fig. 10). Those relationships tended to take on a triangular form, as there were fish with high levels of infection in the glomeruli that did not have high levels of other pathologies, but rarely did the reverse situation occur. Most fish that died before spawning had high levels of infection in glomeruli and nonzero renal and gill scores. Gill pathology and gill *P. minibicornis* scores were also positively correlated (Spearman's $\rho = 0.75$, $P < 0.001$, $N = 82$).

Discussion

Our investigations have extended our understanding of causes of mortality in late-run Fraser River sockeye salmon in a number of ways. Our data from the captive broodstock are the first that show a clear difference in *P. minibicornis* infections and related pathology between fish that died prematurely and those that successfully matured, providing correlative evidence for the role of *P. minibicornis* as a factor in premature mortality. Our finding of significant inflammation of gill tissue in many fish associated with *P. minibicornis* raises the possibility that impaired gill function may play a role in the premature mortality of Fraser River sockeye salmon.

The freshwater habitats used by adult Cultus Lake salmon have changed considerably with the change of timing of entry to the river that began in 1995. Although direct information on the timing of migration is not available because of their relative rarity compared with other late-run populations, observations of fish first arriving at Cultus Lake in late July suggest that their migration to freshwater has

Fig. 6. Sockeye salmon kidney infected with *P. minibicornis*. (*a*) A renal tubule and the two glomeruli with abundant eosinophilic material (asterisk). Scale bar = 50 μm. (*b*) A glomerulus at higher magnification with a *P. minibicornis* infection (arrows) and dense eosinophilic material (asterisk) throughout. Scale bar = 10 μm.

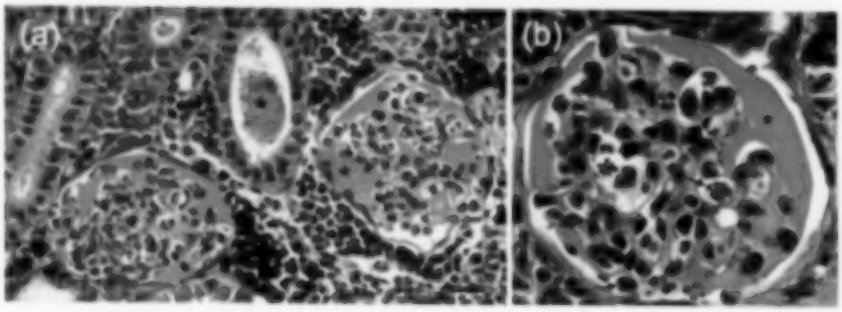

Fig. 7. In situ hybridization and staining of *P. minibicornis* (in blue) in gills of adult sockeye salmon with mild hypertrophy of the lamellar epithelium.

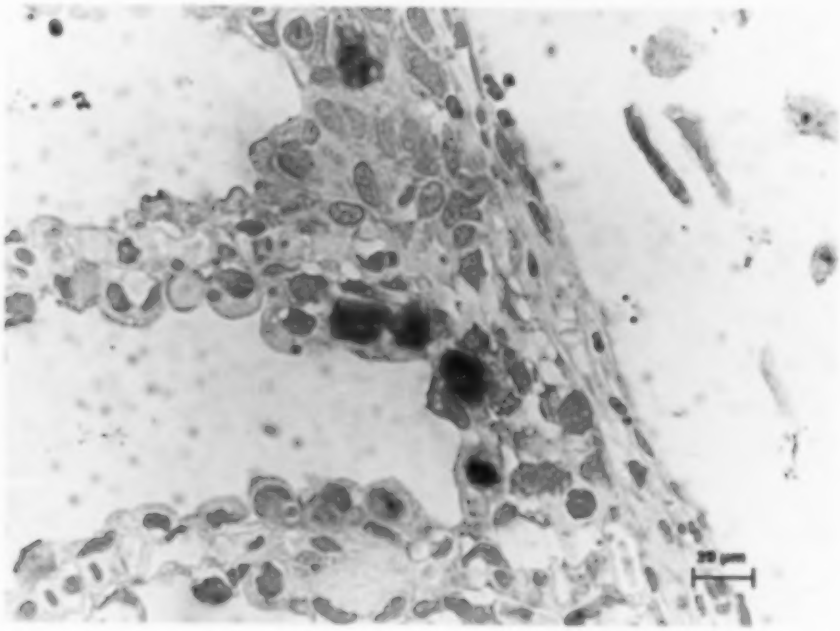

Table 1. Prevalence of *P. minibicornis*, *Loma*, and related pathologies in adult sockeye salmon from Cultus Lake in 2007.

	Egg take	Brood PSM	Lake PSM
Mean date of sampling	8 December	7 November	8 November
P. minibicornis in glomeruli	27/60 (45%)	16/16 (100%)	17/17 (100%)
P. minibicornis in renal tubules	13/59 (22%)	16/17 (94%)	8/8 (100%)
Gill pathology	15/57 (26%)	12/13 (92%)	11/12 (92%)
P. minibicornis in gill	7/58 (12%)	11/15 (73%)	13/15 (87%)
Loma in heart	7/59 (12%)	1/17 (6%)	3/20 (15%)

Note: Egg take refers to spawners that were successfully spawned in the captive broodstock program; the other columns are data from prespawning mortalities in the captive broodstock (brood PSM) and in the lake (lake PSM). Sample sizes vary among metrics because of poor tissue preservation.

advanced much like other late runs (Cooke et al. 2004). Upon entry to the Fraser River, fish are immediately exposed to warm water and *P. minibicornis* actinospores (Wagner et al. 2005) produced by its alternate invertebrate host (Bartholomew et al. 2006). We infer from the timing of arrival at Cultus Lake that most individuals now move

Fig. 8. Mean pathology scores (±SE) for 2007 adult Cultus Lake sockeye salmon. Data are organized by lake and broodstock pre-spawning mortality (PSM) and for fish sacrificed for egg takes from the captive broodstock program.

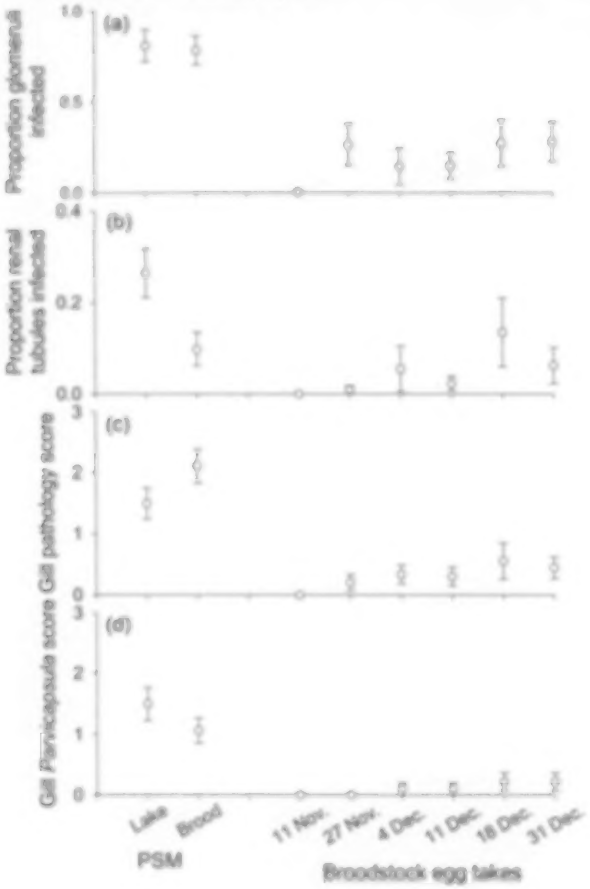

relatively quickly to the lake and hold in the hypolimnion up to 3 months before spawning. Based on our observations on captive broodstock fish, this behaviour appears to retard the progression of disease and increase the probability of survival. Whether the recent change in the location of holding for Cultus Lake sockeye is an adaptive response to disease or a fortunate outcome of the overall change of migration timing from the ocean is currently unknown; however, it would appear to be advantageous from a disease perspective, as most fish enter the lake early enough to be able to mature successfully.

We think that fish that arrived at the lake in late October or November (which is the historical timing) probably held in warmer downstream habitats and that allowed *P. minibicornis* and possibly other infections to develop, reducing the likelihood of successful reproduction in the lake. This behaviour is somewhat different from that observed for the nearby Weaver Creek population where later migrants were found to be more likely to spawn than early ones (Mathes et al. 2010). Mathes et al. (2010) proposed that successful migrants delayed their entry into the Fraser River until later in the season and were exposed to lower water temperatures in the river, which reduced the risk of disease in these fish. Our disease data suggest that most Cultus Lake fish enter the river relatively early in the season, and variation in survival is a consequence of variation in the length of residence in the Fraser River.

Fig. 9. Relationship between the proportion of kidney glomeruli infected with *P. minibicornis* at the time of death and the date of collection from the Sweltzer Creek weir for captive broodstock fish in 2007. Open circles represent fish that were spawned successfully and solid circles represent fish that died before spawning. The line is a logistic regression fit by nonlinear parameter estimation.

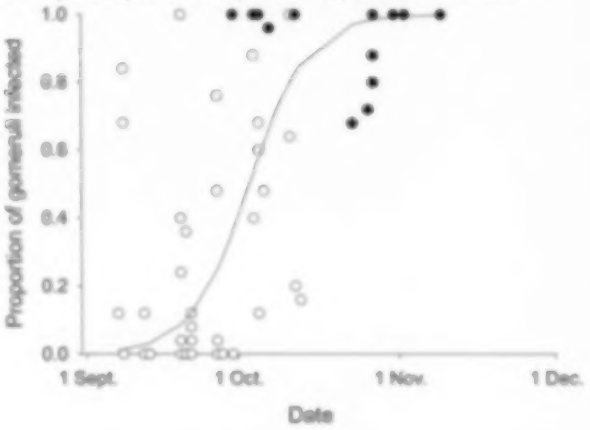

The increased mortality of 2008 broodstock fish that arrived at Cultus Lake before mid-August suggests that other agents of mortality may also be involved. These early migrants are unlikely to have been in the Fraser River long enough to allow *P. minibicornis* to fully develop, although they would have been exposed to peak temperatures in the Fraser River and Sweltzer Creek during their migration. Most of these fish died within 2–3 weeks after capture, despite being held in the relatively cool water of the holding ponds. For other late-run sockeye populations, the earliest migrants suffer high mortality and it has been conjectured that this is the result of exposure to higher than normal river flows and temperature (Gilhousen 1990; English et al. 2005; Farrell et al. 2008). It is also possible that these very early fish are in a stressed condition as a result of their abnormal migration timing from the ocean and may be susceptible to a number of factors that could contribute to their death (Mathes et al. 2010). A larger sample and a thorough examination of the physiology and histology of the earliest migrants are needed to determine the cause of death.

We found a large difference in the intensity of infection by *P. minibicornis* for adults that died before spawning compared with those that successfully matured. Previous investigators have not been able to identify differences in prevalence or intensity of infections between successful spawners and premature mortalities (St-Hilaire et al. 2002; Jones et al. 2003); however, those studies relied on samples from postspawning fish for which the disease may have progressed significantly after the start of spawning. Sockeye salmon can survive for a week or more after spawning (Foerster 1968), and the rapid senescence of fish during

Fig. 10. Relationship between the (*a*) proportion of renal tubules infected with *P. minibicornis*, (*b*) gill pathology score, and (*c*) gill *P. minibicornis* score and the proportion of kidney glomeruli infected with *P. minibicornis* for individual Cultus Lake sockeye salmon in 2007. Open circles represent fish that were spawned successfully in the captive brood stock, solid circles represent captive broodstock fish that died before spawning, and triangles represent prespawning mortalities from Cultus Lake. Numerals indicate the number of overlapping points. In some cases, points were jittered on the *x*-axis to reduce overlap.

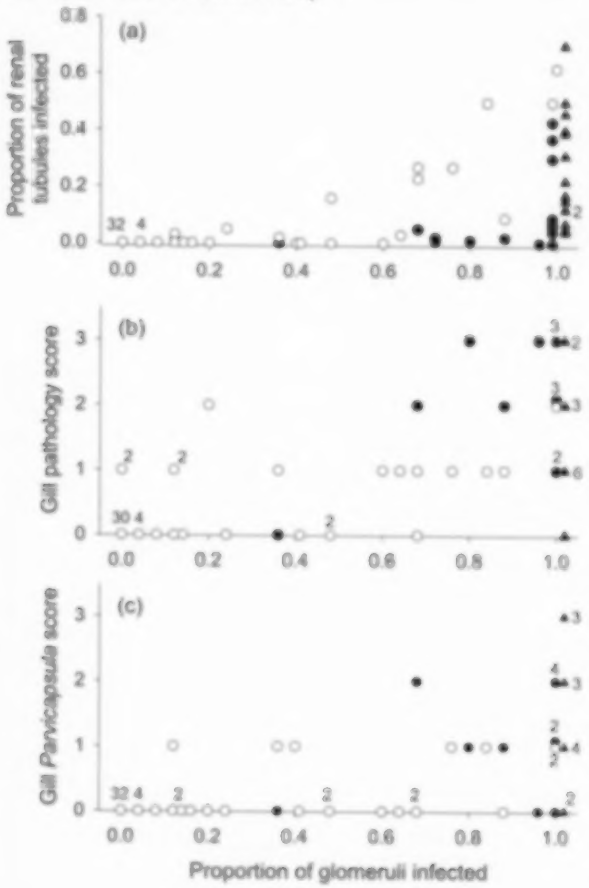

their final days may contribute to an increase in the severity of disease.

The similarity in disease scores between prespawning mortalities in the lake and captive brood ponds as well as the similarity in the median time to death suggest that our conclusions from broodstock data can be cautiously extrapolated to wild fish. However, there are a number of factors that could cause the progression of disease in the rearing ponds to be different from that in the lake. Confinement in ponds likely induces stress in these fish and requires the use of prophylactic drug treatments to prevent the outbreak of bacterial and fungal infections. In other fish, oxytetracycline has been shown to cause a depression in the immune response (Lundén et al. 1998), which may affect susceptibility to disease. Nonetheless, there were both successful spawners and premature mortalities, large variations in the severity of infection and disease, and associations between the timing of arrival, disease, and fate that suggest that the drug treatments did not significantly affect the range of outcomes in the broodstock population. Unfortunately, it is very difficult to sample actively spawning fish in Cultus Lake to evaluate infection and disease because of the depth at which they spawn.

The prevalence and severity of infection of *P. minibicornis* in kidneys were very high among many of our samples. The eosinophilic material seen throughout glomeruli was first reported by Kent et al. (1997) as an eosinophilic fibrinoid exudate that resembles basement membrane thickening. In order for the parasite to become released into Bowman's space and into the renal tubules and urine, it must cause a breach in the glomerular basement membrane, and that may be the cause of the exudate. Diffuse thickening of the glomerular basement membrane is observed with other diseases such as viral hemorrhagic scepticaemia and bacterial kidney disease (Reimschuessel and Ferguson 2006). However, in our samples, we did not observe the wire loop pattern of membrane thickening often associated with those diseases. Presporogonic stages and myxospores were visible in renal tubules once the parasite was widespread in the glomeruli, and this was a condition that was commonly associated with premature death.

Parvicapsula minibicornis has previously been observed in gills of sockeye salmon (St-Hilaire et al. 2002), but the present investigation is the first to observe an association between the severity of the infection and significant histological changes in gills. We observed diffuse lamellar fusion and inflammatory infiltrate throughout the gill filament and lamellae in severe cases. Lamellar fusion is a common response in gills to a number of pathogens and irritants, likely to reduce the surface area exposed to pathogens or toxins (Mallatt 1985; Lewis et al. 2009), although it is often difficult to determine the cause of these changes in an uncontrolled environment. In this study, much of the affected gill tissue contained developmental stages of *P. minibicornis*, and the severity of the gill pathology was correlated with *P. minibicornis* levels in the kidney and gills. Thus, the evidence suggests that the parasite could be the cause of gill disease, although we cannot rule out some other unidentified agent. Controlled infections in an experimental environment such as those conducted by Wagner et al. (2005) are needed to confirm our hypothesis.

Based on observations of developmental stages of a myxosporean parasite in gill tissue and a positive polymerase chain reaction test for *P. minibicornis*, St-Hilaire et al. (2002) proposed that gills may serve as a point of entry for the parasite as is observed for other myxosporeans (Kallert et al. 2009). Our observation that heavy gill infections and associated pathologies occurred after the parasite first appeared in kidney suggests that parasites were accumulating in gills during later stages of infection. The presence of parasite stages within pillar channels of gills demonstrates that the pathogen is in blood, but it is unclear if *P. minibicornis* stages that we found in gills are the result of direct transmission from the environment or were carried from kidneys through the blood to the gills. Pillar channels that were affected by the parasite were fully obstructed with an eosino-

philic material, which is probably the result of parasite presence in the blood as well as basement membrane damage caused by the parasite crossing the membrane when travelling to or from gill epithelium.

Our finding of gill pathology that is potentially related to the presence of *P. minibicornis* raises the potential for respiratory impairment to affect migration and survival. Wagner et al. (2005) found that adult Fraser River sockeye salmon that were infected with *P. minibicornis* took longer to recover from exercise, which they ascribed to a deterioration in renal function. However, these effects may also have been the consequence of reduced function of gills for either gas exchange or osmoregulation. Reductions in the maximal uptake of oxygen during exercise have been observed in rainbow trout (*Oncorhynchus mykiss*) when gill surface area was experimentally reduced (Duthie and Hughes 1987). Similar reductions in performance were observed in trout exposed to zinc or nickel, which were attributed to a reduction in gas exchange caused by lamellar thickening (Lappivaara et al. 1995; Pane et al. 2004). In 2006, we observed fish attempting to swim up highly aerated ephemeral creeks and at the surface of Cultus Lake. Surfacing behaviour was confirmed in a concurrent telemetry study (Pon et al. 2010) that found that death usually followed surface swimming. These observations suggest that gill impairment may have been extremely significant for some fish.

The temperature of the hypolimnetic water in Cultus Lake (<8 °C) appears to suppress further development of the disease, as we found little effect of the length of holding in the captive broodstock ponds in similar water on disease scores. Farrell et al. (2008) also found that sockeye salmon adults from nearby Weaver Creek that held in the hypolimnion of Harrison Lake were more likely to spawn successfully than those that held in much warmer streams near the spawning ground. In Cultus Lake, adults entering the lake remain almost entirely in cold water until the time of spawning, at which point the lake has become isothermal at <8 °C (Pon et al. 2010). Temperature plays a major role in the development of myxosporidian diseases, although threshold temperatures for development have not yet been identified for *P. minibicornis*. Further work using degree-day accumulations to relate river water temperatures to disease progression (e.g., Wagner et al. 2005) should consider using a threshold in the 8 °C range in those calculations.

In summary, our investigations provide correlative evidence for the link between the severity of *Parvicapsula*-related pathology in kidney and gill and premature mortality in adult sockeye salmon. In the case of the Cultus Lake population, negative implications of early entry into the Fraser River for disease development experienced by many late-run populations were offset by the extended use of the hypolimnion of the lake for holding before spawning. Our finding of a relationship between survival and date of arrival at the lake provides some guidance for managers wanting to reduce risk to the population from fishing or habitat impacts in the migration corridor. We recognize that *Parvicapsula* is unlikely to be the sole source of mortality for adult sockeye, and there are likely complex interactions between the parasite, its invertebrate host, the state of fish entering the river, and environmental factors that create the conditions for increased mortality in some years but not in others. Given our findings and the continuing large losses of late-run sockeye salmon in recent years, further investigation of the dynamics of the parasite and its impacts on salmon physiology and performance seem warranted.

Acknowledgements

We thank Dave Barnes, Gary Boak, Ken Peters, Stu Barnetson, and Stephanie Wall for their assistance in the collection of samples, Simon Jones, Dorothee Keiser, and Christine MacWilliams for their help with the histopathology and diagnostic tests, and Sue Grant, Merran Hague, Ron Valet, and Dave Willis for the provision of data. This work was funded by Fisheries and Oceans Canada's Species at Risk and Environmental Watch programs.

References

Bartholomew, J.L., Atkinson, S.D., and Hallett, S.L. 2006. Involvement of *Manayunkia speciosa* (Annelida: Polychaeta: Sabellidae) in the life cycle of *Parvicapsula minibicornis*, a myxozoan parasite of Pacific salmon. J. Parasitol. **92**(4): 742–748. doi:10.1645/GE-781R.1. PMID:16995391.

Brannon, E.L. 1987. Mechanisms stabilizing salmonid fry emergence timing. *In* Sockeye salmon (*Oncorhynchus nerka*) population biology and future management. *Edited by* H.D. Smith, L. Margolis, and C.C. Wood. Can. Spec. Publ. Fish. Aquat. Sci. 96. pp. 120–124.

Ching, H.L., and Munday, D.L. 1984. Geographic and seasonal distribution of the infectious stages of *Ceratomyxa shasta* Noble, 1950, a myxozoan salmonid pathogen in the Fraser River system. Can. J. Zool. **62**(6): 1075–1080. doi:10.1139/z84-154.

Committee on the Status of Endangered Wildlife in Canada. 2003. COSEWIC assessment and status report on the sockeye salmon *Oncorhynchus nerka* (Cultus population) in Canada. Committee on the Status of Endangered Wildlife in Canada, Ottawa, Ont.

Cooke, S.J., Hinch, S.G., Farrell, A.P., Lapointe, M.F., Jones, S.R.M., Macdonald, J.S., Patterson, D.A., Healey, M.C., and Van Der Kraak, G. 2004. Abnormal migration timing and high en route mortality of sockeye salmon in the Fraser River, British Columbia. Fisheries, **29**(2): 22–33. doi:10.1577/1548-8446(2004)29[22:AMTAHE]2.0.CO;2.

Duthie, G.G., and Hughes, G.M. 1987. The effects of reduced gill area and hyperoxia on the oxygen consumption and swimming speed of rainbow trout. J. Exp. Biol. **127**: 349–354.

English, K.K., Koski, W.R., Sliwinski, C., Blakley, A., Cass, A., and Woodey, J.C. 2005. Migration timing and river survival of late-run Fraser River sockeye salmon estimated using radiotelemetry techniques. Trans. Am. Fish. Soc. **134**(5): 1342–1365. doi:10.1577/T04-119.1.

Farrell, A.P., Hinch, S.G., Cooke, S.J., Patterson, D.A., Crossin, G.T., Lapointe, M., and Mathes, M.T. 2008. Pacific salmon in hot water: applying aerobic scope models and biotelemetry to predict the success of spawning migrations. Physiol. Biochem. Zool. **81**(6): 697–708. doi:10.1086/592057.

Foerster, R.E. 1936. The return from the sea of sockeye salmon (*Oncorhynchus nerka*) with special reference to the percentage survival, sex proportions and progress of migration. J. Biol. Board Can. **3**: 421–438.

Foerster, R.E. 1968. The sockeye salmon, *Oncorhynchus nerka*. Bull. Fish. Res. Board Can. 162.

Gilhousen, P. 1990. Prespawning mortalities of sockeye salmon in the Fraser River and possible causal factors. Int. Pac. Salmon Fish. Comm. Bull. XXVI.

Jones, S.R.M., Prosperi-Porta, G., Dawe, S.C., and Barnes, D.P.

2003. Distribution, prevalence and severity of *Parvicapsula minibicornis* infections among anadromous salmonids in the Fraser River, British Columbia, Canada. Dis. Aquat. Organ. **54**(1): 49–54. doi:10.3354/dao054049. PMID:12718470.

Jones, S., Prosperi-Porta, G., Dawe, S., Taylor, K., and Goh, B. 2004. *Parvicapsula minibicornis* in anadromous sockeye (*Oncorhynchus nerka*) and coho (*Oncorhynchus kisutch*) salmon from tributaries of the Columbia River. J. Parasitol. **90**(4): 882–885. doi:10.1645/GE-210R1.

Kallert, D.M., Eszterbauer, E., Grabner, D., and El-Matbouli, M. 2009. *In vivo* exposure of susceptible and non-susceptible fish species to *Myxobolus cerebralis* actinospores reveals non-specific invasion behaviour. Dis. Aquat. Organ. **84**(2): 123–130. doi:10.3354/dao02034. PMID:19476282.

Kent, M.L., Whitaker, D.J., and Dawe, S.C. 1997. *Parvicapsula minibicornis* n. sp. (Myxozoa, Myxosporea) from the kidney of sockeye salmon (*Oncorhynchus nerka*) from British Columbia, Canada. J. Parasitol. **83**(6): 1153–1156. doi:10.2307/3284376.

Lappivaara, J., Nikinmaa, M., and Tuurula, H. 1995. Arterial oxygen tension and the structure of the secondary lamellae of the gills in rainbow trout (*Oncorhynchus mykiss*) after acute exposure to zinc and during recovery. Aquat. Toxicol. **32**(4): 321–331. doi:10.1016/0166-445X(94)00097-A.

Lewis, J.W., Morley, N.J., Drinkall, J., Jamieson, B.J., Wright, R., and Perry, J.D. 2009. Toxic effects of *Streptomyces griseus* spores and exudates on gill pathology of freshwater fish. Ecotoxicol. Environ. Saf. **72**: 173–181.

Lundén, T., Miettinen, S., Lönnström, L.G., Lilius, E.-M., and Bylund, G. 1998. Influence of oxytetracyline and oxolinic acid on the immune response of rainbow trout (*Oncorhynchus mykiss*). Fish Shellfish Immunol. **8**: 217–230. doi:10.1006/fsim.1998.0142.

Mallatt, J. 1985. Fish gill structural changes induced by toxicants and other irritants: a statistical review. Can. J. Fish. Aquat. Sci. **42**(4): 630–648. doi:10.1139/f85-083.

Mathes, M.T., Hinch, S.G., Cooke, S.J., Crossin, G.T., Patterson, D.A., Lotto, A.G., and Farrell, A.P. 2010. Effect of water temperature, timing and physiological condition and lake thermal refugia on migrating adult Weaver Creek sockeye salmon (*Oncorhynchus nerka*). Can. J. Fish. Aquat. Sci. **67**(1): 70–84. doi:10.1139/F09-158.

Pane, E.F., Haque, A., Goss, G.G., and Wood, C.M. 2004. The physiological consequences of exposure to chronic, sublethal waterborne nickel in rainbow trout (*Oncorhynchus mykiss*): exercise vs resting physiology. J. Exp. Biol. **207**(Pt. 7): 1249–1261. doi:10.1242/jeb.00871. PMID:14978065.

Pascho, R.J., Elliott, D.G., and Streufert, J.M. 1991. Brood stock segregation of spring chinook salmon *Oncorhynchus tshawytscha* by the use of the enzyme-linked immunosorbent assay (ELISA) and the fluorescent antibody technique (FAT) affects the prevalence and levels of *Renibacterium salmoninarum* infection in progeny. Dis. Aquat. Organ. **12**: 25–40. doi:10.3354/dao012025.

Patterson, D.A., Macdonald, J.S., Skibo, K.M., Barnes, D.P., Guthrie, I., and Hills, J. 2007. Reconstructing the summer thermal history for the lower Fraser River, 1941–2006 and implications for sockeye salmon (*Oncorhynchus nerka*) spawning migration. Can. Tech. Rep. Fish. Aquat. Sci. 2724.

Pon, L.B., Tovey, C.P., Bradford, M.J., MacLellan, S., and Hume, J.M.B. 2010. Depth and thermal histories of adult sockeye salmon (*Oncorhynchus nerka*) in Cultus Lake in 2006 and 2007. Can. Tech. Rep. Fish. Aquat. Sci. 2867.

Raverty, S., Kieser, D., Bagshaw, J., and St-Hilaire, S. 2000. Renal infestation with *Parvicapsula minibicornis* in wild sockeye salmon from the Harrison and Adams rivers in British Columbia. Can. Vet. J. **41**: 317–318. PMID:10769771.

Reimschuessel, R., and Ferguson, H.W. 2006. Kidney. *In* Systemic pathology of fish: a text and atlas of normal tissues in teleosts and their responses in disease. *Edited by* H.W. Ferguson. Scotian Press, London, U.K. pp. 91–119.

Schubert, N.D., Beacham, T.D., Cass, A., Cone, T.E., Fanos, B.P., Foy, M., Gable, J.H., Grout, J.A., Hume, J.M.B., Johnson, M., Morton, K.F., Shortreed, K.S., Staley, M.J., and Withler, R.E. 2002. Status of Cultus Lake sockeye salmon (*Oncorhynchus nerka*). Can. Sci. Advis. Secr. Res. Doc. 2002/064.

Shortreed, K.S. 2007. The limnology of Cultus Lake. Can. Tech. Rep. Fish. Aquat. Sci. 2753.

St-Hilaire, S., Boichuk, M., Barnes, D., Higgins, M., Devlin, R., Withler, R., Khattra, J., Jones, S., and Kieser, D. 2002. Epitzootiology of *Parvicapsula minibicornis* in Fraser River sockeye salmon, *Oncorhynchus nerka* (Walbaum). J. Fish Dis. **25**(2): 107–120. doi:10.1046/j.1365-2761.2002.00344.x.

Traxler, G.S., Roome, J.R., Lauda, K.A., and LaPatra, S. 1997. Appearance of infections hematopoietic necrosis virus (IHNV) and neutralizing antibodies in sockeye salmon *Oncorhynchus nerka* during their migration and maturation period. Dis. Aquat. Organ. **28**: 31–38. doi:10.3354/dao028031.

Wagner, G.N., Hinch, S.G., Kuchel, L.J., Lotto, A., Jones, S.R.M., Patterson, D.A., Macdonald, J.S., Van Der Kraak, G., Shrimpton, M., English, K.K., Larsson, S., Cooke, S.J., Healey, M.C., and Farrell, A.P. 2005. Metabolic rates and swimming performance of adult Fraser River sockeye salmon (*Oncorhynchus nerka*) after a controlled infection with *Parvicapsula minibicornis*. Can. J. Fish. Aquat. Sci. **62**(9): 2124–2133. doi:10.1139/F05-126.

Potential and realized interactions between two aquatic invasive species: Eurasian watermilfoil (*Myriophyllum spicatum*) and rusty crayfish (*Orconectes rusticus*)

Maria José Maezo, Henri Fournier, and Beatrix E. Beisner

Abstract: With multiple invasions, the potential arises for interactions between invasives inhibiting or promoting spread. Our goal was to investigate the interaction between two invasives, Eurasian watermilfoil (*Myriophyllum spicatum*) and rusty crayfish (*Orconectes rusticus*), which co-occur in several lakes in western Quebec, Canada, and to determine their overlap with littoral fish communities. Crayfish potentially aid milfoil dispersal by fragmentation or, alternatively, inhibit its proliferation through destruction and direct consumption. With a mesocosm experiment, we quantified milfoil fragment production versus biomass reduction by crayfish. More fragments were produced at medium to high crayfish densities, with a significant reduction of milfoil only at the highest densities, demonstrating the potential for both positive and negative interactions. Second, we determined the habitat preferences of each species by conducting a survey in the same lake. There was little overlap in the species' distributions, with each preferring different habitat features, indicating either a low probability of interaction or that interaction occurred historically, resulting in a contemporary exclusion pattern. While our experiment showed a potential for significant interaction, the low natural co-occurrence of these species suggests that they do not currently influence each other or that they previously excluded each other.

Résumé : L'interaction entre de multiples espèces envahissantes peut inhiber ou favoriser leur dispersion. L'objectif de notre étude était de déterminer l'interaction entre deux espèces envahissantes, le myriophylle à épis (*Myriophyllum spicatum*) et l'écrevisse à taches rouges (*Orconectes rusticus*), introduites dans plusieurs lacs de l'ouest du Québec, Canada, et de déterminer leur chevauchement avec les poissons littoraux. Les écrevisses peuvent favoriser la dispersion du myriophylle par fragmentation, mais aussi diminuer sa prolifération par leur consommation et leur destruction. Une expérience en mésocosmes fut réalisée pour quantifier la production de fragments et la réduction de la biomasse des myriophylles par les écrevisses. Plus de fragments furent produits à des densités d'écrevisses moyennes et élevées alors que seules des densités élevées réduisirent significativement la biomasse, démontrant un potentiel d'interactions positives comme négatives. Ensuite, leurs habitats préférentiels furent déterminés par un échantillonnage dans le même lac. Il y avait peu de chevauchement dans leurs répartitions, chacune préférant différentes caractéristiques de l'habitat, ce qui indique une faible probabilité d'interaction ou alors une interaction historique ayant mené à l'exclusion actuelle. Alors que les expériences indiquent la possibilité d'une interaction significative entre ces deux espèces envahissantes, le faible chevauchement et les densités dans le milieu naturel suggèrent qu'elles ne s'influencent pas pour l'instant ou qu'elles se sont exclues l'une l'autre dans le passé.

Introduction

Invasive species are currently one of the major global threats to biodiversity with the potential to dramatically alter community structure and ecosystem functioning (Mack et al. 2000; Sala et al. 2000; Lawler et al. 2006). One of the major challenges to ecologists is to predict the joint impacts and the potential for facilitative synergies that invasive species may have when they co-occur, an idea embodied in the invasional meltdown hypothesis (Simberloff and Von Holle 1999). This study concerns two of the most studied invasive species of freshwater systems in North America: the Eurasian watermilfoil (*Myriophyllum spicatum*) and the rusty crayfish (*Orconectes rusticus*). Impacts of these species when encountered alone are well known (see below), whereas the importance of their interaction when encountered together in the same lake has not been addressed to date, despite the fact that both species already co-occur in some lakes (H. Fournier, unpublished data) and are likely to have strongly overlapping distributions in the near future, given their invasion trajectories and vectors. These species are likely to co-occur in many lakes because both are introduced primarily by people carrying propagules and travelling from lake to lake, either purposefully (i.e., rusty crayfish for live bait) or accidentally (i.e., macrophyte fragments on boats or trailers) (Johnson et al. 2001; Puth and Allen 2005). Further spread within watersheds can also oc-

Received 1 April 2009. Accepted 9 February 2010. Published on the NRC Research Press Web site at cjfas.nrc.ca on 17 March 2010.
J21137

M.J. Maezo and B.E. Beisner.[1] Department of Biological Sciences, Université du Québec at Montreal, C.P. 8888, Succ. Centre Ville, Montréal, QC H3C 3P8, Canada.
H. Fournier. Ministère des Ressources naturelles et de la Faune, Direction de l'expertise Faune-Forêts, 16 impasse de la Gare-Talon, RC 100, Gatineau, QC J8T 0B1, Canada.

[1]Corresponding author (e-mail: beisner.beatrix@uqam.ca).

cur naturally via waterways or through biotic vectors. Thus, the chances that these species will be introduced into the same lakes are high, rendering the understanding of the ecological interactions between these invasives and their impacts on the littoral fish community necessary.

Eurasian watermilfoil (hereafter referred to as milfoil) was introduced from Eurasia into North America in the 1940s and has been considered a very problematic invasive aquatic plant since the 1970s (Grace and Wetzel 1978; Crow and Hellquist 2000). Local expansion occurs mainly via stolon production (Madsen and Smith 1997) and dispersal is primarily accomplished by fragmentation, which allows for interlake colonization (Nichols and Shaw 1986). As a result, milfoil is now widespread in North America (Smith and Barko 1990; Crow and Hellquist 2000). It invades the littoral zone of lakes by forming extensive monotypic stands and outcompetes many other submersed species, thus reducing the biodiversity of macrophytes (Smith and Barko 1990; Madsen et al. 1991; Boylen et al. 1999). The loss of native macrophytes, or the change in total plant biomass in a lake, can cause changes in invertebrate communities and affect littoral fish communities, including young-of-year pelagic species that use plants as habitat, refuge, or reproduction sites (Smith and Barko 1990).

Predictive models of milfoil presence or dominance suggest that lakes with greater human impact are more vulnerable to invasion, specifically mesotrophic to eutrophic lakes (Smith and Barko 1990; Madsen 1998) or in landscapes with little forest cover (Buchan and Padilla 2000). It has been predicted that milfoil should be restricted to locations with nutrient-rich sediments or with heavy public use (Smith and Barko 1990). The mechanisms allowing the recent dominance and proliferation of milfoil in several oligotrophic lakes of the Outaouais region in Quebec, Canada (H. Fournier and P. Houde, Ministère des Ressources naturelles et de la Faune, unpublished data), are therefore not well understood and are of increasing concern to prevent further spread. As a result of the invasion of milfoil into oligotrophic lakes, where aquatic vegetation is usually sparse, shifts to phytophilic fish species are likely to be favoured (Randall et al. 1996; Weaver et al. 1997; Pratt and Smokorowski 2003) at the expense of lithophilic species typical of such environments (Auger 2006). Dense growth of macrophytes, as has been observed with Eurasian milfoil in our study area, should promote proliferation of littoral fish species (Randall et al. 1996; Weaver et al. 1997) with consequences for important pelagic sportfish species like lake trout (*Salvelinus namaycush*). Pelagic fish could be affected by milfoil growth indirectly through changes in the littoral fish community composition affecting prey availability or via increased predation risk on young-of-year of pelagic species. The effects of milfoil on pelagic fish species may also be a direct one with a reduction in spawning habitat quality because of dense macrophyte proliferation (Auger 2006). One of the goals of our study was to determine whether an interaction with an invasive species of crayfish could help explain the proliferation of milfoil throughout these oligotrophic lakes.

The rusty crayfish is native to the Ohio River basin but its use as live bait has permitted it to colonize up to 20 states in the United States as well as the Canadian provinces of Ontario and Quebec (Hobbs and Jass 1988; Taylor and Redmer 1996; Dubé and Desroches 2007). It can invade both lakes and streams where it displaces native congeners (Capelli 1982; Hill and Lodge 1999; Wilson et al. 2004) because of its higher fecundity, earlier reproduction, and faster growth of eggs and young-of-year compared with native species (i.e., *Orconectes propinquus* or *Orconectes virilis*) (Lodge et al. 1985; Olsen et al. 1991). Rusty crayfish is also more aggressive (Capelli and Munjal 1982), has a higher ingestion rate of snails (Olsen et al. 1991), and is less sensitive to predation by fish (DiDonato and Lodge 1993; Hill and Lodge 1995; Kuhlmann et al. 2008). As a result, it has been shown to displace native species both by competition for refuges (Hill and Lodge 1994) and by hybridization (Perry et al. 2001). Based on pH and calcium concentrations, 70% of Canadian Shield lakes provide suitable chemical conditions for *O. rusticus* (Vander Zanden et al. 2004).

Because crayfish are omnivorous and are often the largest invertebrates in freshwater systems, changes in their guild composition can have significant impacts at multiple trophic levels (Nyström et al. 1996; Guan and Wiles 1997; Hamr 2002). They reduce densities of snails and other aquatic invertebrates (Wilson et al. 2004; McCarthy et al. 2006; Johnson et al. 2009) and can thereby have negative impacts on competing littoral fishes (e.g., *Lepomis* spp.) (Wilson et al. 2004; Willis and Magnuson 2006). Rusty crayfish can reach high densities in rocky habitats (Lorman 1980; Garvey et al. 2003), becoming important predators on fish eggs of species that spawn in such habitats, including the economically important lake trout (Horns and Magnuson 1981; Jonas et al. 2005). Rusty crayfish are well known to dramatically reduce native macrophyte biomass and richness in invaded lakes (Lodge et al. 1994; Wilson et al. 2004; Rosenthal et al. 2006). Impacts can be very evident, for example, Lodge and Lorman (1987) showed that >5 crayfish·m^{-2} could completely eliminate macrophytes in 7 weeks and that a single adult crayfish per square metre could cause a 64% reduction in their biomass. Also, Magnuson et al. (1975) observed that macrophytes disappeared in parts of a lake where rusty crayfish densities were between 4 and 6·m^{-2} but that macrophytes were still abundant in places where crayfish densities were between 1.5 and 2·m^{-2}. Some studies have shown that other species of the genus *Myriophyllum* are eliminated by rusty crayfish (Lorman 1980; Rosenthal et al. 2006), while others have found that milfoil persists, and even dominates, in the presence of other crayfish species (Magnuson et al. 1975; Nyström and Strand 1996). Thus, the impact of rusty crayfish on milfoil remains unclear and deserves further study.

The nature of the ecological interaction between these two species could potentially influence their individual impacts in invaded lakes. Rusty crayfish could interfere with milfoil invasion by directly reducing its biomass, thereby precluding the formation of very dense stands. The control of milfoil by rusty crayfish (an antagonistic interaction) could reduce the previously mentioned impacts of milfoil dominance on the ecosystem. In this way, one invasive species could help control another. However, crayfish could also help spread milfoil in invaded lakes (a synergistic interaction) because they generally produce many uneaten cut fragments (Lorman 1980; Lodge and Lorman 1987; Lodge 1991). Because mil-

foil disperses mainly by fragmentation and vegetative reproduction, rusty crayfish could positively affect the macrophyte with an increase in its recruitment rate, perhaps compensating for the mortality induced by crayfish consumption. As mentioned previously, this mechanism could help explain the proliferation success of milfoil in oligotrophic lakes in this region. Finally, there also exists the possibility that these two species do not interact in a significant manner. Such might be the case when some predatory fish species occupy macrophyte stands, thereby deterring rusty crayfish from consuming milfoil, or because of different preferences for substrate types. Where there is no interaction between the invasives because of habitat segregation, impacts of the invasions may be predicted from the direct effects of each species alone (additive effect) in habitats they occupy.

The primary goal of this study was to determine which one of these three types of interaction (antagonistic, synergistic, or additive) occurs between these two invasive species in a large oligotrophic lake using a field mesocosm experiment and a survey of habitat use and overlap. Because both of these invasives occupy the littoral zone, they will overlap with littoral fish communities. As a secondary goal, therefore, we also explore the co-occurrence patterns with littoral fish in the same lake.

Materials and methods

Study site

Lake Pemichangan (46°03′N, 75°51′W) is located in the Gatineau River basin, Outaouais region of Quebec, Canada. This oligotrophic lake (total phosphorus <10 $\mu g \cdot L^{-1}$) has a surface area of 15.44 km^2, a mean depth of 16.8 m, a maximum depth of 59 m, and a littoral zone (<5m deep) that occupies 24.7% of the total lake area. The lake is divided into two large basins, east and west (Fig. 1), each with multiple bays. Some bays are heavily inhabited, while others are completely free of human development. Generally, the east basin has steep sides with rockier substrate and very little human habitation. Most of the Gatineau River watershed is covered by metamorphic rock typical of the Canadian Shield. Coverage by marine tropical waters 570 million years ago, however, contributed to the formation of sedimentary rocks (limestone and sandstone), which are more characteristic of the Lake Pemichangan watershed. Thus, this lake's water is more mineralized (23 mg $Ca \cdot L^{-1}$) than typical Canadian Shield lakes. Between 1987 and 2006, Secchi depth varied from 5 to 8 m, conductivity varied from 110 to 190 $\mu S \cdot cm^{-1}$, and pH varied from 7.8 to 8.5 (data from Québec Ministère des Ressources naturelles et de la Faune). Milfoil was probably introduced in the 1990s and is now the dominant plant in the lake. The date of introduction of rusty crayfish is unknown, but the first confirmed specimen was found in 2001 (Dubé et al. 2002).

Experiment: impact of rusty crayfish on milfoil

To evaluate the impact of rusty crayfish on milfoil, in situ mesocosm experiments were conducted in 16 circular 2 m^2 cages. They were installed in a dense milfoil bed located in the southeast zone (Fig. 1) of the west basin where there was neither human habitation nor disturbance to the riparian zone. Treatments consisted of a cageless reference area and adult crayfish densities of 0 (absent), 0.5 (low), 2 (medium), and 8 (high) individuals$\cdot m^{-2}$, which are well within the range of natural densities of adult crayfish (Capelli 1975; Lodge et al. 1994). The cageless references were sites without cages located at a distance from, but in between, caged treatments that served as a control for the cage effect. Four cages and one reference area were clustered into four blocks and treatments were randomized within blocks. Distance between individual cages and from cageless references were 4–8 m. Cages were positioned in dense milfoil beds in such a way as to exclude logs or rocks on the lake bottom and at depths between 1.45 and 1.6 m. Presence of other macrophytes under the milfoil canopy was also noted (mainly *Elodea canadensis* and several *Potamogeton* spp.), but these were always at very low densities.

Cylindrical cages were built of 0.85 mm thick galvanized steel sheets and galvanized steel mesh (mesh size = 5.71 mm). The top and bottom of the cage walls consisted of solid metal sheets of 15 and 46 cm high, respectively, and the middle part was a 1.1 m high mesh sheet for a total height of 171 cm. Cages were buried 5–10 cm in the sediment and protruded 10–20 cm above the water surface. Additional mesh was added around the top of cages once in place to prevent waves from removing milfoil fragments from or adding them to the cages. This design prevented crayfish escape from the cages because they could neither climb over the sheet nor burrow under the cage. The large mesh size allowed for good water circulation; conditions inside the cages were similar for all treatments even if they differed slightly from those of the cageless conditions. The mesh part of each cage was scrubbed twice during the experiment to remove periphyton.

Crayfish were collected for stocking the experimental cages from 11 to 13 June 2007 in an almost completely isolated bay of the west basin (Ritchie's Bay; Fig. 1) to ensure little interference with the survey part of the study. Because most of the crayfish captured were actually hybrid *O. rusticus* × *O. propinquus* males (see crayfish identification section), we added only adult hybrid males to the cages, excluding females and pure *O. rusticus* to ensure a similar population of crayfish throughout. Prior to the start of the experiment, crayfish were separated into three size categories according to their carapace lengths (small (31–36 mm), medium (37–41 mm), and large (42–46 mm)), kept in three different outdoor tanks, and fed beef liver. The experiment started 15 June 2007 and lasted 8 weeks. One medium crayfish was placed in each of the low-crayfish treatments. One small, two medium, and one large crayfish were placed in the medium-crayfish treatments. Six small, six medium, and four large crayfish were placed in the high-crayfish treatments. To monitor crayfish densities, we used minnow traps baited with beef liver, which were left in the cages overnight, three times during the experiment (every 2–3 weeks). That same night, crayfish were captured from Ritchie's Bay to replace missing experimental crayfish the next morning (see Appendix A). In adding new crayfish, we could not be sure that we maintained the original size distribution exactly.

This experimental design probably represents an overestimate of actual consumption rates by crayfish compared with

Fig. 1. Map of Lake Pemichangan showing the east (E) and west (W) main basins. Black patches indicate milfoil beds as measured in 2007. Mapping was accomplished by slowly travelling the circumference of the lake and surveying with an aquascope (reverse periscope) from a boat and tracing contours using a global positioning system. H represents the 127 sampling points. The site of the experiment and of Ritchie's Bay (source of experimental crayfish) are both indicated. The inset map of eastern Canada shows the approximate location of Lake Pemichangan in the Province of Quebec.

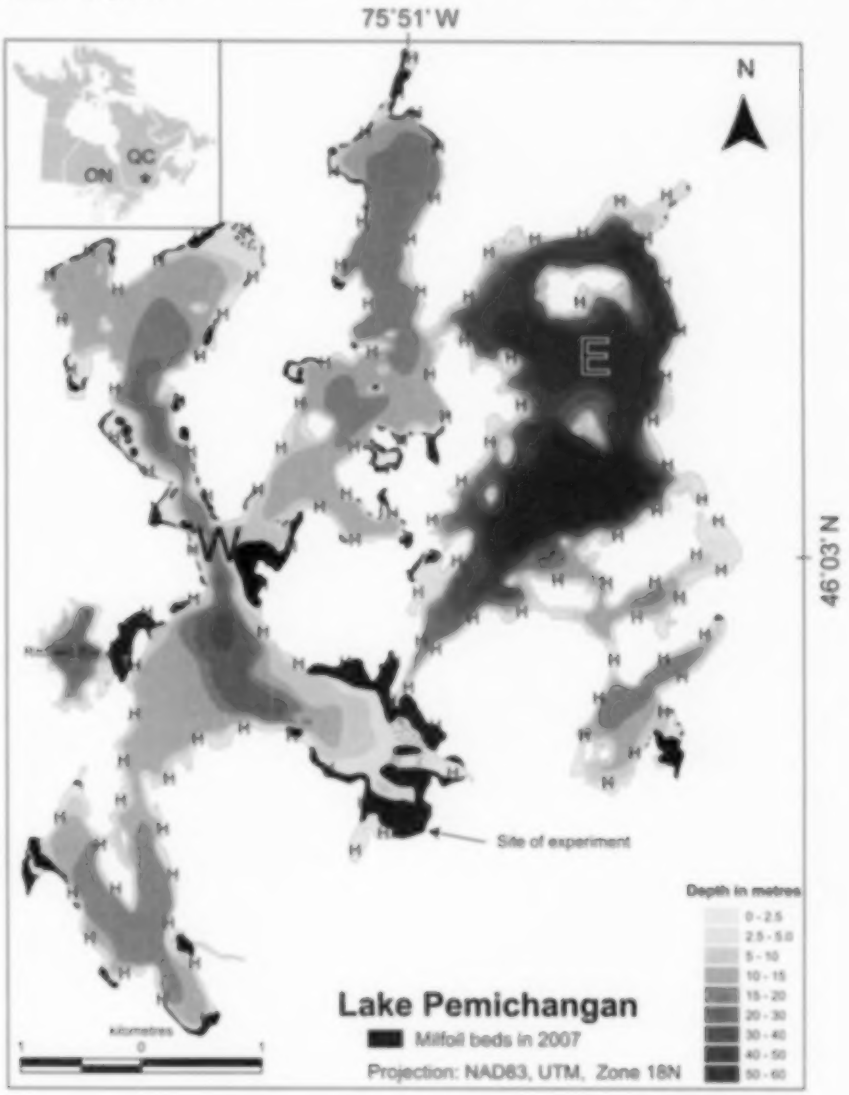

natural conditions because crayfish were restricted to the same 2 m^2 environment for 8 weeks, and thus, it provides an estimate of the potential impacts of crayfish at the applied abundances. Because the cages were small, we could not measure milfoil biomass inside the cages before or during the experiment without perturbing the experiment itself. However, treatments were randomized within blocks, allowing for variation to be evenly distributed, so densities were assumed to be equal across treatments at the beginning of the experiment. Milfoil fragments floating on the water surface of each cage were collected weekly; these were counted, washed, and dried at 80 °C to constant weight. At the end of the experiment, in each cage and cageless reference area, three randomly placed 25 cm × 25 cm quadrats were sampled for their total aboveground biomass. Plants were separated by species, washed, and dried at 80 °C for at least 24 h to a constant weight to estimate dry biomass (±0.005 g).

To provide relative estimates of milfoil fragment production by anthropogenic sources (to compare with biotic production by crayfish in our experiment), we sampled the fragments produced by our 9.9 hp motorboat when tracing

four 50 m transects across dense milfoil beds in early August. We also collected fragments produced by six throws of a 2 kg fluke-style anchor in dense milfoil beds.

Experimental data analyses

Prior to running a one-way ANOVA to compare final milfoil standing biomass and fragment production in the experiment, we ran a nested ANOVA to determine whether there were outlier replicates. One cage from the crayfish-absent treatment was discovered in this way to have significantly lower milfoil biomass than the other replicates in the same treatment (its lower density had also been noted during setup of the experiment) and it was eliminated from subsequent analyses. We then performed a one-way ANOVA followed by a Tukey test on the experimental data to compare mean standing macrophyte biomass as well as mean total number of fragments between treatments using JMP 5.1 (SAS Institute Inc., Cary, North Carolina). Final milfoil biomass data were not transformed (as they satisfied assumptions of homogeneity of variance and normality), but other macrophyte biomass and the number of fragments were square root transformed.

Lake survey: co-occurrence of the two invasives

To establish the co-occurrence of milfoil and rusty crayfish, we conducted a survey of the littoral zone of Lake Pemichangan. In the littoral zone of the lake, 127 sites, linearly situated 400 ±10 m apart (Fig. 1), were systematically sampled for environmental variables, crayfish, and macrophytes. Depending on the slope and the presence of woody debris, site distance from shore varied from 1 to 30 m to sample at a depth of 1.5–2 m. A subset of 42 sites was also sampled for fish to establish the possible co-occurrence with the two invasive species.

Assessing habitat and macrophytes

In May (19–21) and July (9–16), each site was sampled using three random tosses of a 1 m^2 quadrat on different sides of the boat at distances of 3–5 m apart. Within each quadrat, the percent cover of different substrate categories and of macrophytes was assessed. Substrate categories consisted of (1) mud, (2) sand (<2 mm diameter), (3) gravel (2–60 mm diameter), (4) small cobble (60–120 mm diameter), (5) large cobble (120–250 mm diameter), (6) boulders (>250 mm diameter), and (7) bedrock. The mean survey values were then used to build a substrate index for each site, as in Bubb et al. (2006), based on the sum of the percent cover (n) of each substrate category (S):

$$\text{SubIndex} = \sum n_S$$

The substrate index varied between 100 and 700 and increased with substrate grain size.

Plants in quadrats sampled in May and July were classified as either milfoil or "other macrophytes" (including *E. canadensis*, *Potamogeton* spp., *Isoetes* sp., *Nuphar* sp., and *Nymphea* sp.). On 1 August, macrophytes were further sampled at each site using a 25 cm × 25 cm quadrat randomly placed twice. Aboveground biomass was harvested, washed, and dried at 80 °C to constant weight to obtain an average biomass for every site. Percent cover of macrophytes was again evaluated at this time and merged with previous observations to provide a summer-long mean of cover.

At each site, submerged lake (littoral zone, 0–5 m) bank slope was calculated in ArcGIS 9 (ESRI, Redlands, California) using the site coordinates taken with the global positioning system and a bathymetric map. Abundance of logs and branches in the water was recorded in a semiquantitative way ranging from 0 (not present) to 3 (very abundant) and presence–absence of leaf litter was also noted. A debris index ranging from 0 to 18 was then constructed by multiplying the log value by 3, branches by 2, and litter by 1. Human riparian impact was the sum of the presence (1) or absence (0) of cottages, docks, and (or) lawns. Degree of forest cover was recorded semiquantitatively, ranging from absent (0) to fully present (3). The presence–absence of still standing dead trees on the shore was also included as an environmental variable.

Crayfish sampling

Crayfish were sampled 9–16 July and 6–11 September 2007. Sampling coincided with weeks when there was a new moon to maximize catch rates because moonlight is known to reduce crayfish activity (Flint 1977). To sample crayfish, we used standard minnow traps with enlarged entrances (4.5 cm diameter) and baited with 120 ± 5 g of beef liver. One trap was installed at 1.5–2 m depth in each site, left overnight (16–19 h), and collected the next day. All crayfish were identified, carapace length was measured to the nearest 0.5 mm with calipers, and sex and reproductive form (I, reproductive; II, nonreproductive) were noted. Crayfish were returned to the lake at the sampling site from which they had been taken.

This trapping method is known to be selective for large males, which can inhibit other crayfish from entering the trap, especially in rusty crayfish (Capelli 1975; Olsen et al. 1991; Hein et al. 2007). Females and other crayfish species may therefore be underestimated in this study by up to a factor of 2 (Olsen et al. 1991). Sex ratios of natural crayfish populations are usually close to 1:1 (Lorman 1980), but female and male catch rates can change during the year (Lodge et al. 1986; Hein et al. 2007). Other studies suggest that trap catches can be a reliable estimate of relative abundance (Capelli and Magnuson 1983). Even if trap catches do not exactly reflect the actual population structure, traps can indicate the relative abundance of rusty crayfish between sites and can be used as indices of population abundance (Capelli 1975; Olsen et al. 1991), which was the main goal of the survey. However, maximum abundances can be difficult to estimate because trap saturation can occur with rusty crayfish at around 15 individuals per trap (Ogle and Kret 2008).

Crayfish were identified following Hobbs and Jass (1988), Hobbs (1989), and Dubé and Desroches (2007) (see Appendix B for details). Individuals that possessed characters of more than one species were considered hybrids (following Dubé and Desroches 2007). For example, as many individuals possessed a carina on the rostrum but had mostly *O. rusticus* characters, this highly suggests that these individuals were hybrids with *O. propinquus* (Capelli and Capelli 1980). Identification of hybrids in this study was based solely on morphological characteristics. Further genetic

studies would be needed to confirm our classifications. Because all hybrids had mainly *O. rusticus* characteristics, we group them together in the rusty crayfish group for further analyses.

Fish sampling

Every third site (42 sites in total) was sampled for fish littoral community composition using a Smith-Root SR-16S electrofishing boat. The boat followed the shore at a depth of 1–3 m for 3 min, covering a distance of 30 ± 5 m at each site. Sampling was done after sunset between 8:30 p.m. and midnight on three different dates (20, 26, and 28 June 2007). The number of fish of each species was recorded and specimens were returned to the water alive at the sampling site. Individuals that could not be identified in the field were euthanized with an overdose of MS-222 (tricaine methanesulfonate) and preserved in 10% formalin for further identification in the laboratory.

Survey data analyses

Principal components analysis (PCA), an indirect gradient analysis, was performed first to determine the amount of variation in species composition (Leps and Smilauer 2003). Redundancy analysis (RDA), a linear multivariate technique for direct gradient analysis (constrained ordination), was then performed to correlate variation in species abundances with environmental gradients and reveal the variation explained by the environmental variables (Leps and Smilauer 2003). Analyses were performed using CANOCO 4.5 (www.pri.wur.nl/uk/products/canoco/). To conduct the analyses of the 127 sites, community response data consisted of mean summer values for percent cover of milfoil (milfoil) or other macrophytes (Other M) and mean (July and September) rusty crayfish abundance (Crayfish) (the sum of crayfish with *O. rusticus* characters). Analyses were also done using macrophyte biomass, giving the same results as with percent cover, so they are not presented. Species variables (crayfish abundance and percent cover of macrophytes) were $\log(y + 1)$ transformed and centred and environmental variables were centred and standardized. To identify significant variables affecting species composition, we used a forward selection with Monte Carlo permutation tests (499 permutations) on the full model. We used a linear transect spatial restriction to account for the spatial structure of the sampling design.

A separate set of multivariate analyses was conducted for the 42 sites where crayfish, macrophytes, and fish data were all available. These were performed with the July data for crayfish and macrophytes and included only fish species that had an average of more than one capture per site: smallmouth bass (*Micropterus dolomieu*), yellow perch (*Perca flavescens*), pumpkinseed (*Lepomis gibbosus*), blackchin shiner (*Notropis heterodon*), bluntnose minnow (*Pimephales notatus*), brown bullhead (*Ameiurus nebulosus*), and banded killifish (*Fundulus diaphanus*).

Results

Experiment: impact of rusty crayfish on milfoil

Minnow trap catches confirmed that no crayfish were present in the absent crayfish treatments. Densities in other treatments varied slightly because of losses of some individuals through time and the addition of crayfish when losses were mistakenly thought to have occurred. Thus, mean density in the low-crayfish treatment was 0.5 individual·m^{-2} (varying in time and between replicates from 0 to 1 individual·m^{-2}), 2.5 individuals·m^{-2} (1.5–3.5 individuals·m^{-2}) in the medium-crayfish treatment, and 7.5 individuals·m^{-2} (5–9 individuals·m^{-2}) in the high-crayfish treatment. Overall, despite some temporal and between-replicate variation, experimental densities remained close to assigned treatment values.

The impact of both consumption and nonconsumptive fragmentation on milfoil biomass varied with crayfish density (ANOVA, $P = 0.0001$) (Fig. 2*a*). However, only in high-crayfish treatments was milfoil biomass significantly reduced (by 68%) at the end of the experiment compared with the absent crayfish treatment. In medium-crayfish treatments, there was a 34% (nonsignificant) reduction and only a 10% reduction in the low-crayfish treatment. Although there was a trend for caged treatments to have lower milfoil biomass than the cageless references, final biomass in the absent and low-crayfish treatments were not statistically different from that of the cageless references, indicating that there was no significant impact of cages on plant growth.

The potential impact of crayfish on milfoil dispersal, measured as the number of unconsumed fragments that can float to the surface and colonize other areas, also varied with crayfish density relative to the no-crayfish controls (ANOVA, $P = 0.0001$) (Fig. 2*b*). The total number of milfoil fragments collected in the high-crayfish treatment was nine times higher than in the absent crayfish treatment and five times higher in the medium-crayfish treatment. The presence of a low number of crayfish, however, did not have a significant effect, even if the mean number of fragments produced was twice as high as in the absent crayfish treatment. This experiment design also provided an estimate of the number of milfoil fragments that can be produced by the plant itself under natural conditions. Assuming that the cage had no significant effect on fragment formation, a 2 m^2 area of milfoil, with a dry weight biomass of a 62 ± 8 g, can produce 70 ± 5 fragments in 8 weeks (from June to August), which provides an estimate of autofragmentation.

The impact of crayfish density on other macrophytes encountered at low densities under the milfoil canopy (i.e., *E. canadensis* and different species of *Potamogeton*) was also measured in this experiment (Fig. 2*a*). These plants were completely eliminated in the high-crayfish treatment and almost eliminated in the medium-crayfish treatment. While biomass of other macrophytes was significantly lower in cages with crayfish than without, it was not significantly lower than for the cageless reference sites.

Although natural processes that can contribute to milfoil dispersal are important to quantify, the comparison with anthropogenic sources of fragments is an important management issue. Passing through dense milfoil beds with a motorboat produced 69.7 ± 23.5 fragments with a maximum of 115 fragments in less than 1 min. Throwing an anchor in the middle of such beds produced 19.9 ± 10.7 fragments with a maximum of 64 fragments, including some with roots.

Fig. 2. (*a*) Final mean biomass (±1 SE) of milfoil (black bars) and other macrophytes (grey bars) at the end of the experiment and (*b*) total abundance (±1 SE) of milfoil fragments produced during the experiment in cageless reference sites (CR) and in absent crayfish (A), low-crayfish (L), medium-crayfish (M), and high-crayfish (H) treatments. Different letters indicate significant differences between treatment combinations within each graph (Tukey's test, $P < 0.05$).

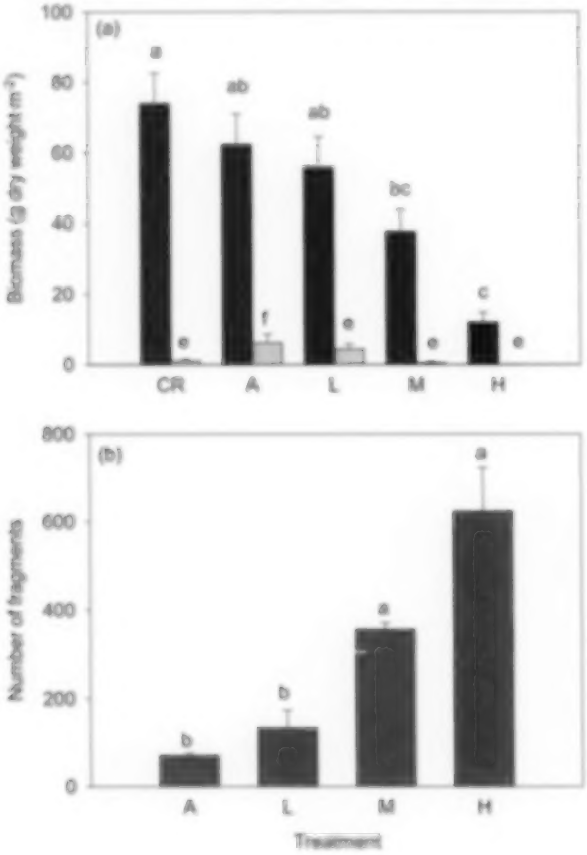

Lake survey

Crayfish captures

In July, more than half (59%) of the captured crayfish consisted of *O. rusticus* × *O. propinquus* hybrids and more than a third (40%) were identified as pure *O. rusticus* (Table 1). Average capture success was 11.58 ± 0.88 crayfish·trap^{-1}, which is below the level of trap saturation detected for rusty crayfish by Ogle and Kret (2008). However, because of this phenomenon, we are likely underestimating crayfish abundances at the most densely populated sites. Eleven individuals had a broken rostrum, making it impossible to determine if they were hybrids or pure rusty crayfish (no evidence for the presence of a carina on the rostrum). Only nine individuals of the native species *O. propinquus* were found. We also discovered another introduced species, *Orconectes immunis*, as well as morphological hybrids of the latter with *O. rusticus*. Hybrids between these two species have not, as far as we know, been previously mentioned in the literature, but genetic analysis would be needed to confirm this statement. Spatially, there were more *O. propinquus* and *O. immunis* in the northern end of the lake, but we also captured some on the eastern side (Appendix C, stars and diamonds on Fig. C1).

Table 1. Total crayfish captures in 127 traps for July and September 2007.

Species	Sex	July	September
OR	Males	430	159
	Females	151	22
OR × OP	Males	664	342
	Females	198	32
OP	Males	8	5
	Females	1	1
OI	Males	3	2
	Females	1	2
OR × OI	Males	2	3
	Females	2	1
OR × OP × OI	Males		1
Unidentified		11	10
Total OR	Males	1096	505
	Females	351	55
Total catch		1471	580

Note: Crayfish: OR, *Orconectes rusticus*; OP, *Orconectes propinquus*; OI, *Orconectes immunis*; OR × OP, *O. rusticus* × *O. propinquus* hybrids; OR × OI, *O. rusticus* × *O. immunis* hybrids; OR × OP × OI, *O. rusticus* × *O. propinquus* × *O. immunis* hybrids. Total OR is the sum of all crayfish having *O. rusticus* characters.

In September, overall capture success was lower (average of 4.5 ± 0.50 crayfish·trap^{-1}). More than half the captures (64%) consisted of *O. rusticus* × *O. propinquus* hybrids, pure *O. rusticus* making up most of the rest of the catch (31%) along with a few individuals each of *O. propinquus*, *O. immunis*, and *O. rusticus* × *O. immunis* (Table 1). We also discovered an apparent hybrid consisting of *O. rusticus* × *O. propinquus* × *O. immunis* that has not yet been reported in the literature to our knowledge. The majority of natives, *O. propinquus*, and the other introduced species, *O. immunis*, were more common along the northern shore of the lake (Appendix C, stars and diamonds on Fig. C2).

In addition to relative densities, estimation of crayfish abundances was important to allow comparisons between experimental and survey components of this study. Capelli (1975) suggested that the effective trapping area of minnow traps was 12.5 m^2. Average catch per unit effort (CPUE) across all sites in July, when capture success was highest, was 11.58 ± 0.88 ind·trap^{-1}, giving an average density of crayfish in the littoral zone of Lake Pemichangan of almost 1 individual·m^{-2}. Of the 127 sites sampled, 35 sites had macrophytes and average CPUE of crayfish was lower (4.29 ± 1.06 individuals·trap^{-1}) in those sites than in those without macrophytes (14.23 ± 0.98 indiduals·trap^{-1}). Given that trap saturation can occur in rusty crayfish, values in sites without macrophytes are likely underestimates of actual densities, making the significant patterns detected in the following analyses conservative estimates. These results suggest that crayfish density was 0.34 individual·m^{-2} in

macrophyte beds and 1.14 individuals·m^{-2} in sites without macrophytes. Most of the sites without macrophytes (85%) had a substrate index superior to 400 (62% of all sites), which means that they had at least some proportion of cobble or other rocky substrate offering cover to the crayfish. Highest CPUEs in macrophyte beds were observed in sites that also offered rocks or logs as shelter (e.g., there were only four sites with milfoil and two with other macrophytes that had a CPUE of >9 individuals·trap^{-1}, with a maximum of 27 individuals·trap^{-1}).

Milfoil and rusty crayfish co-occurrence

Joint distribution patterns of crayfish, milfoil, and other macrophytes were determined using ordination (Leps and Smilauer 2003). The results obtained for both PCA and RDA were very similar for both July and September. Therefore, here, we present mean crayfish captures over the 2 months (Fig. 3). The eigenvalues and the cumulative percentage of variation explained by axes 1 and 2 for both PCA and RDA analyses are shown in Table 2. The first two axes of the PCA captured a very high proportion (92.0%) of the species variation and clearly showed a separation between the three species groups: milfoil, other macrophytes, and crayfish all reached high abundances in different sites (Fig. 3*a*). The first axis contained 94.6% of the variation explained by the environmental variables. In the RDA, although the two first axes only explained 43.1% of species variation, the positions of the species did not fundamentally change, meaning that we still captured the variation in species composition (Fig. 3*b*) (Leps and Smilauer 2003). Again, the first axis captured most of the variation (42.1%) and interpretation of the second axis was limited because it only explained another 0.01% of species variation. Significant variables selected were substrate index (Monte Carlo, P = 0.004), which explained 38% of species variation, followed by debris (P = 0.01), which explained another 4%. Other variables were not significant but were left in the RDA biplot (Fig. 3*b*) to reveal the correlation between variables. Macrophytes, including milfoil, were encountered in sites with low substrate index (mud and sand), while crayfish were more associated with higher substrate index (gravel, cobble, and boulders) and the abundance of debris (logs, branches, and leaves). Note also that milfoil was particularly associated with riparian use. Even if this was simply an artefact arising due to a negative correlation with substrate index and that riparian use was not selected as a significant variable, it still suggests that milfoil and riparian use are closely related in this lake.

Littoral fish

The total catch in the 42 sites sampled consisted of 16 species (Table 3) with pumpkinseed and yellow perch as dominants. Seven species made up 93.8% of the catch and only these species were used in the ordinations. Among sites, fish abundance ranged from 5 to 257 and richness ranged from two to eight species (average of 4.6 ± 0.3).

Littoral community structure

We detected two distinct littoral community types in this lake using ordination methods on the 42 sites where fish, crayfish, and macrophytes were sampled. The first two axes

Fig. 3. Biplot from the (*a*) PCA and (*b*) RDA of macrophytes and crayfish at 127 sites with all environmental variables. Species response variables: Crayfish (sum of *Orconectes rusticus* and *Orconectes rusticus* × *Orconectes propinquus* hybrids, males and females), Milfoil (*Myriophyllum spicatum*), and OtherM (sum of all other macrophytes). Environmental variables: SubIndex (substrate index, increasing with grain size of sediments), Slope (slope of the littoral zone), Riparian (riparian use by humans, sum of the presence of cottages, docks, and lawn), Debris (sum of logs, branches, and leaves), Forest (forest abundance on shore), and Trees (presence of standing dead trees).

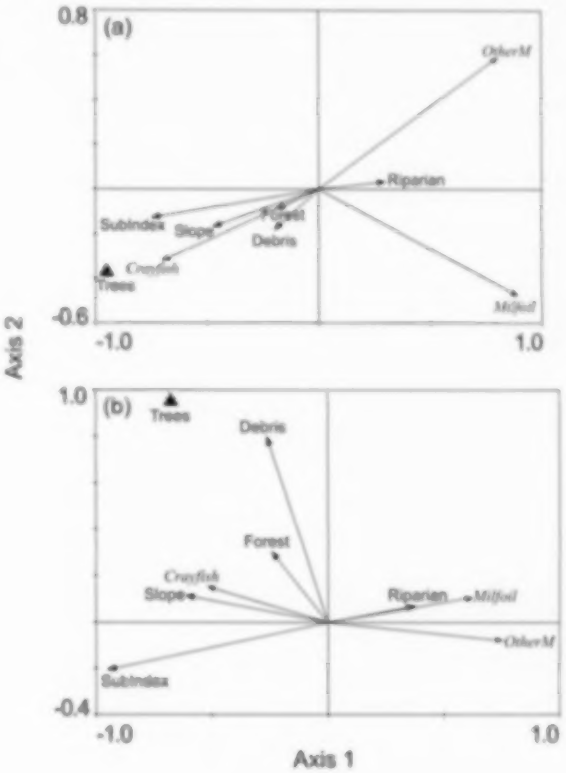

in the PCA explained 67.8% of total species variation, 89.7% of it being related to species–environment relationships (Table 4; Fig. 4*a*). The first axis of the RDA explained 41.1% of species variation and 88.1% of species–environment relationships (Table 4; Fig. 4*b*). The second axis only captured 2.6% more species variation. Again, we limited our interpretations, therefore, to species positions only with respect to the first axis. Both the PCA and RDA clearly separated two distinct littoral assemblages: smallmouth bass, associated with crayfish on one side, and all of the other fish species associated with macrophytes on the other, without any significant separation between milfoil and other macrophytes. Significant forward-selected variables were substrate index, which explained 33% of species variation (P = 0.012), and debris, which explained another 8% of species variation (P = 0.028). Crayfish and smallmouth bass were encountered at higher abundances in sites with high

Table 2. Summary of results for the PCA and RDA of average densities of milfoil, crayfish, and other macrophytes at 127 sampling sites in relation to environmental variables.

	PCA		RDA	
Variable	Axis 1	Axis 2	Axis 1	Axis 2
Eigenvalues	0.672	0.248	0.421	0.010
Species–environment correlations	0.784	0.253	0.796	0.207
Cumulative percent variance of species data	67.2	92.0	42.1	43.1
Cumulative percent variance of species–environment relationships	94.6	98.2	96.3	98.7
Sum of all canonical eigenvalues	0.437	0.437	0.437	0.437

Table 3. Total and mean number (and SE) of fish captured per site by electrofishing in 42 sites in late June 2007.

			Captures per site	
Common name	Latin name	Total captures	Mean	SE
Smallmouth bass	*Micropterus dolomieu*	215	4.89	0.70
Yellow perch	*Perca flavescens*	554	12.59	3.76
Pumpkinseed	*Lepomis gibbosus*	1443	32.80	4.12
Bluntnose minnow	*Pimephales notatus*	233	5.30	1.44
Blackchin shiner	*Notropis heterodon*	290	6.59	2.52
Brown bullhead	*Ameiurus nebulosus*	66	1.50	0.49
Banded killifish	*Fundulus diaphanus*	46	1.04	0.50
Blacknose shiner	*Notropis heterolepis*	30	0.68	0.23
Rainbow smelt	*Osmerus mordax*	11	0.25	0.14
Golden shiner	*Notemigonus crysoleucas*	15	0.34	0.17
Central mudminnow	*Umbra limi*	13	0.30	0.16
White sucker	*Catostomus commersoni*	6	0.14	0.12
Fallfish	*Semotilus corporalis*	2	0.05	0.05
Northern pike	*Esox lucius*	3	0.07	0.04
Iowa darter	*Etheostoma exile*	7	0.16	0.16
Logperch	*Percina caprodes*	1	0.02	0.02
Total		2934	66.68	8.94

Note: Only species with more than one capture per site were included in the RDAs (first seven species listed).

Table 4. Summary of results for the PCA and RDA of communities consisting of fish, crayfish, and macrophytes at 42 sites in July 2007 in relation to environmental variables.

	PCA		RDA	
Variable	Axis 1	Axis 2	Axis 1	Axis 2
Eigenvalues	0.561	0.116	0.411	0.026
Species–environment correlations	0.851	0.318	0.86	0.553
Cumulative percent variance of species data	56.1	67.8	41.1	43.7
Cumulative percent variance of species–environment relationships	87.2	89.7	88.1	93.7
Sum of all canonical eigenvalues	0.467	0.467	0.467	0.467

substrate index (higher proportion of gravel, cobble, and boulders). This variable was also correlated with slope and forested sites. On the other hand, macrophytes (both milfoil and other plants) and all other fish (e.g., yellow perch, pumpkinseed, bluntnose minnow, blackchin shiner, brown bullhead, and banded killfish) were all related to a lower substrate index (i.e., mud and sand). The second most important variable, debris, which represents the presence of logs, branches, and litter, was also related to high crayfish abundance.

Discussion

Rusty crayfish impacts on milfoil

Our experiment suggests that crayfish can have both positive and negative proximate effects on milfoil. Negative effects through consumption occur at higher densities of adult rusty crayfish, as we observed experimentally. Crayfish at medium to high experimental densities also increased the quantity of fragments produced, increasing by five- to ninefold the dispersal potential of milfoil over crayfish-absent

Fig. 4. Biplots of the (*a*) PCA and (*b*) RDA for the 42 sites sampled for fish. Symbol names are as in Fig. 3 with the addition of fish species: Mido, *Micropterus dolomieu*; Pefl, *Perca flavescens*; Legi, *Lepomis gibbosus*; Pino, *Pimephales notatus*; Nobd, *Notropis heterodon*; Amne, *Ameiurus nebulosus*; Fudi, *Fundulus diaphanus*.

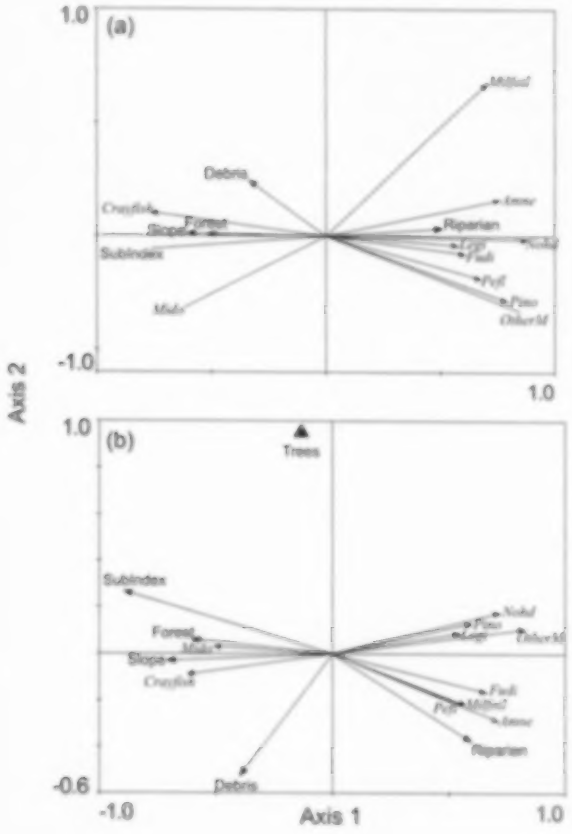

conditions. Our experimental results suggest, therefore, that direct negative impacts of crayfish on milfoil will dominate at higher crayfish densities. At medium densities, more positive impacts are probable, while no significant interaction between the two is expected at low crayfish densities. However, because of fragmentation, even at high abundances of crayfish, negative predation impacts could be compensated for by the increase in dispersal potential for the plant if establishment of propagules is successful.

Madsen and Smith (1997) calculated that less than half (46%) of milfoil fragments that settled onto sediments successfully established. The overall impact of the fragmentation potential observed in our experiment for the lake will thus depend both on the establishment success of fragments and on the densities of crayfish at all sites where milfoil can grow. We believe that for crayfish to control milfoil by reducing bed sizes, crayfish would have to be at very high abundances across the entire lake. At more intermediate crayfish densities, our experimental results suggest that if crayfish and milfoil co-occur in the same sites, crayfish will more likely contribute to milfoil dispersal than to controlling its biomass. Thus, our experimental results support the idea that crayfish should not be introduced as biological control for macrophytes (Magnuson et al. 1975), and especially not for milfoil.

Not to be neglected, however, is the role of human activity on lakes where the species have already been introduced. We showed that medium and intermediate abundances of rusty crayfish should increase the dispersal potential of milfoil. However, it is important to recognize that this effect may be negligible compared with what humans can do with motorboats or anchors. Travelling through a dense milfoil bed with a motor can create more than a hundred fragments in less than 1 min, which is equivalent or superior to what dense aggregations of crayfish can do in 1 week or to what a 2 m^2 milfoil bed can produce in 8 weeks by autofragmentation (as estimated by the cageless references). Thus, the human impact on milfoil is likely to remain much more significant than that of crayfish.

Additive effects on native macrophytes

It is well documented that milfoil has a negative impact on native macrophytes (Smith and Barko 1990; Madsen et al. 1991; Boylen et al. 1999), even though other species can be encountered under its canopy, as we observed in our experiments. All other species of macrophytes were almost eliminated at medium crayfish densities and completely eliminated at high crayfish densities. Rusty crayfish have been shown experimentally to prefer *Myriophyllum* spp. to the same degree as other lesser-branched or nonrosulate species (Lodge and Lorman 1987). Our results suggest that the combined presence of both milfoil and rusty crayfish could increase the negative impact on native macrophytes over that of either invasive species alone. At medium to high crayfish densities, we thus expect to observe at least an additive effect of the two species on richness and abundance of native macrophytes.

Milfoil and rusty crayfish co-occurrence

Survey data indicated that the actual co-occurrence of milfoil and crayfish was low in this lake. Crayfish did not reach high abundances in macrophyte sites and this pattern was consistent all summer long. The availability of different substrate types in this lake seems to be the major factor explaining this separation. Milfoil and other macrophytes were encountered in muddy and sandy sites, whereas crayfish were more common in sites made up of gravel, cobble, and boulders. The mean abundance of crayfish in macrophyte beds was <5 individuals·trap^{-1} with densities therefore lower than 0.5 individual·m^{-2} (the lowest density in our experiments). Experimentally, no significant impacts on milfoil were observed at such low densities, and thus, we conclude that rusty crayfish should not currently have any significant effect on milfoil in this lake either through consumption or through fragmentation. In only one site, which had both milfoil and cobble, were crayfish densities high enough (27 individuals·trap^{-1} or ~2.16 individuals·m^{-2}) to enable a potential interaction. Based on our experiment, crayfish could potentially contribute to milfoil dispersal in these types of sites; however, for this to have an impact on the entire lake, these sites would have to be very abundant, and according to our survey, they are not. Therefore, the presence of rusty crayfish is probably not the reason for the suc-

cessful spread and dominance of milfoil in this lake. However, the possibility remains that if historic crayfish densities were higher, rocky sites could have been even more unfavourable sites for milfoil colonization, implying an interaction between the species. Unfortunately, no past data on the distribution of these two species exist for this lake, making this hypothesis impossible to verify.

At the actual observed abundances in most macrophyte beds, rusty crayfish are also probably not having a significant impact on other macrophytes in this lake. Wilson et al. (2004) proposed a threshold value of >9 individuals·trap^{-1} at which to expect observable changes in invaded systems, and crayfish densities tended to be much higher (up to 60 individuals·trap^{-1}) in sites where consistently significant reductions of macrophyte abundance were observed (Wilson et al. 2004; Roth et al. 2007). In this lake, only two sites with other macrophytes had ≥9 individuals·trap^{-1}. It appears, therefore, that crayfish abundances in Lake Pemichangan are not currently high enough in most macrophyte sites to produce a significant herbivory impact.

Crayfish in Lake Pemichangan do not reach abundances in macrophyte beds that are as high as those seen in other studies (Magnuson et al. 1975; Lorman 1980; Wilson et al. 2004) because in this lake, they are mainly using sites with a high cobble content (high substrate index). Preferential use of cobble habitats by crayfish has been observed in several studies (Hill and Lodge 1994; Kershner and Lodge 1995; Garvey et al. 2003), and in at least one other study, it also corresponded to a low use of macrophyte beds (Kershner and Lodge 1995). Kershner and Lodge (1995) also attributed increasing use of cobble habitats with increasing predator density, including smallmouth bass and yellow perch. Lake Pemichangan has important populations of fish predators as well as a high proportion (62%) of sampled sites that contained cobble and other rocky substrates. Thus, according to previous work, the high availability of cobble coupled with the presence of fish predators could explain the low abundance of crayfish in macrophyte beds in our survey.

Another reason for the low use of macrophyte beds by crayfish could be that the substrate, which was muddy for most sites with macrophytes in our study, impedes crayfish movement, as also suggested by Kershner and Lodge (1995). Further, lower dissolved oxygen and pH can be observed under dense macrophytes canopies (Frodge et al. 1990), which can represent a stress for crayfish and lead to population declines (e.g., Hessen et al. 2004). It is possible that milfoil has the same effect; however, we cannot conclude that milfoil itself is excluding crayfish because crayfish densities were low under all macrophyte species. Also, because most crayfish survived in our experiment, it means that even if conditions under a milfoil canopy might be stressful, they are certainly not lethal. It appears that in this lake, most macrophyte beds, including milfoil, are not a preferred habitat for crayfish.

However, many studies have demonstrated that macrophytes harbour, but are also consumed by, crayfish (Wilson et al. 2004; Hein et al. 2007; Roth et al. 2007), as they also appear to offer shelter from fish predation (Kershner and Lodge 1995; Garvey et al. 2003). This seems to be more likely the case in (*i*) smaller lakes, where crayfish reach similar densities in cobble and macrophytes (e.g., Hein et al. 2007), (*ii*) in lakes where cobble is less available (e.g., Lorman 1980), or (*iii*) in lakes where the abundance of crayfish is higher (Wilson et al. 2004; Roth et al. 2007). Taken together, the results of previous studies and our survey suggest, therefore, that only when crayfish actually shelter in macrophyte beds do they have important negative impacts on macrophytes, as observed in our experiments. Higher impacts of rusty crayfish on macrophytes should therefore be expected in lakes with less cobble habitat, with smaller populations of fish predators, or with higher abundances of crayfish than observed in Lake Pemichangan. These conditions could lead to higher co-occurrence of rusty crayfish and macrophytes, including milfoil. More significant interactions (positive and negative) could also occur if rocks and logs are also found in macrophyte beds. Such sites would provide refuge for crayfish during the day but allow them to feed in macrophyte beds (antagonistic effect) and to cut fragments during the night, thereby increasing the dispersal potential of macrophytes like milfoil (synergistic effect).

Invasive species and the littoral fish community

Two types of fish assemblages were identified in this lake, one group (mainly represented by pumpkinseed and yellow perch) associated with all macrophytes and another group dominated by smallmouth bass, that were associated with rusty crayfish. This suggests that, at the present moment, fish communities do not differ between milfoil beds and those composed of other macrophytes and that crayfish do not co-occur with pumpkinseed, a fish species known to be negatively affected by rusty crayfish invasion (Wilson et al. 2004; Roth et al. 2007). Further studies are needed to understand how changes in the littoral area caused by both milfoil and rusty crayfish are likely to influence fish communities. At the moment, however, we find that rusty crayfish in this lake are likely not having a negative impact on *Lepomis* sp., as observed in other lakes (Roth et al. 2007), although it is possible that negative interactions occurred historically, leading to the nonoverlapping pattern we detected. Currently, crayfish in this lake are at low densities and found in rocky areas that are not the preferred habitats of *Lepomis* (Roth et al. 2007), thereby precluding strong contemporary interactions. Nor do we see gross changes in fish communities across the lake associated with milfoil replacing native macrophytes. However, the overall increase in macrophyte cover in this lake, owing to milfoil invasion, should eventually favour some increases in phytophilic fish species abundances because we observe higher fish densities in macrophyte-covered sites in this lake (data not shown).

Rusty crayfish invasion in Lake Pemichangan and Quebec

Our results clearly demonstrate that across the lake, *O. rusticus* has almost entirely replaced the native species *O. propinquus*, as both are very successful in rocky habitats (Hill and Lodge 1994). However, some of the genetic diversity from *O. propinquus* remains integrated in the hybrid population of the lake (introgression), but this genotype will likely disappear with time (Perry et al. 2001). *Orconectes rusticus* is larger than *O.propinquus* and is also more aggressive (Capelli and Munjal 1982), has a higher ingestion rate of snails (Olsen et al. 1991), and is less sensitive to predation by fish (Garvey et al. 1994; Hill and Lodge 1995; Kuhlmann et al.

2008). Therefore, the potential extirpation of *O. propinquus* not only results in a loss of the native diversity (although according to the biological species concept *O. rusticus* and *O. propinquus* are not true distinct species because hybrids are viable) but also can cause changes in ecosystem functioning because these species are not ecologically equivalent.

The date of introduction of rusty crayfish into this lake is unknown. Wilson et al. (2004) showed that rusty crayfish took 19 years to completely invade Trout Lake, Wisconsin, USA, with an invasion rate of 0.68 km·year^{-1}. Given this rate and the fact that the size of Trout Lake (16.08 km^2, 16.2 km of shoreline) is similar to that of Lake Pemichangan (although it has a longer perimeter of 80 km because of its many distinct bays), we believe that rusty crayfish has been present for at least 20 years, and probably longer, assuming that there was only one point of introduction and that humans have not moved rusty crayfish around the lake. This hypothesized date is further supported by the fact that an *O. rusticus* × *O. propinquus* hybrid from Heney Lake (also in the Gatineau River basin and close to Lake Pemichangan) that was sampled in 1982 exists in museum samples (J. Dubé, Ministère des Ressources naturelles et de la Faune, 201 place Charles-LeMoyne, Longueuil, QC J4K 2T5, Canada, personal communication). It is likely, therefore, that rusty crayfish have been present in the region for at least 25 years.

Lake management implications

To date, there exist no cost-effective methods of control of either of these two invasive species that have been demonstrated to work over the medium to long term. For rusty crayfish, 5 years of intensive trapping (exceeding 13 000 trap-days in some years) associated with restricted fishing regulations (to increase crayfish predator abundance) were shown to be effective (Hein et al. 2007). However, it is still unclear if such labour-intensive trapping efforts need to be sustained to maintain low abundances of rusty crayfish. Furthermore, this control was pursued in a research context in a small lake (0.64 km^2) and it is unlikely that this control effort could reasonably be applied in many more lakes, unless massive economic investments are directed towards invasive species control. For milfoil, millions of dollars are spent annually on harvesting, herbicides, and other nonspecific control methods, but these are usually effective only in the short term (Smith and Barko 1990; Sheldon and Creed 1995; Eiswerth et al. 2000). There is also hope for the success of the North American aquatic weevil (*Euhrychiopsis lecontei*) as a biological control agent (Sheldon 1987; Sheldon and Creed 1995, 2003), but its control abilities have been shown to be very limited so far in this region (Lavoie 2009).

Although synergistic effects are possible between invasive species, as we have shown potential for here, the human impact on milfoil (mainly through boat activity) is likely to be much more significant than that of crayfish. We believe that human activity can be modified to mitigate the success of these species individually and in conjunction with each other. For example, milfoil success in this lake is highly associated with riparian use. One important human activity is the creation of beaches and grassy lawns in riparian areas next to cottages. This activity not only increases the proportion of sandy sediment cover through active deposition of sand in such areas, but the "cleaning up" of waterfronts through the removal of coarse woody debris and leaves opens up habitat that is preferred by the milfoil. Further, it is in such areas close to cottages and boat launches where heavy boating activity is likely to occur, further enhancing the spread potential of milfoil through fragment creation. In our study, milfoil beds were very abundant in boat launch areas.

Our study of the distribution of crayfish and macrophytes in a lake with very diverse habitats has shown that more untouched natural areas offer preferred habitats for rusty crayfish, thereby decreasing their interaction potential and impact on both native and invasive macrophytes. Were the more pristine areas of the lake (without human habitation and boat launches, mainly the entire east basin) to be converted to human-occupied areas, as is the case with the rest of the lake, there would likely be an increased overlap in the distribution of macrophytes and crayfish, as has been observed in other more inhabited lakes (e.g., Trout Lake; Wilson et al. 2004). If this were to occur, we predict an increase in dispersal and domination by milfoil, in part owing to greater interaction with the moderately sized rusty crayfish populations we observed. However, there does remain an upper limit to milfoil populations because very high densities of rusty crayfish can control milfoil, as we demonstrated experimentally.

Acknowledgments

Thanks to E. Boucher, T. Lachartre, M. Dappen, P. Durand, M. Guay, A. Isabelle, M.-H. Jodoin, and J. Piché for field assistance and to J. Dubé for advice. We would also like to acknowledge the generous logistical support provided by the Friends of Lake Pemichangan, in particular the family of E. Isabelle, and the Gatineau Fish and Game Club, especially E. Gow. We also thank two anonymous reviewers for their comments on an earlier version of this manuscript. Funding was provided by an FQRNT postgraduate scholarship to M.J.M., a Natural Sciences and Engineering Research Council of Canada Discovery Grant to B.E.B., and the Ministère des Ressources naturelles et de la Faune du Québec to H.F.

References

Auger, I. 2006. Évaluation du risque de l'introduction du myriophylle à épis sur l'offre de pêche et la biodiversité des eaux à touladi. Report for the Ministère des Ressources naturelles et de la Faune, Outaouais, Qué.

Boylen, C.W., Eichler, L.W., and Madsen, J.D. 1999. Loss of native aquatic plant species in a community dominated by Eurasian watermilfoil. Hydrobiologia, **415**: 207–211. doi:10.1023/A:1003804612998.

Bubb, D.H., Thom, T.J., and Lucas, M.C. 2006. Movement, dispersal and refuge use of co-occurring introduced and native crayfish. Freshw. Biol. **51**(7): 1359–1368. doi:10.1111/j.1365-2427.2006.01578.x.

Buchan, L.A.J., and Padilla, D.K. 2000. Predicting the likelihood of Eurasian watermilfoil presence in lakes, a macrophyte monitoring tool. Ecol. Appl. **10**(5): 1442–1455. doi:10.1890/1051-0761(2000)010[1442:PTLOEW]2.0.CO;2.

Capelli, G.M. 1975. Distribution, life history, and ecology of crayfish in northern Wisconsin, with emphasis on *Orconectes propinquus* (Girard). Ph.D. thesis, University of Wisconsin, Madison, Wis.

Capelli, G.M. 1982. Displacement of native crayfish by *Orconectes rusticus* in northern Wisconsin. Limnol. Oceanogr. **27**: 741–745.

Capelli, G.M., and Capelli, J.F. 1980. Hybridization between crayfish of the genus *Orconectes*: morphological evidence. Crustaceana, **39**(2): 121–132. doi:10.1163/156854080X00021.

Capelli, G.M., and Magnuson, J.J. 1983. Morpho-edaphic and biogeographic analysis of crayfish distribution in northern Wisconsin. J. Crustac. Biol. **3**(4): 548–564. doi:10.2307/1547950.

Capelli, G.M., and Munjal, B.L. 1982. Agressive interactions and resource competition in relation to species displacement among crayfish of the genus *Orconectes*. J. Crustac. Biol. **2**(4): 486–492. doi:10.2307/1548090.

Crow, G.E., and Hellquist, C.B. 2000. Aquatic and wetland plants of Northeastern North America. Vol. 1. University of Wisconsin Press, Madison, Wis.

DiDonato, G.T., and Lodge, D.M. 1993. Species replacements among *Orconectes* crayfishes in Wisconsin lakes: the role of predation by fish. Can. J. Fish. Aquat. Sci. **50**(7): 1484–1488. doi:10.1139/f93-169.

Dubé, J., and Desroches, J.-F. 2007. Les écrevisses du Québec: Biologie, identification et répartition géographique. Ministère des Ressources Naturelles et de la Faune du Québec, Longueuil, Qué.

Dubé, J., Pariseau, P., and St-Hilaire, D. 2002. Première mention de l'écrevisse *Orconectes rusticus* (Girard) au Québec. Nat. Can. **126**: 45–47.

Eiswerth, M.E., Donaldson, S.G., and Johnson, W.S. 2000. Potential environmental impacts and economic damages of eurasian watermilfoil (*Myriophyllum spicatum*) in western Nevada and northeastern California. Weed Technol. **14**(3): 511–518. doi:10.1614/0890-037X(2000)014[0511:PEIAED]2.0.CO;2.

Flint, R.W. 1977. Seasonal activity, migration and distribution of the crayfish, *Pacificatus leniusculus*, in Lake Tahoe. Am. Midl. Nat. **97**(2): 280–292. doi:10.2307/2425094.

Frodge, J.D., Thomas, G.L., and Pauley, G.B. 1990. Effects of canopy formation by floating and submergent aquatic macrophytes on the water quality of two shallow Pacific Northwest lakes. Aquat. Bot. **38**(2–3): 231–248. doi:10.1016/0304-3770(90)90008-9.

Garvey, J.E., Stein, R.A., and Thomas, H.M. 1994. Assessing how fish predation and interspecific prey competition influence a crayfish assemblage. Ecology, **75**(2): 532–547. doi:10.2307/1939556.

Garvey, J.E., Rettig, J.E., Stein, R.A., Lodge, D.M., and Klosiewski, S.P. 2003. Scale-dependent associations among fish predation, littoral habitat, and distributions of crayfish species. Ecology, **84**(12): 3339–3348. doi:10.1890/02-0444.

Grace, J.B., and Wetzel, R.G. 1978. The production biology of eurasian watermilfoil (*Myriophyllum spicatum* L.): a review. J. Aquat. Plant Manag. **16**: 1–11.

Guan, R.Z., and Wiles, P.R. 1997. Ecological impact of introduced crayfish on benthic fishes in a British lowland river. Conserv. Biol. **11**(3): 641–647. doi:10.1046/j.1523-1739.1997.96073.x.

Hamr, P. 2002. *Orconectes*. *In* Biology of freshwater crayfish. *Edited by* D.M. Holdich. Blackwell Science, Oxford, U.K. pp. 585–608.

Hein, C.L., Vander Zanden, M.J., and Magnuson, J.J. 2007. Intensive trapping and increased fish predation cause massive population decline of an invasive crayfish. Freshw. Biol. **52**(6): 1134–1146. doi:10.1111/j.1365-2427.2007.01741.x.

Hessen, D.O., Skurdal, J., and Braathen, J.E. 2004. Plant exclusion of a herbivore: crayfish population decline caused by an invading waterweed. Biol. Invasions, **6**(2): 133–140. doi:10.1023/B:BINV.0000022131.40783.f0.

Hill, A.M., and Lodge, D.M. 1994. Diel changes in resource demand: competition and predation in species replacement among crayfishes. Ecology, **75**(7): 2118–2126. doi:10.2307/1941615.

Hill, A.M., and Lodge, D.M. 1995. Multi-trophic-level impact of sublethal interactions between bass and omnivorous crayfish. J. North Am. Benthol. Soc. **14**(2): 306–314. doi:10.2307/1467782.

Hill, A.M., and Lodge, D.M. 1999. Replacement of resident crayfishes by an exotic crayfish: the roles of competition and predation. Ecol. Appl. **9**(2): 678–690. doi:10.1890/1051-0761(1999)009[0678:RORCBA]2.0.CO;2.

Hobbs, H.H., Jr. 1989. An illustrated checklist of the American crayfishes (Decapoda: Astacidae, Cambaridae and Parastacidae). Smithson. Contrib. Zool. **480**: 1–236.

Hobbs, H.H., and Jass, J.P. 1988. The crayfishes and shrimp of Wisconsin. Spec. Publ. Biol. Geol. Milwaukee Public Museum, Milwaukee, Wis.

Horns, W.H., and Magnuson, J.J. 1981. Crayfish predation on lake trout eggs in Trout Lake, Wisconsin. Rapp. P.-v. Réun. Cons. Int. Explor. Mer, **178**: 299–303.

Johnson, L.E., Ricciardi, A., and Carlton, J.T. 2001. Overland dispersal of aquatic invasive species: a risk assessment of transient recreational boating. Ecol. Appl. **11**(6): 1789–1799. doi:10.1890/1051-0761(2001)011[1789:ODOAIS]2.0.CO;2.

Johnson, P.T.J., Olden, J.D., Solomon, C.T., and Vander Zanden, M.J. 2009. Interactions among invaders: community and ecosystem effects of multiple invasive species in an experimental aquatic system. Oecologia (Berl.), **159**(1): 161–170. doi:10.1007/s00442-008-1176-x.

Jonas, J.L., Claramunt, R.M., Fitzsimons, J.D., Marsden, J.E., and Ellrott, B.J. 2005. Estimates of egg deposition and effects of lake trout (*Salvelinus namaycush*) egg predators in three regions of the Great Lakes. Can. J. Fish. Aquat. Sci. **62**(10): 2254–2264. doi:10.1139/F05-141.

Kershner, M.W., and Lodge, D.M. 1995. Effects of littoral habitat and fish predation on the distribution of an exotic crayfish, *Orconectes rusticus*. J. North Am. Benthol. Soc. **14**(3): 414–422. doi:10.2307/1467207.

Kuhlmann, M.L., Budylak, S.M., and Carvin, E.L. 2008. Testing the differential predation hypothesis for the invasion of rusty crayfish in a stream community: laboratory and field experiments. Freshw. Biol. **53**: 113–128.

Lavoie, M. 2009. L'utilisation du charançon pour le biocontrôle du myriophylle à épis. M.Sc. thesis, Département des sciences biologiques, Université du Québec à Montréal, Montréal, Qué.

Lawler, J.J., Aukema, J.E., Grant, J.B., Halpern, B.S., Kareiva, P., Nelson, C.R., Ohleth, K., Olden, J.D., Schlaepfer, M.A., Silliman, B.R., and Zaradic, P. 2006. Conservation science: a 20-year report card. Front. Ecol. Environ. **4**(9): 473–480. doi:10.1890/1540-9295(2006)4[473:CSAYRC]2.0.CO;2.

Leps, J., and Smilauer, P. 2003. Multivariate analysis of ecological data using CANOCO. Cambridge University Press, New York.

Lodge, D.M. 1991. Herbivory on fresh-water macrophytes. Aquat. Bot. **41**(1–3): 195–224. doi:10.1016/0304-3770(91)90044-6.

Lodge, D.M., and Lorman, J.G. 1987. Reductions in submersed macrophyte biomass and species richness by the crayfish *Orconectes rusticus*. Can. J. Fish. Aquat. Sci. **44**(3): 591–597. doi:10.1139/f87-072.

Lodge, D.M., Beckel, A.L., and Magnuson, J.J. 1985. Lake-bottom tyrant. Nat. Hist. **94**: 33–37.

Lodge, D.M., Kratz, T.K., and Capelli, G.M. 1986. Long-term dynamics of three crayfish species in Trout Lake, Wisconsin. Can. J. Fish. Aquat. Sci. **43**: 993–998. doi:10.1139/f86-122.

Lodge, D.M., Kershner, M.W., Aloi, J.E., and Covich, A.P. 1994. Effects of an omnivorous crayfish (*Orconectes rusticus*) on a freshwater littoral food web. Ecology, **75**(5): 1265–1281. doi:10.2307/1937452.

Lorman, J.G. 1980. Ecology of the crayfish *Orconectes rusticus* in Northern Wisconsin. Ph.D. thesis, University of Wisconsin, Madison, Wis.

Mack, R.N., Simberloff, D., Lonsdale, W.M., Evans, H., Clout, M.,

and Bazzaz, F.A. 2000. Biotic invasions: causes, epidemiology, global consequences, and control. Ecol. Appl. **10**(3): 689–710. doi:10.1890/1051-0761(2000)010[0689:BICEGC]2.0.CO;2.

Madsen, J.D. 1998. Predicting invasion success of eurasian watermilfoil. J. Aquat. Plant Manag. **36**: 28–32.

Madsen, J.D., and Smith, D.H. 1997. Vegetative spread of Eurasian watermilfoil colonies. J. Aquat. Plant Manag. **35**: 63–68.

Madsen, J.D., Sutherland, J.W., Bloomfield, J., Eichler, L.W., and Boylen, C.W. 1991. The decline of native vegetation under dense Eurasian watermilfoil canopies. J. Aquat. Plant Manag. **29**: 94–99.

Magnuson, J.J., Capelli, G.M., Lorman, J.G., and Stein, R.A. 1975. Consideration of crayfish for macrophyte control. Proceedings of the Symposium on Water Quality Management through Biological Control (23–30 January 1975). Rep. No. ENV 07-75-1. University of Florida, Gainsville, Fla. pp. 66–74.

McCarthy, J.M., Hein, C.L., Olden, J.D., and Jake Vander Zanden, M. 2006. Coupling long-term studies with meta-analysis to investigate impacts of non-native crayfish on zoobenthic communities. Freshw. Biol. **51**(2): 224–235. doi:10.1111/j.1365-2427.2005.01485.x.

Nichols, S.A., and Shaw, B.H. 1986. Ecological life histories of the threee aquatic nuisance plants, *Myriophyllum spicatum*, *Potamogeton crispus*, and *Elodea canadensis*. Hydrobiologia, **131**(1): 3–21. doi:10.1007/BF00008319.

Nyström, P., and Strand, J.A. 1996. Grazing by a native and an exotic crayfish on aquatic macrophytes. Freshw. Biol. **36**(3): 673–682. doi:10.1046/j.1365-2427.1996.d01-508.x.

Nyström, P., Brönmark, C., and Graneli, W. 1996. Patterns in benthic food webs: a role for omnivorous crayfish? Freshw. Biol. **36**(3): 631–646. doi:10.1046/j.1365-2427.1996.d01-528.x.

Ogle, D.H., and Kret, L. 2008. Experimental evidence that captured rusty crayfish (*Orconectes rusticus*) exclude uncaptured rusty crayfish from entering traps. J. Freshwat. Ecol. **23**: 123–129.

Olsen, T.M., Lodge, D.M., Capelli, G.M., and Houlihan, R.J. 1991. Mechanisms of impact of an introduced crayfish (*Orconectes rusticus*) on littoral congeners, snails, and macrophytes. Can. J. Fish. Aquat. Sci. **48**(10): 1853–1861. doi:10.1139/f91-219.

Perry, W.L., Feder, J.L., and Lodge, D.M. 2001. Implications of hybridization between introduced and resident *Orconectes* crayfishes. Conserv. Biol. **15**(6): 1656–1666. doi:10.1046/j.1523-1739.2001.00019.x.

Pratt, T.C., and Smokorowski, K.E. 2003. Fish habitat management implications of the summer habitat use by littoral fishes in a north temperate, mesotrophic lake. Can. J. Fish. Aquat. Sci. **60**(3): 286–300. doi:10.1139/F03-022.

Puth, L.M., and Allen, T.F.H. 2005. Potential corridors for the rusty crayfish, *Orconectes rusticus*, in northern Wisconsin (USA) lakes: lessons for exotic invasions. Landsc. Ecol. **20**(5): 567–577. doi:10.1007/s10980-004-5649-y.

Randall, R.G., Minns, C.K., Cairns, V.W., and Moore, J.E. 1996. The relationship between an index of fish production and submerged macrophytes and other habitat features at three littoral areas in the Great Lakes. Can. J. Fish. Aquat. Sci. **53**(Suppl. 1): 35–44. doi:10.1139/cjfas-53-S1-35.

Rosenthal, S.K., Stevens, S.S., and Lodge, D.M. 2006. Whole-lake effects of invasive crayfish (*Orconectes* spp.) and the potential for restoration. Can. J. Fish. Aquat. Sci. **63**(6): 1276–1285. doi:10.1139/F06-037.

Roth, B.M., Tetzlaff, J.C., Alexander, M.L., and Kitchell, J.F. 2007. Reciprocal relationships between exotic rusty crayfish, macrophytes, and *Lepomis* species in northern Wisconsin lakes. Ecosystems (N.Y., Print), **10**(1): 75–86. doi:10.1007/s10021-006-9004-9.

Sala, O.E., Chapin, F.S., III, Armesto, J.J., Berlow, E., Bloomfield, J., Dirzo, R., Huber-Sanwald, E., Huenneke, L.F., Jackson, R.B., Kinzig, A., Leemans, R., Lodge, D.M., Mooney, H.A., Oesterheld, M., Poff, N.L., Sykes, M.T., Walker, B.H., Walker, M., and Wall, D.H. 2000. Global biodiversity scenarios for the year 2100. Science, **287**(5459): 1770–1774. doi:10.1126/science.287.5459.1770. PMID:10710299.

Sheldon, S.P. 1987. The effect of herbivorous snails on submerged macrophyte communities in Minnesota lakes. Ecology, **68**(6): 1920–1931. doi:10.2307/1939883.

Sheldon, S.P., and Creed, R.P., Jr. 1995. Use of a native insect as a biological control for an introduced weed. Ecol. Appl. **5**(4): 1122–1132. doi:10.2307/2269359.

Sheldon, S.P., and Creed, R.P., Jr. 2003. The effect of a native biological control agent for Eurasian watermilfoil on six North American watermilfoils. Aquat. Bot. **76**(3): 259–265. doi:10.1016/S0304-3770(03)00055-X.

Simberloff, D., and Von Holle, B. 1999. Positive interactions of nonindigenous species: invasional meltdown? Biol. Invasions, **1**(1): 21–32. doi:10.1023/A:1010086329619.

Smith, C.S., and Barko, J.W. 1990. Ecology of eurasian watermilfoil. J. Aquat. Plant Manag. **28**: 55–64.

Taylor, C.A., and Redmer, M. 1996. Dispersal of the crayfish *Orconectes rusticus* in Illinois, with notes on species displacement and habitat preference. J. Crustac. Biol. **16**(3): 547–551. doi:10.2307/1548745.

Vander Zanden, M.J., Wilson, K.A., Casselman, J.M., and Yan, N.D. 2004. Species introductions and their impacts in North American Shield lakes. *In* Boreal Shield watersheds: lake trout ecosystems in a changing environment. *Edited by* J.M. Gunn, R.J. Steedman, and R.A. Ryder. CRC Press, New York. pp. 239–264.

Weaver, M.J., Magnuson, J.J., and Clayton, M.K. 1997. Distribution of littoral fishes in structurally complex macrophytes. Can. J. Fish. Aquat. Sci. **54**(10): 2277–2289. doi:10.1139/cjfas-54-10-2277.

Willis, T.V., and Magnuson, J.J. 2006. Response of fish communities in five north temperate lakes to exotic species and climate. Limnol. Oceanogr. **51**: 2808–2820.

Wilson, K.A., Magnuson, J.J., Lodge, D.M., Hill, A.M., Kratz, T.K., Perry, W.L., and Willis, T.V. 2004. A long-term rusty crayfish (*Orconectes rusticus*) invasion: dispersal patterns and community change in a north temperate lake. Can. J. Fish. Aquat. Sci. **61**(11): 2255–2266. doi:10.1139/F04-170.

Appendix A

Table A1. Schedule of rusty crayfish additions to each experimental treatment indicating the number of new individuals added to each cage.

Crayfish treatment	Replicate	20 June	6 July	3 August
Low	1	0	1	1
	2	0	1	0
	3	0	1	1
	4	0	1	0
Medium	1	1	2	0
	2	0	2	0
	3	0	1	0
	4	1	0	0
High	1	9	16	0
	2	0	0	3
	3	5	5	0
	4	1	0	0

Appendix B

Fig. B1. Crayfish characteristics used for identification (modified from Dubé and Desroches 2007, adapted from Hobbs 1989). A, location of rust-coloured marks on the carapace of *Orconectes rusticus*; B, black bands on the tips of the chelae fingers of *O. rusticus*; C, carina on the rostrum of *Orconectes propinquus*; D, distinct notch at the base of chelae fingers in *Orconectes immunis*. (*a*) Dorsal view of carapace; (*b*) mesial view of first pleopod in form I male; (*c*) lateral view of first pleopod in form I male; (*d*) lateral view of form II male; (*e*) dorsal view of distal podomers of chelae in form I male.

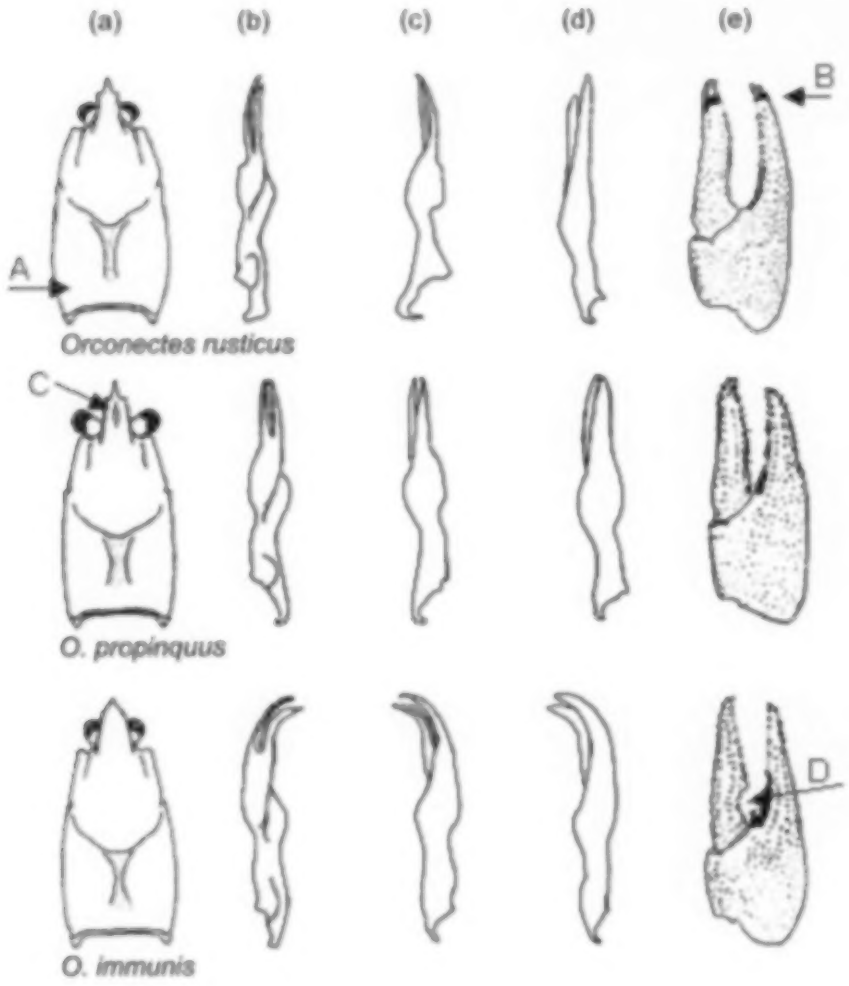

References

Dubé, J., and Desroches, J.-F. 2007. Les écrevisses du Québec: biologie, identification et répartition géographique. Ministère des Ressources Naturelles et de la Faune du Québec, Longueuil, Qué.

Hobbs, H.H., Jr. 1989. An illustrated checklist of the American crayfishes (Decapoda: Astacidae, Cambaridae and Parastacidae). Smithson. Contrib. Zool. **480**: 1–236.

Appendix C

In Figs. C1 and C2, the size of the symbol and its associated number represent the total number of crayfish captured. Proportions of each species and hybrid are shown by circles with sizes proportional to the total number of captures of the OR and OR × OP types. Species and hybrid names are *Orconectes rusticus* (OR), *Orconectes propinquus* (OP), *Orconectes immunis* (OI), *O. rusticus* × *O. propinquus* hybrids (OR × OP), *O. propinquus* × *O. immunis* hybrids (OR × OI), and *O. propinquus* × *O. propinquus* × *O. immunis* hybrids (OR × OP × OI) for which presence is shown with different symbols (see legends).

Fig. C1. Crayfish captures in July 2007.

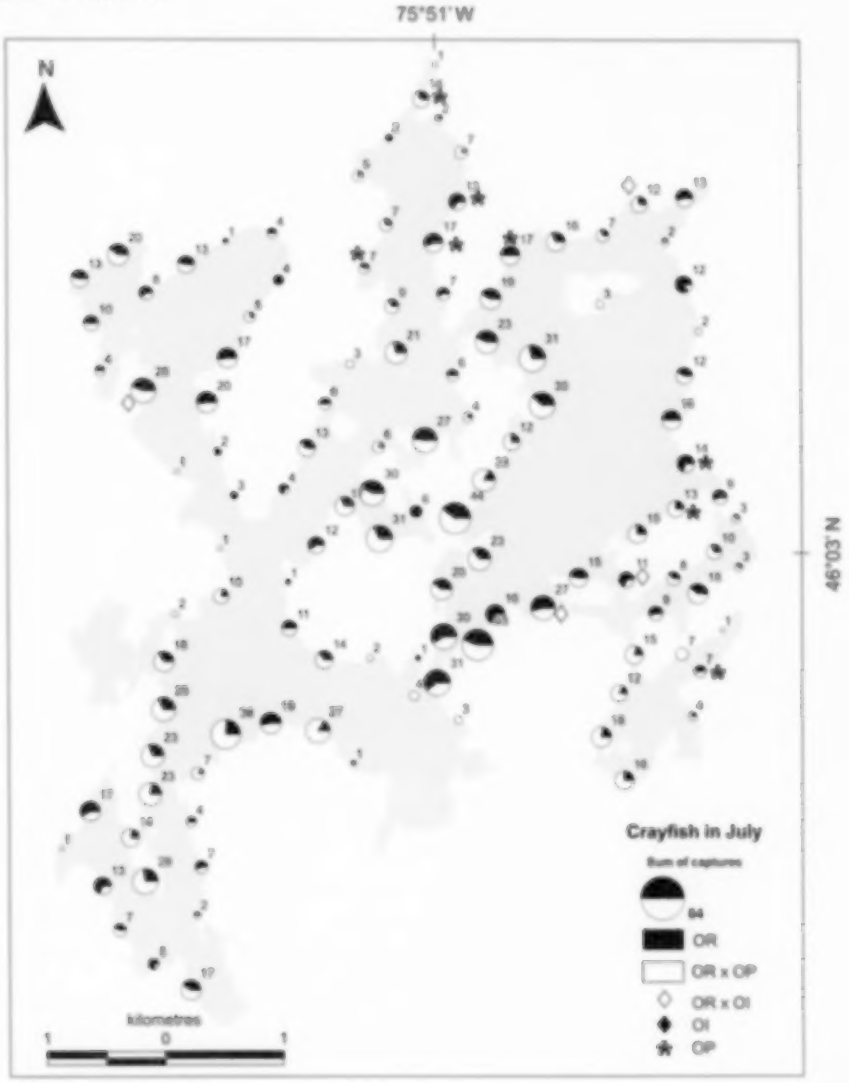

Fig. C2. Crayfish captures in September 2007.

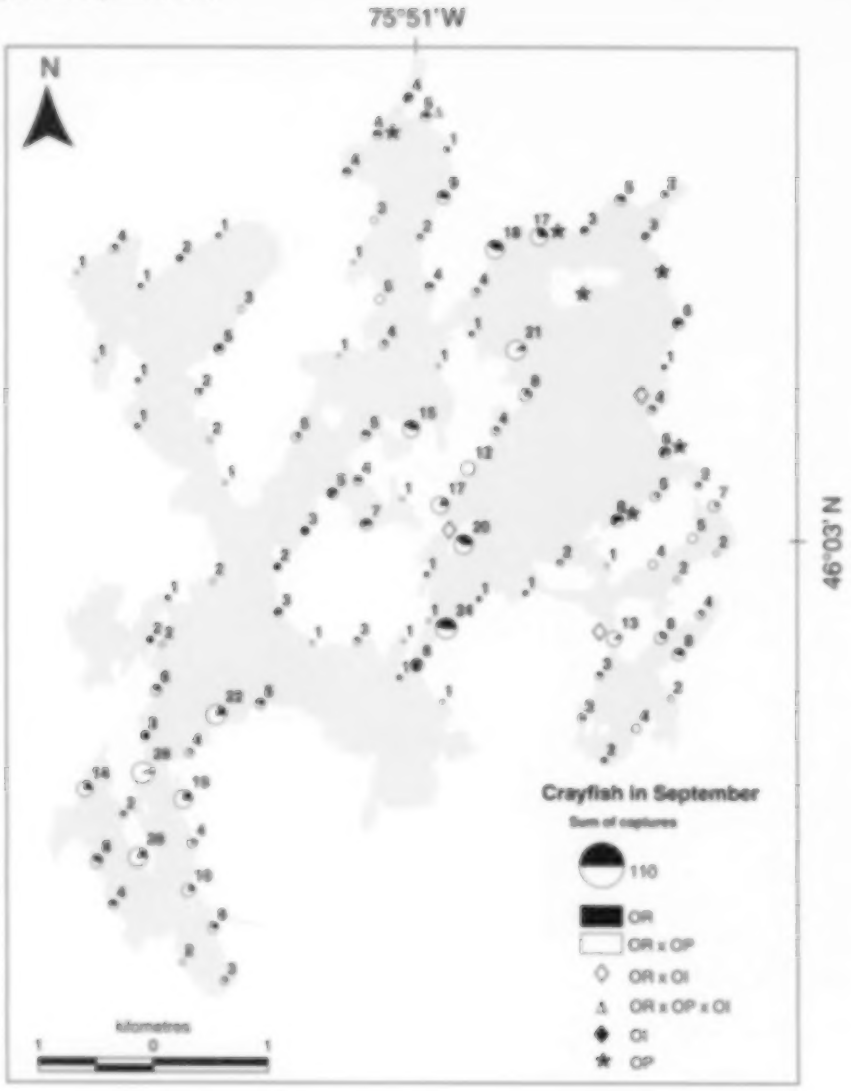

Identification of ecological structure and species relationships along an oceanographic gradient in the Gulf of Maine using multivariate analysis with bootstrapping

Adrian Jordaan, Yong Chen, David W. Townsend, and Sally Sherman

Abstract: Ecosystem-based fisheries management requires a fundamental understanding of ecosystem boundaries and interspecies interactions. We report a delineation of fish and invertebrate data collected by trawl survey along the Maine, USA, coast. Principal components analysis (PCA) reduced the multidimensionality of the data and created new variables from correlations among species. Bootstrapped PCA was employed to assess PCA structure using eigenvalue variation and species associations using eigenvector variation. A general linear model related structure of fish community identified in PCA to depth, temperature, longitude, and interactions among these variables. Generally, alongshore and onshore–offshore assemblage patterns related to oceanographic gradients, with seasonal variation. PCA-created variables act as indicators of biodiversity and are related to the scale of observation, allowing for multiple scales to be integrated if data are available. Species targeted and gear used along with spatial extent and sampling density must be considered when management zonation is to be undertaken but would allow boundaries to follow biological and physical gradients rather than relying on the typical political and economic variables, avoiding ecologically deleterious spatial patterns in fishing pressure or other instances of *de facto* zoning. Regardless, this study describes some contributing factors causing division of species assemblages that should be considered.

Résumé : La gestion des pêches basée sur les écosystèmes nécessite une compréhension fondamentale des frontières entre les écosystèmes et des interactions entre les espèces. Nous présentons une délimitation des données sur les poissons et les invertébrés récoltées par inventaire au chalut le long de la côte du Maine, É.-U. Une analyse des composantes principales (PCA) a réduit la nature multidimensionnelle des données et a créé de nouvelles variables à partir des corrélations entre les espèces. Une PCA avec bootstrap a servi à estimer la structure de la PCA, ainsi que les associations d'espèces, d'après la variation des valeurs propres. Un modèle linéaire général a relié la structure de la communauté de poissons identifiée dans la PCA à la profondeur, à la température, à la longitude et aux interactions entre ces variables. En général, les patrons de regroupements le long de la côte et entre la côte et le large sont associés à des gradients océaniques avec une variation saisonnière. Les variables créées par la PCA servent d'indicateurs de la biodiversité et sont reliées à l'échelle d'observation, ce qui permet l'intégration de plusieurs échelles lorsque les données sont suffisantes. Il est nécessaire de tenir compte des espèces ciblées et des engins de pêche utilisés, de même que de l'étendue spatiale et de la densité d'échantillonnage, afin d'entreprendre un zonage de gestion; celui-ci doit permettre aux frontières de suivre les gradients biologiques et physiques plutôt que de se baser sur les variables politiques et économiques habituelles; ainsi, il est possible d'éviter les effets spatiaux néfastes de la pression de pêche et des autres circonstances du zonage *de facto*. Néanmoins, notre étude décrit certains facteurs à considérer qui contribuent à la division des regroupements d'espèces.

[Traduit par la Rédaction]

Introduction

Biodiversity is a structural characteristic describing ecosystems that provides information on the state (Slocombe 1998) as well as the adaptive capacity and robustness of the ecosystem to external impacts including anthropogenic activities and climate change (Levin and Lubchenco 2008). Detailing biodiversity with a spatial perspective and translating the results into a framework that allows for spatially specific management of human actions within ecological systems at the appropriate scale will minimize unintended deleterious impacts on ecosystem function (see Berkes et al.

Received 5 February 2009. Accepted 31 December 2009. Published on the NRC Research Press Web site at cjfas.nrc.ca on 26 March 2010.
J21047

A. Jordaan.[1] School of Marine Sciences, University of Maine, Orono, ME 04469, USA; Marine Sciences Research Center, School of Marine and Atmospheric Sciences, Stony Brook University, Stony Brook, NY 11794-5000, USA.
Y. Chen and D.W. Townsend. School of Marine Sciences, University of Maine, Orono, ME 04469, USA.
S. Sherman. Department of Marine Resources, West Boothbay Harbor, ME 04575, USA.

[1]Corresponding author (e-mail: Adrian.Jordaan@stonybrook.edu).

2006; Crowder et al. 2006). Commercial and recreational fishing as well as other anthropogenic disturbances such as aquaculture, oil and gas extraction/production, wind farms, and coastal development tend to cluster spatially by stakeholder preference for certain oceanographic conditions, benthic habitats, and location relative to human development (see Crowder et al. 2006). Thus, application of single-species and site-by-site management techniques has allowed *de facto* zoning, where political boundaries and stakeholder preferences dictate spatial organization of anthropogenic impacts, to be the rule. Comprehensive planning using spatial trends in biodiversity and abundance of species will help curtail *de facto* zoning whose case-by-case style of management results in spatially fragmented conservation efforts (Crowder et al. 2006). Such is the case when marine reserves shift fishing effort (Hilborn 2003) onto other fishing grounds that are important habitat (Hinrichsen et al. 2009; Suuronen et al. 2010). By considering spatial structure in species assemblages, we propose proxies for biodiversity as indicators in the application of zoning within ecosystem-based management strategies.

For fisheries management purposes, Northeastern US stocks are divided into two populations: one occupying shallow, productive, glacially derived Georges Bank and another the sheltered, but deeper, Gulf of Maine (Fig. 1). This simply recognizes the fundamental divergent physical and biological properties of the two environments and the resulting productivity differences between them (see Townsend et al. 2006). While ecosystem structure is often delineated along boundaries produced by gradients in the physical environment (Strayer et al. 2003), the designation ignored structure of organisms occurring at a larger scale (Frisk et al. 2008) and finer scale (Ames 2004), often with negative consequences such as extirpation of unrecognized subpopulations (see Ames 2004). Historic cod metapopulation dynamics along the coastal waters of the Gulf of Maine (Ames 2004) and an oceanographic gradient created by a coastal current system (Pettigrew et al. 2005; Townsend et al. 2006) both demonstrate the presence of finer-scale, biologically relevant gradients within the Gulf of Maine that were not recognized until recently. Ecosystem-based management policies support structuring basic units of management along ecological gradients as opposed to political ones (US Commission on Ocean Policy 2004), hence matching the spatial scales of management and ecological processes.

There has been substantial effort to classify areas of the ocean based on a variety of characteristics that consider spatial structure of biodiversity in support of geographically based management. First attempts used ordination techniques to demonstrate persistent biological structure along environmental discontinuities on the Northwest Atlantic continental shelf using trawl survey data (Overholtz and Tyler 1985; Gabriel 1992; Mahon et al. 1998). While the assemblage designations of Mahon et al. (1998) have been generally supported (Jørgensen et al. 2005), one valid critique of these techniques is the subjectivity with which cutoffs in eigenvalues and eigenvectors were made (Souissi et al. 2001). Bootstrapped and standard principal components analysis (PCA_{BTSP} and PCA, respectively) were employed to tackle analysis of a multivariable ecological data sets to address this very deficiency (Jackson 1993; Jackson 1995; Pillar 1999). Despite criticism for allowing axis reversal among bootstrap runs (Mehlman et al. 1995), PCA_{BTSP}-based techniques have been shown, using both simulated and real data, to outperform other methods in determining the number of nontrivial components (Jackson 1993, 1995; Pillar 1999) and eigenvector loadings (Peres-Neto et al. 2003). As such, the PCA_{BTSP} provides a methodology for determining the cutoff (stopping rule) and determining relationships among species using a probability-based method. This method has significant advantage in that each new variable (principal component) is uncorrelated with others and can be statistically tested against physical variables. This is particularly helpful in dealing with multiple scales within data sets and the multifactor interacting influences of physical variables in determining species' distributions.

Other analyses exist that also have the same general characteristics, such as hierarchal clustering analyses (Souissi et al. 2001; Jørgensen et al. 2005). Jørgensen et al. (2005), for example, examined the fish assemblages of Davis Strait and southern Baffin Bay using two survey trips analyzed by cluster analysis and Bayesian multinomial logit models with assumed probability distribution functions to assign survey trawls to the clusters. Then, assemblages were mapped using a spherical variogram model and a kriging method. However, species in low numbers need to be excluded from the analyses to keep the model stable (Jørgensen et al. 2005). This is not the case with PCA_{BTSP}, which can handle rarer species as long as there are common trends in variation with other species. PCA_{BTSP} will exclude rarer species among bootstrap runs, thereby reducing their impact in determining assemblages probabilistically during evaluation of eigenvectors. Furthermore, PCA_{BTSP} does not depend on distributional assumptions.

Here, we attempt to discern multispecies structure along a small section of coastline within the Gulf of Maine, long assumed to constitute a single ecosystem. The existence of the Eastern and Western Maine Coastal Currents (EMCC and WMCC, respectively) creates strong physical gradients in temperature, salinity, stratification, and productivity. The EMCC is driven by tidal energy and to lesser degree wind stress that vertically mix the water column bringing deeper, nutrient-rich cold water to the surface and lower-salinity, warmer temperature to depth (Pettigrew et al. 2005). The mixed water then flows along the edge of the coastal shelf break as the EMCC (Pettigrew et al. 2005). The greater tidal mixing of the EMCC contrasts the increased stratification of the WMCC's and resulting warmer surface and colder benthos with a division between the two water masses roughly in midcoast Maine at Penobscot Bay (Fig. 1) (Pettigrew et al. 2005; Townsend et al. 2006). As such, a gradient in biodiversity and a discernable pattern in ecosystem structure are expected across the EMCC–WMCC boundary, although such an observation has never been evaluated quantitatively. To test whether fish species display common trends of variation such that biodiversity is structured along physical characteristics of the coastal waters of Maine, which is the objective of this study, a PCA_{BTSP}-based technique is used to characterize relative abundance data obtained from an inshore trawl survey. Using new variables derived from the PCA, fish assemblages are identified and related to physical

Fig. 1. Gulf of Maine depth contours (50, 100, 200, and 300 m), idealized western and eastern Maine coastal current (WMCC and EMCC, respectively) pathways, and relative location of the region in North America (inset).

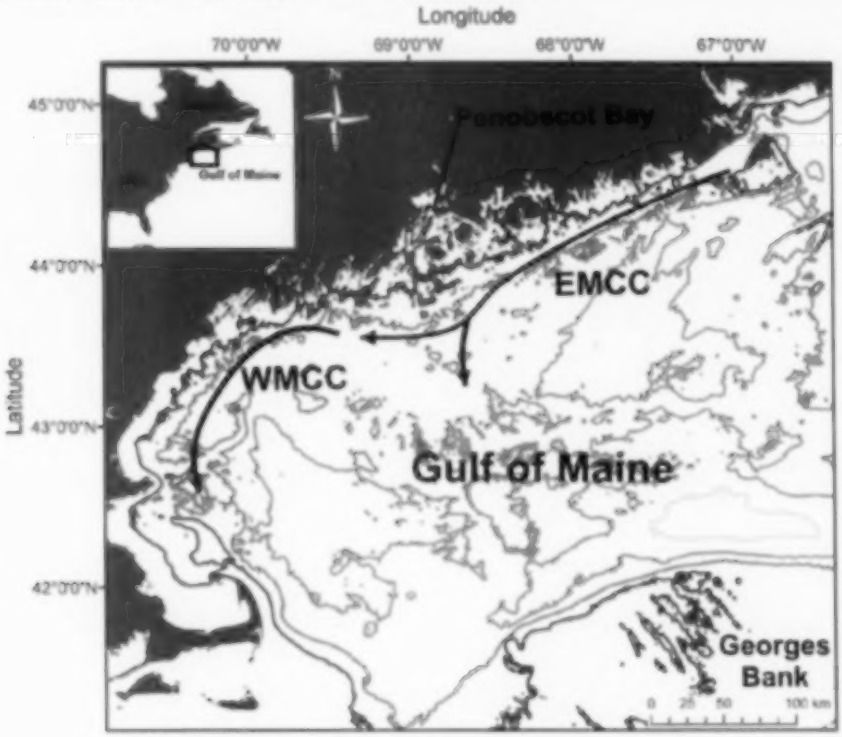

variables and plotted as biodiversity maps for use in geographically based management strategies.

Materials and methods

The Maine–New Hampshire inshore trawl survey has been conducted every fall and spring since fall 2000. It has a stratified random design modeled after the National Marine Fisheries Service bottom trawl surveys (Sherman et al. 2005) and includes four depth strata: 9–37, 37–64, 64–100, and >100 m (its outer boundary roughly delineated by the 12 mi. or 22 km limit; Chen et al. 2006). The fourth stratum was added in the spring of 2003. Additionally, five longitudinal strata were added based on oceanographic, geologic, and biological features, resulting in 20 separate strata. To randomize the survey area (~13 720 km^2), each stratum is divided into 1 nautical mile (i.e., 1.85 km) sampling grids. A target of 100 stations in each survey results in a sampling density of about one station per 137 km ^{2} in comparison with the National Oceanic and Atmospheric Administration National Marine Fisheries Service surveys' one station per 892 km^2. Number of tows conducted per stratum was apportioned according to its total area.

Survey tows are conducted as consistently as possible in a straight line at 2.5 kn for 20 min duration (range 2.3–2.8 kn over the entire survey of 80–100 tows; tow speeds are adjusted slightly due to tidal currents to keep net fishing properly). The 20 min duration runs from the time the brakes are set on the winches until the brakes are released to start hauling back. Tows of shorter or longer durations that are deemed representative standardize the numbers of fish caught to 20 min. Tows not deemed representative are rejected and repeated.

The net is a modified version of the shrimp net design used in Maine waters designed to fish for a variety of near-bottom-dwelling species without targeting any specific species. The net is constructed of 5 cm No. 24 polyethylene mesh with a 2.5 cm (stretched measure) mesh liner in the cod end. The 2003 survey, which we isolated for this analysis, included 101 sites sampled in the spring and 78 in the fall sample period (Sherman et al. 2005).

Principal components analysis with bootstrapping

The data set was divided into three different groups, benthic vertebrates, benthic invertebrates, and pelagic species (both vertebrate and invertebrate), since each represents generally divergent behavioural tendencies related directly to habitat use. Benthic vertebrates are generally more mobile, benthic invertebrates are sessile or slow moving, and pelagic species use the water column as primary habitat. Species that only occurred once in the data set were removed. PCA was applied to each of the three categories. The resultant principal components (PCs) were interpreted with respect to the original data. We used the following three-step procedure (Fig. 2) for analyzing the results of the PCA_{BTSP} and a "normal" PCA (PCA_{NRML}).

Step 1. Evaluate PCA_{BTSP} eigenvalues and establish stopping rules. Derive eigenvalues and confidence intervals and

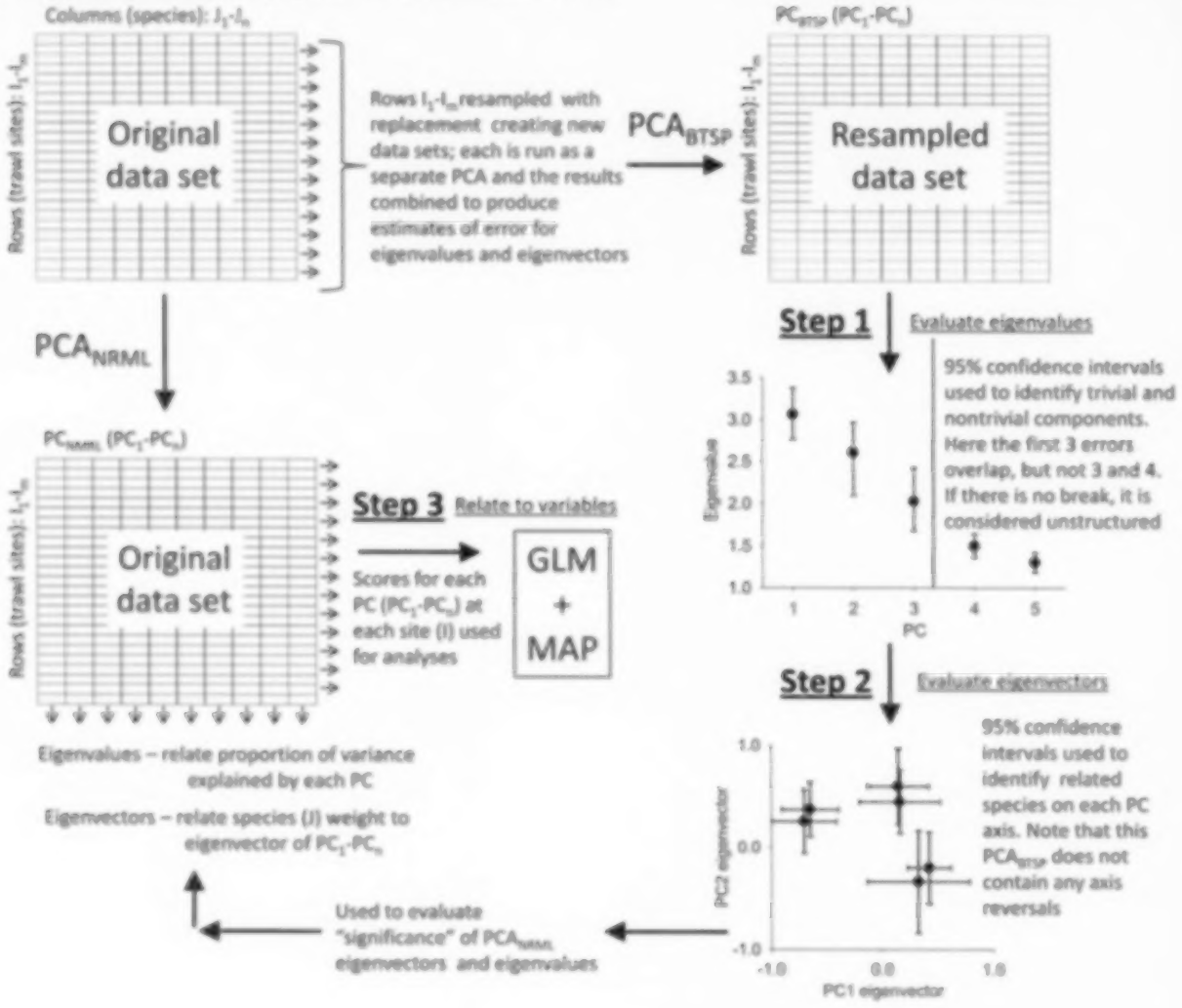
Columns (species): J_1-J_n
Rows (trawl sites): I_1-I_n
Original data set
Rows I_1-I_n resampled with replacement creating new data sets; each is run as a separate PCA and the results combined to produce estimates of error for eigenvalues and eigenvectors
PCA_{BTSP}
PC_{BTSP} (PC_1-PC_n)
Resampled data set
PCA_{NRML}
PC_{NRML} (PC_1-PC_n)
Step 1
Evaluate eigenvalues
95% confidence intervals used to identify trivial and nontrivial components. Here the first 3 errors overlap, but not 3 and 4. If there is no break, it is considered unstructured
Eigenvalue
PC
Step 2
Evaluate eigenvectors
95% confidence intervals used to identify related species on each PC axis. Note that this PCA_{BTSP} does not contain any axis reversals
PC2 eigenvector
PC1 eigenvector
Step 3
Relate to variables
Scores for each PC (PC_1-PC_n) at each site (I) used for analyses
GLM + MAP
Eigenvalues – relate proportion of variance explained by each PC
Eigenvectors – relate species (J) weight to eigenvector of PC_1-PC_n
Used to evaluate "significance" of PCA_{NRML} eigenvectors and eigenvalues

Fig. 2. Flowchart of PCA used in study. The difference between PCA_{BTSP} and PCA_{NRML} simply revolves around the resampling of rows with replacement, hence developing a measure of variation in the former.

determine which PCs provide a meaningful dissection of the data and which are equivalent to random noise. PCs are judged based on 95% confidence limits (95% CLs). Once the 95% CLs for successive PCs overlap, they are judged to no longer produce a meaningful dissection of the data (Jackson 1993). Only PCs identified as unique for each group (benthic vertebrates, benthic invertebrates, and pelagic species) by the PCA_{BTSP} for both the spring and fall surveys were used in further analysis.

Step 2. Evaluate PCA_{BTSP} eigenvectors and species dependence. Derive distribution of eigenvector scores and evaluate for understanding of species contributing to meaningful components. Determine which species have statistically overlapping distributions and hence are correlated in abundance (i.e., form assemblages). Again, 95% CLs are used to determine overlapping eigenvector scores and hence which (groups of) species are driving the patterns for PCs identified as relevant in step 1. There has not been adequate work to determine which method of assessing and correcting axis reversals–reflections in bootstrapped PCA is best (Jackson 1995); hence, we do not try to correct for this, but rather acknowledge the phenomena and treat the bimodality of eigenvectors within the analyses and interpretation. The bootstrap eigenvector loading distributions were compared with one another for species with similar distributions using Kolmogorov–Smirnov (KS) two-sample tests (SYSTAT version 10.2) (SYSTAT, Chicago, Illinois). Groupings of fish were designated based on the KS test, which determines statistically whether two sampled frequency distributions are from the same population. Additionally, the two species with each of the highest and lowest component loading scores were compared for trends in species correlations against the full group of species using the mean bootstrapped Pearson correlation coefficients and 95% CLs.

Step 3. Relate to variables and test structure. Relate relevant PC scores at each site to potential independent variables and use spatial data to map biodiversity indices. Once PCs that are relevant are determined (step 1) and the species that drive patterns are identified (step 2), the PC scores calculated for each site are tested against physical data using a general linear model (GLM) and mapped using the ending latitude and longitude. The scores generated in PCA_{NRML} for each site were compared for differences in relation to longitude, depth, and temperature (and interactions) using the GLM analysis. Furthermore, natural neighbor interpolation (Sibson 1981) using ArcMap ArcToolbox spatial analysis software (ESRI, Redlands, California), which interpolates a surface from points, was employed to demonstrate spatial patterns of PC scores. Natural neighbor interpolation is based on the Thiessen polygon network created from the Delaunay triangulation of the data points and uses a weighted average of the neighboring data points to calculate the interpolation point (Sibson 1981).

Steps 1 and 2 use the PCA_{BTSP} technique, while step 3 uses results from PCA_{NRML}, since each bootstrap run resamples (with replacement) the trawl stations. The PCA_{BTSP} was implemented using SAS version 9.1 (SAS Institute Inc., Cary, North Carolina) and 1000 bootstrap runs were completed. The analyses included 29 species of benthic vertebrates (Table 1), 24 species of benthic invertebrates (Table 2), and 10 pelagic species in the spring survey and 11 in the fall (Table 3).

Results

Evaluating eigenvalues and stopping rules (step 1)

The eigenvalues indicate that the first PC of each species group explained 16%–23% of the total variance in the spring survey and 17%–24% in the fall survey (Table 4). The eigenvalue scores were higher for PCA_{BTSP} than for PCA_{NRML} in all but one case (Table 4), although not significantly, since PCA_{NRML} scores were within the PCA_{BTSP} 95% CLs. The analysis of benthic vertebrate data demonstrated that the eigenvalues scores for PC1, PC2, and PC3 were all different from one another and those for PC4 onwards were similar for both the spring and fall surveys. An analysis of the pelagic data identified PC1 and PC2 as unique eigenvalues. Neither benthic invertebrate data set (spring or fall) provided unique values, suggesting a lack of structure in the data. As a result, benthic invertebrates were not considered further in the results.

Evaluating eigenvectors and species correlations (step 2)

Eigenvectors generated by PCA_{BTSP} and PCA_{NRML} demonstrated agreement in the division of species, but with dampened PCA_{BTSP} values compared with PCA_{NRML}-generated loadings (Figs. 3, 4, 5, and 6). Component eigenvector loadings alternated between negative and positive scores in different bootstrap runs; however, where individual species toggle between positive and negative eigenvectors in different bootstrap runs, the distances (vector) among species are conserved (Jackson 1993, 1995; Mehlman et al. 1995). The flip-flop highlights the arbitrary nature of assigning positive and negative values, also demonstrated by two other examples. First, for benthic vertebrates in the fall sample period, PCA_{NRML} scores were opposite to scores given by PCA_{BTSP} but identified the same pattern in species loadings (Fig. 6). Second, PCA_{NRML} has opposite eigenvector loadings in the spring (Fig. 4) and fall (Fig. 6) as evidenced by the species *Lophius americanus*.

Table 1. Species list for the benthic vertebrate group.

Species	Common name
Aspidophoroides monopterygius	Alligatorfish
Cryptacanthodes maculatus	Wrymouth
Cyclopterus lumpus	Lumpfish
Enchelyopus cimbrius	Fourbeard rockling
Gadus morhua	Atlantic cod
Glyptocephalus cynoglossus	Witch flounder
Hemitripterus americanus	Sea raven
Hippglossus hippoglossus	Atlantic halibut
Hippoglossoides platessoides	American plaice
Limanda ferruginea	Yellowtail flounder
Lophius americanus	Goosefish/monkfish
Lumpenus lumpretaeformis	Snakeblenny
Macrozoarces americanus	Ocean pout
Melanogrammus aeglefinus	Haddock
Merluccius bilinearis	Silver hake
Myoxocephalus octodecemspinosus	Longhorn sculpin
Myoxocephalus scorpius	Shorthorn sculpin
Paralichthys oblongus	Fourspot flounder
Pollachius virens	Pollock
Pseudopleuronectes americanus	Winter flounder
Raja erinacea	Little skate
Raja radiata	Thorny skate
Raja senta	Smooth skate
Reinhardtius hippoglossoides	Greenland halibut
Scophthalmus aquosus	Windowpane flouder
Sebastes fasciatus	Acadian redfish
Tautogolabrus adspersus	Cunner
Urophycis chuss	Red hake
Urophycis tenuis	White hake

In the spring sampling, patterns in pelagic species were generally driven by positive loadings (Fig. 3*a*) among the highly correlated (Fig. 3*b*) *Alosa aestivalis*, *Alosa pseudoharengus*, and *Clupea harengus*, although the species were not identified as similar KS groups (KS test determined groupings, center of Fig. 3). The particularly strong agreement among the species with positive loadings was weaker with *Osmerus mordax* and *Alosa sapidissima*. The negative loading species *Euphausiid* spp. and *Maurolicus muelleri* had little correlation with one another (Fig. 3*b*).

The spring sampled benthic vertebrate eigenvector loadings were strongly driven by the species group of *Lophius americanus*, *Sebastes fasciatus*, and *Hippoglossoides platessoides* and to a lesser degree the other species that are correlated (Fig. 4). Weak correlation coefficients amongst these species did not impact the KS groupings (Fig. 4*b*). KS group A were often more highly correlated (correlation coefficient > 0.5) with species with lesser eigenvectors such as *Lophius americanus* and *Merluccius bilinearis* (Fig. 4*b*). *Myoxocephalus scorpius* had a correlation coefficient $-1 <$ correlation coefficient < 1 with large error bars (Fig. 4*b*), which results from being sampled inconsistently among bootstrap runs. If a species, by not being contained in the

Table 2. Species list for the benthic invertebrate group.

Species	Common name
Arctica islandica	Ocean quahog
Astarte undata	Waved astarte
Cancer borealis	Jonah crab
Cancer irroratus	Rock crab
Caudina arenata	Rat-tail cucumber
Cephalopoda spp.	Octopus (unclassified)
Chionecetes opilio	Snow crab
Crangon septemspinosa	Sevenspine Bay shrimp, sandshrimp
Cucumaria frondosa	Sea cucumber
Dichelopandalus leptocerus	Bristled longbeak
Echinoidae sp.	Sand dollar
Geryon quinquedens	Red crab
Homarus americanus	American lobster
Hyas araneus	Toad crab
Lithodes sp.	Northern stone crab
Mytilus edulis	Blue mussel
Pandalus borealis	Northern shrimp
Pandalus montagui	Aesop shrimp
Pasiphaea multidentata	Pink glass shrimp
Placopecten magelanicus	Sea scallop
Stomatopod sp.	Mantis shrimp
Strongylocentrotus droebachiensis	Sea urchin
Venericardia borealis	Northern cardita
Yoldia thraciaeformis	Ax head clam

Table 3. Species list for the pelagic group.

Species	Common name
Alosa aestivalis	Blueback herring
Alosa pseudoharengus	Alewife
Alosa sapidissima	American shad
Brevoortia tyrannus	Atlantic menhaden
Clupea harengus	Atlantic herring
Euphausiid spp.	Krill
Loligo pealei	Longfin squid
Maurolicus muelleri	Pearlsides
Osmerus mordax	Rainbow smelt
Scomber scombrus	Atlantic mackerel
Squalus acanthias	Spiny dogfish

bootstrap subsample, receives a coefficient of 0 when excluded in bootstrap runs, 95%CL error bars will relate the frequency of absence. This is also reflected in eigenvector frequencies (Fig. 4*a*).

In the analysis of pelagic species from the fall sampling, using PCA_{NRSM}, separated *Osmerus mordax* and *Brevoortia tyrannus* from each other and the rest of the species, although they maintain high correlations with *Clupea harengus* and *Alosa pseudoharengus* (Fig. 5*b*). The species with the most negative eigenvectors, *Squalus acanthias* and *Maurolicus muelleri*, had only a weak relationship with each other, and *Maurolicus muelleri* had a number of 0 scores, indicating infrequency in capture (Fig. 5*a*), and in fact was only captured in two tows. There was significant variation in eigenvector loadings, with most species showing uniform or wide distributions, with the uniformly distributed species grouping together in KS tests (Fig. 5).

The PCA_{BTSP} of fall-sampled benthic vertebrate species demonstrates a more polarized pattern with negative and positive eigenvectors (Fig. 6*a*). Furthermore, both positive and negative species sets show significant correlations with one another and negative correlations with species of the opposing sign (Fig. 6*b*). A bimodal distribution in eigenvector loadings, due to axis reversals, occurs (Fig. 6*a*), but the magnitude of vectors among species is conserved (Jordaan 2006). The species group *Lophius americanus*, *Glyptocephalus cynoglossus*, *Hippoglossoides platessoides*, *Enchelyopus cimbrius*, and *Urophycis chuss* are all highly correlated with one another and negatively correlated with the group consisting of *Pseudopleuronectes americanus*, *Myoxocephalus octodecemspinosus*, *Raja erinacea*, and *Scophthalmus aquosus* (Fig. 6).

Relate to variables, spatial biological structure, and physical correlates (step 3)

The results of the GLM demonstrate that there were differences in the structure of the data sets associated with longitude, temperature, depth, and their interactions. For the spring pelagics, PC1 produced a significant model with longitude, depth, and the depth–longitude interaction all significant factors and with temperature and all other interactions not significant (Table 5). For the spring pelagics, PC2 also produced a significant model with all factors and interactions significantly contributing to the model, except for temperature and the temperature–longitude interaction (Table 5). For the spring benthic vertebrates, PC1 produced a significant model with longitude, temperature, and the temperature–longitude interaction as significant contributors to the model with depth and all other interactions not significant (Table 5). PC2 and PC3 produced a significant model but with no significant contributory factors (Table 5).

For the fall benthic vertebrates, PC1 produced a significant model; only longitude was near significance (Table 6). By removing all depth-associated factors (none had $P < 0.68$), the model remains significant ($F_{[3,66]} = 28.6$, $P < 0.001$, $r^2 = 0.55$) with longitude ($T = -3.1$, $P = 0.003$), temperature ($T = -2.6$, $P = 0.013$), and the temperature–longitude interaction ($T = 2.7$, $P = 0.01$) as significant factors. The benthic vertebrate PC2 was also significantly explained by the model (Table 6). Only the depth–temperature interaction and longitude–depth–temperature interactions (Table 6) were significant, but depth and the longitude–depth interaction were marginal. Depth and the longitude–depth interaction were significant for the PC3 benthic vertebrate GLM (Table 6). The GLM for the pelagic PC1 analysis produced a significant model ($F_{[7,66]} = 20.0$, $P < 0.001$, $r^2 = 0.68$) with all factors and interactions being significant ($P < 0.001$).

The spatial distribution of species assemblages, using the scores for each site generated by PCA_{NRSM}, suggests a complex mosaic with general onshore–offshore and east–west gradients (Figs. 7, 8, 9, and 10). The spring pelagic species PC1 follows a general onshore–offshore gradient and has similar assemblages in eastern and western Maine, with separation in the Penobscot region (Fig. 7*a*). PC2 also demonstrates an onshore–offshore gradient and some east–west

Table 4. Eigenvalues (EV) and percent explained variance (%) for the first three PCs generated for the three species groupings benthic vertebrates (VERT), benthic invertebrates (INV), and pelagic species (PEL) for the spring and fall surveys.

		Spring						Fall					
		PC1		PC2		PC3		PC1		PC2		PC3	
		EV	%	EV	%	EV	%	EV	%	EV	%	EV	%
PCA_{NRML}	VERT	4.7	16	3.2	11	2.3	8	5.5	19	3.3	11	2.7	9
	INV	4.3	18	2.9	12	2.5	11	4.2	17	3.0	12	2.5	10
	PEL	2.3	23	1.6	16	1.2	12	2.7	24	2.2	20	1.3	12
PCA_{BTSP}	VERT	5.1	18	3.4	12	2.5	9	5.9	20	3.6	12	2.8	10
	INV	4.5	19	3.0	12	2.3	10	4.5	19	3.2	13	2.5	10
	PEL	2.4	24	1.7	17	1.2	12	2.9	26	2.2	20	1.4	12

Note: Both the SYSTAT generated and SAS bootstrap generated values are given.

Fig. 3. (*a*) Species eigenvectors and (*b*) Pearson correlation coefficients for spring pelagic species generated by PCA_{BTSP} for PC1 only. The species list located in the middle is ordered by increasing loading frequencies. The loading calculated by PCA_{NRML} and grouping based on KS tests of eigenvector probability frequency distributions are also given (U, unique distribution; letters indicate like distributions). Pearson correlation coefficients include mean and standard deviation for two species at the top and bottom of the list; see legend for species and symbols.

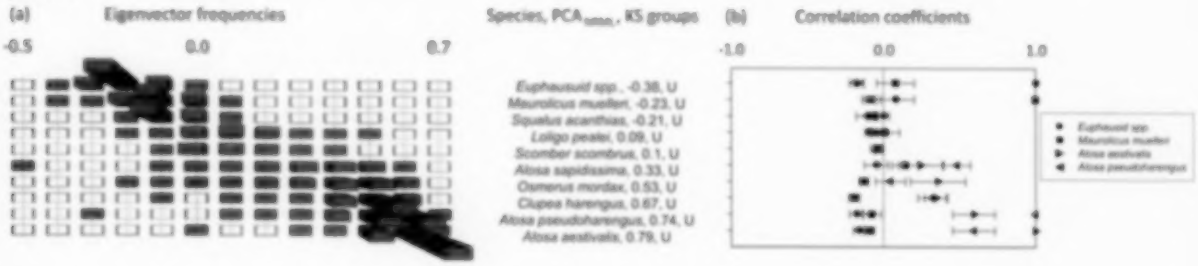

Fig. 4. (*a*) Species eigenvectors and (*b*) Pearson correlation coefficients for spring benthic vertebrate species generated by PCA_{BTSP} for PC1 only. The species list located in the middle is ordered by increasing loading frequencies. The loading calculated by PCA_{NRML} and grouping based on KS tests of eigenvector probability frequency distributions are also given (U, unique distribution; letters indicate like distributions). Pearson correlation coefficients include mean and standard deviation for two species at the top and bottom of the list; see legend for species and symbols.

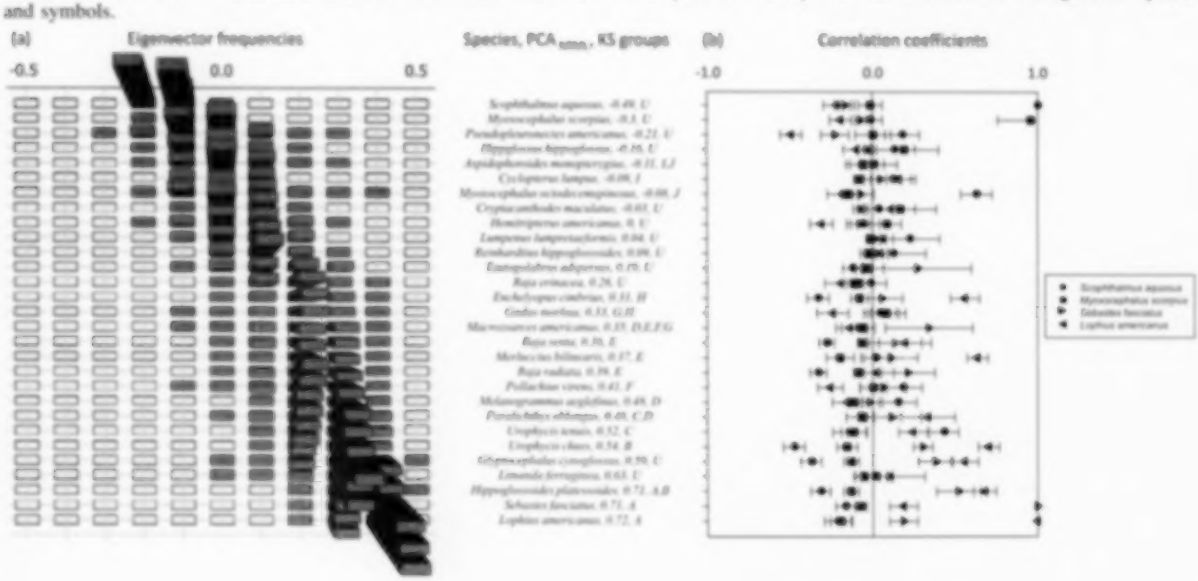

Fig. 5. (*a*) Species eigenvectors and (*b*) Pearson correlation coefficients for fall pelagic species generated by PCA_{BTSP} for PC1 only. The species list located in the middle is ordered by increasing loading frequencies. The loading calculated by PCA_{NRSR} and grouping based on KS tests of eigenvector probability frequency distributions are also given (U, unique distribution; letters indicate like distributions). Pearson correlation coefficients include mean and standard deviation for two species at the top and bottom of the list; see legend for species and symbols.

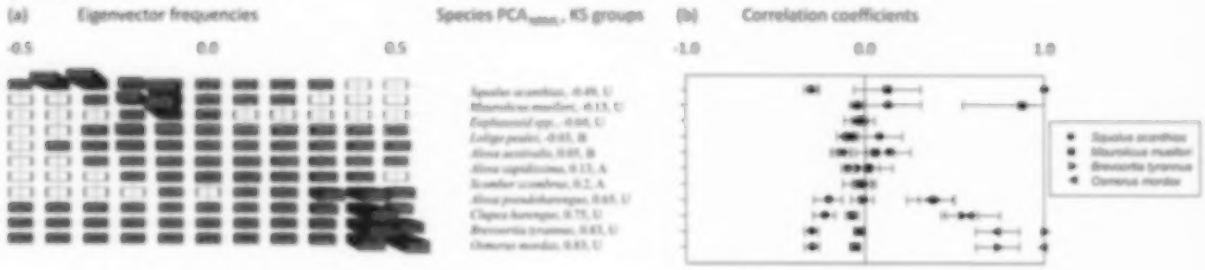

Fig. 6. (*a*) Species eigenvectors and (*b*) Pearson correlation coefficients for fall benthic vertebrate species generated by PCA_{BTSP} for PC1 only. The species list located in the middle is ordered by increasing loading frequencies. The loading calculated by PCA_{NRSR} and grouping based on KS tests of eigenvector probability frequency distributions are also given (U, unique distribution; letters indicate like distributions). Pearson correlation coefficients include mean and standard deviation for two species at the top and bottom of the list; see legend for species and symbols.

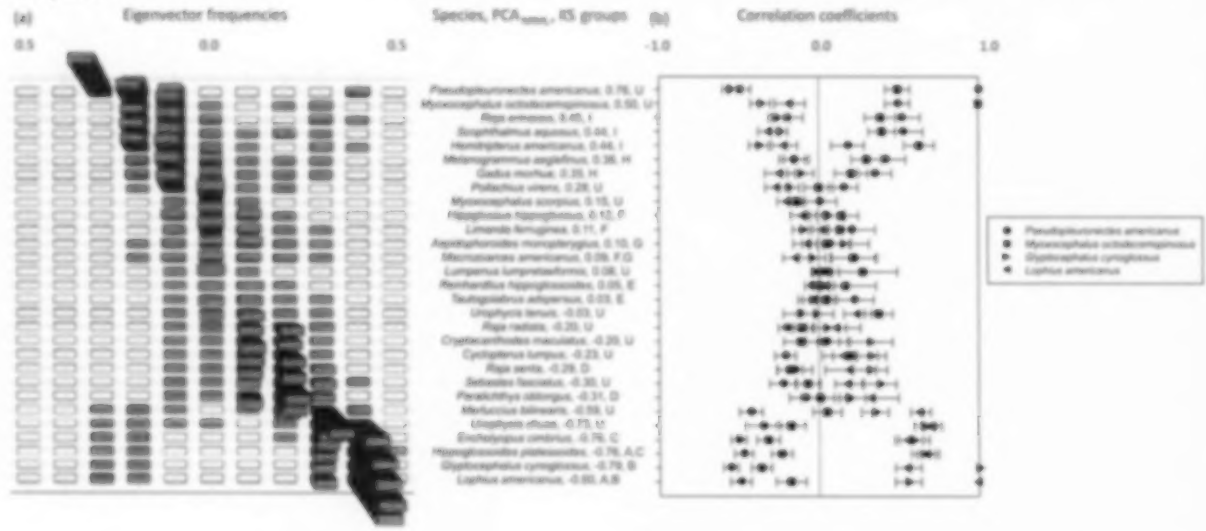

similarity (Fig. 7*b*). The spatial distribution of spring benthic vertebrate scores demonstrates a primary onshore–offshore and east–west gradient (Fig. 8*a*). PC2 and PC3 each contrast an area in the eastern survey region with patches of habitat throughout the rest of the survey area (Figs. 8*b* and 8*c*).

The spatial distribution of the fall pelagic species suggests a divergence in the assemblages of eastern and western Maine across the Penobscot region boundary with the maintenance of some similarities within the coastal zone in PC1 (Fig. 9*a*). PC1 and PC2 appear to represent the east and west coastline, respectively (Fig. 9). The spatial distribution of fall benthic vertebrate scores demonstrates a general onshore–offshore and east–west gradient as well as some uniqueness about the Penobscot region (Fig. 10*a*). PC1 contrasts a coastal and offshore plume in the east that becomes coastally bound in the west, with an offshore region in the west. PC2 contrasts the far eastern and western areas with the center of the survey region (Fig. 10*b*). PC3 demonstrates an onshore–offshore gradient focused along the eastern Maine coast (Fig. 10*c*).

Discussion

This study presents a previously unidentified division of species assemblages along a regional oceanographic gradient within the inshore Gulf of Maine. Individual and sets of species are organized in a non-uniform manner across a physical environment resulting in concordance between biological structuring and physical gradients. This provides an opportunity to account for trends in biodiversity in developing area-based management strategies.

Oceanographic processes associated with two water masses, the WMCC and EMCC, along coastal Maine exert primary control over ecological patterns, demonstrated by

Table 5. Spring 2003 general linear model results for each relevant PC for benthic vertebrates and pelagic species and the associated df, F ratio, p value, and r^2 for each test.

	Benthic vertebrates			Pelagic species	
	PC1	PC2	PC3	PC1	PC2
df	100	100	100	100	100
F	29.9	3.92	13.10	11.78	3.38
p	<0.0001	0.0009	<0.0001	<0.0001	0.0029
r^2	0.69	0.23	0.49	0.49	0.20
Longitude	**0.0035**	0.4782	0.5515	**0.0277**	**0.0163**
Temperature	**0.0153**	0.7963	0.6733	0.0997	0.0698
Depth	0.9766	0.6975	0.3112	**0.0363**	**0.0061**
Longitude × temperature	**0.0158**	0.8030	0.6917	0.0998	0.0702
Longitude × depth	0.9545	0.7040	0.3338	**0.0350**	**0.0064**
Temperature × depth	0.9919	0.7895	0.9968	0.1111	**0.0328**
Longitude × depth × temperature	0.9905	0.7727	0.9766	0.1148	**0.0343**

Note: The independent variables and p values with bolded values significant at the $\alpha < 0.05$ value are listed.

Table 6. Fall 2003 general linear model results for each relevant PC for benthic vertebrates and pelagic species and the associated df, F ratio, p value, and r^2 for each test.

	Benthic vertebrates			Pelagic species	
	PC1	PC2	PC3	PC1	PC2
df	73	73	73	73	73
F	23.91	3.82	6.87	20.03	14.92
p	<0.0001	0.0015	<0.0001	<0.0001	<0.0001
r^2	0.72	0.29	0.42	0.68	0.61
Longitude	0.0807	0.6182	0.1418	**<0.0001**	0.8019
Temperature	0.7475	0.0720	**0.0300**	**0.0003**	0.2931
Depth	0.1491	0.2651	0.1586	**<0.0001**	0.0663
Longitude × temperature	0.1425	0.2765	0.1693	**<0.0001**	0.0726
Longitude × depth	0.7581	0.0709	**0.0333**	**0.0003**	0.3064
Temperature × depth	0.6918	**0.0162**	0.0622	**0.0002**	0.0716
Longitude × depth × temperature	0.6897	**0.0154**	0.0704	**0.0003**	0.0738

Note: The independent variables and p values with bolded values significant at the $\alpha < 0.05$ value are listed.

the consistency with which temperature, longitude, and their interaction were significant in the GLM analyses. Water temperatures are highly correlated with species abundances and fluctuation in fisheries landings regionally along the Maine coast (Dow 1981) and locally influence fish presence and absence in Maine tidal coves and embayments (Targett and McCleave 1974; Jordaan 2010). Thermal tolerance of a species, particularly during planktonic early life stages, is a critical component in development, growth, and survival (Jordaan and Kling 2003). It is not clear what component(s) of the water mass accounts for differences in the species assemblage structure, in particular because of large numbers of interacting variables. For example, cooler bottom temperatures occur beneath the vertically stratified WMCC, as opposed to warmer bottom water in the EMCC where the tidal currents effectively mix heating from solar energy throughout the water column and nutrients from depth to the surface (Townsend 1991). Differences in dissolved inorganic nutrient loads between the two coastal current systems, being highest in the east, result in lower overall primary productivity with a greater fraction of that productivity being recycled in the WMCC (Townsend 1991). Productivity varies substantially along the northeast US continental shelf due to variation in physical forces and inputs from different water masses; continental shelf waters of southern New England and Georges Bank generally have higher primary productivity than Gulf of Maine waters and substantial differences exist along the Gulf of Maine coastline (Townsend et al. 2006). Thus, it is not surprising that bottom-up processes driving recruitment of New England groundfish stocks also appear to differ by region (Brodziak et al. 2001).

Because fish assemblages are related to temperature, it will be important to consider decadal cycles in coupled ocean–atmosphere systems. The North Atlantic Oscillation (NAO), which is related to anthropogenic-driven climate change (Hoerling et al. 2001), influences the makeup of source waters entering the Gulf of Maine with low NAO years correlated with colder, fresher, and nutrient-depleted water compared with warmer, high-nutrient waters during positive NAO events (Thomas et al. 2003; Townsend et al. 2006; Townsend and Ellis 2010). Thus, shifts due to climate and NAO impacts are expected through changes in sources waters and their related physical properties.

Species assemblage structure shifted from a temperature–depth–longitude-based relationship during spring to a temperature–longitude-related ecological pattern in the fall. Seasonal shifts are not uncommon, for example, Georges Bank cod and haddock tend to occupy shifting temperature and

Fig. 7. Spring pelagic species biodiversity maps from (*a*) PC1 and (*b*) PC2 scores. Symbols represent PC scores classified into five categories from negative scores (triangles) to positive scores (circles) with larger symbols indicating larger absolute values. Contour plots are results of natural neighbor interpolation reflecting the spatial variation in scores with dark shading representing positive scores and light shading negative scores. Neutral scores are given by hexagons and lack of any shading.

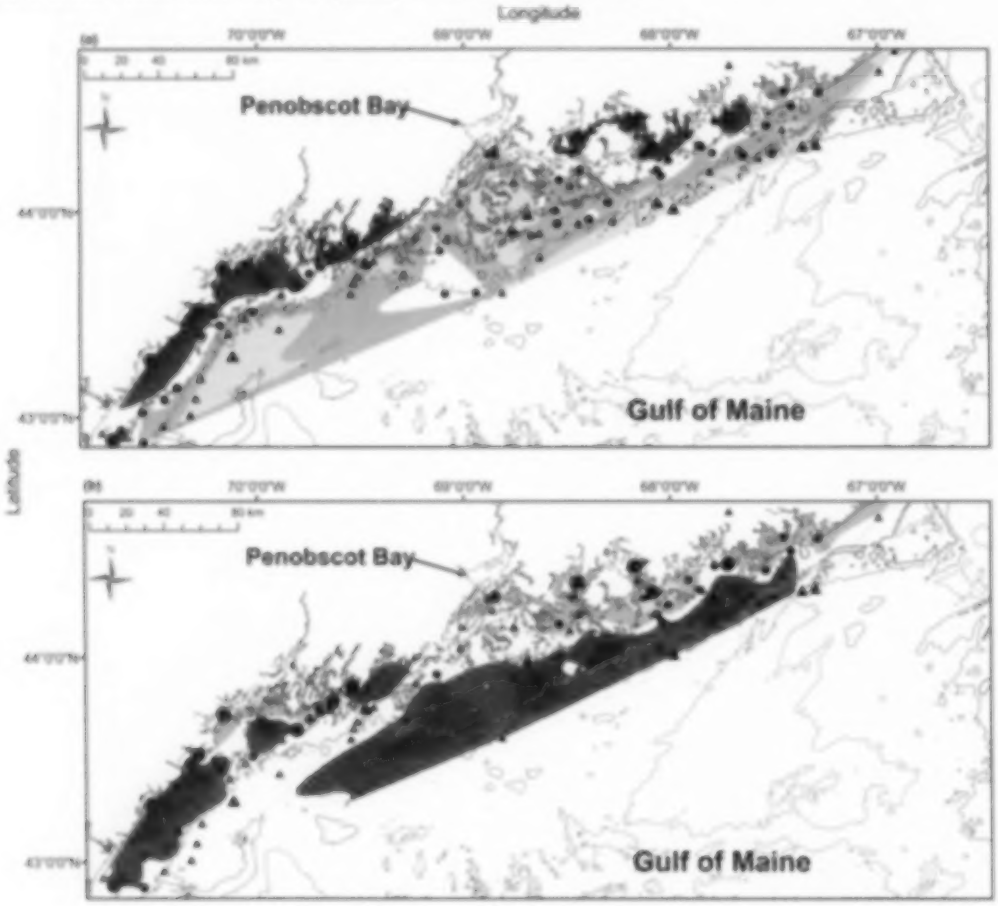

depth preferences while maintaining preference for coarse sand or gravel bottom sediments (Sundermeyer et al. 2005) or by remaining within temperature ranges from winter through summer by altering depth, as shown for haddock (Perry and Smith 1994). As a result, many species movement patterns and observed distributions may demonstrate a relationship among depth, temperature, and season (Methratta and Link 2007). Discordance among species between spring and fall surveys (see cod and haddock, Table 7) may be due to seasonal shifts of habitat choice. It is precisely these relationships that become important in designing a geographically based management scheme.

While some species showed shifts, others did not. Both spring and fall structure of benthic vertebrates was strongly driven by monkfish, with this monkfish species group distribution matching that of monkfish caught by the shrimp survey in the Gulf of Maine (Northeast Data Poor Stocks Working Group 2007). During the spring survey, there were two pockets of the monkfish species group located in the deeper basins along with Acadian redfish, a deepwater fish found inshore in colder months (Collette and Klein-MacPhee 2002), as a correlated species. The monkfish group contrasted a coastal species group with a spatial distribution that resembles the trajectory of the eastern Maine coastal current (see Pettigrew et al. 2005). The fall survey demonstrates reinforcement of the pattern seen in the spring with a larger number of species, including American plaice, witch flounder, fourbeard rockling, and red hake, becoming significantly correlated with monkfish. The strength of species–species relationships implies a connection to the seasonal pattern in the coastal currents and robustness of structure in communities around them. Secondarily, over this mesoscale structure is a mosaic of habitats that appear to be important in the structuring of fish populations with a uniqueness of areas near the Bay of Fundy (benthics) and the mouth of the Penobscot River (pelagics). Historically and presently, the coastal Maine fishery focuses effort on a select few species, of which a number figured prominently in the results, including monkfish, redfish, gadids, flatfish, herring, and alewife (Table 7). While pelagic species are not caught with

Fig. 8. Spring benthic vertebrate species biodiversity maps from (*a*) PC1, (*b*) PC2, and (*c*) PC3 scores. Symbols represent PC scores classified into five categories from negative scores (triangles) to positive scores (circles) with larger symbols indicating larger absolute values. Contour plots are results of natural neighbor interpolation reflecting the spatial variation in scores with dark shading representing positive scores and light shading negative scores. Neutral scores are given by hexagons and lack of any shading.

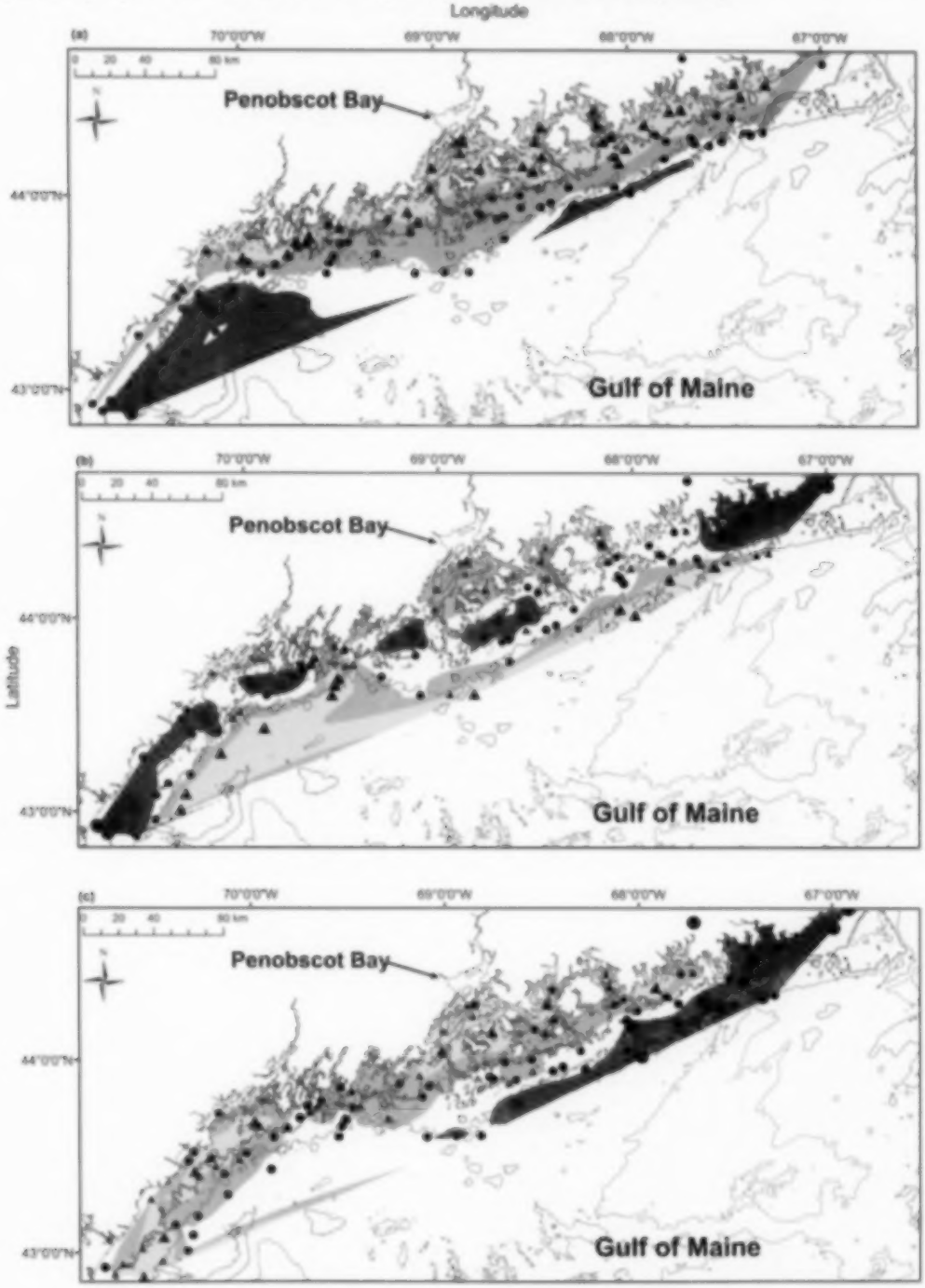

Fig. 9. Full pelagic species biodiversity maps from (*a*) PC1 and (*b*) PC2 scores. Symbols represent PC scores classified into five categories from negative scores (triangles) to positive scores (circles) with larger symbols indicating larger absolute values. Contour plots are results of natural neighbor interpolation reflecting the spatial variation in scores with dark shading representing positive scores and light shading negative scores. Neutral scores are given by hexagons and lack of any shading.

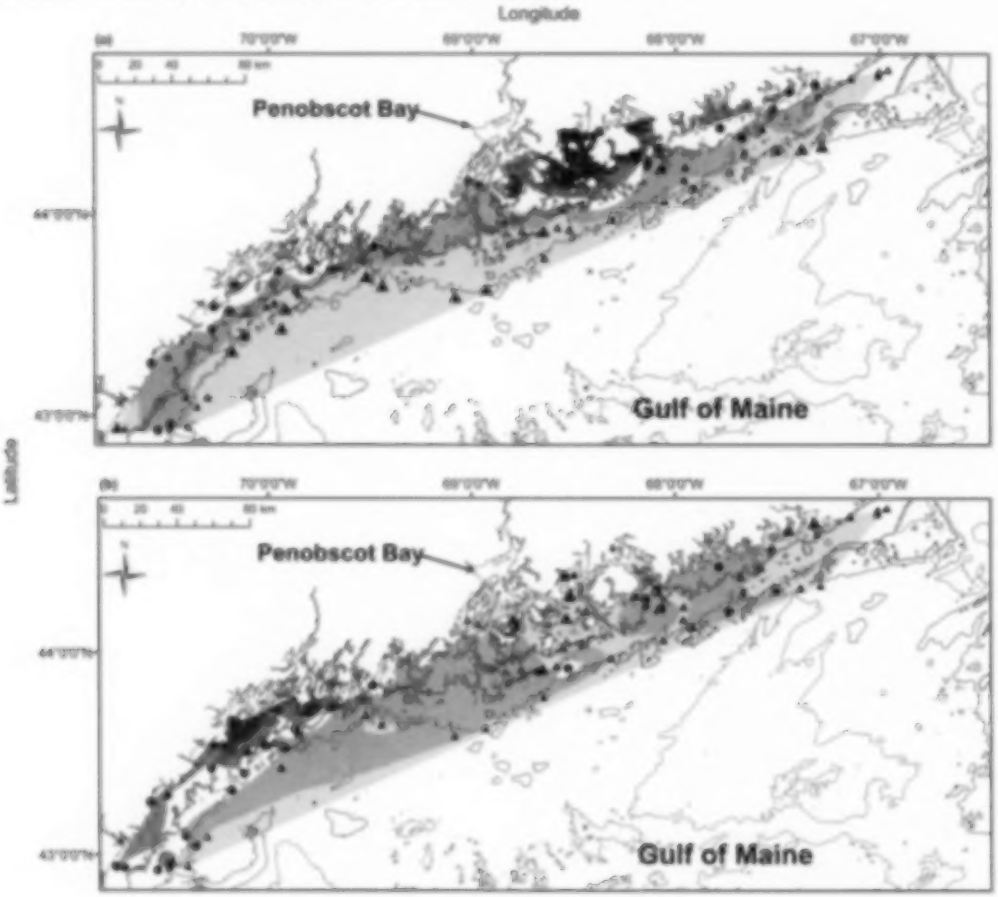

high efficiency in bottom trawls, their abundance, frequency of capture, and structured data set identified by PCA_{BTSP} were such that we felt impelled to include them. Presently, herring fisheries have the largest landings by weight along coastal Maine. Pelagic and primarily anadromous nearshore herring-like forage fish (alewife, blueback herring, and Atlantic herring) spatially contrasted an offshore euphausiids and pearlside group in the spring survey. Pearlsides are a deepwater bathypelagic fish and euphausiids are common large-bodied invertebrates that are an important predator of copepods (Baumgartner et al. 2003). There is little broadscale distribution information regarding euphausiids, although they are known to exhibit vertical migration and surface swarming behavior in response to internal waves interacting with banks (Stevick et al. 2008). In the fall, Atlantic herring remained an important nearshore species with menhaden and smelt and to a lesser degree the anadromous alosids. The nearshore pelagic group appeared to be focused just east of Penobscot Bay and contrasted an offshore predatory dogfish distribution. Timing and routes of migration by alewife, Atlantic herring, menhaden, and dogfish likely contribute to the observed assemblage patterns, with species that overwinter in the mid-Atlantic bight arriving in the western Gulf of Maine earliest (Collette and Klein-MacPhee 2002). The pelagic species schooling behavior (Collette and Klein-MacPhee 2002), complex patterns in behavior such as diel vertical distributions, and the resulting patchy distributions are likely responsible for the poor ability of any one variable to describe assemblage patterns. As a result, a large number of interacting variables appear to be responsible. Thus, interpretation of pelagic species assemblages should be approached with caution at finer scales but does demonstrate broad assemblage differences between inshore–offshore regions and along the coast. The distribution of forage fish has an inverse relationship to the mobile pelagic predatory spiny dogfish. A high degree of structure of assemblages is corroborated by the ability to create feeding guilds using dendrogram analysis of stomach contents from fishes in the Gulf of Maine (Garrison and Link 2000). These results suggest that predator–prey relationships are also captured to some degree by measures of assemblage structure. The relationship between diet-based grouping of fish and assemblage structure should be further studied.

Fig. 10. Fall benthic vertebrate species biodiversity maps from (*a*) PC1, (*b*) PC2, and (*c*) PC3 scores. Symbols represent PC scores classified into five categories from negative scores (triangles) to positive scores (circles) with larger symbols indicating larger absolute values. Contour plots are results of natural neighbor interpolation reflecting the spatial variation in scores with dark shading representing positive scores and light shading negative scores. Neutral scores are given by hexagons and lack of any shading.

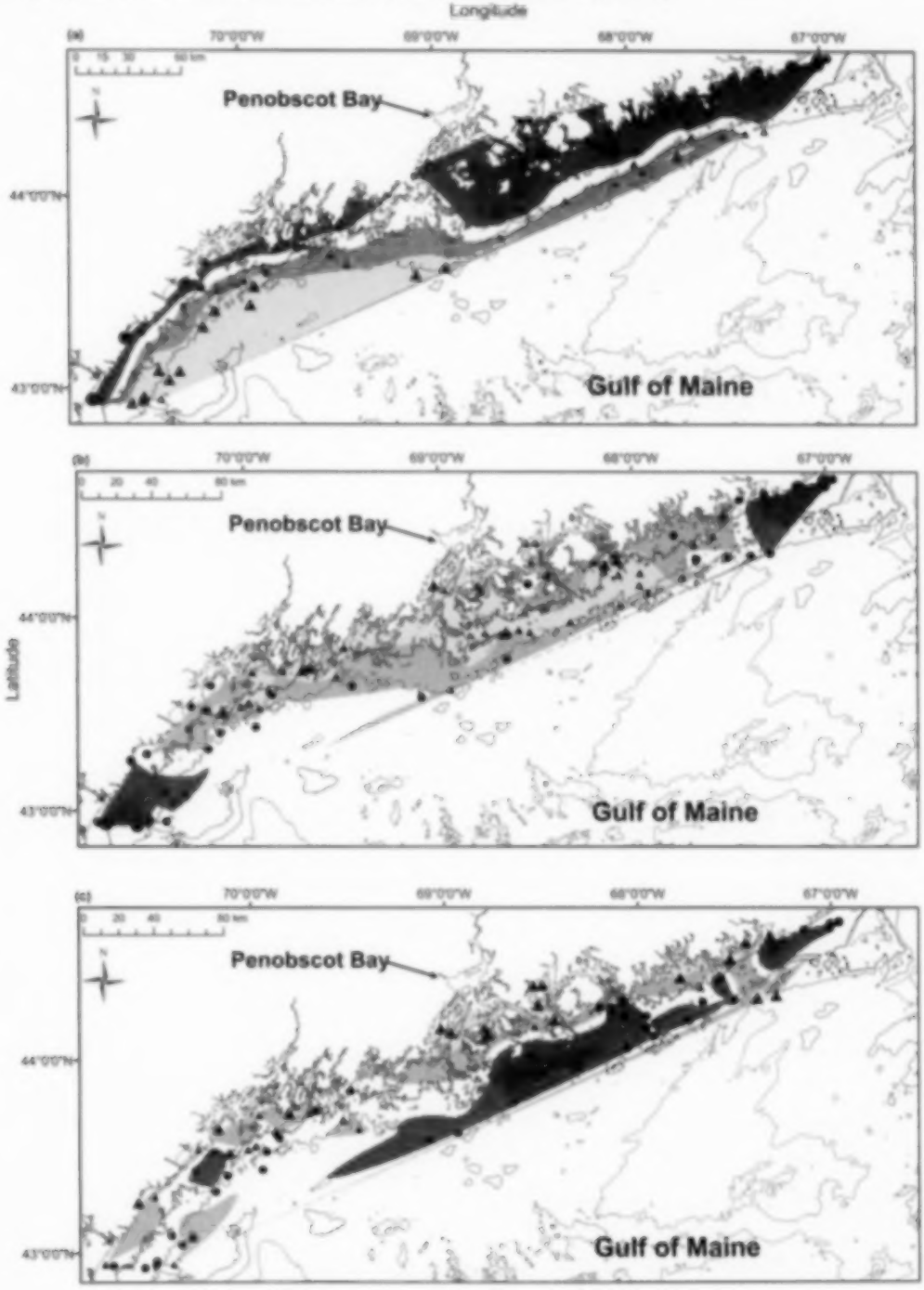

Table 7. Spring and fall species groupings for analyses of vertebrate and pelagic data.

	Positive loading	Negative loading
Spring		
Vertebrate	*Lophius americanus*	*Scophthalmus aquosus*
	Sebastes fasciatus	
	Hippoglossoides platessoides	*Myoxocephalus octodecemspinosus*
	Urophycis chuss	
		Pseudopleuronectes americanus
	Limanda ferruginea	
		Hippglossus hippoglossus
	Urophycis tenuis	
	Paralichthys oblongus	
	Melanogrammus aeglefinus	
Pelagic	*Clupea harengus*	*Squalus acanthias*
	Alosa pseudoharengus	Euphausiid spp.
	Alosa aestivalis	
Fall		
Vertebrate	*Pseudopleuronectes americanus*	*Lophius americanus*
		Glyptocephalus cynoglossus
	Myoxocephalus octodecemspinosus	*Hippoglossoides platessoides*
		Enchelyopus cimbrius
	Raja erinacea	
	Hemitripterus americanus	*Urophycis chuss*
	Scophthalmus aquosus	
	Gadus morhua	
	Melanogrammus aeglefinus	
Pelagic	*Osmerus mordax*	*Squalus acanthias*
	Brevoortia tyrannus	
	Clupea harengus	
	Alosa pseudoharengus	

Note: Species are listed starting with the highest loadings with spaces in the list indicating weaker associations.

We found groups of co-occurring species distributed unevenly across spatial gradients in physical characteristics, including temperature. New PC variables showed primary east–west and onshore–offshore differences in community structure and a secondary mosaic of patches along the coast of Maine. Placing the results within the context of hierarchical patch dynamics (Wu and Loucks 1995) helps to elucidate key ecosystem boundaries. Concordance between the pattern in species assemblages and surface currents of the interior Gulf of Maine strengthen in the fall. The matching physical structure and species eigenvectors lead us to nominate ocean mixing regimes, generated by a gradient in tidal current and other forces (see Pettigrew et al. 2005), as the primary driver of community structure when viewed at the scale of the inshore waters of the Gulf of Maine. However, it should be remembered that this regional structuring is embedded within a broader division along the continental shelf (Mahon et al. 1998; Jordaan et al. 2007), among Georges Bank and the deeper basins and coastal areas of the Gulf of Maine (Overholtz and Tyler 1985; Gabriel 1992; A. Jordaan unpublished data) and overlooks finer-scale local patterns that occur within and among coastal embayments (Jordaan 2010).

Most benthic vertebrate and invertebrate species sampled possess typical broadcast spawning and pelagic egg and larval life history characteristics suggesting that responses to the environment should be similar between the two groups; however, this was not the case. The lack of coherence by invertebrates, many of which are sessile or have limited potential for movement, suggests that differences between invertebrate and vertebrate analyses reflect differences in adult mobility as opposed to dispersal. It appears that patterns in sediment type and other static physical properties were not strong enough to create consistent patterns at the measurement scale employed in this study. The concordance between the EMCC and the benthic vertebrate structure strengthening over the summer suggests that more mobile species adjust their distributions. Structuring of invertebrates may occur at scales within or beyond the scope of this survey, for example, associated significantly with either benthic heterogeneity (Wahle and Steneck 1992; Poppe et al. 2003) or global distributions in fishing effort (Berkes et al. 2006). Further, low catchability of benthic invertebrates by sampling gear and lack of trawl coverage of more complex habitats, which may not be trawlable, may be playing an important role in observations of invertebrate and pelagic species assemblages. Different survey designs would be required to accomplish more comprehensive analysis.

Eastwood et al. (2006) mapped benthic assemblages to find only minor differences in top-down or bottom-up classification of assemblages and the resulting assemblage maps but indicated that bottom-up approaches seem to improve as more physical acoustic-derived data are made available. We did not include any acoustic data but rather focused on bio-

logical data only using what is a top-down division of the data set into new principal components, largely because fisheries survey data are collected frequently and reliably and thus will eventually allow for a strong time series analysis that can begin to parse out seasonal trends. With only a handful of years with consistent data available, there is no advantage to including a temporal component at this point but rather to introduce the spatial variation in assemblage structure in a single year. However, we must recognize the limitations of the analysis focusing on three factors and their interactions. Habitat types, and other data, would improve the detection of trends in assemblage structure.

The methods applied here depend on correlations among species to generate new variables. The addition of bootstrap-generated stopping rules and identification of significant species–species relationships have improved the application of PCA to this end; however it is not the only method available. We agree with Field et al. (1982) that patterns in species should be examined prior to determining important physical factors, which precludes the use of canonical correlation analysis. Current ecological classification has widely adopted nonparametric ranking of similarities to create a matrix that can identify geographically related divisions in assemblages and species that contribute to patterns (Field et al. 1982). Heavy computing loads were identified as a limitation in classification analysis and stopping rules (Field 1969; Field et al. 1982), a factor that no longer exists. The commonly employed Bray–Curtis measure of similarity and nonmetric multidimensional scaling ordination accommodate robustness and flexibility but sacrifice information by using rank data (Field et al. 1982). PCA_{BTSP}, on the other hand, will sacrifice some flexibility and robustness to gain a more quantitative edge. It is unfortunately not possible to identify the most appropriate techniques without a systematic evaluation of each combined with input from stakeholders who depend on the results being applied appropriately. This line of research should be examined, as should the refinement of postclassification analyses.

Management implications

An important element to this work is the application to area- and ecosystem-based management in the Gulf of Maine. Due to dependence of species distributions on bottom type, Auster et al. (2001) suggested that trawl survey data can be used as proxies for distribution of seafloor habitats and used to infer habitat requirements of co-occurring species. Across the Gulf of Maine, Georges Bank, and Scotian Shelf, depth and temperature are related more strongly to species distributions than substrate type (Mahon and Smith 1989; Methratta and Link 2007), but thus, it is more helpful to recognize the sum total of "habitat" and not concentrate on one physical factor. Our results suggest a number of distributional relationships between species and physical variables and agree with the assertion that survey data can be used to infer patterns in habitat and biodiversity because correlation of species' distributions provides a proxy for the physical environment. However, interpretations will be entirely dependent on the scale and effort of sampling. A more detailed investigation relating variability of temperatures, current patterns, and species abundances and assemblage distributions will be necessary to understand spatial structuring of ecosystems.

Fisheries in the past 50 years have been typified by boom–bust cycles, with effort shifting to new species after the completion of a cycle, reflected in the commercial landings (Fig. 11). It is thought that by matching the scales of management to those of ecological structure, management will be more effective. Part of this is the recognition that a large number of differing habitats will have to be included to provide for species year-to-year variation in movements and distributions. Species that were structured at scales that match the extent and sampling density of the data used in this analysis and were involved in driving patterns in assemblage structure along the Maine coastal area include monkfish (Table 7), the most recent Maine groundfish fishery (Fig. 11), and Acadian redfish (Table 7), one of the older fisheries (Fig. 11). Compared with historical conditions, cod are no longer playing any structuring role along the Maine coast largely due to managers ignoring and fishers targeting finer-scale metapopulations that removed the species from coastal Maine (Ames 2004), as is the case for a number of other species. The present analysis suggests that a spatially explicit management of benthic vertebrates is possible and that many commercially and ecologically relevant groundfish species can be spatially managed at far smaller scales than the two-stock paradigm of today.

It is important to consider the method of capture, in particular how interpretation differs between fisheries-dependent and fisheries-independent catches. If the analysis were performed on fisheries-dependent data, correlations among species and similar eigenvector loadings would indicate increasing likelihood of capture; therefore, the approach could also be used to identify bycatch risk. For example, the analysis of fisheries-independent data in this work suggests a high likelihood of bycatch of the anadromous river herrings (alewife and blueback herring) during hypothetical spring menhaden and smelt and fall herring fisheries. In contrast, the fall benthic vertebrates have a large number of species susceptible to catch as a nontargeted species if any one of the correlated species is targeted by a hypothetical fishery. Because fishing effort is unevenly distributed (Murawski et al. 2005; Mills et al. 2007) and impacts could be either amplified or diminished, there is opportunity for overfishing or a system of area-based management that satisfies ecosystem-based principals to develop.

The periodicity of sampling and selectivity of gear will always be a consideration in interpretation of results for directing management. This study used data collected from a fisheries-independent survey that employs the same sampling protocol over sampling seasons and years. The selectivity of sampling gear is different from species to species. Thus, the composition of fish species abundance observed in the survey data may differ from that of the actual fish community in the ecosystem. However, because the standard sampling protocol is used throughout the sampling program, the selectivity of each species is the same over time, which makes the correlations or covariance between species abundance indices consistent over time. The proposed approach used the correlations, which makes the results derived from this study robust with respect to differences in selectivity among species. The associations between the highest loading

Fig. 11. Fisheries landings for the State of Maine from 1950 to the present organized according to maximum historic peak landings: (*a*) <5000 metric tons, (*b*) 5000–10 000 metric tons, and (*c*) >10 000 metric tons. Landings data do not translate into a measure of abundance but rather show the progression of fisheries from redfish through a variety of other groundfish, flatfish, and invertebrates and ending with only herring and lobster making contributions in the final years. Herring is the only species that contributes substantial landings through the entire time period. Note that Maine fisheries only represent a fraction of total landings in the Gulf of Maine but are expected to reflect dynamics along the Maine coast. Data available at www.maine.gov/dmr/commercialfishing/historicaldata.htm (Maine Department of Marine Resources).

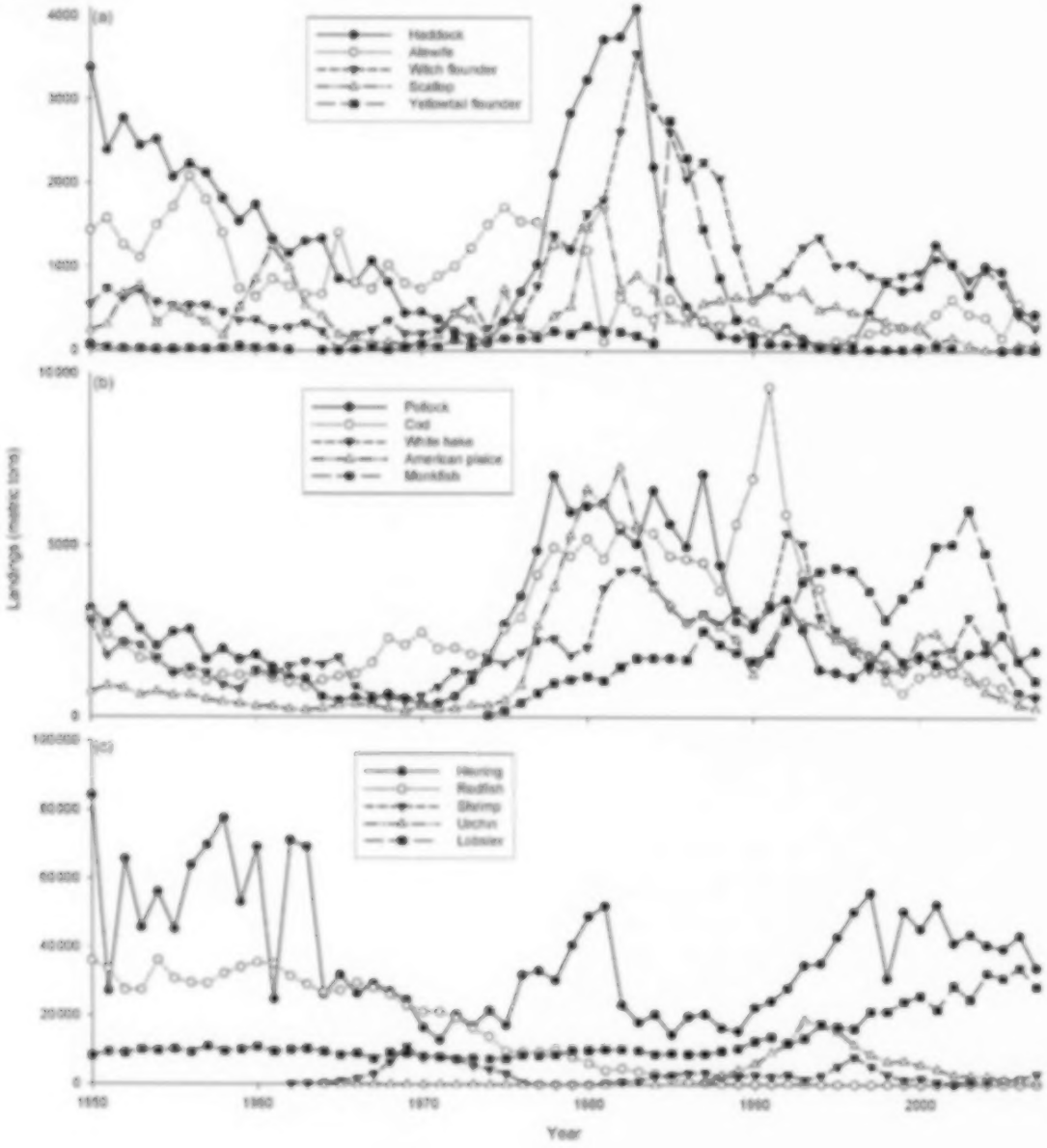

species and correlation coefficients were consistent, suggesting that groups of species are important in determining structure rather than any one species. O'Neill (2001) argued that ecosystems, by definition, include biases regarding spatial coverage by assuming a closed system. The analyses presented here constitute a methodology for determining structure in populations of organisms. By doing so, biases imposed by prior assumptions of ecosystem boundaries are removed in favor of designating structure based on biological variables. No-take marine reserves or marine protected areas have been advocated as integral components of ecosystem-based zoning, but there has also been considerable

debate regarding their effectiveness in that capacity (Norse et al. 2003). Smith et al. (2008) found that the western Gulf of Maine closure was having no appreciable effect on monkfish population recovery. Since monkfish became the active groundfish fishery after the loss of coastal cod, managers should consider guarding against overcapitalized fleets shifting effort from failing fisheries. One mechanism to accomplish this is to restrict effort spatially. Our results indicate that the western Gulf of Maine closure is small compared with the region associated with the monkfish-dominated assemblage. To designate an effective plan that includes monkfish and other species, a larger, more comprehensive closure system is required.

To use the methods outlined in this paper as a mechanism for identifying appropriate management scales within a broad area-based management scheme will require further steps, including the establishment and management of a marine protected area network. The challenge that remains is achieving a shared vision in management that is adequately geographically based (Murawski 2007). It will be necessary to incorporate other ecological and socioeconomic indicators that consider such attributes as local (genetic) stocks, species dispersal potentials, size and age structure, and fleet dynamics. Furthermore, specific plans should be tested through multispecies modeling such as available in the Ecospace model (Walters et al. 1999). Still, the analysis presented here can determine expansion of species groups or shifts in interactions with other species and, when combined with process-oriented indicators that register changes in trophic interactions, can add valuable information to the management of fisheries. Developing plans without basing them on the underlying biodiversity could lead to potentially serious consequences of overfishing or otherwise impact certain specific or underrepresented species and habitats, a principal that is consistent for all forms of *de facto* zoning.

While devising species-specific plans is required to stave off extinction of species at critically low abundances (Bain et al. 2007), there are situations where the full life cycle or a critical prey resource is not adequately protected. For example, Baltic Sea marine protected areas have been criticized for shifting fishing effort onto smaller juvenile fishes, resulting in higher discard rates and other negative consequences (Hinrichsen et al. 2009; Suuronen et al. 2010). Thus, achieving a geographically based system will require all habitats to be represented under a flexible, but comprehensive, plan. A major step toward this is recognizing the gradients in biodiversity. The development of techniques for uncovering spatial structure in marine assemblages and defining the limitations and advantages of each will be critical to appropriately partitioning the marine environment.

Acknowledgements

We thank Maine Sea Grant and Paul Anderson for funding A.J. and further Maine Sea Grant/NOAA funding through grant NA03OAR4170084. We express our appreciation to past and present Department of Marine Resources employees for time spent collecting and processing the data used in this manuscript and the captain and crew of the F/V *Robert Michael* for their efforts in contributing to the survey. The inshore trawl surveys are funded by the Northeast Consortium and National Marine Fisheries Service. We thank Heather Deese-Riordan, Jeanne Brown, and two anonymous reviewers for constructive comments that improved earlier versions of this manuscript.

References

Ames, E.P. 2004. Atlantic cod stock structure in the Gulf of Maine. Fisheries, **29**(1): 10–28. doi:10.1577/1548-8446(2004)29[10:ACSSIT]2.0.CO;2.

Auster, P.J., Joy, K., and Valentine, P.C. 2001. Fish species and community distributions as proxies for seafloor habitat distributions: the Stellwagen Bank National Marine Sanctuary example (Northwest Atlantic, Gulf of Maine). Environ. Biol. Fishes, **60**(4): 331–346. doi:10.1023/A:1011022320818.

Bain, M.B., Haley, N., Peterson, D.L., Arend, K.K., Mills, K.E., Sullivan, P.J., and Lusseau, D. 2007. Recovery of a US endangered fish. PLoS One, **2**(1): e168. doi:10.1371/journal.pone.0000168. PMID:17245444.

Baumgartner, M.F., Cole, T.V.N., Campbell, R.G., Teegarden, G.J., and Durbin, E.G. 2003. Associations between North Atlantic right whales and their prey, *Calanus finmarchicus*, over diel and tidal time scales. Mar. Ecol. Prog. Ser. **264**: 155–166. doi:10.3354/meps264155.

Berkes, F., Hughes, T.P., Steneck, R.S., Wilson, J.A., Bellwood, D.R., Crona, B., Folke, C., Gunderson, L.H., Leslie, H.M., Norberg, J., Nyström, M., Olsson, P., Osterblom, H., Scheffer, M., and Worm, B. 2006. Ecology. Globalization, roving bandits, and marine resources. Science, **311**(5767): 1557–1558. doi:10.1126/science.1122804. PMID:16543444.

Brodziak, J.K., Overholtz, W.J., and Rago, P.J. 2001. Does spawning stock affect recruitment of New England groundfish? Can. J. Fish. Aquat. Sci. **58**(2): 306–318. doi:10.1139/cjfas-58-2-306.

Chen, Y., Sherman, S., Wilson, C., Sowles, J., and Kanaiwa, M. 2006. A comparison of two fishery independent survey programs used to define the population structure of American lobster (*Homarus americanus*) in the Gulf of Maine. Fish. Bull. (Wash., D.C.), **104**: 247–255.

Collette, B.B., and Klein-MacPhee, G. 2002 Bigelow and Schroeder's Fishes of the Gulf of Maine. 3rd ed. Smithsonian Institution Press, Washington, D.C.

Crowder, L.B., Osherenko, G., Young, O.R., Airamé, S., Norse, E.A., Baron, N., Day, J.C., Douvere, F., Ehler, C.N., Halpern, B.S., Langdon, S.J., McLeod, K.L., Ogden, J.C., Peach, R.E., Rosenberg, A.A., and Wilson, J.A. 2006. Sustainability. Resolving mismatches in U.S. ocean governance. Science, **313**(5787): 617–618. doi:10.1126/science.1129706. PMID:16888124.

Dow, R.L. 1981. Influence of sea temperature cycles on the abundance and availability of marine and estuarine species of commerce. *In* Proceedings of the Oceans 1981 Conference Record, Boston, Massachusetts, 16–18 September 1981. The Ocean: An International Workplace. Vol. 2. IEEE, New York. pp. 775–779.

Eastwood, P.D., Souissi, S., Rogers, S.I., Coggan, R.A., and Brown, C.J. 2006. Mapping seabed assemblages using comparative top-down and bottom-up classification approaches. Can. J. Fish. Aquat. Sci. **63**(7): 1536–1548. doi:10.1139/F06-058.

Field, J.G. 1969. The use of the information statistic in the numerical classification of heterogeneous systems. J. Ecol. **57**(2): 565–569. doi:10.2307/2258400.

Field, J.G., Clarke, K.R., and Warwick, R.M. 1982. A practical strategy for analysing multispecies distribution patterns. Mar. Ecol. Prog. Ser. **8**: 37–52. doi:10.3354/meps008037.

Frisk, M.G., Miller, T.J., Martell, S.J.D., and Sosebee, K. 2008. New hypothesis helps explain elasmobranch "outburst" on

Georges Bank in the 1980s. Ecol. Appl. **18**(1): 234–245. doi:10.1890/06-1392.1. PMID:18372569.

Gabriel, W. 1992. Persistence of demersal fish assemblages between Cape Hatteras and Nova Scotia, Northwest Atlantic. J. Northwest Atl. Fish. Sci. **14**: 29–46.

Garrison, L.P., and Link, J.S. 2000. Dietary guild structure of the fish community in the Northeast United States continental shelf ecosystem. Mar. Ecol. Prog. Ser. **202**: 231–240. doi:10.3354/meps202231.

Hilborn, R. 2003. Forum. Marine reserves: the best option for our oceans? Front. Ecol. Environ. **1**(9): 497.

Hinrichsen, H.H., Krauss, G., Böttcher, U., and Köster, F. 2009. Identifying eastern Baltic cod nursery grounds using hydrodynamic modelling: knowledge for the design of Marine Protected Areas. ICES J. Mar. Sci. **66**(1): 101–108. doi:10.1093/icesjms/fsn207.

Hoerling, M.P., Hurrell, J.W., and Xu, T. 2001. Tropical origins for recent North Atlantic climate change. Science, **292**(5514): 90–92. doi:10.1126/science.1058582. PMID:11292869.

Jackson, D.A. 1993. Stopping rules in principal components analysis: a comparison of heuristical and statistical approaches. Ecology, **74**(8): 2204–2214. doi:10.2307/1939574.

Jackson, D.A. 1995. Bootstrapped principal component analysis — reply to Mehlman et al. Ecology, **76**(2): 644–645. doi:10.2307/1941220.

Jordaan, A. 2006. Determining environmental drivers of fish community structure along the coast of Maine. Ph.D. thesis, University of Maine, Orono, Maine.

Jordaan, A. 2010. Fish assemblages spatially structure along a multi-scale wave energy gradient. Environ. Biol. Fishes, **87**(1): 13–24. doi:10.1007/s10641-009-9537-9.

Jordaan, A., and Kling, L.J. 2003. Determining the optimal temperature range for Atlantic cod (*Gadus morhua*) during early life. *In* Proceedings of the 26th Annual Larval Fish Conference, Oslo, Norway, 22–26 July 2002. The Big Fish Bang. Institute of Marine Research, Bergen, Norway. pp. 45–62. ISBN 82-7461-059-8. Available from www.fishlarvae.com/e/Book_Reader.asp?pg=/e/BigBang/Jordaan.pdf&pgid=223.

Jordaan, A., Frisk, M.G., Wolff, N.H., Incze, L.S., Hamlin, L., and Chen, Y. 2007. Structure of fish assemblages along the northeastern United States based on trawl survey data: indicators of biodiversity and a basis for ecosystem and area-based management. International Council for the Exploration of the Sea, Copenhagen, Denmark. CM 2007/A:05. Available from www.ices.dk/products/CMdocs/CM-2007/A/A0507.pdf

Jørgensen, O.A., Hvingel, C., Møller, P.R., and Treble, M.A. 2005. Identification and mapping of bottom fish assemblages in Davis Strait and southern Baffin Bay. Can. J. Fish. Aquat. Sci. **62**(8): 1833–1852. doi:10.1139/f05-101.

Levin, S.A., and Lubchenco, J. 2008. Resilience, robustness, and marine ecosystem-based management. Bioscience, **58**(1): 27–32. doi:10.1641/B580107.

Mahon, R., and Smith, R.W. 1989. Demersal fish assemblages on the Scotian Shelf, northwest Atlantic: spatial distribution and persistence. Can. J. Fish. Aquat. Sci. **46**(Suppl. 1): s134–s152. doi:10.1139/f89-285.

Mahon, R., Brown, S.K., Zwanenburg, K.C.T., Atkinson, D.B., Buja, K.R., Claflin, L., Howell, G.D., Monaco, M.E., O'Boyle, R.N., and Sinclair, M. 1998. Assemblages and biogeography of demersal fishes of the East Coast of North America. Can. J. Fish. Aquat. Sci. **55**(7): 1704–1738. doi:10.1139/cjfas-55-7-1704.

Mehlman, D.W., Shepherd, U.L., and Kelt, D.A. 1995. Bootstrapping principal components analysis: a comment. Ecology, **76**(2): 640–643. doi:10.2307/1941219.

Methratta, E.T., and Link, J.S. 2007. Ontogenetic variation in habitat association for four groundfish species in the Gulf of Maine–Georges Bank region. Mar. Ecol. Prog. Ser. **338**: 169–181. doi:10.3354/meps338169.

Mills, C.M., Townsend, S.E., Jennings, S., Eastwood, P.D., and Houghton, C.A. 2007. Estimating high resolution trawl fishing effort from satellite-based vessel monitoring system data. ICES J. Mar. Sci. **64**(2): 248–255. doi:10.1093/icesjms/fsl026.

Murawski, S.A. 2007. Ten myths concerning ecosystem approaches to marine resource management. Mar. Policy, **31**(6): 681–690. doi:10.1016/j.marpol.2007.03.011.

Murawski, S.A., Wigley, S.E., Fogarty, M.J., Rago, P.J., and Mountain, D.G. 2005. Effort distribution and catch patterns adjacent to temperate MPAs. ICES J. Mar. Sci. **62**: 1150–1167.

Norse, E.A., Grimes, C.B., Ralston, S., Hilborn, R., Castilla, J.C., Palumbi, S.R., Fraser, D., and Kareiva, P. 2003. Marine reserves: the best option for our oceans? Front. Ecol. Environ. **1**(9): 495–502. doi:10.2307/3868117.

Northeast Data Poor Stocks Working Group. 2007. Monkfish assessment report for 2007. Reference Document 07-21. US Department of Commerce, Northeast Fish Science Center, Woods Hole, Mass.

O'Neill, R.V. 2001. Is it time to bury the ecosystem concept? (with full military honors, of course!). Ecology, **82**(12): 3275–3284.

Overholtz, W.J., and Tyler, A.V. 1985. Long-term responses of the demersal fish assemblages of Georges Bank. Fish. Bull. (Wash., D.C.), **83**: 507–520.

Peres-Neto, P.R., Jackson, D.A., and Somers, K.M. 2003. Giving meaningful interpretation to ordination axes: assessing loading significance in principal component analysis. Ecology, **84**(9): 2347–2363. doi:10.1890/00-0634.

Perry, R.I., and Smith, S.J. 1994. Identifying habitat associations of marine fishes using survey data: an application to the Northwest Atlantic. Can. J. Fish. Aquat. Sci. **51**(3): 589–602. doi:10.1139/f94-061.

Pettigrew, N.R., Churchill, J.H., Janzen, C.D., Mangum, L.J., Signell, R.P., Thomas, A.C., Townsend, D.W., Wallinga, J.P., and Xue, H. 2005. The kinematic and hydrographic structure of the Gulf of Maine Coastal Current. Deep-Sea Res. II: Top. Stud. Oceanogr. **52**(19–21): 2369–2391. doi:10.1016/j.dsr2.2005.06.033.

Pillar, V.D. 1999. The bootstrapped ordination re-examined. J. Veg. Sci. **10**(6): 895–902. doi:10.2307/3237314.

Poppe, L.J., Paskevich, V.F., Williams, S.J., Hastings, M.E., Kelley, J.T., Belknap, D.F., Ward, L.G., FitzGerald, D.M., and Larsen, P.F. 2003. Surficial sediment data from the Gulf of Maine, Georges Bank, and vicinity: a GIS compilation. U.S. Geol. Surv. Open-File Rep. 03-001. Available from http://pubs.usgs.gov/of/2003/of03-001/index.htm.

Sherman, S.A., Stepanek, K., and Sowles, J. 2005. Maine–New Hampshire inshore groundfish trawl survey. Procedures and protocols. Res. Ref. Doc. 05/01. Maine Department of Marine Resources. Available from www.maine.gov/dmr/rm/trawl/reports/proceduresandprotocols.pdf.

Sibson, R. 1981. Interpolating multivariate data. John Wiley & Sons, New York.

Slocombe, D.S. 1998. Defining goals and criteria for ecosystem-based management. Environ. Manag. **22**(4): 483–493. doi:10.1007/s002679900121. PMID:9582385.

Smith, M.D., Grabowski, J.H., and Yund, P.O. 2008. The role of closed areas in rebuilding monkfish populations in the Gulf of Maine. ICES J. Mar. Sci. **65**(7): 1326–1333. doi:10.1093/icesjms/fsn137.

Souissi, S., Ibanez, F., Hamadou, R.B., Boucher, J., Cathelineau,

A.C., Blanchard, F., and Poulard, J.C. 2001. A new multivariate mapping method for studying species assemblages and their habitats: example using bottom trawl surveys in the Bay of Biscay (France). Sarsia, **86**: 527–542.

Stevick, P.T., Incze, L.S., Kraus, S.D., Rosen, S., Wolff, N., and Baukus, A. 2008. Trophic relationships and oceanography on and around a small offshore bank. Mar. Ecol. Prog. Ser. **363**: 15–28. doi:10.3354/meps07475.

Strayer, D.L., Power, M.E., Fagan, W.F., Pickett, S.T.A., and Belnap, J. 2003. A classification of ecological boundaries. Bioscience, **53**(8): 723–729. doi:10.1641/0006-3568(2003)053[0723:ACOEB]2.0.CO;2.

Sundermeyer, M.A., Rothschild, B.J., and Robinson, A.R. 2005. Using commercial landings data to identify environmental correlates with distributions of fish stocks. Fish. Oceanogr. **14**(1): 47–63. doi:10.1111/j.1365-2419.2004.00302.x.

Suuronen, P., Jounela, P., and Tschernij, V. 2010. Fishermen responses on marine protected areas in the Baltic cod fishery. Mar. Policy, **34**(2): 237–243. doi:10.1016/j.marpol.2009.07.001.

Targett, T.E., and McCleave, J.D. 1974. Summer abundance of fishes in a Maine tidal cove with special reference to temperature. Trans. Am. Fish. Soc. **103**(2): 325–330. doi:10.1577/1548-8659(1974)103<325:SAOFIA>2.0.CO;2.

Thomas, A.C., Townsend, D.W., and Weatherbee, R. 2003. Satellite measured phytoplankton variability in the Gulf of Maine. Cont. Shelf Res. **23**(10): 971–989. doi:10.1016/S0278-4343(03)00086-4.

Townsend, D.W. 1991. Influences of oceanographic processes on the biological productivity of the Gulf of Maine. Rev. Aquat. Sci. **5**: 211–230.

Townsend, D.W., and Ellis, W.G. 2010. Primary production and nutrient cycling on the Northwest Atlantic continental shelf. *In* Carbon and nutrient fluxes in continental margins: a global synthesis. *Edited by* K.-K. Liu, L. Atkinson, R. Quiñones, and L. Talaue-McManus. IGBP Book Series. Springer, Berlin. pp. 234–248.

Townsend, D.W., Thomas, A.C., Mayer, L.M., Thomas, M., and Quinlan, J. 2006. Oceanography of the Northwest Atlantic Continental Shelf. *In* The sea. Vol. 14. *Edited by* A.R. Robinson and K.H. Brink. Harvard University Press, Boston, Mass. pp. 119–168.

U.S. Commission on Ocean Policy. 2004. An ocean blueprint for the 21st century. Final report. U.S. Commission on Ocean Policy, Washington, D.C.

Wahle, R.A., and Steneck, R.S. 1992. Habitat restrictions in early benthic life: experiments on habitat selection and in situ predation with the American lobster. J. Exp. Mar. Biol. Ecol. **157**(1): 91–114. doi:10.1016/0022-0981(92)90077-N.

Walters, C., Pauly, D., and Christensen, V. 1999. Ecospace: prediction of mesoscale spatial patterns in trophic relationships of exploited ecosystems, with emphasis on the impacts of marine protected areas. Ecosystems (N.Y., Print), **2**(6): 539–554. doi:10.1007/s100219900101.

Wu, J., and Loucks, O.L. 1995. From balance of nature to hierarchal patch dynamics: a paradigm shift in ecology. Q. Rev. Biol. **70**(4): 439–466. doi:10.1086/419172.

The role of dispersal and retention in the early life stages of shrimp in a lowland river

Amina E. Price and Paul Humphries

Abstract: This study investigated the importance of dispersal and retention processes during early ontogeny for three caridean shrimp species that complete their entire life history in freshwater. Directional traps were used to examine the small-scale movement patterns of shrimp into and out of nursery habitat patches (slackwaters) in a small lowland river in south-eastern Australia. Movement patterns provided evidence for two contrasting life history based dispersal and retention strategies. For the two smaller atyid species, *Paratya australiensis* and *Caridina mccullochi*, the majority of larvae remained within the slackwater in which they were hatched until the final stage of development, at which point dispersal, either among slackwaters or out of slackwaters to faster-flowing pool and run habitats, occurred. For the larger palaemonid species, *Macrobrachium australiense*, larvae were hatched into slackwaters and dispersal occurred predominately during the first stage of larval development and then decreased as development progressed. Despite the differences in dispersal strategies among species, movement was mostly associated with a particular larval stage and thus emphasizes the importance of retention during critical developmental periods and of the potential impact that flow alteration could have on these and other species with similar life histories.

Résumé : Notre étude examine l'importance des processus de dispersion et de rétention durant le début de l'ontogenèse chez trois espèces de crevettes caridéennes qui complètent tout leur cycle biologique en eau douce. Des pièges directionnels ont servi à déterminer les patrons de déplacement des crevettes à petite échelle à l'entrée et la sortie des taches d'habitat de nourricerie (étales de courant) dans une petite rivière de plaine dans le sud-est de l'Australie. Les patrons de déplacement démontrent l'existence de deux stratégies bien disctinctes de dispersion et de rétention basées sur les cycles biologiques. Chez les deux espèces plus petites d'atyidés, *Paratya australiensis* et *Caridina mccullouchi*, la majorité des larves demeure dans l'étale où elles ont éclos jusqu'aux derniers stades de leur développement; à ce moment a lieu la dispersion, soit entre les étales, soit des étales vers les habitats d'eau plus rapide des profonds et des rapides. Chez l'espèce de palaemonidé de plus grande taille, *Macrobrachium australiense*, les larves éclosent dans les étales et la dispersion se fait surtout durant le premier stade du développement larvaire pour ensuite diminuer au cours du développement. Malgré les différences de stratégie de dispersion entre les espèces, les déplacements sont surtout associés à des stades larvaires particuliers. Cela souligne l'importance de la rétention durant les périodes critiques du développement et l'impact potentiel des modifications de débit sur ces espèces et sur d'autres espèces à cycle biologique semblable.

[Traduit par la Rédaction]

Introduction

The early life phases of many aquatic animals are characterized by poorly developed swimming abilities (Chia et al. 1984; Werner 2002; Bauer 2004). Consequently, movement is perilous, as larvae risk becoming displaced and entrained by the flow into unsuitable nursery habitats (Urho 1999; Houde 2002; Bauer 2004). Thus dispersal to, and retention in, suitable nursery habitat has long been recognized as a key factor in determining recruitment success (Sinclair 1988; Urho 1999; Largier 2004). A variety of life history strategies have evolved that minimize the risk of displacement and maximize the chances of retention in suitable nursery habitats. These include adults spawning in sites that are also suitable as nursery habitat and the same habitat being used throughout the life cycle, thereby removing the requirement for larvae to disperse into suitable nursery habitat (Werner 2002). For many species, however, the nursery habitat is different from the breeding or spawning habitat (e.g., Bauer 2004; O'Connell et al. 2005; Rome et al. 2009) or movement may be required in response to changes in habitat requirements and (or) suitability (Brittain and Eikeland 1988; Frid and Townsend 1989; Schlosser and Angermeier 1995). This has been noted for a number of

Received 30 April 2009. Accepted 10 February 2010. Published on the NRC Research Press Web site at cjfas.nrc.ca on 24 March 2010. J21175

Paper handled by Associate Editor John Richardson.

A.E. Price.[1,2] Cooperative Research Centre for Freshwater Ecology, University of Canberra, 2601, ACT, Australia.
P. Humphries. Institute for Land, Water and Society, School of Environmental Sciences, Charles Sturt University, P.O. Box 789, Albury, NSW, 2640, Australia.

[1]Corresponding author (e-mail: amina.price@latrobe.edu.au).
[2]Present address: The Murray–Darling Freshwater Research Centre, La Trobe University, Department of Environmental Management and Ecology, P.O. Box 991, Wodonga, Victoria, 3689, Australia.

amphidromous shrimp species with larvae that hatch in freshwaters and develop in saline waters and juveniles that then migrate upstream into adult freshwater habitats (Bauer 2004).

Within rivers, movement and retention are significantly influenced by flow (Pavlov 1994; Wiens 2002). The unidirectional nature of river flow requires organisms to be able to maintain position to avoid being flushed out of otherwise suitable habitat patches. Thus, habitat selection at the meso-scale is frequently determined by velocity thresholds for many organisms, with those species and life stages that have limited swimming ability frequently selecting low- or zero-flow habitat patches such as slackwaters (Humphries et al. 1999; Keckeis and Schiemer 2002; King 2004).

Slackwaters, also termed backwaters, dead water zones, inshore bays, or embayments, are areas with little or no directional flow and represent an important patch type in riverine ecosystems (Humphries et al. 2006; Thorp et al. 2006). Within the main channel of rivers, slackwaters typically form in slow-flowing littoral zones, in areas where flow is restricted by obstructions such as snags, and in semi-enclosed areas where rising water backs up (Thorp et al. 2006). Slackwaters act as retention zones and are believed to influence the structure and function of river ecosystems in relation to nutrient cycling, productivity, and trophic food webs (Schiemer et al. 2001; Thorp et al. 2006). Slackwaters also serve as crucial habitat for many stream-dwelling organisms, particularly the early life stages of wholly freshwater species of fish and shrimp (Richardson et al. 2004; Thorp et al. 2006). Although the importance of slackwaters as nursery habitat has been well established, for the majority of species that utilize them as nursery habitat, there is a paucity of information regarding dispersal and retention processes. We have some knowledge of downstream dispersal patterns for fish and invertebrate species with a larval drifting phase; however, there is little information regarding retention patterns for these species. In addition, dispersal and retention patterns are largely unknown for species that do not have a larval drifting phase. For these species, it is not known whether larvae disperse from spawning habitat into slackwater habitat, or whether larvae disperse among slackwaters and, if so, at what stage of development. Also, for species that experience ontogenetic changes in habitat requirements, it is not known at what stage of development dispersal out of slackwaters occurs.

In lowland rivers in which overbank flooding is relatively unpredictable or aseasonal, a number of riverine species breed under low flow conditions (Humphries et al. 2002; Nunn et al. 2007; Zeug and Winemiller 2008). Under these conditions, slackwaters, which are often ephemeral by nature, become relatively temporally stable. In addition, the larvae of a number of fish and shrimp species appear to preferentially use larger, more temporally stable slackwaters (Price 2007). The timing of spawning to coincide with low flows and the preferential use of temporally stable nursery habitat suggest that movement may be limited until swimming ability has developed, and in these systems, retention of weakly swimming larvae within slackwaters may be an important aspect of recruitment success. Thus, for species that spawn during low flow conditions and whose larvae utilize slackwaters as nursery habitat, we hypothesize that there would be limited movement by larvae. Specifically, we hypothesize that (*i*) spawning habitat would be the same as nursery habitat and, thus, there would be movement of ripe–berried adults into slackwaters, with no net movement of early-stage larvae into slackwaters, and (*ii*) there would be limited larval movement out of slackwaters until late stages of development or until recruitment to the juvenile stage.

This study investigated the role of dispersal and retention in the early life history of lowland riverine shrimp by testing these hypotheses in an Australian lowland river. The study used shrimp as model organisms as they occur in much higher abundances than fish in Australian lowland rivers and their early life history is similar to that of the fish species that utilize slackwaters as nursery habitats.

Materials and methods

Study location

The study was conducted in the lowland reaches of the Broken River, which is located in the southern Murray–Darling Basin in southeastern Australia (Fig. 1). The Broken River is a tributary of the Goulburn River, which in turn flows into the Murray River. The Murray River flows into the ocean approximately 2000 km downstream from the confluence with the Goulburn River. The Broken River has an approximate mean daily discharge of 10.28 $m^3 \cdot s^{-1}$. Throughout the study period, the mean daily discharge ranged from 1.2 to 3.1 $m^3 \cdot s^{-1}$. The flow regime of the river has been somewhat modified, however; only about 10% of the river's mean annual discharge is diverted for off-stream use and the lower reaches have predominantly retained the natural seasonal hydrological cycle.

In the lowland reaches of the catchment, the Broken River runs through a broad alluvial floodplain, which is periodically inundated. In this section of the catchment, riparian vegetation is mainly continuous, although quite narrow in many sections. The main channel in the lowland reaches is generally 10–30 m wide, and the riverine substrate is largely dominated by sand with occasional patchy areas of clay and bedrock. The river contains a diverse range of aquatic habitat types, including deep pools, run sequences, and a variety of slackwater habitat. This river was chosen for the study because of its relatively natural flow regime and the diversity of habitats and because it is known to support a high diversity of fish and shrimp species.

Sampling was conducted at two reaches (Scholes Road, 36°30′60.5″S, 145°57′22.1″E; Quinn Road, 36°27′57.4″S, 145°53′56.3″E) in the lowland section of the river, between the townships of Benalla and Shepparton (Fig. 1). The distance between slackwaters varies depending on river discharge and channel morphology; however, on average, slackwater density ranged from approximately 1 slackwater per 2 m to 1 slackwater per 4 m at the two study reaches.

Study species

Three species of caridean shrimp (*Paratya australiensis*, *Caridina mccullochi*, and *Macrobrachium australiense*) are collected in relatively high abundances in the Broken River as larvae, juveniles, and adults (Richardson et al. 2004). Both *M. australiense* and *C. mccullochi* are entirely freshwater species. *Paratya australiensis* can also complete its

Fig. 1. Location of the Broken River in the southern Murray–Darling Basin, southeastern Australia. Study reaches are indicated by Xs.

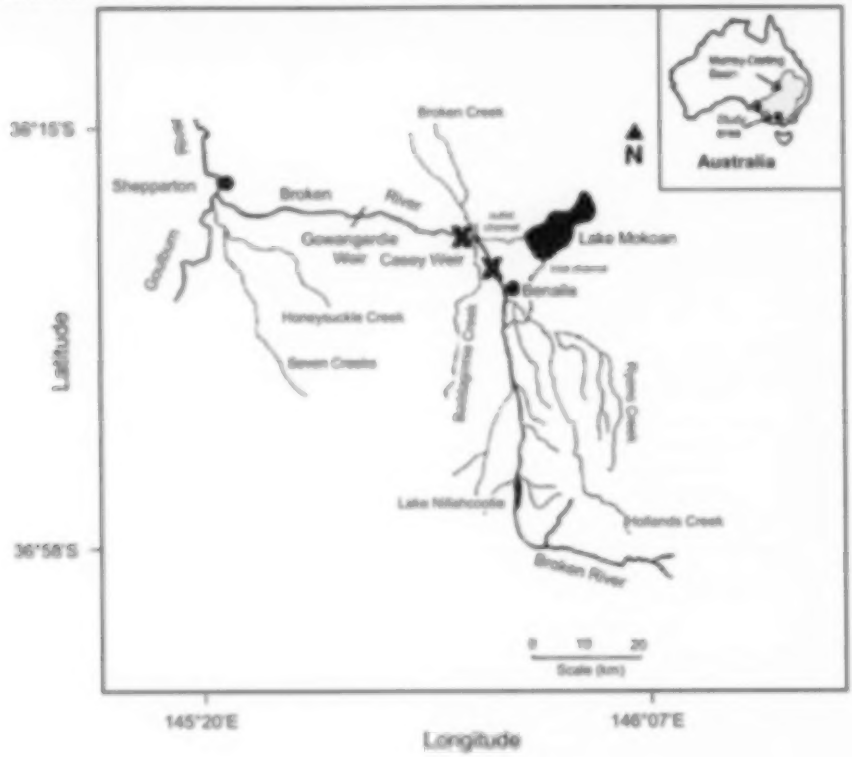

life cycle in freshwater and is described as being primarily a freshwater species; however, *P. australiensis* has also been found to occur in some estuaries (Walsh and Mitchell 1998). All three species have been shown to utilize slackwater habitats for at least part of their life histories (Richardson et al. 2004). *Caridina mccullochi* occur primarily in slackwater habitats throughout all stages of development (Richardson et al. 2004). *Paratya australiensis* and *M. australiense* larvae occur almost exclusively in slackwaters; however, juveniles and adults of both species are also found in a variety of other faster-flowing habitats (Richardson et al. 2004). Both *P. australiensis* and *C. mccullochi* larvae have an extended development of eight and seven stages, respectively (Benzie 1982; Walsh 1993). *Macrobrachium australiense* larvae have an abbreviated development of only three larval stages (Fielder 1970).

Recent genetic studies have led to uncertainty regarding the taxonomic status of *P. australiensis* and *C. mccullochi* (Page et al. 2005; Cook et al. 2006). *Paratya australiensis* is currently considered a complex of cryptic species, and this may also be the case for *C. mccullochi*. In this study, we identified species using current morphological keys (see Sample preservation and laboratory methods), and as such, we treat the species complexes as single entities but recognise that there could be some variation in our results because of small differences among lineages.

Directional trap design

The directional traps were designed to target all life stages of the three shrimp species known to occur in the lowland reaches of the Broken River. The directional traps were cylindrical in shape, 1 m in length, and 26 cm in diameter (Fig. 2). The entrance to the trap was funnelled, with a gap of ~7 cm in diameter. The walls of the traps were made of clear polycarbonate, as previous studies have shown that traps made of translucent materials are more effective than those made of opaque materials (Casselman and Harvey 1978; Culp and Glozier 1989). The bottoms of the traps consisted of 250 μm netting, which allowed water to flow through the trap, and were removable, making emptying of the traps relatively quick and easy. The traps were divided into two sections by a removable divider, which allowed animals smaller than 2 mm (i.e., larvae) to move into the bottom section of the trap, while keeping larger animals confined in the top section, thus preventing potential predation of larvae by juveniles and adults while in the trap.

Sampling methodology

Directional traps were set three times over two days from 10 to 30 November 2004 at Quinn Road and from 6 to 20 December 2004 at Scholes Road. Traps were set at different times at the two reaches as previous work had shown temporal differences in spawning times among sites (Price 2007). At each reach, traps were set in five slackwaters previously found to have consistently high diversity and abundances of shrimp (Price 2007). The same slackwaters were used for each consecutive trip at each reach. Slackwater areas were identified by placing a sweep net in the water and observing

Fig. 2. Placement of directional traps: (*a*) position of traps in slackwaters in relation to flow direction (DS, downstream; US, upstream; LAT, middle of entrance of slackwater); (*b*) trap direction. (*c*) Diagram showing design of directional traps.

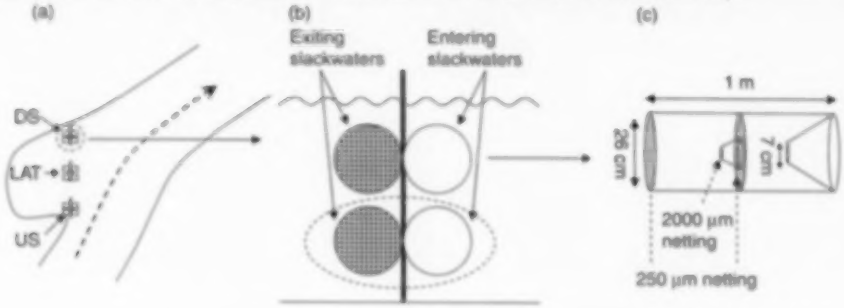

any ballooning of the net (sensu King 2004). If no movement of the net occurred, the habitat was considered "still" (Copp 1992; King 2004). This method was tested by King (2004), and velocities in still habitats were found to range from 0 to 0.02 $m \cdot s^{-1}$. For some slackwaters, the edges of the slackwater were evident with an abrupt change to faster-flowing water. For other slackwaters, however, the boundaries were not as obvious and the edges of the slackwater were determined using the above method.

Between 6 and 12 traps were set in each slackwater, depending on the depth of the water. Each trap was attached to one of three pairs of metal stakes, which were placed at the upstream and downstream ends and in the middle of the entrance of the slackwater (Fig. 2). On each stake, one trap was placed facing into the slackwater and another was set facing out of the slackwater. Two traps were set for each direction (i.e., two traps facing in and two traps facing out), where water depth allowed, with one set of traps sitting just above the substratum and the other set just below surface. Traps were set such that one end of the trap was located within the boundaries of the slackwater and the other end of the trap was outside the edge of the slackwater. Thus, although it is possible that the traps may have been collecting individuals that were exiting and then re-entering the slackwaters, the positioning of the traps across the edge of the slackwaters allowed for net movement to be measured. On each occasion, traps were set throughout the course of each day, emptied after 24 h, and then re-set for a further 24 h.

Sample preservation and laboratory methods

Upon collection, all samples were preserved in 95% ethanol. Samples were sorted in the laboratory, and all shrimp were removed under a dissecting microscope. Shrimp were identified to species (Hawking et al. 2004) and were classified into one of five stages for *M. australiense* (larval stages 1–3, nonberried juvenile–adult, and berried females), nine stages for *C. mccullochi* (larval stages 1–7, nonberried juvenile–adult, and berried females), and 10 stages for *P. australiensis* (larval stages 1–8, nonberried juvenile–adult, and berried females) using a key by J.E. Growns and A.J. Richardson (unpublished data, The Murray–Darling Freshwater Research Centre, P.O. Box 91 Wodonga, 3689, Australia).

Data analysis

There were too few berried *P. australiensis* and *C. mccullochi* collected for statistical analysis. There were, however, sufficient numbers of juveniles–adults and larvae of all three shrimp species and sufficient numbers of berried *M. australiense* collected for the analyses. Because the primary aim of this study was to examine movement patterns into and out of slackwaters, the data were pooled from the different sampling trips and reaches and from traps set at different depths and at different positions across slackwater entrances. A chi-square analysis, using SYSTAT (version 10, Systat Software, Inc., Chicago, Illinois), was used to determine whether the proportion of individuals entering and exiting slackwaters differed significantly.

Table 1. Numbers of total larvae, each larval stage, nonberried juveniles–adults, and berried adults of the three shrimp species collected in directional traps.

Stage	*Paratya australiensis*	*Caridina mccullochi*	*Macrobrachium australiense*
Total larvae	93	78	320
Larval stage			
I	15	5	234
II	4	8	49
III	1	8	37
IV	2	7	NA
V	—	9	NA
VI	2	10	NA
VII	9	31	NA
VIII	60	NA	NA
Juveniles–adults	192	115	531
Berried adults	6	14	30
Species total	291	207	881

Results

Species composition

A total of 1379 shrimp from three species (*P. australiensis*, *C. mccullochi*, and *M. australiense*) were collected (Table 1). All species were present as larvae and juveniles and adults. The relative abundances of juveniles and adults to larvae were similar for all three species, with juveniles comprising approximately 65% of the species total. *Macrobrachiium australiense* was the dominant species (64%), followed by *P. australiensis* (21%). Final-stage larvae dominated the larval samples for *P. australiensis* and *C. mccullochi*, contributing

Fig. 3. Total abundance of individuals collected from directional traps entering and exiting slackwaters. Significant differences, as determined by chi-square analysis, are indicated by asterisks (*, $P < 0.05$; ***, $P < 0.001$). J/A, juveniles–adults.

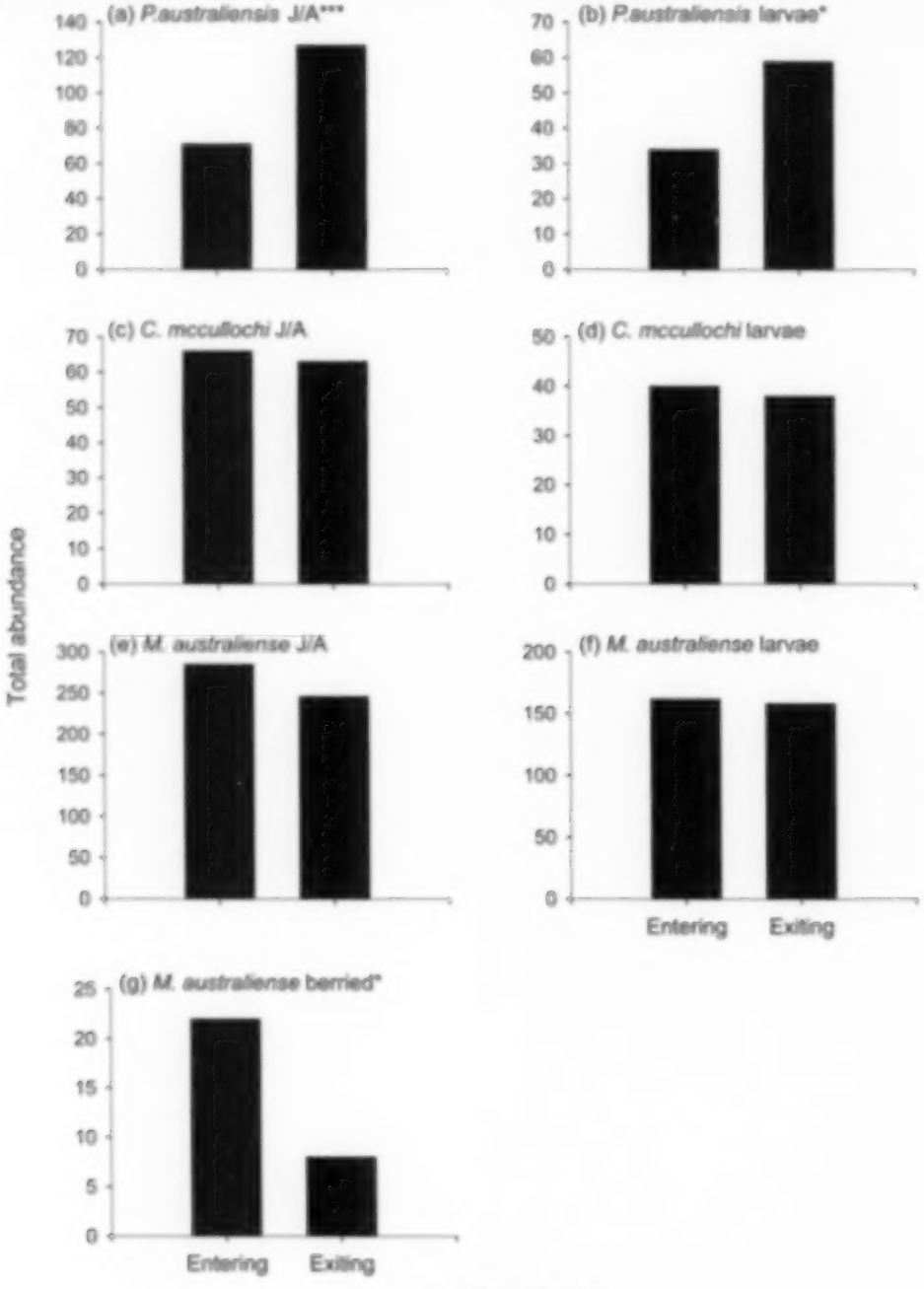

65% and 40%, respectively. However, early-stage larvae were dominant (73%) for *M. australiense* (Table 1).

Directional movement patterns

Significantly more *P. australiensis* juveniles–adults and larvae (total) were collected moving out of slackwaters than moving into them (Fig. 3). Furthermore, significantly greater numbers of stages I, II, VII, and VIII *P. australiensis* larvae were collected exiting than entering slackwaters (Fig. 4). By contrast, the number of *C. mccullochi* juveniles–adults and

Fig. 4. Total abundance of larvae of (*a*) *P. australiensis*, (*b*) *C. mccullochi*, and (*c*) *M. australiense*, by stage of development, collected from directional traps entering (solid bars) and exiting (open bars) slackwaters.

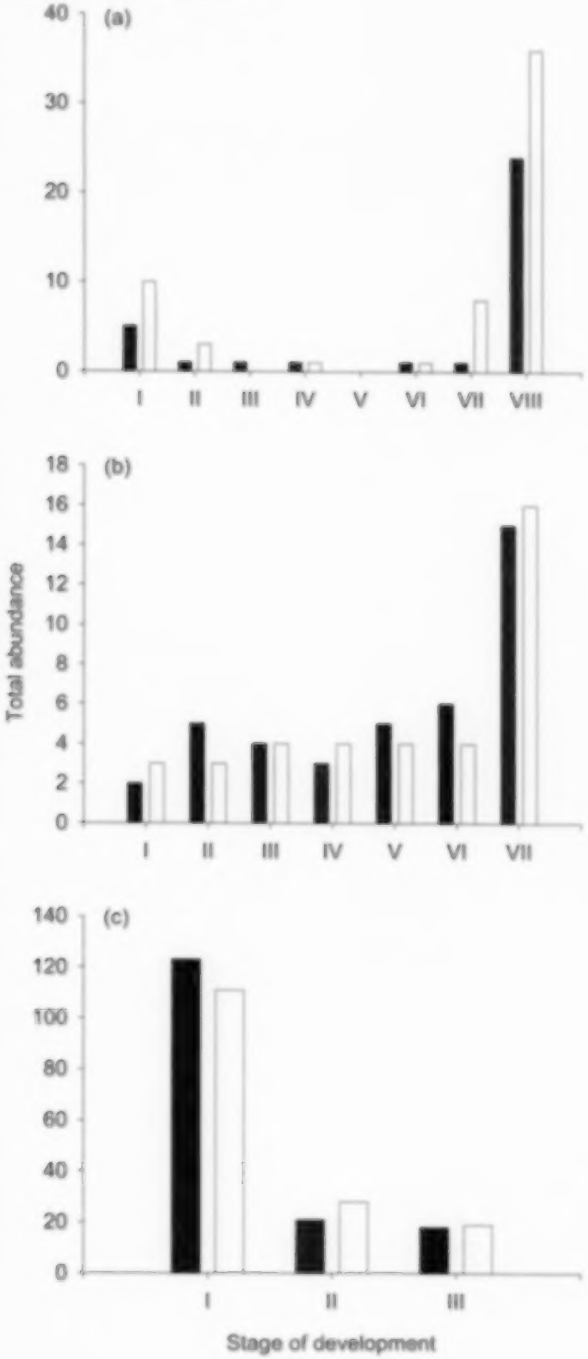

larvae (total and each developmental stage) moving into and out of slackwaters was similar (Figs. 3 and 4). Similarly, the number of *M. australiense* juveniles–adults and larvae (total and each developmental stage) moving into and out of slackwaters was similar (Figs. 3 and 4); however, significantly more berried females were collected moving in than out (Fig. 3).

Discussion

Do early-stage larvae or ripe–berried adults move into slackwaters?

There are two possible mechanisms available for larvae to access nursery habitat: (*i*) adults select a breeding site that is also suitable as nursery habitat and (*ii*) eggs or larvae disperse into nursery habitats from breeding habitats. For lowland riverine shrimp, we predicted that breeding habitat would be the same as nursery habitat and, thus, that there would be no evidence of net movement of early-stage larvae into slackwaters and that berried females would be captured entering slackwaters to hatch larvae.

The first prediction — that there would be no evidence of net movement of early-stage larvae into slackwaters — was borne out for the larvae of all three species of shrimp. For *C. mccullochi* and *M. australiense*, the proportion of individuals captured entering and exiting slackwaters was similar for all larval stages and for early-stage larvae specifically. For *P. australiensis*, a greater number of individuals overall, and early-stage *P. australiensis* larvae in particular, were collected exiting than entering slackwaters. Thus, there was no indication of net movement into slackwaters from other habitat types for the larvae of these species, suggesting that larvae are hatched in slackwaters.

For *P. australiensis* and *C. mccullochi*, insufficient numbers of ripe–berried adults were collected to be able to determine whether adults were entering slackwaters to hatch larvae. This may indicate that females become berried while in slackwater habitat and remain within that habitat patch until larvae are hatched. The results for berried *M. australiense*, however, allow some conclusions to be drawn. These results supported the prediction that adults hatch larvae in slackwaters, as a significantly greater number of berried females were captured entering slackwaters than exiting them. Although berried *P. australiensis* and *C. mccullochi* females are frequently collected from slackwaters, large adults and berried *M. australiense* females have been found to occur more commonly in faster-flowing areas (Richardson et al. 2004), which suggests that the observed movement patterns may be spawning-related. In the Broken River, the peak spawning period for *M. australiense* is in December (Richardson et al. 2004), and this correlates well with the findings from the current study in which berried *M. australiense* females were collected in the directional traps from early December onwards. These results strongly suggest that berried *M. australiense* females migrate from their preferred faster-flowing habitats into slackwaters where larvae are hatched. Migration by females to hatch larvae has also been documented for some species of amphidromous *Macrobrachium* (Bauer and Delahoussaye 2008; Rome et al. 2009). For these species, females migrate downstream from their normal freshwater habitat to place larvae in saline en-

vironments (Bauer and Delahoussaye 2008; Rome et al. 2009).

Do larvae move out of slackwaters and, if so, when?

It was predicted that for species such as those collected in the present study, which breed during low flow conditions and whose larvae utilize slackwaters as nursery habitat, there would be limited movement of larvae into and out of slackwaters. Overall, this was not shown to be the case in this study, as shrimp larvae were captured in relatively large numbers both entering and exiting slackwaters. This indicates that movement among slackwaters routinely occurs for all three species. For many organisms, small-scale movement between patches occurs frequently and may be in response to changes in resource availability, predator densities, or abiotic conditions such as temperature (McIntosh and Townsend 1998; Lucas and Baras 2001; Hay et al. 2008). This may present particular challenges to early life stages with limited swimming ability. Although there is little information regarding small-scale movement patterns of shrimp larvae, there is evidence of this type of movement for at least one species of fish. Tyus (1991) examined the movement patterns of young Colorado squawfish (*Ptychocheilus lucius*) at two sites in the Green River in North America and found that young fish used backwaters but moved between different shoreline habitats, possibly in search of more suitable habitats. The results of the present study suggest that similar movements may occur for the larvae of all three shrimp species.

Movement patterns differed among the three shrimp species, with the majority of *M. australiense* larvae captured being early-stage and the majority of *P. australiensis* and *C. mccullochi* larvae being late-stage. Following the hatching of *M. australiensis* larvae in slackwaters, stage I larvae appear to then readily move into and out of these habitats. The low numbers of later-stage larvae indicate that movement then decreases. Given that sampling was conducted during the peak spawning period for *M. australiense* (Richardson et al. 2004), the paucity of later-stage larvae relative to early-stage larvae captured in directional traps in the present study may be a result of the timing of sampling (as sampling concluded in mid- to late December) rather than an indication of the movement patterns of later-stage larvae. However, this seems unlikely, as the larval stage of *M. australiense* is relatively short (approximately six days; Fielder 1970). The low numbers of later-stage larvae may also be attributable to mortality of larvae as they age. However, although mortality may be a contributing factor, it is unlikely to be the only explanation for the observed patterns, as later-stage larvae of the two other species should also have been collected in decreasing abundances and this was not the case (see below).

In contrast to *M. australiense* larvae, the majority of *P. australiensis* and *C. mccullochi* larvae collected were in the final stage of development. Although there were no significant differences in the proportions of *C. mccullochi* larvae entering and exiting slackwaters, a significantly greater proportion of *P. australiensis* larvae were captured exiting slackwaters, which suggests that some larvae were dispersing from slackwaters. Richardson et al. (2004) note that although *P. australiensis* is most abundant in slow-flowing habitats, it also occurs in faster currents as well. They suggest that unlike *C. mccullochi*, which remains in slackwaters throughout its life history, and *M. australiense*, whose larvae require slackwaters, slackwaters are not essential for *P. australiensis* to complete its life history. Thus, it is logical that of the three species, *P. australiensis* was the only species that showed evidence of larval dispersal out of slackwaters into the main channel.

Dispersal and retention models

Directional trapping of nursery habitat entrances in a lowland river provided evidence for two contrasting life history based dispersal and retention models (Fig. 5). For two of the three species of shrimp collected (*P. australiensis* and *C. mccullochi*), retention was the key process throughout larval development (model 1). Larvae were hatched in slackwaters, and the majority of these larvae then remained within the slackwater in which they were hatched until the final stage of development, at which point they dispersed out of and (or) among slackwaters. This suggests that movement is minimal until larvae are larger and more developed, at which stage swimming ability is likely to be improved (Chia et al. 1984; Fuiman 2002; Werner 2002) and the risk of transport-related mortality is therefore reduced. Although there is no information regarding the swimming ability of *C. mccullochi* larvae, for *P. australiensis*, this conclusion is supported by the findings of Hancock and Bunn (1999), who found that stage III and stage IV *P. australiensis* larvae are washed downstream by even low current velocities. This model was consistent with our prediction that given the inherent risk of transport-related mortality, in species that breed during low flows and preferentially use temporally stable slow-flowing nursery habitat, retention rather than dispersal would be the key strategy until later life stages, when swimming ability has developed.

For the third species, *M. australiense*, dispersal and retention were important at different stages throughout larval development (model 2). Female *M. australiense* apparently became berried in faster-flowing adult habitats and then undertook a small-scale migration into slackwaters where larvae were hatched. This was followed by early-stage larvae moving among slackwaters, with movement decreasing markedly as development progressed. This second model did not support our predictions regarding larval retention in slackwaters but was consistent with the ontogenetic movement patterns of several other freshwater macroinvertebrate species. Ontogenetic changes in dispersal patterns have been shown to occur for some species of Ephemeroptera and Plecoptera (Elliott 1967), Trichoptera (Elliott 1968, 1981; Fjellheim 1980), and Coleoptera (Elliott 2008). In particular, similar patterns as those found in this study for *M. australiense* have been found for non-case-building larvae of several species of Trichoptera and for four species of elmid beetles in which dispersal rates are high for early instars and decrease until the larvae have reached either the final instar or adulthood (e.g., Fjellheim 1980; Elliott 1981, 2008). Periods of high dispersal for early-stage larvae have been shown to coincide with periods of rapid growth (Elliott 1968, 1981, 2008). It is thought that distribution patterns of early-stage larvae are highly aggregated and that during periods of rapid growth, dispersal is required to reduce levels

Fig. 5. Schematic diagram of a river reach with two slackwaters, showing the two proposed early life history dispersal and retention models.

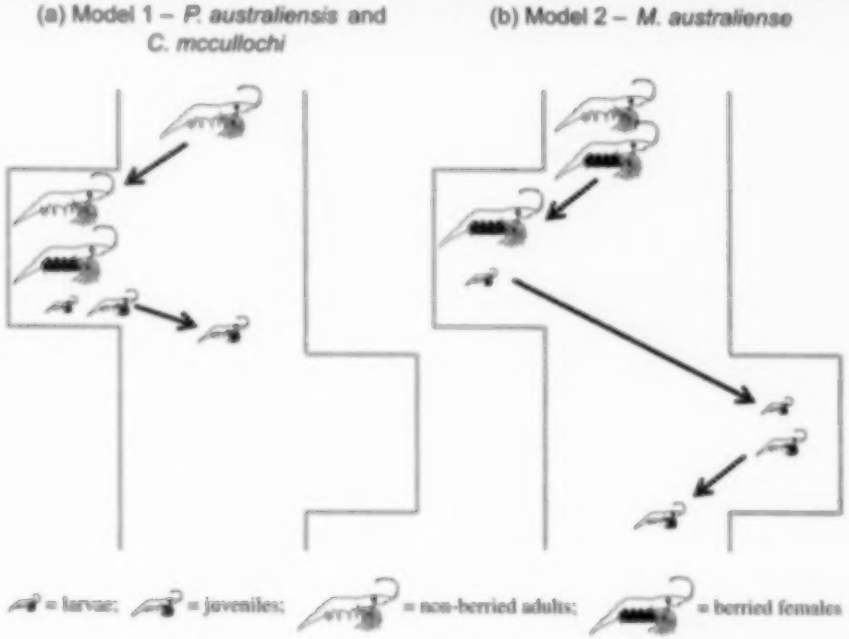
(a) Model 1 – P. australiensis and C. mccullochi
(b) Model 2 – M. australiense
= larvae; = juveniles; = non-berried adults; = berried females

of intraspecific competition for food and space (Elliott 1968; Fjellheim 1980). This may also explain the early dispersal of *M. australiense* larvae.

Although there is no reason to suppose that intraspecific competition is not also a problem for *P. australiensis* and *C. mccullochi* larvae, we propose that for early life stages of species for which movement between breeding and nursery habitat is not required, dispersal versus retention may be seen as a trade-off in risk between transport-related mortality and the need to minimize mortality arising from suboptimal ambient conditions (e.g., high levels of competition). As transport-related mortality is strongly linked to swimming ability, which in turn is frequently related to body size for some aquatic organisms (Chia et al. 1984; Luckenbach and Orth 1992; Fuiman 2002), we suggest that for smaller-sized larvae such as early-stage *P. australiensis* and *C. mccullochi*, the risk of mortality through displacement into unsuitable habitats is greater than that from intraspecific competition. However, for species with larger-sized larvae such as *M. australiense*, movement among nursery habitat patches along the slower-flowing littoral zone may be less risky.

Implications

Although dispersal and retention patterns are well documented for many aquatic species, particularly those that occur in marine and estuarine systems and those that undertake large-scale movements, this study represents a first attempt to develop small-scale dispersal and retention models for some of the many freshwater species that utilize slackwaters as nursery habitat. Despite the differences in dispersal strategies among species, the results from this study indicate that for all three species of shrimp, movement appeared to be predominantly associated with a certain period of larval development and thus highlight the importance of retention during critical developmental periods. The impacts of river regulation and flow modification on habitat availability and large-scale longitudinal dispersal and migration are well documented (see Bunn and Arthington 2002; Lytle and Poff 2004; Murchie et al. 2008). However, these impacts in relation to the dispersal and retention characteristics of low flow adapted species and life stages remain poorly understood (Schiemer et al. 2001; Keckeis and Schiemer 2002; Lytle and Poff 2004). The early life stages of riverine organisms typically are only able to maintain their position at considerably slower current velocities than adults (Corbett and Powles 1986; Franzin and Harbicht 1992) and can be displaced from nursery habitats if velocities increase rapidly (Harvey 1987; Pavlov 1994; Humphries et al. 2006). Thus, increased flows arising from river regulation, resulting in higher velocities throughout the channel and littoral zones and greater temporal variability in slow-flowing areas such as slackwaters, may result in larvae that are not adapted to moving being flushed out of slackwaters and entrained in the flow. In turn, this may result in high mortality rates, poor recruitment, and over time, significant population declines.

Acknowledgements

We thank Ben Gawne, Kathie and Raine Le Busque, Nick May, Rochelle Petrie, Jeremy Philp, Elizabeth Price, and Susanne Watkins for assistance with fieldwork and trap construction. Ben Gawne and Martin Thoms provided valuable advice throughout the study, and Sally Hladyz provided advice on the manuscript. We also thank the property owners for allowing us access to the field sites. This study was funded by a Co-operative Research Centre for Freshwater

Ecology postgraduate scholarship. Additional funding was provided by The Murray–Darling Freshwater Research Centre.

References

Bauer, R.T. 2004. Remarkable shrimps: adaptations and natural history of the Caridea ns. University of Oklahoma Press, Norman, Oklahoma.

Bauer, R.T., and Delahoussaye, J. 2008. Life history migrations of the amphidromous river shrimp *Macrobrachium ohione* from a continental large river system. J. Crustac. Biol. **28**(4): 622–632. doi:10.1651/08-2977.1.

Benzie, J.A.H. 1982. The complete larval development of *Caridina mccullochi* Roux, 1926 (Decapoda, Atyidae) reared in the laboratory. J. Crustac. Biol. **2**(4): 493–513. doi:10.2307/1548091.

Brittain, J.E., and Eikeland, T.J. 1988. Invertebrate drift — a review. Hydrobiologia, **166**(1): 77–93. doi:10.1007/BF00017485.

Bunn, S.E., and Arthington, A.H. 2002. Basic principles and ecological consequences of altered flow regimes for aquatic biodiversity. Environ. Manage. **30**(4): 492–507. doi:10.1007/s00267-002-2737-0. PMID:12481916.

Casselman, J.M., and Harvey, H.H. 1973. Fish traps of clear plastic. Prog. Fish-Cult. **35**(4): 218–220. doi:10.1577/1548-8659(1973)35[218:FTOCP]2.0.CO;2.

Chia, F.-S., Buckland-Nicks, J., and Young, C.M. 1984. Locomotion of marine invertebrate larvae: a review. Can. J. Zool. **62**(7): 1205–1222. doi:10.1139/z84-176.

Cook, B.D., Baker, A.M., Page, T.J., Grant, S.C., Fawcett, J.H., Hurwood, D.A., and Hughes, J.M. 2006. Biogeographic history of an Australian freshwater shrimp, *Paratya australiensis* (Atyidae): the role life history transition in phylogeographic diversification. Mol. Ecol. **15**(4): 1083–1093. doi:10.1111/j.1365-294X.2006.02852.x. PMID:16599968.

Copp, G.H. 1992. Comparative microhabitat use of cyprinid larvae and juveniles in a lotic floodplain channel. Environ. Biol. Fishes, **33**(1–2): 181–193. doi:10.1007/BF00002563.

Corbett, B.W., and Powles, P.M. 1986. Spawning and larval drift of sympatric walleyes and white suckers in a Ontario stream. Trans. Am. Fish. Soc. **115**(1): 41–46. doi:10.1577/1548-8659(1986)115<41:SALDOS>2.0.CO;2.

Culp, J.M., and Glozier, N.E. 1989. Experimental evaluation of a minnow trap for small lotic fish. Hydrobiologia, **175**(1): 83–87. doi:10.1007/BF00008477.

Elliott, J.M. 1967. Life histories and drifting of Plecoptera and Ephemeroptera in a Dartmoor stream. J. Anim. Ecol. **36**(2): 343–362. doi:10.2307/2918.

Elliott, J.M. 1968. The life histories and drifting of Trichoptera in a Dartmoor stream. J. Anim. Ecol. **37**(3): 615–625. doi:10.2307/3078.

Elliott, J.M. 1981. A quantitative study of the life cycle of the net-spinning caddis *Philopotamus montanus* (Trichoptera: Philopotamidae) in a Lake District stream. J. Anim. Ecol. **50**(3): 867–883. doi:10.2307/4143.

Elliott, J.M. 2008. Ontogenetic shifts in drift periodicity and benthic dispersal in elmid beetles. Freshw. Biol. **53**(4): 698–713. doi:10.1111/j.1365-2427.2007.01927.x.

Fielder, D.R. 1970. The larval development of *Macrobrachium australiense* Holthius, 1950 (Decapoda, Palaemonidae) reared in the laboratory. Crustaceana, **18**(1): 60–74. doi:10.1163/156854070X00077.

Fjellheim, A. 1980. Differences in drifting of larval stages of *Rhyacophila nubila* (Trichoptera). Holarct. Ecol. **3**: 99–103.

Franzin, W.G., and Harbicht, S.M. 1992. Tests of drift samplers for estimating abundance of recently hatched walleye larvae in small rivers. N. Am. J. Fish. Manage. **12**(2): 396–405. doi:10.1577/1548-8675(1992)012<0396:TODSFE>2.3.CO;2.

Frid, C.L.J., and Townsend, C.R. 1989. An appraisal of the patch dynamics concept in stream and marine benthic communities whose members are highly mobile. Oikos, **56**(1): 137–141. doi:10.2307/3566098.

Fuiman, L.A. 2002. Special considerations of eggs and larvae. *In* Fishery science — the unique contributions of early life stages. *Edited by* L.A. Fuiman and R.G. Werner. Blackwell Science, Oxford, UK. pp. 1–32.

Hancock, M.A., and Bunn, S.E. 1999. Swimming response to water current in *Paratya australiensis* Kemp, 1917 (Decapoda, Atyidae) under laboratory conditions. Crustaceana, **72**(3): 313–323. doi:10.1163/156854099503393.

Harvey, B.C. 1987. Susceptibility of young-of-the-year fishes to downstream displacement by flooding. Trans. Am. Fish. Soc. **116**(6): 851–855. doi:10.1577/1548-8659(1987)116<851:SOYFTD>2.0.CO;2.

Hawking, J.H., Smith, L.M., and Le Busque, K. 2004. Identification and ecology of Australian freshwater invertebrates. Available at http://www.mdfrc.org.au/bugguide [accessed January 2004].

Hay, C.H., Franti, T.G., Marx, D.B., Peters, E.J., and Hesse, L.W. 2008. Macroinvertebrate drift density in relation to abiotic factors in the Missouri River. Hydrobiologia, **598**(1): 175–189. doi:10.1007/s10750-007-9149-3.

Houde, E.D. 2002. Mortality. *In* Fishery science — the unique contributions of early life stages. *Edited by* L.A. Fuiman and R.G. Werner. Blackwell Science, Oxford, UK. pp. 64–87.

Humphries, P., King, A.J., and Koehn, J.D. 1999. Fish, flows and floodplains: links between freshwater fishes and their environment in the Murray–Darling River system, Australia. Environ. Biol. Fishes, **56**(1–2): 129–151. doi:10.1023/A:1007536009916.

Humphries, P., Serafini, L.G., and King, A.J. 2002. River regulation and fish larvae: variation through space and time. Freshw. Biol. **47**(7): 1307–1331. doi:10.1046/j.1365-2427.2002.00871.x.

Humphries, P., Cook, R.A., Richardson, A.J., and Serafini, L.G. 2006. Creating a disturbance: manipulating slackwaters in a lowland river. River Res. Appl. **22**(5): 525–542. doi:10.1002/rra.920.

Keckeis, H., and Schiemer, F. 2002. Understanding conservation issues of the Danube River. *In* Fishery science — the unique contributions of early life stages. *Edited by* L.A. Fuiman and R.G. Werner. Blackwell Science, Oxford, UK. pp. 272–288.

King, A.J. 2004. Ontogenetic patterns of habitat use by fishes within the main channel of an Australian floodplain river. J. Fish Biol. **65**(6): 1582–1603. doi:10.1111/j.0022-1112.2004.00567.x.

Largier, J. 2004. The importance of retention zones in the dispersal of larvae. Am. Fish. Soc. Symp. **42**: 105–122.

Lucas, M.C., and Baras, E. 2001. Migration of freshwater fishes. Blackwell Science, Oxford, UK.

Luckenbach, M.W., and Orth, R.J. 1992. Swimming velocities and behaviour of blue crab (*Callinectes sapidus* Rathbun) megalopae in still and flowing water. Estuaries, **15**(2): 186–192. doi:10.2307/1352691.

Lytle, D.A., and Poff, N.L. 2004. Adaptation to natural flow regimes. Trends Ecol. Evol. **19**(2): 94–100. doi:10.1016/j.tree.2003.10.002. PMID:16701235.

McIntosh, A.R., and Townsend, C.R. 1998. Do different predators affect distance, direction, and destination of movements by a stream mayfly? Can. J. Fish. Aquat. Sci. **55**(8): 1954–1960. doi:10.1139/cjfas-55-8-1954.

Murchie, K.J., Hair, K.P.E., Pullen, C.E., Redpath, T.D., Stephens,

H.R., and Cooke, S.J. 2008. Fish response to modified flow regimes in regulated rivers: research methods, effects and opportunities. River Res. Appl. **24**(2): 197–217. doi:10.1002/rra.1058.

Nunn, A.D., Harvey, J.P., Britton, J.R., Frear, P.A., and Cowx, I.G. 2007. Fish, climate and the Gulf Stream: the influence of abiotic factors on the recruitment success of cyprinid fishes in lowland rivers. Freshw. Biol. **52**(8): 1576–1586. doi:10.1111/j.1365-2427.2007.01789.x.

O'Connell, M.T., Franze, C.D., Spalding, E.A., and Poirrier, M.A. 2005. Biological resources of the Louisiana Coast. Part 2. Coastal animals and habitat associations. J. Coast. Res. **44**: 146–161.

Page, T.J., Choy, S.C., and Hughes, J.M. 2005. The taxonomic feedback loop: symbiosis of morphology and molecules. Biol. Lett. **1**(2): 139–142. doi:10.1098/rsbl.2005.0298. PMID: 17148149.

Pavlov, D.S. 1994. The downstream migration of young fishes in rivers: mechanisms and distribution. Folia Zool. (Brno), **43**: 193–208.

Price, A. 2007. Utilisation of still-water patches by fish and shrimp in a lowland river, with particular emphasis on early-life stages. Ph.D. thesis, School of Resource, Environmental and Heritage Sciences, University of Canberra, Canberra, ACT, Australia.

Richardson, A.J., Growns, J.E., and Cook, R.A. 2004. Distribution and life history of caridean shrimps in regulated lowland rivers in southern Australia. Mar. Freshw. Res. **55**(3): 295–308. doi:10.1071/MF03126.

Rome, N.E., Conner, S.L., and Bauer, R.T. 2009. Delivery of hatching larvae to estuaries by an amphidromous river shrimp: test of hypotheses based on larval moulting and distribution. Freshw. Biol. **47**: 501–515.

Schiemer, F., Keckeis, H., Reckendorfer, W., and Winkler, G. 2001. The inshore retention concept and its significance for large rivers. Arch. Hydrobiol. Suppl. **135**: 509–516.

Schlosser, I.J., and Angermeier, P.L. 1995. Spatial variation in demographic processes of lotic fishes: conceptual models, empirical evidence, and implications for conservation. Am. Fish. Symp. No. 17. pp. 392–401.

Sinclair, M. 1988. Marine populations: an essay on population regulation and speciation. Washington Sea Grant Press, Seattle, Washington.

Thorp, J.H., Thoms, M.C., and Delong, M.D. 2006. The riverine ecosystem synthesis: biocomplexity in river networks across space and time. River Res. Appl. **22**(2): 123–147. doi:10.1002/rra.901.

Tyus, H.M. 1991. Movements and habitat use of young Colorado squawfish in the Green River, Utah. J. Freshwat. Ecol. **6**: 43–51.

Urho, L. 1999. Relationship between dispersal of larvae and nursery areas in the Baltic Sea. ICES J. Mar. Sci. **56**(Suppl.): 114–121. doi:10.1006/jmsc.1999.0634.

Walsh, C.J. 1993. Larval development of *Paratya australiensis* Kemp, 1917 (Decapoda, Caridea, Atyidae) reared in the laboratory, with comparisons of fecundity and egg and larval size between estuarine and riverine environments. J. Crustac. Biol. **13**(3): 456–480. doi:10.2307/1548788.

Walsh, C.J., and Mitchell, B.D. 1998. Factors associated with variations in abundance of epifaunal caridean shrimps between and within estuarine seagrass meadows. Mar. Freshw. Res. **49**(8): 769–777. doi:10.1071/MF97101.

Werner, R.G. 2002. Habitat requirements. *In* Fishery science — the unique contributions of early life stages. *Edited by* L.A. Fuiman and R.G. Werner. Blackwell Science, Oxford, UK. pp. 161–182.

Wiens, J.A. 2002. Riverine landscapes: taking landscape ecology into the water. Freshw. Biol. **47**(4): 501–515. doi:10.1046/j.1365-2427.2002.00887.x.

Zeug, S.C., and Winemiller, K.O. 2008. Relationships between hydrology, spatial heterogeneity, and fish recruitment dynamics in a temperate floodplain river. River Res. Appl. **24**(1): 90–102. doi:10.1002/rra.1061.

Incorporating temporal variation in the growth of red abalone (*Haliotis rufescens*) using hierarchical Bayesian growth models

Yan Jiao, Laura Rogers-Bennett, Ian Taniguchi, John Butler, and Paul Crone

Abstract: Many marine species exhibit temporal variation in individual growth. Yearly variation in growth has been identified for red abalone (*Haliotis rufescens*) in southern California, USA, but has not been previously incorporated into growth models. In this study, Bayesian hierarchical models were developed to describe variability in growth rates for the Johnsons Lee red abalone population. Although the Bayesian hierarchical modeling estimates are close to estimates of the nonhierarchical highly parameterized model that assigns an estimate of parameters to each data period when the sample sizes are high, the hyperparameters in the hierarchical model are more useful in incorporating the temporal variability into the stock assessment. By ignoring temporal variability, confidence intervals of the estimates of growth can be unrealistically narrow, possibly leading to bias when these models are used for developing biological reference points such as $F_{0.1}$, F_{max}, or $F_{x\%}$. The use of a Bayesian hierarchical approach is generally suggested for future growth modeling and for per-recruitment models that include growth when determining precautionary management decisions.

Résumé : Plusieurs espèces marines accusent des variations temporelles dans leur croissance individuelle. Des variations annuelles de croissance ont été signalées chez les ormeaux rouges (*Haliotis rufescens*) dans le sud de la Californie, É.-U., mais elles n'ont jamais été incorporées aux modèles de croissance. Nous avons mis au point, dans notre étude, des modèles hiérarchiques bayésiens pour décrire la variation des taux de croissance dans la population d'ormeaux rouges de Johnsons Lee. Bien que les estimations produites par la modélisation hiérarchique bayésienne soient proches des estimations d'un modèle non hiérarchique fortement paramétrisé qui assigne une estimation des paramètres à chaque période de données lorsque les tailles des échantillons sont fortes, les hyperparamètres du modèle hiérarchique sont plus commodes pour incorporer la variabilité temporelle dans l'évaluation des stocks. Lorsqu'on néglige la variabilité temporelle, les intervalles de confiance des estimations de la croissance peuvent être de façon irréaliste trop étroits, ce qui peut mener à des erreurs lorsque ces modèles servent à la détermination de points de référence biologiques, tels que $F_{0.1}$, F_{max} ou $F_{x\%}$. Nous suggérons donc d'utiliser de façon générale une méthode hiérarchique bayésienne pour la modélisation de la croissance et dans les modèles par recrutement qui incluent la croissance lorsqu'on prend des décisions préventives de gestion.

[Traduit par la Rédaction]

Introduction

The growth of marine fishes and mollusks is highly variable. Temperature, food availability, and population density are considered to be dominant factors in large growth rate differences among different populations of the same species (Krohn et al. 1997; Swain et al. 2003). Differences also exist in length at age within and among year classes of a population, with differences in invertebrates being very large (Pearse and Cameron 1991). Large variations in growth among year classes are often hypothesized to result from variability in ocean conditions such as water temperature (Hutchings and Myers 1994) and food availability (Krohn et al. 1997). Other factors that can cause variation in growth include size-selective mortality (Myers 1989; Hanson and Chouinard 1992), energy allocation (Chen and Mello 1999), population stress as a result of overexploitation (Beacham 1983; Trippel 1995), population structure (Lilly 1996), and genetics.

Red abalone (*Haliotis rufescens*) is the largest abalone and the basis for an important recreational fishery in California. Haaker et al. (1998) developed and supported the hy-

Received 2 July 2009. Accepted 10 February 2010. Published on the NRC Research Press Web site at cjfas.nrc.ca on 26 March 2010. J21291

Paper handled by Associate Editor Ray Hilborn.

Y. Jiao.[1] Department of Fisheries and Wildlife Sciences, Virginia Polytechnic Institute and State University, Blacksburg, VA 24061-0321, USA.
L. Rogers-Bennett. California Department of Fish and Game, Bodega Marine Laboratory, 2099 Westside Road, Bodega Bay, CA 94923-0247, USA.
I. Taniguchi. California Department of Fish and Game, Marine Region, 4665 Lampson Avenue, Suite C, Los Alamitos, CA 90720, USA.
J. Butler and P. Crone. NOAA, NMFS, Southwest Fisheries Science Center, La Jolla, CA 92037-1022, USA.

[1]Corresponding author (e-mail: yjiao@vt.edu).

pothesis that growth of red abalone varies significantly in different years, associated with temperature changes during El Niño ocean climate oscillations. Although Haaker et al. (1998) detected temporal variation in individual growth, no model has been developed to date to effectively incorporate this type of variation. The traditional von Bertalanffy model, which assumes constant parameters in the model, cannot accommodate temporal changes in growth even when multiyear data are included in the analysis (Clark 2003).

In this research, a multilevel prior in a hierarchical approach is used to address the problem of describing growth rates and their associated uncertainty when multiyear data are included and indicate substantial variability in growth over time. Models with multilevel priors are called hierarchical models (Gelman et al. 2004). Multilevel priors have been used to represent inter- or intra-species differences when data are hierarchical (Clark 2003; Gelman et al. 2004). Hierarchical models accommodate temporal differences but assume that these differences derive from an underlying distribution (Gelman et al. 2004).

In this study, a hierarchical growth model was used to simulate temporal variation of red abalone growth (Gelman et al. 2004). The estimated hyperparameters, the parameters that further specify the priors of the parameters in the model, capture the temporal and spatial variations and provide a more comprehensive representation of important variation in growth compared with traditional constant growth rate models. Ultimately, growth models that address such variation are likely the most useful for describing a species' overall population dynamics and providing stock status determinations in formal assessments. Per-recruit models have been widely used in fisheries stock assessment, including assessment of abalone species (Shepherd et al. 1991; Nash 1992; Shepherd et al. 1995), and to determine biological reference points (BRP), e.g., $F_{0.1}$, $F_{\%}$, $F_{\%\,\mathrm{SSB}}$ (Caddy and Mahon 1995; Food and Agricultural Organisation of the United Nations (FAO) 1995; Quinn and Deriso 1999). Failure to incorporate or model the temporal variations of growth may result in biased BRP estimation associated with per-recruit methods.

To evaluate the potential benefits of a hierarchical modeling approach, the goodness of fit of three hierarchical models was compared with that of a nonhierarchical model. In the hierarchical models, the data sets were restructured such that (*i*) hierarchical growth differed each year (model M1), (*ii*) hierarchical growth differed every two years (model M2), and (*iii*) hierarchical growth was the same over all years (model M3). We also compared the above hierarchical models with the nonhierarchical models that fit to the data of all the years cumulated (model M4) and to the data of each time period (model M5). Deviance information criterion (DIC; Spiegelhalter et al. 2002) was used to compare model goodness of fit as it incorporates both model fit and model complexity. The hierarchically structured models were implemented in a Bayesian framework and analyzed using Markov chain Monte Carlo (MCMC) simulation. Bayesian methods have been shown to be effective approaches in solving hierarchical models (Gelman et al. 2004).

Materials and methods

Tag-recapture data from red abalone at Johnsons Lee (33°54′N, 120°06′W) on the south side of Santa Rosa Island, California, USA, were collected from 1978 to 1984 by California Department of Fish and Game personnel and used to measure growth (Haaker et al. 1998). SCUBA divers collected red abalone and brought them to the vessel, where they were placed in flowing-seawater tanks. Abalone were marked with numbered stainless steel tags secured with stainless steel wire through two open shell apertures (Haaker et al. 1986). Shell length (maximum shell dimension) was measured to the nearest millimetre with calipers. Abalone were marked and visited in 1978, 1979, 1980, 1981, 1982, and 1984. In each year, both tagged and additional untagged abalone were collected and measured and retagged if appropriate. Recapture information is as follows: from 1978 to 1979, 158 red abalones were recaptured; from 1979 to 1980, 86 were recaptured; from 1980 to 1981, 210 were recaptured; from 1981 to 1982, 361 were recaptured; and from 1982 to 1984, 59 were recaptured (Fig. 1). Individuals recaptured more than once were very limited. There were five individuals recaptured four times (0.2%), 24 individuals recaptured three times (1.1%), and 177 individuals recaptured twice (8.3%).

We determined growth curves from annual increments in length of tagged individuals. We used the nonlinear methodology for mark–recapture data to estimate the parameters and standard errors for the von Bertalanffy growth model (Fabens 1965; Kirkwood and Somers 1984; Quinn and Deriso 1999). The von Bertalanffy growth model can be written as

$$(1)\qquad L_t = L_\infty(1 - e^{-Kt}),\ \text{or}$$
$$dL = L_{t+\Delta t} - L_t = (L_\infty - L_t)(1 - e^{-K\Delta t})$$

where L_∞ and K are parameters in the von Bertalanffy growth model, L_∞ represents the asymptotic length of red abalone, K is the Brody growth coefficient (Ricker 1975), t_0 is assumed to be 0 as used in Haaker et al. (1998), L_t is the length at time t, and $L_{t+\Delta t}$ is the length at time $t + \Delta t$. A hierarchical growth model (Gelman et al. 2004) developed in this study can be written as

$$(2)\qquad dL_s = L_{s,t+\Delta t} - L_{s,t} = (L_{s,\infty} - L_{s,t})(1 - e^{-K_s\Delta t})$$
$$L_{s,\infty} \sim N(\overline{L}_\infty, \overline{\sigma}^2_{L_\infty})$$
$$K_s \sim N(\overline{K}, \overline{\sigma}^2_K)$$

where the subscript s represents temporal-specific parameters. The hierarchical population structure is implemented in this model through a multilevel prior of temporal-specific parameters in the growth model. dL_s were assumed to follow normal distributions with mean $(L_{s,\infty} - L_{s,t})(1 - e^{-K_s\Delta t})$ and variance $\sigma^2_{dL_s}$.

The Bayesian approach uses a probability rule (Bayes' theorem) to calculate a "posterior distribution" from the observed data and a "prior distribution", which summarizes the prior knowledge of the parameters (Berger 1985; McAllister and Kirkwood 1998; Gelman et al. 2004). This approach was used to estimate the uncertainty in parameter estimates. A nonhierarchical Bayesian model describes a

Fig. 1. Observed red abalone (*Haliotis rufescens*) length at time t versus the length at time $t + \Delta t$. Lines are the $L_t \sim L_t$ points; solid circles are the $L_t \sim L_{t+\Delta t}$ points. (*a*) 1978–1979; (*b*) 1979–1980; (*c*) 1980–1981; (*d*) 1981–1982; (*e*) 1982–1984.

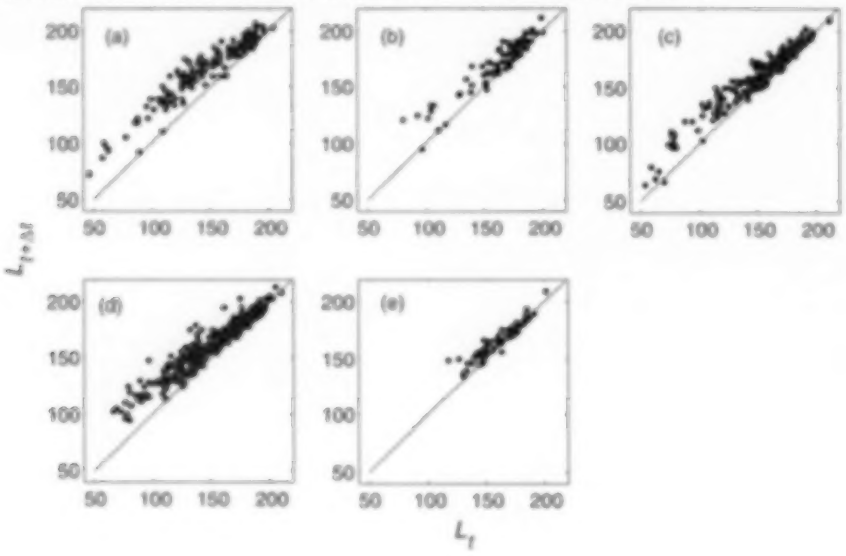

posterior density for parameters ($p(\theta|dL_t)$) using Bayes' theorem as

$$(3)\quad p(\theta = L_\infty, K|dL_t) = \frac{\prod_t f(dL_t|\theta)\,\pi(\theta)}{\int_{-\infty}^{+\infty}\prod_t f(dL_t|\theta)\,\pi(\theta)\,d\theta}$$

whereas a hierarchical Bayesian method assigns priors of hyperparameters to yield the joint posterior:

$$(4)\quad p(\theta' = L_{\infty,\infty}, K_\infty, \overline{L}_\infty, \overline{K}, \overline{\sigma}_{L_\infty}, \overline{\sigma}_K|dL) = \frac{\prod_t f(dL_t|L_{\infty,\infty}, K_t)\,\pi_1(L_{\infty,t}|\overline{L}_\infty, \overline{\sigma}_{L_\infty})\,u_1(\overline{L}_\infty)\,v_1(\overline{\sigma}_{L_\infty})\,\pi_2(K_t|\overline{K}, \overline{\sigma}_K)\,u_2(\overline{K})\,v_2(\overline{\sigma}_K)}{\int_{-\infty}^{+\infty}\prod_t f(dL_t|L_{\infty,\infty}, K_t)\,\pi_1(L_{\infty,t}|\overline{L}_\infty, \overline{\sigma}_{L_\infty})\,u_1(\overline{L}_\infty)\,v_1(\overline{\sigma}_{L_\infty})\,\pi_2(K_t|\overline{K}, \overline{\sigma}_K)\,u_2(\overline{K})\,v_2(\overline{\sigma}_K)\,d\theta'}$$

In the above equations, $f(dL_t|\theta)$ is the probability density function of dL_t on parameter vector θ; $u_1(\overline{L}_\infty)$ and $v_1(\overline{\sigma}_{L_\infty})$ are the probability density functions of $\overline{L}_\infty$ and $\overline{\sigma}_{L_\infty}$, respectively; and $u_2(\overline{K})$ and $v_2(\overline{\sigma}_K)$ are the probability density functions of $\overline{K}$ and $\overline{\sigma}_K$, respectively.

Bayesian implementation of these models requires specification of prior distributions on all unobserved quantities. Noninformative priors (here, wide uniform distributions) were used for variances $\overline{\sigma}^2_{L_\infty}$, $\overline{\sigma}^2_K$ and $\sigma^2_{dL_\infty}$. Uniform prior distributions work better as noninformative priors than inverse-gamma distributions for variance parameters when dealing with hierarchical models (Gelman 2006).

A critical issue in using Markov chain Monte Carlo (MCMC) methods is how to determine when random draws have converged to the posterior distribution. Here, three methods were considered: monitoring the trace for key parameters, diagnosing the autocorrelation plot for key parameters, and using the Gelman and Rubin statistic (Gelman and Rubin 1992; Cowles and Carlin 1996; Spiegelhalter et al. 2004). A detailed description of the use of these methods in fisheries can be found in Su et al. (2001). In this study, three Markov chains generated using WinBugs were used (Spiegelhalter et al. 2004). The three chains converged after 50 000 iterations with a thinning interval of 5 based on the convergence criteria and were discarded. A thinning interval of 5 was then used to avoid parameter autocorrelation. Another 20 000 iterations were used to generate the posterior distributions. The posterior distributions of the key parameters were obtained through a kernel smoothing approach (Bowman and Azzalini 1997).

To compare the performance of the hierarchically structured model with the commonly used nonhierarchical von Bertalanffy growth model, another three hierarchical models were developed (Table 1). In the first hierarchical model (M1),

Table 1. Model comparison among hierarchical and nonhierarchical growth models of red abalone (*Haliotis rufescens*). Priors of the hierarchical models are $\overline{L}_\infty \sim U(180, 250)$ $I(150, 400)$, $\overline{K} \sim U(0.15, 0.35)$. Priors for the nonhierarchical model are $L_\infty \sim U(150, 400)$, $K \sim U(0.15, 0.40)$.

		Parameter estimates	
Model	DIC	L_∞ (mean, median, SD, 95% CI)	K (mean, median, SD, 95% CI)
M1	5938.7	$\overline{L}_\infty$ (200.3, 199.9, 9.3, 183.4, 220.5)	$\overline{K}$ (0.239, 0.237, 0.039, 0.165, 0.323)
		$\overline{\sigma}^2_{L_\infty}$ (484, 452, 237, 123, 957)	$\overline{\sigma}^2_K$ (0.013, 0.007, 0.015, 0.001, 0.059)
		$L_{1,\infty}$ (223.0, 222.8, 5.5, 213.0, 234.7)	K_1 (0.285, 0.284, 0.022, 0.244, 0.329)
		$L_{2,\infty}$ (205.6, 205.1, 6.6, 194.3, 220.2)	K_2 (0.217, 0.216, 0.031, 0.161, 0.281)
		$L_{3,\infty}$ (196.8, 196.6, 4.4, 189.0, 206.2)	K_3 (0.212, 0.212, 0.018, 0.176, 0.249)
		$L_{4,\infty}$ (194.8, 194.7, 2.6, 189.9, 200.3)	K_4 (0.293, 0.293, 0.017, 0.260, 0.326)
		$L_{5,\infty}$ (177.3, 177.3, 3.5, 170.6, 184.4)	K_5 (0.172, 0.167, 0.019, 0.151, 0.221)
M2	6018.4	$\overline{L}_\infty$ (197.8, 196.6, 10.5, 181.5, 221.7)	$\overline{K}$ (0.246, 0.245, 0.049, 0.158, 0.339)
		$\overline{\sigma}^2_{L_\infty}$ (495, 468, 253, 104, 968)	$\overline{\sigma}^2_K$ (0.026, 0.017, 0.024, 0.002, 0.089)
		$L_{1,\infty}$ (211.6, 211.4, 3.6, 205.1, 219.0)	K_1 (0.297, 0.296, 0.018, 0.261, 0.333)
		$L_{2,\infty}$ (195.4, 195.4, 2.2, 191.3, 200.0)	K_2 (0.262, 0.262, 0.012, 0.238, 0.286)
		$L_{3,\infty}$ (177.4, 177.3, 3.4, 170.8, 184.2)	K_3 (0.170, 0.165, 0.017, 0.151, 0.214)
M3	6262.1	$\overline{L}_\infty$ (202.0, 199.0, 15.0, 181.3, 238.2)	$\overline{K}$ (0.255, 0.258, 0.055, 0.156, 0.344)
		$\overline{\sigma}^2_{L_\infty}$ (462, 442, 292, 20, 972)	$\overline{\sigma}^2_K$ (0.039, 0.034, 0.029, 0.001, 0.096)
		L_∞ (194.1, 194.1, 1.5, 191.2, 197.2)	K (0.282, 0.281, 0.010, 0.262, 0.301)
M4	10614.6	L_∞ (191.7, 191.7, 1.1, 189.6, 194.0)	K (0.278, 0.277, 0.008, 0.262, 0.292)
M5	1117.9	$L_{1,\infty}$ (224.2, 223.7, 6.9, 212.1, 239.4)	K_1 (0.282, 0.282, 0.026, 0.232, 0.335)
	597.4	$L_{2,\infty}$ (207.2, 206.7, 7.0, 193.7, 223.7)	K_2 (0.212, 0.208, 0.035, 0.156, 0.288)
	1421.1	$L_{3,\infty}$ (196.9, 196.6, 4.5, 188.8, 206.5)	K_3 (0.211, 0.211, 0.019, 0.175, 0.249)
	2430.7	$L_{4,\infty}$ (194.3, 194.2, 2.5, 189.6, 199.5)	K_4 (0.296, 0.296, 0.016, 0.265, 0.329)
	368.7	$L_{5,\infty}$ (177.2, 177.2, 2.8, 171.8, 182.8)	K_5 (0.163, 0.160, 0.012, 0.150, 0.195)
	Total = 5935.8		

Note: All negative growth data are included. Deviance information criterion (DIC) and posterior mean, median, standard deviation (SD), and 95% credible interval (95% CI) of the parameter estimates are provided.

each year's data, except 1983 because no tagging occurred that year, were assumed to be hierarchically structured as

$$
\begin{aligned}
(5)\quad & L_{t+\Delta t} - L_t = (L_\infty - L_t)(1 - e^{-K\Delta t}) \\
& L_{1,\infty} \sim N(\overline{L}_\infty, \overline{\sigma}^2_{L_\infty})|_{1982-1984} I(150, 400) \\
& \vdots \\
& L_{5,\infty} \sim N(\overline{L}_\infty, \overline{\sigma}^2_{L_\infty})|_{1982-1984} I(150, 400) \\
& \overline{L}_\infty \sim U(180, 250) \\
& \overline{\sigma}^2_{L_\infty} \sim U(1, 1000) \\
& K_1 \sim N(\overline{K}, \overline{\sigma}^2_K)|_{1978-1979} I(0.15, 0.40) \\
& \vdots \\
& K_5 \sim N(\overline{K}, \overline{\sigma}^2_K)|_{1982-1984} I(0.15, 0.40) \\
& \overline{K} \sim U(0.15, 0.35) \\
& \overline{\sigma}^2_K \sim U(0.0001, 0.1)
\end{aligned}
$$

Here I represents the boundary of the distribution in WinBUGS, i.e., $I(150, 400)$ means that the boundary of the random variable L_∞ is between 150 and 400.

In the second hierarchical model (M2), the data for every two-year period are assumed to be hierarchically structured as

$$
\begin{aligned}
(6)\quad & L_{t+\Delta t} - L_t = (L_\infty - L_t)(1 - e^{-K\Delta t}) \\
& L_{1,\infty} \sim N(\overline{L}_\infty, \overline{\sigma}^2_{L_\infty})|_{1978-1980} I(150, 400) \\
& L_{2,\infty} \sim N(\overline{L}_\infty, \overline{\sigma}^2_{L_\infty})|_{1980-1982} I(150, 400) \\
& L_{3,\infty} \sim N(\overline{L}_\infty, \overline{\sigma}^2_{L_\infty})|_{1982-1984} I(150, 400) \\
& \overline{L}_\infty \sim U(180, 250) I(150, 400) \\
& \overline{\sigma}^2_{L_\infty} \sim U(1, 1000) \\
& K_1 \sim N(\overline{K}, \overline{\sigma}^2_K)|_{1978-1980} I(0.15, 0.40) \\
& K_2 \sim N(\overline{K}, \overline{\sigma}^2_K)|_{1980-1982} I(0.15, 0.40) \\
& K_3 \sim N(\overline{K}, \overline{\sigma}^2_K)|_{1982-1984} I(0.15, 0.40) \\
& \overline{K} \sim U(0.15, 0.35) \\
& \overline{\sigma}^2_K \sim U(0.0001, 0.1)
\end{aligned}
$$

In the third hierarchical model (M3), the model is hierarchically structured but the data were not assumed to be hierarchical:

$$
\begin{aligned}
(7)\quad & L_{t+\Delta t} - L_t = (L_\infty - L_t)(1 - e^{-K\Delta t}) \\
& L_\infty \sim N(\overline{L}_\infty, \overline{\sigma}^2_{L_\infty})|_{1978-1984} I(150, 400) \\
& \overline{L}_\infty \sim U(180, 250) \\
& \overline{\sigma}^2_{L_\infty} \sim U(1, 1000) \\
& K \sim N(\overline{K}, \overline{\sigma}^2_K)|_{1978-1984} I(0.15, 0.40) \\
& \overline{K} \sim U(0.15, 0.35) \\
& \overline{\sigma}^2_K \sim U(0.0001, 0.1)
\end{aligned}
$$

$\overline{L}_\infty$, the hyperparameter of the mean of L_∞, was assumed to

follow a uniform distribution between 180 mm and 250 mm. This range was based on L_∞ estimates from other studies on red abalone populations (Haaker et al. 1998; Rogers-Bennett et al. 2007). The hyperparameter of the variance of L_∞, $\bar{\sigma}^2_{L_\infty}$, was modeled as noninformative, with a wide uniform distribution between 1 and 1000. The hyperparameter of $\overline{K}$ was assumed to follow a uniform distribution between 0.15 and 0.35 based on K estimates from other studies (Haaker et al. 1998; Rogers-Bennett et al. 2007). The hyperparameter of the variance of K, $\bar{\sigma}^2_K$, was modeled as noninformative, with a wide uniform distribution between 0.0001 and 1.

The nonhierarchical von Bertalanffy growth model is

$$(8)\quad \begin{aligned} L_{t+\Delta t} - L_t &= (L_\infty - L_t)(1 - e^{-K\Delta t}) \\ L_\infty &\sim U(150, 400) \\ K &\sim U(0.15, 0.40) \end{aligned}$$

The priors of L_∞ and K in this model are wider than the priors of their mean values in the hierarchical models. The range of L_∞ is as wide as the range of L_t in the hierarchical models to prevent the influence of the informative priors. We also added the model that assigns an estimate of parameters to each data period (M5). Sensitivities of the results to prior assumption of both parameters and hyperparameters were analyzed by changing the lower limits of $\overline{L}_\infty$ and $\overline{K}$ to 50% of the ones used above and by changing the high limit to 150% of the ones used above. Changes to both the posterior mean and variance were compared. We also analyzed the growth based on the data set with the negative growth records not incorporated.

The goodness of fit of the Bayesian hierarchical models was compared with the classical nonhierarchical model based on the estimates of the DIC (Spiegelhalter et al. 2002). DIC can be written as

$$(9)\quad \begin{aligned} &\mathrm{DIC} = 2\overline{D} - \hat{D} \quad \text{or} \quad \overline{D} + p_D \\ &D(y, \theta) = -2\log\text{-likelihood}(y|\theta) \\ &p_D = \overline{D} - \hat{D} \end{aligned}$$

where D is deviance, a measurement of prediction of goodness for our models, p_D is the effective number of parameters in a Bayesian model, $\overline{D}$ is the posterior mean of the deviance, and $\hat{D}$ is the deviance of the posterior mean. The DIC is a hierarchical modeling generalization of the AIC (Akaike information criterion) and BIC (Bayesian information criterion, also known as the Schwarz criterion). It is particularly useful in Bayesian model selection problems in which the posterior distributions of the models have been obtained by MCMC simulation. Like AIC and BIC, it is an asymptotic approximation as the sample size becomes large. It is only valid when the posterior distribution is approximately multivariate normal (Spiegelhalter et al. 2002, 2004).

Results

The Gelman and Rubin statistics for all of the parameters, including all variance terms, equaled 1, which indicated convergence of the Markov chains. Further, the autocorrelation function plot indicated that a thinning interval of 5 was large enough to address potential autocorrelation in the MCMC runs (Fig. 2).

Among the 5 models, M5, the model that assigns the estimate of parameters to each data period, had the lowest DIC value (Table 1), with model M1 associated with generally similar DIC values. Among the three hierarchical models tested, M1, the model with data from each year treated as hierarchical, performed the best, resulting in the lowest DIC. Models M2 and M3, the other two models with multilevel priors of the von Bertalanffy growth parameters, also resulted in lower DIC values than the nonhierarchical model (M4). The large differences in DIC values among models used to describe population growth indicate that temporal changes in growth of red abalone can be significant and ultimately should be considered in population assessments of this species.

Using a hierarchically structured model generally resulted in parameter estimates of L_∞ and K with wider credible intervals than using a nonhierarchical model (Table 1). The credible intervals and standard deviations of L_∞ and K were considerably larger for the hierarchical von Bertalanffy models M1, M2, and M3 than the nonhierarchical model M4, which is illustrated in Table 1.

The hierarchically structured models not only describe the growth of all the individuals tagged, but also simulate the growth differences among sampling years. The hierarchical models M1 and M2 clearly indicated temporal differences in red abalone growth (Table 1). Results from the model with the best fit, M1, showed that the joint posterior distributions of L_∞ and K differed substantially between 1978–1979 (i.e., the highest growth period), 1982–1984 (i.e., the lowest growth period), and the three intermediate periods (Table 1; Fig. 3). Parameter L_∞ exhibited a decreasing trend over time (1978 to 1984). Parameter K varied also, with K_1 (0.285) and K_4 (0.293) resulting in relatively high estimates, K_2 (0.217) and K_3 (0.212) at an intermediate level, and K_5 (0.172) at the lowest value. The overall posterior von Bertalanffy growth curve showed that abalone grew faster and larger in 1978–1979, but more slowly in 1982–1984. Results from M2, when every two years of data were combined, also indicated that red abalone growth differed markedly between 1978–1980, 1982–1984, and the 1980–1982 intermediate periods (Table 1).

Residuals, estimated as the differences of the posterior mean of the length increase with the observed length increase, were plotted against the fitted growth increase (dL_t) when hierarchical model M1 was used. No obvious patterns were observed in the residual plot of model M1, with the exception of uneven sample sizes among groups of dL_t (Fig. 4). Also, residual diagnostics for model M5 revealed no visible patterns of statistical violation.

The posteriors of the hyperparameters and key parameters for most of the years in all of the hierarchical models were stable when the priors of $\overline{L}_\infty$ widened from $U(180, 250)$/$U(150, 400)$ to $U(90, 375)$/$U(50, 400)$ and when $\overline{K}$ widened from $U(0.15, 0.35)$ to $U(0.075, 0.525)$ (Tables 1 and 2; Fig. 5). The posteriors of the key parameters of the nonhierarchical models were also stable when L_∞ widened from U (150, 400) to $U(50, 400)$, and K widened from $U(0.15, 0.40)$ to $U(0.075, 0.575)$ (Tables 1 and 2). The parameters of the period of 1982–1984 were less stable and were influenced by the boundary of K (Table 2; Fig. 3).

The percentages of negative growth data were 2%, 17%,

Fig. 2. Autocorrelation function plots of parameters when M1 is used with prior stated in Table 1 and text: (*a*) $\overline{L}_\infty$; (*b*) $\overline{\sigma}^2_{L_\infty}$; (*c*) $\overline{K}$; and (*d*) $\overline{\sigma}^2_K$.

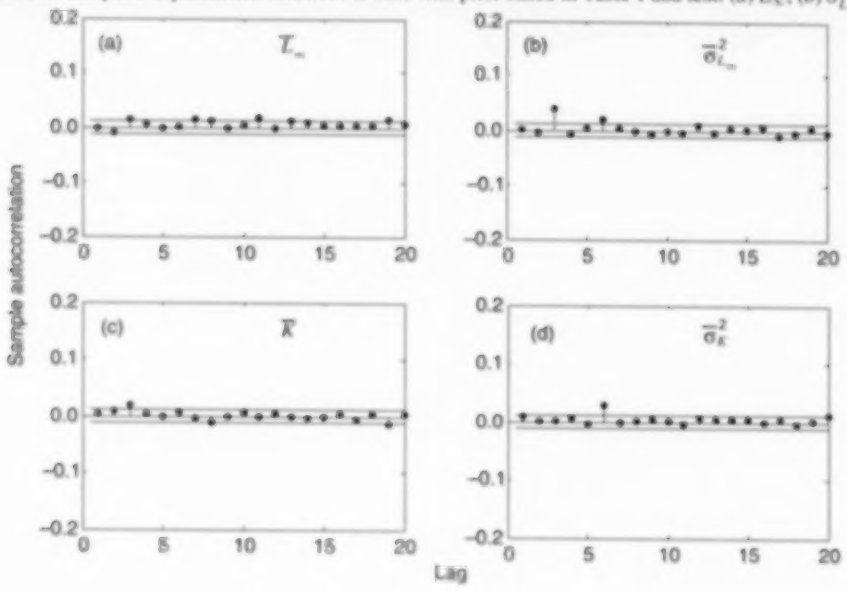

Fig. 3. Joint posterior distributions of K and L_∞ from 1978 to 1984 based on the hierarchical growth model M1 with prior stated in Table 1: red, 1978–1979; magenta, 1979–1980; yellow, 1980–1981; green, 1981–1982; blue, 1982–1984.

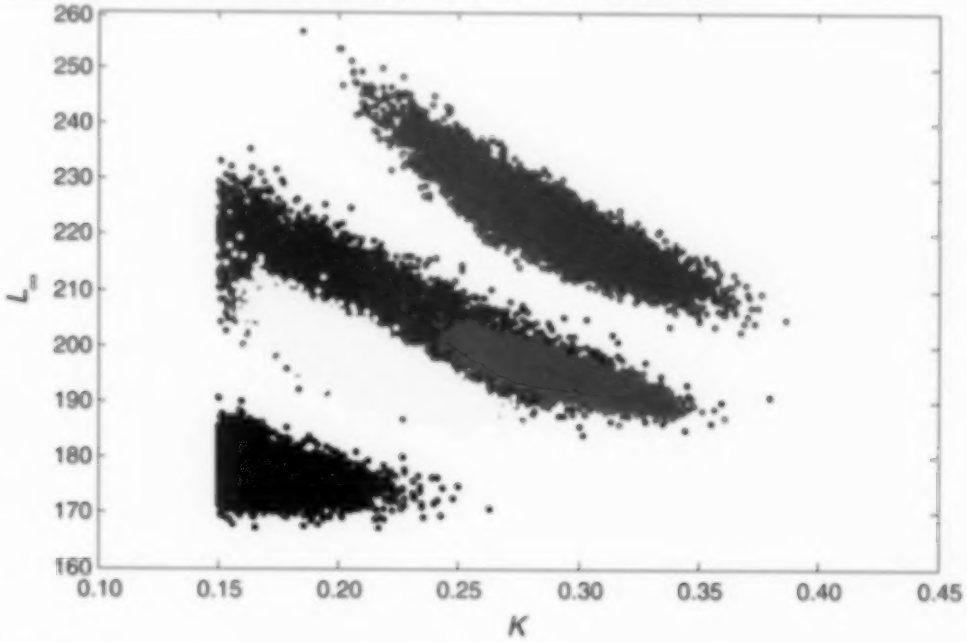

18%, 12%, and 23% during the 5-year tagging periods. In all of the models, omission of the negative data resulted in changes to the estimated growth parameters, depending on the amount of negative values in the total data set for each tag–recapture period, e.g., period 1982–1984 had highest percentage of negative values and resulted in the largest differences (Table 3). Finally, inclusion or omission of the negative growth information in the modeling analyses conducted here indicated that temporal variation in the growth of red abalone is likely a significant attribute in this species' biology off the southern California coast (San Miguel Island).

Discussion

Although the Bayesian hierarchical modeling estimates are close to estimates of the nonhierarchical model that as-

Fig. 4. Residuals plots when model M1 is used with prior stated in Table 1 and the text: (*a*) 1978–1979; (*b*) 1979–1980; (*c*) 1980–1981; (*d*) 1981–1982; and (*e*) 1982–1984.

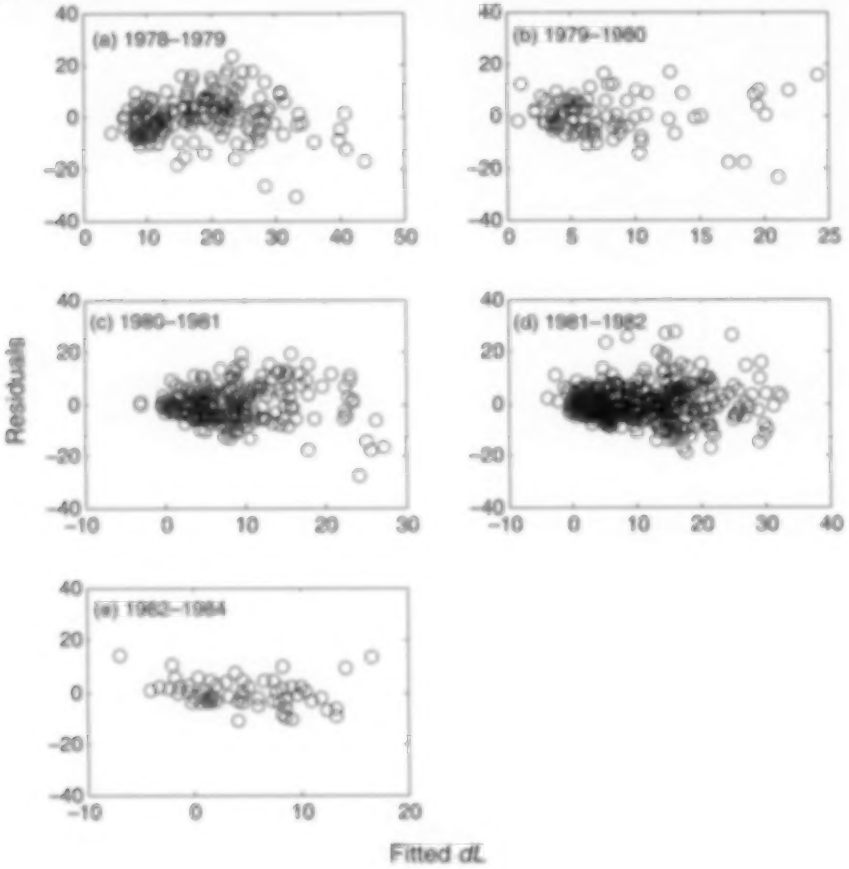

signs an estimate of parameters to each data period in this study, the hyperparameters in the hierarchical model are often very useful in incorporating the temporal variability into the stock assessment (Gelman et al. 2004). The goodness of fit of the hierarchical models can be worse than that of the highly parameterized model when the number of data groups is small. The fits for each data group are not as good because the hierarchical model assumes that the differences among the data groups are from the same underlying distribution; at the same time, the number of parameters in the hierarchical models is not much less than in the highly parameterized model because the number of groups is low. In this study, there were five years of recaptures; the fits using M1 and M5 were close, with M5 being slightly better. When the number of years of recaptures increases, say to 10 years or more, the goodness of fit using hierarchical models will be much better because of better parsimony. In spite of the goodness of fit, the hierarchical models always estimate the parameters of all data groups simultaneously, and the hyperparameters can be used in future stock assessment when the specific temporal change is less predictable.

The hierarchical growth model captured the dramatic temporal variation in growth including years of warm and normal sea surface temperatures (SST) in southern California. Slow growth rates from 1982 to 1984 occurred during a major El Niño event (Figs. 6 and 7). We found that L_∞ had a significant negative relationship with average SST anomalies ($p = 0.0081$; Fig. 7). More work is needed to investigate the impacts of cold sea surface conditions on the growth of red abalone. We suggest that this relationship between SST and red abalone growth could be factored into future management algorithms and decisions. Currently, few fishery management plans explicitly incorporate SST (or other measures of ocean productivity) into fishery models. One exception is the management of Pacific sardines in which it is widely hypothesized that ocean warming greatly influences sardine productivity and abundance and, therefore, SST is used formally when setting harvest guidelines for this species (Conser et al. 2002). For red abalone, we see that few individuals will grow into the legal size (197 mm for commercial fisheries and 178 mm for recreational fishery) during warm-water years. As a result, if fishing effort remains unchanged and population dynamics models ignore this growth variation, then exploitation rate, the percent taken, will be higher in these years than anticipated (Parma 2002).

Warm water also impacts food availability, having a negative effect on kelp growth (Leighton 1974; Tegner and Dayton 1987; Tegner et al. 1992). In laboratory experiments,

Table 2. Model comparison among hierarchical and nonhierarchical growth models of red abalone (*Haliotis rufescens*). Priors of the hierarchical models are $\overline{L}_\infty \sim U(90, 375)$ $I(50, 400)$, $\overline{K} \sim U(0.075, 0.525)$. Priors for the nonhierarchical model are $L_\infty \sim U(50, 400)$, $K \sim U(0.075, 0.525)$.

		Parameter estimates	
Model	DIC	L_∞ (mean, median, SD, 95% CI)	K (mean, median,SD, 95% CI)
M1	5936.2	$\overline{L}_\infty$ (200.8, 200.8, 9.9, 181.3, 220.9)	$\overline{K}$ (0.230, 0.229, 0.058, 0.116, 0.361)
		$\sigma^2_{L_\infty}$ (447, 404, 247, 88, 953)	σ^2_K (0.020, 0.013, 0.019, 0.002, 0.077)
		$L_{1,\infty}$ (222.6, 222.3, 5.6, 212.5, 234.6)	K_1 (0.286, 0.286, 0.022, 0.243, 0.331)
		$L_{2,\infty}$ (206.5, 205.7, 7.3, 194.4, 223.1)	K_2 (0.213, 0.212, 0.033, 0.150, 0.279)
		$L_{3,\infty}$ (197.0, 196.7, 4.4, 189.0, 206.4)	K_3 (0.211, 0.210, 0.019, 0.176, 0.248)
		$L_{4,\infty}$ (194.7, 194.6, 2.6, 189.9, 200.1)	K_4 (0.294, 0.294, 0.017, 0.261, 0.327)
		$L_{5,\infty}$ (183.6, 182.7, 6.7, 172.7, 198.4)	K_5 (0.126, 0.122, 0.031, 0.079, 0.194)
M2	6016.7	$\overline{L}_\infty$ (196.8, 196.9, 12.7, 170.2, 222.6)	$\overline{K}$ (0.243, 0.234, 0.088, 0.095, 0.449)
		$\sigma^2_{L_\infty}$ (465, 431, 265, 69, 965)	σ^2_K (0.036, 0.029, 0.026, 0.004, 0.094)
		$L_{1,\infty}$ (211.4, 211.2, 3.6, 204.8, 219.0)	K_1 (0.297, 0.297, 0.019, 0.261, 0.335)
		$L_{2,\infty}$ (195.5, 195.4, 2.2, 191.3, 200.1)	K_2 (0.261, 0.261, 0.012, 0.238, 0.286)
		$L_{3,\infty}$ (183.7, 183.0, 6.6, 172.9, 198.1)	K_3 (0.122, 0.119, 0.029, 0.078, 0.188)
M:	6261.7	$\overline{L}_\infty$ (194.0, 193.9, 22.6, 147.4, 241.0)	$\overline{K}$ (0.292, 0.289, 0.113, 0.093, 0.504)
		$\sigma^2_{L_\infty}$ (502, 503, 287, 26, 977)	σ^2_K (0.044, 0.041, 0.029, 0.002, 0.097)
		L_∞ (194.0, 194.0, 1.5, 191.2, 197.1)	K (0.282, 0.282, 0.010, 0.262, 0.302)
M4	10614.5	$\overline{L}_\infty$ (191.7, 191.7, 1.1, 189.6, 193.9)	K (0.278, 0.278, 0.008, 0.263, 0.293)
M5	1117.9	$L_{1,\infty}$ (224.1, 223.6, 6.9, 212.0, 239.0)	K_1 (0.282, 0.282, 0.027, 0.232, 0.335)
	597.9	$L_{2,\infty}$ (209.2, 207.6, 10.4, 194.0, 234.3)	K_2 (0.204, 0.204, 0.040, 0.126, 0.284)
	1421.2	$L_{3,\infty}$ (196.9, 196.6, 4.5, 188.8, 206.6)	K_3 (0.211, 0.211, 0.019, 0.175, 0.249)
	2430.64	$L_{4,\infty}$ (194.3, 194.2, 2.5, 189.6, 199.5)	K_4 (0.297, 0.296, 0.016, 0.265, 0.329)
	367.2	$L_{5,\infty}$ (182.9, 182.3, 5.2, 174.3, 194.5)	K_5 (0.120, 0.119, 0.023, 0.081, 0.170)
	Total = 5934.8		

Note: All the negative growth data are included. Deviance information criterion (DIC) and posterior mean, median, standard deviation (SD), and 95% credible interval (95% CI) of the parameter estimates are provided.

Fig. 5. Posterior probability density functions of hyperparameters when model M1 is used under three situations corresponding to Tables 1–3 (S1, S2, and S3): (*a*) $\overline{L}_\infty$; (*b*) $\sigma^2_{L_\infty}$; (*c*) $\overline{K}$; and (*d*) σ^2_K. S1, continuous line; S2, dotted line; S3, dotted–dashed line.

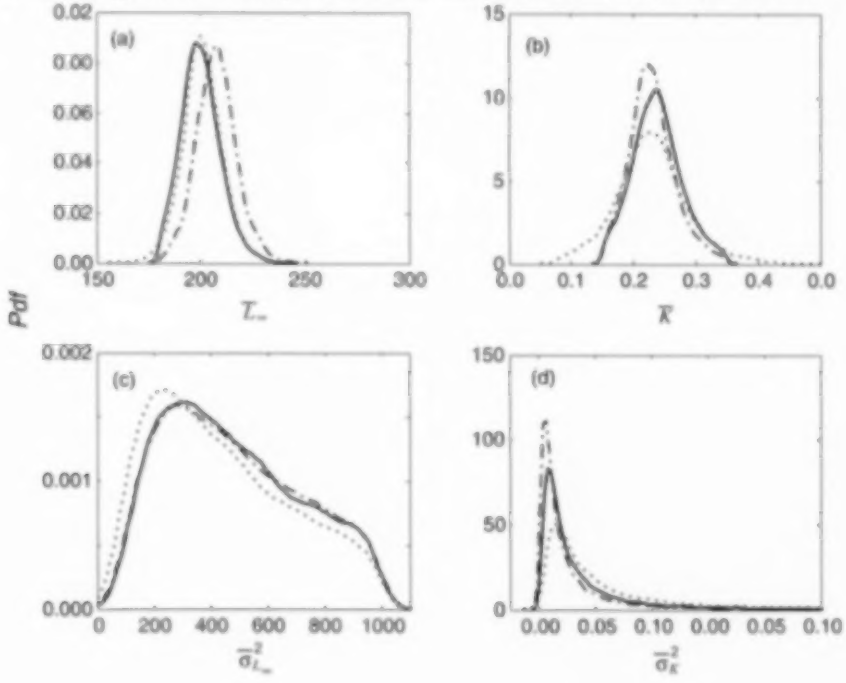

Table 3. Model comparison among hierarchical and nonhierarchical growth models of red abalone (*Haliotis rufescens*). Priors of the hierarchical models are $\overline{L}_\infty \sim U(180, 250)$ $I(150, 400)$, $\overline{K} \sim U(0.15, 0.35)$. Priors for the nonhierarchical model are $L_\infty \sim U(150, 400)$, $K \sim U(0.15, 0.40)$.

		Parameter estimates	
Model	*DIC*	L_∞ (mean, median, SD, 95% CI)	K (mean, median, SD, 95% CI)
M1	4935.1	$\overline{L}_\infty$ (207.4, 207.2, 9.9, 187.9, 228.0)	$\overline{K}$ (0.231, 0.229, 0.036, 0.164, 0.313)
		$\sigma^2_{L_\infty}$ (486, 453, 239, 118, 958)	σ^2_K (0.010, 0.005, 0.014, 0.001, 0.054)
		$L_{1,\infty}$ (228.4, 228.0, 6.2, 217.3, 241.9)	K_1 (0.269, 0.269, 0.021, 0.228, 0.312)
		$L_{2,\infty}$ (212.3, 211.6, 7.3, 200.0, 228.4)	K_2 (0.239, 0.237, 0.034, 0.176, 0.308)
		$L_{3,\infty}$ (208.4, 208.0, 6.2, 197.4, 221.8)	K_3 (0.201, 0.200, 0.019, 0.164, 0.240)
		$L_{4,\infty}$ (204.7, 204.5, 3.9, 197.8, 212.7)	K_4 (0.259, 0.259, 0.017, 0.225, 0.293)
		$L_{5,\infty}$ (182.6, 182.6, 4.5, 174.0, 191.6)	K_5 (0.171, 0.166, 0.019, 0.151, 0.221)
M2	4973.1	$\overline{L}_\infty$ (203.8, 203.2, 11.9, 183.0, 229.5)	$\overline{K}$ (0.240, 0.237, 0.048, 0.158, 0.337)
		$\sigma^2_{L_\infty}$ (520, 501, 251, 112, 970)	σ^2_K (0.025, 0.015, 0.024, 0.002, 0.089)
		$L_{1,\infty}$ (218.3, 218.2, 4.4, 210.4, 227.6)	K_1 (0.285, 0.285, 0.019, 0.249, 0.324)
		$L_{2,\infty}$ (205.8, 205.7, 3.4, 199.7, 212.8)	K_2 (0.237, 0.237, 0.013, 0.211, 0.264)
		$L_{3,\infty}$ (182.7, 182.7, 4.4, 174.2, 191.5)	K_3 (0.169, 0.164, 0.018, 0.151, 0.216)
M3	5193.7	$\overline{L}_\infty$ (207.4, 205.5, 15.4, 182.5, 241.7)	$\overline{K}$ (0.252, 0.252, 0.055, 0.156, 0.345)
		$\sigma^2_{L_\infty}$ (466, 447, 288, 22, 970)	σ^2_K (0.039, 0.033, 0.029, 0.001, 0.096)
		L_∞ (203.4, 203.4, 2.2, 199.2, 208.0)	K (0.258, 0.258, 0.011, 0.237, 0.280)
M4	8707.5	L_∞ (200.6, 200.6, 1.7, 197.5, 204.0)	K (0.255, 0.255, 0.008, 0.239, 0.272)
M5	1076.2	$L_{1,\infty}$ (229.4, 228.8, 7.7, 215.9, 246.1)	K_1 (0.268, 0.267, 0.026, 0.218, 0.320)
	458.3	$L_{2,\infty}$ (212.9, 212.0, 8.4, 199.0, 232.0)	K_2 (0.238, 0.237, 0.038, 0.168, 0.316)
	1099.6	$L_{3,\infty}$ (209.4, 209.0, 6.4, 197.9, 223.0)	K_3 (0.197, 0.197, 0.019, 0.161, 0.237)
	2047.8	$L_{4,\infty}$ (204.1, 203.9, 3.9, 197.0, 212.5)	K_4 (0.262, 0.262, 0.018, 0.227, 0.297)
	251.1	$L_{5,\infty}$ (182.5, 182.5, 3.6, 175.3, 189.7)	K_5 (0.164, 0.160, 0.013, 0.150, 0.198)
	Total = 4932.9		

Note: All the negative growth data are deleted. Deviance information criterion (DIC) and posterior mean, median, standard deviation (SD), and 95% credible interval (95% CI) of the parameter estimates are provided.

warm water temperatures halted growth, reduced reproduction, and increased the onset of a lethal abalone disease, withering syndrome (WS) (Vilchis et al. 2005). To distinguish the impacts of warm water from other factors, laboratory experiments with abundant kelp in WS disease free conditions were conducted that resulted in the cessation of abalone growth (Rogers-Bennett et al. 2010). These laboratory-based growth results correspond to results for red abalone in the field, which further supports their incorporation into the growth modeling work.

Negative growth data were recorded in this study. Reasons for this negative growth can be both measurement error and real negative growth caused by conditions of poor food and physiological stress. L. Rogers-Bennett (personal observation) has seen this negative growth in the lab in warm water and poor food conditions. Haaker et al. (1998) concluded that there was no significant effect caused by the tagging performance. We suggest considering the negative growth values in the modeling analysis in this situation. A possible supplementary approach is to use a measurement error model, which does not assume that the length measurements are perfect but with measurement errors (Jiao et al. 2006; Cope and Punt 2007).

Potential effects from both sampling selectivity and fishery selectivity can be a problem (Myers 1989; Sinclair et al. 2002). If the fastest-growing individuals reached the legal size sooner, they would be differentially removed, and growth estimation would become negatively biased over time. Conversely, if larger abalone are easier to locate (size-selective sampling), then the fastest-growing small abalone would have a higher probability of recapture during subsequent sampling, and growth rates for small (but fast-growing) individuals could be overestimated. Although the study site was open to extraction, with commercial minimum catchable size of 197 mm and recreational minimum catchable size of 178 mm, Haaker et al. (1998) and Tegner et al. (1989) concluded that there was no obvious effect caused by the sampling selectivity and fishing selectivity based on length sampling during this time period on this population.

Individual-level hierarchical models may be used when the percentage of multiple recaptures is high, because if a single abalone contributes to more than one data point in the analysis, then each point is not strictly independent and the potential correlation among replicate observations from each individual needs to be accounted for (Gelman et al. 2004; Zhang et al. 2009). However, in this study, the percentage of recaptures, including abalone captured more than once, in the 6 years of the recapture study was very low, and therefore, we did not consider this effect. It may be explored in a future study.

Some other modeling approaches may be considered in the future based on the characteristics of this red abalone population. Growth parameters L_∞ and K are strongly correlated, so models with explicit treatments of the known strong correlations among growth parameters may be used for red abalone growth in this population (Helser and Lai 2004; He and Bence 2007). A "random-walk" approach

Fig. 6. Sea surface temperature anomalies of ENSO (Joint Institute for the Study of the Atmosphere and Ocean 2007). Global ENSO SST (tropics minus extratropics) (C) 1950 – July 2007. The rectangle indicates the period when the red abalone (*Haliotis rufescens*) were tagged at Johnsons Lee.

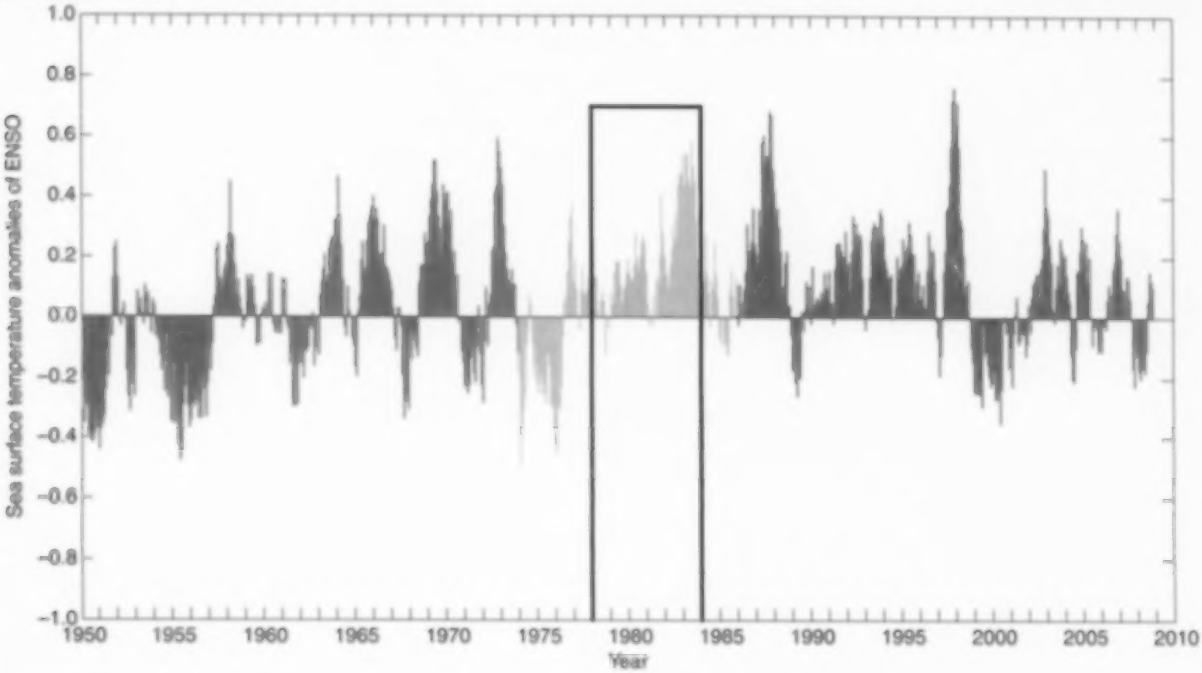

Fig. 7. Analysis between sea surface temperature (SST) anomalies and growth parameters (posterior means from model M1). Average anomalies of SST are calculated as the mean SST anomalies over years. For example, for individuals tagged in 1978 and recaptured at 1979, the corresponding average SST anomaly equals the mean SST anomalies of 1978 and 1979. (*a*) $L_{\infty,i}$ ~ averaged SST anomaly; (*b*) K_i ~ averaged SST anomaly.

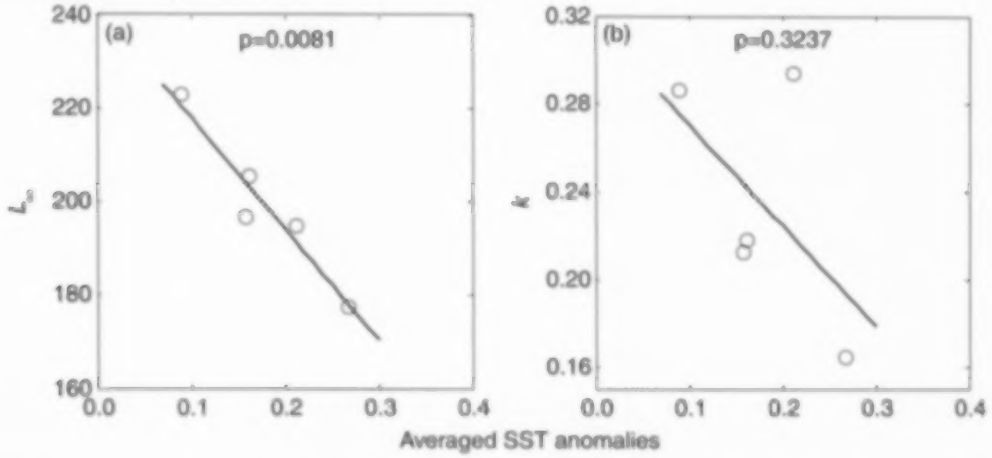

(Szalai et al. 2003; Jiao et al. 2009) might be better suited to time-varying parameters that can describe trends of the parameters. Also the very strong relationship between L_∞, K, and SST anomaly suggests that it might be effectively used as a direct covariate in the hierarchical analysis. Introducing categorical or continuous covariates into this type of analysis is relatively straightforward and may be much more parsimonious than allowing additional parameters for variable growth over years or arbitrary groupings of years (Helser et al. 2007). We need to select the type of models to explore according to the data characteristics and our preliminary knowledge of the effects of the possible covariates. In situations when either the data for each time period were not balanced, with some years having small sample size or narrow

length range, or the relationship between growth parameters and covariate is possibly nonlinear, which is usually true, the use of hierarchical models is suggested. The hierarchical model would allow the years with low sample size or narrow length range to borrow strength from other years with large sample size in the first situation. It would estimate the time-changing parameters and then look into the relationship between parameters and the covariates.

In this study, the base growth curve considered is the von Bertalanffy curve, but other growth curves can perform better or are worthwhile to be explored in the future (Katsanevakis 2006; Rogers-Bennett et al. 2007; Haddon et al. 2008). Uncertainty in model selection can be high when different growth curves are used. Model averaging and Bayesian model averaging can be alternative approaches to incorporate this model selection uncertainty (Burnham and Anderson 2002; Jiao et al. 2008).

Temporal variation of red abalone growth has been determined to be an important biological feature of these long-lived marine invertebrates (Haaker et al. 1998; Hobday and Tegner 2002). A model that can incorporate these temporal variations is needed to better capture abalone growth dynamics. For long-term management purposes, these variations need to be included in the stock assessment of abalone. When yield-per-recruit (YPR) and egg-per-recruit (EPR) models are used for stock assessment purposes, a hierarchical growth model as developed in this study may be used instead of nonhierarchical models that are more generally employed. YPR and EPR models are sensitive to growth variation and are certainly not safe to be used for abalone stock assessment (Tegner et al. 1989). A nonhierarchical model can underestimate the uncertainty caused by growth variation over time, which could contribute to overfishing during periods of low ocean productivity.

Growth during 1982 to 1984 was reduced to such a level that most abalone would not grow to the minimum legal size at that rate. This result is a challenge for stock assessment modeling and management because growth is widely used in developing biological reference points from per-recruitment analyses. Lower growth rates in the population than used in the modeling work could result in high $F_{0.1}$ and $F_{\%}$ estimates from YPR and EPR models given the same minimum catchable size limit because most would be smaller than the size limit. However, the availability of abalone of catchable sizes would be low. A comprehensive modeling system that is capable of recognizing and incorporating important variability in growth rates and its relation with ocean climate if possible is needed for abalone and other species that exhibit highly variable growth rates. Hierarchical growth modeling may be a component of an ecosystem-based fishery management approach that can incorporate important changes in vital rates as they respond to fluctuations in oceanographic conditions.

Acknowledgements

This project was supported in part by the USDA Cooperative State Research, Education and Extension Service (Hatch Project No. 0210510) and a grant from Concur for red abalone stock assessment to Y. Jiao. This publication is a contribution of the Bodega Marine Laboratory, University of California at Davis. We thank the California Department of Fish and Game Marine Region for supporting this work, especially T. Barnes. We also thank Paul Breen and two anonymous reviewers for constructive comments and suggestions.

References

Beacham, T.D. 1983. Growth and maturity of Atlantic cod (*Gadus morhua*) in the southern Gulf of St. Lawrence. Can. Tech. Rep Fish. Aquat. Sci. No. 1142.

Berger, J.O. 1985. Statistical decision theory and Bayesian analysis. Springer-Verlag, New York.

Bowman, A.W., and Azzalini, A. 1997. Applied smoothing techniques for data analysis. Oxford University Press, Oxford, UK.

Burnham, K.P., and Anderson, D.R. 2002. Model selection and multimodel inference: a practical information-theoretic approach. 2nd ed. Springer, New York.

Caddy, J.F., and Mahon, R. 1995. Reference points for fisheries management. FAO (Food and Agricultural Organisation of the United Nations) Fish. Tech. Pap. No. 347.

Chen, Y., and Mello, L.G.S. 1999. Growth and maturation of cod (*Gadus morhua*) of different year classes in the Northwest Atlantic, NAFO subdivision 3Ps. Fish. Res. **42**(1–2): 87–101. doi:10.1016/S0165-7836(99)00036-3.

Clark, J.S. 2003. Uncertainty and variability in demography and population growth: a hierarchical approach. Ecology, **84**(6): 1370–1381. doi:10.1890/0012-9658(2003)084[1370:UAVIDA]2.0.CO;2.

Conser, R.J., Hill, K.T., Crone, P.R., and Bergen, D. 2002. Stock assessment of Pacific sardine with management recommendations for 2003: executive summary. Pacific States Fishery Management Council, Portland, OR 97220, USA.

Cope, J.M., and Punt, A.E. 2007. Admitting ageing error when fitting growth curves: an example using the von Bertalanffy growth function with random effects. Can. J. Fish. Aquat. Sci. **64**(2): 205–218. doi:10.1139/F06-179.

Cowles, M.K., and Carlin, B.P. 1996. Markov chain Monte Carlo convergence diagnostics: a comparative review. J. Am. Stat. Assoc. **91**(434): 883–904. doi:10.2307/2291683.

Fabens, A.J. 1965. Properties and fitting of the von Bertalanffy growth curve. Growth, **29**(3): 265–289. PMID:5865688.

Food and Agricultural Organisation of the United Nations. 1995. Precautionary approach to fisheries. Part 1. Guidelines on the precautionary approach to capture fisheries and species introductions, United Nations. FAO (Food and Agricultural Organisation of the United Nations) Fish. Tech. Pap. No. 350/1.

Gelman, A. 2006. Prior distributions for variance parameters in hierarchical models (comment on article by Browne and Draper). Bayesian Anal. **1**(3): 515–534.

Gelman, A., and Rubin, D.B. 1992. Inference from iterative simulation using multiple sequences (with discussion). Stat. Sci. **7**(4): 457–472. doi:10.1214/ss/1177011136.

Gelman, A., Carlin, J.B., Stern, H.S., and Rubin, D.B. 2004. Bayesian data analysis. Chapman & Hall, Boca Raton, Florida.

Haaker, P.L., Parker, D.O., and Henderson, K.C. 1986. Red abalone size data from Johnsons Lee, Santa Rosa Island, collected from 1978 to 1984. Marine Resources Tech. Rep. No. 53. Available at aquacomm.fcla.edu/720/ [accessed 12 November 2009].

Haaker, P.L., Parker, D.O., Barsky, K.C., and Chun, C.S. 1998. Growth of the red abalone, *Haliotis rufescens* (Swainson), at Johnsons Lee, Santa Rosa Island, California. J. Shellfish Res. **17**(3): 747–753.

Haddon, M., Mundy, C., and Tarbath, D. 2008. Using an inverse-

logistic model to describe growth increments of blacklip abalone (*Haliotis rubra*) in Tasmania. Fish. Bull. (Washington, D.C.), **106**(1): 58–71.

Hanson, J.M., and Chouinard, G.A. 1992. Evidence that size-selectivity mortality affects growth of Atlantic cod (*Gadus morhua* L.) in the southern Gulf of St. Lawrence. J. Fish Biol. **41**(1): 31–41. doi:10.1111/j.1095-8649.1992.tb03168.x.

He, J.X., and Bence, J.R. 2007. Modeling annual growth variation using a hierarchical Bayesian approach and the von Bertalanffy growth function, with application to lake trout in southern Lake Huron. Trans. Am. Fish. Soc. **136**(2): 318–330. doi:10.1577/T06-108.1.

Helser, T.E., and Lai, H.L. 2004. A Bayesian hierarchical meta-analysis of fish growth, with an example for North American largemouth bass, *Micropterus salmoides*. Ecol. Model. **178**(3–4): 399–416. doi:10.1016/j.ecolmodel.2004.02.013.

Helser, T.E., Stewart, I.J., and Lai, H.L. 2007. A Bayesian hierarchical meta-analysis of growth for the genus *Sebastes* in the eastern Pacific ocean. Can. J. Fish. Aquat. Sci. **64**(3): 470–485. doi:10.1139/F07-024.

Hobday, A.J., and Tegner, M.J. 2002. Influence of temperature and fishing on local population dynamics of red abalone. CCOFI Rep. **43**: 74–96.

Hutchings, J.A., and Myers, R.A. 1994. Timing of cod reproduction: interannual variability and the influence of temperature. Mar. Ecol. Prog. Ser. **108**(5): 21–31. doi:10.3354/meps108021.

Jiao, Y., Reid, K., and Nudds, T. 2006. Variation in the catchability of yellow perch (*Perca flavescens*) in the fisheries of Lake Erie using a Bayesian error-in-variable approach. ICES J. Mar. Sci. **63**: 1695–1704. doi:10.1016/j.icesjms.2006.07.002.

Jiao, Y., Neves, R., and Jones, J. 2008. Models and model selection uncertainty in estimating growth rates of endangered freshwater mussel populations. Can. J. Fish. Aquat. Sci. **65**(11): 2389–2398. doi:10.1139/F08-141.

Jiao, Y., Reid, K., and Smith, E. 2009. Model selection uncertainty and Bayesian model averaging in fisheries recruitment modeling. *In* The future of fisheries science in North America. *Edited by* R.J. Beamish and B.J. Rothschild. Fish and Fisheries Book Series No. 31, Springer, New York. pp. 505–524.

Joint Institute for the Study of the Atmosphere and Ocean (JISAO). 2007. Global SST-ENSO index, 1817 to November 2008. Available at jisao.washington.edu/data_sets/globalsstenso/ [accessed 12 April 2008].

Katsanevakis, S. 2006. Modelling fish growth: model selection, multi-model inference and model selection uncertainty. Fish. Res. **81**(2–3): 229–235. doi:10.1016/j.fishres.2006.07.002.

Kirkwood, G.P., and Somers, I.F. 1984. Growth of two species of tiger prawn, *Penaeus esculentus* and *P. semisulcatus*, in the western Gulf of Carpentaria. Aust. J. Mar. Freshwater Res. **35**(6): 703–712. doi:10.1071/MF9840703.

Krohn, M., Reidy, S., and Kerr, S. 1997. Bioenergetic analysis of the effects of temperature and prey availability on growth and condition of northern cod (*Gadus morhua*). Can. J. Fish. Aquat. Sci. **54**(S1): 113–121. doi:10.1139/cjfas-54-S1-113.

Leighton, D.H. 1974. The influence of temperature on larval and juvenile growth in three species of southern California abalones. Fish. Bull. (Washington, D.C.), **72**(4): 1137–1145.

Lilly, G.R. 1996. Growth and condition of cod in subdivision 3Ps as determined from trawl surveys (1972–1996) and sentinel surveys (1995). DFO Atl. Fish. Res. Doc. No. 96/69.

McAllister, M.K., and Kirkwood, G.P. 1998. Using Bayesian decision analysis to help achieve a precautionary approach for managing developing fisheries. Can. J. Fish. Aquat. Sci. **55**(12): 2642–2661. doi:10.1139/cjfas-55-12-2642.

Myers, R.A. 1989. Estimating bias in growth caused by size-selective fishing mortality. ICES CM 1989/D:8.

Nash, W. 1992. An evaluation of egg-per-recruit analysis as a means of assessing size limits for blacklip abalone (*Haliotis rubra*) in Tasmania. *In* Abalone of the world: biology, fisheries and culture. *Edited by* S.A. Shepherd, M.J. Tegner, and S.A. Guzmán del Próo. Blackwell Scientific Publication, Oxford, UK. pp. 318–38.

Parma, A.M. 2002. In search of robust harvesting rules for Pacific halibut in the face of uncertain assessments and decadal changes in productivity. Bull. Mar. Sci. **70**(2): 423–453.

Pearse, J.S., and Cameron, R.A. 1991. Echinodermata: Echinoid. *In* Reproduction of marine invertebrates. VI. *Edited by* A.C. Giese, J.S. Pearse, and V.B. Pearse. Boxwood Press, Pacific Grove, California. pp. 514–664.

Quinn, T.J., and Deriso, R.B. 1999. Quantitative fish dynamics. Oxford University Press, New York.

Ricker, W.E. 1975. Computation and interpretation of biological statistics of fish populations. Bull. Fish. Res. Board Can. No. 191.

Rogers-Bennett, L., Rogers, D.W., and Schultz, S. 2007. Modeling growth and mortality of red abalone (*Haliotis rufescens*) in northern California. J. Shellfish Res. **26**(3): 719–727. doi:10.2983/0730-8000(2007)26[719:MGAMOR]2.0.CO;2.

Rogers-Bennett, L., Dondenville, R., Moore, J.D., Ignacio Vilchis, L. 2010. Sublethal impacts on reproduction in red abalone exposed to warm water, starvation and disease: implications of ocean warming. J. Shell. Res. In press.

Shepherd, S.A., Guzmán del Próo, S.A., Turrubiates, J., Belmar, J., Baker, J.L., and Sluczanowski, P.R. 1991. Growth, size at sexual maturity, and egg-per-recruit analysis of the abalone *Haliotis fulgens* in Baja California. Veliger, **34**: 324–330.

Shepherd, S.A., Baker, L., and Johnson, D.W. 1995. Yield-per-recruit and egg-per-recruit analyses of the Omani abalone, *Haliotis mariae*. Mar. Freshw. Res. **46**(3): 663–668. doi:10.1071/MF9950663.

Sinclair, A.F., Swain, D.P., and Hanson, J.M. 2002. Disentangling the effects of size-selective mortality, density and temperature on length at age. Can. J. Fish. Aquat. Sci. **59**(2): 372–382. doi:10.1139/f02-014.

Spiegelhalter, D.J., Best, N.G., Carlin, B.P., and van der Linde, A. 2002. Bayesian measures of model complexity and fit (with discussion). J. Roy. Stat. Soc. Ser. B, **64**(4): 583–639. doi:10.1111/1467-9868.00353.

Spiegelhalter, D.J., Thomas, A., Best, N., and Lunn, D. 2004. WinBUGS user manual. Version 1.4.1. MRC Biostatistics Unit, Cambridge, UK.

Su, Z., Adkison, M.D., and Van Alen, B.W. 2001. A hierarchical Bayesian model for estimating historical salmon escapement and escapement timing. Can. J. Fish. Aquat. Sci. **58**(8): 1648–1662. doi:10.1139/cjfas-58-8-1648.

Swain, D.P., Sinclair, A.F., Castonguay, M., Chouinard, G.A., Drinkwater, K.F., Fanning, L.P., and Clark, D.S. 2003. Density-versus temperature-dependent growth of Atlantic cod (*Gadus morhua*) in the Gulf of St. Lawrence and on the Scotian Shelf. Fish. Res. **59**(3): 327–341. doi:10.1016/S0165-7836(02)00027-9.

Szalai, E.B., Fleischer, G.W., and Bence, J.R. 2003. Modeling time-varying growth using a generalized von Bertalanffy model with application to bloater (*Coregonus hoyi*) growth dynamics in Lake Michigan. Can. J. Fish. Aquat. Sci. **60**(1): 55–66. doi:10.1139/f03-003.

Tegner, M.J., and Dayton, P.K. 1987. El Nino effects on southern California kelp forest communities. Adv. Ecol. Res. **17**: 243–279. doi:10.1016/S0065-2504(08)60247-0.

Tegner, M.J., Breen, P.A., and Lennert, C.E. 1989. Population biology of red abalones (*Haliotis rufescens*) in southern California and management of the red and pink (*H. corrugata*) abalone fisheries. Fish. Bull. (Washington, D.C.), **87**(2): 313–339.

Tegner, M.J., DeMartini, J.D., and Karpov, K.A. 1992. The California red abalone fishery: a case study in complexity. *In* Abalone of the world: biology, fisheries and culture. *Edited by* S.A. Shepherd, M.J. Tegner, and S.A. Guzman del Prom. Blackwell Scientific Publications, Oxford, UK. pp370–383.

Trippel, E.A. 1995. Age-at-maturity as a stress indicator in fisheries. Bioscience, **45**(11): 759–771. doi:10.2307/1312628.

Vilchis, L.I., Tegner, M.J., Moore, J.D., Friedman, C.S., Riser, K.L., Robbins, T.T., and Dayton, P.K. 2005. Ocean warming effects on growth, reproduction, and survivorship of southern California abalone. Ecol. Appl. **15**(2): 469–480. doi:10.1890/03-5326.

Zhang, Z., Lessard, J., and Campbell, A. 2009. Use of Bayesian hierarchical models to estimate northern abalone, *Haliotis kamtschatkana*, growth parameters from tag-recapture data. Fish. Res. **95**(2–3): 289–295. doi:10.1016/j.fishres.2008.09.035.

Patterns in nutrient limitation and chlorophyll *a* along an anthropogenic eutrophication gradient in French Mediterranean coastal lagoons

Philippe Souchu, Béatrice Bec, Val H. Smith, Thierry Laugier, Annie Fiandrino, Laurent Benau, Valérie Orsoni, Yves Collos, and André Vaquer

Abstract: A cross-ecosystem comparison of data obtained from 20 French Mediterranean lagoons with contrasting eutrophication status provided the basis for investigating the variables that best predict chlorophyll *a* (Chl *a*) concentrations and nutrient limitation of phytoplankton biomass along a strong nutrient enrichment gradient. Summer concentrations of dissolved inorganic nitrogen (DIN) and phosphorus (DIP) comprised only a small fraction of total nitrogen (TN) and total phosphorus (TP). On the basis of inorganic nutrient concentrations, the most oligotrophic lagoons appeared to be phosphorus-limited, with a tendency towards the development of nitrogen limitation as eutrophication increased, as evidenced by decreasing DIN:DIP ratios. A weak but significantly positive relationship was found between dissolved silicate (DSi) and Chl *a*, reflecting DSi accumulation in the water column along the trophic state gradient and implying a progressive shift away from potential Si limitation of phytoplankton growth. Observed concentrations of Chl *a* were far better explained by TN and TP than by DIN and DIP concentrations, suggesting that a total nutrient based approach is likely to be the most appropriate for managing eutrophication in Mediterranean lagoons and other coastal waters. These results give credence to the idea that marine and freshwater environments respond in a similar fashion to nutrient enrichment.

Résumé : Une comparaison inter-sites des concentrations de nutriments et de chlorophylle *a* (Chl *a*) issues de 20 lagunes de Méditerranée française de degrés divers d'eutrophisation a été menée afin de rechercher la meilleure variable expliquant le niveau de Chl *a* et d'explorer la limitation de la production primaire par les nutriments au long d'un fort gradient d'enrichissement en azote et phosphore. En été, l'azote et le phosphore inorganiques dissous (DIN et PID respectivement) constituaient une faible fraction des concentrations d'azote et de phosphore totaux (TN et TP respectivement). Sur la base des concentrations en nutriments inorganiques, la plupart des lagunes oligotrophes semblaient limitées par le phosphore avec une tendance vers des rapports DIN:DIP décroissants, et donc une limitation par l'azote, lorsque l'eutrophisation augmentait. Une corrélation positive mais faible a aussi été obtenue entre les concentrations de silicates (DSi) et Chl *a*, indiquant une accumulation de DSi dans la colonne d'eau et donc une diminution de la limitation de la croissance du phytoplancton par la silice au fur et à mesure que l'eutrophisation augmentait. Le fait que Chl *a* était beaucoup mieux expliquée par TN et TP que par DIN et DIP suggère même que l'approche limnologique basée sur l'ensemble des nutriments est vraisemblablement la meilleure pour gérer l'eutrophisation dans les lagunes méditerranéennes et dans d'autres écosystèmes marins côtiers. Ces constats renforcent l'idée que les écosystèmes marins et d'eau douce répondent de façon similaire à l'enrichissement en nutriments.

Introduction

The over-enrichment of lakes, inland water courses, and coastal waters with nitrogen (N) and phosphorus (P) has been one of the major effects of human activity on aquatic ecosystems during the past 50 years (Nixon 1995; Cloern 2001). Cultural eutrophication presents a major problem for most of Europe's regional seas, including the Mediterranean (Ignatiades 2005). However, most eutrophication-related problems in the Mediterranean region currently are confined to limited areas, rather than being widespread phenomena (European Environment Agency 1999). For example, Mediterranean coastal lagoons exhibit a wide range of trophic states, and reductions in anthropogenic N and P inputs will be necessary to attain the desired levels of water quality that have recently been specified by the Water Framework Directive for European water bodies (European Economic Community 2000).

Received 6 July 2009. Accepted 10 February 2010. Published on the NRC Research Press Web site at cjfas.nrc.ca on 25 March 2010. J21297

P. Souchu,[1,2] **T. Laugier, A. Fiandrino, and L. Benau.** Ifremer, Laboratoire Environnement Ressource Languedoc–Roussillon, BP 171, Avenue Jean Monnet 34203 Sète CEDEX, France.
B. Bec, Y. Collos, and A. Vaquer. Université Montpellier 2, CNRS, Ifremer, UMR 5119 Ecosystèmes Lagunaires, CC093, 34095 Montpellier CEDEX 5, France.
V.H. Smith. Department of Ecology and Evolutionary Biology, University of Kansas, Lawrence, KS 66045, USA.
V. Orsoni. Ifremer, Laboratoire Environnement Ressource Corse, Immeuble Agostini, Zone industrielle de Furiani, 20600 Bastia, France.

[1]Corresponding author (e-mail: psouchu@ifremer.fr).
[2]Present address: Ifremer, LER/MPL/NT, Rue de l'Ile d'Yeu, BP 21105, 44311 Nantes CEDEX 03, France.

Historically, N has been considered to be the primary growth-limiting nutrient in marine ecosystems (Ryther and Dunstan 1971), and P has been considered to be the principal limiting nutrient in lakes (Schindler 1977). However, this paradigm has been increasingly called into question in recent years as evidence has accumulated for widespread occurrences of both N and P limitation in lakes and streams (Elser et al. 1990, 2007; Lewis and Wurtsbaugh 2008), as well as frequent P limitation in the oceans (Downing et al. 1999; Elser et al. 2007). Downing et al. (1999) have observed through bioassay experiments that P limitation was strongest in unpolluted ecosystems, whereas N limitation was more frequent in relatively polluted coastal waters.

In marine waters, measurements of dissolved inorganic nitrogen, inorganic phosphorus, and silicate concentrations (DIN, DIP, and DSi, respectively) are often used as a measure of eutrophication status, and ratios between dissolved nutrients have long been used to indicate which of these three nutrients is likely to be growth-limiting (Fisher et al. 1995; Justić et al. 1995). In contrast, total nitrogen (TN) and total phosphorus (TP) are considered to be the best indicators of eutrophication status and nutrient limitation in freshwater lakes and rivers (Dodds 2003). However, this more limnological approach using relationships between phytoplankton biomass and total nutrients has been applied to marine waters with success to predict eutrophication (Downing 1997; Meeuwig et al. 2000; Smith 2003), suggesting a common response of marine and freshwater systems to nutrient enrichment (Guildford and Hecky 2000; Smith 2006). A water quality database developed for 20 Mediterranean coastal lagoons exhibiting a wide range of external nutrient loading provided the basis for a comparative assessment of nutrient limitation and the controls of algal biomass along this eutrophication gradient, using both marine (dissolved inorganic nutrients) and limnological (total forms of N and P) approaches.

Materials and methods

Studied sites

A database was developed during 1998–2002 for 18 lagoons in the Languedoc–Roussillon (LR) region of France and two lagoons in Corsica (Fig. 1). All marine water bodies (median salinity in summer > 20 psu) presenting an annually persistent water volume of $\geq 0.5 \times 10^6$ m^3 were included in the database (Table 1). Some lagoons were divided into sectors corresponding to hydrodynamic boxes empirically defined on the basis of their bottom contours and depth. The aim was to individualize sectors belonging to the same lagoon but display significant differences (see BS, BM, and BN in Bages lagoon; Fig. 1). Depending on the lagoon size and shape, one to three stations were located in the middle of each sector.

Salses-Leucate (L) lagoon, the second largest LR lagoon after Thau (T), has permanent karstic water inputs (Boutière et al. 1982). La Palme lagoon (LP) also features a karstic watershed but its inputs from karst aquifers are weaker than at L (Wilke and Boutière 2000). The Bages-Sigean (B) lagoon is made up of several smaller basins and has only one opening to the sea at the southernmost end (Jacques et al. 1975). Ayrolle (AY) lagoon is directly connected to the sea, whereas Gruissan (GR) lagoon is connected to the sea by a 2.5 km channel that can receive freshwater from a diversion canal. Vendres (VE) lagoon is a complex wetland-like system with a hydraulic management that is made difficult by marine water inflows and the Aude River flash floods (Aloisi and Gadel 1992).

The Thau (T) lagoon is the largest and deepest LR lagoon (Souchu et al. 2001). The digging of the Sète to Rhone canal has split in half four lagoons located to the east of Thau (Ingril to Méjean–Grec). These eight lagoons are called "palavasian" because of their proximity to the coastal resort of Palavas-les-Flots. Lagoons located landward (Ingril North (IN), Vic (VC), Arnel (AR), and Méjean (M)) are bordered by wetlands and can communicate with seafront lagoons (Ingril South (IS), Pierre Blanche (PB), Prévost (PR), and Grec (GE)) through numerous openings in the Sète to Rhone canal. Or (O) lagoon is bordered by a wetland with a steady supply of freshwater from the northeast. Ponant (PO) lagoon receives freshwater inflow all year round. The small Médard (MD) lagoon is an old-feed pond for salt marshes. The two Corsican lagoons, Diana (D) and Urbino (U), which have a maximum depth of 10 m and mean depth ≥4 m, could be classified as "deep lagoons," as could Thau (Frisoni et al. 1983).

Field observations also allowed us to assign to each lagoon a trophic status (Fig. 1) according to their phanerogam–macroalgae and (or) phytoplankton succession (Duarte 1995; Schramm 1999). The oligotrophic lagoons corresponded to transparent waters with a dominance of marine phanerogams with associated macroalgae. The mesotrophic lagoons included climax species but also proliferating macroalgae. The eutrophic lagoons exhibited a disappearance of phanerogams, but proliferating macroalgae could still develop. The hypertrophic lagoons exhibited quasi-exclusive dominance by phytoplankton.

Data collection

This study was focused on the summer period during which primary production is maximum. The 29 stations (Table 1) were sampled in June, July, and August 1999, 2001, and 2002, except for 10 stations in 1999 and 4 stations in 2001. Periods of temporary sediment resuspension were avoided by not sampling for three days following any period of wind speed exceeding 25 m·s^{-1}. Temperature and salinity were measured with a WTW LF 197 field sensor (precision, ±0.5%) calibrated monthly with salinity standards (IAPSO 38H5; Ocean Scientific International Ltd., Havant, Hampshire, UK). Subsurface water samples were taken by boat between the hours of 1000 and 1600 in 2 L polypropylene bottles prewashed with 1 mol·L^{-1} HCl and then copiously rinsed with deionized water.

In the laboratory, water was prefiltered less than 3 h after sampling through 200 µm mesh to remove most zooplankton. The prefiltered water was transferred to ashed (450 °C for 6 h) Pyrex bottles and stored at –20 °C for further analyses of total nitrogen (TN) and total phosphorus (TP) (see below). For analyses of dissolved inorganic nutrients, the prefiltered water was filtered through Whatman GF/F membranes with an all-glass filtering system and a vacuum of less than 10 cm Hg. The whole apparatus and the membrane were prerinsed twice before filtration. Ammonium concen-

Fig. 1. Location of sampling stations and limits of sectors (dotted line) in oligotrophic (□), mesotrophic (△), eutrophic (■), and hypertrophic (▲) lagoons of the Languedoc–Roussillon (LR) region and Corsica. See Materials and methods for an explanation of codes.

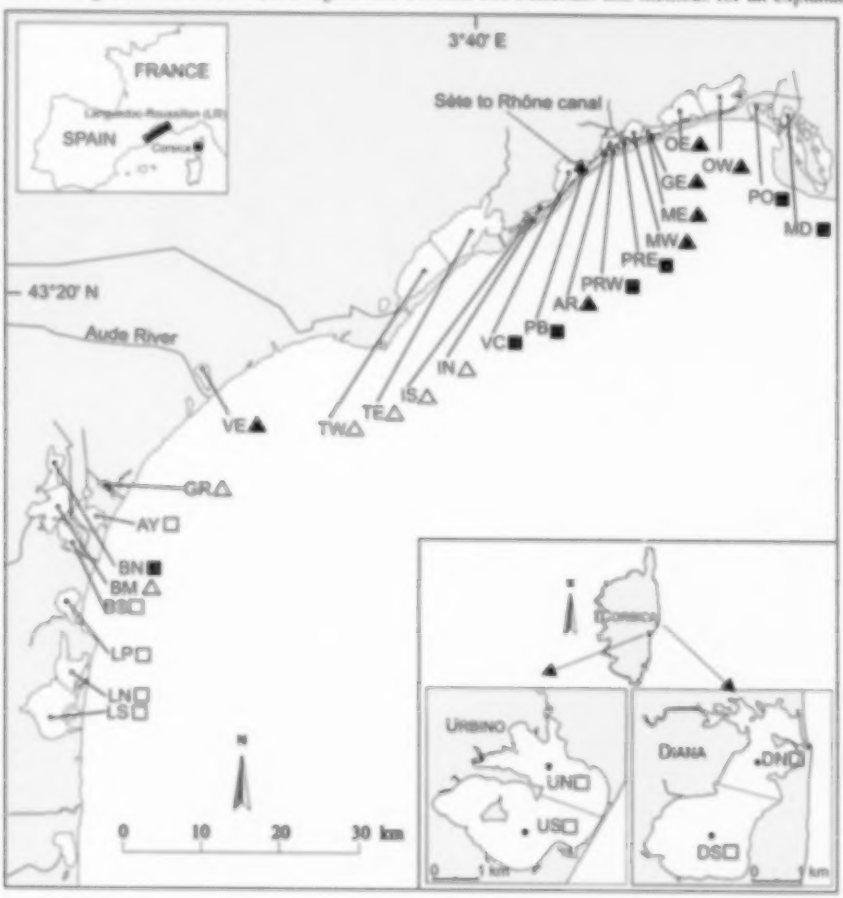

trations (NH_4^+) were measured according to the manual method of indophenol blue (Aminot and Kérouel 2004). Nitrate (NO_3^-), nitrite (NO_2^-), and dissolved inorganic phosphorus (DIP) samples were frozen at –20 °C in Pyrex bottles before their analyses on a segmented flow analyzer (Tréguer and Le Corre 1975). Dissolved inorganic nitrogen concentration was expressed as DIN = NH_4^+ + NO_3^- + NO_2^-. Samples for dissolved silicate (DSi) analysis were stored at 4 °C in polycarbonate bottles and analysed on a segmented flow analyzer according to Tréguer and Le Corre (1975) in the following weeks. DSi was analyzed only during annual cycles. Although the filtration of water through Whatman GF/F membranes and using an all-glass filtering system potentially could lead to overestimates of DSi, the similarity of these results to those obtained from 2003 to 2006 using nitrate cellulose filter filtration and an all-polycarbonate filtering system leads us to believe that our glass-filtered DSi data are valid.

Concentrations of TN were measured in prefiltered water by chemical oxidation with potassium persulfate in a hot alkaline medium in Teflon vials (adapted from Raimbault and Slawyk 1991). Reagent mix (5 mL) was added to 40 mL of the sample and then autoclaved in Teflon vials at 120 °C (1 bar) for 1 h. The various N forms (except N_2) were oxidized to nitrate, which was then measured according to Tréguer and Le Corre (1975). For analyses of TP, the potassium persulfate oxidation was carried out in acid medium according to Menzel and Corwin (1965). DIP concentrations were then measured according to Tréguer and Le Corre (1975). Measurements of TP in Corsican lagoons were limited to the summer of 2002 because of the use of faulty vials during annual cycle sampling. However, results of TP measurements in 2002 were confirmed by those obtained between 2003 and 2006 (T. Laugier, unpublished).

Chlorophyll *a* (Chl *a*) concentrations, described in B. Bec (unpublished data), were analyzed in all samples. On return to the laboratory, 5–50 mL (depending on the phytoplankton abundance) were filtered under a vacuum of less than 10 cm Hg on Whatman GF/F membranes and stored at –20 °C in glass tubes. Filters were ground in acetone (90%) and extracted during 24 h in the dark at 4 °C. Pigments were measured by spectrofluorimetry (Neveux and Lantoine 1993) and are expressed in micrograms per litre (precision, ±5%).

Median values for the above water quality parameters were calculated for the pooled data from each lagoon or from each individual sector of lagoons within which the sec-

Table 1. Summary characteristics of the 20 studied lagoons (see Fig. 1 for station locations).

Lagoon	Label	Mean depth (m)	Area (km^2)	Volume ($\times 10^6$ m^3)	Station	Station depth (m)
Salse-Leucate	L	2.0	54	90	LS	3.0
					LN	2.6
La Palme	LP	0.5	6.0	3.3	LP	1.5
					BS	1.3
Bages-Sigean	B	1.3	37	49	BM	2.0
					BN	2.1
Ayrolle	AY	0.5	13.2	9.0	AY	0.9
Gruissan	GR	0.5	1.4	1.0	GR	0.7
Vendres	VE	0.9	4.8/10	1.4/3.0	VE	0.8
Thau	T	4.0	75	260	TW	5.5
					TE	9.0
Palavasian						
Ingril South	IS	0.6	3.6	2.2	IS	1.0
Ingril North	IN	0.6	3.2	1.9	IN	1.0
Pierre Blanche	PB	0.4	3.7	1.5	PB	0.9
Vic	VC	1.2	11.5	13.8	VC	1.6
Prévost	PR	0.75	3.8	2.9	PRW	0.8
					PRE	0.9
Arnel	AR	0.40	4.7	1.9	AR	0.7
Grec	GE	0.30	2.7	0.7	GE	0.7
Méjean	M	0.75	5.5	4.1	MW	0.8
					ME	0.9
Or (Mauguio)	O	0.8	32	24	OW	1.2
					OE	1.2
Ponant	PO	2.7	2.0	5.4	PO	3.5
Médard	MD	0.6	1.4	0.9	MD	0.8
Corsican						
Diana	D	6.0	5.7	10.2	DS	8.0
					DN	7.0
Urbino	U	5.0	7.6	33	US	7.5
					UN	7.5

tor median water quality was found to differ significantly (Kruskal–Wallis, $p < 0.05$). Individual sectors were then kept for Bages-Sigean and Méjean lagoons, which both had significant between-station differences for both TN and TP.

Results

All DIN concentrations were close to 1 µmol·L^{-1}, except for lagoons Grec and Médard (Fig. 2), and the contribution of DIN to TN remained below 6% except at Diana. DIP concentrations ranged from low values of ≤0.12 µmol·L^{-1} in oligotrophic lagoons Salses-Leucate, La Palme, Bages South, Ayrolle, Diana, and Urbino to much higher values of >1 µmol·L^{-1} in hypertrophic lagoons Vendres and Méjean West (Fig. 2). The contribution of DIP to TP remained below 15% except at Bages Middle, Bages North, Thau, and Ponant. DSi ranged between 0.5 µmol·L^{-1} at Diana and 204 µmol·L^{-1} at Vendres. DSi individual concentrations remained at <2 µmol·L^{-1} in 11% of samples (16 out of 144 samples). Reflecting the strong eutrophication gradient in these lagoons, TN varied from 16 µmol·L^{-1} at Diana to 452 µmol·L^{-1} at Vendres, whereas TP varied from 0.14 µmol·L^{-1} at Diana to 28 µmol·L^{-1} at Vendres. Salinity ranged from 21.3 psu at Or to a maximum of 40.1 psu at Prévost. DIP, TN, and TP were inversely correlated with salinity (Table 2, eqs. 1 to 5).

Fig. 2. Log-scaled plot of dissolved inorganic nitrogen (DIN) on dissolved inorganic phosphorus (DIP) in oligotrophic (□), mesotrophic (△), eutrophic (■), and hypertrophic (▲) lagoons of the Languedoc–Roussillon (LR) region and Corsica. See Materials and methods for an explanation of codes.

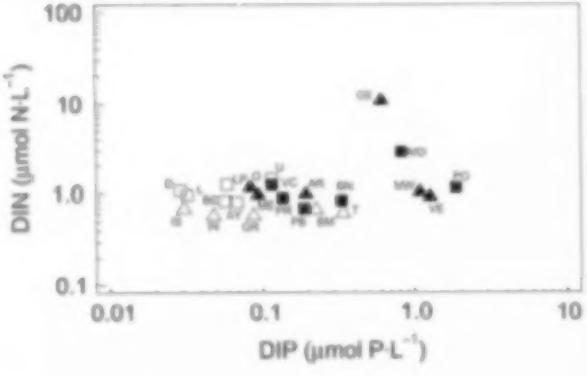

DIN:DIP ratios varied from 1.1, by moles, at Vendres and Ponant to 40 at Diana. No significant correlation was found between the DIN:DIP ratio and DIN; instead, the observed variability in DIN:DIP was largely explained by variations in DIP (Table 2, eqs. 9 and 10; Fig. 2). DIN:DIP was inver-

Table 2. Empirical models and summary statistics for the relationships between salinity, nutrients, and Chl *a* in the 20 studied lagoons.

Equation	Regression model	*n*	r^2	*p*
1	$\log_{10}$DIN on $\log_{10}$Sal	23	NS	0.29
2	$\log_{10}$DIP = 4.8 – 3.7 $\log_{10}$Sal	23	0.39	0.001
3	$\log_{10}$DSi = 5.8 – 3.1 $\log_{10}$Sal	23	NS	0.12
4	$\log_{10}$TN = 5.3 – 2.3 $\log_{10}$Sal	23	0.25	0.01
5	$\log_{10}$TP = 5.8 – 3.7 $\log_{10}$Sal	23	0.30	0.006
6	$\log_{10}$DIN on $\log_{10}$DIP	23	NS	0.08
7	$\log_{10}$DIN on $\log_{10}$DSi	23	NS	0.38
8	$\log_{10}$DSi on $\log_{10}$DIP	23	NS	0.05
9	$\log_{10}$DIN:DIP on $\log_{10}$DIN	23	NS	0.56
10	$\log_{10}$DIN:DIP = 0.30 – 0.69 $\log_{10}$DIP	23	0.76	0.0001
11	$\log_{10}$DIN:DIP = 1.24 – 0.34 $\log_{10}$DSi	23	0.19	0.04
12	$\log_{10}$DIN:DIP = 1.67 – 0.47 $\log_{10}$TN	23	0.20	0.03
13	$\log_{10}$DIN:DIP = 0.97– 0.45 $\log_{10}$TP	23	0.34	0.003
14	$\log_{10}$TN = 1.64 + 0.65 $\log_{10}$TP	23	0.92	0.0001
15	$\log_{10}$TN:TP = 2.2 – 0.37 $\log_{10}$TN	23	0.52	0.0001
16	$\log_{10}$TN:TP = 1.63 – 0.30 $\log_{10}$TP	23	0.77	0.0001
17	$\log_{10}$TN:TP = 1.24 + 0.34 $\log_{10}$DIN:DIP	23	0.48	0.0003
18	$\log_{10}$Chl *a* on $\log_{10}$DIN	23	NS	0.22
19	$\log_{10}$Chl *a* = 1.60 + 0.72 $\log_{10}$DIP	23	0.27	0.001
20	$\log_{10}$Chl *a* = –0.23 +0.70 $\log_{10}$DSi	23	0.23	0.02
21	$\log_{10}$Chl *a* = –1.96 + 1.62 $\log_{10}$TN	23	0.81	0.0001
22	$\log_{10}$Chl *a* = 0.69 + 1.08 $\log_{10}$TP	23	0.78	0.0001

Note: *n*, sample size; r^2, coefficient of determination; *p*, significance level of *r*; NS, not significant ($p \geq 0.05$); sal, salinity; DIN, dissolved inorganic nitrogen; DIP, dissolved inorganic phosphorus; DSi, dissolved silicate; TN, total nitrogen; TP, total phosphorus; Chl *a*, chlorophyll *a*.

sely correlated with both TN and TP (Table 2, eqs. 12 and 13). Similarly, DIN:DIP was inversely correlated with DSi (Table 2, eq. 11), reflecting the almost significant correlation between DIP and DSi (Table 2, eq. 7). DSi:DIN ratios ranged from 0.5 at Diana to 267 at Vic, but Diana was the only lagoon with a DSi:DIN ratio <1. DSi:DIP ratios ranged from 17 at Bages Middle to 1640 at Salses-Leucate.

A strong positive relationship was found between TN and TP (Table 2, eq. 14). TN:TP ratios decreased from about 75 in the less eutrophic lagoons (TP < 0.80 μmol·L^{-1}) to the Redfield ratio (16:1 by moles) in the most eutrophic systems (Fig. 3; Table 2, eq. 15 and 16). There was also a significant and positive covariance between TN:TP and DIN:DIP (Table 2, eq. 17; Fig. 4).

Chl *a* varied along the eutrophication gradient from <2 μg·L^{-1} at Salses-Leucate, La Palme, Bages South, and Ayrolle to >270 μg·L^{-1} at Vendres. There was no significant correlation between DIN and Chl *a* (Table 2, eq. 18; Fig. 5). However, both DIP and DSi exhibited weak but significant correlations with Chl *a* (Table 2, eqs. 19 and 20; Fig. 5). In contrast, both TN and TP were very strongly correlated with Chl *a*, with much higher coefficients of determination than for dissolved nutrients (Table 2, eqs. 21 and 22; Fig. 6).

Discussion

Nutrient limitation assessments using dissolved inorganic nutrients

Inorganic nutrient concentrations in coastal waters reflect the integrated sum of riverine, sewage, atmospheric, and oceanic inputs, uptake, sorption, grazing, sedimentation, re-

Fig. 3. Relationship between total nitrogen (TN) and total phosphorus (TP) in oligotrophic (□), mesotrophic (△), eutrophic (■), and hypertrophic (▲) lagoons of the Languedoc–Roussillon (LR) region and Corsica. The dotted line corresponds to the Redfield ratio (16:1 by moles). See Table 2 for regression parameters and Materials and methods for an explanation of codes.

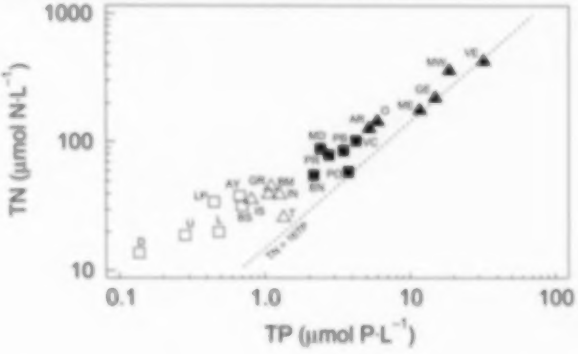

generation, burial, etc. (Fisher et al. 1992). We found that summer DIN remained at low concentrations in virtually all lagoons, whereas DIP and DSi varied largely along a range of concentrations resembling those typically found in coastal and oceanic waters (Nixon 1982; Ragueneau et al. 2002).

When compared with the dissolved nutrient based criteria for nutrient limitation suggested by Justić et al. (1995),

(1) N limitation: DIN < 1 μmol · L^{-1}; DIN:DIP < 10; DSi:DIN > 1

Fig. 4. Relationship between TN:TP and DIN:DIP in oligotrophic (□), mesotrophic (△), eutrophic (■), and hypertrophic (▲) lagoons of the Languedoc–Roussillon (LR) region and Corsica. The solid and the dotted lines correspond, respectively, to the ratios used by Justić et al. (1995) for dissolved inorganic nutrients and by Guildford and Hecky (2000) for total nutrients to discriminate phosphorus limitation from nitrogen limitation. See Table 2 for regression equations and Materials and methods for an explanation of codes.

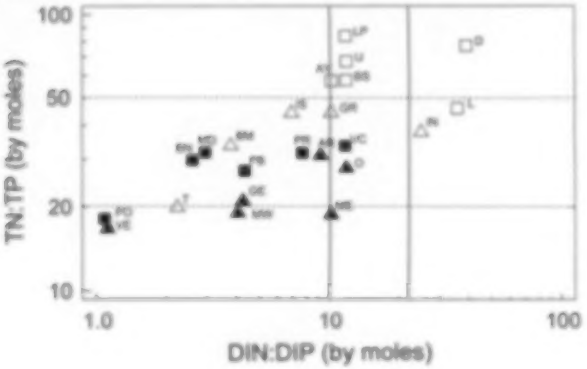

(2) P limitation: $DIP < 0.1\ \mu mol \cdot L^{-1}$; $DIN:DIP < 22$; $DSi:DIP > 22$

(3) Si limitation: $DSi < 2\ \mu mol \cdot L^{-1}$; $DSi:DIN < 1$; $DSi:DIP < 10$

the consistently high DIN:DIP ratios observed in the oligotrophic lagoons (range: 11 to 40, by moles) suggest that P was most likely to be the primary limiting nutrient for algal growth in these systems. This conclusion is consistent with the data of Souza et al. (2003) for the oligotrophic Araruama Lagoon (Brazil), as well as the conclusions of Murrell et al. (2006) and Johnson et al. (2006) for several coastal waters in Florida. These general conclusions also are consistent with Downing et al. (1999), who suggested that the role of P in primary production limitation in nonpolluted coastal waters may have been underestimated. Summer limitation by nitrogen alone seemed to become apparent above a certain level of eutrophication in the studied lagoons. Experimental nutrient enrichment bioassays carried out in parallel with this study confirmed that both nitrogen and phosphorus limit summer pelagic primary production in the oligotrophic lagoon Salses-Leucate (B. Bec, unpublished data) and that nitrogen alone was limiting in the mesotrophic lagoon Thau (Fouilland et al. 2002).

The observed accumulation of DIP along the eutrophication gradient and the inverse correlation between DIP and salinity could be explained by invoking progressively lower N:P supply ratios that reflect an increasing influence of sewage inputs on the total nutrient load (Downing and McCauley 1992). However, nowadays, sewage can be richer in N than in P because of a more effective removal of P, as is the case for the eight Palavasian and Or lagoons (Table 3). Moreover, the range of N:P loading ratios for the 13 lagoons

Fig. 5. Relationships between Chl *a* and (*a*) dissolved inorganic nitrogen (DIN), (*b*) dissolved inorganic phosphorus (DIP), and (*c*) dissolved silicate (Dsi) in oligotrophic (□), mesotrophic (△), eutrophic (■), and hypertrophic (▲) lagoons of the Languedoc–Roussillon (LR) region and Corsica. The lines in parts *b* and *c* correspond to regression equations in Table 2. See Materials and methods for an explanation of codes.

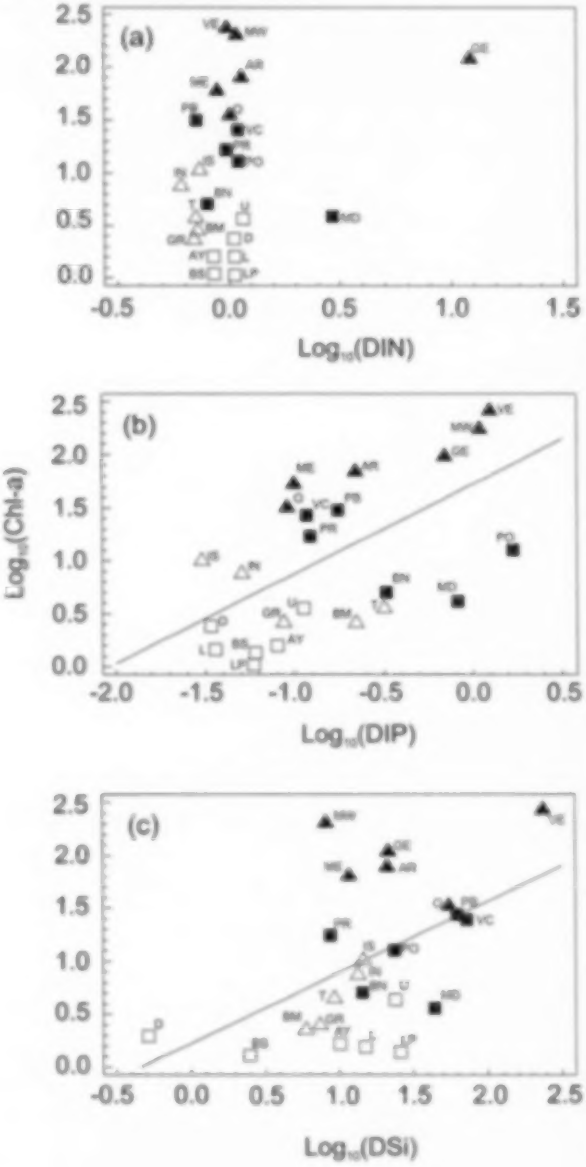

for which N and P loading data are available is narrower than the ranges of DIN:DIP and TN:TP in the water column. We tentatively conclude that the observed increase of DIP along the eutrophication gradient is better explained by the P content of lagoon sediments than by salinity and that recycling processes strongly affect inorganic nutrient concentrations in the water column (P. Souchu, unpublished data).

Fig. 6. Relationships between Chl *a* and (*a*) total nitrogen (TN) and (*b*) total phosphorus (TP) in oligotrophic (□), mesotrophic (△), eutrophic (■), and hypertrophic (▲) lagoons of the Languedoc–Roussillon (LR) region and Corsica. The lines correspond to regression equations in Table 2. See Materials and methods for an explanation of codes.

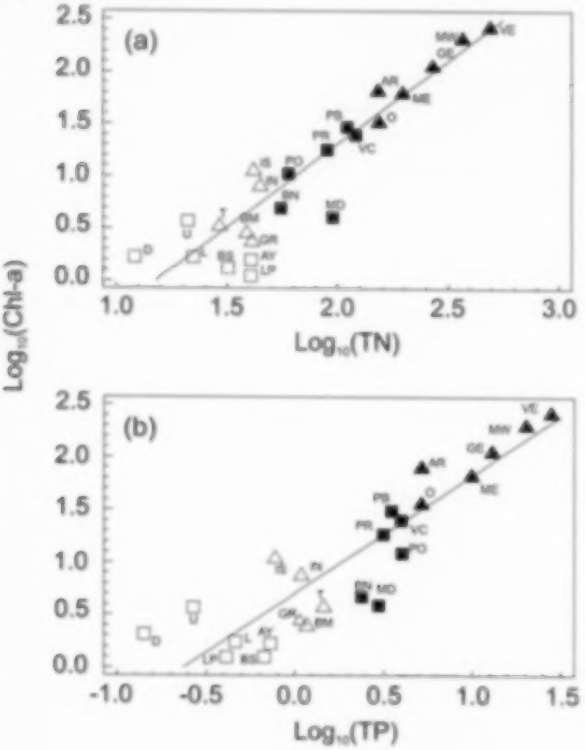

Egge and Aksnes (1992) have shown that diatoms often dominated the phytoplankton community when DSi concentrations exceeded 2 μmol·L^{-1}. However, few samples in the pooled database exhibited DSi concentrations <2 μmol·L^{-1} (13%). Moreover, based the empirical criteria in eqs. 1–3 above, the relatively high observed ratios of DSi:DIN (range: 0.5 to 267, by moles) and DSi:DIP (range: 17 to 1640, by moles) together suggest that DSi was very unlikely to limit algal growth in the studied lagoons, even at extreme levels of nutrient enrichment. The trend for DSi to accumulate along the eutrophication gradient was unexpected because DSi typically is not increased by any significant extent during anthropogenic N and P enrichment (Conley et al. 1993). Indeed, several authors have reported a pattern of species shifts towards phytoplankton species other than diatoms as a consequence of DSi depletion in nutrient-enriched waters (Anderson et al. 2002; Turner 2002). However, phytoplanktonic proliferation induces an accumulation in sediments of diatom frustules, the dissolution of which can lead to summer DSi maxima (Aller and Benninger 1981). The similarity of DIP and DSi relationships with Chl *a* (see below), which suggests the accumulation of both dissolved nutrients along the eutrophication gradient, could potentially result from the recycling of phytoplankton at the water–sediment interface in the studied lagoons (P. Souchu, unpublished data.).

Nutrient limitation assessments using total nutrients

Guildford and Hecky (2000) proposed the following criteria for N and P limitation assessment in lake and ocean waters, using molar ratios of total nitrogen and total phosphorus (eqs. 4–6):

(4) N limitation: TN:TP < 20

(5) N and P limitation: TN:TP = 20 – 40

(6) P limitation: TN:TP > 50

Based on these empirical thresholds, we conclude that the most oligotrophic lagoons in this study were consistently limited by P. For a majority of the studied lagoons, the phytoplankton production was likely limited by both N and P (TN:TP = 20–50). The three lagoons having TN:TP < 20 (Vendres, Méjean West, and Ponant) were also those for which the median summer DIP concentration was in excess (>1 μmol·L^{-1}), providing additional evidence that P was unlikely to limit net primary production in these low N:P ratio systems. Summer limitation of algal growth by N thus may only occur in more mesotrophic Mediterranean coastal lagoons with a tendency towards increasingly likelihood of N limitation as eutrophication increases; consequently, transitions from limitation by P to limitation by N may be considered as an indication of anthropogenic eutrophication in these systems.

The convergence of the limnological and marine approaches in lagoons is evident from the positive and high correlation between DIN:DIP and TN:TP (Table 2, eq. 17). The relationship suggests that TN:TP = 45 when DIP:DIN is 16, a value that is close to the empirical TN:TP threshold proposed by Guildford and Hecky (2000). However, if the decrease of DIN:DIP along the eutrophication gradient (Table 2, eq. 13) is clearly due to DIP accumulation, the TN:TP ratio decrease (Table 2, eq. 16) is more difficult to explain as TN and TP are a mixture of inorganic nutrients, dissolved organic matter (DOM), and seston. In the study lagoons, regarding the low contribution of inorganic nutrients to TN and TP (ca. 10%), TN and TP can be considered as essentially made up of seston and DOM. The N:P ratios in DOM are largely higher than the Redfield ratio (Hopkinson and Vallino 2005), whereas the TN:TP ratios in sestonic organic matter would display values closer to the Redfield ratio (Hall et al. 2005). As Chl *a* concentrations increase, TN and TP are increasingly determined by the N and P content of the phytoplankton cells (see Wetzel (2001) for DON and PON in lakes). This trend may help to explain why TN:TP ratios move closer to the Redfield ratio as eutrophication increases. In hypertrophic lagoons (Vendres), the planktonic biomass is high enough that TN:TP ratios are close to 16.

Nutrient controls of algal biomass

The predictive power of using a total nutrient based approach for the prediction of summer median algal biomass is strongly evident in the lagoons studied here: total N and total P based regression models for summer median Chl *a*

Table 3. Contribution of sewage to total inputs of N and P in 13 lagoons for which the watershed is well defined (N. Dupré, unpublished data).

	Contribution of sewage to total inputs (%)					
Lagoons	N	P	TN:TP in sewage	TN:TP in total inputs	DIN:DIP in water	TN:TP in water
Bages-Sigean	39	12	26.5	33.1	4.9	41
La Palme	37	14	3.4	16.0	11.4	85
Leucate	39	21	8.9	16.5	36.5	46
Or	49	55	24.0	27.4	11.5	29
Palavasian (8)	87	77	26.2	23.0	7.7	29
Thau	34	46	10.7	14.7	2.2	21

Note: N:P ratios (by moles) in sewage and inputs are compared with ratios in lagoon waters. For Bages-Sigean and the eight Palavasian lagoons, N:P ratios in the water correspond to pooled data from all stations.

were consistently more superior to comparable DIN- and DIP-based models (compare Figs. 5 and 6). In fact, there was no correlation between concentrations of DIN and Chl *a* (Table 2, eq. 18), and both DIP and DSi exhibited only weak correlations with Chl *a* (Table 2, eqs. 19 and 20). It is also very important to note that the simple regression model reported here for summer median TP and Chl *a* in coastal Mediterranean lagoons,

$$(7) \quad \log \text{Chl}\,a = 0.690 + 1.08 \log \text{TP}, \quad r^2 = 0.78$$

confirms the strongly positive relationship observed by Knoppers et al. (1991; data not shown) for annual average TP and Chl *a* in six coastal lagoons in Brazil:

$$(8) \quad \log \text{Chl}\,a = 0.017 + 2.02 \log \text{TP}, \quad r^2 = 0.92$$

as well as that observed between annual median TP and summer median Chl *a* in 15 coastal embayments in Germany (Sagert et al. 2008; data not shown):

$$(9) \quad \log \text{Chl}\,a = 0.601 + 1.24 \log \text{TP}, \quad r^2 = 0.83$$

A similarly strong relationship has been found between summer mean concentrations of TP and Chl *a* in the hypertrophic Vistonis Lagoon, Greece (Gikas et al. 2006; data not shown):

$$(10) \quad \log \text{Chl}\,a = 0.300 + 2.367 \log \text{TP}, \quad r^2 = 0.92$$

as well as in numerous other comparative analyses of freshwater and marine ecosystems (Prairie et al. 1989; Champion and Currie 2000; Smith 2006).

Moreover, Boynton et al. (1996) found significant relationships between annual TN loading rates and average TN and Chl *a* concentrations for Maryland coastal bays, even without making any adjustments for hydraulic residence time. We found very significant relationships between annual total N and P loading rates and median TN and TP concentrations for the 13 lagoons with well-defined watersheds (Table 3), without making any adjustments for their hydraulic residence time ($r^2 = 0.85$ and 0.94 for N and P, respectively; ANOVA $p < 0.05$; N. Dupré, unpublished data, available from author T. Laugier). Soballe and Kimmel (1987) have suggested that algal production per unit P in water increases in the sequence rivers < impoundments < natural lakes and suggested that we view aquatic systems as occupying positions along a continuum ordered by water residence time. The Mediterranean lagoons studied here appear to behave very similarly to lakes because they have relatively long hydraulic residence times due to their low tidal amplitudes (Bacher et al. 1995).

Implications for eutrophication management

As noted by Rabalais et al. (2009), coastal water quality is currently on the decline, and excessive exports of nutrients from the land to the world's coastal oceans will almost certainly continue to occur unless societal intervention or changes in human culture are successfully pursued. Our cross-system comparison of Chl *a* and nutrients from 20 coastal Mediterranean lagoons suggests that the identity of the primary growth-limiting nutrient in these systems may shift from P alone in oligotrophic lagoons to N alone as eutrophication proceeds. We tentatively conclude that like most unenriched freshwater systems, pristine coastal French Mediterranean lagoons may typically be P-limited.

A critical need remains for water resource managers to reduce nutrient loads to reduce the negative effects of global eutrophication and prevent further degradation (Rabalais et al. 2009). The management of eutrophication will require careful assessments of whether N, P, or both N and P should be controlled to develop successful and cost-effective strategies for the control of coastal zone eutrophication. We note, however, that Elser et al. (2007) found that although enrichment by either N or P can increase autotroph production, a simultaneous increase in both nutrients leads to dramatically higher levels of production in nearly all situations. We surmise that the converse response also can be expected to occur (i.e., simultaneous reductions in both N and P will minimize algal production), and we thus favor joint N and P loading control to protect estuarine and coastal marine environments. However, such management decisions will need to be based on careful syntheses of current and historical data (e.g., Conley et al. 2009; Paerl 2009), as well as quantitative and objective frameworks for the assessment of coastal zone water quality.

Strong relationships between Chl *a* and total nutrient and empirical models predicting in-lake P concentrations as a function of annual P load have been essential tools for management of eutrophication in lakes for more than three decades (Vollenweider 1976; OECD 1982). We concur with Hoyer et al. (2002) that an approach using total nutrients is

similarly valid for eutrophication modeling in marine systems, and as shown by the data presented here, it is in fact superior to approaches that rely on concentrations and ratios of dissolved inorganic nutrients. However, Cloern (2001) has suggested that differences between the eutrophication response of lakes and coastal waters to eutrophication potentially may result from system-specific attributes acting as filters that may modulate their respective responses to enrichment. We thus urge other researchers worldwide to test the utility of this empirical approach in coastal waters that exhibit a wide range of physicochemical, biological, and hydrological characteristics to confirm if the tools and methods that have been so very successful in the management of freshwater eutrophication are also broadly applicable to coastal marine ecosystems.

Acknowledgements

This paper uses unpublished raw data from the Lagoon Monitoring Network (Réseau de Suivi Lagunaire) financed by Agence de l'Eau, Région Languedoc–Roussillon and Ifremer. This paper also was supported in part by NSF DMS–0342239 to Val H. Smith. We thank the staff of the Ifremer laboratories in Corsica and Languedoc–Roussillon and of the Parc Naturel Régional de la Narbonnaise. The authors are grateful to anonymous reviewers for their comments on the paper. This paper is dedicated to Nicolas Dupré (1978–2008).

References

Aller, R.C., and Benninger, L.K. 1981. Spatial and temporal patterns of dissolved ammonium, manganese and silica fluxes from bottom sediments in Long Island Sound, U.S.A. J. Mar. Res. **39**: 295–314.

Aloisi, J.C., and Gadel, F. 1992. Mécanismes sédimento–génétiques et évolution d'un écosystème lagunaire Méditerranéen: L'étang de Vendres (Hérault). Vie Milieu, **42**: 165–183.

Aminot, A., and Kérouel, R. 2004. Hydrologie des écosystèmes marins. Paramètres et analyses. Ifremer, Brest, France.

Anderson, D.M., Glibert, P.M., and Burkholder, J.M. 2002. Harmful algal blooms and eutrophication: nutrient sources, composition, and consequences. Estuaries, **25**(4): 704–726. doi:10.1007/BF02804901.

Bacher, C., Bioteau, H., and Chapelle, A. 1995. Modelling the impact of a cultivated oyster population on the nitrogen dynamics: the Thau lagoon case (France). Ophelia, **42**: 29–54.

Boutière, H., de Bovée, F., Delille, D., Fiala, M., Gros, C., Jacques, G., Knoepffler, M., Labat, J.P., Panouse, M., and Soyer, J. 1982. Effet d'une crise dystrophique dans l'étang de Salses–Leucate. *In* Proceedings International Symposium on Coastal Lagoons, SCOR/IABO/UNESCO (Bordeaux, 8–14 September 1981). Oceanol. Acta, **4**(Suppl.): 231–242.

Boynton, W.R., Murray, L., Hagy, J.D., Stokes, C., and Kemp, W.M. 1996. A comparative analysis of eutrophication patterns in a temperate coastal lagoon. Estuaries, **19**(2): 408–421. doi:10.2307/1352459.

Champion, M., and Currie, D.J. 2000. Phosphorus–chlorophyll relationships in lakes, rivers, and estuaries. Verh. Int. Ver. Theor. Angew. Limnol. **27**: 1986–1989.

Cloern, J.E. 2001. Our evolving conceptual model of the coastal eutrophication problem. Mar. Ecol. Prog. Ser. **210**: 223–253. doi:10.3354/meps210223.

Conley, D.J., Schelske, C.L., and Stoermer, E.F. 1993. Modification of the biogeochemical cycle of silica with eutrophication. Mar. Ecol. Prog. Ser. **101**: 179–192. doi:10.3354/meps101179.

Conley, D.J., Paerl, H.W., Howarth, R.W., Boesch, D.F., Seitzinger, S.P., Havens, K.E., Lancelot, C., and Likens, G.E. 2009. Ecology. Controlling eutrophication: nitrogen and phosphorus. Science (Washington, D.C.), **323**(5917): 1014–1015. doi:10.1126/science.1167755. PMID:19229022.

Dodds, W.K. 2003. Misuse of inorganic N and soluble reactive P concentrations to indicate nutrient status of surface waters. J. N. Am. Benthol. Soc. **22**(2): 171–181. doi:10.2307/1467990.

Downing, J.A. 1997. Marine nitrogen:phosphorus stoichiometry and the global N:P cycle. Biogeochemistry, **37**(3): 237–252. doi:10.1023/A:1005712322036.

Downing, J.A., and McCauley, E. 1992. The nitrogen:phosphorus relationship in lakes. Limnol. Oceanogr. **37**: 936–945.

Downing, J.A., Osenberg, C.W., and Sarnelle, O. 1999. Meta-analysis of marine nutrient-enrichments: variations in the magnitude of nutrient limitation. Ecology, **80**(4): 1157–1167. doi:10.1890/0012-9658(1999)080[1157:MAOMNE]2.0.CO;2.

Duarte, C.M. 1995. Submerged aquatic vegetation in relation to different nutrient regimes. Ophelia, **41**: 87–112.

Egge, J.K., and Aksnes, D.L. 1992. Silicate as regulating nutrient in phytoplankton competition. Mar. Ecol. Prog. Ser. **83**: 281–289. doi:10.3354/meps083281.

Elser, J.J., Marzolf, E.R., and Goldman, C.R. 1990. Phosphorus and nitrogen limitation of phytoplankton growth in the freshwaters of North America: a review and critique of experimental enrichments. Can. J. Fish. Aquat. Sci. **47**(7): 1468–1477. doi:10.1139/f90-165.

Elser, J.J., Bracken, M.E.S., Cleland, E.E., Gruner, D.S., Harpole, W.S., Hillebrand, H., Ngai, J.T., Seabloom, E.W., Shurin, J.B., and Smith, J.E. 2007. Global analysis of nitrogen and phosphorus limitation of primary producers in freshwater, marine and terrestrial ecosystems. Ecol. Lett. **10**(12): 1135–1142. doi:10.1111/j.1461-0248.2007.01113.x. PMID:17922835.

European Economic Community. 2000. Directive 2000/60/EC of the European parliament and of the Council of 23 October 2000 establishing a framework for Community action in the field of water policy. Official Journal of the European Community, 22/12/2000, L327, volume 43. Available at http://eur-lex.europa.eu/LexUriServ/LexUriServ.do?uri=OJ:L:2000:327:0001:0072:EN:PDF.

European Environment Agency. 1999. State and pressures of the marine and coastal Mediterranean environment. European Environment Agency, Copenhagen, Denmark.

Fisher, T.R., Peele, E.R., Ammerman, J.W., and Harding, L.W., Jr. 1992. Nutrient limitation of phytoplankton in Chesapeake Bay. Mar. Ecol. Prog. Ser. **82**: 51–63. doi:10.3354/meps082051.

Fisher, T.R., Melack, J.M., Grobbelaar, J.U., and Howarth, R.W. 1995. Nutrient limitation of phytoplankton and eutrophication of inland, estuarine, and marine waters. *In* Phosphorus in the global environment: transfers, cycles and management. *Edited by* H. Tiessen. Wiley and Sons, New York. pp. 301–322.

Fouilland, E., Descolas-Gros, C., Collos, Y., Vaquer, A., Souchu, P., Gasc, A., Bibent, B., and Pons, V. 2002. Influence of nitrogen enrichment on size-fractionated in vitro carboxylase activities of phytoplankton from Thau lagoon (Coastal Mediterranean Lagoon, France). J. Exp. Mar. Biol. Ecol. **275**(2): 147–171. doi:10.1016/S0022-0981(02)00235-6.

Frisoni, G.F., Guelorget, O., Ximenes, M.C., and Perthuisot, J.P. 1983. Etude écologique de trois lagunes de la plaine orientale Corse (Biguglia, Diana, Urbino): expressions biologiques qualitatives et quantitatives du confinement. J. Rech. Oceanogr. **8**: 57–80.

Gikas, G.D., Yiannakopoulou, T., and Tsihrintzis, V.A. 2006.

Water quality trends in a coastal lagoon impacted by non-point source pollution after implementation of protective measures. Hydrobiologia, **563**(1): 385–406. doi:10.1007/s10750-006-0034-2.

Guildford, S.J., and Hecky, R.E. 2000. Total nitrogen, total phosphorus, and nutrient limitation in lakes and oceans: is there a common relationship? Limnol. Oceanogr. **45**: 1213–1223.

Hall, S.R., Smith, V.H., Lythe, D.A., and Leibold, M.A. 2005. Constraints on primary producer N:P stoichiometry along N:P supply ratio gradients. Ecology, **86**(7): 1894–1904. doi:10.1890/04-1045.

Hopkinson, C.S., Jr., and Vallino, J.J. 2005. Efficient export of carbon to the deep ocean through dissolved organic matter. Nature (London), **433**(7022): 142–145. doi:10.1038/nature03191. PMID:15650735.

Hoyer, M.V., Frazer, T.K., Notestein, S.K., and Canfield, D.E., Jr. 2002. Nutrient, chlorophyll, and water clarity relationships in Florida's nearshore coastal waters with comparisons to freshwater lakes. Can. J. Fish. Aquat. Sci. **59**(6): 1024–1031. doi:10.1139/f02-077.

Ignatiades, L. 2005. Scaling the trophic status of the Aegean Sea, eastern Mediterranean. J. Sea Res. **54**(1): 51–57. doi:10.1016/j.seares.2005.02.010.

Jacques, G., Cahet, G., Fiala, M., Neveux, J., and Panouse, M. 1975. Caractéristiques du milieu pélagique des étangs de Bages-Sigean et de Salses-Leucate pendant l'été 1974. Vie Milieu, **25**: 1–18.

Johnson, M.W., Heck, K.L., Jr., and Fourqurean, J.W. 2006. Nutrient content of seagrasses and epiphytes in the northern Gulf of Mexico: evidence of phosphorus and nitrogen limitation. Aquat. Bot. **85**(2): 103–111. doi:10.1016/j.aquabot.2006.02.003.

Justić, D., Rabalais, N.N., Turner, E., and Dortch, Q. 1995. Changes in nutrient structure of river-dominated coastal waters: stoichiometric nutrient balance and its consequences. Estuar. Coast. Shelf Sci. **40**(3): 339–356. doi:10.1016/S0272-7714(05)80014-9.

Knoppers, B., Kjerfve, B., and Carmouze, J.-P. 1991. Trophic state and water turn-over time in six choked coastal lagoons in Brazil. Biogeochemistry, **14**(2): 149–166. doi:10.1007/BF00002903.

Lewis, W.M., Jr., and Wurtsbaugh, W.A. 2008. Control of lacustrine phytoplankton by nutrients: erosion of the phosphorus paradigm. Int. Rev. Hydrobiol. **93**(4-5): 446–465. doi:10.1002/iroh.200811065.

Meeuwig, J.J., Kauppila, P., and Pitkänen, H. 2000. Predicting coastal eutrophication in the Baltic: a limnological approach. Can. J. Fish. Aquat. Sci. **57**(4): 844–855. doi:10.1139/cjfas-57-4-844.

Menzel, D.W., and Corwin, N. 1965. The measurement of total phosphorus in seawater based on the liberation of organically bound fractions by persulfate oxidation. Limnol. Oceanogr. **10**: 280–282.

Murrell, M.C., Stanley, R.S., Lores, E.M., DiDonato, G.T., Smith, L.M., and Flemer, D.A. 2006. Evidence that phosphorus limits phytoplankton growth in a Gulf of Mexico estuary: Pensacola Bay, Florida, USA. Bull. Mar. Sci. **79**: 155–167.

Neveux, J., and Lantoine, F. 1993. Spectrofluorimetric assay of chlorophylls and phaepigments using the least squares approximation technique. Deep-Sea Res. **40**(9): 1747–1765. doi:10.1016/0967-0637(93)90030-7.

Nixon, S.W. 1982. Nutrient dynamics, primary production and fisheries yields of lagoons. *In* Proceedings of International Symposium on Coastal Lagoons, SCOR/IABO/UNESCO (Bordeaux, France, 8–14 September 1981). Oceanol Acta. **4**(Suppl.): 357–371.

Nixon, S.W. 1995. Coastal marine eutrophication: a definition, social causes, and future concerns. Ophelia, **41**: 199–219.

Organisation for Economic Cooperation and Development. 1982. Eutrophication of waters: monitoring, assessment and control. Organisation for Economic Cooperation and Development (OECD), Paris, France.

Paerl, H.W. 2009. Controlling eutrophication along the freshwater–marine continuum: dual nutrient (N and P) reductions are essential. Estuaries Coasts, **32**(4): 593–601. doi:10.1007/s12237-009-9158-8.

Prairie, Y.T., Duarte, C.M., and Kalff, J. 1989. Unifying nutrient–chlorophyll relationships in lakes. Can. J. Fish. Aquat. Sci. **46**(7): 1176–1182. doi:10.1139/f89-153.

Rabalais, N.N., Turner, R.E., Díaz, R.J., and Justić, D. 2009. Global change and eutrophication of coastal waters. ICES J. Mar. Sci. **66**(7): 1528–1537. doi:10.1093/icesjms/fsp047.

Ragueneau, O., Lancelot, C., Egorov, V., Vervlimmeren, J., Cociasu, A., Déliat, G., Krastev, A., Daoud, N., Rousseau, V., Popovitchev, V., Brion, N., Popa, L., and Cauwet, G. 2002. Biogeochemical transformations in inorganic nutrients in the mixing zone between the Danube River and the north-western Black Sea. Estuar. Coast. Shelf Sci. **54**(3): 321–336. doi:10.1006/ecss.2000.0650.

Raimbault, P., and Slawyk, G. 1991. A semiautomatic, wet-oxidation method for the determination of particulate organic nitrogen collected on filters. Limnol. Oceanogr. **36**: 405–408.

Ryther, J.H., and Dunstan, W.M. 1971. Nitrogen, phosphorus, and eutrophication in the coastal marine environment. Science (Washington, D.C.), **171**(975): 1008–1013. doi:10.1126/science.171.3975.1008. PMID:4993386.

Sagert, S., Rieling, T., Eggert, A., and Schubert, H. 2008. Development of a phytoplankton indicator system for the ecological assessment of brackish coastal waters (German Baltic Sea coast). Hydrobiologia, **611**(1): 91–103. doi:10.1007/s10750-008-9456-3.

Schindler, D.W. 1977. Evolution of phosphorus limitation in lakes. Science (Washington, D.C.), **195**(4275): 260–262. doi:10.1126/science.195.4275.260. PMID:17787798.

Schramm, W. 1999. Factors influencing seaweed responses to eutrophication: some results from EU-project EUMAC. J. Appl. Phycol. **11**(1): 69–78. doi:10.1023/A:1008076026792.

Smith, V.H. 2003. Eutrophication of freshwater and coastal marine ecosystems: a global problem. Environ. Sci. Pollut. Res. **10**(2): 126–139. doi:10.1065/espr2002.12.142.

Smith, V.H. 2006. Responses of estuarine and coastal marine phytoplankton to nitrogen and phosphorus enrichment. Limnol. Oceanogr. **51**: 377–384.

Soballe, D.M., and Kimmel, B.L. 1987. A large-scale comparison of factors influencing phytoplankton abundance in rivers, lakes and impoundments. Ecology, **68**(6): 1943–1954. doi:10.2307/1939885.

Souchu, P., Vaquer, A., Collos, Y., Landrein, S., Deslous-Paoli, J.-M., and Bibent, B. 2001. Influence of shellfish farming activities on the biogeochemical composition of the water column in Thau lagoon. Mar. Ecol. Prog. Ser. **218**: 141–152. doi:10.3354/meps218141.

Souza, M.F.L., Kjerfve, B., Knoppers, B., Landim de Souza, W.F., and Damasceno, R.N. 2003. Nutrient budgets and trophic states in a hypersaline coastal lagoon: Lagoa de Araruama, Brazil. Estuar. Coast. Shelf Sci. **57**(5-6): 843–858. doi:10.1016/S0272-7714(02)00415-8.

Tréguer, P., and Le Corre, P. 1975. Manuel d'analyse des sels nutritifs dans l'eau de mer. Utilisation de l'auto analyseur II, Technicon. L.O.C. Université Bretagne Occidentale, Brest, France.

Turner, R.E. 2002. Element ratios and aquatic food webs. Estuaries, **25**(4): 694–703. doi:10.1007/BF02804900.

Vollenweider, R.A. 1976. Advances in defining critical loading levels of phosphorus in lake eutrophication. Mem. Ist. Ital. Idrobiol. **33**: 53–83.

Wetzel, R.G. 2001. Limnology: lake and river ecosystems. Academic Press, San Diego, California.

Wilke, M., and Boutière, H. 2000. Hydrobiological, physical and chemical characteristics and spatio-temporal dynamics of an oligotrophic Mediterranean lagoon: The étang de La Palme (France). Vie Milieu, **50**: 101–115.

A comparison of pre-industrial and present-day changes in *Bosmina* and *Daphnia* size structure from soft-water Ontario lakes

Jennifer B. Korosi, Andrew M. Paterson, Anna M. DeSellas, and John P. Smol

Abstract: Understanding the long-term controls on cladoceran size structure has important implications for aquatic ecosystems. Although there has been considerable interest in zooplankton size trends for Canadian Shield lakes, data are not available for zooplankton size structure prior to the period of anthropogenic disturbances. Here, we present pre- and post-impact size data for the common pelagic cladocerans *Bosmina* and *Daphnia* for 44 well-studied Shield lakes in south-central Ontario (Canada). We show that *Daphnia* were larger and that the length of *Bosmina* body appendages (mucrones and antennules) was longer in pre-industrial times than they are today. The reduction in *Bosmina* appendage length we observed may suggest a reduction in copepod predation pressure since pre-industrial times. Reduced maximum body size in *Daphnia* is a predicted response to a warming climate in north temperate lakes; however, we suggest that alternate explanations, specifically acidification and subsequent recovery following emission reductions, should also be explored as the primary drivers of *Daphnia* size changes in this lake set. Overall, our results highlight the importance of pre-impact data for understanding the long-term controls on cladoceran body size from pre-1850 to present.

Résumé : La compréhension des facteurs qui contrôlent à long terme la structure en taille des cladocères peut avoir des incidences importantes sur l'étude des écosystèmes aquatiques. Bien que l'on se soit beaucoup intéressé aux tendances dans la taille du zooplancton dans les lacs du Bouclier canadien, il n'existe pas de données sur la structure en taille du zooplancton pour la période antérieure aux perturbations anthropiques. Nous présentons ici des données d'avant et d'après l'impact sur les cladocères pélagiques communs *Bosmina* et *Daphnia* dans 44 lacs bien étudiés du bouclier dans le centre-sud de l'Ontario (Canada). Nous montrons que les *Daphnia* étaient plus grands et que la longueur des appendices corporels (mucrons et antennules) des *Bosmina* étaient plus importante durant la période préindustrielle qu'actuellement. La réduction de la longueur des appendices des *Bosmina* que nous observons peut laisser croire à une réduction de la pression de prédation de la part des copépodes depuis la période préindustrielle. La réduction de la taille maximale chez *Daphnia* est une réaction prédite au réchauffement climatique dans les lacs tempérés boréaux; cependant, nous suggérons que des explications de rechange, en particulier l'acidification et le rétablissement qui a suivi la réduction des émissions, devraient aussi être explorées comme facteurs explicatifs principaux des changements de taille des *Daphnia* dans cet ensemble de lacs. Globalement, nos résultats soulignent l'intérêt des données d'avant l'impact pour comprendre les facteurs qui contrôlent à long terme la taille corporelle des cladocères d'avant 1850 jusqu'à aujourd'hui.

[Traduit par la Rédaction]

Introduction

Body size of the pelagic cladocerans *Daphnia* and *Bosmina* are useful indicators of ecosystem status. Predation on Cladocera is largely size-selective, and fish predation in particular is often strongest on larger-bodied daphniid taxa (Brooks and Dodson 1965). Furthermore, increases in the length of *Bosmina* body appendages (mucrones and antennules) typically reflect higher abundances of invertebrate predators, as these features increase predator handling time and provide *Bosmina* with escape opportunities (Kerfoot 1974, 1978). Body size also has implications for nutrient cycling in lakes, as smaller individuals cycle nutrients less efficiently, but at a faster rate (Gliwicz 1990). In recognition of the importance of size structure to ecosystem functioning, the long-term zoological monitoring program of lakes in the Muskoka–Haliburton region of south-central Ontario, Canada (Dorset Environmental Science Centre, Ontario Ministry of the Environment), has collected size data regularly since the ~1980s. These data sets are important for lake managers

Received 1 April 2009. Accepted 29 December 2009. Published on the NRC Research Press Web site at cjfas.nrc.ca on 25 March 2010. J21135

J.B. Korosi,[1] A.M. DeSellas,[2] and J.P. Smol. Paleoecological Environmental Assessment and Research Laboratory (PEARL), Department of Biology, Queen's University, Kingston, ON K7L 3N6, Canada.
A.M. Paterson. Ontario Ministry of the Environment, Dorset Environmental Science Centre, 1026 Bellwood Acres Road, P.O. Box 39, Dorset, ON P0A 1E0, Canada.

[1]Corresponding author (e-mail: Jennifer.Korosi@queensu.ca).
[2]Present address: Ontario Ministry of the Environment, Dorset Environmental Science Centre, 1026 Bellwood Acres Road, P.O. Box 39, Dorset, ON P0A 1E0, Canada.

Fig. 1. Map of south-central Ontario, Canada, with solid circles representing the locations of the 44 study lakes.

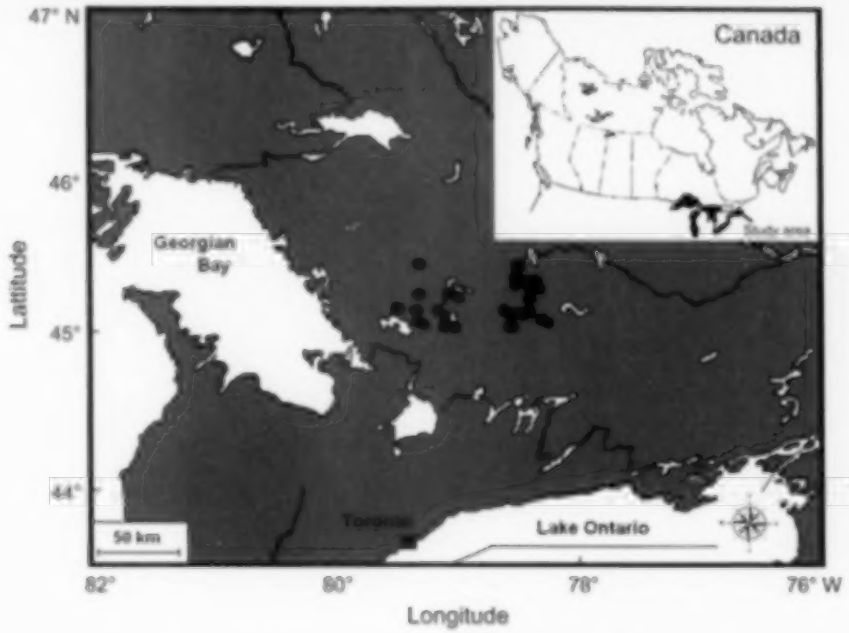

attempting to assess the impacts of multiple anthropogenic stressors on aquatic ecosystems. Nonetheless, pre-impact (i.e., prior to ~1850) data on cladoceran body size are required to put modern-day changes in a long-term context (Smol 2008).

Bosmina and *Daphnia* are usually well represented in lake sediment records, and the potential exists to apply paleolimnological techniques to provide missing regional pre-impact size data. To date, however, relatively few paleolimnological studies on cladoceran body size have been conducted, with most examining changes in size structure through time in relation to a known lake event (e.g., lake fertilization (Hann et al. 1994) and fish introductions (Salo et al. 1989)). The applicability of size structure as a regional indicator of ecosystem change has received considerably less attention. For example, Korosi et al. (2008) relate the size of *Bosmina* and *Daphnia* microfossils in the surface sediments of 42 south-central Ontario lakes to pH, dissolved organic carbon (DOC), and total phosphorus, whereas Alexander and Hotchkiss (2010) provide a surface sediment calibration set for the reconstruction of zooplankton community size structure using *Bosmina* mucro and antennule lengths. Collectively, these two studies highlight the potential applications of cladoceran body size as a regional indicator of ecosystem change.

Our main objective in this present study was to provide (using paleolimnological techniques) pre- and post-impact data on *Bosmina* and *Daphnia* body size in 44 lakes in south-central Ontario (Fig. 1) and, consequently, further insights on the factors influencing zooplankton communities in Shield lakes. Lakes in south-central Ontario have undergone known changes in water quality since the onset of anthropogenic stressors (e.g., Hall and Smol 1996). Furthermore, *Bythotrephes longimanus*, a predatory Cladocera, had invaded eight of these study lakes, including Devine, Harp, Kimball, Nunikani, Leonard, Red Pine, Sherborne, and Young at the time of sediment collection (M. Palmer and N.D. Yan, Department of Biology, York University, 4700 Keele Street Toronto, ON M3J 1P3, Canada, unpublished data). Therefore, we expect significant, directional changes in *Bosmina* and *Daphnia* size measurements to have occurred in the region since pre-industrial times, although the interaction of multiple stressors in nature can make it difficult to predict the direction and magnitude of change. To assess these hypotheses, we initiated a paleolimnological study designed to determine changes in size structure between present-day (2004–2005) and pre-industrial times (pre-1850s) in this well-studied set of 44 Shield lakes from south-central Ontario.

Materials and methods

Forty-four study lakes were sampled within the Muskoka–Haliburton region of south-central Ontario (Fig. 1). Climate in this region is north temperate, and the catchment is comprised of mixed coniferous–deciduous forests with moderate shoreline development related to cottage use on many lakes. This region is underlain by granitic Precambrian Shield bedrock with thin, glacial tills and a naturally low buffering capacity, resulting in soft-water lakes that are sensitive to acidic deposition (Chapman and Putnam 1984). The 44 study lakes are mostly oligotrophic, with circumneutral pH, and range broadly in maximum depth (5.8–61.0 m) and surface area (5.4–679.0 ha; Table 1). These lakes are currently subjected to several interacting anthropogenic stressors that have changed the ecological characteristics of these systems considerably. Acidic deposition from long-range sources is still impacting this region (Neary et al. 1990), although pH

Table 1. Physical and chemical data for the 44 study lakes in south-central Ontario.

Lake	Latitude (°N)	Longitude (°W)	Area (ha)	Z_{max} (m)	TP_{avg} (μg·L^{-1})	pH	DOC (mg·L^{-1})
Axe	45.23	79.30	264.0	15.0	12.0	5.2	10.3
Bassbaum	45.07	78.28	47.3	24.0	6.1	6.6	4.7
Bigwind	45.03	79.03	110.0	32.0	6.0	6.4	3.8
BlueChalk	45.12	78.56	52.4	23.0	7.0	6.8	2.4
Bonnechere	45.28	78.35	105.0	21.4	5.9	6.1	4.2
Brandy	45.06	79.31	108.0	7.5	27.8	6.7	12.7
Buck	45.23	79.00	40.3	30.0	6.5	6.4	3.3
Chub	45.13	78.59	34.4	27.0	9.5	5.8	5.8
Cinder E.	45.04	78.56	50.1	36.5	12.3	5.7	6.8
Cinder W.	45.04	78.56	26.9	16.0	13.4	5.9	6.5
Cradle	45.28	78.35	17.9	33.3	6.5	6.1	2.2
Crosson	45.05	79.02	56.7	25.0	9.5	5.8	7.4
Crown	45.26	78.40	136.0	30.0	4.8	6.4	2.7
Delano	45.31	78.36	23.9	18.6	8.3	6.1	6.5
Devine*	45.12	79.14	40.1	8.8	11.5	6.2	6.4
Dickie	45.09	79.05	93.6	12.0	9.6	6.0	5.9
Glen	45.08	78.30	16.3	15.0	8.9	8.0	4.4
Hamer	45.14	79.48	35.2	8.5	12.2	6.0	9.0
Harp*	45.23	79.07	71.4	37.5	6.3	6.4	4.2
Healey	45.05	79.11	122.0	7.0	10.4	6.4	6.5
Henry	45.08	79.06	21.4	5.8	6.2	5.9	3.8
Kimball*	45.21	78.41	213.0	61.0	3.6	6.2	3.1
Leech	45.03	79.06	82.0	13.7	7.9	6.2	5.3
Leonard*	45.04	79.27	195.0	15.2	6.9	6.4	4.2
Little Clear	45.24	79.00	10.9	25.0	7.0	6.6	3.0
Maggie	45.30	78.52	138.6	31.0	4.5	5.8	2.4
McKay	45.03	79.10	121.5	19.5	8.9	6.6	5.5
Moot	45.09	79.10	46.2	7.9	13.0	5.9	6.8
Nunikani*	45.12	78.44	116.0	24.0	4.6	6.4	3.7
Pearceley	45.42	79.30	44.1	8.1	4.8	5.5	1.9
Pincher	45.34	78.51	42.1	15.5	4.5	5.8	2.5
Plastic	45.11	78.50	32.1	16.3	6.3	5.6	2.4
Poker East	45.03	78.56	5.4	20.5	10.6	6.2	6.8
Poker West	45.03	78.56	15.3	17.5	10.3	6.5	6.3
Red Chalk E.	45.11	78.56	13.1	19.0	6.1	6.5	3.2
Red Chalk M.	45.11	78.56	44.1	38.0	11.1	5.9	3.4
Red Pine*	45.12	78.42	365.0	38.7	4.3	6.2	3.3
Saw	45.03	79.02	27.7	13.1	14.6	6.1	8.3
Sherborne*	45.11	78.47	252.0	35.1	4.4	6.2	3.4
Smoke	45.31	78.41	679.0	55.0	5.0	6.5	3.7
Solitaire	45.22	79.00	124.0	31.0	7.6	6.5	2.4
Timberwolf	45.41	78.48	167.0	20.4	5.9	6.3	4.7
Walker	45.24	79.05	68.2	17.0	5.2	6.7	4.1
Young*	45.13	79.33	105.9	21.1	7.9	6.8	3.4

Note: Lakes denoted by an asterisk (*) had the invasive cladoceran *Bythotrephes longimanus* present at the time of sediment collection (M. Palmer and N.D. Yan, York University, Toronto, Ontario, unpublished data).

is rising in many lakes in response to reductions in SO_2 emissions (Dillon et al. 2007). However, acidification processes and recent warming, combined with reforestation following clear-cutting that occurred in the mid- to late 1800s, have likely contributed to declining total phosphorus (TP) levels in several of these lakes (Hall and Smol 1996; Quinlan et al. 2008). Decades of acidic deposition have also depleted calcium (Ca) reserves in watershed soils (Watmough and Aherne 2008) and lakes (Jeziorski et al. 2008).

In the autumns of 2004 and 2005, replicate sediment cores were obtained from the deepest basin of each of the 44 lakes using a Glew (1989) gravity corer or a miniature Glew (1991) gravity corer (DeSellas et al. 2008). Cores were sectioned into 1 cm intervals using a Glew (1988) vertical extruder. The top 1 cm was analyzed to represent present-day conditions in the lakes, and an additional 1 cm interval at a core depth of 15–20 cm was also analyzed to represent pre-industrial conditions (see Hall and Smol 1996). Numerous paleolimnological studies have been completed in this region, and available Pb^{210} dating profiles for lakes examined in these studies effectively demonstrate that 15–20 cm reliably corresponds to pre-1850 in south-central

Fig. 2. Drawings demonstrating how size measurements were obtained for (*a*) *Bosmina* antennule length (AL), (*b*) *Bosmina* carapace (CL) and mucro (ML) lengths, and (*c*) *Daphnia* post-abdominal claw length (PL). Modified from Kerfoot (1981) and Witty (2004).

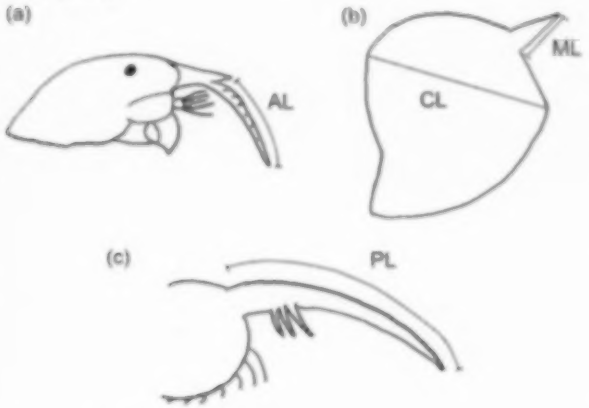

Ontario. This "top–bottom" paleolimnological approach has been widely used to assess a number of limnological issues across North America, including changes in lake-water pH (e.g., Cumming et al. 1992; Dixit et al. 1992; Smol et al. 1998) and other water quality variables (Dixit and Smol 1994; Dixit et al. 1999), changes in taste and odour causing algae (e.g., Paterson et al. 2004), and shifts in algal (e.g., Rühland et al. 2003; Betts-Piper et al. 2004) and cladoceran communities (e.g., Sweetman et al. 2008) in response to recent climate changes.

Microscope slides were prepared for top and bottom sediment intervals for each lake using standard techniques outlined in Korhola and Rautio (2001). Sediments were deflocculated in 10% KOH at 80 °C for ~30 min and passed through a 37 μm sieve, and the residue retained on the sieve was transferred to a vial by rinsing with deionized water (DeSellas et al. 2008). Ethanol was added to prevent fungal growth, and a safranin–glycerin solution was added to stain cladoceran remains. Finally, 50 μL subsamples were pipetted onto glass slides and mounted using glycerine jelly.

Cladoceran remains were identified using a Leica DMRB light microscope with bright field optics (20–40× objective, 15× ocular lenses) equipped with a digital camera, with Witty (2004) and Taylor et al. (2002) as taxonomic sources. *Daphnia* post-abdominal claws were classified as belonging to either the *Daphnia pulex* complex (*D. pulex*, *D. pulicaria*, *D. catawba*, and *D. minnehaha*), the *Daphnia retrocurva* complex (*D. parvula* and *D. retrocurva*), or the *Daphnia ambigua* complex (*D. ambigua*, *D. dentifera*, *D. mendotae*, *D. dubia*, and *D. longiremis*) depending on the morphology of the middle pectin (Witty 2004). The *Daphnia retrocurva* complex was rare in these lakes and was not included in subsequent analyses. When possible, the first 50 *Bosmina* carapaces, 50 *Bosmina* headshields, and 50 *Daphnia* post-abdominal claws were measured per sample, consistent with previous paleolimnological size investigations (Manca et al. 2000; Korosi et al. 2008). Measurements were made (straight line or digitized curve measurements, depending on the degree of curvature of the remains) using Northern Eclipse image analysis software, version 6.0 (Empix Imaging Inc., Mississauga, Ontario). For *Bosmina*, antennule length (AL) and mucro length (ML) (Figs. 2*a* and 2*b*, respectively) were measured to infer changes in invertebrate predation regimes (Kerfoot 1974), whereas carapace length (CL; Fig. 2*b*) was measured as a general estimate of total body length. Daphniid body remains are poorly preserved in lake sediments, and as a result, we were unable to measure *Daphnia* carapaces to estimate body length. However, *Daphnia* post-abdominal claws are well preserved and can be used as a substitute for carapace length, as strong correlations have been documented for *Daphnia* post-abdominal claw length with both *Daphnia* carapace length (Hrbáček 1969) and total body length (Manca and Comoli 1996). Consistent with these studies, we measured *Daphnia* post-abdominal claws (referred to as pecten length in Korosi et al. 2008) as a proxy for *Daphnia* body length (PL; Fig. 2*c*)

Means of lengths were calculated for *Bosmina* CL, ML, and AL and *Daphnia* PL (with *D. ambigua* and *D. pulex* considered both separately and combined in one *Daphnia* category) size measurements for each lake. Changes in the mean size of these measures since the onset of anthropogenic stressors in ~1850 were examined and visually represented using 1:1 plots made with SigmaPlot for Windows (version 10.0, SPSS Inc., Chicago, Illinois). To determine if any observed changes were statistically significant, a non-parametric Wilcoxon's signed-rank test (Sokal and Rohlf 1981) was used, as the distribution of lake size means for top and bottom samples was not normally distributed (Systat for Windows, version 11.0, Systat Software Inc., Chicago, Illinois).

Results and discussion

Bosmina size changes

Size distributions for pre-industrial and present-day assemblages are shown (Table 2). No significant changes in *Bosmina* carapace length were detected between present-day and pre-industrial sediment intervals (Wilcoxon's signed-rank test, $p = 0.68$; Fig. 3*a*); however, a significant decrease was detected in *Bosmina* antennule length (Wilcoxon's signed-rank test, $p < 0.001$; Fig. 3*c*). A similar trend of decreasing *Bosmina* mucro length was also observed; however, this was not statistically significant at $\alpha = 0.05$ (Wilcoxon's signed-rank test, $p = 0.09$; Fig. 3*b*). Long *Bosmina* body appendages are a specific defence response to the presence of predatory copepods (Kerfoot 1975; Kappes and Sinsch 2002; Sweetman and Finney 2003), as the copepods must be able to manoeuvre their bosminiid prey in such a way as to expose the soft, ventral body surface for ingestion (Kerfoot 1975).

Kerfoot (1975) categorized *Bosmina* spp. in Lake Washington as belonging to one of three morph types (small, intermediate, or long) depending on the length of the mucro. Long *Bosmina* morphs are more difficult to handle, providing *Bosmina* with increased escape opportunities when attacked by copepods. Based on this system of organization, the mucro lengths for both the top and bottom samples (median values of 72.89 and 75.51 μm, respectively) would be categorized as "long." Perhaps, then, the modest change in mucro length we observed in this study is not biologically

Table 2. Comparison of *Bosmina* and *Daphnia* size distribution between present-day and pre-industrial sediment intervals for the 44 study lakes.

		Median (μm)	Upper quartile (μm)	Lower quartile (μm)
Bosmina CL	Pre-industrial	257.42	284.85	240.76
	Present day	259.64	285.35	243.66
Bosmina ML	Pre-industrial	75.51	82.48	63.26
	Present day	72.89	86.24	56.85
Bosmina AL	Pre-industrial	124.79	144.30	111.35
	Present day	113.96	127.18	107.65
Daphnia PL	Pre-industrial	153.99	163.96	139.12
	Present day	141.30	154.00	133.47

Note: CL, carapace length; ML, mucro length; AL, antennule length; PL, post-abdominal claw length.

Fig. 3. Plots comparing mean (*a*) *Bosmina* carapace length (CL), (*b*) *Bosmina* mucro length (ML), (*c*) *Bosmina* antennule length (AL), and (*d*) *Daphnia* post-abdominal claw length (PL) in pre-industrial (pre-1850s) and present-day (2004–2005) sediment samples from 44 lakes in south-central Ontario. Results of the Wilcoxon's signed-rank test are also shown. Diagonal line represents the 1:1 line. Solid squares represent lakes that had been invaded by *Bythotrephes longimanus* at the time of sediment collection.

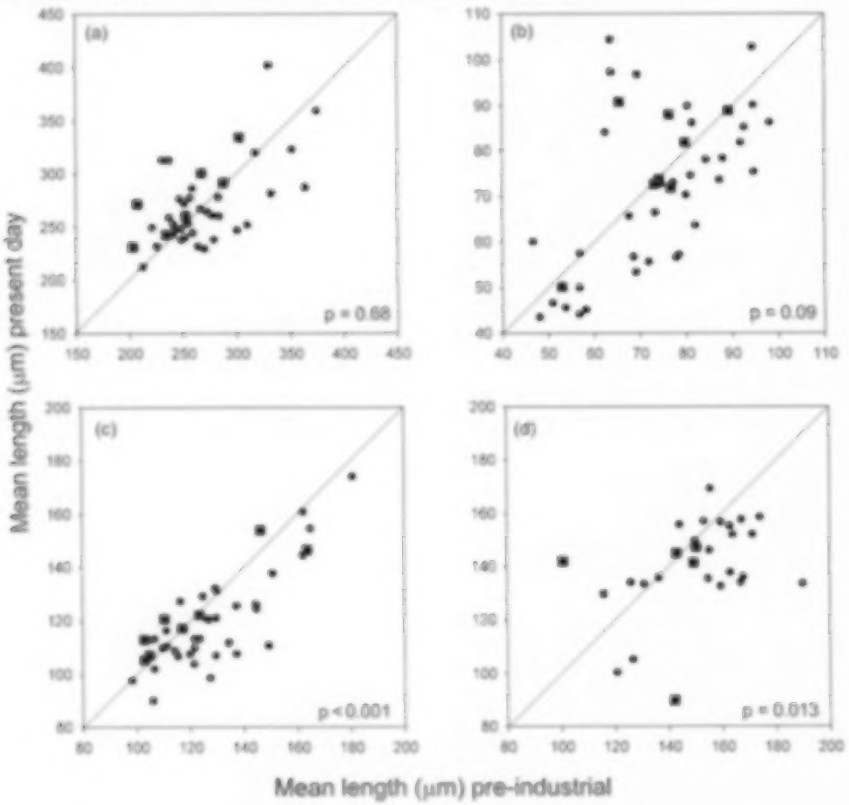

significant. To our knowledge, however, data on the effects of modest increases in *Bosmina* mucro length on copepod predation success are not yet available, although Alexander and Hotchkiss (2010) have documented general positive correlations for mucro length of sedimentary *Bosmina* remains with extant populations of *Epischura lacustris*, *Diacyclops thomasi*, and *Leptodiaptomus minutus*.

The decline in antennule length we observed between top and bottom samples is more appreciable (median values of 113.96 and 124.79 μm, respectively) and also suggests a decrease in copepod predation, as long stout antennules protect vulnerable swimming appendages from damage during an attack (Kerfoot 1975). Interestingly, the difference in antennule length between top and bottom sedimentary samples are comparable with differences in antennule length observed by Sakamoto et al. (2007) between two different types of *Bosmina*: *B. cornuta* and *B. pellucida*. The *B. cornuta* type, which was categorized by a hooked antennule and had an observed length ~110–115 μm, was more vulnerable to copepod predation than the *B. pellucida* type, which had a

slightly curved antennule with an observed length of ~115–123 μm (Sakamoto et al. 2007). This suggests that the actual reduction in antennule length we observed in this study should reflect decreased copepod predation pressure; however, this conclusion should be viewed with caution. Sakamoto and Hanazato (2008) demonstrate that antennule shape, not included as a parameter here, is also important in determining vulnerability of *Bosmina* to copepod predation. Furthermore, confirming a link between copepods and size of appendages of *Bosmina* microfossils is difficult due to the inherent limitations in our methodology. Soft-bodied copepods do not preserve well in lake sediments, and consequently, we have no pre-impact data on zooplankton community structure to compare with.

Daphnia size changes

Across all lakes, the length of *Daphnia* (*D. ambigua* and *D. pulex* grouped together) post-abdominal claws are significantly ($p \leq 0.05$) smaller, on average, in present-day assemblages in comparison with *Daphnia* post-abdominal claw length in pre-industrial assemblages (Wilcoxon's signed-rank test, $p = 0.013$; Fig. 3*d*). When separated into species groups, both the *D. ambigua* and *D. pulex* complexes showed the same trend of decreased size in present-day assemblages (for *D. pulex*, median size is 149.23 μm in the top interval versus 158.41 μm in the bottom interval; for *D. ambigua*, median size is 134.32 μm in the top interval versus 147.32 μm in the bottom interval). This decrease was significant for the *D. ambigua* complex (Wilcoxon's signed-rank test, $p < 0.0001$), but not for the *D. pulex* complex (Wilcoxon's signed-rank test, $p = 0.314$); however, we only found *D. pulex* in the bottom interval of 9 of our 44 study lakes (compared with 30 of 44 lakes in the top interval), and so size changes between top and bottom samples for *D. pulex* cannot reliably be compared. Because *D. pulex* are significantly larger than *D. ambigua* in the top interval (sign test, $p = 0.02$), the increase in relative abundance of *D. pulex* cannot account for the observed decrease in overall *Daphnia* size in present-day sediments. However, we cannot rule out the possibility that species replacement is occurring within both the *D. ambigua* and *D. pulex* complexes in favour of smaller species.

The interaction of multiple stressors over time can make it difficult to assign specific causes for *Daphnia* size changes. Given what is known about regional water quality stressors in these lakes and the factors that can influence size, we can still offer several plausible explanations as to why these changes have occurred. Similar to *Bosmina* appendage changes, the decrease in *Daphnia* size could reflect a shift in the intensity of fish and invertebrate predation, as an increase in visual planktivorous fish predators would select for decreased body size (Brooks and Dodson 1965). However, smallmouth bass and other piscivorous fish populations have been spreading in south-central Ontario lakes over the past few decades, which can reduce the abundance of planktivorous fish (Vander Zanden et al. 2004). This would be expected, through trophic cascades, to result in an increase in *Daphnia* size, contrary to the decrease we observed (Brooks and Dodson 1965).

Several studies are available that have examined the general relationships between zooplankton size and water temperature (e.g., Moore and Folt 1993; Atkinson 1994; Moore et al. 1996), and there is evidence that smaller *Daphnia* taxa survive exposure to elevated temperatures better than larger taxa (Craddock 1976; LaBerge and Hann 1990). Higher temperatures are thought to increase growth rate and the number of moults per individual but lead to a smaller body size at maturity (Moore and Folt 1993; Manca and Comoli 1999). Respiration rates often increase more rapidly than ingestion rates over the same temperature range, and therefore, a decrease in feeding efficiency at higher temperatures may account for smaller body sizes (Lehman 1988; Büns and Ratte 1991). Furthermore, there is evidence that temperature may elicit a size response on time scales as short as a summer heat wave (7–10 days; Moore et al. 1996). In a fishless mountain lake, this size–temperature relationship was applied in a paleolimnological study that used size of *Daphnia* microfossils in the sediments to reconstruct summer temperatures and the length of the productive season (Manca and Comoli 2004). Larger size, in addition to a narrow range of body size, was considered an indication of a short productive season during which *Daphnia* displayed fewer moults (Manca and Comoli 2004).

Daphnia size structure has not yet been tested against climate variables for this lake set; however, Yan et al. (2008) presented some contemporary zooplankton size data for a subset of these same lakes that may, when compared with our present-day and pre-industrial size data, provide further insights on the drivers of *Daphnia* size changes in Shield lakes. They observed increases in body size over time from 1980 to 2003 for *D. ambigua*, *D. longiremus*, and the *D. pulex* complex for eight of the lakes included in this study (Blue Chalk, Chub, Crosson, Dickie, Harp, Heney, Plastic, and Red Chalk Main). Based on the monitoring data gathered by Yan et al. (2008) and our paleolimnological data presented here, we suggest that *Daphnia* may be returning to their pre-industrial size structure. If this is the case, then climate-related changes are unlikely to have been an important factor behind our observed size changes.

Perhaps a more plausible explanation for the decrease in size between present-day and pre-industrial times is related to acidification and subsequent recovery. The lakes in this region have experienced some anthropogenic acidification (Hall and Smol 1996), although to a much lesser extent compared with other acid-sensitive areas such as Sudbury, Ontario (Dixit et al. 1992), and some lakes in eastern Canada (Ginn et al. 2007). *Daphnia mendotae* is one of the larger species in the *D. ambigua* complex and is also very acid-sensitive (B. Keller, Ontario Ministry of the Environment, Cooperative Freshwater Ecology Unit, Laurentian University, Sudbury, ON P3E 2C6, Canada, personal communication, 2009). A decrease in the abundance of *D. mendotae* could potentially account for the decrease in size since pre-industrial times in the *D. ambigua* complex. Within the *D. pulex* complex, the smaller-bodied *D. catawba* is acid-tolerant, and an increase in the abundance of this species in response to acidification could be indicated by the decrease in size within the *D. pulex* complex (B. Keller, personal communication, 2009). Therefore, the decrease in overall *Daphnia* body size we observed may be reflecting a response to lake-water acidification. Recent reductions in SO_2 emissions have reduced acid stress in this region, and there

is evidence that water chemistry and biological communities in these lakes are recovering from the effects of acidification (Bowman et al. 2006; Dillon et al. 2007; Lento et al. 2008). Recent increases in *Daphnia* body size observed by Yan et al. (2008) may be detecting biological recovery within *Daphnia* since the implementation of emission restrictions. Future research on these lakes should focus on detailed core analyses to provide information on the timing of size shifts and which environmental stressors (e.g., climate or acidification) are most likely to be driving the changes.

At the time of this study, eight of the investigated lakes had been invaded by *Bythotrephes longimanus*, yet no trend in size change was seen for either *Daphnia* or *Bosmina* between invaded and noninvaded lakes since pre-industrial times (Fig. 3). Unlike *Leptodora*, another predatory cladoceran, *Bythotrephes* do not use a feeding basket and thus are able to consume larger prey items. In laboratory experiments, *Bythotrephes* have been shown to select medium-sized daphniids, even consuming daphniids larger than 2 mm in some trials (Schulz and Yurista 1999). However, following its invasion into Harp Lake in 1993, larger cladocerans increased in abundance while smaller species declined or disappeared (Yan and Pawson 1997). The lack of size trend observed in this study could suggest that *Bythotrephes* are not having an impact on *Bosmina* and *Daphnia* size or that its effects on size are not detectable at this scale.

Contemporary size data cannot be effectively interpreted without an appropriate point of reference. We demonstrate here the usefulness and sensitivity of paleolimnological techniques for reconstructing historical cladoceran size structure and present pre-impact size data for a set of lakes where modern size trends are continually being monitored by limnologists associated with the Dorset Environmental Science Centre (Ontario Ministry of the Environment). These data have provided some meaningful insights on the environmental factors structuring cladoceran size in Shield lakes that can be further refined by continuing studies (both contemporary and paleolimnological) on long-term size trends.

Acknowledgements

We thank Carole Cheung, Bev Clark, Adam Jeziorski, Michelle Palmer, and Ron Ingram for their participation in the fieldwork. We also thank Norman Yan at York University, Joshua Thienpont, Adam Jeziorski, and several anonymous reviewers for their comments and insights, which improved the quality of the manuscript. This project was funded by an Ontario Ministry of the Environment Best in Science Grant and Natural Sciences and Engineering Research Council of Canada (NSERC) grants to J.P.S.

References

Alexander, M.L., and Hotchkiss, S.C. 2010. *Bosmina* remains in lake sediments as indicators of zooplankton community composition. J. Paleolimnol. **43**(1): 51–59. doi:10.1007/s10933-009-9312-0.

Atkinson, D. 1994. Temperature and organism size — a biological law for ectotherms? Adv. Ecol. Res. **25**: 1–58. doi:10.1016/S0065-2504(08)60212-3.

Betts-Piper, A., Zeeb, B.A., and Smol, J.P. 2004. Chrysophyte cysts from High Arctic Svalbard lakes: preliminary evidence of recent environmental change. J. Paleolimnol. **31**(4): 467–481. doi:10.1023/B:JOPL.0000022546.21996.41.

Bowman, M.F., Somers, K.M., Reid, R.A., and Scott, L.D. 2006. Temporal response of stream benthic macroinvertebrate communities to the synergistic effects of anthropogenic acidification and natural drought events. Freshw. Biol. **51**(4): 768–782. doi:10.1111/j.1365-2427.2006.01516.x.

Brooks, J.L., and Dodson, S.I. 1965. Predation, body size, and composition of plankton. Science (Washington, D.C.), **150**(3692): 28–35. doi:10.1126/science.150.3692.28. PMID:17829740.

Büns, M., and Ratte, H.T. 1991. The combined effects of temperature and food consumption on body weight, egg production, and developmental time in *Chaoborus crystallinus* De Geer (Diptera: Chaoboridae). Oecologia (Berl.), **88**: 470–476.

Chapman, L.J., and Putnam, D.F. 1984. The physiography of southern Ontario special. Vol. 2. Ontario Geological Survey, Sudbury, Ontario.

Craddock, D.R. 1976. Effects of increased water temperature on *Daphnia pulex*. Fish. Bull. (Washington, D.C.), **74**: 403–407.

Cumming, B.F., Smol, J.P., Kingston, J.C., Charles, D.F., Birks, H.J.B., Camburn, K.E., Dixit, S.S., Uutala, A.J., and Selle, A.R. 1992. How much acidification has occurred in Adirondack region lakes (New York, USA) since preindustrial times? Can. J. Fish. Aquat. Sci. **49**: 128–141. doi:10.1139/f92-015.

DeSellas, A.M., Paterson, A.M., Sweetman, J.N., and Smol, J.P. 2008. Cladocera assemblages from the surface sediments of south-central Ontario (Canada) lakes and their relationships to measured environmental variables. Hydrobiologia, **600**(1): 105–119. doi:10.1007/s10750-007-9180-4.

Dillon, P.J., Watmough, S.A., Eimers, M.C., and Aherne, J. 2007 Long-term changes in boreal lake and stream chemistry: recovery from acid deposition and the role of climate. *In* Acid in the environment: lessons learned and future prospects. *Edited by* G.R. Visgilio and D.M. Whitelow. Springer, New York. pp. 59–75.

Dixit, S.S., and Smol, J.P. 1994. Diatoms as environmental indicators in the Environmental Monitoring and Assessment — Surface Waters (EMAP–SW) program. Environ. Monit. Assess. **31**: 275–306.

Dixit, S.S., Dixit, A.S., and Smol, J.P. 1992. Assessment of changes in lake water chemistry in Sudbury area lakes since preindustrial times. Can. J. Fish. Aquat. Sci. **49**(S1): 8–16. doi:10.1139/f92-295.

Dixit, S.S., Smol, J.P., Charles, D.F., Hughes, R.M., Paulsen, S.G., and Collins, G.B. 1999. Assessing water quality changes in the lakes of the northeastern United States using sediment diatoms. Can. J. Fish. Aquat. Sci. **56**(1): 131–152. doi:10.1139/cjfas-56-1-131.

Ginn, B.K., Cumming, B.F., and Smol, J.P. 2007. Assessing pH changes since pre-industrial times in 51 low-alkalinity lakes in Nova Scotia, Canada. Can. J. Fish. Aquat. Sci. **64**(8): 1043–1054. doi:10.1139/F07-078.

Glew, J. 1988. A portable extruding device for close interval sectioning of unconsolidated core samples. J. Paleolimnol. **1**(3): 235–239. doi:10.1007/BF00177769.

Glew, J. 1989. A new trigger mechanism for sediment samplers. J. Paleolimnol. **2**(4): 241–243. doi:10.1007/BF00195474.

Glew, J. 1991. Miniature gravity corer for recovering short sediment cores. J. Paleolimnol. **5**(3): 285–287. doi:10.1007/BF00200351.

Gliwicz, Z.M. 1990. Food thresholds and body size in cladocerans. Nature (London), **343**(6259): 638–640. doi:10.1038/343638a0.

Hall, R.I., and Smol, J.P. 1996. Paleolimnological assessment of long-term water quality changes in south-central Ontario lakes affected by cottage development and acidification. Can. J. Fish. Aquat. Sci. **53**(1): 1–17. doi:10.1139/cjfas-53-1-1.

Hann, B.J., Leavitt, P.R., and Chang, P.S.S. 1994. Cladocera community response to experimental eutrophication in Lake 227 as recorded in laminated sediments. Can. J. Fish. Aquat. Sci. **51**(10): 2312–2321. doi:10.1139/f94-234.

Hrbáček, J. 1969. On the possibility of estimating predation pressure and nutrition level of populations of *Daphnia* (Crust., Cladoc.) from their remains in sediments. Mitt. Int. Ver. Theor. Angew. Limnol. **17**: 269–274.

Jeziorski, A., Yan, N.D., Paterson, A.M., Desellas, A.M., Turner, M.A., Jeffries, D.S., Keller, B., Weeber, R.C., McNicol, D.K., Palmer, M.E., McIver, K., Arseneau, K., Ginn, B.K., Cumming, B.F., and Smol, J.P. 2008. The widespread threat of calcium decline in fresh waters. Science (Washington, D.C.), **322**(5906): 1374–1377. doi:10.1126/science.1164949. PMID:19039134.

Kappes, H., and Sinsch, U. 2002. Temperature- and predator-induced phenotypic plasticity in *Bosmina cornuta* and *B. pellucida* (Crustacea: Cladocera). Freshw. Biol. **47**(10): 1944–1955. doi:10.1046/j.1365-2427.2002.00943.x.

Kerfoot, W.C. 1974. Net accumulation rates and the history of cladoceran communities. Ecology, **55**(1): 51–61. doi:10.2307/1934617.

Kerfoot, W.C. 1975. The divergence of adjacent populations. Ecology, **56**(6): 1298–1313. doi:10.2307/1934698.

Kerfoot, W.C. 1978. Combat between predatory copepods and their prey: *Cyclops*, *Epischura*, and *Bosmina*. Limnol. Oceanogr. **23**: 1089–1102.

Kerfoot, W.C. 1981. Long-term replacement cycles in cladoceran communities: a history of predation. Ecology, **62**(1): 216-233.

Korhola, A., and Rautio, M. 2001. Cladocera and other brachiopod crustaceans. *In* Tracking environmental change using lake sediments. Vol. 4. Zoological indicators. *Edited by* J.P. Smol, H.J.B. Birks, and W.M. Last. Kluwer Academic Publishers, Dordrecht, the Netherlands. pp. 5–41.

Korosi, J.B., Paterson, A.M., DeSellas, A.M., and Smol, J.P. 2008. Linking mean body size of pelagic Cladocera to environmental variables in Precambrian Shield lakes: a paleolimnological approach. J. Limnol. **67**: 22–34.

LaBerge, S., and Hann, B.J. 1990. Acute temperature and oxygen stress among genotypes of *Daphnia pulex* and *Simocephalus vetulus* (Cladocera: Daphniidae) in relation to environmental conditions. Can. J. Zool. **68**(11): 2257–2263. doi:10.1139/z90-314.

Lehman, J.T. 1988. Ecological principles affecting community structure and secondary production by zooplankton in marine and freshwater environments. Limnol. Oceanogr. **33**: 931–945.

Lento, J., Dillon, P.J., Somers, K.M., and Reid, R.A. 2008. Changes in littoral benthic macroinvertebrate communities in relation to water chemistry in 17 Precambrian Shield lakes. Can. J. Fish. Aquat. Sci. **65**(5): 906–918. doi:10.1139/F08-033.

Manca, M., and Comoli, P. 1996. Reconstructing population size structure in Cladocera by measuring their body remains. Mem. Ist. Ital. Idrobiol. **54**: 61–67.

Manca, M., and Comoli, P. 1999. Studies on zooplankton of Lago Paione Superiore. J. Limnol. **58**: 131–135.

Manca, M., and Comoli, P. 2004. Reconstructing long-term changes in *Daphnia*'s body size from subfossil remains in sediments of a small lake in the Himalayas. J. Paleolimnol. **32**(1): 95–107. doi:10.1023/B:JOPL.0000025295.04832.77.

Manca, M., Ramoni, C., and Comoli, P. 2000. The decline of *Daphnia hyaline galeata* in Lago Maggiore: a comparison of the population dynamics before and after oligotrophication. Aquat. Sci. **62**(2): 142–153. doi:10.1007/PL00001328.

Moore, M., and Folt, C. 1993. Zooplankton body size and community structure: effects of thermal and toxicant stress. Trends Ecol. Evol. **8**(5): 178–183. doi:10.1016/0169-5347(93)90144-E.

Moore, M.V., Folt, C.L., and Stemberger, R.S. 1996. Consequences of elevated temperatures for zooplankton assemblages in temperate lakes. Arch. Hydrobiol. **135**: 289–319.

Neary, B.P., Dillon, P.J., Munro, J.R., and Clark, B.J. 1990. The acidification of Ontario lakes: an assessment of their sensitivity and current status with respect to biological damage. Ontario Ministry of the Environment, Dorset, Ontario.

Paterson, A.M., Cumming, B.F., Smol, J.P., and Hall, R.I. 2004. Marked recent increases of colonial scaled chrysophytes in boreal lakes: implications for the management of taste and odour events. Freshw. Biol. **49**(2): 199–207. doi:10.1046/j.1365-2427.2003.01170.x.

Quinlan, R., Hall, R.I., Paterson, A.M., Cumming, B.F., and Smol, J.P. 2008. Long-term assessments of ecological effects of anthropogenic stressors on aquatic ecosystems from paleoecological analyses: challenges to perspectives of lake management. Can. J. Fish. Aquat. Sci. **65**(5): 933–944. doi:10.1139/F08-027.

Rühland, K., Priesnitz, A., and Smol, J.P. 2003. Paleolimnological evidence from diatoms for recent environmental changes in 50 lakes the across Canadian arctic treeline. Arct. Antarct. Alp. Res. **35**: 110–123. doi:10.1657/1523-0430(2003)035[0110:PEFDFR]2.0.CO;2.

Sakamoto, M., and Hanazato, T. 2008. Antennule shape and body size of *Bosmina*: key factors determining its vulnerability to predacious Copepoda. Limnology, **9**(1): 27–34. doi:10.1007/s10201-007-0231-3.

Sakamoto, M., Kwang-Hyeon, C., and Hanazato, T. 2007. Plastic phenotypes of antennule shape in *Bosmina longirostris* controlled by physical stimuli from predators. Limnol. Oceanogr. **52**: 2072–2078.

Salo, J., Walls, M., Rajasilta, M., Sarvala, J., Räsänen, M., and Salonen, V.-P. 1989. Fish predation and reduction in body size in a cladoceran population: palaeoecological evidence. Freshw. Biol. **21**(2): 217–221. doi:10.1111/j.1365-2427.1989.tb01360.x.

Schulz, K.L., and Yurista, P.M. 1999. Implications of an invertebrate predator's (*Bythotrephes cederstroemi*) atypical effects on a pelagic community. Hydrobiologia, **380**(1/3): 179–193. doi:10.1023/A:1003484813672.

Smol, J.P. 2008. Pollution of lakes and rivers: a paleoenvironmental perspective. 2nd ed. Blackwell, Oxford, UK.

Smol, J.P., Cumming, B.F., Dixit, A.S., and Dixit, S.S. 1998. Tracking recovery patterns in acidified lakes: a paleolimnological perspective. Restor. Ecol. **6**(4): 318–326. doi:10.1046/j.1526-100X.1998.06402.x.

Sokal, R.R., and Rohlf, F.J. 1981. Biometry. Freeman, New York.

Sweetman, J.N., and Finney, B.P. 2003. Differential responses of zooplankton populations (*Bosmina longirostris*) to fish predation and nutrient loading in an introduced and natural sockeye salmon nursery lake on Kodiak Island, Alaska, USA. J. Paleolimnol. **30**(2): 183–193. doi:10.1023/A:1025543421436.

Sweetman, J.N., LaFace, E., Rühland, K.M., and Smol, J.P. 2008. Evaluating the response of Cladocera to recent environmental change in lakes from the Canadian Arctic treeline region. Arct. Antarct. Alp. Res. **40**(3): 584–591. doi:10.1657/1523-0430(06-118)[SWEETMAN]2.0.CO;2.

Taylor, D.J., Ishikane, C.R., and Haney, R.A. 2002. The systematics of Holarctic Bosminids and a revision that reconciles molecular and morphological evolution. Limnol. Oceanogr. **47**: 1486–1495.

Vander Zanden, M.J., Olden, J.D., Thorne, J.H., and Mandrak, N.E. 2004. Predicting occurrences and impacts of smallmouth bass introductions in north temperate lakes. Ecol. Appl. **14**(1): 132–148. doi:10.1890/02-5036.

Watmough, S.A., and Aherne, J. 2008. Estimating calcium weath-

ering rates and future lake calcium concentrations in the Muskoka–Haliburton region of Ontario. Can. J. Fish. Aquat. Sci. **65**(5): 821–833. doi:10.1139/F07-196.

Witty, L.M. 2004. Practical guide to identifying freshwater crustacean zooplankton. Cooperative Freshwater Ecology Unit, Department of Biology, Laurentian University. Sudbury, Ontario.

Yan, N.D., and Pawson, T.W. 1997. Changes in the crustacean zooplankton community of Harp Lake, Canada, following invasion by *Bythotrephes cederstroemi*. Freshw. Biol. **37**(2): 409–425. doi:10.1046/j.1365-2427.1997.00172.x.

Yan, N.D., Somers, K.M., Girard, R.E., Paterson, A.M., Keller, W., Ramcharan, C.W., Rusak, J.A., Ingram, R., Morgan, G.E., and Gunn, J.M. 2008. Long-term trends in zooplankton of Dorset, Ontario, lakes: the probable interactive effects of changes in pH, total phosphorus, dissolved organic carbon, and predators. Can. J. Fish. Aquat. Sci. **65**(5): 862–877. doi:10.1139/F07-197.

DISCUSSION / DISCUSSION

Comment on "Differences in predicted catch composition between two widely used catch equation formulations"[1]

R.I.C. Chris Francis

Abstract: Branch (2009. Can. J. Fish. Aquat. Sci. **66**: 126–132) described the two most common catch equation formulations in stock assessment models: the continuous (Baranov) one, which represents fishing mortality as an instantaneous rate, F, and the discrete one, in which it is represented as an exploitation rate, u. He claimed that the continuous formulation is preferable at high fishing mortality where a fish could encounter multiple sets of gear within a year. This claim is wrong for two reasons. First, it is based on the false supposition that the discrete catch equations require the assumption that fish encounter at most only one set of fishing gear in a year. Second, it is not possible to determine, for a specific stock assessment, whether one formulation is preferable to another solely on the basis of information about the fishery. The appropriate way to make this decision is to see which fits the data better.

Résumé : Branch (2009. J. can. sci. halieut. aquat. **66** : 126–132) a décrit les deux formulations de l'équation des captures les plus usitées dans les modèles d'évaluation des stocks, soit la continue (de Baranov) qui représente la mortalité due à la pêche comme un taux instantané, F, et la discontinue qui la représente comme un taux d'exploitation, u. Il soutient que la formulation continue est préférable aux forts taux de mortalité lorsque le poisson peut faire face à plusieurs ensembles d'engins de pêche pendant une année. Cette assertion est fausse pour deux raisons. D'abord, elle est basée sur la présomption erronée que les équations discontinues des captures présupposent que les poissons rencontrent au plus un ensemble d'engins de pêche au cours d'une année. Deuxièmement, il est impossible de déterminer, pour une évaluation de stock donnée, si l'une des formulations est préférable à l'autre seulement d'après les renseignements sur la pêche. La façon appropriée d'arriver à cette décision est de voir laquelle s'ajuste le mieux aux données.

[Traduit par la Rédaction]

Branch (2009*a*) (with corrections in Branch 2009*b*) described the two most commonly used catch equation formulations in stock assessment models as follows. The continuous (or Baranov) formulation, which dates back to Baranov (1918) with modifications due to Pope (1974), can be written as

$$(1) \quad N_{a+1,t+1} = N_{a,t}\, e^{-M - S_a F_t}$$

$$(2) \quad C_{a,t} = \frac{S_a F_t}{M + S_a F_t} N_{a,t}\left(1 - e^{-M - S_a F_t}\right)$$

$$(3) \quad A^C_{a,t} = \frac{\frac{S_a}{S_a F_t + M} N_{a,t}\left(1 - e^{-S_a F_t - M}\right)}{\sum_{a'}\left[\frac{S_{a'}}{S_{a'} F_t + M} N_{a',t}\left(1 - e^{-S_{a'} F_t - M}\right)\right]}$$

where, for age a and year t, N is the beginning-of-year number in the population, M and F are instantaneous rates of natural and fishing mortality, respectively, S describes the fishery selectivity, C is the catch (in numbers), and A^C is the catch composition (the proportions at age in the catch). The first equation describes how the number of fish in the population is changed by mortality; the second and third show how to calculate the numbers and proportions of fish

Received 18 May 2009. Accepted 1 December 2009. Published on the NRC Research Press Web site at cjfas.nrc.ca on 26 March 2010. J21208

Paper handled by Associate Editor Terrance Quinn II.

R.I.C.C. Francis. National Institute of Water and Atmospheric Research, Private Bag 14901, Wellington, New Zealand (e-mail: c.francis@niwa.co.nz).

[1]Appears in Can. J. Fish. Aquat. Sci. **66**: 126–132.

of each age in the catch. The analogous equations for the discrete formulation of the catch equations are

$$N_{a+1,t+1} = N_{a,t}(1 - S_a u_t)e^{-M} \quad (4)$$

$$C_{a,t} = N_{a,t} S_a u_t e^{-(t^* - t)M} \quad (5)$$

$$A^c_{a,t} = \frac{S_a N_{a,t}}{\sum_{a'} S_{a'} N_{a',t}} \quad (6)$$

where u is the annual exploitation rate (for selected fish), and the fishery is assumed to occur in an instant at time t^*. These are slight modifications to the equations of Pope (1972) (whose equations assumed that $t^* - t = 0.5$), which are generally known as Pope's approximation (see last paragraph below for a discussion of the significance of the word "approximation" here).

The aims of the present paper are twofold. The first is to dispute the claim by Branch (2009*a*) that the continuous formulation is preferable to the discrete formulation at high fishing mortality where a fish could encounter multiple sets of fishing gear within a year. That claim was based, at least in part, on the false supposition that the discrete formulation precludes multiple encounters. The second aim is to argue that the appropriate way to decide whether one set of catch equations is better than another for a specific stock assessment is by examining model outputs.

The two formulations, as presented above, differ in two ways, only one of which is relevant to the disputed claim. The difference that is relevant is that the selectivity, S_a, is sometimes exponentiated in the continuous form, but never in the discrete form. As Branch (2009*a*) showed, this leads to an important difference in the predicted catch compositions. With the continuous formulation, the catch composition depends on the level of fishing mortality (see eq. 3). As the level of fishing mortality increases, the proportion of the catch that comes from the less-selected age classes will increase. In contrast, the catch composition for the discrete formulation is independent of the level of fishing mortality (see eq. 6), as was well illustrated in fig. 2 of Branch (2009*a*). The second difference between the two formulations is in the relative timing of natural and fishing mortality. In eqs. 1–3, the two types of mortality occur simultaneously, whereas in eqs. 4–6, they occur sequentially (first proportion $(t^* - t)$ of natural mortality, then fishing mortality, and then the rest of natural mortality). This second difference is not relevant to the disputed claim because the argument of Branch (2009*a*) is not affected if we change eqs. 1–3 to create a modified continuous formulation in which the timing of mortality is like that in eqs. 4–6. (Branch (2009*a*) discussed such a modification, which changes the above eq. 6 to his eq. 20.)

Branch (2009*a*) pointed out another consequence of the difference between the two formulations in the treatment of selectivity. This concerns the maximum mortality that is possible in a year. With the continuous catch equations, there is, at least theoretically, no limit to the proportion of the population that could die (through natural or fishing mortality) in a year. We can express this mathematically by saying that $N_{a+1,t+1} \to 0$ as $F_t \to \infty$. With the discrete equation, there *is* a limit, which is achieved when $u_t = 1$. At this limit, $N_{a+1,t+1} = N_{a,t}(1 - S_a)e^{-M}$, which will be greater than 0 for all age classes for which $S_a < 1$.

Selectivity is an important consideration when we are asking whether one set of catch equations might be preferable to another. This becomes clear when we look at what happens when all fish are equally selected (i.e., $S_a = 1$ for all a). In this case, the key differences between the equations disappear: for both formulations, the catch composition becomes independent of the level of fishing mortality, and there is no theoretical limit to the proportion of the population that could die in a year.

There are two major mechanisms underlying selectivity: fishing gear and spatiotemporal separation. I will show that the former is more consistent with the continuous formulation, and the latter with the discrete. The fishing-gear mechanism for selectivity was well described by Branch (2009*a*). In a scenario in which this was the only selectivity mechanism, the continuous formulation would be appropriate. All fish would be equally available to the fishing gear, but some would more easily escape an encounter with the gear (e.g., smaller fish can more easily escape through the meshes of a trawl net). However, even the less-selected fish would eventually be caught if they were subject to multiple encounters with the gear. The second selectivity mechanism is a consequence of the age-dependent spatiotemporal distribution of fish. For many fish populations, the size and age of fish that you catch will depend, often strongly, on when and where you choose to fish. Fishers' decisions about when and where to fish may be influenced by a wide range of factors, including a preference for a certain size of fish and (or) higher catch rates and (or) distance from ports. Given the complexity of both the fish distributions and fishers' decisions, it is highly unlikely that all ages of fish would be equally available to the fishing gear. Now, consider a second scenario in which a fish population occurs in two areas, but fishing takes place in only one of these. Area 1, where the fishery is, contains all of the adult fish but only some of the juveniles, and area 2 contains the rest of the juveniles. The only movement between areas occurs between fishing seasons and serves to maintain the proportion of juveniles in area 1. If spatial separation were the only selectivity mechanism acting in this fishery, then all fish in area 1 would be equally available to be caught, regardless of age, but no fish in area 2 would be available. This means that, for the whole population, juvenile fish would be partially selected (because those in area 2 are protected from fishing) but adults would be fully selected (because they are all in the fished area). The catch composition would not depend on the exploitation rate because the proportions at age in the catch would be exactly the same as those in area 1, no matter how high the exploitation rate. This scenario is consistent with the discrete catch equations. Because there is no gear selectivity, the probability of a fish being caught when it encounters fishing gear is independent of its age. If that probability were less than 1, then there would be no reason to rule out multiple encounters within a year. Thus, contrary to the assertion of Branch (2009*a*), the discrete catch equations do not preclude multiple encounters.

Because the real world is much more complex than either of these simple scenarios, neither formulation, discrete or

continuous, will ever be correct. In most fisheries, selectivity will be determined by both mechanisms: gear and spatio-temporal separation. Branch (2009*a*) recommended a hybrid formulation (his eqs. 5 and 6) for this situation, with separate parameters for the two mechanisms (S_a for the former, A_a for the latter). I suspect that there would often be some practical difficulties with this formulation because of confounding between the S_a and the A_a (i.e., the data may not contain sufficient information to estimate both the S_a and the A_a). However, even if these equations, or any others, perfectly matched the mix of selectivity mechanisms that were active in our fishery, we could still not say that they were correct because there are other assumptions to consider. For example, both the discrete and continuous formulations above make the highly simplistic assumption that natural mortality is independent of age and year, and also that selectivity does not vary from year to year. Modellers know that these assumptions are not true, but have sometimes found them to be useful approximations. Thus the question to ask when choosing between catch equations is not which one is correct, but which one provides the better approximation to reality for the fishery we are modelling.

How are we to decide whether one formulation for the catch equations is preferable to another for a specific stock assessment? I maintain that the only scientific way to make this decision is to construct two models that differ only in their catch equations, fit both models to the stock assessment data, and examine the model outputs. That is, we should make the decision on the basis of fits to the data rather than on some hypothesis about the mechanisms underlying selectivity. There are two questions to ask. First, do the outputs from the two models differ in any significant way? (i.e., would they lead to different management advice?). If not, then neither formulation is preferable. If there *is* a significant difference in outputs, then we should ask our second question: which model fits the data better? If there is a clear-cut answer to this question, then we can say, with some confidence, which formulation is better for this assessment. However, it is quite possible that the answer will not be clear cut (for example, some data sets may be better fit in one model, and some in the other). In this case we should conclude that neither formulation is clearly preferable, and that both model outputs lie within the range of uncertainty for our assessment.

I am not arguing that we should ignore fishery information in choosing a set of catch equations. Nor do I want to say that the continuous formulation is never preferable for fisheries in which fish encounter multiple sets of gear within a year. My point is simply that any definitive statement about which formulation is better for a specific stock assessment must be based on model outputs.

Finally, I would like to make a comment about Pope's approximation, which, in the current context, refers to eqs. 4–6 in the special case that $t^{\circ} - t = 0.5$. There have been several attempts either to quantify the supposed error in this approximation (e.g., table 1 in Pope (1972); table 1 in Sims (1982); table 10.4 in Hilborn and Walters (1992)) or to reduce this error by modifying the equations (MacCall 1986; Allen and Hearn 1989). All of these attempts seem to me to have been misguided because they have implicitly assumed that the Baranov equations (eqs. 1–3) were true. It is certainly true that Pope's equations were intended as approximations to the Baranov equations. However, it is surely of no more than academic interest to ask how close this approximation is. What we really need to know is which set of equations provides a better approximation to the truth for a specific fishery.

References

Allen, K.R., and Hearn, W.S. 1989. Some procedures for use in cohort analysis and other population simulations. Can. J. Fish. Aquat. Sci. **46**(3): 483–488. doi:10.1139/f89-064.

Baranov, F.I. 1918. On the question of the biological basis of fisheries. Nauch. Issledov. Iktiol. Inst. Izv. 1 (1), Moscow. pp. 81–128.

Branch, T.A. 2009*a*. Differences in predicted catch composition between two widely used catch equation formulations. Can. J. Fish. Aquat. Sci. **66**(1): 126–132. doi:10.1139/F08-196.

Branch, T.A. 2009*b*. Corrigendum: Differences in predicted catch composition between two widely used catch equation formulations. Can. J. Fish. Aquat. Sci. **66**(9): 1631. doi:10.1139/F09-107.

Hilborn, R., and Walters, C.J. 1992. Quantitative fisheries stock assessment. Chapman & Hall, New York.

MacCall, A.D. 1986. Virtual population analysis (VPA) equations for nonhomogeneous populations, and a family of approximations including improvements on Pope's cohort analysis. Can. J. Fish. Aquat. Sci. **43**: 2406–2409. doi:10.1139/f86-298.

Pope, J.G. 1972. An investigation of the accuracy of virtual population analysis using cohort analysis. Int. Comm. Northwest Atl. Fish. Res. Bull. **9**: 65–74.

Pope, J.G. 1974. A possible alternative method to virtual population analysis for the calculation of fishing mortality from catch at age data. International Commission for the Northwest Atlantic Fisheries, Dartmouth, Nova Scotia. Annual Meeting, June 1974. Res. Doc. No. 74/20. Ser. No. 3166.

Sims, S.E. 1982. Algorithms for solving the catch equation forward and backward in time. Can. J. Fish. Aquat. Sci. **39**(1): 197–202. doi:10.1139/f82-023.

DISCUSSION / DISCUSSION

Reply to the comment by Francis on "Differences in predicted catch composition between two widely used catch equation formulations"[1]

Trevor A. Branch

Abstract: Francis (2010. Can. J. Fish. Aquat. Sci. **67**: 763–765) writes a thoughtful response detailing concerns with my suggestion that the continuous (Baranov) catch formulation is preferable to the discrete catch formulation when fishing mortality is high (T.A. Branch. 2009. Can. J. Fish. Aquat. Sci. **66**: 126–132). He suggests the discrete formulation allows for multiple gear encounters and that formulation choice should depend on which formulation better fits the data. Here I first distinguish between gear selectivity and availability and then show that our two views are complementary: the original assumes fish groups with differing gear selectivity but full availability, whereas Francis assumes fish groups fully selected by fishing gear but with differing availability. I maintain that the discrete formulation only models a single instantaneous interaction between fish and fishing gear and therefore only part of the population can be caught if fish groups have equal gear selectivity that is less than 100%, whereas under the same assumptions, the continuous formulation would allow the entire population to be caught. Finally, when the balance between gear selectivity and availability is unknown, I agree that formulation choice could be driven by model fits to the data, although formulation choice could also be based on how the fishery operates.

Résumé : Francis (2010. J. can. sci. halieut. aquat. **67** : 763–765) a répondu de façon bien argumentée en exprimant ses inquiétudes concernant ma suggestion que la formulation continue (de Baranov) des captures est préférable à la formulation discontinue lorsque la mortalité due à la pêche est élevée (T. A. Branch. 2009. J. can. sci. halieut. aquat. **66** : 126–132). Il indique que la formulation discontinue peut être utilisée lorsque les poissons font face à plusieurs engins de pêche et que le choix de formulation devrait dépendre de quelle formulation s'accorde mieux aux données. Je distingue ici d'abord entre la sélectivité et la disponibilité des engins et démontre ensuite que nos vues sont complémentaires : l'original présuppose des groupes de poissons avec une sélectivité différente des engins de pêche, mais avec une pleine disponibilité, alors que Francis présuppose des groupes de poissons avec une pleine sélectivité des engins, mais avec différentes disponibilités. Je maintiens que la formulation discontinue ne modélise qu'une seule interaction instantanée entre les poissons et les engins de pêche et qu'en conséquence seulement une partie de la population peut être capturée si les sélectivités des engins sont égales pour les groupes de poissons et inférieures à 100 %; avec les mêmes présuppositions, la formulation continue permettrait la capture de l'ensemble de la population. Enfin, lorsque l'équilibre entre la sélectivité des engins et la disponibilité est inconnue, je suis d'accord que le choix de la formulation pourrait se baser sur l'ajustement du modèle aux données, bien que le choix de la formulation puisse aussi se baser sur le mode d'opération de la pêche.

[Traduit par la Rédaction]

In my original paper (Branch 2009*a*, 2009*b*), I discussed how the choice of catch equation (continuous vs. discrete) has a marked impact on predicted catch composition when gear selectivity differs among groups of fish. These groups could be species, length, sex, or age groups, but in the general discussion that follows, I will refer to them as age groups for simplicity. Given differences between the two catch formulations in both predicted catch composition and the proportion of the stock that can be caught at high fishing mortality, I suggested that the continuous formulation was preferable at high fishing mortality levels where multiple gear encounters could occur. Francis (2010) responds with two particular criticisms: first that the discrete formulation does not in fact preclude multiple gear encounters, and sec-

Received 2 January 2010. Accepted 8 March 2010. Published on the NRC Research Press Web site at cjfas.nrc.ca on 26 March 2010. J21596

Paper handled by Associate Editor Terrance Quinn II.

T.A. Branch. School of Aquatic and Fishery Sciences, Box 355020, University of Washington, Seattle, WA 98195, USA (e-mail: tbranch@gmail.com).

[1]Appears in Can. J. Fish. Aquat. Sci. **66**: 126–132.

ond, that the choice between the two formulations should be based on which one fits the data better. In this response, I first define gear selectivity and availability, show that the arguments advanced by Branch (2009*a*) and Francis (2010) are not in opposition but are complementary, and show how the two approaches can be combined by including parameters for both gear selectivity and availability.

To understand the complementary nature of the two papers, some clarification is needed on the definition of "selectivity". Branch (2009*a*) defined "selectivity" to be synonymous with gear selectivity (the relative proportion of fish of different ages available to the fishing gear that are caught), whereas Francis (2010) defined "selectivity" as encompassing both gear selectivity and availability (where availability is the absolute proportion of fish of different ages that are in the same area as the fishing fleet and not separated spatiotemporally). Here I will specifically refer to these two components as "gear selectivity" and "availability", while calling their combined effects "catchability" (the relative proportion of fish of different ages in the entire population that are caught by the fishing gear). In doing so, I gloss over a long history of debate over these terms that is touched on by Marr (1951), Beverton and Holt (1957), MacCall (1986), and Millar and Fryer (1999).

Having defined these terms, Branch (2009*a*) can be seen as focusing on the case in which gear selectivity (S_a) differs among ages, but all ages are fully available to the fishing fleet ($A_a = 1$), whereas Francis (2010) focuses on the case in which all fish are fully selected by the fishing gear ($S_a = 1$) but they differ in their availability to the fishing fleet ($0 \leq A_a \leq 1$). If gear selectivity differs among ages, then the continuous and discrete formulations give different predictions. However, if all ages have a gear selectivity of one and availability differs, then both formulations predict the same catch composition, as pointed out by Francis (2010), and he is correct in saying that the discrete formulation is a better choice than the continuous formulation. However, his first criticism, that the discrete formulation can model multiple interactions with the fishery within each time period, is incorrect. That the two formulations predict the same catch composition for full gear selectivity ($S_a = 1$ for all a) does not imply that the discrete formulation allows for multiple interactions with the fishery within each time period. On the contrary, the discrete formulation explicitly models the population first being affected by natural mortality, followed by an instantaneous single pulse of fishing at time t^* (one interaction), and finally further natural mortality until the end of the time period. The effects of this assumption are most easily seen with a contrived example in which all ages are equally but not fully selected by the fishing gear (e.g., $S_a = 0.5$ for all a). In this case, the two formulations would predict identical catch compositions, but the discrete formulation would allow 50% of the available population to be harvested at the maximum exploitation rate ($u_t = 1$), in contrast to the continuous formulation that would allow the entire available population to be harvested at maximum instantaneous fishing mortality ($F_t \to \infty$). These predictions differ because the discrete formulation only allows for a single interaction between fish and fishery.

The second criticism of Francis (2010) is that the choice of formulation should not be based on assumptions regarding the conduct of the fishery (i.e., whether multiple gear interactions occur), but on whichever formulation fits the data better. In light of the above discussion about gear selectivity and availability, our respective views are complementary. If gear selectivity is the most important facet of catchability, then the continuous catch formulation is preferable at high fishing mortalities (Branch 2009*a*), whereas if availability is the most important facet of catchability, then the discrete catch formulation should be used (Francis 2010). But what should we do when both gear selectivity and availability are important, or we do not know their relative importance? In Branch (2009*a*, 2009*b*), I proposed using a hybrid formulation from Megrey (1989) that combines the features of the continuous and discrete formulations, i.e., gear selectivity is exponentiated together with fishing mortality, whereas availability is not exponentiated,

$$(1) \quad N_{a+1,t+1} = N_{a,t} A_a e^{-M - S_a F_t} + N_{a,t}(1 - A_a)e^{-M} \qquad 0 \leq A_a \leq 1,\ 0 \leq S_a$$

$$(2) \quad C_{a,t} = \frac{S_a F_t}{M + S_a F_t} A_a N_{a,t}(1 - e^{-M - S_a F_t})$$

which shows how numbers N at age a and time t change for given gear selectivity S, availability A, fishing mortality F, and natural mortality M, and how these quantities affect catches C over the time period from t to $t + 1$. Francis (2010) correctly points out that in practice, the gear selectivity and availability parameters in eqs. 1–2 are likely to be confounded and difficult to estimate separately and therefore recommends choosing whichever of the continuous or discrete formulations fits the data better. As an inveterate modeler, I generally support this view, which seems a reasonable way forward for most stock assessments given that some stock assessment programs such as CASAL (Bull et al. 2005) and Stock Synthesis II (Methot 2005) allow for easy switching between the discrete and continuous formulations. However, I have some sympathy for the alternative argument that formulation choice should arise from basic assumptions about how a particular fishery operates, not just model fits to the data.

In a few instances, there may be data to model both gear selectivity and availability. Pribac et al. (2005) included a fixed (not estimated) gear selectivity curve based on previous gear experiments and then estimated availability from the data. The gillnets used in this fishery for gummy sharks (*Mustelus antarcticus*) are known to be highly size selective, and availability clearly also differs by age, given marked discrepancies between fishery length frequencies and survey length frequencies. Dorn and Methot (1990) and Methot and Dorn (1995) describe a complementary model for Pacific whiting (*Merluccius productus*) in which gear selectivity is estimated, whereas the relative availability of Pacific whiting to the Canadian and US fisheries in a given year is prespecified using data from acoustic surveys. Hybrid models of this kind may become more common in the future when, for example, gear selectivity is estimated externally to the model using gear experiments (Millar and Fryer 1999) and availability is estimated internally in the model, or alternatively availability is estimated externally and gear selectivity is estimated within the model.

The logical end point of this progression is a model that internally estimates both gear selectivity and availability from available data. I have a paper in preparation that models both for run reconstructions of Bristol Bay sockeye salmon (*Oncorhynchus nerka*) in which gear selectivity can be estimated from differences between catch length frequencies and escapement length frequencies (Kendall and Quinn 2009; Kendall et al. 2009), and availability by stock (fish headed for different rivers) can be estimated from genetic data allocating catches to each stock (Dunn et al. 2009).

References

Beverton, R.J.H., and Holt, S.J. 1957. On the dynamics of exploited fish populations. Fisheries Investigations, Ministry of Agriculture, Fisheries and Food (G.B.), Series II, Vol. 19.

Branch, T.A. 2009*a*. Differences in predicted catch composition between two widely used catch equation formulations. Can. J. Fish. Aquat. Sci. **66**: 126–132. doi:10.1139/F08-196.

Branch, T.A. 2009*b*. Corrigendum: Differences in predicted catch composition between two widely used catch equation formulations. Can. J. Fish. Aquat. Sci. **66**: 1631. doi:10.1139/F09-107.

Bull, B., Francis, R.I.C.C., Dunn, A., McKenzie, A., Gilbert, D.J., and Smith, M.H. 2005. CASAL (C++ algorithmic stock assessment laboratory): CASAL user manual v2.07–2005/06/23. NIWA Technical Report No. 126.

Dunn, T.H., Habicht, C., Jasper, J.R., Hoyt, H.A., Barclay, A.W., Templin, W.D., Baker, T.T., West, F.W., and Fair, L.F. 2009. Genetic stock composition of the commercial harvest of sockeye salmon in Bristol Bay, Alaska, 2006–2008. Alaska Department of Fish and Game Fishery Manuscript Series No. 09-06.

Dorn, M.W., and Methot, R.D. 1990. Status of the Pacific whiting resource in 1989 and recommendations to management in 1990. Alaska Fisheries Science Center, National Marine Fisheries Service, National Oceanic and Atmospheric Administration, NOAA Tech. Memo. NMFS F/NWC-182.

Francis, R.I.C.C. 2010. Comment on "Differences in predicted catch composition between two widely used catch equation formulations". Can. J. Fish. Aquat. Sci. **67**: 763–765.

Kendall, N.W., and Quinn, T.P. 2009. Effects of population-specific variation in age and length on fishery selection and exploitation rates of sockeye salmon (*Oncorhynchus nerka*). Can. J. Fish. Aquat. Sci. **66**: 896–908. doi:10.1139/F09-047.

Kendall, N.W., Hard, J.J., and Quinn, T.P. 2009. Quantifying six decades of fishery selection for size and age at maturity in sockeye salmon. Evol. Appl. **2**: 523–536. doi:10.1111/j.1752-4571.2009.00086.x.

MacCall, A.D. 1986. Virtual population analysis (VPA) equations for nonhomogeneous populations, and a family of approximations including improvements on Pope's cohort analysis. Can. J. Fish. Aquat. Sci. **43**: 2406–2409.

Marr, J.C. 1951. On the use of the terms *abundance*, *availability* and *apparent abundance* in fishery biology. Copeia, **1951**: 163–169. doi:10.2307/1437549.

Megrey, B.A. 1989. Review and comparison of age-structured stock assessment models from theoretical and applied points of view. *In* Mathematical analysis of fish stock dynamics. *Edited by* E.F. Edwards and B.A. Megrey. American Fisheries Society, Bethesda, Maryland. pp. 8–48.

Methot, R. 2005. Technical description of the Stock Synthesis II assessment program. NOAA Fisheries, Seattle, Washington, SEDAR 16-AW-04.

Methot, R.D., and Dorn, M.W. 1995. Biology and fisheries of North Pacific hake (*M. productus*). *In* Hake: biology, fisheries and markets. *Edited by* J. Alheit and T.J. Pitcher. Chapman & Hall, London, UK. pp. 389–414.

Millar, R.B., and Fryer, R.J. 1999. Estimating the size-selection curves of towed gears, traps, nets and hooks. Rev. Fish Biol. Fish. **9**: 89–116. doi:10.1023/A:1008838220001.

Pribac, F., Punt, A.E., Taylor, B.L., and Walker, T.I. 2005. Using length, age and tagging data in a stock assessment of a length selective fishery for gummy shark (*Mustelus antarcticus*). J. Northwest Atl. Fish. Sci. **35**: 267–290. doi:10.2960/J.v35.m521.

NRC·CNRC

National Research Council Canada | Conseil national de recherches Canada

Canadian Journal of Fisheries and Aquatic Sciences 1980–1995 back issues now available on the Web!

Archives du Journal canadien des sciences halieutiques et aquatiques (1980–1995) maintenant accessibles sur le Web!

NRC Research Press is currently taking orders for the one-time purchase of the *Canadian Journal of Fisheries and Aquatic Sciences* back files (1980–1995), 15 years of fully indexed digitized articles are available!

This monthly journal publishes manuscripts reporting significant new knowledge and understanding of fisheries and aquatic sciences. They cover a range of disciplines including biology and ecology of marine and freshwater organisms, limnology, oceanography, physiology, toxicology, genetics, economics, disease, and management. CJFAS is one of 16 journals published by NRC Research Press, Canada's foremost scientific publisher.

Since this is a cost-recovery initiative, once costs are fully recovered, we would like to make our content more widely available by making the back files completely open in late 2009. We hope that libraries and the STM community share this goal and will partner with us to make this initiative a success.

ISSN: 1205-7533

CJFAS Web site: cjfas.nrc.ca

Frequency: Monthly (12 times/year)

Price: $2000.00

Les Presses scientifiques du CNRC acceptent maintenant les commandes pour l'achat en bloc des archives du *Journal canadien des sciences halieutiques et aquatiques* (1980–1995), 15 années d'articles numérisés et indexés!

Cette revue mensuelle publie des articles contribuant, via l'apport de nouvelles connaissances d'importance ou d'une compréhension approfondie, à l'enrichissement des sciences halieutiques et aquatiques. Ceux-ci traitent de disciplines variées, y compris la biologie et l'écologie des organismes d'eau douce et d'eau salée, la limnologie, l'océanographie, la physiologie, la toxicologie, la génétique, l'économie, les maladies et la gestion. Elle est l'une des 16 revues des Presses scientifiques du CNRC, la maison d'édition scientifique la plus importante au Canada.

Il s'agit d'une initiative en recouvrement de coûts. Ainsi, nous aimerions élargir l'accès à nos collections en offrant les archives tout à fait gratuitement vers la fin de 2009, une fois les coûts entièrement recouvrés. Nous espérons que le milieu STM et les bibliothèques appuieront notre objectif et contribueront au succès de cette initiative.

ISSN : 1205-7533

Site Web : jcsha.cnrc.ca

Fréquence : mensuelle (12 numéros par année)

Tarif : 2000 $

Contact **Mike Boroczki** at **613-993-9108**
or mike.boroczki@nrc-cnrc.gc.ca for further information.

Communiquez avec **Mike Boroczki** au **613-993-9108**
ou mike.boroczki@nrc-cnrc.gc.ca pour obtenir des renseignements supplémentaires.

Schindler Endowed Professorship in Aquatic Science

TRENT UNIVERSITY invites applications for a tenured/tenure-track appointment in the Department of Biology to start July 1st 2010, subject to budgetary approval. Appointment will be at the rank of Assistant or Associate Professor. Applicants must have a PhD and a record of outstanding scholarly activity; preference will be given to those with a strong teaching record. The successful candidate is expected to establish an externally-funded research program in an aspect of fresh water Biology and to supervise MSc and PhD students in the Environmental and Life Sciences Graduate Program and/or the proposed Biology Graduate Program. The successful candidate will be provided with a research laboratory in the new Department of Biology building that will open in spring 2011.

The Schindler Endowed Professorship was established to honour Dr. David Schindler, one of the world's leading fresh water biologists. The title and an annual discretionary budget of $10,000 will be for a 5-year term, renewable for a further 5 years following review. Trent University is located on the Otonabee River in a region of numerous lakes and streams. It offers a broad range of research opportunities including a 100 hectare field station, on-campus nature areas, analytical inorganic and organic chemical equipment with an extensive mass spectrometry centre, environmental chambers, major facilities for DNA sequencing and profiling, and imaging facilities. The DNA Building also houses scientists in the Ontario Ministry of Resources that are engaged in broad array of aquatic research programs.

Completed applications should comprise a curriculum vitae, a summary of research plans, an outline of teaching philosophy and names and contact information of three references. Review of applications will begin March 2010 and will continue until the position is filled.

Applications should be sent to
Bradley White, Chair, Department of Biology,
Trent University, 1600 West Bank Drive,
Peterborough, Ontario, Canada K9J 7B8.
For more information, e-mail bwhite@trentu.ca,
call 705-748-1011 ext. 7113, or visit
www.trentu.ca/biology

Trent University is an employment equity employer and especially invites applications from women, Aboriginal people, visible minorities and persons with disabilities. All qualified candidates are encouraged to apply; however, Canadians and permanent residents will be given priority.

TRENT UNIVERSITY

Trent University ad
Canadian Journal of Fisheries and Aquatic Science 7 1/8" x 4 3/4"

Yan Jiao, Laura Rogers-Bennett, Ian Taniguchi, John Butler, and Paul Crone	**730–742**	Incorporating temporal variation in the growth of red abalone (*Haliotis rufescens*) using hierarchical Bayesian growth models
Philippe Souchu, Béatrice Bec, Val H. Smith, Thierry Laugier, Annie Fiandrino, Laurent Benau, Valérie Orsoni, Yves Collos, and André Vaquer	**743–753**	Patterns in nutrient limitation and chlorophyll *a* along an anthropogenic eutrophication gradient in French Mediterranean coastal lagoons
Jennifer B. Korosi, Andrew M. Paterson, Anna M. DeSellas, and John P. Smol	**754–762**	A comparison of pre-industrial and present-day changes in *Bosmina* and *Daphnia* size structure from soft-water Ontario lakes
	DISCUSSION	DISCUSSION
R.I.C. Chris Francis	**763–765**	Comment on "Differences in predicted catch composition between two widely used catch equation formulations"
Trevor A. Branch	**766–768**	Reply to the comment by Francis on "Differences in predicted catch composition between two widely used catch equation formulations"

National Research Council Canada
Ottawa, Canada K1A 0R6

Conseil national de recherches Canada
Ottawa, Canada K1A 0R6

Postage paid at Ottawa
Publications mail
Registration No. 40062591

Port payé à Ottawa
Poste-publication
Enregistrement n° 40062591

USPS periodical postage paid at Plattsburgh, NY 12901, USA

Canadian Journal of

FISHERIES AND AQUATIC SCIENCES

Volume 67, Number 4, April 2010

Journal canadien des

SCIENCES HALIEUTIQUES ET AQUATIQUES

Volume 67, numéro 4, avril 2010

	ARTICLES	ARTICLES
Karin E. Limburg and Mikael Elfman	**597–604**	Patterns and magnitude of Zn:Ca in otoliths support the recent phylogenetic typology of Salmoniformes and their sister groups
Olav Sigurd Kjesbu, David Righton, Maria Krüger-Johnsen, Anders Thorsen, Kathrine Michalsen, Merete Fonn, and Peter R. Witthames	**605–625**	Thermal dynamics of ovarian maturation in Atlantic cod (*Gadus morhua*)
Jeffrey G. Shellberg, Susan M. Bolton, and David R. Montgomery	**626–640**	Hydrogeomorphic effects on bedload scour in bull char (*Salvelinus confluentus*) spawning habitat, western Washington, USA
Michael C. Melnychuk and Carl J. Walters	**641–658**	Estimating detection probabilities of tagged fish migrating past fixed receiver stations using only local information
Aurélie Descroix, Christian Desvilettes, Alexandre Bec, Patrick Martin, and Gilles Bourdier	**659–672**	Impact of macroinvertebrate diet on growth and fatty acid profiles of restocked 0+ Atlantic salmon (*Salmo salar*) parr from a large European river (the Allier)
Michael J. Bradford, Jan Lovy, David A. Patterson, David J. Speare, William R. Bennett, Allen R. Stobbart, and Christine P. Tovey	**673–683**	*Parvicapsula minibicornis* infections in gill and kidney and the premature mortality of adult sockeye salmon (*Oncorhynchus nerka*) from Cultus Lake, British Columbia
Maria José Maezo, Henri Fournier, and Beatrix E. Beisner	**684–700**	Potential and realized interactions between two aquatic invasive species: Eurasian watermilfoil (*Myriophyllum spicatum*) and rusty crayfish (*Orconectes rusticus*)
Adrian Jordaan, Yong Chen, David W. Townsend, and Sally Sherman	**701–719**	Identification of ecological structure and species relationships along an oceanographic gradient in the Gulf of Maine using multivariate analysis with bootstrapping
Amina E. Price and Paul Humphries	**720–729**	The role of dispersal and retention in the early life stages of shrimp in a lowland river

Continued on inside back cover / Suite au verso

Front cover: Boko Saito/Toshiyuki Tajima/Dex Image/Getty Images.

Page couverture : Boko Saito/Toshiyuki Tajima/Dex Image/Getty Images.

Canada

Printed in Canada by / Imprimé au Canada par
NRC Reprographic Services / Service de reprographie CNRC
Page production by / Mise en page par
NRC Research Press / Presses scientifiques du CNRC

0706-652X(20100467:4:1-G